

Editorial

Channelopathies and drug discovery in the postgenomic era

Dayue Darrel DUAN^{1, *}, Tong-hui MA^{2, *}

¹Laboratory of Cardiovascular Phenomis, Center of Biomedical Research Excellence, Department of Pharmacology, Center for Molecular Medicine, University of Nevada School of Medicine, Reno, Nevada 89557, USA; ²Central Research Laboratory, Jilin University Bethune Second Hospital, Changchun 130041, China

Acta Pharmacologica Sinica (2011) 32: 673–674; doi: 10.1038/aps.2011.73

Ion channels are a diverse group of pore-forming proteins that provide selective pathways for the movement of ions (Na^+ , K^+ , Ca^{2+} , Cl^- , etc) across the lipid membrane barrier. Aquaporins facilitate water movement across cell membranes in response to osmotic gradients. There is an increasing body of information on the molecular structure and functional roles of ion and water channels in health and disease, linking channel function at the molecular level to organ physiology. Because ion channels play essential roles in all cells, defects in ion channels are associated with a wide variety of pathophysiological conditions and human diseases. Diseases caused by disturbed function of ion channel subunits or regulatory proteins have been defined as “channelopathies”^[1,2]. In the postgenomic era the rapid progress in the molecular identification of genes for new ion channels and elucidation of their transport properties, physiological functions, and disease relevant mutations has significantly advanced the knowledge of channelopathies and potential new therapies^[3–9]. For examples, the discovery of aquaporin water channels, a family of integral membrane proteins that selectively transport water, has led to the identification of water channelopathies including autosomal dominant and recessive forms of hereditary nephrogenic diabetes insipidus caused by aquaporin-2 mutations^[10], congenital cataracts incurred by aquaporin-0 mutations^[11] and acquired neuronal inflammatory disease neuromyelitis optica in which pathogenic autoantibodies target aquaporin-4^[12]. Impaired Cl^- transport caused by mutations in genes belonging to distinct Cl^- channel families has been found to cause diverse diseases such as cystic fibrosis, myotonia, epilepsy, hyperekplexia, lysosomal storage disease, deafness, renal salt loss, kidney stones,

osteopetrosis, and cardiovascular diseases^[7,13,14]. In addition, the studies on the role of ion channel regulatory proteins, including the sub-membrane adapter ankyrins and alpha-1 syntrophin, membrane coat protein caveolin-3, signaling platform yotiao, and lamins, have also provided novel insights into understanding of human diseases^[15].

In the international symposium on “Channelopathy and Drug Discovery” held in Jilin University Bethune Second Hospital, Changchun, Jilin, China on October 14–16, 2010, about 40 accomplished scientists from the United States, United Kingdom, Canada, Germany, Italy, South Korea, and different regions of China were invited to present their latest research in the fields of channelopathies, with particular focus on aquaporins and chloride channels. In facing the challenges of developing novel pharmacological therapies targeting channelopathies, new strategies of modern drug discovery, including methodology of high throughput screening from natural products and approaches of combinatorial and medicinal chemistry were also discussed. This symposium provided an important platform for domestic and overseas scientists to communicate on the latest academic achievements in channelopathies and drug discovery.

In this Special Issue of Acta Pharmacologica Sinica we have assembled a series of review articles, original research contributions, and perspectives from the speakers of the international symposium to provide the most up-to-date information on our understanding of the mechanisms of aquaporin and Cl^- channelopathies and related new strategies and targets for drug discovery. To cover the topics of channelopathies other than aquaporin and Cl^- channels we extended the invitation to contribute papers from several leading scientists who did not attend the symposium. These articles in this special issue impart a summary of the recent advances in the study of molecular mechanisms and functional roles of a variety of ion channels including Na^{+16} , K^{+17-20} , Ca^{2+21} , Cl^{-22-26} ,

* To whom correspondence should be addressed.

E-mail dduan@medicine.nevada.edu (Dayue Darrel DUAN);

math108@gmail.com (Tong-hui MA)

Received 2011-05-14 Accepted 2011-05-16

TRP^[27, 28], TREK^[29] and acid-sensing Ca²⁺-permeable channels^[30], and aquaporins^[31–35]. Advances are reported in channel integrated physiology, pharmacology and pathophysiology, and in channelopathies of the nervous^[27–28, 30, 34–35], cardiovascular^[15–18, 22, 25, 36–37], renal^[20], and reproductive^[29, 31–33] systems. In addition, the role of pathological release of Ca²⁺ from the sarcoplasmic reticulum via cardiac ryanodine receptors (RyR2) in cardiac arrhythmias and RyR2 as a promising novel target for antiarrhythmic therapy are also discussed^[36].

We believe that publication of this special issue will also highlight the impact of Chinese scientists in this field and promote international academic exchange and collaborations to accelerate understanding of human disease mechanisms and discovery of new treatments.

References

- Hoffman EP. Voltage-gated ion channelopathies: inherited disorders caused by abnormal sodium, chloride, and calcium regulation in skeletal muscle. *Annu Rev Med* 1995; 46: 431–41.
- Wang J, Zhou J, Todorovic SM, Feero WG, Barany F, Conwit R, *et al*. Molecular genetic and genetic correlations in sodium channelopathies: lack of founder effect and evidence for a second gene. *Am J Hum Genet* 1993; 52: 1074–84.
- Andavan GS, Lemmens-Gruber R. Voltage-gated sodium channels: mutations, channelopathies and targets. *Curr Med Chem* 2011; 18: 377–97.
- Dudley SC Jr. Ion channelopathies: a tapped-out mine? *Am J Physiol Heart Circ Physiol* 2011; 300: H716–H717.
- Kass RS. The channelopathies: novel insights into molecular and genetic mechanisms of human disease. *J Clin Invest* 2005; 115: 1986–9.
- Mohler PJ, Bennett V. Ankyrin-based cardiac arrhythmias: a new class of channelopathies due to loss of cellular targeting. *Curr Opin Cardiol* 2005; 20: 189–93.
- Planells-Cases R, Jentsch TJ. Chloride channelopathies. *Biochim Biophys Acta* 2009; 1792: 173–89.
- Tfelt-Hansen PC, Koehler PJ. One hundred years of migraine research: major clinical and scientific observations from 1910 to 2010. *Headache* 2011; 51: 752–78.
- Zhou P, Wang J. Genetic testing for channelopathies, more than ten years progress and remaining challenges. *J Cardiovasc Dis Res* 2010; 1: 47–9.
- Loonen AJ, Knoers NV, van Os CH, Deen PM. Aquaporin 2 mutations in nephrogenic diabetes insipidus. *Semin Nephrol* 2008; 28: 252–65.
- Chepelinsky AB. Structural function of MIP/aquaporin 0 in the eye lens; genetic defects lead to congenital inherited cataracts. *Handb Exp Pharmacol* 2009; 265–97.
- Jarius S, Paul F, Franciotta D, Waters P, Zipp F, Hohlfield R, *et al*. Mechanisms of disease: aquaporin-4 antibodies in neuromyelitis optica. *Nat Clin Pract Neurol* 2008; 4: 202–14.
- Duan D. Phenomics of cardiac chloride channels: the systematic study of chloride channel function in the heart. *J Physiol* 2009; 587: 2163–77.
- Duan DY, Liu LL, Bozeat N, Huang ZM, Xiang SY, Wang GL, *et al*. Functional role of anion channels in cardiac diseases. *Acta Pharmacol Sin* 2005; 26: 265–78.
- Boudoulas KD, Mohler PJ. Beyond membrane channelopathies: alternative mechanisms underlying complex human disease. *Acta Pharmacol Sin* 2011; 32: 798–804.
- Sun Y, Zhang JN, Zhao D, Wang QS, Gu YC, Ma HP, *et al*. Role of the epithelial sodium channel in salt-sensitive hypertension. *Acta Pharmacol Sin* 2011; 32: 789–97.
- Liu Q, Kong AL, Chen R, Qian C, Liu SW, Sun BG, *et al*. Propofol and arrhythmias: two sides of the coin. *Acta Pharmacol Sin* 2011; 32: 817–23.
- Zhou P, Babcock J, Liu LQ, Li M, Gao ZB. Activation of human ether-a-go-go related gene (hERG) potassium channels by small molecules. *Acta Pharmacol Sin* 2011; 32: 781–8.
- Quan Y, Barszczyk A, Feng ZP, Sun HS. Current understanding of K_{ATP} channels in neonatal diseases related to insulin secretion disorders. *Acta Pharmacol Sin* 2011; 32: 765–80.
- Sun Y, Zhou H, Yang BX. Drug discovery for polycystic kidney disease. *Acta Pharmacol Sin* 2011; 32: 805–16.
- Nejatbakhsh N, Feng ZP. Calcium binding protein-mediated regulation of voltage-gated calcium channels linked to human diseases. *Acta Pharmacol Sin* 2011; 32: 741–8.
- Duan DD. The CIC-3 chloride channels in cardiovascular disease. *Acta Pharmacol Sin* 2011; 32: 675–84.
- Yang H, Xu LN, He CY, Liu X, Fang RY, Ma TH. CFTR chloride channel as a molecular target of anthraquinone compounds in herbal laxatives. *Acta Pharmacol Sin* 2011; 32: 834–9.
- Duran C, Hartzell HC. Physiological roles and diseases of tmem16/anoctamin proteins: are they all chloride channels? *Acta Pharmacol Sin* 2011; 32: 685–92.
- Xiang SY, Ye LL, Duan LM, Liu LH, Ge ZD, Auchampach JA, *et al*. Characterization of a critical role for CFTR chloride channels in cardioprotection against ischemia/reperfusion injury. *Acta Pharmacol Sin* 2011; 32: 824–33.
- Cai ZW, Liu J, Li HY, Sheppard DN. Targeting F508del-CFTR to develop rational new therapies for cystic fibrosis. *Acta Pharmacol Sin* 2011; 32: 693–701.
- Yu SQ, Wang DH. Enhanced salt sensitivity following shRNA silencing of neuronal TRPV1 in rat. *Acta Pharmacol Sin* 2011; 32: 845–52.
- Bae CY, Sun HS. TRPM7 in cerebral ischemia and potential target for drug development in stroke. *Acta Pharmacol Sin* 2011; 32: 725–33.
- Buxton ILO, Heyman N, Wu YY, Barnett S, Ulrich C. A role for stretch-activated potassium currents in the regulation of uterine smooth muscle contraction. *Acta Pharmacol Sin* 2011; 32: 758–64.
- Li MH, Inoue K, Si HF, Xiong ZG. Calcium-permeable ion channels involved in glutamate receptor-independent ischemic brain injury. *Acta Pharmacol Sin* 2011; 32: 734–40.
- Sha XY, Xiong ZF, Liu HS, Zheng Z, Ma TH. Pregnant phenotype in aquaporin 8-deficient mice. *Acta Pharmacol Sin* 2011; 32: 840–4.
- Chen Q, Duan EK. Aquaporins in sperm osmoadaptation: an emerging role for volume regulation. *Acta Pharmacol Sin* 2011; 32: 721–4.
- Sha XY, Xiong ZF, Liu HS, Di SD, Ma TH. Maternal-fetal fluid balance and aquaporins: from molecule to physiology. *Acta Pharmacol Sin* 2011; 32: 716–20.
- Verkman AS, Ratelade J, Rossi A, Zhang H, Tradtrantip H. Aquaporin-4: orthogonal array assembly, CNS functions, and role in neuromyelitis optica. *Acta Pharmacol Sin* 2011; 32: 702–10.
- Ma TH, Gao HW, Fang XD, Yang H. Expression and function of aquaporins in peripheral nervous system. *Acta Pharmacol Sin* 2011; 32: 711–5.
- McCauley MD, Wehrens XHT. Targeting ryanodine receptors for antiarrhythmic therapy. *Acta Pharmacol Sin* 2011; 32: 749–57.
- Yang RG, Xi N, Lai KW, Zhong BH, Fung CK, Qu CG, *et al*. Nano-mechanical analysis of insulinoma cells by atomic force microscopy after glucose and capsaicin stimulation. *Acta Pharmacol Sin* 2011; 32: 853–60.

Review

The ClC-3 chloride channels in cardiovascular disease

Dayue Darrel DUAN*

Laboratory of Cardiovascular Phenomics, Center of Biomedical Research Excellence, Department of Pharmacology, University of Nevada School of Medicine, Reno, NV 89557, USA

ClC-3 is a member of the ClC voltage-gated chloride (Cl⁻) channel superfamily. Recent studies have demonstrated the abundant expression and pleiotropy of ClC-3 in cardiac atrial and ventricular myocytes, vascular smooth muscle cells, and endothelial cells. ClC-3 Cl⁻ channels can be activated by increase in cell volume, direct stretch of β 1-integrin through focal adhesion kinase and many active molecules or growth factors including angiotensin II and endothelin-1-mediated signaling pathways, Ca²⁺/calmodulin-dependent protein kinase II and reactive oxygen species. ClC-3 may function as a key component of the volume-regulated Cl⁻ channels, a superoxide anion transport and/or NADPH oxidase interaction partner, and a regulator of many other transporters. ClC-3 has been implicated in the regulation of electrical activity, cell volume, proliferation, differentiation, migration, apoptosis and intracellular pH. This review will highlight the major findings and recent advances in the study of ClC-3 Cl⁻ channels in the cardiovascular system and discuss their important roles in cardiac and vascular remodeling during hypertension, myocardial hypertrophy, ischemia/reperfusion, and heart failure.

Keywords: ClC; chloride channels; heart disease; apoptosis; oxidative stress; remodeling; hypertension

Acta Pharmacologica Sinica (2011) 32: 675–684; doi: 10.1038/aps.2011.30; published online 23 May 2011

Introduction

ClC-3 is a member of the ClC voltage-gated chloride (Cl⁻) channel gene superfamily^[1]. In 1994, ClC-3 cDNA was first cloned from rat kidney by Kawasaki *et al* using a polymerase chain reaction (PCR) cloning strategy^[2]. ClC-3 is also abundantly expressed in brain^[3], lung, kidney^[4], heart^[5, 6], and vasculature^[7] of many species, including human^[4, 6, 8]. Expression of the cloned rat ClC-3 yielded an outwardly-rectifying Cl⁻ current in *Xenopus* oocytes^[2] and in somatic cell lines^[3], which was completely inhibited by activation of protein kinase C (PKC)^[2] or increased intracellular Ca²⁺ concentration^[3]. The Cl⁻ currents produced by expression of cardiac ClC-3 in mammalian cells are also outwardly-rectifying and inhibited by PKC and share many biophysical and pharmacological characteristics with the volume-regulated Cl⁻ currents ($I_{Cl, vol}$) in cardiac myocytes^[5, 9, 10–13], vascular smooth muscle cells^[7], and many other cell types^[14–16]. ClC-3 Cl⁻ channels can be activated also by direct stretch of β 1-integrin through focal adhesion kinase and many active molecules or growth factors including angiotensin II (Ang II) and endothelin-1 mediated

signaling pathways^[17–20], Ca²⁺/calmodulin-dependent protein kinase II (CaMKII)^[21] and reactive oxygen species^[22, 23]. In the past 15 years, accumulated experimental data has shown that ClC-3 proteins are expressed in sarcolemmal membranes and intracellular organelles of cardiac myocytes, vascular smooth muscle cells, and endothelial cells^[24–27]. Numerous studies have demonstrated the pleiotropy of ClC-3 in many cellular functions, including 1) as a key component of the volume-regulated Cl⁻ channels (VRCCs) to strengthen the regulatory volume decrease (RVD) and protect cardiac myocytes from excessive increase in cell volume during hypoxia, ischemia, or hypertrophy; 2) as a regulator of the redox signaling pathway through interaction with NADPH oxidase (Nox) and/or as a superoxide anion (O₂⁻) transporter to improve myocyte viability against oxidative damage; 3) as an anti-apoptotic mechanism through regulation of cell volume and intracellular pH; and 4) as a regulator of other transport functions involved in the etiology of myocardial damage, heart failure, and hypertension (Figure 1).

This review will highlight the major findings and recent advances in the study of ClC-3 Cl⁻ channels in the cardiovascular system and discuss their important roles in cardiac and vascular remodeling during hypertension, myocardial ischemia/reperfusion, hypertrophy, and heart failure.

* To whom correspondence should be addressed.

E-mail dduan@medicine.nevada.edu

Received 2011-02-16 Accepted 2011-03-14

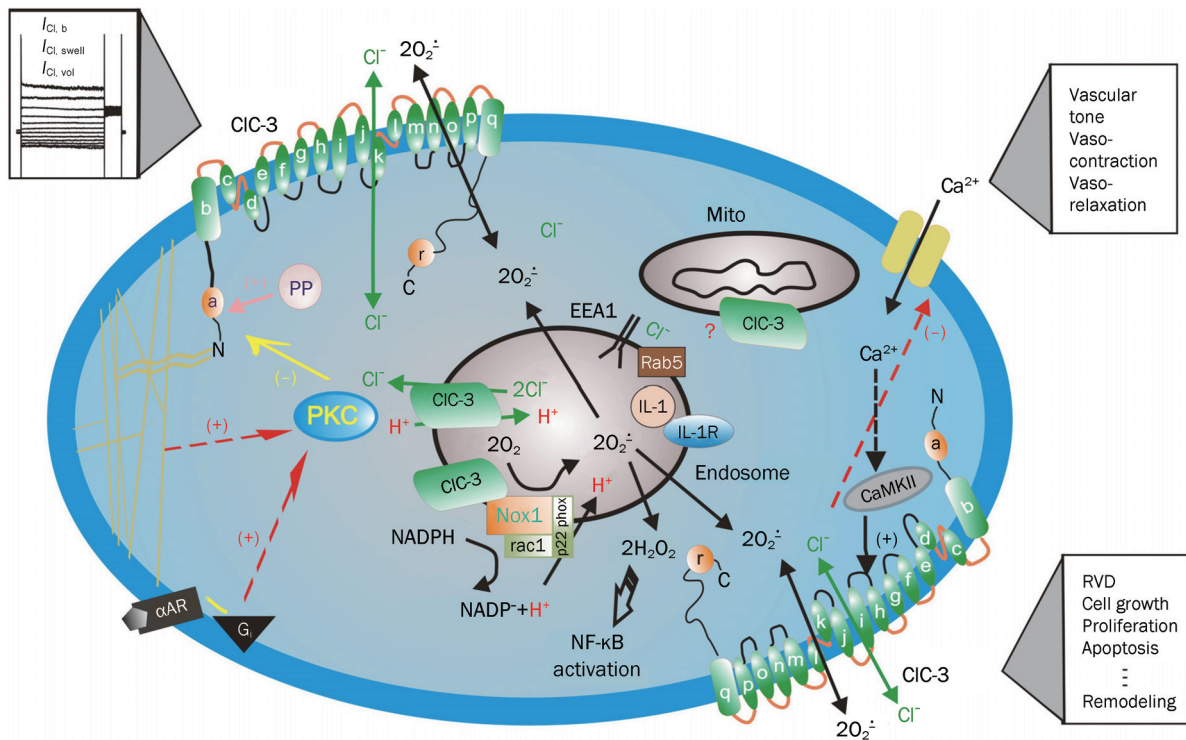


Figure 1. Schematic representation of regulation and function of CIC-3 Cl^- channels in cardiac myocytes and vascular smooth muscle cells. CIC-3, a member of voltage-gated CIC Cl^- channel family, encodes Cl^- channels in cardiac myocytes and vascular smooth muscle cells that are volume regulated ($I_{\text{Cl, vol}}$) and can be activated by cell swelling ($I_{\text{Cl, swell}}$) induced by exposure to hypotonic extracellular solutions or possibly membrane stretch. $I_{\text{Cl, b}}$ is a basally activated CIC-3 Cl^- current. Membrane topology model (α -helices a–r) for CIC-3 is modified from Dutzler *et al.*^[100]. CIC-3 proteins are expressed on both sarcolemmal membrane and intracellular organelles including mitochondria (mito) and endosomes. The proposed model of endosome ion flux and function of Nox1 and CIC-3 in the signaling endosome is modified from Miller Jr *et al.*^[101]. Binding of IL-1 β or TNF- α to the cell membrane initiates endocytosis and formation of an early endosome (EEA1 and Rab5), which also contains NADPH oxidase subunits Nox1 and p22phox, in addition to CIC-3. Nox1 is electrogenic, moving electrons from intracellular NADPH through a redox chain within the enzyme into the endosome to reduce oxygen to superoxide. CIC-3 functions as a chloride-proton exchanger, required for charge neutralization of the electron flow generated by Nox1. The ROS generated by Nox1 result in NF- κ B activation. Both CIC-3 and Nox1 are necessary for generation of endosomal ROS and subsequent NF- κ B activation by IL-1 β or TNF- α in VSMCs. PKC, protein kinase C; PP, serine-threonine protein phosphatases; α -AR, α -adrenergic receptor; G, heterodimeric inhibitory G protein; Nox: NADPH oxidase; CaMKII: Ca^{2+} /calmodulin-dependent protein kinase II; (+) stimulation; (-) inhibition.

CIC-3 and VRCCs

Under osmotic, metabolic, and/or oxidative stress mammalian cells are able to precisely maintain their size through the regulated loss or gain of intracellular ions or other osmolytes to avoid excessive alterations of cell volume that may jeopardize structural integrity and a variety of cellular functions^[28–31]. Even under physiological conditions, volume constancy of any mammalian cell is challenged by the transport of osmotically active substances across the cell membrane and alterations in cellular osmolarity by metabolism^[28]. Thus, the continued operation of cell volume regulatory mechanisms, such as activation of VRCCs, is required for cell volume homeostasis in many mammalian cells, including cardiac myocytes and vascular smooth muscle cells (VSMCs)^[12, 24, 32, 33]. Acute increase in cell volume (or cell swelling) initiates the regulatory volume decrease (RVD) process to bring the cells back to their initial volume, which is achieved by the opening of VRCCs and other channels and transporters mediating Cl^- ,

K^+ , and taurine efflux that in turn drives water exit^[28].

Although the exact identification of the protein(s) responsible for VRCCs has proven to be elusive, CIC-3 has been proposed to be the molecular correlate of the native VRCCs in cardiac myocytes^[5] and VSMCs^[7]. But the role of CIC-3 as a constituent of native VRCCs became an issue of debate owing to inconsistent and conflicting data collected from some laboratories^[34–36]. Specially, the presence of the native VRCCs in two different cell types from the global CIC-3 knockout (*Clcn3*^{-/-}) mice^[35] casts considerable doubt on the role of CIC-3 as a molecular component of VRCCs. However, later additional experiments using *Clcn3*^{-/-} mice revealed that the properties of native VRCCs in the *Clcn3*^{-/-} heart were significantly altered and the expression of a variety of membrane proteins other than CIC-3 was also markedly changed, raising fundamental questions about the usefulness of the *Clcn3*^{-/-} mouse model to assess CIC-3 function^[37]. A series of recent independent studies from many laboratories further strongly corroborated the

hypothesis that CIC-3 encoded a key component of the native VRCCs in a variety of cell types ranging from normal cardiac myocytes to cancer cells^[16, 20, 37-46]. Knockdown of CIC-3 by siRNA^[41, 42, 47], shRNA^[48, 49], and antisense^[20, 39, 43, 45] and intracellular dialysis of anti-CIC-3 antibody (Ab)^[16, 37, 38, 44-46] all consistently eliminated VRCC currents in many types of cells. A recent study using the inducible heart-specific CIC-3 knockout mouse found that a time-dependent inactivation of CIC-3 gene expression was correlated with an elimination of the endogenous VRCCs (Figure 2) and significantly compromised cardiac function (Figure 2)^[50]. Therefore, CIC-3 remains a strong and viable candidate for VRCCs in the heart and may contribute to normal cardiac function.

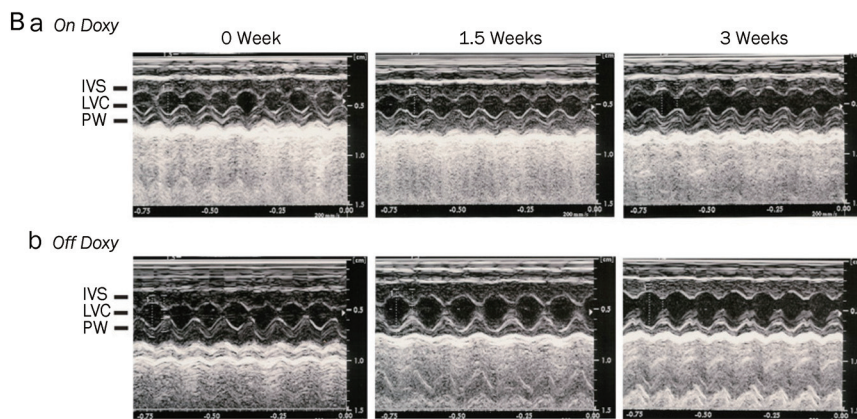
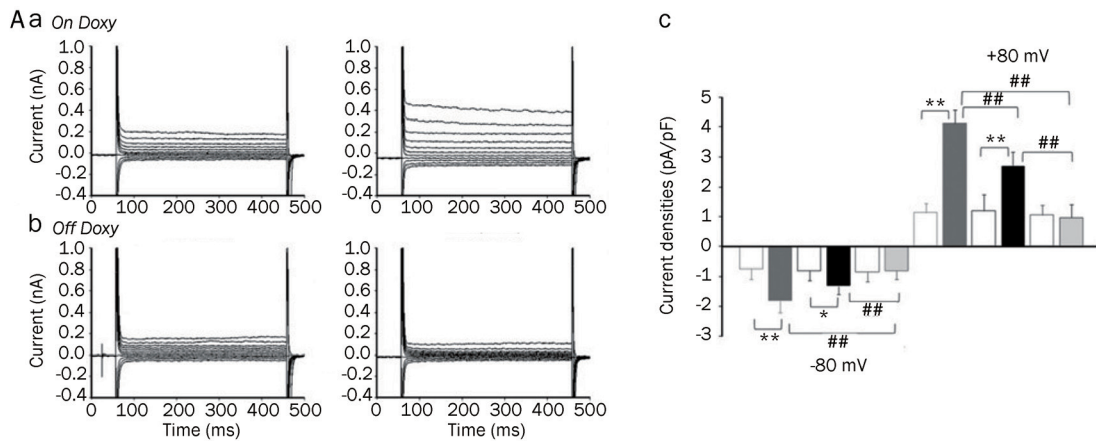
VRCCs and CIC-3 in cardioprotection induced by ischemic preconditioning (IPC)

Ischemic preconditioning (IPC) is a phenomenon in which brief episodes of ischemia dramatically reduce myocardial infarction caused by a subsequent sustained ischemia^[51]. IPC has an early phase (lasting 1-2 h) and a late phase or "second window" (lasting 24-72 h) of protection^[52]. It has been reported that the block of $I_{Cl, \text{swell}}$ in rabbit cardiac myocytes inhibits IPC by brief ischemia, hypo-osmotic stress^[53, 54] and adenosine receptor agonists^[55]. These studies were solely based on the use of several Cl⁻ channel blockers, such as anthracene-9-carboxylic acid (9-AC) and 4-acetamide-4'-isothiocyanatostilbene-2,2'-disulfonic acid (SITS). These pharmacological tools lack specificity to a particular Cl⁻ channel in the heart and may also act on other ion channels or transporters^[56, 57]. Therefore the causal role of $I_{Cl, \text{swell}}$ in IPC has been very difficult to be confirmed^[58]. To specifically test whether the VRCCs are indeed involved in IPC, we have recently established *in vitro* and *in vivo* models of early IPC and late IPC in *CICn3*^{-/-} mice. Our preliminary results indicate that targeted inactivation of CIC-3 gene prevented protective effects of late IPC but not of early IPC, suggesting that CIC-3/VRCCs may contribute differently to early and late IPC^[59, 60]. The underlying mechanisms for these differential effects are currently unknown. Recent reports, however, suggest that VRCCs and CIC-3 may play an important role in apoptosis^[61] and inflammation^[62]. Cl⁻ channel blockers DIDS and NPPB were as potent as a broad-spectrum caspase inhibitor in preventing apoptosis and elevation of caspase-3 activity and improved cardiac contractile function after ischemia and *in vivo* reperfusion^[63]. Transgenic mice overexpressing Bcl-2 in the heart had significantly smaller infarct size and reduced apoptosis of myocytes after ischemia and reperfusion^[64]. It has been shown that Bcl-2 induces up-regulation of $I_{Cl, \text{vol}}$ by enhancing CIC-3 expression in human prostate cancer epithelial cells^[65]. Cell shrinkage is an integral part of apoptosis, suggesting that $I_{Cl, \text{vol}}$ and CIC-3 might be intimately linked to apoptotic events through regulation of cell volume homeostasis^[61, 65, 66].

VRCCs and CIC-3 in myocardial hypertrophy and heart failure

Structural remodeling of myocardial hypertrophy and dilated cardiomyopathy involves oxidative stress and hypertrophic cell volume increase or dilated myocyte membrane stretch, which alters cell volume homeostasis and many cellular functions including cell proliferation, differentiation, and apoptosis. $I_{Cl, \text{swell}}$ is persistently activated in ventricular myocytes from a canine pacing-induced dilated cardiomyopathy model^[67]. Using the perforated patch-clamp technique, Clemons *et al* found that, even in isotonic solutions, a large 9-AC-sensitive, outwardly rectifying Cl⁻ current was recorded in failing cardiac myocytes but not in normal cardiac myocytes. Graded hypotonic cell swelling (60%-90% hypotonic) failed to activate additional current while graded hypertonic cell shrinkage caused an inhibition of the "basal" Cl⁻ current in failing myocytes. Moreover, the maximum current density of the $I_{Cl, \text{swell}}$ in failing myocytes was about 40% greater than that in osmotically swollen normal myocytes. Constitutive activation of $I_{Cl, \text{swell}}$ is also observed in several other animal models of heart failure, such as a rabbit aortic regurgitation model of dilated cardiomyopathy^[68], a dog model of heart failure caused by myocardial infarction^[69], and a mouse model of myocardial hypertrophy by aorta binding^[70]. In human atrial myocytes obtained from patients with right atrial enlargement and/or elevated left ventricular end-diastolic pressure, a tamoxifen sensitive $I_{Cl, \text{swell}}$ was also found to be persistently activated^[67]. Therefore, it is possible that persistent activation of $I_{Cl, \text{swell}}$ is a common response of cardiac myocytes to hypertrophy or heart failure-induced remodeling.

The mechanism for persistent activation of $I_{Cl, \text{swell}}$ in hypertrophied or failing cardiac myocytes is still not clear. Perhaps the increase in cell volume caused by hypertrophy and the stretch of cell membrane caused by dilation are both involved in the activation of $I_{Cl, \text{swell}}$. Alternatively, the persistent activation of $I_{Cl, \text{swell}}$ may be caused by signaling cascades activated during hypertrophy independent of changes in cell length and volume, or both. $I_{Cl, \text{swell}}$ could be activated by direct stretch of β 1-integrin through focal adhesion kinase (FAK) and/or Src^[49]. Mechanical stretch of myocytes also releases Ang II, which binds to AT1 receptors (AT1R) and stimulates FAK and Src in an autocrine-paracrine loop. A recent study by Browe and Baumgarten suggests that the stretch of β 1-integrin in cardiac myocytes activates $I_{Cl, \text{swell}}$ by activating AT1R and NADPH oxidase and, thereby, producing reactive oxygen species (ROS). In addition, a potent NADPH oxidase inhibitor, diphenyleneiodonium (DPI), and a structurally unrelated NADPH oxidase inhibitor, 4-(2-aminoethyl) benzenesulfonyl fluoride (AEBSF), rapidly and completely blocked both background and stretch-activated Cl⁻ currents in cardiac myocytes^[19]. Therefore, NADPH oxidase may be intimately coupled to the channel responsible for $I_{Cl, \text{vol}}$, providing a second regulatory pathway for this channel through membrane stretch or oxidative stress^[19]. This finding is very important for further understanding of the mechanism for hypertrophy activa-



	0 week		1.5 weeks		3 weeks	
	<i>On Doxy</i> n=8	<i>Off Doxy</i> n=15	<i>On Doxy</i> n=4	<i>Off Doxy</i> n=12	<i>On Doxy</i> n=5	<i>Off Doxy</i> n=9
IVSs (mm)	1.64±0.05	1.61±0.03	1.60±0.07	1.49±0.04*	1.61±0.05	1.48±0.04*
LVIDs (mm)	0.95±0.11	0.98±0.08	1.02±0.15	1.51±0.09***#	1.01±0.11	1.57±0.10***,##
LVPWs (mm)	1.41±0.07	1.45±0.05	1.18±0.10	1.33±0.06	1.35±0.08	1.31±0.07
Systole Area (mm ²)	2.61±0.52	2.93±0.38	1.89±0.73	3.77±0.42	2.41±0.55	3.16±0.49
IVSd (mm)	0.81±0.02	0.81±0.02	0.76±0.03	0.76±0.02	0.80±0.02	0.80±0.02
LVIDd (mm)	2.86±0.12	2.94±0.08	2.81±0.16	3.26±0.09*#	2.94±0.12	3.21±0.11
LVPWd (mm)	1.08±0.05	1.08±0.04	1.02±0.07	1.08±0.04	0.98±0.05	1.07±0.05
Diastole Area (mm ²)	11.36±1.29	13.26±0.94	13.83±1.83	14.44±1.05	12.07±1.38	12.09±1.22
FS (%)	66.88±2.12	67.08±1.55	63.65±3.00	54.36±1.73***,##	65.35±2.27	51.62±2.00***,###
LVEF (%)	79.01±2.16	78.11±1.58	85.21±3.06	74.25±1.76**	80.02±2.31	75.20±2.04
Mass (mg/mm ²)	89.06±4.36	92.33±3.18	78.65±6.16	103.08±3.56***,###	83.93±4.66	102.02±4.11***,##
Body Weight (g)	34.86±2.55	43.10±1.86#	33.15±3.61	41.21±2.08	35.04±2.73	36.34±2.40
Mass/BW Ratio	2.69±0.18	2.17±0.13	2.37±0.26	2.55±0.15*	2.38±0.12	2.86±0.17***,##

* $P < 0.05$, ** $P < 0.01$, *** $P < 0.001$ vs *off Doxy* 0 week; # $P < 0.05$, ## $P < 0.01$, ### $P < 0.001$ vs *on Doxy* at the same time point.

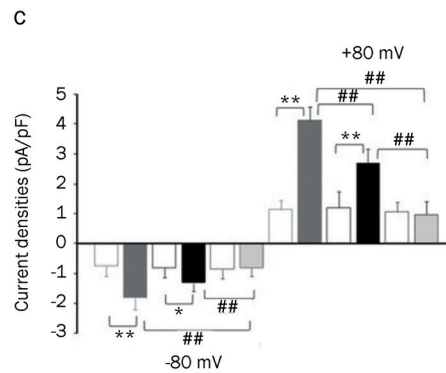
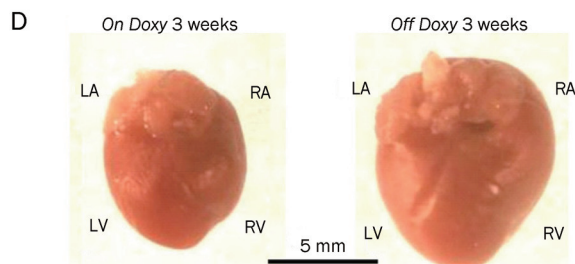


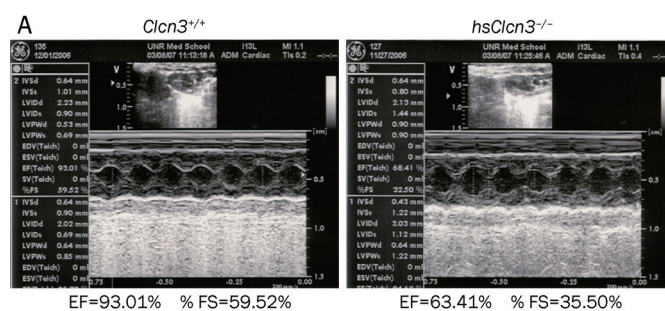
Figure 2. Effects of inducible heart-specific CIC-3 knockout on cardiac volume-regulated Cl⁻ current (VRCC) and heart function. (A) Representative current traces in freshly isolated atrial myocytes from the inducible heart-specific CIC-3 knockout (*doxyhsCIC-3^{-/-}*) mice with doxycycline (*on Doxy*) in the diet (panel a), or after withdraw of doxycycline (*off Doxy*) from the diet for 3 weeks (panel b). (c) Summary of VRCC current densities in isotonic and hypotonic solutions, recorded at +80 mV and -80 mV. Open boxes, under isotonic conditions; filled boxes under hypotonic conditions; Grey boxes, on doxycycline; black boxes, off doxycycline 1.5 weeks; pale grey boxes, off doxycycline for 3 weeks. ** $P < 0.01$, hypotonic-induced VSOAC current densities compared to isotonic conditions. ## $P < 0.01$, hypotonic-induced VSOAC current densities compared between *on Doxy* and 1.5 weeks *off Doxy*, and between 1.5 and 3 weeks *off Doxy* using ANOVA. (B) Representative M-mode echocardiography from *on Doxy* (a) and *off Doxy* (b) mice. (C) Time-dependent changes in M-mode echocardiogram of age-matched *on Doxy* or *off Doxy* for 1.5 and 3 weeks. (D) Comparison of hearts isolated from age-matched (11-week old) *doxyhsClcn3^{-/-}* mice *on Doxy* or *off Doxy* for 3 weeks. Hearts were cleaned up blood and connective tissues and fixed in 4% paraformaldehyde. (Adapted from Xiong et al.^[50]).

tion of $I_{Cl,swell}$ and CIC-3 channels and their relationship with hypertrophy and heart failure as it is very well known that Ang II plays a crucial role in myocardial hypertrophy and heart failure^[71]. Interestingly, Miller and colleagues recently found that Cl⁻ channel inhibitors and knockout of CIC-3 abolished cytokine-induced generation of ROS in endosomes and ROS-dependent NF- κ B activation in vascular smooth muscle cells^[37], suggesting a potential close interaction between NADPH oxidase and CIC-3 (Figure 1). In human corneal keratocytes and human fetal lung fibroblasts CIC-3 knockdown by a short hairpin RNA (shRNA) significantly decreased VRCC and lysophosphatidic acid (LPA)-activated Cl⁻ current ($I_{Cl,LPA}$) in the presence of transforming growth factor- β 1 (TGF- β 1) compared with controls, whereas CIC-3 overexpression resulted in increased $I_{Cl,LPA}$ in the absence of TGF- β 1^[72]. CIC-3 knockdown also resulted in a reduction of α -smooth muscle actin (α -SMA) protein levels in the presence of TGF- β 1, whereas CIC-3 overexpression increased α -SMA protein expression in the absence of TGF- β 1. In addition, keratocytes transfected with CIC-3 shRNA had a significantly blunted regulatory volume decrease response following hyposmotic stimulation compared with controls. These data not only confirm that CIC-3 is important in VRCC function and cell volume regulation, but also provides new insight into the mechanism for the CIC-3-mediated fibroblast-to-myofibroblast transition^[15].

The functional and clinical significance of VRCCs in the hypertrophied and dilated heart is currently unknown. Using a mouse aortic binding model of myocardial hypertrophy, we have found that globally targeted disruption of *CIC-3* gene (*CICn3*^{-/-}) accelerated the development of myocardial hypertrophy and the discompensatory process, suggesting that activation of $I_{Cl,vol}$ might be important in the adaptive remodeling of the heart during pressure overload^[73]. Interestingly, heart failure was found to be accompanied by a reduced $I_{Cl,vol}$ density in rabbit cardiac myocytes^[43]. Our recent studies on the conditional heart-specific CIC-3 knockout (*hsCICn3*^{-/-}) mice (Figure 3) support the crucial functional role of CIC-3 channels in the adaptive remodeling of the heart against pressure overload^[72]. As shown in Figure 3, echocardiography revealed marked signs of myocardial hypertrophy (a significant increase in left ventricular mass LVM) and heart failure (a significant increase in LVIDs and reduction in IVSs, LVEF, and %FS) in the *hsCICn3*^{-/-} mice compared to their age-matched wild-type control mice (Figure 3B). In addition, both left and right atria were significantly enlarged (Figure 3C). These data strongly suggest that CIC-3 may play an important role in maintaining normal structure and function of the mammalian heart.

VRCCs and CIC-3 in electrophysiology and electrical remodeling

Activation of VRCCs is expected to produce depolarization of the resting membrane potential and significant shortening of action potential duration (APD) because of its strong outwardly rectifying property^[5, 11, 24, 74, 75]. The Cl⁻ current through



B

	<i>CICn3</i> ^{+/+} (n=8)	<i>hsCICn3</i> ^{-/-} (n=8)
IVSd (mm)	0.54±0.02	0.56±0.02
IVSs (mm)	1.31±0.09	1.01±0.04*
LVIDd (mm)	2.63±0.16	2.69±0.09
LVIDs (mm)	0.84±0.07	1.52±0.09***
LVPWd (mm)	0.74±0.05	0.81±0.05
LVPWs (mm)	1.22±0.05	1.23±0.05
LVEF	0.97±0.04	0.80±0.03***
% FS	67.05±3.57	43.88±2.85***
HR (bpm)	495.71±22.58	396.13±19.11**
LVM (mg)	40.58±4.33	52.22±2.91*

P*<0.05, *P*<0.01, ****P*<0.001 vs *CICn3*^{+/+}.

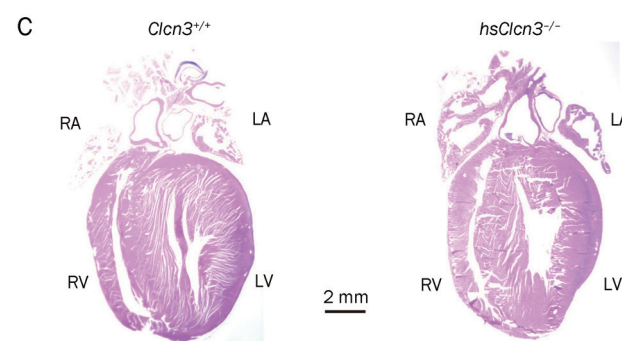


Figure 3. Echocardiography of cardiac function of wild type and heart-specific CIC-3 knockout mice. (A) Representative M-mode echocardiography from wild-type (*CICn3*^{+/+}; left) and heart-specific CIC-3 knockout (*hsCICn3*^{-/-}; right) mice. (B) Echocardiographic measurements in *CICn3*^{+/+} and *hsCICn3*^{-/-} mice. IVSd, interventricular septum thickness at the end of diastole; LVIDd, left ventricular (LV) dimension at the end of diastole; LVPWd, LV posterior wall thickness at the end of diastole; IVSs, interventricular septum thickness at the end of systole; LVIDs, LV dimension at the end of systole; LVPWs, LV posterior wall thickness at the end of systole; LVEF, calculated LV ejection fraction; %FS, LV fractional shortening; Estimated LV mass, LVM (mg)=1.05[(IVS+LVID+LVPW)³-(LVID)³], where 1.05 is the specific gravity of the myocardium. (C) Single longitudinal section (8 μ m) of hearts to demonstrate all four heart chambers. Longitudinal were stained with hematoxylin and eosin (Bar=2 mm) (Ye L and Duan DD. unpublished data).

the VRCCs under basal or isotonic conditions is small^[10, 11, 76] but can be further activated by stretching of the cell mem-

brane by inflation^[77] or direct mechanical stretch of membrane β_1 -integrin^[78] and/or cell swelling induced by exposure to hypoosmotic solutions^[5, 9-13]. The consequences of activation of $I_{Cl, vol}$ are very complex. It may be detrimental, beneficial, or both simultaneous in different parts of the heart, depending on environmental influences.

Because cardiac myocytes swell during hypoxia and ischemia, and the washout of hyperosmotic extracellular fluid after reperfusion induces further cell swelling, activation of VRCCs may contribute to APD shortening and arrhythmias induced by hypoxia, ischemia and reperfusion^[79]. Shortening of APD and, therefore, the effective refractory period (ERP) reduces the length of the conducting pathway needed to sustain reentry (wavelength). In principle, this favors the development of atrial fibrillation (AF) or ventricular fibrillation (VF), depending on the presence of multiple reentrant circuits or rotating spiral waves. Activation of $I_{Cl, vol}$ may slow or enhance the conduction of early extrasystoles, depending on the timing. In guinea-pig heart, hypo-osmotic solution shortened APD and increased APD gradients between right and left ventricles. In burst stimulation-induced VF, exposure to hypo-osmotic solution increased VF frequencies, transforming complex fast Fourier transformation spectra to a single dominant high frequency on the left but not the right ventricle^[19]. Perfusion with the VRCC blocker indanyloxyacetic acid-94 reversed organized VF to complex VF with lower frequencies, indicating that VRCC underlies the changes in VF dynamics. Consistent with this interpretation, CIC-3 channel protein expression is 27% greater on left than right ventricles, and computer simulations showed that insertion of $I_{Cl, vol}$ transformed complex VF to a stable spiral. Therefore, activation of $I_{Cl, vol}$ has a major impact on VF dynamics by transforming random multiple wavelets to a highly organized VF with a single dominant frequency.

In the case of myocardial hypertrophy and heart failure, ionic remodeling is one of the major features of pathophysiological changes^[80]. Under these conditions, $I_{Cl, vol}$ is constitutively active^[69]. The persistent activation of $I_{Cl, vol}$ may limit the APD prolongation and make it more difficult to elicit early after depolarization (EAD). Indeed, in myocytes from failing hearts, blocking $I_{Cl, vol}$ by tamoxifen significantly prolonged APD and decreased the depolarizing current required to elicit EAD by about 50%. And hyper-osmotic cell shrinkage, which also inhibits $I_{Cl, vol}$, was almost equivalent to the effect of tamoxifen on APD and EAD in these myocytes^[79]. It has been shown that mechanical stretching or dilation of the atrial myocardium is able to cause arrhythmias. Since $I_{Cl, vol}$ was also found in sino-atrial (S-A) nodal cells, VRCCs may serve as a mediator of mechanotransduction and play a significant role in the pacemaker function if they act as the stretch-activated channels in these cells^[79, 81]. Baumgarten's laboratory has recently demonstrated that $I_{Cl, vol}$ in ventricular myocytes can be directly activated by mechanical stretch through selectively stretching β_1 -integrins with mAb-coated magnetic beads^[19, 79]. Although it has been suggested that stretch and swelling activate the same anion channel in some non-cardiac cells, further

study is needed to determine whether this is true in cardiac myocytes and VSMCs.

VRCC and CIC-3 in vasculature and hypertensive vascular remodeling

It has been demonstrated that VRCCs and CIC-3 are expressed in aortic and pulmonary VSMCs of human and several other species^[20, 82, 83] and have been implicated in a number of vital cellular functions including vascular myogenic tone, cell volume regulation, cell proliferation and apoptosis^[7, 26, 61, 84].

Membrane stretch or increases in transmural pressure cause contraction of vascular smooth muscle cells, *ie*, myogenic response^[85]. Early studies revealed that the myogenic response was associated with membrane depolarization^[86]. Ion channels sensitive to mechanical stimuli have been suggested to serve as the sensor element of the myogenic response of vascular smooth muscle. Mechano-sensitive Cl^- channels and VRCCs have been observed in vascular smooth muscle cells^[7, 87] and a pressure-induced Cl^- efflux was reported^[88]. Activation of VRCCs and CIC-3 has been postulated to participate in the myogenic response^[7, 84, 86, 87], such as in the membrane depolarization and contraction mediated by activation of α_1 -adrenoceptors and vascular wall distension due to increased transmural pressure^[89]. However, convincing functional evidence for the functional role of VRCCs or CIC-3 in myogenic response and myogenic tone is still lacking due to the lack of specific Cl^- channel blockers^[90]. Further study using the CIC-3 knockout or transgenic mice may provide more insights into the functional role of CIC-3 and VRCCs in the regulation of myogenic response to mechanical stretch.

Arterial VSMC proliferation is a key event in the development of hypertension-associated vascular disease^[83]. Recent accumulating evidence suggests an important role of CIC-3 and VRCCs in the regulation of cell proliferation induced by numerous mitogenic factors^[61]. The magnitude of VRCC currents in actively growing VSMCs is higher than in growth-arrested or differentiated VSMCs, suggesting that VRCCs may be important for VSMC proliferation^[91]. Antisense oligonucleotide-mediated downregulation of CIC-3 dramatically inhibits cell proliferation of rat aortic VSMCs^[20]. A recent study found that static pressure increased VRCCs and CIC-3 expression and promoted rat aortic VSMC proliferation and cell cycle progression^[83]. Inhibition of VRCCs with pharmacological blockers (such as DIDS or the NADPH oxidase inhibitor DPI) or knockdown of CIC-3 with CIC-3 antisense oligonucleotide transfection attenuated pressure evoked cell proliferation and cell cycle progression. Static pressure enhanced the production of ROS in aortic smooth muscle cells. DPI or apocynin pretreatment inhibited pressure-induced ROS production as well as cell proliferation. Furthermore, DPI or apocynin attenuated the pressure-induced upregulation of CIC-3 protein and VRCC current. These data suggest that VRCCs may play a critical role in static pressure-induced cell proliferation and cell cycle progression. Therefore, VRCCs may be of unique therapeutic importance for treatment of hypertension attendant vascular complications.

Cerebral resistance arteries undergo remodeling of the vascular walls during chronic hypertension, which is caused by the coordination of vascular smooth muscle cell proliferation and migration, endothelial cell dysfunction, inflammation and fibrosis. A very recent study demonstrated that the expression of CIC-3 and VRCC activity were increased in basilar artery during hypertension and simvastatin, an inhibitor of 3-hydroxy-3-methylglutaryl coenzyme A (HMG-CoA) reductase widely used in clinics for the treatment of hypercholesterolemia, normalized the upregulation of CIC-3^[92]. Furthermore, simvastatin ameliorated hypertension-caused cerebrovascular remodeling through inhibition of VRCCs and CIC-3 and cell proliferation^[92]. These effects of simvastatin were abolished by pretreatment with mevalonate or geranylgeranyl pyrophosphate. In addition, Rho A inhibitor C3 exoenzyme and Rho kinase inhibitor Y-27632 both reduced cell proliferation and activation of VRCCs. CIC-3 overexpression decreased the suppressive effect of simvastatin on endothelin-1 and hypoosmolarity-induced cell proliferation. These results provided novel mechanistic insight into the beneficial effects of statins in the treatment of hypertension and stroke through an inhibition of CIC-3 and VRCC function.

CIC-3 and superoxide transport and interaction with NADPH oxidase

ROS has been implicated in cellular signaling processes as well as a cause of oxidative stress-induced cell proliferation^[93]. One of the major sources of ROS in the heart and vasculature is through one or more isoforms of the phagocytic enzyme NADPH oxidase, a membrane-localized protein which generates the superoxide ($O_2^{\cdot-}$) anion on the extracellular surface of the plasma membrane (Figure 1). As a charged and short lived anion, it is believed that $O_2^{\cdot-}$ flux is insufficient to initiate intracellular signaling due to the combination of poor permeability through the phospholipid bilayer^[94] and a rapid dismutation to its uncharged and more stable derivative, hydrogen peroxide^[95, 96]. However, recent evidence has indicated discrete signaling roles for both O_2 and H_2O_2 ^[97].

In response to monocrotaline-induced pulmonary hypertension the expression of *Cicn3* gene was upregulated in rat pulmonary artery^[98]. In canine cultured pulmonary arterial smooth muscle cells (PASMCs) incubated with inflammatory mediators *Cicn3* gene was also upregulated^[98]. Overexpression of CIC-3 in PASMCs enhanced viability of the cells against H_2O_2 , thus suggesting that CIC-3 may improve the resistance of VSMCs to ROS in an environment of elevated inflammatory cytokines in hypertensive pulmonary arteries^[98]. It was found that extracellular $O_2^{\cdot-}$, but not H_2O_2 , led to Ca^{2+} signaling and apoptosis in pulmonary endothelial cells^[99]. This indicates that extracellular $O_2^{\cdot-}$ produced by NADPH oxidase or other sources either crosses the plasma membrane or modifies cell surface proteins to mediate cell signaling (Figure 1).

Recently, Hawkins *et al* studied the transmembrane flux of $O_2^{\cdot-}$ in pulmonary microvascular endothelial cells^[17]. Application of an extracellular bolus of $O_2^{\cdot-}$ resulted in rapid and concentration-dependent transient $O_2^{\cdot-}$ -sensitive fluorophore

hydroethidine (HE) oxidation that was followed by a progressive and nonreversible increase in nuclear HE fluorescence. These fluorescence changes were inhibited by superoxide dismutase (SOD), and the Cl^- channel blocker DIDS, and selective silencing of CIC-3 by treatment with siRNA. Extracellular $O_2^{\cdot-}$ triggered Ca^{2+} release, in turn triggered mitochondrial membrane potential alterations that were followed by mitochondrial $O_2^{\cdot-}$ production and cellular apoptosis. These "signaling" effects of $O_2^{\cdot-}$ were prevented by DIDS, by depletion of intracellular Ca^{2+} stores with thapsigargin and by chelation of intracellular Ca^{2+} . This study demonstrates that $O_2^{\cdot-}$ flux across the endothelial cell plasma membrane occurs through CIC-3 channels and induces intracellular Ca^{2+} release, which activates mitochondrial $O_2^{\cdot-}$ generation. These and other studies suggest that activation of CIC-3 may indeed play a role in cell proliferation, growth, volume regulation and apoptosis of VSMCs.

Conclusion

Regulation of CIC-3 functions in the cardiovascular system is emerging as a novel and important mechanism for the electrical and structural remodeling of the heart and vasculature. However, the integrated function of CIC-3 as a key component of VRCC and Nox1 and as a transport of superoxide needs to be further explored. Although specific gene targeting and transgenic approaches have been proven very powerful for specifically addressing the questions, it will be ideal if specific compounds for CIC-3 can be developed as pharmacological tools to answer these questions and to develop drugs targeting CIC-3 as novel therapeutic tools for the treatment of many cardiac and vascular diseases such as myocardial hypertrophy, ischemia, heart failure, and hypertension.

Acknowledgements

The research is supported by grants from the National Institutes of Health (HL63914 and HL106256), National Center of Research Resources (NCR, P20RR15581), and American Diabetes Association Innovation Award (#07-8-IN-08).

References

- 1 Jentsch TJ. ClC chloride channels and transporters: from genes to protein structure, pathology and physiology. *Crit Rev Biochem Mol Biol* 2008; 43: 3-36.
- 2 Kawasaki M, Suzuki M, Uchida S, Sasaki S, Marumo F. Stable and functional expression of the CIC-3 chloride channel in somatic cell lines. *Neuron* 1995; 14: 1285-91.
- 3 Kawasaki M, Uchida S, Monkawa T, Miyawaki A, Mikoshiba K, Marumo F, *et al*. Cloning and expression of a protein kinase C-regulated chloride channel abundantly expressed in rat brain neuronal cells. *Neuron* 1994; 12: 597-604.
- 4 Sasaki S, Uchida S, Kawasaki M, Adachi S, Marumo F. CIC family in the kidney. *Jpn J Physiol* 1994; 44: S3-8.
- 5 Duan D, Winter C, Cowley S, Hume JR, Horowitz B. Molecular identification of a volume-regulated chloride channel. *Nature* 1997; 390: 417-21.
- 6 Britton FC, Hatton WJ, Rossow CF, Duan D, Hume JR, Horowitz B. Molecular distribution of volume-regulated chloride channels (CIC-2

- and CIC-3) in cardiac tissues. *Am J Physiol Heart Circ Physiol* 2000; 279: H2225–33.
- 7 Yamazaki J, Duan D, Janiak R, Kuenzli K, Horowitz B, Hume JR. Functional and molecular expression of volume-regulated chloride channels in canine vascular smooth muscle cells. *J Physiol (Lond)* 1998; 507: 729–36.
- 8 Borsani G, Rugarli EI, Tagliatalata M, Wong C, Ballabio A. Characterization of a human and murine gene (CLCN3) sharing similarities to voltage-gated chloride channels and to a yeast integral membrane protein. *Genomics* 1995; 27: 131–41.
- 9 Du XY, Sorota S. Cardiac swelling-induced chloride current depolarizes canine atrial myocytes. *Am J Physiol* 1997; 272: H1904–16.
- 10 Duan D, Fermini B, Nattel S. Alpha-adrenergic control of volume-regulated Cl⁻ currents in rabbit atrial myocytes. Characterization of a novel ionic regulatory mechanism. *Circ Res* 1995; 77: 379–93.
- 11 Duan D, Hume JR, Nattel S. Evidence that outwardly rectifying Cl⁻ channels underlie volume-regulated Cl⁻ currents in heart. *Circ Res* 1997; 80: 103–13.
- 12 Duan D, Cowley S, Horowitz B, Hume JR. A serine residue in CIC-3 links phosphorylation-dephosphorylation to chloride channel regulation by cell volume. *J Gen Physiol* 1999; 113: 57–70.
- 13 Sorota S. Swelling-induced chloride-sensitive current in canine atrial cells revealed by whole-cell patch-clamp method. *Circ Res* 1992; 70: 679–87.
- 14 Dick GM, Bradley KK, Horowitz B, Hume JR, Sanders KM. Functional and molecular identification of a novel chloride conductance in canine colonic smooth muscle. *Am J Physiol Cell Physiol* 1998; 275: C940–50.
- 15 Hermoso M, Satterwhite CM, Andrade YN, Hidalgo J, Wilson SM, Horowitz B, et al. CIC-3 is a fundamental molecular component of volume-sensitive outwardly rectifying Cl⁻ channels and volume regulation in HeLa cells and *Xenopus laevis* oocytes. *J Biol Chem* 2002; 277: 40066–74.
- 16 Wang GX, Hatton WJ, Wang GL, Zhong J, Yamboliev I, Duan D, et al. Functional effects of novel anti-CIC-3 antibodies on native volume-sensitive osmolyte and anion channels in cardiac and smooth muscle cells. *Am J Physiol Heart Circ Physiol* 2003; 285: H1453–63.
- 17 Hawkins BJ, Madesh M, Kirkpatrick CJ, Fisher AB. Superoxide flux in endothelial cells via the chloride channel-3 mediates intracellular signaling. *Mol Biol Cell* 2007; 18: 2002–12.
- 18 Hiramatsu M, Furukawa T, Sawanobori T, Hiraoka M. Ion channel remodeling in cardiac hypertrophy is prevented by blood pressure reduction without affecting heart weight increase in rats with abdominal aortic banding. *J Cardiovasc Pharmacol* 2002; 39: 866–74.
- 19 Browe DM, Baumgarten CM. Angiotensin II (AT1) receptors and NADPH oxidase regulate Cl⁻ current elicited by {beta}1 integrin stretch in rabbit ventricular myocytes. *J Gen Physiol* 2004; 124: 273–87.
- 20 Wang GL, Wang XR, Lin MJ, He H, Lan XJ, Guan YY. Deficiency in CIC-3 chloride channels prevents rat aortic smooth muscle cell proliferation. *Circ Res* 2002; 91: E28–E32.
- 21 Huang P, Liu J, Di A, Robinson NC, Musch MW, Kaetzel MA, et al. Regulation of human CLC-3 channels by multifunctional Ca²⁺/calmodulin-dependent protein kinase. *J Biol Chem* 2001; 276: 20093–100.
- 22 Browe DM, Baumgarten CM. EGFR kinase regulates volume-sensitive chloride current elicited by integrin stretch via PI-3K and NADPH oxidase in ventricular myocytes. *J Gen Physiol* 2006; 127: 237–51.
- 23 Matsuda JJ, Filali MS, Moreland JG, Miller FJ, Lamb FS. Activation of swelling-activated chloride current by tumor necrosis factor-alpha requires CIC-3-dependent endosomal reactive oxygen production. *J Biol Chem* 2010; 285: 22864–73.
- 24 Duan D. Phenomics of cardiac chloride channels: the systematic study of chloride channel function in the heart. *J Physiol (Lond)* 2009; 587: 2163–77.
- 25 Duan DY, Liu LL, Bozeat N, Huang ZM, Xiang SY, Wang GL, et al. Functional role of anion channels in cardiac diseases. *Acta Pharmacol Sin* 2005; 26: 265–78.
- 26 Hume JR, Duan D, Collier ML, Yamazaki J, Horowitz B. Anion transport in heart. *Physiol Rev* 2000; 80: 31–81.
- 27 Hume JR, Wang GX, Yamazaki J, Ng LC, Duan D. CLC-3 chloride channels in the pulmonary vasculature. *Adv Exp Med Biol* 2010; 661: 237–47.
- 28 Hoffmann EK, Lambert IH, Pedersen SF. Physiology of cell volume regulation in vertebrates. *Physiol Rev* 2009; 89: 193–277.
- 29 Lang F. Mechanisms and significance of cell volume regulation. *J Am Coll Nutr* 2007; 26: 613S–623S.
- 30 Strange K. Cellular volume homeostasis. *Adv Physiol Educ* 2004; 28: 155–9.
- 31 Cala PM, Maldonado H, Anderson SE. Cell volume and pH regulation by the *Amphiuma* red blood cell: a model for hypoxia-induced cell injury. *Comp Biochem Physiol Comp Physiol* 1992; 102: 603–8.
- 32 Xiong D, Wang GX, Burkin DJ, Yamboliev IA, Singer CA, Rawat S, et al. Cardiac-specific overexpression of the human short CLC-3 chloride channel isoform in mice. *Clin Exp Pharmacol Physiol* 2009; 36: 386–93.
- 33 Zhang J, Lieberman M. Chloride conductance is activated by membrane distention of cultured chick heart cells. *Cardiovasc Res* 1996; 32: 168–79.
- 34 Li X, Shimada K, Showalter LA, Weinman SA. Biophysical properties of CIC-3 differentiate it from swelling-activated chloride channels in Chinese hamster ovary-K1 cells. *J Biol Chem* 2000; 275: 35994–8.
- 35 Stobrawa SM, Breiderhoff T, Takamori S, Engel D, Schweizer M, Zdebik AA, et al. Disruption of CIC-3, a chloride channel expressed on synaptic vesicles, leads to a loss of the hippocampus. *Neuron* 2001; 29: 185–96.
- 36 Weylandt KH, Valverde MA, Nobles M, Raguz S, Amey JS, Diaz M, et al. Human CIC-3 is not the swelling-activated chloride channel involved in cell volume regulation. *J Biol Chem* 2001; 276: 17461–7.
- 37 Yamamoto-Mizuma S, Wang GX, Liu LL, Schegg K, Hatton WJ, Duan D, et al. Altered properties of volume-sensitive osmolyte and anion channels (VSOACs) and membrane protein expression in cardiac and smooth muscle myocytes from *Cln3*^{-/-} mice. *J Physiol (Lond)* 2004; 557: 439–56.
- 38 Duan D, Zhong J, Hermoso M, Satterwhite CM, Rossow CF, Hatton WJ, et al. Functional inhibition of native volume-sensitive outwardly rectifying anion channels in muscle cells and *Xenopus* oocytes by anti-CIC-3 antibody. *J Physiol (Lond)* 2001; 531: 437–44.
- 39 Vessey JP, Shi C, Jollimore CA, Stevens KT, Coca-Prados M, Barnes S, et al. Hyposmotic activation of I_{Cl,swell} in rabbit nonpigmented ciliary epithelial cells involves increased CIC-3 trafficking to the plasma membrane. *Biochem Cell Biol* 2004; 82: 708–18.
- 40 Tang YB, Zhou JG, Guan YY. Volume-regulated chloride channels and cerebral vascular remodelling. *Clin Exp Pharmacol Physiol* 2010; 37: 238–42.
- 41 Tang YB, Liu YJ, Zhou JG, Wang GL, Qiu QY, Guan YY. Silence of CIC-3 chloride channel inhibits cell proliferation and the cell cycle via G/S phase arrest in rat basilar arterial smooth muscle cells. *Cell Prolif* 2008; 41: 775–85.
- 42 Tao R, Lau CP, Tse HF, Li GR. Regulation of cell proliferation by intermediate-conductance Ca²⁺-activated potassium and volume-

- sensitive chloride channels in mouse mesenchymal stem cells. *Am J Physiol Cell Physiol* 2008; 295: C1409–16.
- 43 Mao J, Chen L, Xu B, Wang L, Li H, Guo J, *et al.* Suppression of CIC-3 channel expression reduces migration of nasopharyngeal carcinoma cells. *Biochem Pharmacol* 2008; 75: 1706–16.
- 44 Do CW, Lu W, Mitchell CH, Civan MM. Inhibition of swelling-activated Cl^- currents by functional anti-CIC-3 antibody in native bovine non-pigmented ciliary epithelial cells. *Invest Ophthalmol Vis Sci* 2005; 46: 948–55.
- 45 Zhou JG, Ren JL, Qiu QY, He H, Guan YY. Regulation of intracellular Cl^- concentration through volume-regulated CIC-3 chloride channels in A10 vascular smooth muscle cells. *J Biol Chem* 2005; 280: 7301–8.
- 46 Jin NG, Kim JK, Yang DK, Cho SJ, Kim JM, Koh EJ, *et al.* Fundamental role of CIC-3 in volume-sensitive Cl^- channel function and cell volume regulation in AGS cells. *Am J Physiol Gastrointest Liver Physiol* 2003; 285: G938–48.
- 47 Tao R, Lau CP, Tse HF, Li GR. Functional ion channels in mouse bone marrow mesenchymal stem cells. *Am J Physiol Cell Physiol* 2007; 293: C1561–7.
- 48 Cuddapah VA, Sontheimer H. Molecular interaction and functional regulation of CIC-3 by Ca^{2+} /calmodulin-dependent protein kinase II (CaMKII) in human malignant glioma. *J Biol Chem* 2010; 285: 11188–96.
- 49 Yin Z, Tong Y, Zhu H, Watsky MA. CIC-3 is required for LPA-activated Cl^- current activity and fibroblast-to-myofibroblast differentiation. *Am J Physiol Cell Physiol* 2008; 294: C535–42.
- 50 Xiong D, Heyman NS, Airey J, Zhang M, Singer CA, Rawat S, *et al.* Cardiac-specific, inducible CIC-3 gene deletion eliminates native volume-sensitive chloride channels and produces myocardial hypertrophy in adult mice. *J Mol Cell Cardiol* 2010; 48: 211–9.
- 51 Murry CE, Jennings RB, Reimer KA. Preconditioning with ischemia: a delay of lethal cell injury in ischemic myocardium. *Circulation* 1986; 74: 1124–36.
- 52 Guo Y, Wu WJ, Qiu Y, Tang XL, Yang Z, Bolli R. Demonstration of an early and a late phase of ischemic preconditioning in mice. *Am J Physiol Heart Circ Physiol* 1998; 275: H1375–87.
- 53 Diaz RJ, Losito VA, Mao GD, Ford MK, Backx PH, Wilson GJ. Chloride channel inhibition blocks the protection of ischemic preconditioning and hypo-osmotic stress in rabbit ventricular myocardium. *Circ Res* 1999; 84: 763–75.
- 54 Diaz RJ, Batthish M, Backx PH, Wilson GJ. Chloride channel inhibition does block the protection of ischemic preconditioning in myocardium. *J Mol Cell Cardiol* 2001; 33: 1887–9.
- 55 Batthish M, Diaz RJ, Zeng HP, Backx PH, Wilson GJ. Pharmacological preconditioning in rabbit myocardium is blocked by chloride channel inhibition. *Cardiovasc Res* 2002; 55: 660–71.
- 56 Heusch G, Liu GS, Rose J, Cohen MV, Downey JM. No confirmation for a causal role of volume-regulated chloride channels in ischemic preconditioning in rabbits. *J Mol Cell Cardiol* 2000; 32: 2279–85.
- 57 Sorota S. Pharmacologic properties of the swelling-induced chloride current of dog atrial myocytes. *J Cardiovasc Electrophysiol* 1994; 5: 1006–16.
- 58 Heusch G, Cohen MV, Downey JM. Ischemic preconditioning through opening of swelling-activated chloride channels? *Circ Res* 2001; 89: E48.
- 59 Bozeat N, Dwyer L, Ye L, Yao T, Duan D. The role of CIC-3 chloride channels in early and late ischemic preconditioning in mouse heart. *FASEB J* 2005; 19: A694–5.
- 60 Bozeat N, Dwyer L, Ye L, Yao TY, Hatton WJ, Duan D. VSOACs play an important cardioprotective role in late ischemic preconditioning in mouse heart. *Circulation* 2006; 114: 272–3.
- 61 Guan YY, Wang GL, Zhou JG. The CIC-3 Cl^- channel in cell volume regulation, proliferation and apoptosis in vascular smooth muscle cells. *Trends Pharmacol Sci* 2006; 27: 290–6.
- 62 Volk AP, Heise CK, Hougén JL, Artman CM, Volk KA, Wessels D, *et al.* CIC-3 and $I_{\text{Cl}^- \text{swell}}$ are required for normal neutrophil chemotaxis and shape change. *J Biol Chem* 2008; 283: 34315–26.
- 63 Mizoguchi K, Maeta H, Yamamoto A, Oe M, Kosaka H. Amelioration of myocardial global ischemia/reperfusion injury with volume-regulatory chloride channel inhibitors *in vivo*. *Transplantation* 2002; 73: 1185–93.
- 64 Chen Z, Chua CC, Ho YS, Hamdy RC, Chua BH. Overexpression of Bcl-2 attenuates apoptosis and protects against myocardial I/R injury in transgenic mice. *Am J Physiol Heart Circ Physiol* 2001; 280: H2313–20.
- 65 Lemonnier L, Shuba Y, Crepin A, Roudbaraki M, Slomianny C, Mauroy B, *et al.* Bcl-2-dependent modulation of swelling-activated Cl^- current and CIC-3 expression in human prostate cancer epithelial cells. *Cancer Res* 2004; 64: 4841–8.
- 66 Wei L, Xiao AY, Jin C, Yang A, Lu ZY, Yu SP. Effects of chloride and potassium channel blockers on apoptotic cell shrinkage and apoptosis in cortical neurons. *Pflügers Arch* 2004; 448: 325–34.
- 67 Patel DG, Higgins RS, Baumgarten CM. Swelling-activated Cl^- current, $I_{\text{Cl}^- \text{swell}}$, is chronically activated in diseased human atrial myocytes. *Biophys J* 2003; 84: 233a.
- 68 Clemo HF, Baumgarten CM. Protein kinase C activation blocks $I_{\text{Cl}^- \text{swell}}$ and causes myocyte swelling in a rabbit congestive heart failure model. *Circulation* 1998; 98: I-695.
- 69 Clemo HF, Stambler BS, Baumgarten CM. Swelling-activated chloride current is persistently activated in ventricular myocytes from dogs with tachycardia-induced congestive heart failure. *Circ Res* 1999; 84: 157–65.
- 70 Duan D, Liu L, Wang GL, Ye L, Tian H, Yao Y, *et al.* Cell volume-regulated ion channels and ionic remodeling in hypertrophied mouse heart. *J Cardiac Failure* 2004; 10: S72.
- 71 van Borren MM, Verkerk AO, Vanharanta SK, Baartscheer A, Coronel R, Ravesloot JH. Reduced swelling-activated Cl^- current densities in hypertrophied ventricular myocytes of rabbits with heart failure. *Cardiovasc Res* 2002; 53: 869–78.
- 72 Xiong D, Ye L, Neveux I, Burkin DJ, Scowen P, Evans R, *et al.* Cardiac specific inactivation of CIC-3 gene reveals cardiac hypertrophy and compromised heart function. *FASEB J* 2008; 22: 970.25.
- 73 Liu LH, Ye L, McGuckin C, Hatton WJ, Duan D. Disruption of *Clcn3* gene in mice facilitates heart failure during pressure overload. *J Gen Physiol* 2003; 122: 33A.
- 74 Hiraoka M, Kawano S, Hirano Y, Furukawa T. Role of cardiac chloride currents in changes in action potential characteristics and arrhythmias. *Cardiovas Res* 1998; 40: 23–33.
- 75 Vandenberg JI, Bett GC, Powell T. Contribution of a swelling-activated chloride current to changes in the cardiac action potential. *Am J Physiol* 1997; 273: C541–7.
- 76 Duan D, Fermi B, Nattel S. Sustained outward current observed after I_{to1} inactivation in rabbit atrial myocytes is a novel Cl^- current. *Am J Physiol* 1992; 263: H1967–71.
- 77 Du XY, Sorota S. Modulation of dog atrial swelling-induced chloride current by cAMP: protein kinase A-dependent and -independent pathways. *J Physiol (Lond)* 1997; 500: 111–22.
- 78 Browe DM, Baumgarten CM. Stretch of beta 1 integrin activates an outwardly rectifying chloride current via FAK and Src in rabbit ventricular myocytes. *J Gen Physiol* 2003; 122: 689–702.
- 79 Baumgarten CM, Clemo HF. Swelling-activated chloride channels in

- cardiac physiology and pathophysiology. *Prog Biophys Mol Biol* 2003; 82: 25–42
- 80 Tomaselli GF, Marban E. Electrophysiological remodeling in hypertrophy and heart failure. *Cardiovasc Res* 1999; 42: 270–83.
- 81 Hagiwara N, Masuda H, Shoda M, Irisawa H. Stretch-activated anion currents of rabbit cardiac myocytes. *J Physiol (Lond)* 1992; 456: 285–302.
- 82 Lamb FS, Clayton GH, Liu BX, Smith RL, Barna TJ, Schutte BC. Expression of CLCN voltage-gated chloride channel genes in human blood vessels. *J Mol Cell Cardiol* 1999; 31: 657–66.
- 83 Qian JS, Pang RP, Zhu KS, Liu DY, Li ZR, Deng CY, *et al.* Static pressure promotes rat aortic smooth muscle cell proliferation via upregulation of volume-regulated chloride channel. *Cell Physiol Biochem* 2009; 24: 461–70.
- 84 Nelson MT. Bayliss, myogenic tone and volume-regulated chloride channels in arterial smooth muscle. *J Physiol (Lond)* 1998; 507: 629.
- 85 Meininger GA, Davis MJ. Cellular mechanisms involved in the vascular myogenic response. *Am J Physiol Heart Circ Physiol* 1992; 263: H647–H659.
- 86 Jackson WF. Ion channels and vascular tone. *Hypertension* 2000; 35: 173–8.
- 87 Nelson MT, Conway MA, Knot HJ, Brayden JE. Chloride channel blockers inhibit myogenic tone in rat cerebral arteries. *J Physiol (Lond)* 1997; 502: 259–64.
- 88 Doughty JM, Langton PD. Measurement of chloride flux associated with the myogenic response in rat cerebral arteries. *J Physiol (Lond)* 2001; 534: 753–61.
- 89 Remillard CV, Lupien MA, Crepeau V, Leblanc N. Role of Ca^{2+} - and swelling-activated Cl^{-} channels in $\alpha 1$ -adrenoceptor-mediated tone in pressurized rabbit mesenteric arterioles. *Cardiovasc Res* 2000; 46: 557–68.
- 90 Doughty JM, Miller AL, Langton PD. Non-specificity of chloride channel blockers in rat cerebral arteries: block of the L-type calcium channel. *J Physiol (Lond)* 1998; 507: 433–9.
- 91 Voets T, Wei L, De SP, Van DW, Eggermont J, Droogmans G, *et al.* Downregulation of volume-activated Cl^{-} currents during muscle differentiation. *Am J Physiol Cell Physiol* 1997; 272: C667–74.
- 92 Liu YJ, Wang XG, Tang YB, Chen JH, Lv XF, Zhou JG, *et al.* Simvastatin ameliorates rat cerebrovascular remodeling during hypertension via inhibition of volume-regulated chloride channel. *Hypertension* 2010; 56: 445–52.
- 93 Taniyama Y, Griendling KK. Reactive oxygen species in the vasculature: molecular and cellular mechanisms. *Hypertension* 2003; 42: 1075–81.
- 94 Tanabe S, Wang X, Takahashi N, Uramoto H, Okada Y. HCO_3^{-} -independent rescue from apoptosis by stilbene derivatives in rat cardiomyocytes. *FEBS Lett* 2005; 579: 517–22.
- 95 Finkel T. Oxidant signals and oxidative stress. *Curr Opin Cell Biol* 2003; 15: 247–54.
- 96 Finkel T, Deng CX, Mostoslavsky R. Recent progress in the biology and physiology of sirtuins. *Nature* 2009; 460: 587–91.
- 97 Devadas S, Zaritskaya L, Rhee SG, Oberley L, Williams MS. Discrete generation of superoxide and hydrogen peroxide by T cell receptor stimulation: selective regulation of mitogen-activated protein kinase activation and fas ligand expression. *J Exp Med* 2002; 195: 59–70.
- 98 Dai YP, Bongalon S, Hatton WJ, Hume JR, Yamboliev IA. CIC-3 chloride channel is upregulated by hypertrophy and inflammation in rat and canine pulmonary artery. *Br J Pharmacol* 2005; 145: 5–14.
- 99 Madesh M, Hawkins BJ, Milovanova T, Bhanumathy CD, Joseph SK, Ramachandrarao SP, *et al.* Selective role for superoxide in InsP3 receptor-mediated mitochondrial dysfunction and endothelial apoptosis. *J Cell Biol* 2005; 170: 1079–90.
- 100 Dutzler R, Campbell EB, Cadene M, Chait BT, MacKinnon R. X-ray structure of a CIC chloride channel at 3.0 Å reveals the molecular basis of anion selectivity. *Nature* 2002; 415: 287–94.
- 101 Miller FJ Jr, Filali M, Huss GJ, Stanic B, Chamseddine A, Barna TJ, *et al.* Cytokine activation of nuclear factor kappa B in vascular smooth muscle cells requires signaling endosomes containing Nox1 and CIC-3. *Circ Res* 2007; 101: 663–71.

Review

Physiological roles and diseases of *tmem16*/*anoctamin* proteins: are they all chloride channels?

Charity DURAN, H Criss HARTZELL*

Emory University School of Medicine, Department of Cell Biology and Center for Neurodegenerative Disease Atlanta, GA 30322, USA

The *Tmem16* gene family was first identified by bioinformatic analysis in 2004. In 2008, it was shown independently by 3 laboratories that the first two members (*Tmem16A* and *Tmem16B*) of this 10-gene family are Ca^{2+} -activated Cl^- channels. Because these proteins are thought to have 8 transmembrane domains and be anion-selective channels, the alternative name, Anoctamin (anion and octa=8), has been proposed. However, it remains unclear whether all members of this family are, in fact, anion channels or have the same 8-transmembrane domain topology. Since 2008, there have been nearly 100 papers published on this gene family. The excitement about *Tmem16* proteins has been enhanced by the finding that *Ano1* has been linked to cancer, mutations in *Ano5* are linked to several forms of muscular dystrophy (LGMDL2 and MMD-3), mutations in *Ano10* are linked to autosomal recessive spinocerebellar ataxia, and mutations in *Ano6* are linked to Scott syndrome, a rare bleeding disorder. Here we review some of the recent developments in understanding the physiology and structure-function of the *Tmem16* gene family.

Keywords: chloride channels; patch clamp; ion channels; channelopathies; ion transport; muscular dystrophy; ataxia; blood clotting

Acta Pharmacologica Sinica (2011) 32: 685–692; doi: 10.1038/aps.2011.48

Introduction

Ca^{2+} -activated Cl^- channels (CaCCs) play manifold roles in cell physiology^[1, 2] including epithelial secretion^[3, 4], sensory transduction and adaptation^[5–8], regulation of smooth muscle contraction^[9], control of neuronal and cardiac excitability^[10], and nociception^[11]. CaCCs were first described in *Xenopus* oocytes^[12, 13] and salamander rods^[14] in the early 1980's, but it was not until 3 years ago that the proteins responsible for these channels were identified. Prior to that, several other proteins were proposed as molecular candidates. These include CIC-3^[15], CLCAs^[16], and bestrophins^[17]. None of these proteins have properties that exactly fit those of classical CaCCs^[1]. Although bestrophins are indeed CaCCs, their expression profile is more restricted and their biophysical properties are different from classical CaCCs^[17]. So, in 2008, the announcements that three labs had cloned genes that encoded classical CaCCs generated considerable excitement^[18–20]. The two genes that have been shown definitively to encode CaCCs are called *Tmem16A* and *Tmem16B*. These are two members of a family that consists of 10 genes in mammals^[21]. Yang *et al*^[19] proposed the new name “anoctamin” or *Ano* (anion+octa=8) and this name is now the official HUGO nomenclature and

has replaced *Tmem16* in Genbank. *Tmem16A* is now *Ano1*, *Tmem16B* is *Ano2*, and so-on except that the letter I is skipped in the *Tmem16* nomenclature so that *Tmem16J* is *Ano 9* and *Tmem16K* is *Ano10*. There is some dissatisfaction in the field with the *Ano* nomenclature because, as discussed below, it is not certain that all the members of this family are anion channels or have the 8-transmembrane topology. Also, the term “*Ano*” has a potentially objectionable meaning in the Spanish language^[22]. For this reason, the *Tmem16* terminology still remains in use in parallel with *Ano*. This review summarizes some of the recent developments in this field. The reader should consult several other outstanding reviews on *Tmem16*/*Ano* proteins for more detail and different perspectives^[22–29].

Structure-function of anoctamins

Hydropathy analysis shows that all anoctamins have eight hydrophobic helices that are likely to be transmembrane domains with cytosolic N- and C-termini. This predicted topology has been confirmed experimentally for *Ano7*, whose topology has been determined using inserted HA epitope tag accessibility and endogenous N-glycosylation^[30]. Although this topology is appealing, the epitope tag accessibility methodology used to identify intracellular domains of *Ano7* does not clearly distinguish between intracellular domains and protein that is not efficiently trafficked to the plasma membrane. Because of this technical limitation and the fact that the topol-

* To whom correspondence should be addressed.

E-mail criss.hartzell@emory.edu

Received 2011-03-15 Accepted 2011-04-05

ogy of other Anos has not been experimentally determined, more investigation is required to establish the topology of these proteins.

The quaternary structure of Ano1 was recently determined to be that of a homodimer using both migration in native gels as well as Förster resonance energy transfer (FRET)^[31, 32]. Ano1 subunits associate before they are trafficked to the plasma membrane. The association of Ano1 subunits is likely due to noncovalent interactions, as the Ano1 assembly cannot be separated into monomers by chemical reduction with DTT. The oligomeric state is not affected by changes in intracellular Ca²⁺, suggesting that the homodimeric structure of Ano1 is not a determinant of channel gating. The homodimeric structure of Ano1 is reminiscent of that of CLC chloride channels, although it is not known whether the channel functions as a dimer or a higher order oligomer that is not detected quantitatively by the techniques used to date. For example, it is possible that the dimer is a biochemically stable form, but that dimerization of the dimers is required to create a functional channel. Further, it is not known whether Ano1 can form heteromers with other Anos or whether it associates with other accessory subunits. It will be interesting to see if Ano1 subunits assemble to form a single functional pore, or if each subunit contains a separate Cl⁻ conduction pathway, similar to the double barrel structure of CLC channels.

Multiple isoforms

At least 4 splice variants have been identified for Ano1^[33] and two splice variants have been found for Ano7^[34]. Human Ano1 has 4 different alternatively-spliced segments, *a*, *b*, *c*, and *d* corresponding, respectively, to an alternative initiation site, exon-6b, exon-13, and exon-15^[33]. Segments *a* and *b* are located in the N-terminus and *c* and *d* are in the first intracellular loop. The variant with all 4 segments is designated as Ano1*abcd*; the variant lacking segments *b* and *d*, for example, is Ano1*ac*. Analysis of ESTs in Genbank predicts that several of the other Anos also have multiple splice variants. Some of these variants may not have channel functions because they are predicted to lack some or all of the transmembrane domains. For example, the short form of Ano7, which has been shown to be translationally expressed, is a short, soluble protein^[34]. The four splice variants of Ano1 exhibit different voltage-dependent and Ca²⁺-dependent gating properties^[33, 35]. Thus, alternative splicing is likely to contribute to the heterogeneity of CaCC currents observed in native tissues.

Gating mechanisms of Ano1

Ano1 is gated by both voltage and Ca²⁺ but examination of the sequence of Ano1 gives few clues about the sites that sense voltage or bind to Ca²⁺. Unlike voltage-gated channels that have amphipathic transmembrane helices with charged amino acids that serve to sense voltage, Ano1 has no such sequences. Furthermore, there are no obvious E-F hands that might serve as Ca²⁺ binding sites or definitive IQ domains for CaM binding. The first intracellular loop, between TMD2 and TMD3, has a large number of acidic amino acids including

a stretch of 5 consecutive glutamates (⁴⁴⁴EEEE₄₄₈) that have attracted attention as a possible Ca²⁺ sensor^[35]. The last glutamate in this sequence is the first residue of a 4-amino acid alternatively-spliced segment (⁴⁴⁸EAVK₄₅₁). Neutralization of the glutamates has little effect on Ca²⁺ sensitivity, although deletion of the alternatively-spliced segment (Δ EAVK) alters both voltage-dependent gating and Ca²⁺ sensitivity^[33, 35]. Thus, although the first intracellular loop plays an important role in coupling both voltage and Ca²⁺ binding to channel opening, it is unlikely to be the binding site for Ca²⁺.

If Ano1 has no Ca²⁺ binding site, perhaps the Ca²⁺ binding site is located on an accessory subunit, such as calmodulin (CaM). A recent paper reports that CaM binds to a 22-amino acid region that overlaps with the *b* segment in the N-terminus called CaM-BD1 and is "essential" for gating Ano1^[36]. This putative CaM binding site is not canonical, but resembles some other CaM binding sites. However, only the Ano1 splice variants containing the *b* segment (*eg*; Ano1*abc*) seems to require CaM. Ano1*ac*, which lacks the CaM-BD1, does not require CaM and is activated directly by Ca²⁺. It is curious that deletion of the *b* segment reveals a Ca²⁺ binding site that is suppressed in the variant having the CaM binding domain. Clearly, additional work is required to clarify the role of CaM in regulation of Ano1. Some endogenous CaCCs are regulated directly by Ca²⁺ and others by CaM-dependent pathways^[2, 37, 38] and this may be explained by expression of different splice variants or isoforms. For example, the Ca²⁺-sensitivity of the CaCC in olfactory receptor neurons, which is now thought to be Ano2, is decreased by a factor of ~2 by over-expression of dominant-negative inactive CaMs, but CaM is not essential for activation^[38].

Functions of Tmem16/Ano paralogs

Anoctamins display differential temporal and spatial expression in a variety of developing tissues, suggesting they may play an important role in development^[39-41]. In murine tissues, Anos 1, 6, 7, 8, 9, and 10 are expressed in a variety of epithelia, while Anos 2, 3, 4, and 5 are more restricted to neuronal and musculoskeletal tissues^[42]. Ano1 and Ano2 are the only two members of the family that have been shown conclusively to be CaCCs.

Ano1 is ubiquitously expressed

Ano1 is widely expressed in virtually every kind of secretory epithelium, for example, salivary gland, pancreas, gut, mammary gland, and airway epithelium^[18, 19, 43-46]. Ano1 knockout mice display defective Ca²⁺ dependent Cl⁻ secretion in a variety of epithelia^[44-46] and Ano1 has been implicated in rotovirus-induced diarrhea^[47]. In addition, Ano1 is expressed in a variety of other cell types including certain smooth muscles and sensory neurons.

Ano1 is a secondary Cl⁻ channel in airway

The major Cl⁻ channel in human airway is cystic fibrosis transmembrane conductance regulator (CFTR), the protein that is defective in cystic fibrosis. CaCCs have long been considered

as a potential target for therapy of cystic fibrosis based on the idea that upregulation or activation of CaCCs might compensate for loss of CFTR in airway fluid secretion^[48]. Two drugs that activate CaCCs by elevating intracellular Ca^{2+} are presently in clinical trials for treating cystic fibrosis^[49, 50]. Recently, however, Namkung *et al*^[51] showed that novel Ano1 inhibitors were rather ineffective in inhibiting CaCCs in airway epithelial cells despite their efficacy in inhibiting heterologously expressed Ano1 as well as native CaCCs in salivary gland. This result is puzzling in light of the reports by several groups that Ano1 is expressed in airway epithelium and that knock-out of Ano1 decreases airway secretion^[43, 44, 46]. One possible explanation is that that Ano1 in airway is a different splice variant or has other accessory proteins that alters its pharmacological profile. Cystic fibrosis affects other tissues in addition to airway – reproductive tract, pancreas, bile duct. Ano1 is expressed in all of these tissues and may be an alternate, non-CFTR Cl^- secretory pathway^[43, 44, 52]. Although Ano1 may represent a potential target for pharmacological treatment of cystic fibrosis, one serious concern is the fact that Ano1 is so widely expressed that systemically administered drugs are likely to have widespread side-effects. Thus, it seems that any therapy that targets Ano1 may require local delivery protocols. However, the differential sensitivity of airway and salivary gland CaCCs to novel Ano1 inhibitors raises the prospect that development of subtype-specific drugs may be feasible.

Ano1 is essential for gut motility

In addition to epithelia, Ano1 is robustly expressed in interstitial cells of Cajal which are responsible for generating pacemaker activity in smooth muscle of the gut^[43, 53, 54]. Mice homozygous for a null allele of Ano1 fail to develop slow wave activity in gastrointestinal smooth muscles. The resulting loss of gastrointestinal motility may be an important contributor to the early death of Ano1 knockout mice^[43] and decreased expression of Ano1 in interstitial cells of Cajal may contribute to gastroparesis common in diabetic patients^[55].

Ano1 is expressed in certain smooth muscle cells

Ano1 is also expressed robustly in various kinds of smooth muscle including vascular smooth muscle cells^[43, 56, 57]. Treatment of rat pulmonary aortic smooth muscle cells with siRNA against Ano1 results in a reduction of CaCCs^[56]. Ano1 is also strongly expressed in airway smooth muscle cells, suggesting the possibility that this channel might be involved in asthma. Asthma is characterized by disorders of smooth muscle Ca^{2+} signaling and remodeling of the airway smooth muscle^[58]. Considering that Ano1 is Ca^{2+} -regulated and implicated in tracheal development^[40], a role for Ano1 in asthma deserves attention.

Ano1 overexpression is associated with cancer

Ano1 originally attracted the interest of cancer biologists because it is upregulated in several cancers^[59-61]. Oncologists have recognized Ano1 by several other names including DOG1 (Discovered On GIST-1 tumor), ORAOV2 (Oral cancer

Overexpressed), and TAOS-2 (Tumor Amplified and Over-expressed). Ano1 may prove a useful tool for the diagnosis of certain cancers. Gene expression profiling identified *Ano1* as being highly expressed in gastrointestinal stromal tumors (GISTs). KIT immunoreactivity has traditionally been used to differentiate GISTs from other tumors that are morphologically similar^[62]. While KIT staining is highly specific for GISTs, not all GISTs display KIT immunoreactivity. Ano1 very specifically identifies a higher percentage of GIST tumors than does KIT, indicating that Ano1 may be a more robust and sensitive diagnostic biomarker for GISTs^[63, 64].

In both oral and head and neck squamous cell carcinomas, amplification of the Ano1 locus is correlated with a poor outcome^[61, 65]. Ano1 expression is significantly increased in patients with a propensity to develop metastases. Given the role that Cl^- channels play in cell proliferation and migration, it is possible that Ano1 overexpression provides a growth or metastatic advantage to cancer cells^[66]. Supporting the role of Ano1 in metastasis is that overexpression of Ano1 stimulates cell movement^[67]. In contrast, silencing of Ano1 decreases cell migration; treatment of cells with CaCC blockers has a similar effect. Overexpression of Ano1 has no marked effect on cell proliferation. Although evidence suggests Ano1 may have a role in metastases, it is still possible that the chromosomal region containing Ano1 (11q13) contains other genes involved in cancer progression.

Ano1 may be involved in nociception

Ano1 is expressed in small dorsal root ganglion neurons and is implicated in mediating nociceptive signals triggered by bradykinin^[11]. Bradykinin is a very potent inflammatory and pain-inducing substance that is released at sites of tissue damage or inflammation. Bradykinin acts on G_q -coupled B2 receptors to stimulate phospholipase-C, IP_3 production, and release of Ca^{2+} from intracellular stores. The elevation of intracellular Ca^{2+} opens CaCCs apparently encoded by Ano1. CaCC current, along with KCNQ channel activation, depolarizes and increases AP firing. Local injection of CaCC inhibitors attenuates the nociceptive effect of local injections of BK.

Ano2 plays a role in sensory transduction

In olfactory sensory neurons, odorants open cyclic nucleotide gated channels by binding to G-protein coupled olfactory receptors that elevate cAMP^[6]. Ca^{2+} influx through the cyclic nucleotide gated channels then activates CaCCs that amplify the receptor potential. From immunostaining studies, it was first suggested that Best2 might be the olfactory CaCC^[68], but electrophysiological recordings from Best2 knockout mice failed to confirm a role for Best2 in mediating the olfactory receptor potential^[69, 70]. It seems Ano2 is now the best candidate for the pore-forming subunit of CaCCs in olfactory sensory neurons^[5-7, 71]. Ano2 generates Ca^{2+} activated chloride currents when expressed in heterologous systems^[20, 72]. Ano2 is localized in the cilia and dendritic knobs of olfactory sensory neurons and displays electrophysiological properties similar to native olfactory CaCCs. Ano2 displays similar halide per-

meability, Ca^{2+} sensitivity, single-channel conductance, and rundown kinetics to native olfactory CaCCs^[5]. However, there are differences in channel inactivation kinetics, suggesting the possible presence of other regulatory subunits.

Release of the neurotransmitter glutamate at photoreceptor synapses is controlled by intracellular Ca^{2+} . Ca^{2+} -activated Cl^- channels located in photoreceptor nerve terminals^[14, 73] have been shown to provide a feedback control on transmitter release^[74]. Ano2 is highly expressed in photoreceptor synaptic terminals^[8]. Ano2 is localized to presynaptic membranes in ribbon synapses, where it co-localizes with the adapter proteins PSD95, MPP4, and VGLL3. Ano2 contains a consensus C-terminal PDZ class I binding motif that interacts with the PDZ domains of PSD95. Through this interaction, Ano2 is tethered to membrane domains along photoreceptor terminals, and may serve to regulate synaptic output in these cells. Ano1 has also been shown to be expressed in photoreceptor terminals, suggesting there may be a contribution by both proteins to CaCCs in photoreceptors^[74].

Are Ano3-Ano10 chloride channels?

With the exception of Ano1 and Ano2, the status of other anoctamin family members as channels is unclear. In the hands of many investigators, including ourselves, many of the heterologously-expressed Anos 3–10 do not produce robust currents because they are not readily trafficked to the plasma membrane. This could indicate that they have intracellular functions or are simply missing the necessary chaperone subunits to help them to the surface. In a study by Scheiber *et al*^[42], it was concluded that in addition to Ano1 and Ano2, Anos 6, 7, and 10 were Cl^- channels. However, in iodide flux assays, the ATP- or ionomycin-stimulated flux reported for Anos 6, 7, and 10 were <10% of those for Ano1. Furthermore, the short form of Ano7 (Ano7S), which is a 179 amino acid protein with no predicted transmembrane domains and very unlikely to be an ion channel, produced approximately the same flux as the long form of Ano7. No patch clamp data were reported for Ano7. Over-expression of Ano10 produced a Cl^- current that was activated slowly over a time frame of 10 min. However, expression of Ano10 also suppressed maximal currents produced by Ano1. To date, no functional data have been published for Anos 3 and 4. Recently, Ano6 was reported by another lab to be a non-selective cation channel that is more permeable to Ca^{2+} than Na^{2+} ^[75]. It will be interesting to discover the functions of these proteins.

Ano5 mutations are linked to musculoskeletal disorders

Mutations in Ano5 result in a spectrum of musculoskeletal disorders. Ano5 was originally identified as GDD1, the gene product mutated in a rare autosomal dominant skeletal syndrome called gnathodiphyseal dysplasia (GDD)^[76]. Mutations in cysteine-356, a highly conserved cysteine in the first extracellular loop of Ano5, results in abnormal bone mineralization and bone fragility. Ano5 resides predominantly in intracellular membrane vesicles, but the nature of these compartments is still unknown^[77]. Although the function of Ano5 remains

to be determined, it clearly plays important roles in musculoskeletal development. Ano5 is expressed in growth-plate chondrocytes and osteoblasts at sites of active bone turnover, indicating an important role in bone formation. Ano5 is also expressed in somites and in developing skeletal muscle, and is upregulated during the skeletal muscle cell line C2C12 myogenic differentiation.

The importance of Ano5 in skeletal muscle physiology is further highlighted by the recent finding that mutations in Ano5 produce several recessive muscular dystrophies^[78–80]. Patients with a proximal limb-girdle muscular dystrophy (LGMD2L) and distal non-dysferlin Miyoshi myopathy (MMD3) carry mutations in Ano5. These mutations include a splice site and base pair duplication that result in premature stop codons, and two missense mutations, R758C and G231V. The phenotypes resulting from these mutations are reminiscent of dysferlinopathies, in which a deficiency in dysferlin causes defective skeletal muscle membrane repair. It has been suggested that chloride currents are important in membrane repair^[81] and Ano5 may be one of the channels involved in this process. Additional evidence implicating Ano5 in the maintenance of skeletal muscle is that Ano5 expression is increased in dystrophin-deficient mdx mice, a mouse model of Duchenne muscular dystrophy. In contrast to the Duchenne muscular dystrophy phenotype, dystrophin-deficient mdx mice maintain their ability to regenerate muscle fibers and have reduced endomysial fibrosis^[82]. The role of Ano5 in muscle membrane repair is still speculative, but determining if Ano5 functions as a chloride channel will be critical for elucidating its role in musculoskeletal pathologies (Figure 1).

Ano6 plays a role in blood clotting

Mutations in Ano6 have recently been implicated in Scott syndrome, a rare congenital bleeding disorder caused by a defect in blood coagulation^[83]. In platelets, like other cell types, phosphatidylserine is located on the inner leaflet of the plasma membrane. When platelets are activated they expose phosphatidylserine on the outer leaflet of the plasma membrane to promote clotting. This redistribution of phosphatidylserine is mediated by phospholipid scramblases that transport phospholipids bidirectionally from one leaflet to the other. In patients with Scott syndrome this mechanism is defective, resulting in impaired blood clotting. Ano6 was found to be critical for Ca^{2+} dependent exposure of phosphatidylserine on the cell surface in Ba/F3 platelet cells. Furthermore, a patient with Scott syndrome harbored a mutation at a splice-acceptor site of Ano6, resulting in premature termination of the protein. Cells derived from this patient did not expose phosphatidylserine in response to a Ca^{2+} ionophore, unlike cells derived from the patient's unaffected parents. These data imply that Ano6 is required for scramblase activity. However, the recent finding that Ano6 is a non-selective cation channel^[75] throws another wrinkle into the interpretation of these data.

Ano7 is highly expressed in prostate

Ano7, which is highly expressed in prostate, was discovered

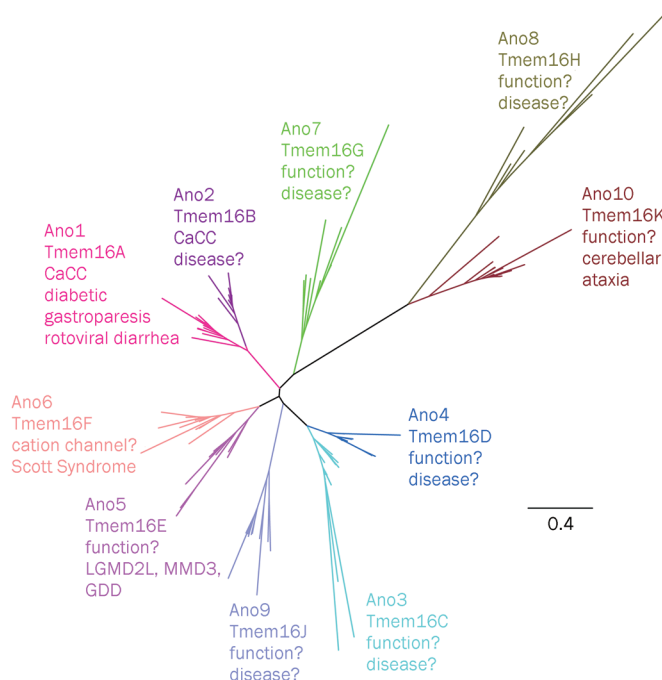


Figure 1. Phylogenetic tree of vertebrate Anoctamins. Each branch is labeled with the Ano and Tmem16 nomenclature, followed by the known or suspected physiological function, and any diseases that have been associated with this protein. GDD: gnathodiphyseal dysplasia; LGMD2L: proximal limb girdle muscular dystrophy; MMD3: distal Miyoshi muscular dystrophy. The tree was computed using 103 vertebrate Anoctamins found in Genbank and Ensembl using nearest neighbor statistics.

in a search for genes whose expression patterns mimicked those of known prostate cancer genes^[34, 84]. Of 40 000 human genes examined, 8 novel genes, including Ano7, were identified as being the most closely linked to known prostate cancer genes. Ano7 is expressed on the apical and lateral membranes of normal prostate. In the prostate LNCaP cell line stably transfected with Ano7, the protein localizes to cell-cell contact regions. It has been suggested that Ano7 promotes cell association because cell association can be reduced with RNAi targeted to Ano7^[84]. The predominant expression in prostate and prostate cancers poise Ano7 as an attractive candidate for immunotherapy^[85, 86], although the role of Ano7 in the development of prostate cancer is uncertain.

Ano10 mutations are linked to ataxia

Mutations in Ano10 have been linked to autosomal-recessive cerebellar ataxias associated with moderate gait ataxia, down-beat nystagmus, and dysarthric speech^[87]. Affected individuals display severe cerebellar atrophy. Two of the mutations introduce premature stop codons, probably leading to null protein expression. The other mutation is a missense mutation, L510R, which is highly conserved among the Anos and lies in the sixth transmembrane domain within the DUF590 domain of unknown function. It remains especially uncertain whether Ano10 is an ion channel, because Ano10 and Ano8

constitute the most divergent branch of the anoctamin family. While there is little functional data for Ano10, a *Drosophila* ortholog of Ano8/10, called Axs, is necessary for normal spindle formation and cell cycle progression^[88]. Axs co-localizes with ER components, and is recruited to microtubules of assembling spindles during mitosis and meiosis. A dominant mutation in Axs causes abnormal segregation of homologous achiasmate chromosomes due to defects in spindle formation, and disrupts cell cycle progression. It remains to be seen if Ano10 plays a similar role in mammalian systems.

Summary

The Tmem16/Anoctamin family promises to reveal many exciting secrets over the next few years. We are impatient to know whether Anos3–10 are anion channels, other types of channel, or something else, such as a phospholipid scramblase. We would also like to know whether some of these proteins have functions in intracellular organelles. It is interesting that in just ~3 years since Ano1 and Ano2 were identified as CaCCs, Anos 5, 6, and 10 have been linked to several serious human diseases, but human diseases caused by mutations in Ano1 and Ano2 have not been found. Certainly in the case of Ano1, this may be because these mutations are lethal, just as the null allele is in mice^[40]. The location of the pore of the Ano1 channel still has not been clearly established. Although mutations between TMD5 and TMD6 point to the putative re-entrant loop here as being part of the pore^[18, 19], the remarkably high conservation in this region between Ano1, which is an anion channel, and Ano6, which is apparently a cation channel, argues against this region as a determinant of ion selectivity. Unravelling the mechanisms of Ano1 regulation by Ca²⁺ and voltage also remain areas that are certain to provide exciting insights.

Acknowledgements

The work in the authors' lab is supported by the National Institutes of Health grants RO1-GM60448, RO1-EY014582, and P30-EY006360. Charity DURAN is supported by an NIH Training Grant T32-EY007092.

The authors would like to thank Drs Qing-huan XIAO, Kuai YU, Patricia PEREZ-CORNEJO, and Jorge ARREOLA for helpful discussion and comments.

References

- Duran C, Thompson CH, Xiao Q, Hartzell HC. Chloride channels: often enigmatic, rarely predictable. *Annu Rev Physiol* 2010; 72: 95–121.
- Hartzell C, Putzier I, Arreola J. Calcium-activated chloride channels. *Annu Rev Physiol* 2005; 67: 719–58.
- Tarran R. Regulation of airway surface liquid volume and mucus transport by active ion transport. *Proc Am Thorac Soc* 2004; 1: 42–6.
- Tarran R, Loewen ME, Paradiso AM, Olsen JC, Gray MA, Argent BE, et al. Regulation of murine airway surface liquid volume by CFTR and Ca²⁺-activated Cl⁻ conductances. *J Gen Physiol* 2002; 120: 407–18.
- Stephan AB, Shum EY, Hirsh S, Cygnar KD, Reiser J, Zhao H. ANO₂ is the ciliary calcium-activated chloride channel that may mediate olfactory amplification. *Proc Natl Acad Sci U S A* 2009; 106: 11776–81.

- 6 Hengl T, Kaneko H, Dauner K, Vocke K, Frings S, Mohrlen F. Molecular components of signal amplification in olfactory sensory cilia. *Proc Natl Acad Sci U S A* 2010; 107: 6052–7.
- 7 Rasche S, Toetter B, Adler J, Tschapek A, Doerner JF, Kurtenbach S, et al. *Tmem16b* is specifically expressed in the cilia of olfactory sensory neurons. *Chem Senses* 2010; 35: 239–45.
- 8 Stohr H, Heisig JB, Benz PM, Schoberl S, Milenkovic VM, Strauss O, et al. *TMEM16B*, a novel protein with calcium-dependent chloride channel activity, associates with a presynaptic protein complex in photoreceptor terminals. *J Neurosci* 2009; 29: 6809–18.
- 9 Large WA, Wang Q. Characteristics and physiological role of the Ca^{2+} -activated Cl^- conductance in smooth muscle. *Am J Physiol* 1996; 271: C435–54.
- 10 Duan D. Phenomics of cardiac chloride channels: the systematic study of chloride channel function in the heart. *J Physiol* 2009; 587: 2163–77.
- 11 Liu B, Linley JE, Du X, Zhang X, Ooi L, Zhang H, et al. The acute nociceptive signals induced by bradykinin in rat sensory neurons are mediated by inhibition of M-type K^+ channels and activation of Ca^{2+} -activated Cl^- channels. *J Clin Invest* 2010; 120: 1240–52.
- 12 Barish ME. A transient calcium-dependent chloride current in the immature *Xenopus oocyte*. *J Physiol* 1983; 342: 309–25.
- 13 Miledi R. A calcium-dependent transient outward current in *Xenopus laevis oocytes*. *Proc R Soc Lond B Biol Sci* 1982; 215: 491–7.
- 14 Bader CR, Bertrand D, Schwartz EA. Voltage-activated and calcium-activated currents studied in solitary rod inner segments from the salamander retina. *J Physiol* 1982; 331: 253–84.
- 15 Huang P, Liu J, Di A, Robinson NC, Musch MW, Kaetzel MA, et al. Regulation of human *CLC-3* channels by multifunctional Ca^{2+} /calmodulin-dependent protein kinase. *J Biol Chem* 2001; 276: 20093–100.
- 16 Loewen ME, Forsyth GW. Structure and function of *CLCA* proteins. *Physiol Rev* 2005; 85: 1061–92.
- 17 Hartzell HC, Qu Z, Yu K, Xiao Q, Chien LT. Molecular physiology of bestrophins: multifunctional membrane proteins linked to best disease and other retinopathies. *Physiol Rev* 2008; 88: 639–72.
- 18 Caputo A, Caci E, Ferrera L, Pedemonte N, Barsanti C, Sondo E, et al. *TMEM16A*, a membrane protein associated with calcium-dependent chloride channel activity. *Science* 2008; 322: 590–4.
- 19 Yang YD, Cho H, Koo JY, Tak MH, Cho Y, Shim WS, et al. *TMEM16A* confers receptor-activated calcium-dependent chloride conductance. *Nature* 2008; 455: 1210–5.
- 20 Schroeder BC, Cheng T, Jan YN, Jan LY. Expression cloning of *TMEM16A* as a calcium-activated chloride channel subunit. *Cell* 2008; 134: 1019–29.
- 21 Milenkovic VM, Brockmann M, Stohr H, Weber BH, Strauss O. Evolution and functional divergence of the anoctamin family of membrane proteins. *BMC Evol Biol* 2010; 10: 319.
- 22 Flores CA, Cid LP, Sepulveda FV, Niemeyer MI. *TMEM16* proteins: the long awaited calcium-activated chloride channels? *Braz J Med Biol Res* 2009; 42: 993–1001.
- 23 Galiotta LJ. The *TMEM16* protein family: a new class of chloride channels? *Biophys J* 2009; 97: 3047–53.
- 24 Ferrera L, Caputo A, Galiotta LJ. *TMEM16A* protein: a new identity for Ca^{2+} -dependent Cl^- channels. *Physiology (Bethesda)* 2010; 25: 357–63.
- 25 Hartzell HC, Yu K, Xiao Q, Chien LT, Qu Z. Anoctamin / *TMEM16* family members are Ca^{2+} -activated Cl^- channels. *J Physiol Online* 2009; 587: 2127–39.
- 26 Kunzelmann K, Kongsuphol P, Aldehni F, Tian Y, Ousingsawat J, Warth R, et al. Bestrophin and *TMEM16-Ca*²⁺ activated Cl^- channels with different functions. *Cell Calcium* 2009; 46: 233–41.
- 27 Braun AP. Cloning and expression of a calcium-activated chloride channel reveal a novel protein candidate. *Channels (Austin)* 2008; 2: 393–4.
- 28 Galindo BE, Vacquier VD. Phylogeny of the *TMEM16* protein family: some members are overexpressed in cancer. *Int J Mol Med* 2005; 16: 919–24.
- 29 Kunzelmann K, Kongsuphol P, Chootip K, Toledo C, Martins JR, Almaca J, et al. Role of the Ca^{2+} -activated Cl^- channels bestrophin and anoctamin in epithelial cells. *Biol Chem* 2011; 392: 125–34.
- 30 Das S, Hahn Y, Walker DA, Nagata S, Willingham MC, Peehl DM, et al. Topology of *NGEP*, a prostate-specific cell:cell junction protein widely expressed in many cancers of different grade level. *Cancer Res* 2008; 68: 6306–12.
- 31 Sheridan JT, Worthington EN, Yu K, Gabriel SE, Hartzell HC, Tarran R. Characterization of the oligomeric structure of the Ca^{2+} -activated Cl^- channel *Ano1/TMEM16A*. *J Biol Chem* 2011; 286: 1381–8.
- 32 Fallah G, Romer T, Detro-Dassen S, Braam U, Markwardt F, Schmalzing G. *TMEM16A(a)/anoctamin-1* shares a homodimeric architecture with *CLC* chloride channels. *Mol Cell Proteomics* 2011; 10: M110.004697.
- 33 Ferrera L, Caputo A, Ubbly I, Bussani E, Zegarra-Moran O, Ravazzolo R, et al. Regulation of *TMEM16A* chloride channel properties by alternative splicing. *J Biol Chem* 2009; 284: 33360–8.
- 34 Bera TK, Das S, Maeda H, Beers R, Wolfgang CD, Kumar V, et al. *NGEP*, a gene encoding a membrane protein detected only in prostate cancer and normal prostate. *Proc Natl Acad Sci U S A* 2004; 101: 3059–64.
- 35 Xiao Q, Yu K, Perez-Cornejo P, Cui Y, Arreola J, Hartzell HC. Voltage- and calcium-dependent gating of *tmem16a/ano1* chloride channels are physically coupled by the first intracellular loop. *Proc Natl Acad Sci U S A* 2011. doi: 10.1073/pnas.1102147108.
- 36 Tian Y, Kongsuphol P, Hug M, Ousingsawat J, Witzgall R, Schreiber R, et al. Calmodulin-dependent activation of the epithelial calcium-dependent chloride channel *TMEM16A*. *FASEB J* 2011; 25: 1058–68.
- 37 Arreola J, Melvin JE, Begenisich T. Differences in regulation of Ca^{2+} -activated Cl^- channels in colonic and parotid secretory cells. *Am J Physiol* 1998; 274: C161–C166.
- 38 Kaneko H, Mohrlen F, Frings S. Calmodulin contributes to gating control in olfactory calcium-activated chloride channels. *J Gen Physiol* 2006; 127: 737–48.
- 39 Gritli-Linde A, Vaziri Sani F, Rock JR, Hallberg K, Iribarne D, Harfe BD, et al. Expression patterns of the *Tmem16* gene family during cephalic development in the mouse. *Gene Expr Patterns* 2009; 9: 178–91.
- 40 Rock JR, Futtner CR, Harfe BD. The transmembrane protein *TMEM16A* is required for normal development of the murine trachea. *Develop Biol* 2008; 321: 141–9.
- 41 Rock JR, Harfe BD. Expression of *TMEM16* paralogs during murine embryogenesis. *Develop Dynamics* 2008; 237: 2566–74.
- 42 Schreiber R, Uliyakina I, Kongsuphol P, Warth R, Mirza M, Martins JR, et al. Expression and function of epithelial anoctamins. *J Biol Chem* 2010; 285: 7838–45.
- 43 Huang F, Rock JR, Harfe BD, Cheng T, Huang X, Jan YN, et al. Studies on expression and function of the *TMEM16A* calcium-activated chloride channel. *Proc Natl Acad Sci U S A* 2009; 106: 21413–8.
- 44 Ousingsawat J, Martins JR, Schreiber R, Rock JR, Harfe BD, Kunzelmann K. Loss of *TMEM16A* causes a defect in epithelial Ca^{2+} -dependent chloride transport. *J Biol Chem* 2009; 284: 28698–703.
- 45 Romanenko VG, Catalan MA, Brown DA, Putzier I, Hartzell HC, Marmorstein AD, et al. *Tmem16A* encodes the Ca^{2+} -activated Cl^- channel in mouse submandibular salivary gland acinar cells. *J Biol Chem* 2010; 285: 12990–3001.

- 46 Rock JR, O'Neal WK, Gabriel SE, Randell SH, Harfe BD, Boucher RC, *et al*. Transmembrane protein 16A (TMEM16A) is a Ca²⁺-regulated Cl⁻ secretory channel in mouse airways. *J Biol Chem* 2009; 284: 14875–80.
- 47 Ousingsawat J, Mirza M, Tian Y, Roussa E, Schreiber R, Cook DI, *et al*. Rotavirus toxin NSP4 induces diarrhea by activation of TMEM16A and inhibition of Na⁺ absorption. *Pflugers Arch* 2011; 461: 579–89.
- 48 Knowles MR, Clarke LL, Boucher RC. Extracellular ATP and UTP induce chloride secretion in nasal epithelia of cystic fibrosis patients and normal subjects *in vivo*. *Chest* 1992; 101: 60S–63S.
- 49 Zeitlin PL, Boyle MP, Guggino WB, Molina L. A phase I trial of intranasal Moli1901 for cystic fibrosis. *Chest* 2004; 125: 143–9.
- 50 Storey S, Wald G. Novel agents in cystic fibrosis. *Nat Rev Drug Discov* 2008; 7: 555–6.
- 51 Namkung W, Phuan PW, Verkman AS. TMEM16A inhibitors reveal TMEM16A as a minor component of calcium-activated chloride channel conductance in airway and intestinal epithelial cells. *J Biol Chem* 2011; 286: 2365–74.
- 52 Dutta AK, Khimji AK, Kresge C, Bugde A, Dougherty M, Esser V, *et al*. Identification and functional characterization of TMEM16A, a Ca²⁺-activated Cl⁻ channel activated by extracellular nucleotides, in biliary epithelium. *J Biol Chem* 2011; 286: 766–76.
- 53 Hwang SJ, Blair PJ, Britton FC, O'Driscoll KE, Hennig G, Bayguinov YR, *et al*. Expression of anoctamin 1/TMEM16A by interstitial cells of Cajal is fundamental for slow wave activity in gastrointestinal muscles. *J Physiol* 2009; 587: 4887–904.
- 54 Zhu MH, Kim TW, Ro S, Yan W, Ward SM, Koh SD, *et al*. A Ca²⁺-activated Cl⁻ conductance in interstitial cells of Cajal linked to slow wave currents and pacemaker activity. *J Physiol* 2009; 587: 4905–18.
- 55 Mazzone A, Bernard CE, Strega PR, Beyder A, Galletta LJ, Pasricha PJ, *et al*. Altered expression of ANO1 variants in human diabetic gastroparesis. *J Biol Chem* 2011; 286: 13393–403.
- 56 Manoury B, Tamuleviciute A, Tammaro P. TMEM16A/anoctamin 1 protein mediates calcium-activated chloride currents in pulmonary arterial smooth muscle cells. *J Physiol* 2010; 588: 2305–14.
- 57 Davis AJ, Forrest AS, Jepps TA, Valencik ML, Wiwchar M, Singer CA, *et al*. Expression profile and protein translation of TMEM16A in murine smooth muscle. *Am J Physiol Cell Physiol* 2010; 299: C948–59.
- 58 Mahn K, Ojo OO, Chadwick G, Aaronson PI, Ward JP, Lee TH. Ca²⁺ homeostasis and structural and functional remodelling of airway smooth muscle in asthma. *Thorax* 2010; 65: 547–52.
- 59 West RB, Corless CL, Chen X, Rubin BP, Subramanian S, Montgomery K, *et al*. The novel marker, DOG1, is expressed ubiquitously in gastrointestinal stromal tumors irrespective of KIT or PDGFRA mutation status. *Am J Pathol* 2004; 165: 107–13.
- 60 Huang X, Gollin SM, Raja S, Godfrey TE. High-resolution mapping of the 11q13 amplicon and identification of a gene, TAOS1, that is amplified and overexpressed in oral cancer cells. *Proc Natl Acad Sci U S A* 2002; 99: 11369–74.
- 61 Carles A, Millon R, Cromer A, Ganguli G, Lemaire F, Young J, *et al*. Head and neck squamous cell carcinoma transcriptome analysis by comprehensive validated differential display. *Oncogene* 2006; 25: 1821–31.
- 62 Espinosa I, Lee CH, Kim MK, Rouse BT, Subramanian S, Montgomery K, *et al*. A novel monoclonal antibody against DOG1 is a sensitive and specific marker for gastrointestinal stromal tumors. *Am J Surg Pathol* 2008; 32: 210–8.
- 63 Hwang DG, Qian X, Hornick JL. DOG1 antibody is a highly sensitive and specific marker for gastrointestinal stromal tumors in cytology cell blocks. *Am J Clin Pathol* 2011; 135: 448–53.
- 64 Lee CH, Liang CW, Espinosa I. The utility of discovered on gastrointestinal stromal tumor 1 (DOG1) antibody in surgical pathology—the GIST of it. *Adv Anat Pathol* 2010; 17: 222–32.
- 65 Huang X, Godfrey TE, Gooding WE, McCarty KS Jr, Gollin SM. Comprehensive genome and transcriptome analysis of the 11q13 amplicon in human oral cancer and synteny to the 7F5 amplicon in murine oral carcinoma. *Genes Chromosomes Cancer* 2006; 45: 1058–69.
- 66 Kunzelmann K. Ion channels and cancer. *J Membr Biol* 2005; 205: 159–73.
- 67 Ayoub C, Wasyluk C, Li Y, Thomas E, Marisa L, Robe A, *et al*. ANO1 amplification and expression in HNSCC with a high propensity for future distant metastasis and its functions in HNSCC cell lines. *Br J Cancer* 2010; 103: 715–26.
- 68 Pifferi S, Pascarella G, Boccaccio A, Mazzatenta A, Gustincich S, Menini A, *et al*. Bestrophin-2 is a candidate calcium-activated chloride channel involved in olfactory transduction. *Proc Natl Acad Sci U S A* 2006; 103: 12929–34.
- 69 Pifferi S, Dibattista M, Sagheddu C, Boccaccio A, Al Qteishat A, Ghirardi F, *et al*. Calcium-activated chloride currents in olfactory sensory neurons from mice lacking bestrophin-2. *J Physiol* 2009; 587: 4265–79.
- 70 Bakall B, McLaughlin PJ, Stanton JB, Hartzell HC, Marmorstein LY, Marmorstein AD. The bestrophin-2 knock-out mouse: histological and functional analysis. *ARVO Meeting Abstracts* 2007; 48: 2983.
- 71 Sagheddu C, Boccaccio A, Dibattista M, Montani G, Tirindelli R, Menini A. Calcium concentration jumps reveal dynamic ion selectivity of calcium-activated chloride currents in mouse olfactory sensory neurons and TMEM16b-transfected HEK 293T cells. *J Physiol* 2010; 588: 4189–204.
- 72 Pifferi S, Dibattista M, Menini A. TMEM16B induces chloride currents activated by calcium in mammalian cells. *Pflugers Arch* 2009; 458: 1023–38.
- 73 MacLeish PR, Nurse CA. Ion channel compartments in photoreceptors: evidence from salamander rods with intact and ablated terminals. *J Neurophysiol* 2007; 98: 86–95.
- 74 Mercer AJ, Rabl K, Riccardi GE, Brecha NC, Stella SL Jr, Thoreson WB. Location of release sites and calcium-activated chloride channels relative to calcium channels at the photoreceptor ribbon synapse. *J Neurophysiol* 2011; 105: 321–35.
- 75 Yang H, Jin T, Cheng T, Jan YN, Jan LY. Scan: a novel small-conductance Ca²⁺-activated non-selective cation channel encoded by TMEM16F. *Biophys J* 2011; 100: 259a.
- 76 Tsutsumi S, Kamata N, Vokes TJ, Maruoka Y, Nakakuki K, Enomoto S, *et al*. The novel gene encoding a putative transmembrane protein is mutated in gnathodiaphyseal dysplasia (GDD). *Am J Hum Genet* 2004; 74: 1255–61.
- 77 Mizuta K, Tsutsumi S, Inoue H, Sakamoto Y, Miyatake K, Miyawaki K, *et al*. Molecular characterization of GDD1/TMEM16E, the gene product responsible for autosomal dominant gnathodiaphyseal dysplasia. *Biochem Biophys Res Commun* 2007; 357: 126–32.
- 78 Hicks D, Sarkozy A, Muelas N, Koehler K, Huebner A, Hudson G, *et al*. A founder mutation in Anoctamin 5 is a major cause of limb-girdle muscular dystrophy. *Brain* 2011; 134: 171–82.
- 79 Bolduc V, Marlow G, Boycott KM, Saleki K, Inoue H, Kroon J, *et al*. Recessive mutations in the putative calcium-activated chloride channel Anoctamin 5 cause proximal LGMD2L and distal MMD3 muscular dystrophies. *Am J Hum Genet* 2010; 86: 213–21.
- 80 Mahjneh I, Jaiswal J, Lamminen A, Somer M, Marlow G, Kiuru-Enari S, *et al*. A new distal myopathy with mutation in anoctamin 5. *Neuromuscul Disord* 2010; 20: 791–5.

- 81 Fein A, Terasaki M. Rapid increase in plasma membrane chloride permeability during wound resealing in starfish oocytes. *J Gen Physiol* 2005; 126: 151–9.
- 82 Sicinski P, Geng Y, Ryder–Cook AS, Barnard EA, Darlison MG, Barnard PJ. The molecular basis of muscular dystrophy in the mdx mouse: a point mutation. *Science* 1989; 244: 1578–80.
- 83 Suzuki J, Umeda M, Sims PJ, Nagata S. Calcium-dependent phospholipid scrambling by TMEM16F. *Nature* 2010; 468: 834–8.
- 84 Das S, Hahn Y, Nagata S, Willingham MC, Bera TK, Lee B, *et al*. NGEP, a prostate-specific plasma membrane protein that promotes the association of LNCaP cells. *Cancer Res* 2007; 67: 1594–601.
- 85 Cereda V, Poole DJ, Palena C, Das S, Bera TK, Remondo C, *et al*. New gene expressed in prostate: a potential target for T cell-mediated prostate cancer immunotherapy. *Cancer Immunol Immunother* 2010; 59: 63–71.
- 86 Williams RM, Naz RK. Novel biomarkers and therapeutic targets for prostate cancer. *Front Biosci (Schol Ed)* 2010; 2: 677–84.
- 87 Vermeer S, Hoischen A, Meijer RP, Gilissen C, Neveling K, Wieskamp N, *et al*. Targeted next-generation sequencing of a 12.5 Mb homozygous region reveals ANO10 mutations in patients with autosomal-recessive cerebellar ataxia. *Am J Hum Genet* 2010; 87: 813–9.
- 88 Kramer J, Hawley RS. The spindle-associated transmembrane protein Axs identifies a membranous structure ensheathing the meiotic spindle. *Nat Cell Biol* 2003; 5: 261–3.

Review

Targeting F508del-CFTR to develop rational new therapies for cystic fibrosis

Zhi-wei CAI, Jia LIU, Hong-yu LI, David N SHEPPARD*

School of Physiology and Pharmacology, University of Bristol, Medical Sciences Building, University Walk, Bristol BS8 1TD, UK

The mutation F508del is the commonest cause of the genetic disease cystic fibrosis (CF). CF disrupts the function of many organs in the body, most notably the lungs, by perturbing salt and water transport across epithelial surfaces. F508del causes harm in two principal ways. First, the mutation prevents delivery of the cystic fibrosis transmembrane conductance regulator (CFTR) to its correct cellular location, the apical (lumen-facing) membrane of epithelial cells. Second, F508del perturbs the Cl⁻ channel function of CFTR by disrupting channel gating. Here, we discuss the development of rational new therapies for CF that target F508del-CFTR. We highlight how structural studies provide new insight into the role of F508 in the regulation of channel gating by cycles of ATP binding and hydrolysis. We emphasize the use of high-throughput screening to identify lead compounds for therapy development. These compounds include CFTR correctors that restore the expression of F508del-CFTR at the apical membrane of epithelial cells and CFTR potentiators that rescue the F508del-CFTR gating defect. Initial results from clinical trials of CFTR correctors and potentiators augur well for the development of small molecule therapies that target the root cause of CF: mutations in CFTR.

Keywords: ATP-binding cassette transporter; epithelial ion transport; cystic fibrosis; CFTR; chloride ion channel; F508del; CFTR corrector; CFTR potentiator

Acta Pharmacologica Sinica (2011) 32: 693–701; doi: 10.1038/aps.2011.71

Introduction

Salty sweat is diagnostic of cystic fibrosis (CF), an autosomal recessive genetic disease common in Caucasians^[1, 2]. The elevated concentration of salt in sweat is indicative of the underlying molecular defect in CF, the loss of chloride ion (Cl⁻) channel function in the apical (lumen-facing) membrane of epithelia lining ducts and tubes throughout the body^[1]. The impermeability of the apical membrane to Cl⁻ in CF disrupts fluid and electrolyte transport across epithelia and, hence, the function of a variety of organs. This leads to the wide-ranging manifestations of the disease, which include chronic lung disease, exocrine pancreatic insufficiency, meconium ileus (blockage of the terminal ileum), male infertility and salty sweat^[1, 2]. The median survival of CF patients in North America and Western Europe is around 40 years^[2].

There are two principal causes of debilitation and death in CF patients^[1, 3, 4]. First, chronic obstructive lung disease caused by thick tenacious mucus that prevents normal mucociliary clearance. Second, persistent bacterial infections, typically

with *Pseudomonas aeruginosa*, which result in bronchiectasis, respiratory failure and eventually death. Current therapies for CF include physiotherapy, mucolytic drugs and antibiotics to treat lung disease, and pancreatic enzyme replacement and supplementary nutrition to overcome gastrointestinal dysfunction^[1, 2]. These therapies treat the symptoms of CF; they do not target the root cause of the disease.

In 1989, the defective gene responsible for CF was identified and predicted to encode a protein with five domains: two membrane-spanning domains (MSDs), two nucleotide-binding domains (NBDs) and a unique regulatory domain (RD)^[5]. Shortly thereafter, the protein product of this gene, the cystic fibrosis transmembrane conductance regulator (CFTR), was demonstrated to be a unique member of the ATP-binding cassette (ABC) transporter superfamily^[6]. Instead of forming an ATP-driven pump like most family members, CFTR was demonstrated to function as an ATP-gated pathway for anion movement driven by the transmembrane electrochemical gradient^[7–10]. Subsequent research has aimed to understand the physiological role of CFTR, learn how CF mutations cause CFTR dysfunction and develop rational new therapies for CF patients. Here, we selectively review progress in the development of drug therapies for CF, focusing on small molecules

* To whom correspondence should be addressed.

E-mail D.N.Sheppard@bristol.ac.uk

Received 2011-03-27 Accepted 2011-04-25

that target the most common CF mutation, F508del, deletion of the three base pairs that result in the loss of the phenylalanine residue at position 508 of the CFTR protein sequence; 90% of CF patients carry at least one copy of the F508del mutation.

The F508del-CFTR mutant retains some residual channel function

When Rich *et al*^[11] found that expression of F508del-CFTR in CF airway epithelial cells failed to correct the defective Cl⁻ permeability of these cells and Cheng *et al*^[12] subsequently demonstrated that the F508del mutation disrupts CFTR biosynthesis and membrane trafficking in COS-7 cells, it was widely assumed that F508del-CFTR had no Cl⁻ channel function. Surprisingly however, Drumm *et al*^[13] demonstrated that F508del-CFTR generates a cAMP-activated Cl⁻ conductance when expressed in *Xenopus* oocytes. Because F508del-CFTR Cl⁻ currents had similar conduction and permeation properties, but reduced magnitude compared with those of wild-type CFTR, Drumm *et al*^[13] speculated that F508del-CFTR forms a channel with attenuated sensitivity to cAMP agonists, a conclusion that was to prove prescient. Concurrently, Dalemans *et al*^[14] used the patch-clamp technique to demonstrate that F508del-CFTR forms a Cl⁻ channel regulated by cAMP-dependent phosphorylation in Vero cells. The authors demonstrated that F508del-CFTR had many properties in common with those of wild-type human CFTR^[14]. However, there was one notable exception, the pattern of channel gating of F508del-CFTR differed dramatically from that of wild-type CFTR^[14].

Biophysical properties of the F508del-CFTR Cl⁻ channel

Like other mutations that affect specific residues within the NBDs^[15], F508del has no discernable effect on the conduction and permeation properties of the CFTR Cl⁻ channel. First, the F508del-CFTR Cl⁻ channel has a small single-channel conductance, which does not differ from that of wild-type CFTR (6–10 pS; *eg* Li *et al*^[16]). Second, like wild-type CFTR (but see^[17]), the current-voltage (I–V) relationship of F508del-CFTR is linear (*eg* Dalemans *et al*^[14]). Third, both wild-type and F508del-CFTR are highly selective for anions over cations ($P_{Na}/P_{Cl}=0.08$; *eg* Li *et al*^[16]). Fourth, wild-type and F508del-CFTR share the identical anion permeability sequence of Br⁻>Cl⁻>I⁻ (*eg* Dalemans *et al*^[14]). Finally, wild-type and F508del-CFTR both exhibit time- and voltage-independent gating behavior (*eg* Denning *et al*^[18]). Consistent with these data, using excised membrane patches from gallbladder epithelial cells of wild-type and F508del-CFTR mice French *et al*^[19] demonstrated that the F508del mutation is without effect on the biophysical properties of murine CFTR. Thus, the data suggest that the F508del mutation does not affect the pore properties of CFTR.

The gating defect of the F508del-CFTR Cl⁻ channel

Figure 1 illustrates the gating pattern of wild-type and F508del-CFTR Cl⁻ channels following phosphorylation by protein kinase A (PKA). The gating behavior of wild-type CFTR is characterized by frequent bursts of channel activity that are interrupted by brief flickery closures and separated

by longer closures between bursts (Figure 1). By contrast, the gating pattern of F508del-CFTR is characterized by infrequent bursts of channel activity that are interrupted by brief flickery closures, but separated by long closures of prolonged duration (Figure 1). Work by a number of investigators using a variety of cells and experimental conditions demonstrate that the open probability (P_o ; a measure of the average fraction of time that a channel is open) of F508del-CFTR is about one third that of wild-type CFTR^[14, 18, 20–23], although Miki *et al*^[24] argue that the P_o of F508del-CFTR is likely to be substantially lower (~fifteen-fold less than that of wild-type CFTR). Surprisingly, and in marked contrast to these data, other authors found that the P_o of F508del-CFTR did not differ from that of wild-type CFTR^[16, 19]. A likely explanation for these differences is that the rate of activation of F508del-CFTR is more than seven-fold slower than that of wild-type CFTR^[25].

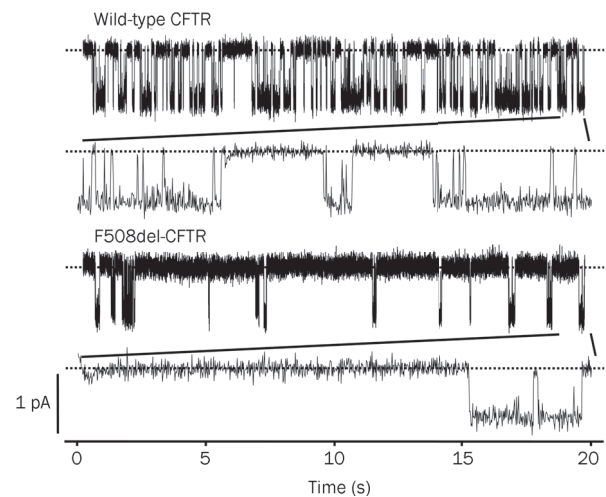


Figure 1. Single-channel activity of wild-type and F508del-CFTR. Representative recordings of wild-type and F508del-CFTR Cl⁻ channels in excised inside-out membrane patches from C127 cells expressing recombinant CFTR. ATP (1 mmol/L) and PKA (75 nmol/L) were continuously present in the intracellular solution, voltage was clamped at -50 mV, and a large Cl⁻ concentration gradient was imposed across the membrane patch ($[Cl^-]_{Ext}=10$ mmol/L; $[Cl^-]_{Int}=147$ mmol/L). Dashed lines indicate where the channels are closed and downward deflections correspond to channel openings. Beneath each of the prolonged 20 s recordings, the last 1 s of the record is shown on an expanded scale. Other details are as described in Cai and Sheppard^[23]. Modified, with permission, from Cai and Sheppard^[23].

To understand how the F508del mutation disrupts CFTR channel gating, several investigators have examined the gating kinetics of the F508del-CFTR Cl⁻ channel. Dalemans *et al*^[14] first demonstrated that in cell-attached membrane patches on Vero cells voltage-clamped at -60 mV, the F508del mutation was without effect on open times, but decreased mean closed times five-fold compared with those of wild-type CFTR. Haws *et al*^[20] and our group^[23, 26] examined the gating kinetics of F508del-CFTR in membrane patches from BHK

and C127 cells. Both groups found that the F508del mutation was without effect on open and closed times within bursts. Instead, F508del caused a large decrease in P_o by (i) markedly prolonging the closed time interval between bursts and (ii) reducing mean burst duration^[20, 23, 26]. These data suggest that the F508del mutation disrupts CFTR channel gating in two ways: first, F508del dramatically slows the rate of entry into a burst of channel activity. Second, F508del accelerates the rate of channel closure.

F508del is located at a critical interface in the CFTR gating pathway

The F508del mutation profoundly disrupts CFTR channel gating by slowing dramatically the rate of channel opening and by accelerating the rate of channel closure. An explanation for the gating behavior of F508del-CFTR is provided by the ATP-driven NBD dimerization model of CFTR channel gating^[27, 28]. This model integrates the results of functional studies of CFTR channel gating with biochemical and structural data. Structural studies of ABC transporters suggest that the NBDs are organized as a head-to-tail dimer with two ATP-binding sites located at the NBD1:NBD2 interface^[29-32]. The data suggest that one ATP-binding site is formed by the Walker A and B motifs of NBD1 and the LSGGQ motif of NBD2 (termed site 1), while the other is formed by the Walker A and B motifs of NBD2 and the LSGGQ motif of NBD1 (termed site 2) (Figure 2). However, photolabeling studies argue that the ATP-binding sites of CFTR are not equivalent in function; site 1 stably binds nucleotides, whereas site 2 rapidly hydrolyses them^[33, 34]. Because CFTR Cl^- channels transit between the closed and open configurations in seconds, Vergani *et al*^[27, 28] interpreted the photolabeling data to suggest that CFTR channel gating

is controlled by ATP binding and hydrolysis at site 2, driving cycles of NBD dimer assembly and disassembly. To test this model, Vergani *et al*^[28] applied mutant cycle analysis to residues predicted to lie on opposite sides of the NBD1:NBD2 dimer interface. Of note, the authors demonstrated that R555 (NBD1) and T1246 (NBD2) are energetically coupled only in open channels, arguing convincingly that the NBDs undergo dynamic reorganization during channel gating^[28]. For further discussion of how ATP gates the CFTR Cl^- channel, see^[35-37].

Using the ATP-driven NBD dimerization model of CFTR channel gating^[27, 28], Roxo-Rosa *et al*^[26] speculated that the exceptionally slow rate of channel opening of F508del-CFTR might be explained by F508del inducing misfolding and/or structural instability of NBD1, which would hamper ATP binding. Moreover, the reduced open time of F508del-CFTR might reflect weakening of the binding energy for stable NBD1:NBD2 dimer formation by the mutation^[26]. In support of this idea, Pissarra *et al*^[38] demonstrated that the solubilizing mutations used to promote crystallization of human NBD1^[32] traffic F508del-CFTR to the surface and abrogate, albeit incompletely, the channel's gating defect. Thus, deletion of F508 might cause intrinsic misfolding and/or structural instability of NBD1^[26].

However, two lines of evidence argue against the idea that deletion of F508 causes misfolding of NBD1. First, F508del perturbs the local topography of NBD1, without affecting domain folding^[32], but see Pissarra *et al*^[38]. Second, F508 is located at the surface of NBD1, where it might interact with the MSDs^[31, 32]. The residue is remote from the NBD1:NBD2 interface, the location of the ATP-binding sites (Figure 2).

Following the elucidation of the atomic structure of the ABC transporter Sav1866, the multidrug transporter of *S aureus*^[39],

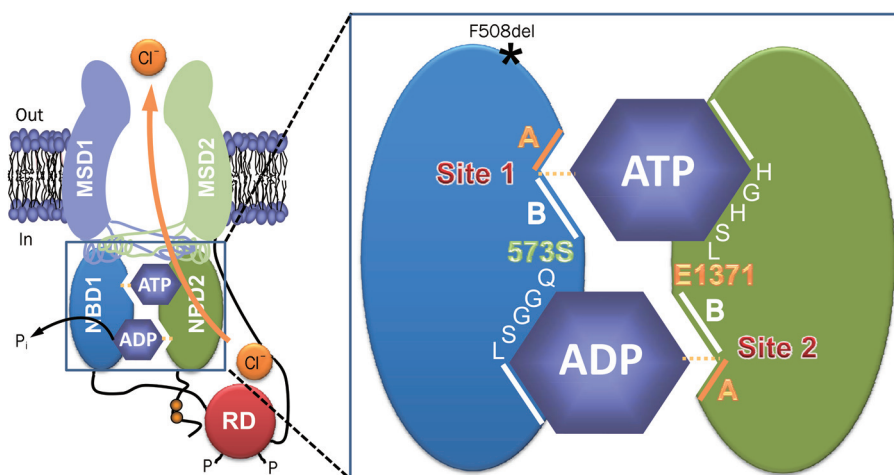


Figure 2. The organization of the ATP-binding sites in CFTR. The simplified model shows the molecular architecture of ATP-binding site 1 (site 1) and ATP-binding site 2 (site 2) in an open CFTR Cl^- channel. Each ATP-binding site is formed by the Walker A and B motifs (labeled A and B, respectively) of one NBD and the LSGGQ motif of the other NBD. Site 2 contains a canonical LSGGQ motif, whereas site 1 contains a non-canonical LSGGH motif. Site 2 also contains a catalytic base (E1371) at the distal end of the Walker B motif, but this residue is absent in site 1 (S573). The location of the CF mutation F508del on the surface of NBD1 opposite intracellular loop 4 (ICL4) is shown by an asterisk. Abbreviations: MSD, membrane-spanning domain; NBD, nucleotide-binding domain; P, phosphorylation of the RD; P_i , inorganic phosphate; RD, regulatory domain. In and out denote the intra- and extracellular sides of the membrane, respectively. See text for further information. Modified, with permission, from Hwang and Sheppard^[36].

structural models of the entire CFTR protein have been developed^[40–42] and used to understand better CFTR function (eg Alexander *et al*^[43]). Of note, these structural models have provided important new insight into how the F508del mutation disrupts CFTR channel gating. They also reveal the function of the four intracellular loops (ICLs), which connect transmembrane segments within the MSDs. Each ICL consists of two long α -helical extensions of transmembrane segments with an intervening short α -helix at its most cytoplasmic location orientated parallel to the plane of the membrane. Because this short α -helix interacts with the NBDs, it is termed the coupling helix^[40, 41].

For two reasons, the positions of the ICLs in structural models of CFTR are notable. First, the ICLs communicate both with the same and the opposite NBD (eg ICL1 (MSD1) with NBD1 and ICL2 (MSD1) with NBD2^[40, 41]). Prior to these structural models, communication between the NBDs and MSDs was presumed to be only vertical (eg NBD1:MSD1). However, the structural models of Serohijos *et al*^[40] and Mornon *et al*^[41] argue that communication between the NBDs and MSDs is both vertical and orthogonal (eg NBD1:MSD1 and NBD1:MSD2). Second, the coupling helix of ICL4 interacts with the surface of NBD1 in the region of F508^[40, 41]. This observation provides an explanation for why the F508del mutation profoundly disrupts CFTR channel gating. The mutation affects a residue located at a critical interface in the CFTR gating pathway, the sequence of conformation changes initiated by ATP-driven NBD dimerization, which leads to opening of the CFTR pore and Cl⁻ flow through the channel. Thus, understanding the interface between the F508 region of NBD1 and the coupling helix of ICL4 is central to the development of drug therapies that target the root cause of CF.

Rational new therapies for CF that target defects in F508del-CFTR

To target the root cause of CF, future therapies should (i) overcome the F508del-CFTR processing defect and traffic the mutant protein to the apical membrane^[12]; (ii) extend the residence time of F508del-CFTR at the apical membrane^[44] and abrogate channel “rundown” (eg Schultz *et al*^[22]) and (iii) rescue the defective channel gating of F508del-CFTR^[14]. Thus, small molecules with two or possibly three types of activity are required to restore function to the F508del-CFTR Cl⁻ channel.

Small molecules that overcome the processing defect of F508del-CFTR and traffic the mutant protein to the apical membrane are termed CFTR correctors because they rescue the cell surface expression of F508del-CFTR^[45, 46]. CFTR correctors might interact with CFTR itself, by acting as either substrate mimics or active site inhibitors. Alternatively, they might target one or more of the many CFTR interacting proteins that orchestrate and control processing of CFTR, its delivery to, and expression at the apical membrane. This latter group of CFTR correctors is termed proteostasis regulators because they aim to treat CF by manipulating the concentration, conformation, quaternary structure and/or location of CFTR^[47].

Small molecules that repair the gating defect of the F508del-CFTR Cl⁻ channel are termed CFTR potentiators because they do not open silent channels, but instead enhance ATP-dependent channel gating following the phosphorylation of F508del-CFTR by PKA^[45]. Although some agents (eg bromotetramisole^[48]) enhance CFTR gating by modulating activity of the protein kinases and phosphatases that control the phosphorylation status of CFTR, CFTR potentiators interact directly with CFTR to enhance channel gating. Interestingly, a small number of compounds have been identified which possess both CFTR corrector and potentiator activity^[49, 50]. These small molecules are termed CFTR corrector-potentiators or dual-acting molecules.

Because there is insufficient information at the present time to design rationally CFTR correctors and potentiators, the strategy of choice to identify drug-like small molecule CFTR modulators is high-throughput screening (HTS)^[45]. HTS exploits a reliable, sensitive, cost-effective assay to screen libraries of chemically diverse small molecules (eg approved drugs^[51], drug-like chemicals^[52] and natural products^[53]) to identify lead compounds for medicinal chemistry optimization. For example, Alan Verkman (UCSF, San Francisco, USA) used Fischer rat thyroid cells, epithelial cells devoid of CFTR expression and cAMP-stimulated Cl⁻ currents^[54] engineered to co-express recombinant human CFTR and a green fluorescent protein (GFP) with ultra high halide sensitivity in a halide flux assay (eg Yang *et al*^[52]). By contrast, Vertex Pharmaceuticals (San Diego, USA) employed NIH-3T3 cells expressing recombinant human CFTR in a fluorescence resonance energy transfer (FRET)-based membrane voltage-sensing assay (eg Van Goor *et al*^[55]). Both of these HTS assays monitor the change in CFTR-mediated anion flux elicited by CFTR modulators in real time.

By screening 150 000 drug-like compounds using F508del-CFTR expressing FRT cells, Verkman's group were the first to identify CFTR correctors using HTS^[56]. Among the chemical scaffolds with CFTR corrector activity, the bisaminomethylthiazole corr-4a (Figure 3) deserves special attention. Pedemonte *et al*^[56] demonstrated that corr-4a is equipotent to low temperature correction at restoring function to F508del-CFTR-expressing human bronchial epithelia (CFBE), achieving levels of CFTR function approximately 8% of that of human bronchial epithelia expressing wild-type CFTR (HBE). Of special note, the aminoarylthiazole corr-2b identified by Pedemonte *et al*^[56] exhibits dual activity as both a CFTR corrector and a CFTR potentiator^[50]. When compared with small molecules that act as CFTR correctors, corr-2b generated double the amount of forskolin-activated CFTR Cl⁻ current (I_{FSK}) relative to the total CFTR Cl⁻ current measured in the presence of forskolin and the CFTR potentiator genistein (I_{TOT}) (CFTR correctors (eg corr-4a): $I_{\text{FSK}}/I_{\text{TOT}} \sim 40\%$; corr-2b: $I_{\text{FSK}}/I_{\text{TOT}} \sim 80\%$; see Figure 1 of Pedemonte *et al*^[50]). Moreover, the authors demonstrated that aminoarylthiazoles do not act as typical CFTR potentiators because they require protein synthesis to exert their effects (see below and^[50]). Elucidation of the mechanism of action of corr-2b and related dual-acting small molecules is

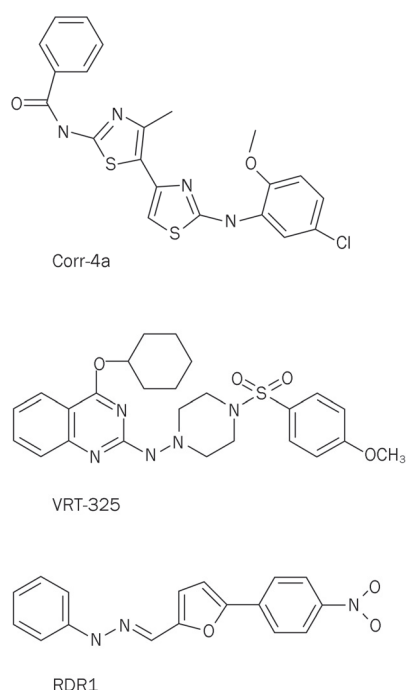


Figure 3. Chemical structures of some CFTR correctors identified by HTS. Abbreviations: Corr-4a, N-[2-(5-Chloro-2-methoxy-phenylamino)-4'-methyl-[4,5']bithiazolyl-2'-yl]-benzamide; VRT-325, 4-Cyclohexyloxy-2-[1-[4-(4-methoxy-benzensulfonyl)-piperazin-1-yl]-ethyl]-quinazoline; RDR1, 5-(4-nitrophenyl)-2-furaldehyde 2-phenylhydrazone.

a priority for future research.

In a ground-breaking program funded by the Cystic Fibrosis Foundation (Bethesda, USA), a nonprofit, donor-supported organization, Vertex Pharmaceuticals identified 13 distinct chemical scaffolds with CFTR corrector activity after screening ~164 000 chemically diverse drug-like small molecules^[55]. Following medicinal chemistry optimization, Vertex Pharmaceuticals identified the quinazoline VRT-325 (Figure 3) as a potent and efficacious CFTR corrector that enhances the maturation of native F508del-CFTR protein and augments CFTR-mediated transepithelial Cl⁻ secretion in CFBE^[55]. Biochemical studies of VRT-325 suggest that it acts at the endoplasmic reticulum to promote CFTR folding^[55]. Because VRT-325 decreases the apparent ATP affinity of purified, reconstituted F508del-CFTR^[57], it might rescue the processing and trafficking of F508del-CFTR, at least in part, by interacting directly with the mutant protein.

To identify CFTR correctors that interact directly with F508del-CFTR, Sampson *et al*^[58] employed differential scanning fluorimetry, which identifies ligands of a target protein by monitoring their effects on the thermal unfolding of the protein. Among 224 hits identified in a previous HTS for CFTR correctors, just one chemical, the substituted phenylhydrazone RDR1 (Figure 3), was able to thermally stabilize murine F508del-CFTR^[58]. As with previous studies of CFTR correctors by the Hanrahan and Thomas groups^[59, 60], the authors deployed a battery of biochemical and functional

assays to investigate F508del-CFTR rescue by RDR1 in heterologous cells, polarized epithelia and genetically-modified mice. The authors' data demonstrate that RDR1 thermally stabilizes murine F508del-NBD1, increases the maturation of human F508del-CFTR protein and augments the function of human CFTR *in vitro* and murine CFTR *in vivo*^[58]. Taken together, these data and the additive effect of RDR1 treatment and low temperature incubation on human F508del-CFTR maturation argue convincingly that RDR1 is a CFTR corrector that targets directly F508del-NBD1 to exert its effects. Identification of the RDR1-binding site on CFTR should be an important goal of future research.

To identify CFTR potentiators that rescue the gating defect of F508del-CFTR, Yang *et al*^[52] studied FRT cells expressing low temperature-corrected F508del-CFTR. A screen of 100 000 compounds identified six novel classes of high-affinity F508del-CFTR potentiators^[52]. However, by screening additional structural analogues, Yang *et al*^[52] discovered tetrahydrobenzothiophenes (*eg* ΔF508_{act}-02; Figure 4), which potentiate F508del-CFTR with $K_d < 100$ nmol/L. Subsequently, Pedemonte *et al*^[61] screened 50 000 compounds searching for further ligands that rescue the gating defect of F508del-CFTR. After secondary analyses, Pedemonte *et al*^[61] identified phenylglycines and sulfonamides that potentiate F508del-CFTR with nanomolar potency. Interestingly, by screening a library of 2000 compounds, including drugs approved for clinical use, Pedemonte *et al*^[51] demonstrated that the antihypertensive drugs 1,4-dihydropyridines (DHPs) act as F508del-CFTR potentiators by a mechanism independent of their effects on voltage-gated Ca²⁺ channels. To identify DHPs that potentiate F508del-CFTR without inhibiting voltage-gated Ca²⁺ channels, Pedemonte *et al*^[62] investigated structure-activity relationships

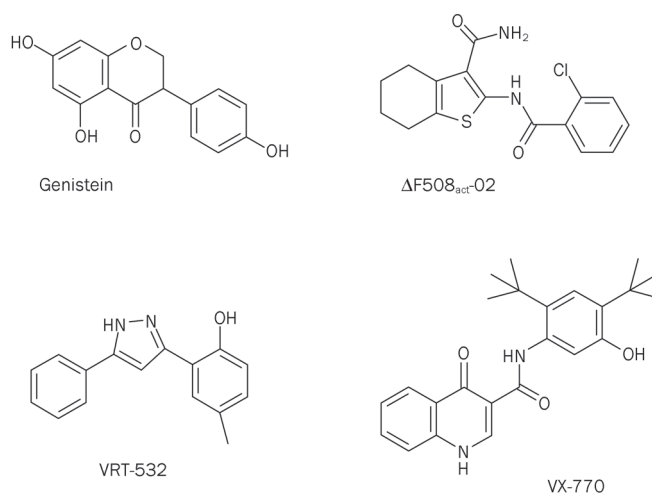


Figure 4. Chemical structures of some CFTR potentiators identified by HTS. Abbreviations: ΔF508_{act}-02, 2-(2-chlorobenzamido)-4,5,6,7-tetrahydro-3H-indene-1-carboxamide; VRT-532, 4-methyl-2-(5-phenyl-1H-pyrazol-3-yl)phenol; VX-770, N-(2,4-di-tert-butyl-5-hydroxyphenyl)-4-oxo-1,4-dihydroquinoline-3-carboxamide. For comparison, the chemical structure of genistein is shown.

using a panel of 333 analogues of felodipine, the most potent CFTR potentiator identified in their original screen. The authors' data demonstrate that substituents with hydrophobic groups enhance the potency of DHPs as CFTR potentiators^[62]. They also reveal that some DHPs are excellent lead compounds for the development of therapeutically active CFTR potentiators.

To identify therapeutically active potentiators of F508del-CFTR, Vertex Pharmaceuticals screened 122000 synthetic compounds from their compound collection using NIH-3T3 cells expressing temperature-corrected F508del-CFTR^[55]. After careful scrutiny, Van Goor *et al*^[55] selected for further study 53 compounds consisting of 10 distinct chemical scaffolds. One compound, the pyrazole VRT-532 (Figure 4), rescued the gating defect of F508del-CFTR by accelerating the rate of channel opening and slowing the rate of channel closure^[55]. Critically, VRT-532 augmented robustly CFTR-mediated transepithelial Cl⁻ secretion in CFBE (EC₅₀, 2.7±0.2 μmol/L^[55]). Importantly, the effects of VRT-532 on CFBE were synergistic with the CFTR corrector VRT-325. CFBE incubated with VRT-325 and then treated with cAMP agonists and VRT-532 generated levels of CFTR-mediated transepithelial Cl⁻ secretion in CFBE >20% of those observed in HBE^[55].

Subsequently, Vertex Pharmaceuticals screened 228 000 chemically diverse drug-like compounds to identify chemical scaffolds for development into therapeutically active CFTR potentiators. Following medicinal chemistry optimization, Vertex Pharmaceuticals identified VX-770 (Figure 4), a potent, selective and orally bioavailable CFTR potentiator^[63]. Interestingly, by increasing the frequency and duration of channel openings, VX-770 (1 μmol/L) restored the channel activity (measured by P_o) of F508del-CFTR to wild-type CFTR levels^[63]. Moreover, treatment of CFBE (genotype F508del/G551D) with VX-770 (10 μmol/L) increased airway surface liquid volume and ciliary beat frequency to levels about half those of HBE^[63].

Based on its performance in preclinical studies, VX-770 became the first CFTR potentiator to be tested in the clinic. The drug was first tested in 39 adult CF patients carrying the CFTR mutation G551D, which has no effect on the processing and trafficking of CFTR, but profoundly disrupts channel gating^[64, 65]. The CF patients in this study took VX-770 orally in a randomized, double-blind, placebo-controlled trial^[66]. VX-770 was well tolerated by CF patients, and at high concentration (150 mg), VX-770 decreased the sweat Cl⁻ concentration to a level approaching the normal range (<60 mmol/L) and improved lung function (measured by forced expiratory volume in one second, FEV₁) by 9%^[66]. Further clinical studies of VX-770 are ongoing. Of special note, initial results from the phase III clinical trial of VX-770 on 83 CF patients with the G551D mutation demonstrated a sustained improvement in lung function at 48 weeks with drug-treated CF patients 55% less likely to experience a pulmonary exacerbation (<http://investors.vrtx.com/releasedetail.cfm?ReleaseID=551869>). Vertex Pharmaceuticals indicate that they plan to apply for US and European drug approval later in 2011 (<http://investors.vrtx.com/releasedetail.cfm?ReleaseID=551869>).

Knowledge of how ATP gates the CFTR Cl⁻ channel, particularly the ATP-driven NBD dimerization model^[27, 28], provides explanations for the mechanism(s) of action of CFTR potentiators. Ai *et al*^[67] first proposed that genistein and other CFTR potentiators might enhance CFTR channel gating by affecting NBD dimerization. The authors speculated first that the binding of genistein at the interface of the NBD dimer might lower the free energy of the transition state and, hence, accelerate channel opening^[67]. Second, the authors proposed that genistein might slow the rate of channel closure by stabilizing the NBD dimer conformation^[67]. Finally, the authors argued that the binding site for genistein might be located at the dimer interface^[67]. Consistent with this idea, Moran *et al*^[68] used a molecular model of the NBD1:NBD2 dimer to show that genistein, apigenin and a series of novel CFTR potentiators identified by HTS bind to CFTR at the dimer interface. As predicted^[69] and verified^[70] by functional data, this drug-binding site is distinct from the two ATP-binding sites of CFTR. Moreover, sequences from both NBD1 (Walker A, Walker B and LSGGQ) and NBD2 (LSGGQ) contribute to the drug-binding site, with those from NBD1 forming a cavity in which CFTR potentiators dock^[68]. Following the development of structural models of the entire CFTR protein^[40-42], *in silico* structure-based screening is likely to become a powerful tool to identify small molecules that interact directly with F508del-CFTR and other CF mutants. Of note, using this approach Kalid *et al*^[49] identified a ligand-binding site in the vicinity of F508 at the interface of the NBDs and MSDs. Finally, differences in the molecular pharmacology of CFTR homologs from different species (eg human and murine CFTR^[63, 71, 72]) argue that chimeric CFTR proteins may be valuable tools to identify where CFTR potentiators dock with CFTR^[73].

Conclusions

Two decades after the identification of the defective gene responsible for CF, therapies based on a molecular understanding of the disease are beginning to be tested in the clinic. Early results from these trials are encouraging. They raise the prospect of personalized medicine, whereby specific therapies are designed to target precisely the genetic defects harbored by individuals afflicted by CF. However, the development of efficacious and safe drug therapies for CF patients will require much more work. For example, it is currently unknown how much CFTR function is required to rescue CF mutants, whether drug therapy for CF is mutation specific and if long-term treatment with CFTR correctors and potentiators causes adverse effects. Answers to these pressing questions will play an important role in shaping future therapeutic strategies for CF.

Acknowledgements

We thank former laboratory colleagues for stimulating discussions. Work in the authors' laboratory is supported by the Cystic Fibrosis Trust and the Engineering and Physical Sciences Research Council [grant no. EP/F03623X/1]. J Liu is supported by scholarships from the University of Bristol and

the Overseas Research Students Awards Scheme of Universities UK.

Author contribution

The authors researched the literature and wrote the review.

References

- 1 Welsh MJ, Ramsey BW, Accurso F, Cutting GR. Cystic fibrosis. In: Scriver CR, Beaudet AL, Sly WS, Valle D, editors. *The Metabolic and Molecular Basis of Inherited Disease*. New York: McGraw-Hill Inc; 2001. p 5121–88.
- 2 Davis PB. Cystic fibrosis since 1938. *Am J Respir Crit Care Med* 2006; 173: 475–82.
- 3 Rowe SM, Miller S, Sorscher EJ. Cystic fibrosis. *N Engl J Med* 2005; 352: 1992–2001.
- 4 Boucher RC. Airway surface dehydration in cystic fibrosis: pathogenesis and therapy. *Annu Rev Med* 2007; 58: 157–70.
- 5 Riordan JR, Rommens JM, Kerem B, Alon N, Rozmahel R, Grzelczak Z, et al. Identification of the cystic fibrosis gene: cloning and characterization of complementary DNA. *Science* 1989; 245: 1066–73.
- 6 Holland IB, Cole SPC, Kuchler K, Higgins CF. *ABC Proteins: from bacteria to man*. London: Academic Press; 2003.
- 7 Anderson MP, Gregory RJ, Thompson S, Souza DW, Paul S, Mulligan RC, et al. Demonstration that CFTR is a chloride channel by alteration of its anion selectivity. *Science*. 1991; 253: 202–5.
- 8 Bear CE, Li CH, Kartner N, Bridges RJ, Jensen TJ, Ramjeesingh M, et al. Purification and functional reconstitution of the cystic fibrosis transmembrane conductance regulator (CFTR). *Cell* 1992; 68: 809–18.
- 9 Anderson MP, Berger HA, Rich DP, Gregory RJ, Smith AE, Welsh MJ. Nucleoside triphosphates are required to open the CFTR chloride channel. *Cell* 1991; 67: 775–84.
- 10 Hwang TC, Nagel G, Nairn AC, Gadsby DC. Regulation of the gating of cystic fibrosis transmembrane conductance regulator C1 channels by phosphorylation and ATP hydrolysis. *Proc Natl Acad Sci U S A* 1994; 91: 4698–702.
- 11 Rich DP, Anderson MP, Gregory RJ, Cheng SH, Paul S, Jefferson DM, et al. Expression of cystic fibrosis transmembrane conductance regulator corrects defective chloride channel regulation in cystic fibrosis airway epithelial cells. *Nature* 1990; 347: 358–63.
- 12 Cheng SH, Gregory RJ, Marshall J, Paul S, Souza DW, White GA, et al. Defective intracellular transport and processing of CFTR is the molecular basis of most cystic fibrosis. *Cell* 1990; 63: 827–34.
- 13 Drumm ML, Wilkinson DJ, Smit LS, Worrell RT, Strong TV, Frizzell RA, et al. Chloride conductance expressed by $\Delta F508$ and other mutant CFTRs in *Xenopus* oocytes. *Science* 1991; 254: 1797–9.
- 14 Dalemans W, Barbry P, Champigny G, Jallat S, Dott K, Dreyer D, et al. Altered chloride ion channel kinetics associated with the $\Delta F508$ cystic fibrosis mutation. *Nature* 1991; 354: 526–8.
- 15 Sheppard DN, Welsh MJ. Structure and function of the CFTR chloride channel. *Physiol Rev* 1999; 79 (1 Suppl): S23–45.
- 16 Li C, Ramjeesingh M, Reyes E, Jensen T, Chang X, Rommens JM, et al. The cystic fibrosis mutation ($\Delta F508$) does not influence the chloride channel activity of CFTR. *Nat Genet* 1993; 3: 311–6.
- 17 Cai Z, Scott-Ward TS, Sheppard DN. Voltage-dependent gating of the cystic fibrosis transmembrane conductance regulator Cl^- channel. *J Gen Physiol* 2003; 122: 605–20.
- 18 Denning GM, Anderson MP, Amara JF, Marshall J, Smith AE, Welsh MJ. Processing of mutant cystic fibrosis transmembrane conductance regulator is temperature-sensitive. *Nature* 1992; 358: 761–4.
- 19 French PJ, van Doorninck JH, Peters RH, Verbeek E, Ameen NA, Marino CR, et al. A $\Delta F508$ mutation in mouse cystic fibrosis transmembrane conductance regulator results in a temperature-sensitive processing defect in vivo. *J Clin Invest* 1996; 98: 1304–12.
- 20 Haws CM, Nepomuceno IB, Krouse ME, Wakelee H, Law T, Xia Y, et al. $\Delta F508$ -CFTR channels: kinetics, activation by forskolin, and potentiation by xanthines. *Am J Physiol* 1996; 270: C1544–55.
- 21 Hwang TC, Wang F, Yang IC, Reenstra WW. Genistein potentiates wild-type and $\Delta F508$ -CFTR channel activity. *Am J Physiol* 1997; 273: C988–98.
- 22 Schultz BD, Frizzell RA, Bridges RJ. Rescue of dysfunctional $\Delta F508$ -CFTR chloride channel activity by IBMX. *J Membr Biol* 1999; 170: 51–66.
- 23 Cai Z, Sheppard DN. Phloxine B interacts with the cystic fibrosis transmembrane conductance regulator at multiple sites to modulate channel activity. *J Biol Chem* 2002; 277: 19546–53.
- 24 Miki H, Zhou Z, Li M, Hwang TC, Bompadre SG. Potentiation of disease-associated cystic fibrosis transmembrane conductance regulator mutants by hydrolyzable ATP analogs. *J Biol Chem* 2010; 285: 19967–75.
- 25 Wang F, Zeltwanger S, Hu S, Hwang TC. Deletion of phenylalanine 508 causes attenuated phosphorylation-dependent activation of CFTR chloride channels. *J Physiol* 2000; 524: 637–48.
- 26 Roxo-Rosa M, Xu Z, Schmidt A, Neto M, Cai Z, Soares CM, et al. Revertant mutants G550E and 4RK rescue cystic fibrosis mutants in the first nucleotide-binding domain of CFTR by different mechanisms. *Proc Natl Acad Sci U S A* 2006; 103: 17891–6.
- 27 Vergani P, Nairn AC, Gadsby DC. On the mechanism of MgATP-dependent gating of CFTR Cl^- channels. *J Gen Physiol* 2003; 121: 17–36.
- 28 Vergani P, Lockless SW, Nairn AC, Gadsby DC. CFTR channel opening by ATP-driven tight dimerization of its nucleotide-binding domains. *Nature* 2005; 433: 876–80.
- 29 Locher KP, Lee AT, Rees DC. The *E. coli* BtuCD structure: a framework for ABC transporter architecture and mechanism. *Science* 2002; 296: 1091–8.
- 30 Smith PC, Karpowich N, Millen L, Moody JE, Rosen J, Thomas PJ, et al. ATP binding to the motor domain from an ABC transporter drives formation of a nucleotide sandwich dimer. *Mol Cell* 2002; 10: 139–49.
- 31 Lewis HA, Buchanan SG, Burley SK, Connors K, Dickey M, Dorwart M, et al. Structure of nucleotide-binding domain 1 of the cystic fibrosis transmembrane conductance regulator. *EMBO J* 2004; 23: 282–93.
- 32 Lewis HA, Zhao X, Wang C, Sauder JM, Rooney I, Noland BW, et al. Impact of the $\Delta F508$ mutation in first nucleotide-binding domain of human cystic fibrosis transmembrane conductance regulator on domain folding and structure. *J Biol Chem* 2005; 280: 1346–53.
- 33 Aleksandrov L, Aleksandrov AA, Chang XB, Riordan JR. The first nucleotide binding domain of cystic fibrosis transmembrane conductance regulator is a site of stable nucleotide interaction, whereas the second is a site of rapid turnover. *J Biol Chem* 2002; 277: 15419–25.
- 34 Basso C, Vergani P, Nairn AC, Gadsby DC. Prolonged nonhydrolytic interaction of nucleotide with CFTR's NH_2 -terminal nucleotide binding domain and its role in channel gating. *J Gen Physiol* 2003; 122: 333–48.
- 35 Gadsby DC, Vergani P, Csanády L. The ABC protein turned chloride channel whose failure causes cystic fibrosis. *Nature* 2006; 440:

- 477–83.
- 36 Hwang TC, Sheppard DN. Gating of the CFTR Cl⁻ channel by ATP-driven nucleotide-binding domain dimerisation. *J Physiol* 2009; 587: 2151–61.
- 37 Kirk K, Wang W. A unified view of cystic fibrosis transmembrane conductance regulator (CFTR) gating: combining the allostereism of a ligand-gated channel with the enzymatic activity of an ATP-binding cassette (ABC) transporter. *J Biol Chem* 2011; 286: 12813–9.
- 38 Pissarra LS, Farinha CM, Xu Z, Schmidt A, Thibodeau PH, Cai Z, et al. Solubilizing mutations used to crystallize one CFTR domain attenuate the trafficking and channel defects caused by the major cystic fibrosis mutation. *Chem Biol* 2008; 15: 62–9.
- 39 Dawson RJ, Locher KP. Structure of a bacterial multidrug ABC transporter. *Nature* 2006 14; 443: 180–5.
- 40 Serohijos AW, Hegedus T, Aleksandrov AA, He L, Cui L, Dokholyan NV, et al. Phenylalanine-508 mediates a cytoplasmic-membrane domain contact in the CFTR 3D structure crucial to assembly and channel function. *Proc Natl Acad Sci U S A* 2008; 105: 3256–61.
- 41 Mornon JP, Lehn P, Callebaut I. Atomic model of human cystic fibrosis transmembrane conductance regulator: membrane-spanning domains and coupling interfaces. *Cell Mol Life Sci* 2008; 65: 2594–612.
- 42 Mornon JP, Lehn P, Callebaut I. Molecular models of the open and closed states of the whole human CFTR protein. *Cell Mol Life Sci* 2009; 66: 3469–86.
- 43 Alexander C, Ivetac A, Liu X, Norimatsu Y, Serrano JR, Landstrom A, et al. Cystic fibrosis transmembrane conductance regulator: using differential reactivity toward channel-permeant and channel-impermeant thiol-reactive probes to test a molecular model for the pore. *Biochemistry* 2009; 48: 10078–88.
- 44 Lukacs GL, Chang XB, Bear C, Kartner N, Mohamed A, Riordan JR, et al. The ΔF508 mutation decreases the stability of cystic fibrosis transmembrane conductance regulator in the plasma membrane. Determination of functional half-lives on transfected cells. *J Biol Chem* 1993; 268: 21592–8.
- 45 Verkman AS, Galiotta LJ. Chloride channels as drug targets. *Nat Rev Drug Discov* 2009; 8: 153–71.
- 46 Amaral MD. Targeting CFTR: How to treat cystic fibrosis by CFTR-repairing therapies. *Curr Drug Targets*. 2011; 12: 683–93.
- 47 Balch WE, Morimoto RI, Dillin A, Kelly JW. Adapting proteostasis for disease intervention. *Science* 2008; 319: 916–9.
- 48 Becq F, Jensen TJ, Chang XB, Savoia A, Rommens JM, Tsui LC, et al. Phosphatase inhibitors activate normal and defective CFTR chloride channels. *Proc Natl Acad Sci U S A* 1994; 91: 9160–4.
- 49 Kalid O, Mense M, Fischman S, Shitrit A, Bihler H, Ben-Zeev E, et al. Small molecule correctors of F508del-CFTR discovered by structure-based virtual screening. *J Comput Aided Mol Des* 2010; 24: 971–91.
- 50 Pedemonte N, Tomati V, Sondo E, Caci E, Millo E, Armirotti A, et al. Dual activity of aminoarylthiazoles on the trafficking and gating defects of the cystic fibrosis transmembrane conductance regulator (CFTR) chloride channel caused by cystic fibrosis mutations. *J Biol Chem* 2011; 286: 15215–26.
- 51 Pedemonte N, Diena T, Caci E, Nieddu E, Mazzei M, Ravazzolo R, et al. Antihypertensive 1,4-dihydropyridines as correctors of the cystic fibrosis transmembrane conductance regulator channel gating defect caused by cystic fibrosis mutations. *Mol Pharmacol* 2005; 68: 1736–46.
- 52 Yang H, Shelat AA, Guy RK, Gopinath VS, Ma T, Du K, et al. Nanomolar affinity small molecule correctors of defective ΔF508-CFTR chloride channel gating. *J Biol Chem* 2003; 278: 35079–85.
- 53 Xu LN, Na WL, Liu X, Hou SG, Lin S, Yang H, et al. Identification of natural coumarin compounds that rescue defective ΔF508-CFTR chloride channel gating. *Clin Exp Pharmacol Physiol* 2008; 35: 878–83.
- 54 Sheppard DN, Carson MR, Ostedgaard LS, Denning GM, Welsh MJ. Expression of cystic fibrosis transmembrane conductance regulator in a model epithelium. *Am J Physiol* 1994; 266: L405–13.
- 55 Van Goor F, Straley KS, Cao D, González J, Hadida S, Hazlewood A, et al. Rescue of ΔF508-CFTR trafficking and gating in human cystic fibrosis airway primary cultures by small molecules. *Am J Physiol Lung Cell Mol Physiol* 2006; 290: L1117–30.
- 56 Pedemonte N, Lukacs GL, Du K, Caci E, Zegarra-Moran O, Galiotta LJ, et al. Small-molecule correctors of defective ΔF508-CFTR cellular processing identified by high-throughput screening. *J Clin Invest* 2005; 115: 2564–71.
- 57 Kim Chiaw P, Wellhauser L, Huan LJ, Ramjeesingh M, Bear CE. A chemical corrector modifies the channel function of F508del-CFTR. *Mol Pharmacol* 2010; 78: 411–8.
- 58 Sampson HM, Robert R, Liao J, Matthes E, Carlile GW, Hanrahan JW, et al. Identification of a NBD1-binding pharmacological chaperone that corrects the trafficking defect of F508del-CFTR. *Chem Biol*. 2011; 18: 231–42.
- 59 Robert R, Carlile GW, Pavel C, Liu N, Anjos SM, Liao J, et al. Structural analog of sildenafil identified as a novel corrector of the F508del-CFTR trafficking defect. *Mol Pharmacol* 2008; 73: 478–89.
- 60 Robert R, Carlile GW, Liao J, Balghi H, Lesimple P, Liu N, et al. Correction of the ΔF508 cystic fibrosis transmembrane conductance regulator trafficking defect by the bioavailable compound glafenine. *Mol Pharmacol*. 2010; 77: 922–30.
- 61 Pedemonte N, Sonawane ND, Taddei A, Hu J, Zegarra-Moran O, et al. Phenylglycine and sulfonamide correctors of defective ΔF508 and G551D cystic fibrosis transmembrane conductance regulator chloride-channel gating. *Mol Pharmacol* 2005; 67: 1797–807.
- 62 Pedemonte N, Boido D, Moran O, Giampieri M, Mazzei M, Ravazzolo R, et al. Structure-activity relationship of 1,4-dihydropyridines as potentiators of the cystic fibrosis transmembrane conductance regulator chloride channel. *Mol Pharmacol* 2007; 72: 197–207.
- 63 Van Goor F, Hadida S, Grootenhuis PD, Burton B, Cao D, Neuberger T, et al. Rescue of CF airway epithelial cell function *in vitro* by a CFTR potentiator, VX-770. *Proc Natl Acad Sci U S A* 2009; 106: 18825–30.
- 64 Cai Z, Taddei A, Sheppard DN. Differential sensitivity of the cystic fibrosis (CF)-associated mutants G551D and G1349D to potentiators of the cystic fibrosis transmembrane conductance regulator (CFTR) Cl⁻ channel. *J Biol Chem* 2006; 281: 1970–7.
- 65 Bompadre SG, Sohma Y, Li M, Hwang TC. G551D and G1349D, two CF-associated mutations in the signature sequences of CFTR, exhibit distinct gating defects. *J Gen Physiol* 2007; 129: 285–98.
- 66 Accurso FJ, Rowe SM, Clancy JP, Boyle MP, Dunitz JM, Durie PR, et al. Effect of VX-770 in persons with cystic fibrosis and the G551D-CFTR mutation. *N Engl J Med* 2010; 363: 1991–2003.
- 67 Ai T, Bompadre SG, Wang X, Hu S, Li M, Hwang TC. Capsaicin potentiates wild-type and mutant cystic fibrosis transmembrane conductance regulator chloride-channel currents. *Mol Pharmacol* 2004; 65: 1415–26.
- 68 Moran O, Galiotta LJ, Zegarra-Moran O. Binding site of activators of the cystic fibrosis transmembrane conductance regulator in the nucleotide binding domains. *Cell Mol Life Sci* 2005; 62: 446–60.
- 69 Wang F, Zeltwanger S, Yang IC, Nairn AC, Hwang TC. Actions of genistein on cystic fibrosis transmembrane conductance regulator channel gating. Evidence for two binding sites with opposite effects. *J Gen Physiol* 1998; 111: 477–90.

- 70 Zegarra-Moran O, Monteverde M, Galiotta LJ, Moran O. Functional analysis of mutations in the putative binding site for cystic fibrosis transmembrane conductance regulator potentiators. Interaction between activation and inhibition. *J Biol Chem* 2007; 282: 9098–104.
- 71 Lansdell KA, Delaney SJ, Lunn DP, Thomson SA, Sheppard DN, Wainwright BJ. Comparison of the gating behaviour of human and murine cystic fibrosis transmembrane conductance regulator Cl⁻ channels expressed in mammalian cells. *J Physiol* 1998; 508: 379–92.
- 72 de Jonge H, Wilke M, Bot A, Sheppard DN. Responsiveness of mouse versus human CFTR-ΔF508 to small molecule correctors and potentiators. *Pediatr Pulmonol Suppl* 2009; 32: 291–92.
- 73 Scott-Ward TS, Cai Z, Dawson ES, Doherty A, Da Paula AC, Davidson H, *et al*. Chimeric constructs endow the human CFTR Cl⁻ channel with the gating behavior of murine CFTR. *Proc Natl Acad Sci U S A* 2007; 104: 16365–70.

Review

Aquaporin-4: orthogonal array assembly, CNS functions, and role in neuromyelitis optica

Alan S VERKMAN*, Julien RATELADE, Andrea ROSSI, Hua ZHANG, Lukmanee TRADTRANTIP

Departments of Medicine and Physiology, University of California, San Francisco, CA 94143-0521, USA

Aquaporin-4 (AQP4) is a water-selective transporter expressed in astrocytes throughout the central nervous system, as well as in kidney, lung, stomach and skeletal muscle. The two AQP4 isoforms produced by alternative splicing, M1 and M23 AQP4, form heterotetramers that assemble in cell plasma membranes in supramolecular structures called orthogonal arrays of particles (OAPs). Phenotype analysis of AQP4-null mice indicates the involvement of AQP4 in brain and spinal cord water balance, astrocyte migration, neural signal transduction and neuroinflammation. AQP4-null mice manifest reduced brain swelling in cytotoxic cerebral edema, but increased brain swelling in vasogenic edema and hydrocephalus. AQP4 deficiency also increases seizure duration, impairs glial scarring, and reduces the severity of autoimmune neuroinflammation. Each of these phenotypes is likely explicable on the basis of reduced astrocyte water permeability in AQP4 deficiency. AQP4 is also involved in the neuroinflammatory demyelinating disease neuromyelitis optica (NMO), where autoantibodies (NMO-IgG) targeting AQP4 produce astrocyte damage and inflammation. Mice administered NMO-IgG and human complement by intracerebral injection develop characteristic NMO lesions with neuroinflammation, demyelination, perivascular complement deposition and loss of glial fibrillary acidic protein and AQP4 immunoreactivity. Our findings suggest the potential utility of AQP4-based therapeutics, including small-molecule modulators of AQP4 water transport function for therapy of brain swelling, injury and epilepsy, as well as small-molecule or monoclonal antibody blockers of NMO-IgG binding to AQP4 for therapy of NMO.

Keywords: AQP4; water transport; transgenic mice; brain edema; astrocyte migration; neuroexcitation; neuroinflammation; epilepsy; neuromyelitis optica

Acta Pharmacologica Sinica (2011) 32: 702–710; doi: 10.1038/aps.2011.27; published online 9 May 2011

Aquaporin-4 identification, distribution, structure and function

Aquaporin-4 (AQP4) was originally cloned by our lab in 1994 from rat lung^[1] and subsequently from different species and tissues^[2]. AQP4 is most strongly expressed in the central nervous system (CNS), but is found as well in kidney collecting duct, gastric parietal cells, skeletal muscle, airway epithelium and various glandular epithelia^[3, 4]. In the CNS, AQP4 is expressed in astrocytes, and is particularly concentrated at pial and ependymal surfaces in contact with the cerebrospinal fluid (CSF) in the subarachnoid space and the ventricles^[5]. At the cell level, AQP4 expression is polarized in astrocytic foot processes in contact with blood vessels.

AQP4 is present in two major isoforms produced by alternative splicing: a relatively long (M1) isoform with translation initiation at Met-1, and a shorter (M23) isoform with transla-

tion initiation at Met-23 (Figure 1A)^[2, 6, 7]. In rat, but not human or mouse, a longer isoform (Mz) is also found, but at very low levels^[8, 9]. The M1 and M23 isoforms of AQP4 associate in membranes as heterotetramers^[10, 11]. AQP4 functions as a water-selective transporter with a relatively high single channel water permeability compared to other aquaporins^[12, 13]. A high-resolution X-ray crystal structure along with molecular dynamics simulations suggest a structural basis of AQP4 water selectivity involving steric and electrostatic factors^[14]. Like other aquaporins^[15, 16], AQP4 monomers, each of about 30 kdalton molecular size, contain 6 membrane-spanning helical domains and two short helical segments surrounding cytoplasmic and extracellular vestibules connected by a narrow aqueous pore.

AQP4 assembly in orthogonal arrays of particles

AQP4 is a structural component of orthogonal arrays of particles (OAPs), which are square arrays of intramembrane particles seen in cell membranes by freeze-fracture electron microscopy (FFEM)^[17, 18]. Based on the finding that AQP4 is

* To whom correspondence should be addressed.

E-mail Alan.Verkmann@ucsf.edu

Received 2011-02-28 Accepted 2011-03-14

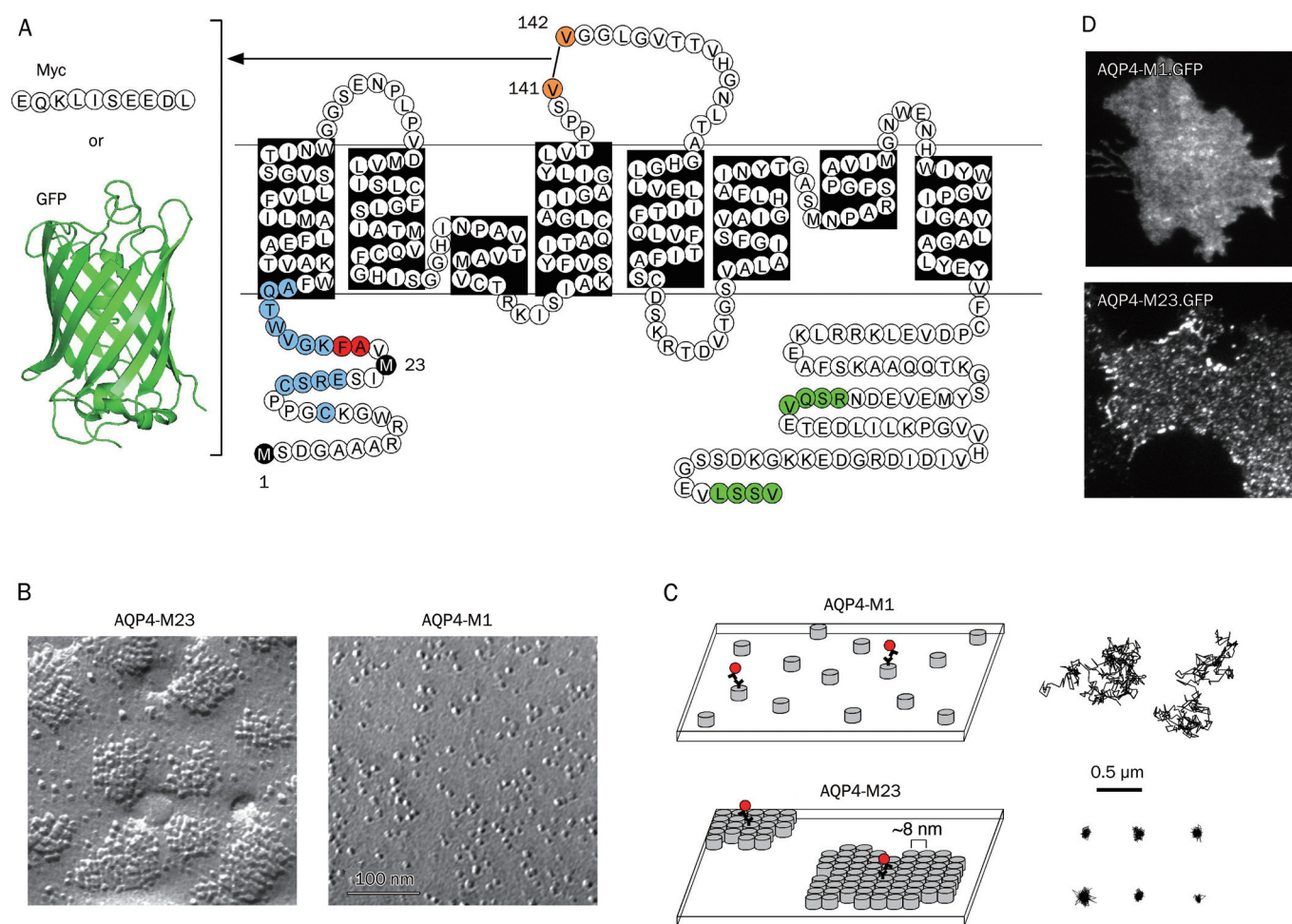


Figure 1. Visualization of AQP4 in OAPs in live cells. (A) AQP4 sequence and topology showing site of Myc or GFP insertion in the second extracellular loop for fluorescence labeling. Black: Met1 and Met23 translation initiation sites; blue: residues where single mutations do not affect OAP formation or disruption; red: residues where single mutations strongly disrupt OAPs; green: C-terminal PDZ-binding domains. (B) Freeze-fracture electron micrographs of COS-7 cells expressing Myc-tagged AQP4-M23 (left) and AQP4-M1 (right). (C) Schematic showing the organization of AQP4 tetramers (left) and representative single particle trajectories (right) of quantum dot-labeled AQP4 molecules in cells expressing AQP4-M1 (top) or AQP4-M23 (bottom). Each grey cylinder represents one AQP4 tetramer. A subset of AQP4 molecules is labeled with quantum dots (red) for single particle tracking. (D) Visualization of AQP4 OAPs by total internal reflection fluorescence microscopy, showing GFP tagged M1 (top) and M23 (bottom) AQP4.

expressed in the same cells in which OAPs were identified, we originally proposed that AQP4 was the OAP protein. Experimental support for this hypothesis came from FFEM on AQP4-transfected CHO cells showing characteristic OAPs^[19], and from the absence of OAPs in brain and other tissues from AQP4 null mice^[20]. Immunogold labeling of AQP4 in OAPs in tissues confirmed the conclusion that AQP4 was the key structural component of OAPs^[21]. The biological significance of OAP formation by AQP4 remains unknown, though it has been proposed that OAPs might facilitate AQP4 water transport, polarization to astrocyte foot processes, and cell-cell adhesion^[12, 22, 23]. As discussed further below, AQP4 OAPs have also been proposed to be the target of neuromyelitis optica (NMO) autoantibodies (NMO-IgG)^[24].

FFEM in cells transfected with the M1 and M23 isoforms of AQP4 show that M23 assembles into large OAPs, whereas

M1 tetramers are largely dispersed (Figure 1B)^[25]. In primary astrocytes, and in cells co-transfected with M1 and M23, OAPs are considerably smaller on average than OAPs in cells expressing only M23^[23, 25], suggesting that M1 interacts with the array-forming M23 in the plasma membrane, limiting the size to which OAPs assemble *in vivo*. Prior to 2008, the only method for identifying OAPs was FFEM. However, various technical challenges limit the usefulness of FFEM when examining questions regarding the mechanisms involved in OAP formation and regulation. Limitations include fixation artifacts, difficulty in obtaining statistically rigorous information about numbers of AQP4 tetramers in OAPs, and difficulty in identifying OAPs in cells expressing low levels of AQP4.

We developed a series of optical methods to study AQP4 OAP assembly in live cells. One method used in our studies has been single particle tracking (SPT), a technique that

is technically and conceptually simple. A c-myc epitope is engineered into the second extracellular loop of the AQP4 molecule (Figure 1A), cells are transiently transfected, and a subset of AQP4 molecules at the plasma membrane in live cells are labeled, via antibody coupling, to fluorescent quantum dots (Figure 1C, left). The movement of individual quantum dots, due to AQP4 diffusion, is followed using a fluorescence microscope, and trajectories of individual quantum dots are reconstructed and analyzed. We initially applied SPT to study AQP1 diffusion, finding long-range free diffusion over a wide variety of conditions, indicating that AQP1 exists in the plasma membrane largely free of specific interactions^[26]. In applying SPT to AQP4, we reasoned that individual AQP4 tetramers should be mobile, whereas AQP4 in large OAPs should be relatively immobile. As expected, in a variety of cell lines and primary astrocytes, we found remarkable immobility of AQP4-M23 and rapid diffusion of AQP4-M1 (Figure 1C, right)^[27].

We exploited AQP4 diffusion as a 'read-out' of OAP assembly in live cells to investigate a series of questions regarding the biophysics and determinants of OAP formation. From measurements on AQP4 mutants and chimeras, we concluded that OAP formation by M23 involved hydrophobic intermolecular interactions of N-terminal AQP4 residues just downstream of Met-23, and that lack of OAP formation by M1 results from non-specific blocking of N-terminal interactions by residues just upstream of Met-23^[28]. We also demonstrated rapid and reversible temperature-dependent assembly into OAPs of certain weakly associating AQP4 mutants^[29], and found that the M1 and M23 isoforms of AQP4 co-mingled in OAPs^[10]. OAPs in live cells were visualized directly by total internal reflection microscopy of GFP-AQP4 chimeras (Figure 1D)^[30]. Single-molecule step-photobleaching and intensity analysis of GFP-labeled M1-AQP4 in the presence of excess unlabeled AQP4 isoforms/mutants indicated heterotetrameric AQP4 association. Time-lapse total internal reflection fluorescence imaging of AQP4-M23 in live cells indicated that OAPs diffused slowly and rearranged over tens of minutes. Together, our measurements in live cells revealed extensive AQP4 monomer-monomer and tetramer-tetramer interactions as well as regulated AQP4 assembly in OAPs. Current work is focused on mathematical modeling of AQP4 assembly in OAPs and super-resolution imaging of individual OAPs.

Functions of AQP4 in the CNS

We have systematically investigated the roles of AQP4 in the CNS utilizing AQP4 knockout mice created in 1997 by targeted gene disruption^[31]. As described below, we confirmed the anticipated involvement of AQP4 in brain water balance, and discovered unexpected roles of AQP4 in astrocyte migration, neuroexcitatory phenomena and neuroinflammation. For each of these phenotypes there is a direct or at least plausible link between AQP4 molecular function as a water channel with the CNS phenotype. AQP4 knockout mice have normal growth and survival, as well as CNS anatomy and histology, vascularity, baseline intracranial pressure and blood-

brain barrier integrity^[32-34]. More recently, Hu and coworkers independently generated AQP4 knockout mice, though they reported significant baseline abnormalities in their mice including impaired blood-brain barrier integrity^[35]. The mice of Hu *et al* manifest a variety of neurochemical and other abnormalities^[36-38], which are difficult to interpret because of their baseline abnormalities and the difficulty in reconciling the various brain phenotypes with the water transporting role of AQP4. There are also confusing data in the literature from Frigeri and coworkers who reported marked abnormalities in cell structure and proliferation in astrocyte cell cultures after AQP4 knockdown^[39]. The original and follow-on data by that group appear to be incorrect, as AQP4 knockdown or knockout in astrocyte cultures does not affect cell growth or morphology^[40-42].

AQP4 and brain edema

The pattern of AQP4 expression in the brain (at interfaces between brain parenchyma and major fluid compartments) as well as regulation studies (correlating AQP4 expression and brain edema) provide indirect evidence for involvement of AQP4 in brain water balance. We thus postulated the involvement of AQP4 in water movement into and out of brain. There are several types of brain edema that can occur independently or together. In cytotoxic (cellular) brain edema, water moves into the brain through an intact blood-brain barrier in response to osmotic driving forces (Figure 2). The archetypal example of cytotoxic edema is water intoxication in which acute serum hyponatremia causes brain swelling by a simple osmotic mechanism. Mice lacking AQP4 show improved clinical outcome and reduced brain water accumulation compared to wildtype mice in water intoxication as well as in other models of primarily cytotoxic brain edema, including ischemic stroke and bacterial meningitis^[32, 43]. Increased AQP4 protein expression in a transgenic AQP4-overexpressing mouse worsens brain swelling in water intoxication^[44]. Recently, an additional mechanism of AQP4-dependent brain swelling has been proposed involving altered cell volume regulation and loss of AQP4-TRPV4 interaction in AQP4 deficiency^[45], though further work is needed to prove the relevance of this mechanism *in vivo*.

In vasogenic (leaky-vessel) brain edema, water moves into the brain by a bulk fluid flow mechanism through a leaky blood-brain barrier, and exits the brain through the AQP4-rich glia limitans lining brain ventricles and the brain surface (Figure 2). When these water exit routes are impaired in obstructive hydrocephalus, water movement out of the brain through microvessels at the blood-brain barrier becomes more significant. The archetypal example of vasogenic edema is brain tumor-associated edema. AQP4 knockout mice manifest worse clinical outcome and greater brain water accumulation in brain tumor edema as well as in other models of vasogenic edema including intraparenchymal fluid infusion, cortical-freeze injury, brain abscess and subarachnoid hemorrhage^[33, 46, 47]. AQP4 null mice also manifest an accelerated course of brain swelling in obstructive hydrocephalus^[48],

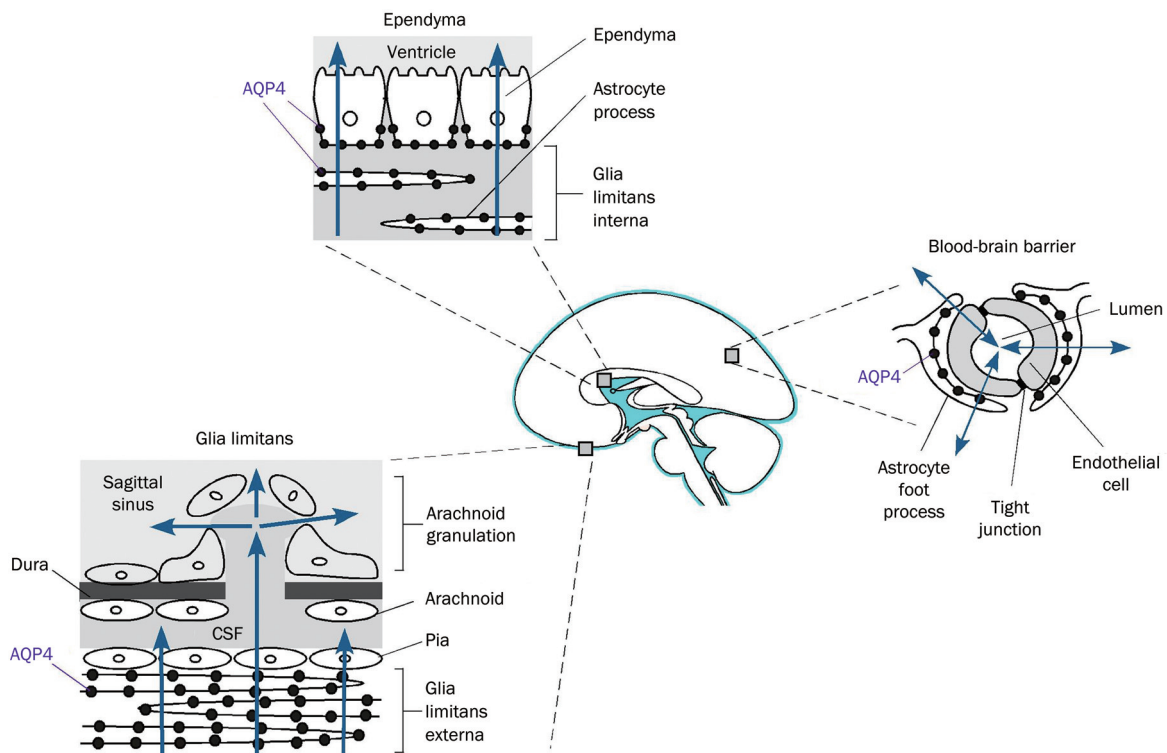


Figure 2. Routes of AQP4-facilitated water entry and exit from the brain, showing blood-brain barrier, ependyma and pial surface.

which is generally classified as a cause of interstitial edema. As a bidirectional water channel, AQP4 thus facilitates brain water accumulation in cytotoxic edema and clearance of excess brain water in vasogenic and interstitial edema. AQP4 appears to play a similar role in spinal cord, with reduced swelling and improved clinical outcome in AQP4 deficiency in spinal cord compression injury^[49], which is primarily associated with cytotoxic edema, while worse swelling and clinical outcome in spinal cord contusion injury^[50], which is primarily vasogenic in nature.

AQP4 and astrocyte migration

Work done by our lab in tumor angiogenesis led to the discovery of AQP4 involvement in astrocyte migration. Motivated by the strong expression of AQP1 in tumor microvessels, we found impaired angiogenesis and tumor growth in AQP1 null mice after subcutaneous or intracranial tumor cell implantation^[51]. Studies in primary aortic endothelial cell cultures from wildtype and AQP1 null mice revealed similar adhesion and proliferation, though impaired cell migration. Supporting a general role of aquaporins in cell migration were the findings that transfection of non-endothelial cells with various AQPs accelerated their migration, and that migrating AQP1-expressing cells had prominent membrane ruffles at their leading edge with polarization of AQP1 protein to lamellipodia. Similar observations were made in brain, where astrocyte migration is important in glial scar formation. Glial scar formation can both be beneficial, by sequestering an acute lesion such as in brain injury, and deleterious, by inhibiting

neuronal regeneration and axonal sprouting^[52]. We found that astrocyte cultures from brains of wildtype and AQP4 knockout mice had similar morphology, proliferation and adhesiveness, but showed markedly impaired migration in the AQP4-deficient cultures in wound healing and transwell Boyden chamber assays^[41]. AQP4 was polarized to the leading edge of migrating cells, with more lamellipodia formed in wildtype *vs* AQP4 null astrocyte cultures. Further, glial scarring was impaired in AQP4 null mice following a stab injury. In a follow-on study, we showed remarkably impaired migration of AQP4-null astrocytes in intact brain in a model of stab injury involving injection of fluorescently labeled astrocytes^[53]. Of relevance to brain, the tumor grade of astrocytomas has been correlated in a number of studies with AQP4 expression^[54]. We found that aquaporin expression in tumor cells increased their extravasation from blood vessels and local invasiveness^[55], providing a potential explanation for the expression of aquaporins in many high-grade tumors.

We propose that aquaporin-facilitated cell migration involves enhanced water movement at the plasma membrane in lamellipodial protrusions^[56]. The importance of water fluxes across the plasma membrane in causing localized swelling of lamellipodia has been considered in the early literature on cell migration^[57]. As diagrammed in Figure 3A, we propose that actin de-polymerization and ion influx at the leading edge of a migrating cell increase cytoplasmic osmolality locally, driving water influx across the cell plasma membrane. Supporting the idea of water flow into and out of migrating cells is evidence that migration can be modulated by changes in

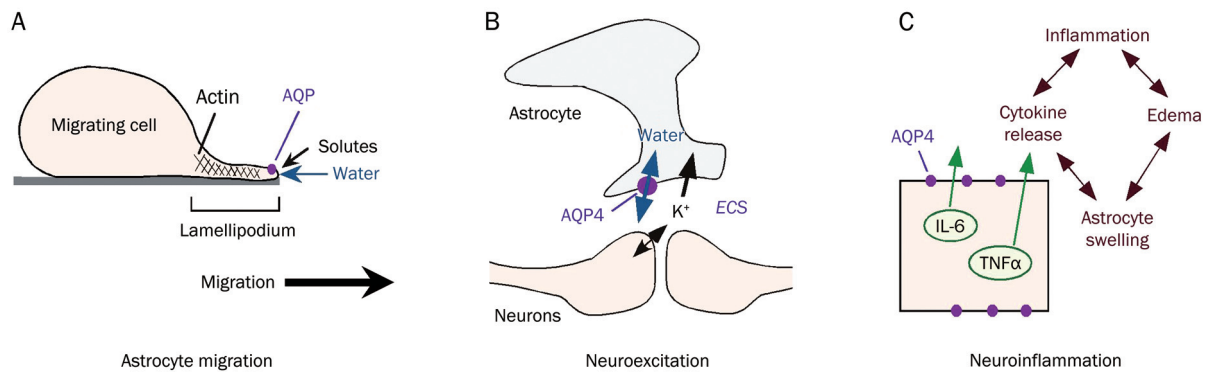


Figure 3. Roles of AQP4 in brain. (A) Proposed mechanism of aquaporin-facilitated cell migration. Aquaporin-facilitated water influx across lamellipodia at the leading edge of a migrating cell promotes membrane protrusion. (B) Proposed pseudo-solvent drag mechanism of AQP4-facilitated neuroexcitation. K⁺ released into the extracellular space (ECS) following neuroexcitation is mainly taken up by astrocytes. K⁺ reuptake results in osmotic water influx into astrocytes and consequent ECS shrinkage, maintaining the electrochemical driving force for K⁺ reuptake. (C) Proposed mechanism for AQP4 involvement in neuroinflammation. AQP4 facilitates cytokine secretion, as well as astrocyte swelling and local cytotoxic edema.

extracellular osmolality and transcellular osmotic gradients^[41]. The resultant water transport and expansion of the adjacent plasma membrane caused by increased hydrostatic pressure is followed by actin re-polymerization to stabilize the cell membrane protrusion. In support of this idea is the observation that regional hydrostatic pressure changes within cells do not equilibrate throughout the cytoplasm on scales of ten microns and ten seconds^[58], and could thus contribute to the formation of localized cell membrane protrusions. Further studies are required to validate our ideas relating aquaporin water permeability to cell migration.

AQP4 and neuroexcitation

The brain extracellular space (ECS) comprises ~20% of brain tissue volume, consisting of a jelly-like matrix in which neurons, glial cells and blood vessels are embedded. The ECS contains ions, neurotransmitters, metabolites, peptides, and extracellular matrix molecules, forming the microenvironment for neurons, astrocytes and other brain cells. During neuronal activity, depolarization of neurons and adjacent glial cells increases extracellular glutamate and K⁺. Excess K⁺ in the ECS is taken up and 'siphoned' largely by astrocytes. AQP4 is expressed in electrically excitable tissues in supportive cells adjacent to excitable cells, including glia but not neurons in brain, Müller but not bipolar cells in retina, supportive but not hair cells in the inner ear, and supportive cells but not olfactory receptor neurons in olfactory epithelium. Postulating from its expression pattern the involvement of AQP4 in neuroexcitatory phenomena, we characterized various neurosensory and neuroexcitatory phenotypes in the AQP4 knockout mice. Electrophysiological measurements showed impaired vision^[59], hearing^[60] and olfaction^[61] in AQP4 null mice, as demonstrated by increased auditory brainstem response thresholds, and reduced electroretinogram and electroolfactogram potentials. Also, seizure threshold is reduced and seizure duration is prolonged in AQP4 knockout mice^[62]. Possible mechanisms for these phenomena supported by

experimental data include delayed K⁺ reuptake by astrocytes in AQP4 deficiency following neuroexcitation^[62, 63], and mild ECS expansion^[64–67]. Delayed K⁺ reuptake was also found in α -synaptrophin null mice in which astrocyte AQP4 is mislocalized^[68]. Slowed K⁺ reuptake in brain would prolong seizure duration, as found experimentally.

The precise link between K⁺ reuptake by astrocytes and AQP4 water permeability remains speculative. It had been postulated that interaction between AQP4 and the inwardly rectifying K⁺ channel, Kir4.1, was responsible^[69]; however, patch-clamp analysis indicated that AQP4 deficiency did not affect Kir4.1 K⁺ channel function in retinal Müller cells or brain astrocytes^[70, 71]. As diagrammed in Figure 3B, we propose a simple mechanism in which AQP4-dependent water permeability enhances K⁺ transport by pseudo-solvent drag. Excess K⁺ released into the ECS by neurons during neuroexcitation is taken up largely by the AQP4-containing astrocytes. Reuptake of K⁺ following neuroexcitation results in osmotic water influx into AQP4-expressing astrocytes and consequent ECS shrinkage, which maintains the electrochemical driving force for K⁺ reuptake. Reduced astrocyte water permeability in AQP4 deficiency would reduce ECS contraction and hence slow K⁺ reuptake. This hypothesis is attractive because it relates the neuroexcitation phenotypes directly to AQP4 water transport.

AQP4 and neuroinflammation

We recently discovered a novel role of AQP4 in neuroinflammation following studies of experimental autoimmune encephalomyelitis (EAE), an extensively used model of neuroinflammatory demyelinating diseases such as multiple sclerosis. EAE is mediated primarily by myelin-specific Th1 or Th17 cells. The motivation for this work is the central involvement of astrocytes in neuroinflammation and evidence, as discussed in the next section, that AQP4 is the target antigen in the neuroinflammatory autoimmune disease neuromyelitis optica (NMO). In an initial phenotype study, we found that compared with wild type mice, AQP4 knockout mice showed

remarkably attenuated EAE following active immunization with myelin oligodendrocyte glycoprotein (MOG) peptide, with reduced motor dysfunction, brain inflammation and myelin loss^[72]. In a follow-on study, potential mechanisms for the protective effect of AQP4 deficiency were investigated, including AQP4-dependent leukocyte and microglia cell function, immune cell entry in the CNS, intrinsic neuroinflammation, and humoral immune response^[40]. As we found with active-immunization EAE, neuroinflammation was greatly reduced in AQP4 knockout mice in adoptive-transfer EAE, which involved injection of MOG-sensitized T-lymphocytes in naïve mice. A series of negative studies ruled out AQP4-dependent differences in immune cell function and CNS entry, microglial function and humoral immune responses: (a) AQP4 was absent in immune cells, including activated T-lymphocytes; (b) CNS migration of fluorescently labeled, MOG-sensitized T-lymphocytes was comparable in wildtype and AQP4 knockout mice; (c) microglia did not express AQP4; and (d) serum anti-AQP4 antibodies were absent in EAE. Remarkably, however, intracerebral injection of lipopolysaccharide produced much greater neuroinflammation in wildtype than in AQP4 knockout mice, indicating an intrinsic pro-neuroinflammatory role of AQP4. In analyzing possible cellular mechanisms, we found that the secretion of the major cytokines TNF- α and IL-6 was reduced in astrocyte cultures from AQP4 knockout mice. Further, adenovirus-mediated expression of AQP4, or of a different aquaporin, AQP1, increased cytokine secretion in astrocyte and non-astrocyte cell cultures, supporting the involvement of aquaporin water permeability in cytokine secretion.

These findings implicated a novel intrinsic pro-inflammatory role of AQP4, which we propose at the cellular level involves AQP4-dependent differences in astrocyte water permeability and consequent cell swelling and cytokine release (Figure 3C). AQP4-dependent neuroinflammation is likely further exaggerated by a positive-feedback cycle of secretion of pro-inflammatory cytokines and local cytotoxic brain swelling, which, as discussed above, is also AQP4-dependent.

AQP4 and neuromyelitis optica

NMO is a neuroinflammatory demyelinating disease that, unlike multiple sclerosis, primarily affects optic nerve and spinal cord, leading to blindness, paralysis and death^[73]. A defining feature of NMO is the presence of serum autoantibodies directed against extracellular epitopes on AQP4^[74]. Recent data suggest that most, if not all NMO patients are seropositive for AQP4 autoantibodies (NMO-IgG), which recognize 3-dimensional epitopes on the extracellular surface of AQP4^[75]. There is emerging evidence for a pathogenic role of NMO-IgG in NMO, as administration of human NMO-IgG to naïve mice or to rats with pre-existing neuroinflammation produces NMO-like pathology^[76-79]. The most compelling evidence to date implicating a pathogenic role of NMO-IgG is the appearance of characteristic NMO lesions, with neuroinflammation, loss of glial fibrillary acidic protein (GFAP) and AQP4 immunoreactivity, demyelination and perivascular

complement deposition, following direct intracerebral injection of NMO-IgG in mice^[79]. As diagrammed in Figure 4, it is thought that NMO-IgG binding to AQP4 in astrocytes initiates an inflammatory cascade involving recruitment of leukocytes (granulocytes, macrophages, NK cells, lymphocytes), cytokine release, and complement and NK cell-mediated astrocyte damage^[80]. The consequent neuroinflammation and myelin loss produce neurological deficits. A glutamate excitotoxicity mechanism for NMO pathogenesis has also been proposed based on NMO-IgG-induced internalization of glutamate transporters in transfected cells^[81]; however, the relevance of glutamate transporter internalization to astrocytes in the CNS remains unproven. The initiating events in NMO-IgG production and CNS penetration remain unknown, as do the reasons why NMO-IgG produces much greater pathology in spinal and optic nerve compared to brain, with no significant pathology in peripheral AQP4-expressing organs.

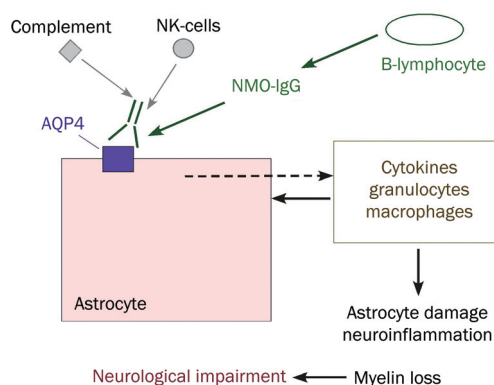


Figure 4. Proposed mechanism of NMO disease pathogenesis. NMO-IgG binding to AQP4 on astrocytes causes complement- and NK-mediated cell injury, resulting in leukocyte recruitment and cytokine release.

There has been recent interest in determining whether NMO-IgG targets the M1 *vs* M23 isoforms of AQP4, and OAP *vs* non-OAP associated AQP4. One report that analyzed NMO serum specimens concluded that OAPs were the exclusive target of NMO-IgG^[24]. However, this conclusion cannot be correct because the clinical assay for serum anti-AQP4 autoantibody uses M1 AQP4^[82], and we^[10] and others^[76, 80] reported strong binding of some NMO autoantibodies to cells expressing only M1 AQP4. The paper of Nicchia^[24] was also flawed in that they reported OAPs sized smaller than the diffraction limit of light, which was not possible. We recently examined the issue of NMO binding specificity utilizing a two-color fluorescence ratio imaging assay of AQP4-expressing cells stained with NMO patient serum or a recombinant monoclonal NMO autoantibody (NMO-rAb), together with a C-terminus anti-AQP4 antibody^[83]. NMO-rAb titrations showed single site binding with dissociation constants down to 44 nmol/L. Different NMO-rAbs and NMO patient sera showed wide variation in NMO-IgG binding to M1 *vs* M23 AQP4. We found that differences in binding affinity rather than stoichiometry

accounted for M23>M1 binding specificity. Binding and OAP measurements in cells expressing M23 AQP4 mutants with OAP-disrupting mutations indicated that the differential binding of NMO-IgG to M1 vs M23 was due to OAP assembly rather than to differences in the M1 vs M23 N-termini. Measurements using purified Fab fragments derived from NMO-rAbs suggested that a structural change in the AQP4 epitope upon array assembly, and not bivalent NMO-IgG binding, accounts for the greater binding affinity to OAPs.

Current NMO therapies are directed toward reducing the inflammatory response (immunosuppression) and the NMO-IgG load (B-cell depletion and plasmapheresis). A complement targeted monoclonal antibody therapy is in clinical trials. Our laboratory has focused on the development of a novel therapeutic approach involving blocking of the binding of pathogenic NMO antibodies to AQP4, which is believed to be the initiating event in NMO pathogenesis. We are currently developing both a monoclonal antibody approach involving tight-binding, non-pathogenic, engineered recombinant NMO antibodies ('aquaporumabs'), as well as drug-like small-molecule blockers identified by high-throughput screening.

Prospects for AQP4-based therapies

In addition to the possibility of NMO-IgG blocker therapy for NMO discussed just above, the involvement of AQP4 in brain water balance, astrocyte migration, neuroexcitation and neuroinflammation suggest the therapeutic potential of AQP4 modulators. Notwithstanding the challenges in drug delivery to the central nervous system and their multiplicity of actions, AQP4 inhibitors have potential utility in reducing cytotoxic brain swelling, seizure intensity, glial scar formation, and neuroinflammation; enhancers of AQP4 expression have potential utility in reducing vasogenic brain swelling. AQP4 modulators may thus offer new therapeutic options for stroke, tumor, infection, hydrocephalus, epilepsy, neuroinflammatory conditions and traumatic brain and spinal cord injury. However, the discovery of potent and selective small-molecule AQP4 inhibitors is a major challenge, as no confirmed small-molecule AQP4 inhibitors have been identified to date and identification of inhibitors of AQP4 by conventional screening methods has so far been unsuccessful. Further, AQP4 inhibitor therapy for brain swelling will require care because cytotoxic and vasogenic edema often coexist in varying proportions during the evolution of a CNS insult. For example, AQP4 inhibition may be beneficial early in the course of spinal cord trauma, but deleterious later on. Because of the involvement of AQP4 in neurosensory phenomena, transient visual, auditory and olfactory impairment are possible with AQP4 inhibition. In epilepsy therapy, while AQP4 inhibition reduces seizure duration and hence severity, it appears to increase seizure susceptibility. Of the various theoretical applications of AQP4-based therapies, the indications with greatest potential for success are likely NMO-IgG/AQP4 blocker therapy for NMO, and AQP4 inhibition therapy for acute cytotoxic cerebral edema in ischemic stroke.

References

- 1 Hasegawa H, Ma T, Skach W, Matthay MA, Verkman AS. Molecular cloning of a mercurial-insensitive water channel expressed in selected water-transporting tissues. *J Biol Chem* 1994; 269: 5497–500.
- 2 Jung JS, Bhat RV, Preston GM, Guggino WB, Baraban JM, Agre P. Molecular characterization of an aquaporin cDNA from brain: candidate osmoreceptor and regulator of water balance. *Proc Natl Acad Sci U S A* 1994; 91: 13052–6.
- 3 Frigeri A, Gropper MA, Turck CW, Verkman AS. Immunolocalization of the mercurial-insensitive water channel and glycerol intrinsic protein in epithelial cell plasma membranes. *Proc Natl Acad Sci U S A* 1995; 92: 4328–31.
- 4 Frigeri A, Gropper MA, Umenishi F, Kawashima M, Brown D, Verkman AS. Localization of MIWC and GLIP water channel homologs in neuromuscular, epithelial and glandular tissues. *J Cell Sci* 1995; 108: 2993–3002.
- 5 Nielsen S, Nagelhus EA, Amiry-Moghaddam M, Bourque C, Agre P, Ottersen OP. Specialized membrane domains for water transport in glial cells: high-resolution immunogold cytochemistry of aquaporin-4 in rat brain. *J Neurosci* 1997; 17: 171–80.
- 6 Lu M, Lee MD, Smith BL, Jung JS, Agre P, Verdijk MA, et al. The human AQP4 gene: definition of the locus encoding two water channel polypeptides in brain. *Proc Natl Acad Sci U S A* 1996; 93: 10908–12.
- 7 Yang B, Ma T, Verkman AS. cDNA cloning, gene organization, and chromosomal localization of a human mercurial insensitive water channel. Evidence for distinct transcriptional units. *J Biol Chem* 1995; 270: 22907–13.
- 8 Moe SE, Sorbo JG, Sogaard R, Zeuthen T, Petter Ottersen O, Holen T. New isoforms of rat Aquaporin-4. *Genomics* 2008; 91: 367–77.
- 9 Rossi A, Crane JM, Verkman AS. Aquaporin-4 Mz isoform: brain expression, supramolecular assembly and neuromyelitis optica antibody binding. *Glia* 2011. doi: 10.1002/glia.21177.
- 10 Crane JM, Bennett JL, Verkman AS. Live cell analysis of aquaporin-4 m1/m23 interactions and regulated orthogonal array assembly in glial cells. *J Biol Chem* 2009; 284: 35850–60.
- 11 Neely JD, Christensen BM, Nielsen S, Agre P. Heterotetrameric composition of aquaporin-4 water channels. *Biochemistry (Mosc)* 1999; 38: 11156–63.
- 12 Yang B, van Hoek AN, Verkman AS. Very high single channel water permeability of aquaporin-4 in baculovirus-infected insect cells and liposomes reconstituted with purified aquaporin-4. *Biochemistry (Mosc)* 1997; 36: 7625–32.
- 13 Yang B, Verkman AS. Water and glycerol permeabilities of aquaporins 1–5 and MIP determined quantitatively by expression of epitope-tagged constructs in *Xenopus* oocytes. *J Biol Chem* 1997; 272: 16140–6.
- 14 Ho JD, Yeh R, Sandstrom A, Chorny I, Harries WE, Robbins RA, et al. Crystal structure of human aquaporin 4 at 1.8 Å and its mechanism of conductance. *Proc Natl Acad Sci U S A* 2009; 106: 7437–42.
- 15 Hub JS, Grubmuller H, de Groot BL. Dynamics and energetics of permeation through aquaporins. What do we learn from molecular dynamics simulations? *Handb Exp Pharmacol* 2009; 190: 57–76.
- 16 Walz T, Fujiyoshi Y, Engel A. The AQP structure and functional implications. *Handb Exp Pharmacol* 2009; 190: 31–56.
- 17 Landis DM, Reese TS. Arrays of particles in freeze-fractured astrocytic membranes. *J Cell Biol* 1974; 60: 316–20.
- 18 Rash JE, Staehelin LA, Ellisman MH. Rectangular arrays of particles on freeze-cleaved plasma membranes are not gap junctions. *Exp Cell Res* 1974; 86: 187–90.
- 19 Yang B, Brown D, Verkman AS. The mercurial insensitive water channel (AQP-4) forms orthogonal arrays in stably transfected Chinese

- hamster ovary cells. *J Biol Chem* 1996; 271: 4577–80.
- 20 Verbavatz JM, Ma T, Gobin R, Verkman AS. Absence of orthogonal arrays in kidney, brain and muscle from transgenic knockout mice lacking water channel aquaporin-4. *J Cell Sci* 1997; 110: 2855–60.
- 21 Rash JE, Yasumura T, Hudson CS, Agre P, Nielsen S. Direct immunogold labeling of aquaporin-4 in square arrays of astrocyte and ependymocyte plasma membranes in rat brain and spinal cord. *Proc Natl Acad Sci U S A* 1998; 95: 11981–6.
- 22 Hiroaki Y, Tani K, Kamegawa A, Gyobu N, Nishikawa K, Suzuki H, *et al*. Implications of the aquaporin-4 structure on array formation and cell adhesion. *J Mol Biol* 2006; 355: 628–39.
- 23 Silberstein C, Bouley R, Huang Y, Fang P, Pastor-Soler N, Brown D, *et al*. Membrane organization and function of M1 and M23 isoforms of aquaporin-4 in epithelial cells. *Am J Physiol Renal Physiol* 2004; 287: F501–11.
- 24 Nicchia GP, Mastrototaro M, Rossi A, Pisani F, Tortorella C, Ruggieri M, *et al*. Aquaporin-4 orthogonal arrays of particles are the target for neuromyelitis optica autoantibodies. *Glia* 2009; 57: 1363–73.
- 25 Furman CS, Gorelick-Feldman DA, Davidson KG, Yasumura T, Neely JD, Agre P, *et al*. Aquaporin-4 square array assembly: opposing actions of M1 and M23 isoforms. *Proc Natl Acad Sci U S A* 2003; 100: 13609–14.
- 26 Crane JM, Verkman AS. Long-range nonanomalous diffusion of quantum dot-labeled aquaporin-1 water channels in the cell plasma membrane. *Biophys J* 2008; 94: 702–13.
- 27 Crane JM, Van Hoek AN, Skach WR, Verkman AS. Aquaporin-4 dynamics in orthogonal arrays in live cells visualized by quantum dot single particle tracking. *Mol Biol Cell* 2008; 19: 3369–78.
- 28 Crane JM, Verkman AS. Determinants of aquaporin-4 assembly in orthogonal arrays revealed by live-cell single-molecule fluorescence imaging. *J Cell Sci* 2009; 122: 813–21.
- 29 Crane JM, Verkman AS. Reversible, temperature-dependent supra-molecular assembly of aquaporin-4 orthogonal arrays in live cell membranes. *Biophys J* 2009; 97: 3010–8.
- 30 Tajima M, Crane JM, Verkman AS. Aquaporin-4 (AQP4) associations and array dynamics probed by photobleaching and single-molecule analysis of green fluorescent protein-AQP4 chimeras. *J Biol Chem* 2010; 285: 8163–70.
- 31 Ma T, Yang B, Gillespie A, Carlson EJ, Epstein CJ, Verkman AS. Generation and phenotype of a transgenic knockout mouse lacking the mercurial-insensitive water channel aquaporin-4. *J Clin Invest* 1997; 100: 957–62.
- 32 Manley GT, Fujimura M, Ma T, Noshita N, Filiz F, Bollen AW, *et al*. Aquaporin-4 deletion in mice reduces brain edema after acute water intoxication and ischemic stroke. *Nat Med* 2000; 6: 159–63.
- 33 Papadopoulos MC, Manley GT, Krishna S, Verkman AS. Aquaporin-4 facilitates reabsorption of excess fluid in vasogenic brain edema. *FASEB J* 2004; 18: 1291–3.
- 34 Saadoun S, Tait MJ, Reza A, Davies DC, Bell BA, Verkman AS, *et al*. AQP4 gene deletion in mice does not alter blood-brain barrier integrity or brain morphology. *Neuroscience* 2009; 161: 764–72.
- 35 Zhou J, Kong H, Hua X, Xiao M, Ding J, Hu G. Altered blood-brain barrier integrity in adult aquaporin-4 knockout mice. *Neuroreport* 2008; 19: 1–5.
- 36 Li Z, Gao L, Liu Q, Cao C, Sun XL, Ding JH, *et al*. Aquaporin-4 knockout regulated cocaine-induced behavior and neurochemical changes in mice. *Neurosci Lett* 2006; 403: 294–8.
- 37 Liu L, Lu Y, Kong H, Li L, Marshall C, Xiao M, *et al*. Aquaporin-4 deficiency exacerbates brain oxidative damage and memory deficits induced by long-term ovarian hormone deprivation and *D*-galactose injection. *Int J Neuropsychopharmacol* 2011. DOI: 10.1017/S1461145711000022.
- 38 Wu N, Lu XQ, Yan HT, Su RB, Wang JF, Liu Y, *et al*. Aquaporin 4 deficiency modulates morphine pharmacological actions. *Neurosci Lett* 2008; 448: 221–5.
- 39 Nicchia GP, Frigeri A, Liuzzi GM, Svelto M. Inhibition of aquaporin-4 expression in astrocytes by RNAi determines alteration in cell morphology, growth, and water transport and induces changes in ischemia-related genes. *FASEB J* 2003; 17: 1508–10.
- 40 Li L, Zhang H, Varrin-Doyer M, Zamvil SS, Verkman AS. Proinflammatory role of aquaporin-4 in autoimmune neuroinflammation. *FASEB J* 2011; 25: 1556–66.
- 41 Saadoun S, Papadopoulos MC, Watanabe H, Yan D, Manley GT, Verkman AS. Involvement of aquaporin-4 in astroglial cell migration and glial scar formation. *J Cell Sci* 2005; 118: 5691–8.
- 42 Badaut J, Ashwal S, Adami A, Tone B, Recker R, Spagnoli D, *et al*. Brain water mobility decreases after astrocytic aquaporin-4 inhibition using RNA interference. *J Cereb Blood Flow Metab* 2011; 31: 819–31.
- 43 Papadopoulos MC, Verkman AS. Aquaporin-4 gene disruption in mice reduces brain swelling and mortality in pneumococcal meningitis. *J Biol Chem* 2005; 280: 13906–12.
- 44 Yang B, Zador Z, Verkman AS. Glial cell aquaporin-4 overexpression in transgenic mice accelerates cytotoxic brain swelling. *J Biol Chem* 2008; 283: 15280–6.
- 45 Benfenati V, Caprini M, Dovizio M, Mylonakou MN, Ferroni S, Ottersen OP, *et al*. An aquaporin-4/transient receptor potential vanilloid 4 (AQP4/TRPV4) complex is essential for cell-volume control in astrocytes. *Proc Natl Acad Sci U S A* 2011; 108: 2563–8.
- 46 Bloch O, Papadopoulos MC, Manley GT, Verkman AS. Aquaporin-4 gene deletion in mice increases focal edema associated with staphylococcal brain abscess. *J Neurochem* 2005; 95: 254–62.
- 47 Tait MJ, Saadoun S, Bell BA, Verkman AS, Papadopoulos MC. Increased brain edema in aqp4-null mice in an experimental model of subarachnoid hemorrhage. *Neuroscience* 2010; 167: 60–7.
- 48 Bloch O, Auguste KI, Manley GT, Verkman AS. Accelerated progression of kaolin-induced hydrocephalus in aquaporin-4-deficient mice. *J Cereb Blood Flow Metab* 2006; 26: 1527–37.
- 49 Saadoun S, Bell BA, Verkman AS, Papadopoulos MC. Greatly improved neurological outcome after spinal cord compression injury in AQP4-deficient mice. *Brain* 2008; 131: 1087–98.
- 50 Kimura A, Hsu M, Seldin M, Verkman AS, Scharfman HE, Binder DK. Protective role of aquaporin-4 water channels after contusion spinal cord injury. *Ann Neurol* 2010; 67: 794–801.
- 51 Saadoun S, Papadopoulos MC, Hara-Chikuma M, Verkman AS. Impairment of angiogenesis and cell migration by targeted aquaporin-1 gene disruption. *Nature* 2005; 434: 786–92.
- 52 Silver J, Miller JH. Regeneration beyond the glial scar. *Nat Rev Neurosci* 2004; 5: 146–56.
- 53 Auguste KI, Jin S, Uchida K, Yan D, Manley GT, Papadopoulos MC, *et al*. Greatly impaired migration of implanted aquaporin-4-deficient astroglial cells in mouse brain toward a site of injury. *FASEB J* 2007; 21: 108–16.
- 54 Verkman AS, Hara-Chikuma M, Papadopoulos MC. Aquaporins — new players in cancer biology. *J Mol Med* 2008; 86: 523–9.
- 55 Hu J, Verkman AS. Increased migration and metastatic potential of tumor cells expressing aquaporin water channels. *FASEB J* 2006; 20: 1892–4.
- 56 Papadopoulos MC, Saadoun S, Verkman AS. Aquaporins and cell migration. *Pflugers Arch* 2008; 456: 693–700.
- 57 Loitto VM, Karlsson T, Magnusson KE. Water flux in cell motility: expanding the mechanisms of membrane protrusion. *Cell Motil Cyto-*

- skeleton 2009; 66: 237–47.
- 58 Charras GT, Yarrow JC, Horton MA, Mahadevan L, Mitchison TJ. Non-equilibration of hydrostatic pressure in blebbing cells. *Nature* 2005; 435: 365–9.
- 59 Li J, Patil RV, Verkman AS. Mildly abnormal retinal function in transgenic mice without Muller cell aquaporin-4 water channels. *Invest Ophthalmol Vis Sci* 2002; 43: 573–9.
- 60 Li J, Verkman AS. Impaired hearing in mice lacking aquaporin-4 water channels. *J Biol Chem* 2001; 276: 31233–7.
- 61 Lu DC, Zhang H, Zador Z, Verkman AS. Impaired olfaction in mice lacking aquaporin-4 water channels. *FASEB J* 2008; 22: 3216–23.
- 62 Binder DK, Yao X, Zador Z, Sick TJ, Verkman AS, Manley GT. Increased seizure duration and slowed potassium kinetics in mice lacking aquaporin-4 water channels. *Glia* 2006; 53: 631–6.
- 63 Padmawar P, Yao X, Bloch O, Manley GT, Verkman AS. K⁺ waves in brain cortex visualized using a long-wavelength K⁺-sensing fluorescent indicator. *Nat Methods* 2005; 2: 825–7.
- 64 Binder DK, Papadopoulos MC, Haggie PM, Verkman AS. *In vivo* measurement of brain extracellular space diffusion by cortical surface photobleaching. *J Neurosci* 2004; 24: 8049–56.
- 65 Yao X, Hrabetova S, Nicholson C, Manley GT. Aquaporin-4-deficient mice have increased extracellular space without tortuosity change. *J Neurosci* 2008; 28: 5460–4.
- 66 Zador Z, Magzoub M, Jin S, Manley GT, Papadopoulos MC, Verkman AS. Microfiber optic fluorescence photobleaching reveals size-dependent macromolecule diffusion in extracellular space deep in brain. *FASEB J* 2008; 22: 870–9.
- 67 Zhang H, Verkman AS. Microfiber optic measurement of extracellular space volume in brain and tumor slices based on fluorescent dye partitioning. *Biophys J* 2010; 99: 1284–91.
- 68 Amiry-Moghaddam M, Williamson A, Palomba M, Eid T, de Lanerolle NC, Nagelhus EA, *et al*. Delayed K⁺ clearance associated with aquaporin-4 mislocalization: phenotypic defects in brains of alpha-syntrophin-null mice. *Proc Natl Acad Sci U S A* 2003; 100: 13615–20.
- 69 Nagelhus EA, Mathiesen TM, Ottersen OP. Aquaporin-4 in the central nervous system: cellular and subcellular distribution and coexpression with KIR4.1. *Neuroscience* 2004; 129: 905–13.
- 70 Ruiz-Ederra J, Zhang H, Verkman AS. Evidence against functional interaction between aquaporin-4 water channels and Kir4.1 potassium channels in retinal Muller cells. *J Biol Chem* 2007; 282: 21866–72.
- 71 Zhang H, Verkman AS. Aquaporin-4 independent Kir4.1 K⁺ channel function in brain glial cells. *Mol Cell Neurosci* 2008; 37: 1–10.
- 72 Li L, Zhang H, Verkman AS. Greatly attenuated experimental autoimmune encephalomyelitis in aquaporin-4 knockout mice. *BMC Neurosci* 2009; 10: 94.
- 73 Wingerchuk DM, Lennon VA, Lucchinetti CF, Pittock SJ, Weinshenker BG. The spectrum of neuromyelitis optica. *Lancet Neurol* 2007; 6: 805–15.
- 74 Lennon VA, Kryzer TJ, Pittock SJ, Verkman AS, Hinson SR. IgG marker of optic-spinal multiple sclerosis binds to the aquaporin-4 water channel. *J Exp Med* 2005; 202: 473–7.
- 75 Mader S, Lutterotti A, Di Pauli F, Kuenz B, Schanda K, Aboul-Enein F, *et al*. Patterns of antibody binding to aquaporin-4 isoforms in neuromyelitis optica. *PLoS One* 2010; 5: e10455.
- 76 Bennett JL, Lam C, Kalluri SR, Saikali P, Bautista K, Dupree C, *et al*. Intrathecal pathogenic anti-aquaporin-4 antibodies in early neuromyelitis optica. *Ann Neurol* 2009; 66: 617–29.
- 77 Bradl M, Misu T, Takahashi T, Watanabe M, Mader S, Reindl M, *et al*. Neuromyelitis optica: pathogenicity of patient immunoglobulin *in vivo*. *Ann Neurol* 2009; 66: 630–43.
- 78 Kinoshita M, Nakatsuji Y, Kimura T, Moriya M, Takata K, Okuno T, *et al*. Neuromyelitis optica: Passive transfer to rats by human immunoglobulin. *Biochem Biophys Res Commun* 2009; 386: 623–7.
- 79 Saadoun S, Waters P, Bell BA, Vincent A, Verkman AS, Papadopoulos MC. Intra-cerebral injection of neuromyelitis optica immunoglobulin G and human complement produces neuromyelitis optica lesions in mice. *Brain* 2010; 133: 349–61.
- 80 Hinson SR, Pittock SJ, Lucchinetti CF, Roemer SF, Fryer JP, Kryzer TJ, *et al*. Pathogenic potential of IgG binding to water channel extracellular domain in neuromyelitis optica. *Neurology* 2007; 69: 2221–31.
- 81 Hinson SR, Roemer SF, Lucchinetti CF, Fryer JP, Kryzer TJ, Chamberlain JL, *et al*. Aquaporin-4-binding autoantibodies in patients with neuromyelitis optica impair glutamate transport by down-regulating EAAT2. *J Exp Med* 2008; 205: 2473–81.
- 82 Wingerchuk DM, Lennon VA, Pittock SJ, Lucchinetti CF, Weinshenker BG. Revised diagnostic criteria for neuromyelitis optica. *Neurology* 2006; 66: 1485–9.
- 83 Crane JM, Lam C, Rossi A, Gupta T, Bennett JL, Verkman AS. Binding affinity and specificity of neuromyelitis optica autoantibodies to aquaporin-4 M1/M23 isoforms and orthogonal arrays. *J Biol Chem* 2011; 286: 16516–24.

Review

Expression and function of aquaporins in peripheral nervous system

Tong-hui MA^{1,*}, Hong-wen GAO¹, Xue-dong FANG¹, Hong YANG²

¹Central Research Laboratory, Jilin University Bethune Second Hospital, Changchun 130041, China; ²School of Life Sciences, Liaoning Provincial Key Laboratory of Biotechnology and Drug Discovery, Liaoning Normal University, Dalian 116029, China

The expression and role of the aquaporin (AQP) family water channels in the peripheral nervous system was less investigated. Since 2004, however, significant progress has been made in the immunolocalization, regulation and function of AQPs in the peripheral nervous system. These studies showed selective localization of three AQPs (AQP1, AQP2, and AQP4) in dorsal root ganglion neurons, enteric neurons and glial cells, periodontal Ruffini endings, trigeminal ganglion neurons and vomeronasal sensory neurons. Functional characterization in transgenic knockout mouse model revealed important role of AQP1 in pain perception. This review will summarize the progress in this field and discuss possible involvement of AQPs in peripheral neuropathies and their potential as novel drug targets.

Keywords: aquaporins; peripheral nervous system; neuronal transduction; gene knockout; gene expression; pain

Acta Pharmacologica Sinica (2011) 32: 711–715, doi: 10.1038/aps.2011.63; published online 23 May 2011

Introduction

Aquaporins (AQPs) are a family of water-transporting proteins selectively expressed in epithelial, endothelial and many other cell types where they play important physiological functions^[1, 2]. In the past two decades, studies on the expression and function of AQPs in the nervous system have been focused mainly in the central nervous system. Numerous studies reported the localization of six AQPs including AQP1, AQP3, AQP4, AQP5, AQP8, and AQP9 in the brain and spinal cord^[3]. Functional studies using transgenic knockout mouse model revealed important roles of AQP1 in cerebral spinal fluid (CSF) secretion and pain sensation and AQP4 in brain edema formation, neuronal transduction, neurogenesis, glioma spreading, neuroinflammation and pain perception^[3–12].

In contrast, the expression and function of AQPs in the peripheral nervous system are less investigated. Until 2004, Matsumoto *et al* first described AQP1 mRNA expression in the trigeminal ganglion by the hierarchical cluster analysis of DNA microarray and *in situ* hybridization^[13]. Since then, significant progress has been made in the immunolocalization, regulation and function of AQPs in the peripheral nervous system. So far studies have reported the expression of three AQPs including AQP1, AQP2, and AQP4 in peripheral neuronal or glial elements such as dorsal root ganglion neu-

rons, enteric neurons and glial cells, periodontal Ruffini endings, trigeminal ganglion neurons and vomeronasal sensory neurons. Functional characterization in transgenic knockout mouse model suggested important role of AQP1 in peripheral pain perception. This review will summarize the progress in this field and discuss possible involvement of AQPs in peripheral neuropathies and their potential as novel drug targets.

Expression and function of AQP1 in peripheral sensory nerves

In a study to identify candidate genes involved in somatosensory functions of cranial sensory ganglia reported in 2004, Matsumoto *et al* first described the expression of AQP1 mRNA in neurons of somatosensation-related ganglia by the hierarchical cluster analysis of DNA microarray^[13]. Further analysis by *in situ* hybridization showed specific expression of AQP1 mRNA in neurons with higher frequencies in trigeminal and petrosal ganglion and with low frequency in nodose ganglia. AQP1 is expressed in small to medium size neurons with a diameter under 30 μm . The expression pattern suggested the involvement of AQP1 in somatosensation in cranial structures such as the face, oral cavity and pharynx. Although there was no protein expression data provided, this is the first report of an AQP expression in peripheral nerve.

Later on, a study conducted by Oshio *et al* reported AQP1 protein localization in nerve fibers in the trigeminal and sciatic nerves as well as in small neurons and nerve fibers in dorsal root ganglia (DRG) in the peripheral nervous system^[14]. Co-

* To whom correspondence should be addressed.

E-mail math108@gmail.com

Received 2011-03-16 Accepted 2011-04-20

localization of AQP1 with substance P and capsaicin receptor TRPV1 in DRG suggested that AQP1 was expressed in C-fiber nociceptive neurons and possibly contributed to the processing of pain signals. They performed a study on the role of AQP1 in pain sensation by comparing acute pain responses to thermal, mechanical, and chemical noxious stimuli in AQP1 knockout (AQP1^{-/-}) and wildtype (AQP1^{+/+}) mice. Although no significant differences were found in the morphology or number of neurons expressing SP or TRPV1 in the DRG between AQP1^{-/-} and AQP1^{+/+} mice, they showed that AQP1^{-/-} mice had reduced responsiveness to thermal and capsaicin chemical stimuli, but not to mechanical stimuli or formalin^[14]. This study was the first evidence for a role of AQP1 in pain signal transduction.

However, a following study reported by Shields *et al* was in marked disagreement with the above functional data^[15]. By more sophisticated expression analysis, they found several lines of evidences suggesting the involvement of AQP1 in pain sensation including: (1) AQP1 protein is present in the spinal cord in laminae associated with nociceptive processing, (2) AQP1 is present on the membrane of DRG neurons neurochemically defined as nociceptors, (3) the onset of AQP1 expression in DRG corresponds temporally to the formation of functional synaptic contacts between nociceptors and their postsynaptic partners in the spinal cord, and (4) AQP1 labeling in the dorsal horn changes after sciatic nerve lesion, a manipulation that results in an altered pain state. They then performed *in vivo* electrophysiological measurements and behavioral analyses in a comprehensive battery of acute and persistent pain tests on AQP1^{-/-} and AQP1^{+/+} mice to evaluate a functional role of AQP1 in nociceptive processing. Unexpectedly, they could not detect a differential phenotype suggesting a functional contribution of AQP1 to nociceptive processing in all the acute and persistent pain tests including Hargreaves test, tail flick test, Hot plate test, von Frey test of mechanical threshold, spared nerve injury model of neuropathic pain, capsaicin test, prostaglandin E2 inflammation and hypoosmolar challenge. They concluded that AQP1 was not required for normal pain processing despite its abundant and restricted expression in nociceptive primary afferent neurons.

To resolve the discrepancy for the role of AQP1 in pain physiology, Zhang and Verkman performed a study with more extensive behavioral testing as well as immunolocalization, water permeability, and patch clamp studies on freshly isolated, dissociated DRG neurons from AQP1^{-/-} and AQP1^{+/+} mice^[16]. They reported greatly reduced behavioral responses to inflammatory thermal and cold pain in litter-matched AQP1^{-/-} mice. In mechanistic studies, they found distinct electrophysiological defects related to impaired Na_v1.8 Na⁺ channel functioning in AQP1-deficient DRG neurons. By patch clamp, immunoprecipitation, and single particle tracking studies in transfected cell models, the researchers identified a novel AQP1-Na_v1.8 interaction that may be responsible, in part, for the impaired pain sensation in AQP1 deficient mice. Based on these results, the researchers proposed potential utility of AQP1 inhibitor to reduce pain nociception as a

novel strategy to achieve analgesia at the presynaptic spinal level.

It is not known why these studies generated conflict results in the same AQP1 knockout mouse model by similar approaches. More investigations will be required to establish a role of AQP1 in peripheral pain perception. Based on some recent studies that indicated functional involvement of AQP1 and AQP4 in pain perception of the central nervous system^[10-12], we have reason to speculate a contribution of AQP1 in certain types of peripheral pain perception.

Expression of AQP1 in enteric nervous system

Gao *et al* first reported the expression pattern of AQP1 in human enteric nervous system by immunolocalization in 2006^[17]. Strong AQP1 expression was identified in the submucosal and myenteric nerve plexuses in the esophagus. AQP1 was localized to the same cell population expressing glial fibrillary acidic protein (GFAP), but clearly not to the neurons in the ganglia, indicating glial cell-specific expression. The same study also described glial selective expression of AQP1 in pancreatic ganglia. AQP4 and AQP9, which are broadly expressed in astroglial cells in brain and spinal cord, were not localized in glial cells or neurons in the peripheral nerve plexuses. The study concluded that AQPs were differentially expressed in the peripheral versus central nervous system and that channel-mediated water transport mechanisms may be involved in peripheral neuronal activity by regulating water homeostasis in the ganglia and nerve fiber bundles.

Some following studies indicated that the expression of AQP1 in the enteric nervous system exhibited species difference. Nagahama *et al* reported the localization of AQP1 protein in a particular neuronal subtype in the enteric nervous system of the rat ileum^[18]. Co-localization study indicated that AQP1-positive neurons simultaneously expressed a neuronal marker HuC/D. AQP1 is expressed in a subpopulation (~9.3%) of the HuC/D-positive neurons. AQP1-positive neurons were classified as Dogiel type I cells, which have several short processes and a single long process. Many AQP1-positive nerve fibers were also found both in the myenteric and submucosal plexuses in all regions of the ileum. The neuronal expression pattern of AQP1 in rat ileum is apparently different from the glial cell-specific expression seen in the nerve plexuses in human esophagus and pancreas^[17].

In consistent with the above study, Ishihara *et al* confirmed the localization of AQP1 in neurons and fibers of rat myenteric plexus^[19]. Based on their analysis, AQP1 is expressed in a subpopulation (about 5.5%) of the HuC/D-positive neurons, slightly different from the data by Nagahama *et al*^[18]. To study the possible involvement of AQP1 in diabetic gastrointestinal dysfunctions, the researchers examined the pathological changes in AQP1-positive neurons in streptozotocin-induced (STZ) diabetic rats. Although the total number of the HuC/D-positive neurons is similar between normal and STZ rats, AQP1-positive neurons in STZ rats were found to be significantly increased by two-fold (11.2% *vs* 5.5% in normal rats). It was also described that many AQP1-positive fibers with

swollen varicosities were seen in the secondary and tertiary myenteric plexus and in the longitudinal and circular muscle layers of STZ rats. The swollen AQP1-positive varicosities and increased AQP1-positive neurons were thought to be the consequence of the long-term diabetic conditions in STZ rats. It was postulated that these pathological changes of AQP1-positive neurons possibly contribute to diabetic gastrointestinal dysfunction in streptozotocin-induced diabetic rats. Therefore, AQP1 may become a potential new therapeutic target for gastrointestinal dysfunction in diabetes.

Recently, another study by Arciszewski *et al* supported the presence of AQP1 in enteric neurons^[20]. However, their results indicated AQP1 expression on submucosal but not myenteric neurons in the sheep duodenum. The vast majority of AQP1-bearing submucosal neurons were immunoreactive to substance P, suggesting that they are probably a subpopulation of sensory neurons. In both the rat and sheep studies, AQP1 expression was not detected in glial elements of submucosal plexus, which is different from the finding by Gao *et al* in the human esophagus^[17]. These results further demonstrate species difference of AQP1 expression in enteric nervous system. The physiological function of AQP1 as a water channel in the enteric nervous system remains unknown. Apparently, more systematic studies are required to clarify the function as well as the expression patterns of AQP1 in the enteric nervous systems in human and different species of animal models.

Expression of AQP1 in the mechanoreceptive periodontal Ruffini endings

Nandasena *et al* reported the immunolocalization of AQP1 in the periodontal Ruffini endings of the rat incisors and trigeminal ganglion^[21]. AQP1 immunostaining was detected in the axon terminals of the periodontal Ruffini endings as well as their associated terminal Schwann cells, as confirmed with a double staining with AQP1 and either a neuronal marker PGP9.5 or a glial marker S-100 protein. In addition, the study determined AQP1 expression in about 16.1% trigeminal neurons and in certain satellite cells which surrounded AQP1-positive or -negative neurons. An analysis of a cross-sectional area of these AQP1-positive neurons demonstrated that approximately 66.9% of the positive neurons were 400–1000 μm^2 (averaged at $671.4 \pm 172.4 \mu\text{m}^2$), indicating that they belong to medium-sized neurons that mediate mechanotransduction. This is the first report confirming that the axon terminals of mechanoreceptors are positive for an AQP. Further investigation is needed for clarifying co-localization of SP/AQP1 or TRPV1/AQP1 in the trigeminal ganglion to determine the proportion of AQP1-positive neurons that are similar to dorsal root ganglion nociceptors. These findings suggest that AQP1 may control water transport in the periodontal Ruffini endings. But whether AQP1 is involved in neural signal transduction in the mechanoreceptive periodontal Ruffini endings remains to be determined.

Expression and regulation of AQP2 in peripheral nervous system

The first report about AQP2 expression in peripheral nervous system was seen in a study of AQP distribution in human tissue microarrays by Mobasher *et al* in 2005^[22]. AQP2 was described to be expressed in peripheral nerve bundles. But no information about tissue origin was provided. In 2009, Radel-la's group reported two studies about regulated expression of AQP2 in rodent peripheral nerve and its possible involvement in pain transmission^[23, 24].

The first study analyzed the expression of AQP2 in the trigeminal ganglia in an mouse model of perioral acute inflammatory pain induced by formalin^[23]. The data showed altered AQP2 expression in trigeminal ganglia in acute inflammatory pain. In the control group, the AQP2 immunostaining showed general labeling in the cytoplasm of each neuronal class that appeared stronger in the medium- and large-sized neurons than in the small neurons. After formalin treatment, there was a marked increase of AQP2 expression in small-sized neurons and a decrease in medium- and large-sized neurons. A strong increase of AQP2 protein in the neuronal membrane of small-sized neurons was seen, suggesting increased expression and intracellular redistribution of AQP2 mainly in small-sized neurons. The expression pattern of AQP1 in the ganglia remained unaltered after formalin treatment. Quantitative immunoblot analysis also indicated increased expression of AQP2, but not AQP1 upon formalin treatment. These data support the hypothesis that AQP2 is involved in pain transmission in the peripheral nervous system.

In the second study, they analyzed the presence and localization of AQP2 in the spinal cord and dorsal root ganglia of normal rats and evaluated AQP2 expression in response to chronic constriction injury of the sciatic nerve, a model of neuropathic pain^[24]. The results showed that although AQP2 expression was not detectable in the dorsal root ganglia of normal rats, a remarkable increase of AQP2 expression in response to chronic constriction injury treatment was seen in small-diameter neurons in dorsal root ganglia. These data suggested that AQP2 expression was involved in neuropathic nerve injuries, although its precise role remains to be determined.

The exact mechanism by which AQP2 is enhanced in DRG neurons is not clear. AQP2 is known as a regulated water channel both at protein translocation and transcriptional level in response to arginine vasopressin (AVP) in the renal collecting ducts through V2 receptor^[25]. AVP and its V1 receptor were reported to present in DRG^[26, 27]. It is not known whether AQP2 is regulated by AVP in DRG. Further studies are warranted to elucidate the mechanism of pain-induced AQP2 expression and function in peripheral sensory ganglia.

Expression of AQP4 in peripheral nervous system

Role of AQP4 in the central nervous system has been a major focus in the aquaporin field. Many important functions of AQP4 have been determined including brain edema formation

and absorption, pathogenesis of neuromyelitis optica, hydrocephalus and pain perception^[3-6, 8-12, 28]. Little is known about the expression and function of AQP4 in the peripheral nervous system.

In a recent study, Thi *et al* identified AQP4 protein expression in the myenteric and submucosal nerve plexuses of the mouse and the rat colon by immunofluorescence^[29]. In the myenteric plexus, about 12% in the mouse and 13% in the rat myenteric neurons were AQP4 positive as revealed by double staining of the enteric ganglia with antibodies to AQP4 and the neuronal marker NF-H (neurofilament-heavy chain 100). In the submucosal plexus, nearly 80% neurons were positive for AQP4 in both the mouse and the rat colon. Double labeling for AQP4 and the glial marker GFAP (glial fibrillary acidic protein) verified that glial cells in the enteric plexuses were not immunoreactive to AQP4. In the same study, they confirmed a neuronal distribution of AQP1 in the myenteric and the submucosal plexuses similar to that reported by Nagahama *et al* in the rat small intestine^[18]. This study clearly indicated that neurons rather than glial cells contained AQP4 in the colonic nerve plexuses, providing the first evidence that AQP4 was differentially expressed in peripheral versus central nervous system. The expression of AQP4 in myenteric and submucosal neurons suggests that AQP4 may be involved in intestinal motility and the neuronal regulation of transport processes in the intestinal mucosa. The researchers did not analyze the colocalization of AQP4 with neuronal markers specific to sensory neurons. Therefore, it is not known whether AQP4 is expressed in enteric sensory neurons.

Another recent study reported by Ablimit *et al* identified AQP4 expression in the neuronal sensory cells of the vomeronasal organ^[30]. Vomeronasal organ is part of the nasal chemosensory system situated at the base of the nasal septum

in the anterior nasal cavity^[31, 32] and is anatomically and physiologically distinct from the olfactory system^[33-35]. The sensory epithelium of the vomeronasal organ is composed of a sensory cell layer and supporting cell layer. AQP4 expression was highly concentrated in the sensory cells of the sensory epithelium. By immunogold electron microscopy, AQP4 protein was localized to the plasma membrane of neuronal sensory cells. Gold labeling representing AQP4 is clearly seen along the entire plasma membrane of the cell body and axons except for the apical membrane facing the surface of the lumen. In contrast to the presence of AQP4 in the axon forming the vomeronasal nerve, nerve fiber bundles running in the lamina propria of the nonsensory mucosa were negative for AQP4, suggesting a specific role of AQP4 in the neuronal transduction of the vomeronasal organ. A previous study indicated impaired olfaction in mice lacking AQP4 water channel^[36]. Vomeronasal organ is regarded as a chemosensory organ for pheromones^[34]. It will be interesting to study the role of AQP4 in the regulation of social behavior and sexual preference in AQP4 knockout mouse model.

Perspectives

The study on the expression and function of AQPs in the peripheral nervous system is still in an early stage although significant progress has been made in this field (summarized in Table 1). The picture on the distribution of AQP family members in the peripheral nervous system is far from complete. The precise cellular localization of AQPs in different types of peripheral nerves requires further systematic studies in human as well as model animals. The functions of AQPs in the peripheral nervous system are still largely unknown. The conflict results on the role of AQP1 in pain perception will await more investigations to clarify before AQP1 can become

Table 1. Expression and function of aquaporins in peripheral nervous system.

AQP	Species	Tissue	Cell type	Function	Reference
AQP1	Human	Pancreatic and enteric ganglia and nerve fiber bundles	Glial cells	Enteric neuronal transduction?	17
	Sheep	Enteric ganglia	Neurons	Enteric neuronal transduction?	20
	Rat	Enteric ganglia and nerve fiber bundles Incisors and trigeminal ganglia	Neurons	Diabetic gastrointestinal dysfunction?	18, 19, 29
			Axon terminals of periodontal Ruffini endings, terminal Schwann cells	Mechanoreception?	21
	Mouse	Trigeminal, petrosal, and nodose ganglia	Small to medium size neurons	Somatosensation in cranial structures?	13, 29
AQP2	Rat	Dorsal root ganglia	Nociceptive neurons	Pain sensation	14-16
	Mouse	Trigeminal ganglia	Small-diameter neurons	Neuropathic nerve injury?	24
AQP4	Rat	Enteric nerve plexus	Neurons	Pain transmission?	23
			Neurons	Neuronal control of intestinal motility and mucosal transport?	29
	Mouse	Vomeronasal organ Enteric nerve plexus	Neuronal sensory cells Neurons	Social behavior and sexual preference? Neuronal control of intestinal motility and mucosal transport?	30 29

a drug target to reduce pain nociception. The physiological functions of AQP1 and AQP4 in enteric nerve plexuses remain to be determined. The role of AQP1 in mechanoreception requires further investigation. The mechanism of regulated AQP2 expression in neurons of peripheral sensory ganglia and its functional significance in pain transmission needs further elucidation. The physiological importance of AQP4 in sensory neurons of vomeronasal organ remains to be uncovered. More functional studies using transgenic AQP knockout mouse models or human subjects with loss-of-function mutations are required to establish the role of AQPs in the peripheral nervous system and evaluate their potential as novel drug targets for peripheral neuropathies.

Acknowledgements

This work was supported by National Natural Science Foundation (No 30670477), Dalian Municipal Science and Technology Fund (2008E11SF162), and National Basic Research Program of China ("973" Program, No 2009CB521908).

References

- 1 Verkman AS. Mammalian aquaporins: diverse physiological roles and potential clinical significance. *Expert Rev Mol Med* 2008; 10: e13.
- 2 Carbrey JM, Agre P. Discovery of the aquaporins and development of the field. *Handb Exp Pharmacol* 2009; 190: 3–28.
- 3 Tait MJ, Saadoun S, Bell BA, Papadopoulos MC. Water movements in the brain: role of aquaporins. *Trends Neurosci* 2008; 31: 37–43.
- 4 Verkman AS, Binder DK, Bloch O, Auguste K, Papadopoulos MC. Three distinct roles of aquaporin-4 in brain function revealed by knockout mice. *Biochim Biophys Acta* 2006; 1758: 1085–93.
- 5 Zador Z, Stiver S, Wang V, Manley GT. Role of aquaporin-4 in cerebral edema and stroke. *Handb Exp Pharmacol* 2009; 190: 159–70.
- 6 Zheng GQ, Li Y, Gu Y, Chen XM, Zhou Y, Zhao SZ, *et al*. Beyond water channel: aquaporin-4 in adult neurogenesis. *Neurochem Int* 2010; 56: 651–4.
- 7 Jarius S, Wildemann B. AQP4 antibodies in neuromyelitis optica: diagnostic and pathogenetic relevance. *Nat Rev Neurol* 2010; 6: 383–92.
- 8 Nesic O, Guest JD, Zivadinovic D, Narayana PA, Herrera JJ, Grill RJ, *et al*. Aquaporins in spinal cord injury: the janus face of aquaporin 4. *Neuroscience* 2010; 168: 1019–35.
- 9 Filippidis AS, Kalani MY, ReKate HL. Hydrocephalus and aquaporins: lessons learned from the bench. *Childs Nerv Syst* 2011; 27: 27–33.
- 10 Bao F, Chen M, Zhang Y, Zhao Z. Hypoalgesia in mice lacking aquaporin-4 water channels. *Brain Res Bull* 2010; 83: 298–303.
- 11 Chen ML, Bao F, Zhang YQ, Zhao ZQ. Effects of aquaporin 4 deficiency on morphine analgesia and chronic tolerance: a study at spinal level. *J Mol Neurosci* 2010; 42: 140–4.
- 12 Xu GY, Wang F, Jiang X, Tao J. Aquaporin 1, a potential therapeutic target for migraine with aura. *Mol Pain* 2010; 6: 68.
- 13 Matsumoto I, Nagamatsu N, Arai S, Emori Y, Abe K. Identification of candidate genes involved in somatosensory functions of cranial sensory ganglia. *Brain Res Mol Brain Res* 2004; 126: 98–102.
- 14 Oshio K, Watanabe H, Yan D, Verkman AS, Manley GT. Impaired pain sensation in mice lacking Aquaporin-1 water channels. *Biochem Biophys Res Commun* 2006; 341: 1022–8.
- 15 Shields SD, Mazario J, Skinner K, Basbaum AI. Anatomical and functional analysis of aquaporin 1, a water channel in primary afferent neurons. *Pain* 2007; 131: 8–20.
- 16 Zhang H, Verkman AS. Aquaporin-1 tunes pain perception by interaction with Na(v)1.8 Na⁺ channels in dorsal root ganglion neurons. *J Biol Chem* 2010; 285: 5896–906.
- 17 Gao H, He C, Fang X, Hou X, Feng X, Yang H, *et al*. Localization of aquaporin-1 water channel in glial cells of the human peripheral nervous system. *Glia* 2006; 53: 783–7.
- 18 Nagahama M, Ma N, Semba R, Naruse S. Aquaporin 1 immunoreactive enteric neurons in the rat ileum. *Neurosci Lett* 2006; 395: 206–10.
- 19 Ishihara E, Nagahama M, Naruse S, Semba R, Miura T, Usami M, *et al*. Neuropathological alteration of aquaporin 1 immunoreactive enteric neurons in the streptozotocin-induced diabetic rats. *Auton Neurosci* 2008; 138: 31–40.
- 20 Arciszewski MB, Stefaniak M, Zacharko-Siembida A, Całka J. Aquaporin 1 water channel is expressed on submucosal but not myenteric neurons from the ovine duodenum. *Ann Anat* 2011; 193: 81–5.
- 21 Nandasena BG, Suzuki A, Aita M, Kawano Y, Nozawa-Inoue K, Maeda T. Immunolocalization of aquaporin-1 in the mechanoreceptive Ruffini endings in the periodontal ligament. *Brain Res* 2007; 1157: 32–40.
- 22 Mobasheri A, Wray S, Marples D. Distribution of AQP2 and AQP3 water channels in human tissue microarrays. *J Mol Histol* 2005; 36: 1–14.
- 23 Borsani E, Bernardi S, Albertini R, Rezzani R, Rodella LF. Alterations of AQP2 expression in trigeminal ganglia in a murine inflammation model. *Neurosci Lett* 2009; 449: 183–8.
- 24 Buffoli B, Borsani E, Rezzani R, Rodella LF. Chronic constriction injury induces aquaporin-2 expression in the dorsal root ganglia of rats. *J Anat* 2009; 215: 498–505.
- 25 Kwon TH, Hager H, Nejsum LN, Andersen ML, Frokiaer J, Nielsen S. Physiology and pathophysiology of renal aquaporins. *Semin Nephrol* 2001; 21: 231–8.
- 26 Horn AM, Lightman SL. Vasopressin-induced turnover of phosphatidylinositol in the sensory nervous system of the rat. *Exp Brain Res* 1987; 68: 299–304.
- 27 Ma KK, Che YM. Distribution of arginine-vasopressin in the trigeminal, dorsal root ganglia and spinal cord of the rat; depletion by capsaicin. *Comp Biochem Physiol A Physiol* 1995; 110: 71–8.
- 28 Verkman AS. Aquaporins: translating bench research to human disease. *J Exp Biol* 2009; 212: 1707–15.
- 29 Thi MM, Spray DC, Hanani M. Aquaporin-4 water channels in enteric neurons. *J Neurosci Res* 2008; 86: 448–56.
- 30 Ablimit A, Aoki T, Matsuzaki T, Suzuki T, Hagiwara H, Takami S, *et al*. Immunolocalization of water channel aquaporins in the vomeronasal organ of the rat: expression of AQP4 in neuronal sensory cells. *Chem Senses* 2008; 33: 481–8.
- 31 Døving KB, Trotier D. Structure and function of the vomeronasal organ. *J Exp Biol* 1998; 201: 2913–25.
- 32 Takami S. Recent progress in the neurobiology of the vomeronasal organ. *Microsc Res Tech* 2002; 58: 228–50.
- 33 Halpern M, Jia C, Shapiro LS. Segregated pathways in the vomeronasal system. *Microsc Res Tech* 1998; 41: 519–29.
- 34 Witt M, Woźniak W. Structure and function of the vomeronasal organ. *Adv Otorhinolaryngol* 2006; 63: 70–83.
- 35 Martinez-Marcos A. On the organization of olfactory and vomeronasal cortices. *Prog Neurobiol* 2009; 87: 21–30.
- 36 Lu DC, Zhang H, Zador Z, Verkman AS. Impaired olfaction in mice lacking AQP4 water channels. *FASEB J* 2008; 22: 3216–23

Review

Maternal-fetal fluid balance and aquaporins: from molecule to physiology

Xiao-yan SHA¹, Zheng-fang XIONG¹, Hui-shu LIU^{1,*}, Xiao-dan DI¹, Tong-hui MA²

¹Department of Obstetrics, Guangzhou Women and Children's Medical Centre, Guangzhou Medical College, Guangzhou 510623, China; ²Central Research Laboratory, Jilin University Bethune Second Hospital, Changchun 130024, China

Maternal-fetal fluid balance is critical during pregnancy, and amniotic fluid is essential for fetal growth and development. The placenta plays a key role in a successful pregnancy as the interface between the mother and her fetus. Aquaporins (AQPs) form specific water channels that allow the rapid transcellular movement of water in response to osmotic/hydrostatic pressure gradients. AQPs expression in the placenta and fetal membranes may play important roles in the maternal-fetal fluid balance.

Keywords: aquaporin; placenta; fetal membranes; maternal-fetal fluid balance

Acta Pharmacologica Sinica (2011) 32: 716–720; doi: 10.1038/aps.2011. 59; published online 23 May 2011

Introduction

Water is the major component of cells and tissues. Although adults contain 55%–65% water, the fetal body consists of about 70%–90% water, with a lower percentage close to term^[1, 2]. Water across the plasma membrane of cells is a fundamental activity of life, and water homeostasis during fetal development is of crucial physiological importance. Fluid balance in the fetus is dependent on its mother. For example, when the mother is dehydrated, the fetal plasma osmolality increases in parallel with the maternal plasma osmolality when the placental function is normal^[3]. Maternal-fetal fluid exchange at the placenta and fetal membranes and through one pathway of exchange between the fetus and amniotic fluid can occur across the skin before full keratinization. Abortion, premature birth, amniotic fluid volume abnormality, malformation and fetal growth restrictions may result when the homeostasis of the maternal-fetal fluid exchange is disrupted. Thus, maternal-fetal fluid balance is critical during pregnancy.

The molecular mechanisms of maternal-fetal fluid balance are not known. According to researchers^[4–6], several mechanisms, including aquaporins, hormones, blood pressure differences, vascular endothelial growth factor (VEGF) and behavioral regulation, play important roles in maternal-fetal fluid balance. Hormonal mechanisms include the renin-angiotensin system, aldosterone and vasopressin regulation, which

are involved in the alteration of fetal renal excretion, water and sodium reabsorption, and the regulation of vascular volume. In addition, elevated levels of angiotensin II in the fetus increase blood pressure and cause diuresis, which contribute to an increase in amniotic fluid volume. Blood pressure regulation also plays a role in sodium/water homeostasis. VEGF is involved in the regulation of intramembranous blood vessel proliferation, membrane transport via passive permeation and the non-passive transcytotic vesicular movement of fluid. In utero behavioral regulations, such as fetal swallowing, are early functional developments in response to dipsogens. Several aquaporins are expressed in placenta, and aquaporins play key roles in the placental mechanism.

Aquaporins (AQPs) are small (about 30 kDa) membrane proteins that are named for their ability to increase the water permeability of the lipid bilayer of plasma membranes. There are 13 known mammalian AQPs, and certain AQPs increase the permeability to small molecules, such as glycerol (AQP3, 7, 9), urea (AQP3, 7, 8, 9) and ammonia (AQP8)^[7]. AQPs are distributed in different cells in various organs and play critical roles in water and other small uncharged molecules transport across cell membranes^[8–14]. AQPs facilitate transepithelial fluid transport and are involved in a variety of physiological and cellular functions, such as peritoneal dialysis^[15], pleural fluid transport^[16], intraocular pressure and aqueous fluid production^[17], corneal endothelium fluid transport^[18] and amniotic fluid volume^[19].

This review discusses the role of AQPs in maternal-fetal fluid balance. The location, expression and regulation of

* To whom correspondence should be addressed.

E-mail huishuliu@hotmail.com

Received 2011-02-15 Accepted 2011-04-18

AQPs in the female reproductive system, placenta and fetal membranes, abnormal amniotic fluid volume combined with direct evidence from AQP knockout mice (AQP-KO) support that AQPs play important roles in maternal-fetal fluid balance.

AQP expression in the female reproductive system

All living things reproduce. The reproductive system is essential for species survival, but it is not essential to keep an individual alive. A normal reproductive system is the basis of pregnancy and is fundamental for the maternal-fetal fluid balance.

Several subtypes of AQPs have been documented in the reproductive system of both male and female humans, rats and mice^[19-28]. In the female reproductive system, AQPs are strongly expressed in the ovary, oviduct, uterus, placenta, amnion and chorion during pregnancy^[19-22, 25-28]. At least nine AQP isoforms (AQP1-9) are expressed in these organs (Figure 1).

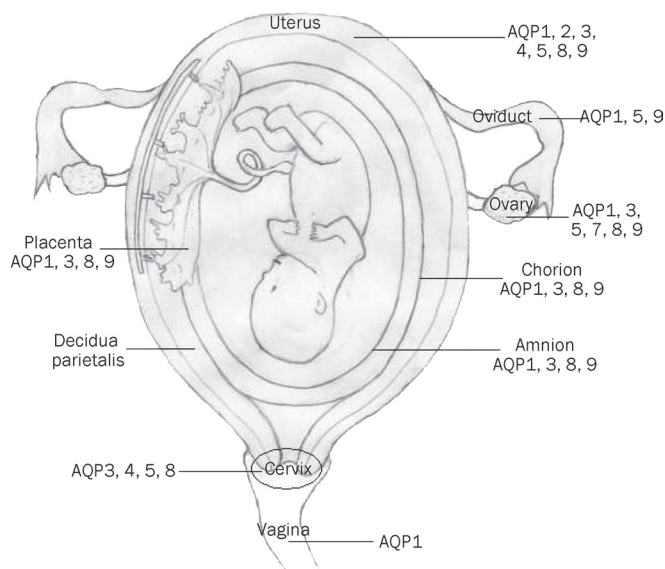


Figure 1. AQPs expression in pregnant female mammalian reproductive system.

The location and expression of AQPs in the female reproductive system suggest that AQPs play important roles in the production of ovum, the secretion of hormones, the regulation of the success of fertilization and early embryonic development^[29-31]. Moreover, these functions of AQPs indicate an involvement in maternal-fetal fluid homeostasis.

Placenta (pregnant temporary organ)

The placenta is a remarkable organ between the mother and her fetus and plays a key role in ensuring a successful pregnancy. During its relatively short life span, the placenta undergoes rapid growth, differentiation and maturation. Nearly all materials that are exchanged between mother and fetus occur at the placenta, and all transport across the

placenta must occur across the syncytial covering of the villous tree, the syncytiotrophoblast, the villous matrix and the fetal endothelium, each of which may impose its own restrictions and selectivity.

Placental transfer

The tissue that separates maternal and fetal blood in the placenta is called the placental barrier. The mature human placenta (hemochorial type) is a discoid organ with an elaborately branched fetal villous tree that is bathed directly by maternal blood. Primates, rodents and lagomorphs have placentas of the hemochorial type.

Paracellular and transcellular are the two pathways of transference across the placenta. The paracellular pathway across the placenta is based on the observation that the placenta is permeable to inert hydrophilic solutes that do not enter cells (eg, inulin), and its existence in the hemochorial placenta is generally accepted^[32]. However, the placental barrier includes a layer of continuous trophoblast syncytium. Therefore, the transcellular route is very important for placental transfer. The existence of transtrophoblastic channels has been demonstrated^[33, 34].

In the transcellular route, molecules pass through the plasma membranes of the cells that constitute the barrier. A transcellular pathway is available for substances such as lipid-soluble molecules, very small hydrophilic molecules and membrane carriers and channels.

Water is transferred across the hemochorial placenta through both the paracellular and transcellular routes, and its transfer may be facilitated by integral membrane water channel proteins (ie, AQPs).

Amniotic fluid (AF) circulation

Because amniotic fluid volume regulation is a key part of the maternal-fetal fluid balance, it has been the focus of research. The amniotic fluid serves as a significant extracorporeal water store for fetal development, including normal anatomic and fetal lung development, and as protection from fetal trauma. A normal amniotic fluid volume is critical for normal fetal growth and symmetrical development. Insufficient (oligohydramnios) or excessive (polyhydramnios) amniotic fluid volume is associated with impaired fetal outcome, including fetal structural or functional abnormalities.

Amniotic fluid volume is dependent on gestational age, and a high regulatory ability maintains the amniotic fluid volume within a fixed range^[35]. Amniotic fluid pathways include the production of fetal urine, fetal swallowing, fetal lung secretion and intramembranous and transmembranous pathways^[36, 37].

A variety of factors, such as postmaturity syndrome, maternal disease, maternal medications, altitude, fetal malformations and abnormal fetal weight, may affect amniotic fluid volume^[36]. Although the regulation of amniotic fluid circulation is poorly understood, the flow of water across biological membranes and the function of membrane water channels is involved.

AQP and maternal-fetal fluid balance

AQP expression in placenta and fetal membranes

Placentation varies in rodents, sheep and humans. Consistent with previous research, our studies^[38–41] have demonstrated that AQP1, 3, 8, and 9 are the major AQPs in the placenta and fetal membranes^[19]. This localization indicates a possible functional role in fluid homeostasis. The location of AQPs in placenta and fetal membranes are summarized in Table 1.

Table 1. AQPs location in placenta and fetal membranes of human, mouse and ovine.

AQP	Species	Location	References
AQP1	Human	vascular endothelial cell, syncytiotrophoblasts, epithelial cells of the amnion, cytotrophoblasts of the chorion	[38] [44]
	Mouse	amnion, vessel walls of placental labyrinth	[19]
	Ovine	vascular endothelial cells, capillary endothelium of the cotyledons	[14]
AQP3	Human	placenta syncytiotrophoblasts, cytotrophoblasts, chorion cytotrophoblasts, amnion HST cells	[39] [55] [56]
	Mouse	amnion, labyrinth trophoblast cells	[14]
	Ovine	cytotrophoblasts of chorion and placenta, fibroblasts of amnion and allantois	[19]
AQP8	Human	amnion and chorion epithelial cells, trophoblasts	[28] [40]
AQP9	Human	amnion epithelial cells, cytotrophoblasts of chorion, trophoblasts	[41] [56]
	Ovine	epithelial cells amnion and allantois	[57]

AQP expression regulation in placenta and fetal membranes

Ontogeny expression of AQPs in placenta and fetal membranes

Several AQP subtypes are expressed in placenta and fetal membranes, and an alteration in the expression of AQPs has been detected during pregnancy. Our previous study^[14] showed that the ontogeny of mRNA expression for AQP1, 3 and 8 in the ovine placenta at different gestational ages (27, 45, 66, 100, and 140 d, where term is ~150 d). AQP1 was the only aquaporin present in the vasculature and was significantly higher at 27 d of gestation compared to the other time points. This result suggested that AQP1 might be related to placental angiogenesis. AQP3 was increased significantly across the gestational period, and the increase in expression coincided with a substantial increase in urea permeability in the ovine placenta.

Beall *et al*^[19] demonstrated that advancing gestation was

associated with an increase in amniotic fluid volume from gestational days e10 to e16 with a marked decrease in amniotic fluid volume from e16 to e19. Fetal membrane AQP1, placental AQP1 and AQP9 expression were negatively correlated with amniotic fluid volume, and placental AQP3 expression was positively correlated with amniotic fluid volume.

The above results indicate that AQPs play roles in placental development and placental functions. Moreover, these results imply that the ontogeny of AQP expression is related to maternal-fetal fluid balance.

AQP expression in placenta with abnormal amniotic fluid volume

Amniotic fluid is essential for the developing fetus to provide the appropriate aquatic environment for symmetrical and normal development. Abnormal amniotic fluid volume induces premature delivery, fetal growth restriction, fetal distress, meconium aspiration syndrome, malformations and fetal death^[42, 43]. Compared to normal amniotic fluid volume, Mann *et al*^[44] detected a significant increase in AQP1 expression, particularly in the amnion (33-fold) of polyhydramnios. Zhu *et al*^[45] also indicated that there was a significant decrease of AQP1 and AQP3 expression in the amnion and chorion of the oligohydramnios group, but AQP3 expression in placenta was significantly increased compared to the normal amniotic fluid volume group.

Our preliminary studies^[46–48] have shown that the expression of AQP1 mRNA is significantly lower in oligohydramnios placenta and fetal membranes than in normal pregnancy at term. The expression of AQP8 mRNA is significantly lower in oligohydramnios placenta than in normal pregnancy placenta at term. The expression of AQP9 mRNA in fetal membranes is significantly higher in polyhydramnios groups than in controls. AQP1, 3, 8, and 9 may play important roles in the maintenance of amniotic fluid volume and the balance of different components in oligohydramnios and polyhydramnios patients.

The above results indicate that the change in AQP expression in human placenta is related to amniotic fluid volume regulation. Furthermore, more evidence at the molecular level demonstrates that AQPs have an important effect on amniotic fluid volume and maternal-fetal fluid balance.

Direct evidence from AQP gene knockout mice

The AQP gene knockout mice (AQP-KO) have been studied for years and have provided direct evidence of their physiological functions. Several analysis of AQP-KO mice have revealed that AQP-knockout mice induce unexpected physiological changes, including an impairment of angiogenesis and cell migration^[49], saliva secretion disability^[50], cerebrospinal fluid (CSF) dynamics^[51], peritoneal dialysis^[52], urinary concentrating ability disturbances^[53, 54] and polyhydramnios^[20].

AQP1 plays an important role in angiogenesis and endothelial cell migration. In AQP1-knockout mice, aortic endothelia migration and wound healing is greatly impaired, but abnormal vessel formation is observed *in vitro*. The mechanism proposed is that water influx at the tip of a lamellipodium results

in membrane protrusion in the direction of cell migration^[49]. AQPs play roles in saliva secretion by transepithelial fluid transport. Osmotic equilibration is impaired in AQP5-knockout mice, which results in a reduced volume of relatively hypertonic fluid secretion^[50]. AQP1 is strongly expressed at the ventricular facing surface of the choroids plexus epithelium (CPE). CSF production and intracranial pressure (ICP) are decreased in AQP1-knockout mice. Water transport by AQP1 is a substantial percentage of choroidal CSF production, and a deficiency of AQP1-mediated transcellular routes may contribute to the decrease in CSF following a reduction in ICP^[51]. AQP1-knockout mice show a decreased initial and cumulative ultrafiltration (UF) without sodium sieving during peritoneal dialysis (PD). This result supports the essential three-pore theory and a similar mechanism in the descending vasa recta^[52]. AQP1 is also strongly expressed in the proximal tubule of the kidney, the descending limb of Henle epithelia and in the vasa recta endothelia. Urinary concentrating ability is severely impaired in AQP1-knockout mice. The primary renal defect in AQP1 knockout mice is the inability to generate a hypertonic medullary interstitium by countercurrent multiplication^[53, 54].

Mann *et al*^[20] have shown that AQP1 gene knockout mice have a greater amniotic fluid volume and lower amniotic fluid osmolality than wild-type and heterozygote counterparts. The result represents the movement of water through the AQP1 channel because of the impaired renal fluid absorption and concentrating ability in AQP1-knockout mice. Moreover, deficiency in the regulation of water movement across the fetal membranes and within the placental trophoblast may be another mechanism for this result. AQP1 in fetal membranes may contribute to amniotic fluid volume regulation, and it is speculated that idiopathic polyhydramnios may be associated with a deficiency in AQP1 in human fetal membranes.

Our research in AQP-knockout pregnant mice is consistent with the above results. For example, our study showed an increase in embryo numbers, heavier placental and fetal/neonatal weight and an increase in the amount of amniotic fluid in AQP8-knockout pregnant mice^[58]. The results of the pregnant phenotypes of AQP-knockout mice provide direct evidence that AQPs play important roles in pregnancy, fetal growth and maternal-fetal fluid balance. Therefore, screening for aquaporin mutations in genetic diseases associated with abnormalities in fluid balance may be required.

In summary, successful pregnancy requires high-quality ovulation, successful fertilization and normal embryonic and fetal development, in which water homeostasis plays a key role throughout pregnancy. The location, expression and regulation of AQPs in the female reproductive system, placenta and fetal membranes, coupled with direct evidence from AQP-knockout mice support the involvement of AQPs in this physiological process and maternal-fetal fluid balance.

Acknowledgements

This study was supported by the National Natural Science Foundation of China (30471828 and 30973206) and the Scien-

tific Research Foundation for the Returned Overseas Chinese Scholars, State Education Ministry [2005]383.

References

- Greizerstein HB. Placental and fetal composition during the last trimester of gestation in the rat. *Biol Reprod* 1982; 26: 847–53.
- Engle WA, Lemons JA. Composition of the fetal and maternal guinea pig throughout gestation. *Pediatr Res* 1986; 20: 1156–60.
- Wintour EM. Water and electrolyte metabolism in the fetal-placental unit. In: Cowett RM, editor. *Principles of perinatal and neonatal metabolism*. Second edition. New York: Springer; 1998. p 511–34.
- Modena AB, Fieni S. Amniotic fluid dynamics. *Acta Biomed* 2004; 75: 11–3.
- Moritz K, Koukoulas I, Albiston A, Wintour EM. Angiotensin II infusion to the midgestation ovine fetus: effects on the fetal kidney. *Am J Physiol Regul Integr Comp Physiol* 2000; 279: R1290–7.
- Daneshmand SS, Cheung CY, Brace RA. Regulation of amniotic fluid volume by intramembranous absorption in sheep: role of passive permeability and vascular endothelial growth factor. *Am J Obstet Gynecol* 2003; 188: 786–93.
- Saparov SM, Liu K, Agre P, Pohi P. Fast and selective ammonia transport by aquaporin-8. *J Biol Chem* 2007; 282: 5296–301.
- Calamita G, Mazzone A, Bizzoca A, Svelto M. Possible involvement of aquaporin-7 and -8 in rat testis development and spermatogenesis. *Biochem Biophys Res Commun* 2001; 288: 619–25.
- Calamita G, Mazzone A, Cho YS, Valenti G, Svelto M. Expression and localization of the aquaporin-8 water channel in rat testis. *Biol Reprod* 2001; 64: 1660–6.
- Elkjaer ML, Nejsum LN, Gresz V, Kwon TH, Jensen UB, Frokiaer J, *et al*. Immunolocalization of aquaporin-8 in rat kidney, gastrointestinal tract, testis, and airways. *Am J Physiol Renal Physiol* 2001; 281: F1047–57.
- Hoque AT, Yamano S, Liu X, Swaim WD, Goldsmith CM, Delporte C, *et al*. Expression of the aquaporin 8 water channel in a rat salivary epithelial cell. *J Cell Physiol* 2002; 191: 336–41.
- Hurley PT, Ferguson CJ, Kwon TH, Andersen ML, Norman AG, Steward MC, *et al*. Expression and immunolocalization of aquaporin water channels in rat exocrine pancreas. *Am J Physiol Gastrointest Liver Physiol* 2001; 280: G701–9.
- Tani T, Koyama Y, Nihei K, Hatakeyama S, Ohshiro K, Yoshida Y, *et al*. Immunolocalization of aquaporin-8 in rat digestive organs and testis. *Arch Histol Cytol* 2001; 64: 159–68.
- Liu H, Koukoulas I, Ross MC, Wang S, Wintour EM. Quantitative comparison of placental expression of three aquaporin genes. *Placenta* 2004; 25: 475–8.
- Ni J, Verbavatz JM, Rippe A, Boisdé I, Moulin P, Rippe B, *et al*. Aquaporin-1 plays an essential role in water permeability and ultrafiltration during peritoneal dialysis. *Kidney Int* 2006; 69: 1518–25.
- Song Y, Yang B, Matthay MA, Ma T, Verkman AS. Role of aquaporin water channels in pleural fluid dynamics. *Am J Physiol Cell Physiol* 2000; 279: C1744–50.
- Zhang D, Vetrivel L, Verkman AS. Aquaporin deletion in mice reduces intraocular pressure and aqueous fluid production. *J Gen Physiol* 2002; 119: 561–9.
- Kuang K, Yiming M, Wen Q, Li Y, Ma L, Iserovich P, *et al*. Fluid transport across cultured layers of corneal endothelium from aquaporin-1 null mice. *Exp Eye Res* 2004; 78: 791–8.
- Beall MH, Wang S, Yang B, Chaudhri N, Amidi F, Ross MG. Placental and membrane aquaporin water channels: correlation with amniotic fluid volume and composition. *Placenta* 2007; 28: 421–8.
- Mann SE, Ricke EA, Torres EA, Taylor RN. A novel model of polyhydramnios: amniotic fluid volume is increased in aquaporin 1 knock-

- out mice. *Am J Obstet Gynecol* 2005; 192: 2041–4.
- 21 Wang S, Chen J, Au KT, Ross MG. Expression of aquaporin 8 and its up-regulation by cyclic adenosine monophosphate in human WISH cells. *Am J Obstet Gynecol* 2003; 188: 997–1001
- 22 Anderson J, Brown N, Mahendroo MS, Reese J. Utilization of different aquaporin water channels in the mouse cervix during pregnancy and parturition and in models of preterm and delayed cervical ripening. *Endocrinology* 2006; 147: 130–40.
- 23 Yeung CH, Callies C, Rojek A, Nielsen S, Cooper TG. Aquaporin isoforms involved in physiological volume regulation of murine spermatozoa. *Biol Reprod* 2009; 80: 350–7.
- 24 Yeung CH, Callies C, Tüttelmann F, Kliesch S, Cooper TG. Aquaporins in the human testis and spermatozoa – identification, involvement in sperm volume regulation and clinical relevance. *Int J Androl* 2010; 33: 629–41.
- 25 McConnell NA, Yunus RS, Gross SA, Bost KL, Clemens MG, Hughes FM Jr. Water permeability of an ovarian antral follicle is predominantly transcellular and mediated by aquaporins. *Endocrinology* 2002; 143: 2905–12.
- 26 Brañes MC, Morales B, Ríos M, Villalón MJ. Regulation of the immunexpression of aquaporin 9 by ovarian hormones in the rat oviductal epithelium. *Am J Physiol Cell Physiol* 2005; 288: C1048–57.
- 27 Jablonski EM, McConnell NA, Hughes FM Jr, Huet-Hudson YM. Estrogen regulation of aquaporins in the mouse uterus: potential roles in uterine water movement. *Biol Reprod* 2003; 69: 1481–7.
- 28 Wang S, Kallichanda N, Song W, Ramirez BA, Ross MG. Expression of aquaporin-8 in human placenta and chorioamniotic membranes: evidence of molecular mechanism for intramembranous amniotic fluid resorption. *Am J Obstet Gynecol* 2001; 185: 1226–31.
- 29 Su W, Qiao Y, Yi F, Guan X, Zhang D, Zhang S, *et al*. Increased female fertility in aquaporin 8-deficient mice. *IUBMB Life* 2010; 62: 852–7.
- 30 Edashige K, Sakamoto M, Kasai M. Expression of mRNAs of the aquaporin family in mouse oocytes and embryos. *Cryobiology* 2000; 40: 171–5.
- 31 Skowronski MT, Kwon TH, Nielsen S. Immunolocalization of aquaporin 1, 5, and 9 in the female pig reproductive system. *J Histochem Cytochem* 2009; 57: 61–7.
- 32 Stulc J. Placental transfer of inorganic ions and water. *Physiol Rev* 1997; 77: 805–36.
- 33 Hedley R, Bradbury MW. Transport of polar non-electrolytes across the intact and perfused guinea-pig placenta. *Placenta* 1980; 1: 277–85.
- 34 Kaufmann P, Schroder H, Leichtweiss HP. Fluid shifts across the placenta. II. Fetomaternal transfer of horseradish peroxidase in the guinea pig. *Placenta* 1982; 3: 339–48.
- 35 Brace RA, Wolf EJ. Normal amniotic fluid volume changes throughout pregnancy. *Am J Obstet Gynecol* 1989; 161: 382–8.
- 36 Sherer DM. A review of amniotic fluid dynamics and the enigma of isolated oligohydramnios. *Am J Perinatol* 2002; 19: 253–66.
- 37 Underwood MA, Gilbert WM, Sherman MP. Amniotic fluid: not just fetal urine anymore. *J Perinatol* 2005; 25: 341–8.
- 38 Liu HS, Song XF, Hao RZ. Expression of aquaporin-1 in human placenta and fetal membranes. *Nan Fang Yi Ke Da Xue Xue Bao* 2008; 28: 333–6.
- 39 Liu HS, Song XF, Yuan WC, Hao RZ. Expression and distribution of aquaporin-3 in human placenta and fetal membranes. *Chin J Biomed Eng* 2007; 13: 210–2.
- 40 Liu HS, Hao RZ, Song XF, Xiong ZF. Aquaporin8 expression in human placenta and fetal membrane. *Chin J Clin Rehab* 2009; 13: 4791–5.
- 41 Liu HS, Song XF, Yuan WC. Expression of aquaporin 9 in human placenta and fetal membranes. *Chin J Perinat Med* 2007; 10: 252–6.
- 42 Manzanares S, Carrillo MP, González-Perán E, Puertas A, Montoya F. Isolated oligohydramnios term pregnancy as an indication for induction of labor. *J Matern Fetal Neonatal Med* 2007; 20: 221–4.
- 43 Daneshmand SS, Cheung CY, Brace RA. Regulation of amniotic fluid volume by intramembranous absorption in sheep: role of passive permeability and vascular endothelial growth factor. *Am J Obstet Gynecol* 2003; 188: 786–93.
- 44 Mann SE, Dvorak N, Gilbert H, Taylor RN. Steady-state levels of aquaporin 1 mRNA expression are increased in idiopathic polyhydramnios. *Am J Obstet Gynecol* 2006; 194: 884–7.
- 45 Zhu XQ, Jiang SS, Zhu XJ, Zou SW, Wang YH, Hu YC. Expression of aquaporin 1 and aquaporin 3 in fetal membranes and placenta in human term pregnancies with oligohydramnios. *Placenta* 2009; 30: 670–6.
- 46 Hao RZ, Liu HS, Xiong ZF. Expression of aquaporin-1 in human oligohydramnios placenta and fetal membranes. *Nan Fang Yi Ke Da Xue Xue Bao* 2009; 29: 1130–2.
- 47 Xiong ZF, Liu HS, Hao RZ. Expressions of aquaporin 3, 8 and 9 mRNA in human oligohydramnios placenta. *Chin J Biomed Eng* 2010; 16: 155–8.
- 48 Liu HS, Hao RZ, Xiong ZF. Expression of aquaporin 1, 3, 8, 9 mRNA in human amniotic membranes in polyhydramnios. *Chin J Perinat Med* 2007; 12: 197–200.
- 49 Saadoun S, Papadopoulos MC, Hara-Chikuma M, Verkman AS. Impairment of angiogenesis and cell migration by targeted aquaporin-1 gene disruption. *Nature* 2005; 434: 786–92.
- 50 Ma T, Song Y, Gillespie A, Carlson EJ, Epstein CJ, Verkman AS. Defective secretion of saliva in transgenic mice lacking aquaporin-5 water channels. *J Biol Chem* 1999; 274: 20071–4.
- 51 Oshio K, Watanabe H, Song Y, Verkman AS, Manley GT. Reduced cerebrospinal fluid production and intracranial pressure in mice lacking choroid plexus water channel Aquaporin-1. *FASEB J* 2005; 19: 76–8.
- 52 Yang B, Folkesson HG, Yang J, Matthay MA, Ma T, Verkman AS. Reduced osmotic water permeability of the peritoneal barrier in aquaporin-1 knockout mice. *Am J Physiol* 1999; 276: C76–81.
- 53 Chou CL, Knepper MA, Hoek AN, Brown D, Yang B, Ma T, *et al*. Reduced water permeability and altered ultrastructure in thin descending limb of Henle in aquaporin-1 null mice. *J Clin Invest* 1999; 103: 491–6.
- 54 Zhao D, Bankir L, Qian L, Yang D, Yang B. Urea and urine concentrating ability in mice lacking AQP1 and AQP3. *Am J Physiol Renal Physiol* 2006; 291: F429–38.
- 55 Wang S, Amidi F, Beall M, Gui L, Ross MG. Aquaporin 3 expression in human fetal membranes and its up-regulation by cyclic adenosine monophosphate in amnion epithelial cell culture. *J Soc Gynecol Invest* 2006; 13: 181–5.
- 56 Damiano A, Zotta E, Goldstein J, Reisin I, Ibarra C. Water channel proteins AQP3 and AQP9 are present in syncytiotrophoblast of human term placenta. *Placenta* 2001; 22: 776–81.
- 57 Wang S, Chen J, Huang B, Ross MG. Cloning and cellular expression of aquaporin 9 in ovine fetal membranes. *Am J Obstet Gynecol* 2005; 193: 841–8.
- 58 Sha XY, Xiong ZF, Liu HS, Zheng Z, Ma TH. Pregnant phenotype in aquaporin 8-deficient mice. *Acta Pharmacol Sin* 2011; 32: 805–16.

Review

Aquaporins in sperm osmoadaptation: an emerging role for volume regulation

Qi CHEN^{1,2}, En-kui DUAN¹, *

¹State Key Laboratory of Reproductive Biology, Institute of Zoology, Chinese Academy of Sciences, Beijing 100101, China; ²Graduate University of Chinese Academy of Sciences, Beijing 100049, China

Upon ejaculation, mammalian sperm experience a natural osmotic decrease during male to female reproductive tract transition. This hypo-osmotic exposure not only activates sperm motility, but also poses potential harm to sperm structure and function by inducing unwanted cell swelling. In this physiological context, regulatory volume decrease (RVD) is the major mechanism that protects cells from detrimental swelling, and is essential to sperm survival and normal function. Aquaporins are selective water channels that enable rapid water transport across cell membranes. Aquaporins have been implicated in sperm osmoregulation. Recent discoveries show that Aquaporin-3 (AQP3), a water channel protein, is localized in sperm tail membranes and that AQP3 mutant sperm show defects in volume regulation and excessive cell swelling upon physiological hypotonic stress in the female reproductive tract, thereby highlighting the importance of AQP3 in the postcopulatory sperm RVD process. In this paper, we discuss current knowledge, remaining questions and hypotheses about the function and mechanistic basis of aquaporins for volume regulation in sperm and other cell types.

Keywords: aquaporins; sperm; water permeability; regulatory volume decrease; osmosensing/mechanosensing; tetrameric structure

Acta Pharmacologica Sinica (2011) 32: 721–724; doi: 10.1038/aps.2011.35; published online 9 May 2011

Efficient sperm volume regulation is a prerequisite for normal sperm function

In most mammalian species studied, the journey of sperm from the male to the female reproductive tract experience a natural osmotic decrease^[1], an evolutionary vestige from freshwater fish species^[2]. Before ejaculation, the mammalian sperm are quiescent in the relatively hypertonic male reproductive tract with no or very low motility. Upon copulation, the sperm enter into the relatively hypotonic female reproductive tract and quickly show motility activation^[3, 4], indicating that osmotic changes are beneficial for initial sperm motility activation. However, postcopulatory hypotonic stress also has a negative effects as it induces osmotic cell swelling, which if uncontrolled, can be detrimental to sperm function and survival^[5]. Mammalian sperm have evolved to effectively reduce the negative impact of hypotonic cell swelling by means of regulatory volume decrease (RVD), which was proposed to involve efficient volume regulation driven by active solute transport and rapid transmembrane water movement^[6].

Functional importance of aquaporins in sperm volume regulation: emerging evidence from AQP3 knockout mice

In the early 1970s, it was demonstrated that the water permeability coefficient of bull spermatozoa was quite high, about four times greater than that of bovine erythrocytes and between ten and thirty times greater than that of artificial bimolecular lipid membranes^[7]. According to these observations, the author made an insightful conclusion that the chief route for the passage of water through the sperm membrane must be via “pores”^[7]. Similar high water permeability coefficients have been discovered in other mammalian species, including humans^[8, 9].

In the past two decades, the understanding of the movement of water through cell membranes has been greatly advanced by the discovery of aquaporins, a family of water-specific membrane channel proteins^[10]. Recently, it was proposed that aquaporins might be active players in sperm volume-regulatory water flux^[11]. Indeed, two aquaporins (AQP7 and 8) were first cloned from rat testes and identified by staining in murine sperm tails^[12–14]. Aquaporin-11 (AQP11) has also been found in the end piece of rat sperm^[15] (although some controversies exist due to variable antibody specificity; for a more detailed description, see the comprehensive review^[14]). However, genetic deletion of AQP7 and 8 in mice did not result in obvious abnormalities in sperm morphology and function^[11, 16, 17],

* To whom correspondence should be addressed.

E-mail duane@ioz.ac.cn

Received 2011-02-13 Accepted 2011-03-17

suggesting that these AQPs are not essential for mouse sperm function or that they can be functionally substituted by other aquaporin members.

After a previous study identified Aquaporin-3 (AQP3) expression in mouse testes^[18], we demonstrated that AQP3 was present in both mouse and human sperm and was located in the plasma membrane of the principle piece of flagellum^[3] (Figure 1A). Further functional studies using AQP3 knockout mice have shown that upon exposure to physiological hypotonic stress, AQP3 mutant sperm show normal initial motility but display increased vulnerability to hypotonic cell swelling characterized by increased tail bending after entering the uterus^[3]. The observed sperm defect was due to impaired cell volume regulation and progressive cell swelling in response to physiological hypotonic stress, as revealed by sperm volume detection using flow cytometry in a population-based manner and by time-lapse imaging of individual sperm^[3]. The tail deformation hampers normal sperm migration into the oviduct, resulting in impaired fertilization and reduced male fertility^[3]. These results provided direct evidence that AQP3 was actively involved in mouse sperm volume regulation during physiological hypotonic stress by protecting sperm from excess cell swelling and, therefore, optimizing postcopulatory sperm behavior.

Notably, it has also been demonstrated that, compared to

mouse sperm, human sperm show a strikingly similar pattern of AQP3 localization^[3], thus providing the intriguing possibility of a similar role for AQP3 in human sperm. On the other hand, we failed to detect AQP3 expression in rat sperm, which is consistent with previous reports^[19]. Indeed, such species-specific expression of AQP3 has been observed in other tissues. For example, AQP3 is expressed in human and rat erythrocytes but not in mouse erythrocytes^[20, 21]. The discrepancies in AQP3 expression patterns between closely related species such as mice and rats suggest a dynamic selection of AQP3 expression during evolution.

How do AQP proteins mediate cell RVD during hypotonic stress?

Despite the observation that AQP3 is important for normal sperm RVD during hypotonic exposure^[3] and the increasing body of evidence that several members of AQPs (AQP1, 2, 3, 4, and 5) are actively involved in RVD of diverse cell types^[22–26], the molecular mechanisms by which AQPs take part in RVD are hard to explain using the “simple permeability” theory, which considers aquaporins as inert pores that simply increase the osmotic permeability of plasma membranes. Under such a “simple permeability” model, RVD begins with a hypotonic stress-induced water influx, followed by active solute transport that enables osmolyte efflux and provides the driving force for water to exit^[27], and the participation of AQPs in RVD is merely to facilitate the time it takes to reach osmotic equilibrium. When applying such a model in the AQP3 mutant sperm, since both water influx and efflux were supposed to be equally diminished, the progressive sperm cell swelling should not have been observed.

Given such a dilemma, it is our belief that AQP3-dependent water permeability in sperm, if any, is not the primary contribution to sperm RVD under hypotonic stress. Alternatively, we hypothesize that AQP3 may function as a part of the membrane osmosensing/mechanosensing system for the initial sensing of cell swelling and therefore, may “trigger” subsequent RVD events such as solute transport and cytoskeleton reconstruction. This hypothesis is supported by the fact that AQP3 is strongly expressed in many organs, such as the bladder, trachea and esophagus, and in olfactory cells^[18, 28, 29], where they seem to have no obvious requirements for rapid water movement but need sensitive perception of tension, shear stress and so on. Moreover, this hypothesis is supported by the recent discovery that AQP5 is actively involved in salivary gland cell RVD by coordinating with TRPV4, a volume sensitive calcium channel, to concertedly regulate cell volume under hypotonic stimulation^[23]. This provides the first mechanistic evidence that AQPs are actively involved in upstream events of cell volume sensing through interaction with other volume-sensitive ion channels. Interestingly, the scenario of volume regulation by AQP5/TRPV4 interaction has recently been expanded for AQP4. As demonstrated in mouse astrocytes, the TRPV4/AQP4 complex plays an important role in the initiation of RVD similar to that of the TRPV4/AQP5 complex in salivary gland cells^[25]. In this regard, it would

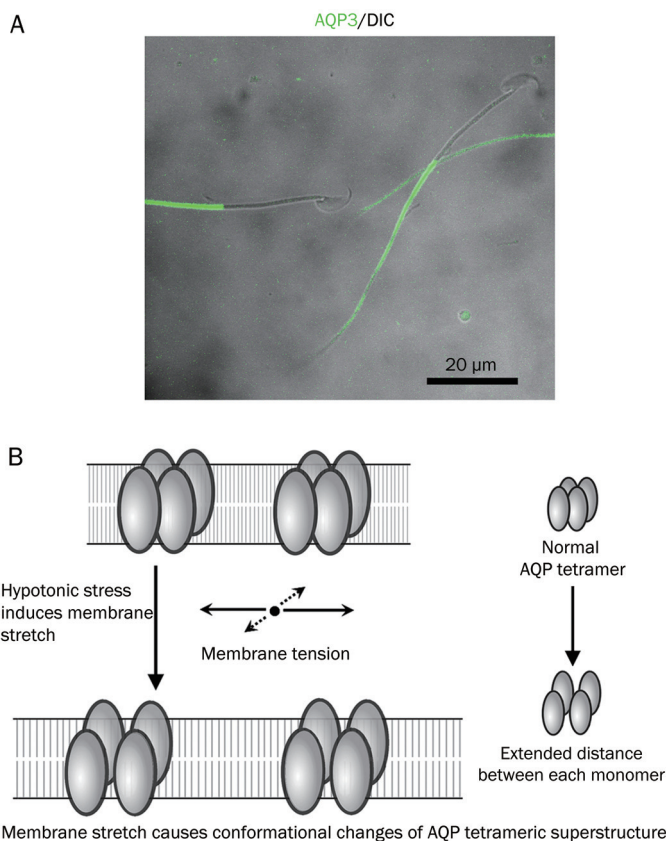


Figure 1. (A) AQP3 localization in mouse sperm. (B) A hypothesized model showing how the AQP tetrameric structure could be involved in cellular mechanosensing during hypotonic stress-induced cell swelling.

not be hard to imagine that AQP3 might also form molecular complexes with other ion channels to mediate sperm RVD. Such candidate molecules may involve the volume sensitive chloride channel CLC-3^[30], which has been observed in mammalian sperm and has been implicated in sperm volume regulation^[31, 32].

Despite the accumulating evidence, a most basic question remains for the involvement of AQPs in RVD: As water channel proteins, by what structural basis do AQPs play a role in osmosensing/mechanosensing? We propose that the answer to this question might reside in the homotetrameric structure of aquaporins, as revealed by molecular crystal structure analysis^[10]. Although it has been established that the water permeability characteristics of AQPs rely on the pores of each monomer, the evolutionary driving force for AQPs to form a tetramer is not understood^[10]. It is hypothesized that the homotetrameric nature of aquaporins could provide a structural base to sense membrane stretching during hypotonic stress-induced cell swelling. As shown in Figure 1B, cell swelling in response to hypotonic stress would increase membrane tension and might result in an extended distance between each AQP monomer and cause conformational changes of the homotetramer. Such changes in molecular structure may initiate downstream signaling cascades for RVD events. This model would be particularly suitable in cases when AQPs form functional complexes with other mechanosensors (such as TRPV4^[23, 25]) or directly interact with cytoskeletal components such as actin filaments (AQP2 has been shown to interact directly with actin^[33]). However, to stringently test such a hypothesis, it would be necessary to create a mutant AQP protein that could not form a tetrameric structure while maintaining the water permeability of each AQP monomer.

There is also a remote possibility that under processes such as sperm RVD under hypotonic stress, AQP3 functions as a unidirectional water channel allowing only water efflux, while other sperm AQPs, such as AQP7 and 8, only allow water influx. Indeed, recent findings have demonstrated that a formate transporter shows an AQP-like channel structure^[34, 35], thus lending support to the radical notion that an aquaporin structure may have the potential to function as a unidirectional water transporter in cooperation with other molecules, at least under certain circumstances.

Conclusion

In summary, the emerging evidence for AQPs in cell volume regulation, including AQP3 in sperm, can not be fully explained by considering AQPs as inert pores simply for water permeability. These phenomena provide future directions for a new round of AQP research focused on AQPs with more fundamental roles as general regulators, such as osmosensors/mechanosensors, possibly with novel mechanisms.

Acknowledgements

We thank Drs Alan S VERKMAN (University of California, San Francisco, USA), Tong-hui MA (Jilin University, Changchun, China) and Dayue Darrel DUAN (University of Nevada,

Reno, USA) for their critical discussions and insightful input into the manuscript. This work was supported by the National Basic Research Program of China (2011CB710905).

References

- 1 Cooper TG, Yeung CH. Acquisition of volume regulatory response of sperm upon maturation in the epididymis and the role of the cytoplasmic droplet. *Microsc Res Tech* 2003; 61: 28–38.
- 2 Alavi SM, Cosson J. Sperm motility in fishes. (II) Effects of ions and osmolality: a review. *Cell Biol Int* 2006; 30: 1–14.
- 3 Chen Q, Peng H, Lei L, Zhang Y, Kuang H, Cao Y, et al. Aquaporin 3 is a sperm water channel essential for postcopulatory sperm osmoadaptation and migration. *Cell Res* 2010. Advance online publication 7 December 2010; doi:10.1038/cr.2010
- 4 Willoughby CE, Mazur P, Peter AT, Critser JK. Osmotic tolerance limits and properties of murine spermatozoa. *Biol Reprod* 1996; 55: 715–27.
- 5 Drevius LO, Eriksson H. Osmotic swelling of mammalian spermatozoa. *Exp Cell Res* 1966; 42: 136–56.
- 6 Yeung CH, Barfield JP, Cooper TG. Physiological volume regulation by spermatozoa. *Mol Cell Endocrinol* 2006; 250: 98–105.
- 7 Drevius LO. Permeability coefficients of bull spermatozoa for water and polyhydric alcohols. *Exp Cell Res* 1971; 69: 212–6.
- 8 Curry MR, Redding BJ, Watson PF. Determination of water permeability coefficient and its activation energy for rabbit spermatozoa. *Cryobiology* 1995; 32: 175–81.
- 9 Noiles EE, Mazur P, Watson PF, Kleinhans FW, Critser JK. Determination of water permeability coefficient for human spermatozoa and its activation energy. *Biol Reprod* 1993; 48: 99–109.
- 10 King LS, Kozono D, Agre P. From structure to disease: the evolving tale of aquaporin biology. *Nat Rev Mol Cell Biol* 2004; 5: 687–98.
- 11 Yeung CH, Callies C, Rojek A, Nielsen S, Cooper TG. Aquaporin isoforms involved in physiological volume regulation of murine spermatozoa. *Biol Reprod* 2009; 80: 350–7.
- 12 Ishibashi K, Kuwahara M, Kageyama Y, Tohsaka A, Marumo F, Sasaki S. Cloning and functional expression of a second new aquaporin abundantly expressed in testis. *Biochem Biophys Res Commun* 1997; 237: 714–8.
- 13 Ishibashi K, Kuwahara M, Gu Y, Kageyama Y, Tohsaka A, Suzuki F, et al. Cloning and functional expression of a new water channel abundantly expressed in the testis permeable to water, glycerol, and urea. *J Biol Chem* 1997; 272: 20782–6.
- 14 Yeung CH. Aquaporins in spermatozoa and testicular germ cells: identification and potential role. *Asian J Androl* 2010; 12: 490–9.
- 15 Yeung CH, Cooper TG. Aquaporin AQP11 in the testis: molecular identity and association with the processing of residual cytoplasm of elongated spermatids. *Reproduction* 2010; 139: 209–16.
- 16 Sohara E, Ueda O, Tachibe T, Hani T, Jishage K, Rai T, et al. Morphologic and functional analysis of sperm and testes in Aquaporin 7 knockout mice. *Fertil Steril* 2007; 87: 671–6.
- 17 Yang B, Song Y, Zhao D, Verkman AS. Phenotype analysis of aquaporin-8 null mice. *Am J Physiol Cell Physiol* 2005; 288: C1161–70.
- 18 Ma T, Song Y, Yang B, Gillespie A, Carlson EJ, Epstein CJ, et al. Nephrogenic diabetes insipidus in mice lacking aquaporin-3 water channels. *Proc Natl Acad Sci U S A* 2000; 97: 4386–91.
- 19 Hermo L, Krzeczunowicz D, Ruz R. Cell specificity of aquaporins 0, 3, and 10 expressed in the testis, efferent ducts, and epididymis of adult rats. *J Androl* 2004; 25: 494–505.
- 20 Yang B, Ma T, Verkman AS. Erythrocyte water permeability and renal function in double knockout mice lacking aquaporin-1 and

- aquaporin-3. *J Biol Chem* 2001; 276: 624–8.
- 21 Roudier N, Bailly P, Gane P, Lucien N, Gobin R, Cartron JP, *et al*. Erythroid expression and oligomeric state of the AQP3 protein. *J Biol Chem* 2002; 277: 7664–9.
 - 22 Galizia L, Flamenco MP, Rivarola V, Capurro C, Ford P. Role of AQP2 in activation of calcium entry by hypotonicity: implications in cell volume regulation. *Am J Physiol Renal Physiol* 2008; 294: F582–90.
 - 23 Liu X, Bandyopadhyay BC, Nakamoto T, Singh B, Liedtke W, Melvin JE, *et al*. A role for AQP5 in activation of TRPV4 by hypotonicity: concerted involvement of AQP5 and TRPV4 in regulation of cell volume recovery. *J Biol Chem* 2006; 281: 15485–95.
 - 24 Kuang K, Yiming M, Wen Q, Li Y, Ma L, Iserovich P, *et al*. Fluid transport across cultured layers of corneal endothelium from aquaporin-1 null mice. *Exp Eye Res* 2004; 78: 791–8.
 - 25 Benfenati V, Caprini M, Dovizio M, Mylonakou MN, Ferroni S, Ottersen OP, *et al*. An aquaporin-4/transient receptor potential vanilloid 4 (AQP4/TRPV4) complex is essential for cell-volume control in astrocytes. *Proc Natl Acad Sci U S A* 2011; 108: 2563–8.
 - 26 Kida H, Miyoshi T, Manabe K, Takahashi N, Konno T, Ueda S, *et al*. Roles of aquaporin-3 water channels in volume-regulatory water flow in a human epithelial cell line. *J Membr Biol* 2005; 208: 55–64.
 - 27 Hoffmann EK, Lambert IH, Pedersen SF. Physiology of cell volume regulation in vertebrates. *Physiol Rev* 2009; 89: 193–277.
 - 28 Matsuzaki T, Suzuki T, Koyama H, Tanaka S, Takata K. Water channel protein AQP3 is present in epithelia exposed to the environment of possible water loss. *J Histochem Cytochem* 1999; 47: 1275–86.
 - 29 Ablimit A, Matsuzaki T, Tajika Y, Aoki T, Hagiwara H, Takata K. Immunolocalization of water channel aquaporins in the nasal olfactory mucosa. *Arch Histol Cytol* 2006; 69: 1–12.
 - 30 Duan D, Winter C, Cowley S, Hume JR, Horowitz B. Molecular identification of a volume-regulated chloride channel. *Nature* 1997; 390: 417–21.
 - 31 Yeung CH, Barfield JP, Cooper TG. Chloride channels in physiological volume regulation of human spermatozoa. *Biol Reprod* 2005; 73: 1057–63.
 - 32 Petrunikina AM, Harrison RA, Ekhlasi-Hundrieser M, Topfer-Petersen E. Role of volume-stimulated osmolyte and anion channels in volume regulation by mammalian sperm. *Mol Hum Reprod* 2004; 10: 815–23.
 - 33 Noda Y, Horikawa S, Katayama Y, Sasaki S. Water channel aquaporin-2 directly binds to actin. *Biochem Biophys Res Commun* 2004; 322: 740–5.
 - 34 Waight AB, Love J, Wang DN. Structure and mechanism of a pentameric formate channel. *Nat Struct Mol Biol* 2010; 17: 31–7.
 - 35 Wang Y, Huang Y, Wang J, Cheng C, Huang W, Lu P, *et al*. Structure of the formate transporter FocA reveals a pentameric aquaporin-like channel. *Nature* 2009; 462: 467–72.

Review

TRPM7 in cerebral ischemia and potential target for drug development in stroke

Christine You-jin BAE², Hong-shuo SUN^{1, 2, 3, 4, *}

Departments of ¹Surgery, ²Physiology, ³Pharmacology, and ⁴Institute of Medical Science, Faculty of Medicine, University of Toronto, 1 King's College Circle, Toronto, Ontario, Canada, M5S 1A8

Searching for effective pharmacological agents for stroke treatment has largely been unsuccessful. Despite initial excitement, antagonists for glutamate receptors, the most studied receptor channels in ischemic stroke, have shown insufficient neuroprotective effects in clinical trials. Outside the traditional glutamate-mediated excitotoxicity, recent evidence suggests few non-glutamate mechanisms, which may also cause ionic imbalance and cell death in cerebral ischemia. Transient receptor potential melastatin 7 (TRPM7) is a Ca²⁺ permeable, non-selective cation channel that has recently gained attention as a potential cation influx pathway involved in ischemic events. Compelling new evidence from an *in vivo* study demonstrated that suppression of TRPM7 channels in adult rat brain *in vivo* using virally mediated gene silencing approach reduced delayed neuronal cell death and preserved neuronal functions in global cerebral ischemia. In this review, we will discuss the current understanding of the role of TRPM7 channels in physiology and pathophysiology as well as its therapeutic potential in stroke.

Keywords: ion channels; TRP; TRPM7; cerebral ischemia; stroke; *in vivo* test; siRNA; neuroprotection

Acta Pharmacologica Sinica (2011) 32: 725–733; doi: 10.1038/aps.2011.60; published online 9 May 2011

Introduction

Stroke is one of the leading causes of death and disability in the world^[1,2]. The disease itself and associated morbidity have caused significant social and economic impacts on society and individuals worldwide. The prevalence of stroke is expected to increase and our aging population is especially vulnerable to stroke insults. The clinical trials of anti-excitotoxic therapies (AET) have failed to benefit stroke patients^[3], thus diminishing the initial excitement of translating research from bench to bedside and using glutamate receptor blockers in treating stroke patients. Even though the mechanisms underlying cerebral ischemia are beginning to be better understood, there is still no clinical or experimental treatment that has shown improved outcome for stroke patients. To ease personal and societal burden of stroke, continuous efforts have been directed towards searching for new therapeutic targets in stroke. This review provides a current view on one of the non-glutamate mechanisms of stroke that mediates through TRPM7 channels from a recent *in vivo* study^[4].

A major event during cerebral ischemia is a concomitant massive release of the excitatory neurotransmitter glutamate,

which results in intracellular calcium overload and eventual cell death^[5]. The excitotoxicity in ischemia has been in the centre of stroke research for a long period of time. Triggered release of excessive glutamate causes cell death following ischemia, which is associated with an increase of the intracellular calcium (Ca²⁺) concentration^[6–8]. Thus, identifying the source of the excessive Ca²⁺ influx and/or release from the intracellular Ca²⁺ stores during ischemia has been a research focus. Traditionally, Ca²⁺-permeable NMDA (*N*-methyl-*D*-aspartic acid), AMPA (*DL*-alpha-amino-3-hydroxy-5-methyl-4-isoxazole propionic acid) receptors^[8] and L-type voltage-dependent Ca²⁺ channels^[9] were considered as the major calcium entry paths and the causes of Ca²⁺ overload during ischemia. This Ca²⁺ overload, or a broad spectrum of ion imbalance, during ischemia is considered to initiate a wide range of sequential events that lead to irreversible damage to protein synthesis, mitochondria, cytoskeleton and plasma membrane, and to eventual cell death. In an ideal scenario, the interruption of this Ca²⁺ overload in ischemia is thought to be clinically beneficial for stroke patients. Blocking these receptor channels prevents the intracellular Ca²⁺ overload and provides significant neuroprotection in the laboratory. Some of the findings from the bench have been translated into many clinical trials in stroke treatment. However, the results of clinical trials testing AET, which include NMDA and AMPA receptor block-

* To whom correspondence should be addressed.

E-mail hss.sun@utoronto.ca

Received 2011-03-14 Accepted 2011-04-18

ers, turned out to be ineffective and even with unwanted side effects^[10–14]. This may be due to multiple factors and it will not be the focus of this review^[15]. Because of the limitation of the glutamate mechanism and the unfavourable outcomes of AET trials, stroke researchers have been seeking for alternative, non-glutamate related therapeutic targets that cause ionic imbalance and cell death. Some of these channels include: acid-sensing ion channels^[16, 17], transient receptor potential (TRP) channels^[4, 7, 18–21], and hemichannels^[22–24], volume-regulated anion channels^[25], sodium-calcium exchangers^[26, 27] and non-selective cation channels^[28].

Based on the recommendations from the Stroke Therapy Academic Industry Roundtable (STAIR) committee, it is important to validate the preclinical development in proof of concept starting with *in vivo* rodent models as experimental animal stroke models^[29]. Recent *in vivo* studies aimed at identifying the non-glutamate mechanisms for stroke have demonstrated the involvement of acid-sensing ion channels^[16, 17] first, and then the TRPM7 (transient receptor potential melastatin 7) channel^[4, 7, 18–21]. In this review, we will mainly focus on the current understanding of the molecular, biophysical, and pharmacological properties of TRPM7 as well as its physiological and pathophysiological roles and its therapeutic potential in stroke.

Classification, structures and distributions

Classification

The TRP superfamily is comprised of a group of non-selective cation channels^[30–33]. Its nomenclature was originated from the first found member of this superfamily, which was identified in a *Drosophila* phototransduction mutant showing transient receptor potential to a continuous light^[34]. Currently, about 30 mammalian TRP channels have been discovered and named according to their sequence homologous structures. They are classified into six subfamilies: 1) TRPC (canonical), 2) TRPM (melastatin), 3) TRPV (vanilloid), 4) TRPA (ankyrin), 5) TRPML (mucolipin) and 6) TRPP (polycystin). Different TRP channels are activated by different physical and chemical stimuli. The diverse gating mechanisms of TRP channels make them good cellular signal integrators critical for physiological and pathological functions^[30–33].

TRPM7 belongs to the melastatin-related subfamily of TRP channels, which is comprised of eight members (eg, TRPM1–8). It was suggested that TRPM7 may also form heteromers with TRPM2 as application of TRPM7 siRNA also down-regulated TRPM2 channel mRNA in an *in vitro* study^[21]. This is important as TRPM2 has also shown to play a role in oxidative stress-mediated cell death, which is a cellular condition shown in stroke.

Gene and protein structures

In human, TRPM7 gene is located on chromosome 15 in the q21.2 region, and encoded by 39 exons that spans about 127 kb of DNA sequence. The mouse TRPM7 gene is 95% identical to human gene^[35]. It is located on chromosome 2 on cytoband F2 and it is also encoded by 39 exons that spans about 85 kb of

DNA sequence.

TRPM7 is a large protein (1864 amino acids in human; 1863 amino acids in mouse) with a predicted molecular weight of approximately 212 kDa. Each subunit has six transmembrane (TM) spanning domains (S1–S6) with a re-entrant pore-forming loop (known as P-loop) between the fifth (S5) and sixth (S6) segments^[32, 33] (Figure 1). The N-terminus has another hydrophobic region (H1) and four regions of TRPM subfamily homology domain (MHD), but their biological significance is largely undefined. The C-terminus contains a TRP box of ~25 highly conserved residues, which may interact with phosphatidylinositol 4,5-bisphosphate (PIP₂), a positive regulator of some TRP channel^[36]. A coiled-coil domain close to the C-terminus may mediate subunit-subunit interactions and tetrameric assembly of TRPM7^[37]. The most unique structural feature of the channel is the enzymatic domain located at the end of C-terminus. In TRPM7, the distal C-terminus has an atypical serine/threonine protein kinase domain that is homologous to a family of α -kinases^[38]. Although this kinase domain does not seem to affect channel activity directly^[33, 39, 40], it may be important for the regulation of channel function by Mg²⁺ nucleotides^[41].

Tissue and cellular distribution

TRPM7 channel mRNA is ubiquitously expressed in almost all tissues^[33, 42, 43]. Recently, real-time quantitative RT-PCR analyses with either Taqman or SYBR Green were used to create comparative distribution profiles of TRPM channels in selected human tissues, including brain, pituitary, heart, lung, liver, fetal liver, skeletal muscle, stomach, intestine, spleen, peripheral blood mononuclear cells, macrophages, pancreas, prostate, placenta, cartilage, bone and bone marrow^[42]. TRPM7 mRNA has the highest expression in heart, pituitary, bone, and adipose tissue^[42]. Similar distribution patterns of TRPM7 were also observed in mouse tissue samples^[44]. Compared to other TRP members, TRPM7 mRNA expression levels were significantly higher in most tissues.

The TRPM7 protein shown by immunofluorescent labeling is strongly expressed at the plasma membrane in N1E-115 neuroblastoma cells^[45], and in vascular smooth muscle cells^[46]. In N1E-115 neuroblastoma cells, HA-tagged TRPM7 antibodies were localized in membrane ruffles^[45]. Similarly, protein expression of TRPM7 is also shown in cell bodies and processes of hippocampal neurons with immunostaining^[4, 47, 48]. In superior cervical ganglion neurons, TRPM7 is exclusively localized within cholinergic vesicles^[49].

Biophysical properties, regulatory mechanisms, pharmacology

Biophysical properties

TRPM7 is a non-selective cation channel that displays several biophysical features that make this channel distinguishable from other TRP members. TRPM7 channel has a reversal potential of approximately 0 mV, and a prominent outward rectification^[30, 33, 43, 50] (Figure 1B). At negative membrane potentials, TRPM7 conducts a small inward current by trans-

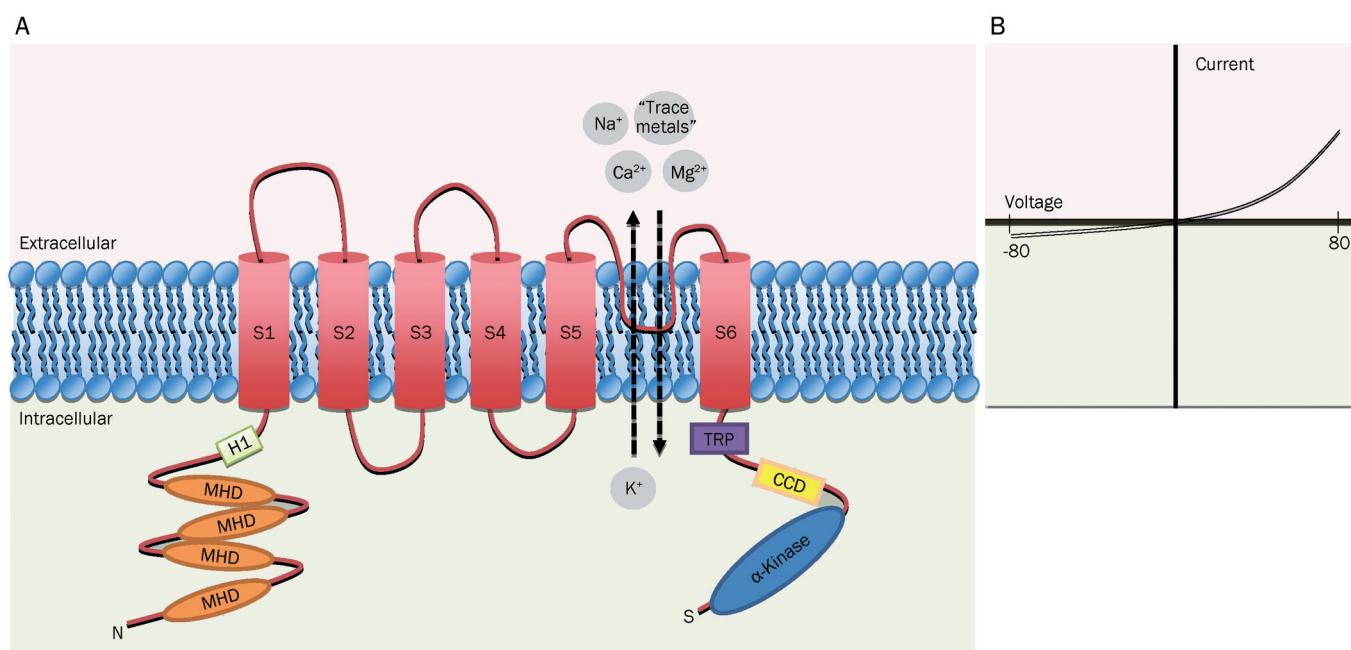


Figure 1. Schematic diagram showing proposed transmembrane topology of TRPM7. (A) The putative membrane topology of a single subunit of TRPM7 is shown. Each subunit has six transmembrane (TM) spanning domains (S1–S6) with a re-entrant pore-forming loop between the fifth (S5) and sixth (S6) segments. The intracellularly located N-terminus has another hydrophobic region (H1) and four regions of TRPM subfamily homology domain (MHD). The intracellularly located C-terminus contains a TRP box of ~25 highly conserved residues (TRP) and a coiled-coil domain (CCD). The distal C-terminus has an atypical serine/threonine protein kinase domain. As indicated in the figure, TRPM7 is a non-selective cation channel that conducts both monovalent ions (eg, Na⁺ and K⁺) and divalent ions (eg, Ca²⁺, Mg²⁺ and other trace metal ions). (B) Representative current-voltage (*I-V*) relationship of TRPM7.

porting divalent cations (eg calcium and magnesium) down their concentration gradients^[35]. TRPM7 current density is usually under 20 pA/pF^[35,50]. At positive membrane potential, TRPM7 conducts a strong outward current as intracellular cations experience strong driving force to exit the cell. This outwardly rectifying property is entirely due to a voltage-dependent block of monovalent cation influx by extracellular divalents. For instance, in the absence of divalent cations, TRPM7 conducts inward monovalent cations^[35]. Consequently, its *I-V* relation becomes quasi-linear suggesting the lack of voltage-dependent gating and channel selectivity (Figure 1B).

Unlike many other Ca²⁺ permeating channels, TRPM7 is characteristically more permeable to a series of trace metal ions. Using equimolar divalent ion substitution approaches, Monteilh-Zoller and colleagues reported a permeation profile for TRPM7 in a sequence of: Zn²⁺ ≈ Ni²⁺ >> Ba²⁺ > Co²⁺ > Mg²⁺ ≥ Mn²⁺ > Sr²⁺ > Cd²⁺ > Ca²⁺^[51]. TRPM7 allows entry of these divalent ions even with physiological levels of extracellular Ca²⁺ and Mg²⁺. TRPM7 is constitutively active and this feature makes TRPM7 a good candidate for both sensing the extracellular concentration of divalents and maintaining intracellular Mg²⁺ homeostasis during ischemic episodes that lead to intense neuronal activity^[47].

TRPM7 channel activity is regulated by extracellular pH. A decrease in extracellular pH (acidic) strongly potentiated current activity of the recombinant TRPM7 channel expressed in HEK-293 cells (~10-fold increase at pH 4.0, and 1-2 fold

increase at pH 6.0)^[52] and in CHOK1 cells (~12-fold increase at pH 4.0)^[53]. However, the TRPM7-like current in the FaDu cell line was insensitive to the acidic condition (pH 5.0)^[54], while the TRPM7-like inward current in human cervical epithelial HeLa cells was increased at pH 4.0^[55]. Protons likely compete with Ca²⁺ and Mg²⁺ for their binding sites, thus increase the inward current by releasing the divalent cation block^[52]. Point mutation of Glu¹⁰⁴⁷ (E1047Q) of TRPM7 channels eliminated the proton-enhanced inward current activity, indicating the residue may be involved in the pH sensitivity of the channels^[53]. Although the effects of protons on endogenous TRPM7 remains controversial, TRPM7 can be regulated in acidic pathophysiological conditions, including ischemic stroke^[56].

TRPM7 is not a mechanosensitive channel, however, shear stress in vascular smooth muscle cells doubled the number of TRPM7 channels near the plasma membrane^[57]. Further studies are required to deduce the mechanism of stress-induced regulation of TRPM7 channels.

Regulatory mechanisms

The heterologously expressed foreign and native TRPM7 channels are constitutively active, and their activities can be modulated by several extracellular and intracellular factors^[43,50]. TRPM7 activities can be tonically inhibited by intracellular Mg²⁺, and Mg-complexed nucleotides, MgATP, MgGTP, and such tonic inhibition is usually less than 10% of maximal

conductance^[35, 41, 50]. Whole-cell patch-clamp recordings have shown that either adding Mg²⁺ chelators (eg HEDTA or Na-ATP) intracellularly or omitting Mg²⁺ and Mg²⁺-complexed nucleotides in intracellular solutions increased activation of TRPM7^[40, 41, 43]. These inhibitory effects may be mediated by binding to C-terminal kinase domain^[39, 43], which in itself is not essential for the activation of TRPM7^[33, 39, 40]. Compared to the wild-type, phosphotransferase-deficient mutant channels (K1648R and G1799D) demonstrated a reduced sensitivity to inhibition by Mg²⁺ at intermediate concentrations close to the IC₅₀^[39]. Moreover, Demeuse and colleagues^[41] reported differential sensitivity to Mg²⁺ and Mg²⁺-nucleotides inhibition in the wild-type, phosphotransferase deficient point mutant (K1648R), and the Δ -kinase truncation mutant. These findings lead to a hypothetical model: only Mg²⁺-nucleotides bind to the kinase domain but this domain interacts with the Mg²⁺ binding site, which is responsible for regulating the channel activity.

Activation of TRPM7 can be regulated via PIP₂, which is a substrate of phospholipase C (PLC)^[58]. The C2 domain of PLC is directly associated with the kinase domain of TRPM7. When carbachol, an agonist for G_{aq}-linked muscarinic type 1 (M1) receptors, was used, PLC-beta was activated. This activation of PLC-beta led to the hydrolysis of localized PIP₂, which caused a rapid decreased I_{TRPM7}.

TRPM7 may also be regulated by phosphorylation. A variant of TRPM7 with a missense mutation (T1482I) is found in a subset of patients with Guamanian amyotrophic lateral sclerosis (ALS-G) and Parkinsonism-dementia (PD-G)^[59]. When recombinant TRPM7s with T1482I mutation were heterologously expressed in HEK-293 cells, these channels were functional but showed increased sensitivity to Mg²⁺ inhibition and reduced phosphorylation compared to wild-type^[59]. Based on the computer analysis of the secondary structure, both Thr-1482 in fish, amphibian, avian, and primate species, and Ser-1482 in murine species are the potential substrates for autophosphorylation by the C-terminus serine/threonine α -kinase domain in TRPM7. Ile-1482 mutation found in these patients, however, cannot be phosphorylated. TRPM6, the closest member to TRPM7, also regulates TRPM7 via cross-phosphorylation, and alters Mg²⁺ homeostasis regulation^[60].

Pharmacological properties

There are currently no selective pharmacological tools (both agonists and antagonists) that can specifically modulate TRPM7 channels^[61]. Gene deletion in global TRPM7 knockout animal is confirmed to be embryonically lethal^[62, 63]. Thus, inability to modulate the TRPM7 channels pharmacologically creates a huge obstacle for investigating the physiological and pathophysiological roles of TRPM7 in stroke. There are some successful studies of gene silencing using small interfering RNA (siRNA) to knockdown the TRPM7 in either mRNA and/or protein expression in central neurons^[4, 21, 47], peripheral neurons^[49], vascular endothelial cells^[64], vascular smooth muscle cells^[65], gastrointestinal tract interstitial pacemaker cells^[66] and human epithelial cells^[67]. TRPM7 can be blocked non-spe-

cifically by trivalent ions, such as Gd³⁺ (IC₅₀ ~1.4-2.5 μ mol/L) and La³⁺ (IC₅₀ ~17 μ mol/L)^[21] and 2-Aminoethoxydiphenyl borate (2-APB) (IC₅₀ ~50 μ mol/L), which is a well known non-specific blocker of many TRP channels^[68]. Recently, it has been reported that inhibitors of 5-lipoxygenase (5-LOX), NDGA (nordihydroguaiaretic acid, IC₅₀ ~6.3 μ mol/L), AA861 (IC₅₀ ~6.0 μ mol/L), and MK886 (IC₅₀ ~8.6 μ mol/L), can suppress the TRPM7 current in HEK-293 cells^[69]. Application of these molecules also prevented some of the phenomena (eg cell death) associated with TRPM7 when exposed to low extracellular divalent cations and other apoptotic stimuli. These effects seem to be independent of their actions on 5-LOX, and the expression level and cellular concentrations of TRPM7 at the plasma membrane were not affected. Previously, studies have reported less tissue damage during cerebral ischemia and myocardial ischemia-reperfusion injury with 5-LOX inhibition^[70, 71]. Although drawing a connection between cellular protective effects during ischemic injury with 5-LOX and blockade of TRPM7 with 5-LOX would be premature, these findings emphasize the importance of future follow-up studies. Thus, there is a pressing need of specific pharmacological agents for studying the physiological and pharmacological roles of the TRPM7 channels *in vivo* and potential therapeutic uses.

Physiological functions

Our current knowledge of the physiological functions of TRPM7 channels has recently been improved, even with limited molecular and specific pharmacological tools. Under physiological conditions, several lines of evidence suggest the role of TRPM7 in cell survival and proliferation^[39, 62, 72]. The early embryonic lethality in global TRPM7 knockout mice hints at the requirement of TRPM7 in cell survival and proliferation as embryonic development involves extensive cell proliferation^[62]. In the same study, TRPM7 gene was selectively deleted in developing thymocytes. These T-cells did not differ in its ability of uptake Mg²⁺ or maintaining global cellular Mg²⁺, but showed defective thymopoiesis. A more recent study showed that knocking out of TRPM7 kinase domain homozygously resulted in embryonic lethality^[63], while heterozygous knockout mice were viable, but exhibited abnormal homeostasis^[63]. TRPM7 knockout in chicken DT40 B cells caused growth arrest and eventual cell death in culture^[39], which may be linked to a regulation of Mg²⁺ homeostasis^[72]. Supplementing TRPM7 knockout cells with a high Mg²⁺ containing medium, but not Ca²⁺ or Zn²⁺, could restore normal cell growth and survival in culture. Knockdown of TRPM7 with RNA interference reduced Ca²⁺ and Mg²⁺ influxes, and decreased cell proliferation in human osteoblast-like cells^[72], and retinoblastoma cells^[73]. TRPM7 dependence for proliferation and differentiation was also shown in zebrafish mutants as they displayed severe growth retardation and general alterations in skeleton development^[74].

Several studies have shown the importance of TRPM7 in cell adhesion. Over-expression of TRPM7 in HEK-293 cells lead to cell rounding, loss of adhesion and cell death^[35]. Consis-

tent with these findings, knockdown of TRPM7 in HEK-293 cells increased cell adhesion^[75]. Over-expression of TRPM7 may produce cell rounding by stimulating the activity of the Ca²⁺-dependent protease m-calpain. TRPM7 has also been implicated in cell motility^[76]. Knockdown of TRPM7 by RNA interference reduced the number of high Ca²⁺ micro-domains induced by platelet-deprived growth factor (PDGF) and disrupted the turning of migrating WI-38 fibroblasts.

It has also been suggested that TRPM7 is involved in the neurotransmitter release by mediating Ca²⁺ influx^[49]. In primary rat superior cervical ganglion neurons, TRPM7 is localized in the synaptic vesicles and interacts with synaptic vesicular snapin, synapsin 1 and synaptotagmin 1. Furthermore, there were some correlations between TRPM7 expression levels and quantal sizes, amplitudes and decay times of the excitatory postsynaptic potential (EPSPs). When TRPM7 specific siRNA was used to suppress endogenous TRPM7 in PC12 cells, acetylcholine-secreted-synaptic-like vesicle fusion was inhibited.

Pathophysiological relevance in cerebral ischemia and stroke

Unregulated monovalent or divalent cation influx is implicated in several different cellular mechanisms (*eg*, excitotoxicity, apoptosis, and oxidative stress) underlying neural cell death during ischemic periods of stroke^[61]. Since cation channels are the main pathways for cation influx from extracellular space, they are closely involved in neuronal cell death. Conventionally, Ca²⁺ permeable NMDA and AMPA receptor channels are widely accepted as the main pathways of Ca²⁺ entrance during ischemia as well as the promising therapeutic targets^[7, 8, 77]. Numerous clinical trials testing AETs in stroke patients, however, yielded disappointing outcomes. The shortcomings of AET led researchers to consider other non-glutamate dependent mechanisms^[10-14], such as non-specific cation channels including acid-sensing ion channels^[16, 17], TRP channels^[4, 7, 18-21], hemichannels^[22-24], volume-regulated anion channels^[25], sodium-calcium exchangers^[26, 27] and non-selective cation channels^[28].

Previous studies demonstrated pathophysiological involvement of TRPM7 in stroke from *in vitro* data. When primary cultured cortical neurons were subjected to oxygen-glucose deprivation (OGD) for a prolonged period, there was an increase in ROS production, a Ca²⁺ influx mediated by TRPM7 and cell deaths^[21]. When the primary mouse cortical neurons were transfected with siRNA vector directed against TRPM7, the TRPM7 mRNA expression was suppressed, ROS-mediated activation was inhibited and subsequent cell death under anoxia was reduced. Such effects were consistently shown with cocktail of blockers for glutamate NMDA and AMPA receptor and L-type calcium channels (MK-801, CNQX, and nimodipine), indicating the independent role of TRPM7 in mediating intracellular Ca²⁺ elevation and subsequent cell death during the prolonged anoxia. In another study, the contribution of TRPM7 channels in cell membrane depolarization, intracellular Ca²⁺ accumulation and cell swelling during the

initial period of brain ischemia is also observed in native CA1 neurons of brain slices^[78].

TRPM7 *in vivo* studies have been scarce for a period of time because both the knockout model and selective pharmacological agents are not available. Eventually, a report demonstrated *in vivo* changes in TRPM7 channels during focal ischemia. Jiang and colleagues^[48] studied the interaction of nerve growth factor (NGF) with TRPM7 channels using both *in vivo* cerebral ischemia-reperfusion and *in vitro* OGD models. NGF, a neurotrophic factor, showed neuroprotective effects during ischemia. In their *in vivo* model, middle cerebral artery occlusion (MCAO) was performed on rats for 1 h and it was followed by reperfusion that lasted for 5, 10, 20, and 30 h. Both mRNA and protein levels of TRPM7 were up-regulated compared with pre-ischemia, peaking at 20 h after the reperfusion with about 2-3 fold increase. Given that there are increases in both mRNA and protein levels of TRPM7, up-regulation of the channels may be another mechanism that increases TRPM7-like current. Interestingly, these expression levels of TRPM7 were close to the normal level when 500 ng of NGF was applied 30 min before ischemia. The effects of NGF on TRPM7, however, disappeared when NGF was introduced after K252a, which is an inhibitor for the NGF-activated TrkA pathway. When wortmannin, which is an inhibitor for phosphatidylinositol-3 kinase (PI-3K) signal pathway, was applied, NGF effects were also abolished. These findings indicate that TRPM7 may be involved in neuronal cell damage *in vivo* during ischemia.

Recently, Sun and colleagues^[4] demonstrated that suppression of TRPM7 channels *in vivo* reduced neuronal cell death and preserved functions after global cerebral ischemia. The study used virally mediated gene silencing with shRNA to knockdown TRPM7 channels in hippocampal CA1 pyramidal neurons of adult rat brains. The viral vectors were delivered *in vivo* using stereotaxic microinjection to CA1 area. First, the authors showed that infecting adult hippocampal CA1 neurons *in vivo* was feasible by using the adeno-associated viral vectors (AAV serotype-1). Secondly, suppression of TRPM7 channels was convincingly demonstrated by measuring: 1) mRNA level in conjunction with the Laser Capture Microdissection for infected hippocampal CA1 cells; 2) protein level with both Western Blot and immunohistochemistry in conjunction with Laser Confocal microscope; and 3) functional level with electrophysiology. Thirdly, the injected viral vectors and transient suppression of TRPM7 channels in the adult rat brains *in vivo* showed no ill effects on cell survival, neuronal and dendritic morphology, neuronal excitability, or synaptic plasticity. Finally, they showed that following fifteen minutes of global cerebral ischemia induced by occluding both common carotid and vertebral arteries, TRPM7 suppression reduced hippocampal CA1 neuronal death *in vivo* and preserved functional outcomes after stroke. The survived neurons preserved their morphological integrity and fine structures, and even maintained their electrophysiological properties (LTP) and hippocampal-dependent behaviours, such as fear-associated and spatial-navigation memory tasks. This is

the first *in vivo* evidence showing the important role of TRPM7 channel in mediating ischemic neuronal cell death in stroke.

Working model of TRPM7 activation during cerebral ischemia

During the initial phase of an ischemic attack, a strong NMDA receptor activation leads to a large influx of Ca^{2+} , and the resulting Ca^{2+} directly stimulates (i) production of nitric oxide (NO) by neuronal nitric oxide synthase (NOS) and (ii) production of superoxide (O_2^-) from mitochondria^[17-19]. When NO and O_2^- are combined, highly reactive species peroxynitrite (ONOO^-) form. Along with other factors, such as decreases in pH and extracellular divalents, that are associated with ischemic episodes, ONOO^- enhances TRPM7 activation. This completes the lethal positive feedback loop of free radical production. In this model, the failure of AET could be partly explained: AET could delay the process but insufficient to ultimately prevent lethal TRPM7 activation (Figure 2).

TRPM7 channels may also be involved in the ischemic lethal process by conducting metal ions other than Ca^{2+} . For instance, Zn^{2+} , which is the most permeable trace ion through TRPM7, is highly toxic to cells if its concentration exceeds the physiological level^[79, 80] and has been implicated in cerebral ischemia. After the brief global ischemic insults, a delayed increase in intracellular Zn^{2+} is observed before cell death in some selective hippocampal CA1 neurons^[81]. Increases in intracellular Zn^{2+} and neuronal cell death were prevented with the application of the membrane-impermeable zinc-chelator calcium-EDTA (calcium-ethylenediaminetetraacetic acid) before the ischemia. Recently, it has been shown that Zn^{2+} -induced neurotoxicity may be mediated by TRPM7^[82]. Both Zn^{2+} -mediated neurotoxicity and neuronal injury associated with oxygen-glucose deprivation (OGD) were reduced by non-specific blockers (Gd^{3+} and 2-APB) and knockdown of TRPM7 by siRNA. Overexpression of TRPM7 in HEK-293 cells led to increase in intracellular Zn^{2+} accumulation and Zn^{2+} -mediated

cell deaths.

Clinical potentials and therapeutic perspectives

To date, therapeutic intervention for stroke is very scarce. The only approved treatment of acute ischemic stroke by the US Food and Drug Administration (FDA) is the tissue plasminogen activator (tPA), which relieves vascular occlusion by dissolving clots^[83]. Although tPA is a potent treatment for stroke, the usage and effectiveness of tPA are still limited by its short therapeutic window, and intrinsic toxicity. With disappointing preliminary clinical results from drugs targeting glutamate-induced excitotoxicity, considerable efforts have been put into searching for alternative targets.

Several lines of evidence support our hypothesis that TRPM7 is involved in ischemic stroke^[77]. Even though findings from cellular and animal studies are compelling, TRP channels should be studied in their native cellular environment, as the specific cellular environment and expression levels seem to be important for the normal physiological functions. It would be necessary to validate their diverse physiological and pathophysiological functions using *in vivo* animal models. For *in vivo* studies, developing tissue-specific or inducible TRPM7 knockout models will be useful as the conventional TRPM7 knockout mouse is not viable^[62, 63].

Without the development of specific pharmacological modulators of TRPM7, we do not expect to see any preliminary clinical trials in the near future. At the initial stage of most drug development, potential therapeutic targets are first identified, and experimental high-throughput screening (HTS) is used to narrow down the drug candidates that bind to the targets and changes their activities^[84]. Hence, in order to design specific and potent inhibitors, it is important to understand their molecular or structural properties in detail^[84, 85]. This is especially true for TRPM7, which seems to have conflicting roles in cell death and cellular survival^[4, 21, 62]. It may be the case that TRPM7 function would have to be regulated sepa-

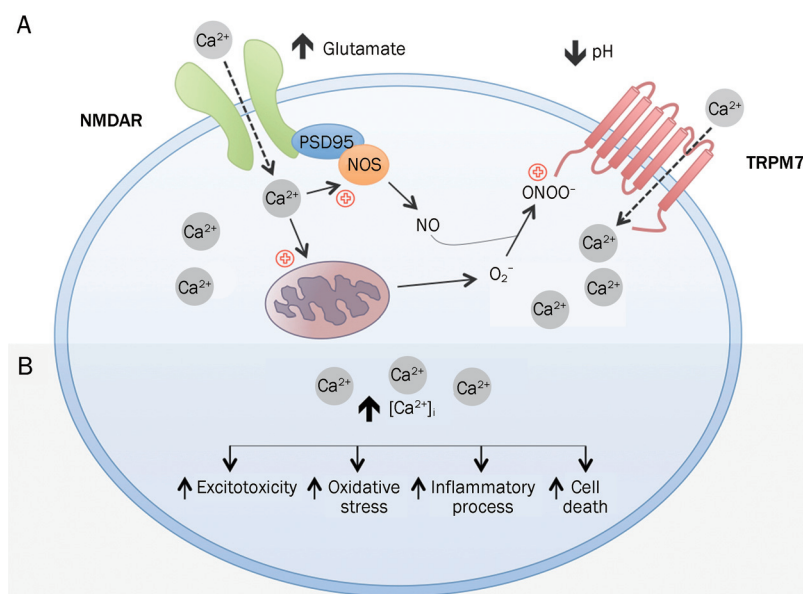


Figure 2. Working model of TRPM7 activation during cerebral ischemia. (A) During the early phase of an ischemic attack, an increase in the extracellular glutamate activates NMDA receptors. Ca^{2+} influx due to activated NMDA receptors stimulates: (i) production of nitric oxide (NO) by nitric oxide synthase (NOS) and (ii) production of superoxide (O_2^-) from mitochondria. NO and O_2^- combine to produce highly reactive species peroxynitrite (ONOO^-). Along with factors, such as decrease in pH, that are associated with ischemia, these free radicals promote sustained activation of TRPM7, which leads to further Ca^{2+} build-up in the intracellular space. (B) Consequences of unchecked Ca^{2+} influx. Increased intracellular Ca^{2+} concentration may lead to excitotoxicity, oxidative stress, inflammatory processes and eventual cell death.

rately, either enhanced or depressed, in different tissues for the prevention of cerebral ischemia and stroke. For instance, Touyz and colleagues^[86] have shown that reduced Mg^{2+} influx in cultured vascular smooth muscle cells (VSMCs) of the spontaneously hypertensive rat (SHR) is associated with down-regulation of TRPM7. Furthermore in the normotensive Wistar-Kyoto rat, TRPM7 expression and activity in VSMCs of the SHR were attenuated by angiotensin II. Since hypertension is a well-known risk factor for cerebral ischemia and stroke, it suggests that TRPM7 channels may enhance cerebral ischemia and stroke by regulation of Mg^{2+} homeostasis^[87]. However, either supplement or depletion of Mg^{2+} showed no effect on hypertension, thus questioning the role of TRPM7 in vasculature regulation^[87]. In contrast, reduction of TRPM7 expression prevented cerebral ischemia and stroke^[4] indicating TRPM7 may play a differential role in vascular smooth muscle cells and neurons. Further investigation is required to evaluate pathophysiological roles of TRPM7 channels in different cell types. Therefore, designing activity-dependent antagonists that preferentially target TRPM7 during stroke is critical in the future study. Understanding its temporal, spatial expressions and interactions with other proteins may aid the development of selective drugs for modulating TRPM7 activity.

When specific TRPM7 channel modulators are developed, these might be added in combination therapy for cerebral ischemic stroke in future. Now it is suspected that, although the recruitment of NMDARs is the key event in the early phase of cell death cascades in cerebral ischemia, there is also progressive recruitment of other non-selective cation channels, such as TRPM7, in the later stages. Based on this hypothesis, combination therapy, which includes drugs that are applied at empirically determined time points for each target, will be more effective in providing neuroprotection and potentially facilitating the recovery of function.

TRPM7 genetic variants may be related to various human diseases. For instance, heterologously expressed T1482I TRPM7 variant was found in a subset of ALS-G (Guamanian amyotrophic lateral sclerosis) and PD-G (Parkinsonism dementia) patients^[59]. The mutation resulted in an increase in sensitivity of the channels to intracellular Mg^{2+} -mediated inhibition, thus the patients were more vulnerable to the diseases^[59]. No test has been performed related to the risk assessment of ischemic stroke. Romero and colleagues^[88], recently conducted a prospective, nested case-control investigation to evaluate the associations of TRPM7 gene variations with the risk of ischemic stroke, and showed that 16 tag-single-nucleotide TRPM7 polymorphisms from 259 Caucasian men had no direct association with the risk assessment of ischemic stroke. However, no test has been done to suggest whether these TRPM7 mutants have neither dysfunction nor abnormality of the expression level of the channels. Thus, these human studies lead to no conclusion between TRPM7 activation and cerebral stroke. Further study is needed to fully understand the biophysical properties of the TRPM7 polymorphisms. Such information will dramatically contribute to our current understanding of the pathophysiological role of TRPM7 in

cerebral ischemia and stroke.

Conclusions

With the failure of using NMDA and AMPA antagonists in clinical trials for stroke treatment, other non-glutamate mechanisms to ischemic cell death have been rigorously investigated. Such disappointing clinical outcomes may originate from the insufficient understanding of non-glutamate mechanisms and their molecular cascades involved in stroke, problems in drug development, delivery of drugs, side effects of drug, or limited time windows for treatment. While the compelling findings from both *in vitro* and *in vivo* studies indicate the involvement of TRPM7 channels in ischemic neuronal injury, further extensive preclinical testing is required to assess the therapeutic potential of the TRPM7 blockade in stroke.

References

- 1 Goldstein LB, Bushnell CD, Adams RJ, Appel LJ, Braun LT, Chaturvedi S, et al. Guidelines for the primary prevention of stroke: a guideline for healthcare professionals from the American Heart Association/American Stroke Association. *Stroke* 2011; 42: 517–84.
- 2 Carandang R, Seshadri S, Beiser A, Kelly-Hayes M, Kase CS, Kannel WB, et al. Trends in incidence, lifetime risk, severity, and 30-day mortality of stroke over the past 50 years. *JAMA* 2006; 296: 2939–46.
- 3 Davis SM, Lees KR, Albers GW, Diener HC, Markabi S, Karlsson G, et al. Selfotel in acute ischemic stroke: possible neurotoxic effects of an NMDA antagonist. *Stroke* 2000; 31: 347–54.
- 4 Sun HS, Jackson MF, Martin LJ, Jansen K, Teves L, Cui H, et al. Suppression of hippocampal TRPM7 protein prevents delayed neuronal death in brain ischemia. *Nat Neurosci* 2009; 12: 1300–7.
- 5 Lipton P. Ischemic cell death in brain neurons. *Physiol Rev* 1999; 79: 1431–568.
- 6 Sattler R, Tymianski M. Molecular mechanisms of calcium-dependent excitotoxicity. *J Mol Med* 2000; 78: 3–13.
- 7 Macdonald J, Xiong Z, Jackson M. Paradox of Ca^{2+} signaling, cell death and stroke. *Trends Neurosci* 2006; 29: 75–81.
- 8 Choi DW. Glutamate neurotoxicity and diseases of the nervous system. *Neuron* 1988; 1: 623–34.
- 9 Horn J, Limburg M. Calcium antagonists for acute ischemic stroke. *Cochrane Database Syst Rev* 2000; (2): CD001928.
- 10 Tymianski M, Charlton MP, Carlen PL, Tator CH. Secondary Ca^{2+} overload indicates early neuronal injury which precedes staining with viability indicators. *Brain Res* 1993; 607: 319–23.
- 11 Manev H, Favaron M, Guidotti A, Costa E. Delayed increase of Ca^{2+} influx elicited by glutamate: role in neuronal death. *Mol Pharmacol* 1989; 36: 106–12.
- 12 Randall RD, Thayer SA. Glutamate-induced calcium transient triggers delayed calcium overload and neurotoxicity in rat hippocampal neurons. *J Neurosci* 1992; 12: 1882–95.
- 13 Lee JM, Zipfel GJ, Choi DW. The changing landscape of ischaemic brain injury mechanisms. *Nature* 1999; 399: A7–14.
- 14 Wahlgren NG, Ahmed N. Neuroprotection in cerebral ischaemia: facts and fancies — the need for new approaches. *Cerebrovasc Dis* 2004; 17: 153–66.
- 15 Fisher M. New approaches to neuroprotective drug development. *Stroke* 2011; 42: S24–7.
- 16 Xiong ZG, Zhu XM, Chu XP, Minami M, Hey J, Wei WL, et al. Neuroprotection in ischemia: blocking calcium-permeable acid-sensing ion

- channels. *Cell* 2004; 118: 687–98.
- 17 Xiong ZG, Chu XP, Simon RP. Ca^{2+} -permeable acid-sensing ion channels and ischemic brain injury. *J Membr Biol* 2006; 209: 59–68.
- 18 McNulty S, Fonfria E. The role of TRPM channels in cell death. *Pflugers Arch* 2005; 451: 235–42.
- 19 Aarts MM, Tymianski M. TRPMs and neuronal cell death. *Pflugers Arch* 2005; 451: 243–9.
- 20 Aarts MM, Tymianski M. TRPM7 and ischemic CNS injury. *Neuroscientist* 2005; 11: 116–23.
- 21 Aarts M, Iihara K, Wei WL, Xiong ZG, Arundine M, Cerwinski W, et al. A key role for TRPM7 channels in anoxic neuronal death. *Cell* 2003; 115: 863–77.
- 22 Thompson RJ, Zhou N, MacVicar BA. Ischemia opens neuronal gap junction hemichannels. *Science* 2006; 312: 924–7.
- 23 de Pina-Benabou MH, Szostak V, Kyrozis A, Rempe D, Uziel D, Urban-Maldonado M, et al. Blockade of gap junctions *in vivo* provides neuroprotection after perinatal global ischemia. *Stroke* 2005; 36: 2232–7.
- 24 Oguro K, Jover T, Tanaka H, Lin Y, Kojima T, Oguro N, et al. Global ischemia-induced increases in the gap junctional proteins connexin 32 (Cx32) and Cx36 in hippocampus and enhanced vulnerability of Cx32 knock-out mice. *J Neurosci* 2001; 21: 7534–42.
- 25 Liu HT, Tashmukhamedov BA, Inoue H, Okada Y, Sabirov RZ. Roles of two types of anion channels in glutamate release from mouse astrocytes under ischemic or osmotic stress. *Glia* 2006; 54: 343–57.
- 26 Matsuda T, Arakawa N, Takuma K, Kishida Y, Kawasaki Y, Sakaue M, et al. SEA0400, a novel and selective inhibitor of the Na^+ - Ca^{2+} exchanger, attenuates reperfusion injury in the *in vitro* and *in vivo* cerebral ischemic models. *J Pharmacol Exp Ther* 2001; 298: 249–56.
- 27 Pignataro G, Tortiglione A, Scorziello A, Giaccio L, Secondo A, Severino B, et al. Evidence for a protective role played by the Na^+ / Ca^{2+} exchanger in cerebral ischemia induced by middle cerebral artery occlusion in male rats. *Neuropharmacology* 2004; 46: 439–48.
- 28 Simard JM, Chen M, Tarasov KV, Bhatta S, Ivanova S, Melnitchenko L, et al. Newly expressed SUR1-regulated NC(Ca-ATP) channel mediates cerebral edema after ischemic stroke. *Nat Med* 2006; 12: 433–40.
- 29 Recommendations for standards regarding preclinical neuroprotective and restorative drug development. *Stroke* 1999; 30: 2752–8.
- 30 Moran M, Xu H, Clapham D. TRP ion channels in the nervous system. *Curr Opin Neurobiol* 2004; 14: 362–69.
- 31 Pedersen S, Owsianik G, Nilius B. TRP channels: an overview. *Cell Calcium* 2005; 38: 233–52.
- 32 Ramsey IS, Delling M, Clapham DE. An Introduction to TRP channels. *Annu Rev Physiol* 2006; 68: 619–47.
- 33 Wu LJ, Sweet TB, Clapham DE. International Union of Basic and Clinical Pharmacology. LXXVI. Current progress in the mammalian TRP ion channel family. *Pharmacol Rev* 2010; 62: 381–404.
- 34 Montell C, Rubin GM. Molecular characterization of the *Drosophila trp* locus: a putative integral membrane protein required for phototransduction. *Neuron* 1989; 2: 1313–23.
- 35 Nadler MJ, Hermosura MC, Inabe K, Perraud AL, Zhu Q, Stokes AJ, et al. LTRPC7 is a Mg^{2+} -ATP-regulated divalent cation channel required for cell viability. *Nature* 2001; 411: 590–5.
- 36 Clapham DE. TRP channels as cellular sensors. *Nature* 2003; 426: 517–24.
- 37 Mei ZZ, Xia R, Beech DJ, Jiang LH. Intracellular coiled-coil domain engaged in subunit interaction and assembly of melastatin-related transient receptor potential channel 2. *J Biol Chem* 2006; 281: 38748–56.
- 38 Yamaguchi H, Matsushita M, Nairn AC, Kuriyan J. Crystal structure of the atypical protein kinase domain of a TRP channel with phosphotransferase activity. *Mol Cell* 2001; 7: 1047–57.
- 39 Schmitz C, Perraud AL, Johnson CO, Inabe K, Smith MK, Penner R, et al. Regulation of vertebrate cellular Mg^{2+} homeostasis by TRPM7. *Cell* 2003; 114: 191–200.
- 40 Kozak JA, Cahalan MD. MIC channels are inhibited by internal divalent cations but not ATP. *Biophys J* 2003; 84: 922–7.
- 41 Demeuse P, Penner R, Fleig A. TRPM7 channel is regulated by magnesium nucleotides via its kinase domain. *J Gen Physiol* 2006; 127: 421–34.
- 42 Fonfria E, Murdock PR, Cusdin FS, Benham CD, Kelsell RE, McNulty S. Tissue distribution profiles of the human TRPM cation channel family. *J Recept Signal Transduct Res* 2006; 26: 159–78.
- 43 Runnels LW, Yue L, Clapham DE. TRP-PLIK, a bifunctional protein with kinase and ion channel activities. *Science* 2001; 291: 1043–7.
- 44 Kunert-Keil C, Bisping F, Kruger J, Brinkmeier H. Tissue-specific expression of TRP channel genes in the mouse and its variation in three different mouse strains. *BMC Genomics* 2006; 7: 159.
- 45 Clark K, Langeslag M, van Leeuwen B, Ran L, Ryazanov AG, Figdor CG, et al. TRPM7, a novel regulator of actomyosin contractility and cell adhesion. *EMBO J* 2006; 25: 290–301.
- 46 Yogi A, Callera GE, Tostes R, Touyz RM. Bradykinin regulates calpain and proinflammatory signaling through TRPM7-sensitive pathways in vascular smooth muscle cells. *Am J Physiol Regul Integr Comp Physiol* 2009; 296: R201–7.
- 47 Wei WL, Sun HS, Olah ME, Sun X, Czerwinska E, Czerwinski W, et al. TRPM7 channels in hippocampal neurons detect levels of extracellular divalent cations. *Proc Natl Acad Sci U S A* 2007; 104: 16323–8.
- 48 Jiang H, Tian SL, Zeng Y, Li LL, Shi J. TrkA pathway(s) is involved in regulation of TRPM7 expression in hippocampal neurons subjected to ischemic-reperfusion and oxygen-glucose deprivation. *Brain Res Bull* 2008; 76: 124–30.
- 49 Krapivinsky G, Mochida S, Krapivinsky L, Cibulsky SM, Clapham DE. The TRPM7 ion channel functions in cholinergic synaptic vesicles and affects transmitter release. *Neuron* 2006; 52: 485–96.
- 50 Penner R, Fleig A. The Mg^{2+} and Mg^{2+} -nucleotide-regulated channel-kinase TRPM7. *Handb Exp Pharmacol* 2007; (179): 313–28.
- 51 Monteilh-Zoller MK, Hermosura MC, Nadler MJ, Scharenberg AM, Penner R, Fleig A. TRPM7 provides an ion channel mechanism for cellular entry of trace metal ions. *J Gen Physiol* 2003; 121: 49–60.
- 52 Jiang J, Li M, Yue L. Potentiation of TRPM7 inward currents by protons. *J Gen Physiol* 2005; 126: 137–50.
- 53 Li M, Du J, Jiang J, Ratzan W, Su LT, Runnels LW, et al. Molecular determinants of Mg^{2+} and Ca^{2+} permeability and pH sensitivity in TRPM6 and TRPM7. *J Biol Chem* 2007; 282: 25817–30.
- 54 Jiang J, Li MH, Inoue K, Chu XP, Seeds J, Xiong ZG. Transient receptor potential melastatin 7-like current in human head and neck carcinoma cells: role in cell proliferation [Research Support, NIH, Extramural]. *Cancer Res* 2007; 67: 10929–38.
- 55 Numata T, Okada Y. Proton conductivity through the human TRPM7 channel and its molecular determinants. *J Biol Chem* 2008; 283: 15097–103.
- 56 Rehncrona S. Brain acidosis. *Ann Emerg Med* 1985; 14: 770–6.
- 57 Oancea E, Wolfe JT, Clapham DE. Functional TRPM7 channels accumulate at the plasma membrane in response to fluid flow. *Circ Res* 2006; 98: 245–53.
- 58 Runnels LW, Yue L, Clapham DE. The TRPM7 channel is inactivated by PIP(2) hydrolysis. *Nat Cell Biol* 2002; 4: 329–36.
- 59 Hermosura MC, Nayakanti H, Dorovkov MV, Calderon FR, Ryazanov AG, Haymer DS, et al. A TRPM7 variant shows altered sensitivity to magnesium that may contribute to the pathogenesis of two Guamanian neurodegenerative disorders. *Proc Natl Acad Sci U S A* 2005; 102: 11510–5.

- 60 Schmitz C, Dorovkov MV, Zhao X, Davenport BJ, Ryazanov AG, Perraud AL. The channel kinases TRPM6 and TRPM7 are functionally nonredundant. *J Biol Chem* 2005; 280: 37763–71.
- 61 Simard JM, Tarasov KV, Gerzanich V. Non-selective cation channels, transient receptor potential channels and ischemic stroke. *Biochim Biophys Acta* 2007; 1772: 947–57.
- 62 Jin J, Desai BN, Navarro B, Donovan A, Andrews NC, Clapham DE. Deletion of *Trpm7* disrupts embryonic development and thymopoiesis without altering Mg^{2+} homeostasis. *Science* 2008; 322: 756–60.
- 63 Ryazanova LV, Rondon LJ, Zierler S, Hu Z, Galli J, Yamaguchi TP, *et al*. TRPM7 is essential for Mg^{2+} homeostasis in mammals. *Nat Commun* 2010; 1: 109.
- 64 Inoue K, Xiong ZG. Silencing TRPM7 promotes growth/proliferation and nitric oxide production of vascular endothelial cells via the ERK pathway. *Cardiovasc Res* 2009; 83: 547–57.
- 65 He Y, Yao G, Savoia C, Touyz RM. Transient receptor potential melastatin 7 ion channels regulate magnesium homeostasis in vascular smooth muscle cells: role of angiotensin II. *Circ Res* 2005; 96: 207–15.
- 66 Kim BJ, Lim HH, Yang DK, Jun JY, Chang IY, Park CS, *et al*. Melastatin-type transient receptor potential channel 7 is required for intestinal pacemaking activity. *Gastroenterology* 2005; 129: 1504–17.
- 67 Numata T, Shimizu T, Okada Y. TRPM7 is a stretch- and swelling-activated cation channel involved in volume regulation in human epithelial cells. *Am J Physiol Cell Physiol* 2007; 292: C460–7.
- 68 Li M, Jiang J, Yue L. Functional characterization of homo- and heteromeric channel kinases TRPM6 and TRPM7. *J Gen Physiol* 2006; 127: 525–37.
- 69 Chen HC, Xie J, Zhang Z, Su LT, Yue L, Runnels LW. Blockade of TRPM7 channel activity and cell death by inhibitors of 5-lipoxygenase. *PLoS ONE* 2010; 5: e11161.
- 70 Jatana M, Giri S, Ansari MA, Elango C, Singh AK, Singh I, *et al*. Inhibition of NF- κ B activation by 5-lipoxygenase inhibitors protects brain against injury in a rat model of focal cerebral ischemia. *J Neuroinflammation* 2006; 3: 12.
- 71 Adamek A, Jung S, Dienesch C, Laser M, Ertl G, Bauersachs J, *et al*. Role of 5-lipoxygenase in myocardial ischemia-reperfusion injury in mice. *Eur J Pharmacol* 2007; 571: 51–4.
- 72 Abed E, Moreau R. Importance of melastatin-like transient receptor potential 7 and cations (magnesium, calcium) in human osteoblast-like cell proliferation. *Cell Prolif* 2007; 40: 849–65.
- 73 Hanano T, Hara Y, Shi J, Morita H, Umebayashi C, Mori E, *et al*. Involvement of TRPM7 in cell growth as a spontaneously activated Ca^{2+} entry pathway in human retinoblastoma cells. *J Pharmacol Sci* 2004; 95: 403–19.
- 74 Elizondo MR, Arduini BL, Paulsen J, MacDonald EL, Sabel JL, Henion PD, *et al*. Defective skeletogenesis with kidney stone formation in dwarf zebrafish mutant for TRPM7. *Curr Biol* 2005; 15: 667–71.
- 75 Su LT, Agapito MA, Li M, Simonson WT, Huttenlocher A, Habas R, *et al*. TRPM7 regulates cell adhesion by controlling the calcium-dependent protease calpain. *J Biol Chem* 2006; 281: 11260–70.
- 76 Wei C, Wang X, Chen M, Ou-Yang K, Song LS, Cheng H. Calcium flickers steer cell migration. *Nature* 2009; 457: 901–5.
- 77 Besancon E, Guo S, Lok J, Tymianski M, Lo EH. Beyond NMDA and AMPA glutamate receptors: emerging mechanisms for ionic imbalance and cell death in stroke. *Trends Pharmacol Sci* 2008; 29: 268–75.
- 78 Lipski J, Park TI, Li D, Lee SC, Trevarton AJ, Chung KK, *et al*. Involvement of TRP-like channels in the acute ischemic response of hippocampal CA1 neurons in brain slices. *Brain Res* 2006; 1077: 187–99.
- 79 Lee JM, Grabb MC, Zipfel GJ, Choi DW. Brain tissue responses to ischemia. *J Clin Invest* 2000; 106: 723–31.
- 80 Lee JM, Zipfel GJ, Park KH, He YY, Hsu CY, Choi DW. Zinc translocation accelerates infarction after mild transient focal ischemia. *Neuroscience* 2002; 115: 871–8.
- 81 Koh JY, Suh SW, Gwag BJ, He YY, Hsu CY, Choi DW. The role of zinc in selective neuronal death after transient global cerebral ischemia. *Science* 1996; 272: 1013–6.
- 82 Inoue K, Branigan D, Xiong ZG. Zinc-induced neurotoxicity mediated by transient receptor potential melastatin 7 channels. *J Biol Chem* 2010; 285: 7430–9.
- 83 Bambauer KZ, Johnston SC, Bambauer DE, Zivin JA. Reasons why few patients with acute stroke receive tissue plasminogen activator. *Arch Neurol* 2006; 63: 661–4.
- 84 Jorgensen WL. The many roles of computation in drug discovery. *Science* 2004; 303: 1813–8.
- 85 Zheng C, Han L, Yap CW, Xie B, Chen Y. Progress and problems in the exploration of therapeutic targets. *Drug Discov Today* 2006; 11: 412–20.
- 86 Touyz RM, He Y, Montezano AC, Yao G, Chubonov V, Gudermann T, *et al*. Differential regulation of transient receptor potential melastatin 6 and 7 cation channels by ANG II in vascular smooth muscle cells from spontaneously hypertensive rats. *Am J Physiol Regul Integr Comp Physiol* 2006; 290: R73–8.
- 87 Yogi A, Callera GE, Antunes TT, Tostes RC, Touyz RM. Transient receptor potential melastatin 7 (TRPM7) cation channels, magnesium and the vascular system in hypertension. *Circ J* 2011; 75: 237–45.
- 88 Romero JR, Ridker PM, Zee RY. Gene variation of the transient receptor potential cation channel, subfamily M, member 7 (TRPM7), and risk of incident ischemic stroke: prospective, nested, case-control study. *Stroke* 2009; 40: 2965–8.

Review

Calcium-permeable ion channels involved in glutamate receptor-independent ischemic brain injury

Ming-hua LI¹, Koichi INOUE², Hong-fang SI³, Zhi-gang XIONG⁴, *

¹Department of Psychology, Washington State University, Vancouver, WA, USA; ²Department of Physiology, Hamamatsu University School of Medicine, Hamamatsu Shizuoka 431–3192, Japan; ³School of Pharmacy, Anhui Medical University, Hefei 230032, China; ⁴Neuroscience Institute, Morehouse School of Medicine, Atlanta, GA 30310, USA

Brain ischemia is a leading cause of death and long-term disabilities worldwide. Unfortunately, current treatment is limited to thrombolysis, which has limited success and a potential side effect of intracerebral hemorrhage. Searching for new cell injury mechanisms and therapeutic interventions has become a major challenge in the field. It has been recognized for many years that intracellular Ca²⁺ overload in neurons is essential for neuronal injury associated with brain ischemia. However, the exact pathway(s) underlying the toxic Ca²⁺ loading remained elusive. This review discusses the role of two Ca²⁺-permeable cation channels, TRPM7 and acid-sensing channels, in glutamate-independent Ca²⁺ toxicity associated with brain ischemia.

Keywords: acid-sensing ion channel; TRPM7; brain ischemia; neurons

Acta Pharmacologica Sinica (2011) 32: 734–740; doi: 10.1038/aps.2011.47; published online 9 May 2011

Introduction

Stroke or cerebral ischemia is a leading cause of death and long-term disabilities worldwide. Although major advances have occurred in the past decades in the prevention of brain ischemia, treatment is limited to the use of tissue plasminogen activator (tPA), which has limited success and a major side effect of intracranial hemorrhage^[1, 2]. Searching for new cell injury mechanisms and effective therapeutic strategies therefore constitutes a major challenge for stroke research.

It has been recognized for several decades that excessive Ca²⁺ entry and resultant cytosolic Ca²⁺ overload play an important role in neuronal injury associated with stroke/brain ischemia^[3]. In the resting condition, free intracellular Ca²⁺ concentration ([Ca²⁺]_i) is maintained at nanomolar levels. Following ischemia, [Ca²⁺]_i can reach as high as several micromoles. Excessive [Ca²⁺]_i loading can activate enzymes such as proteases, phospholipases, and endonucleases. Over-activation of these enzymes causes breakdown of proteins, lipids and nucleic acids, which leads to destruction of neurons^[4–6]. In addition, overloading Ca²⁺ in mitochondria can cause opening of mitochondria permeability transition pore (PTP), a large

conductance channel residing in mitochondrial membrane^[7, 8], promoting apoptosis through release of cytochrome *c* and activation of caspases^[9–11].

Ca²⁺ may enter neurons through various Ca²⁺-permeable ion channels (*eg* voltage-gated or ligand-gated channels) or through ion exchange systems (*eg* reverse Na⁺/Ca²⁺ exchanger). Accumulation of [Ca²⁺]_i can also occur through Ca²⁺ release from intracellular stores (*eg* endoplasmic reticulum, ER). The exact source(s) of Ca²⁺ loading responsible for ischemic brain injury, however, remains unclear. This review discusses the involvement of two novel Ca²⁺-permeable cation channels, TRPM7 channels and acid-sensing ion channels, in ischemic brain injury.

Glutamate mediated Ca²⁺-toxicity

Glutamate is the major excitatory neurotransmitter in the central nervous system (CNS)^[12–14]. Its receptors are widely expressed at soma and dendrites of the CNS neurons. Activation of these receptors is involved in a variety of physiological functions of neurons including synaptic transmission/plasticity, learning/memory, neuronal development and differentiation^[12, 15]. Glutamate receptors are classified into two major categories: ionotropic receptors, which are ligand-gated cation channels; and metabotropic receptors, which are coupled through G proteins to second messenger systems^[16].

* To whom correspondence should be addressed.

E-mail zxiong@msm.edu

Received 2011-03-13 Accepted 2011-04-11

One subtype of ionotropic glutamate receptors, the *N*-methyl-D-aspartate (or NMDA) receptor, is highly permeable to Ca^{2+} ions. Activation of these receptors has been considered to play a critical role in Ca^{2+} toxicity associated with ischemic brain injury^[3, 17-20]. Accordingly, blocking these receptors has been shown to be neuroprotective in cell culture and animal models of brain ischemia. Unfortunately, none of the human trials using the antagonists of glutamate receptors showed a satisfactory protection for stroke patients. Although multiple factors, including difficulty in early initiation of treatment and intolerance of severe side effects, may have contributed to the failure of the trials^[4, 21-24], recent studies suggest that Ca^{2+} entry through glutamate-independent pathways, *eg* TRPM7 channels and Ca^{2+} -permeable acid-sensing ion channels (ASICs), may contribute to the injury of neurons associated with brain ischemia.

TRPM channels and ischemic neuronal injury

Transient receptor potential (TRP) channels belong to a novel family of cation channels that are highly expressed in various tissues including the brain^[25, 26]. Several members of TRP family can be activated by oxidative stress and oxygen free radicals, both of which play important roles in neuronal injury associated with stroke/brain ischemia. Recent work has indicated that members of the melastatin subfamily (TRPM) of the TRP channels, particularly the TRPM7, play a key role in neuronal cell death associated with brain ischemia^[27-31].

The TRP superfamily is a diverse group of voltage-independent calcium-permeable cation channels expressed in mammalian cells^[25, 26]. These channels have been divided into six subfamilies, and two of them, TRPC and TRPM, have members that are widely expressed and activated by oxidative stress. TRPC3 and TRPC4 are activated by oxidants, which induce Na^+ and Ca^{2+} entry into cells through phospholipase C-dependent mechanisms. TRPM2 is activated by oxidative stress or TNF α , and the mechanism involves production of ADP-ribose, which binds to an ADP-ribose binding cleft in the TRPM2 C-terminus. Treatment of neurons or HEK 293T cells expressing TRPM2 with H_2O_2 resulted in Ca^{2+} influx and increased susceptibility to cell death^[27]. Inhibition of endogenous TRPM2 function, in contrast, protected cell viability^[27, 32]. Nevertheless, the exact role of TRPM2 in Ca^{2+} toxicity associated with ischemic brain injury remains to be explored.

The potential role of TRPM7 channels in ischemic neuronal death has been described recently^[30, 31]. Aarts and colleagues first examined the mechanism of neuronal cell death in ischemic conditions in the presence of glutamate antagonists. Cultured mouse cortical neurons were exposed to oxygen-glucose deprivation (OGD), an *in vitro* model of ischemia reported to mediate neuronal death through NMDA receptor activation^[33, 34]. Blocking the glutamate excitotoxicity in these cultures, however, unmasked a potent, previously unappreciated mechanism of non-excitotoxic neuronal cell death, which became increasingly responsible for neurodegeneration as the duration of OGD was prolonged^[30]. Further studies demonstrated that the mechanism of cell death involved activation

of a non-selective cation current with high permeability to Ca^{2+} . The current showed outward rectifying properties, was potentiated by reactive oxygen/nitrogen species (ROS), and was blocked by Gd^{3+} . The electrophysiological characteristics and pharmacological properties of the current suggested the involvement of TRPM7 channels. Indeed, molecular biological approaches (*eg* siRNA) confirmed the involvement of TRPM7 channels in glutamate-independent anoxic neuronal injury^[30]. Although a specific agonist remains to be determined, these studies suggest that, in ischemic conditions, TRPM7 channels could be activated by ROS. Ca^{2+} entry through these channels participates in neuronal injury. A lethal positive feedback loop is established when Ca^{2+} influx through TRPM7 channels stimulates additional ROS production, causing further TRPM7 activation^[30]. Blocking TRPM7 channels or suppressing its expression by RNA interference was effective in preventing the death of neurons by OGD.

Very recent studies by Sun and colleagues also demonstrated involvement of TRPM7 channels in the injury of hippocampal neurons *in vivo* in rat model of global ischemia^[31]. Suppressing TRPM7 expression in CA1 neurons by intrahippocampal injections of viral vectors bearing shRNA specific for TRPM7 channels had no ill effect on animal survival, neuronal and dendritic morphology, neuronal excitability, or synaptic plasticity. However, TRPM7 suppression made neurons resistant to ischemic injury and preserved neuronal morphology and function. Also, it prevented ischemia-induced deficits in long-term potentiation and preserved performance in fear-associated and spatial-navigational memory tasks. Thus, regional suppression of TRPM7 is feasible, well tolerated and inhibits delayed neuronal death *in vivo*. In addition to Ca^{2+} toxicity mediated by TRPM7 channels, studies by Inoue and colleagues have suggested that Zn^{2+} permeability of these channels also plays a role in ischemic brain injury^[35].

Acid-sensing ion channels and ischemic brain injury

In acute neurological conditions such as brain ischemia, marked reduction of tissue pH takes place^[36-41]. Following ischemia, shortage of oxygen supply promotes anaerobic glycolysis, leading to lactic acid accumulation and resultant decrease in brain pH^[42, 43]. Increased ATP hydrolysis and release of H^+ also contributes to pH drop. At the same time, cessation of local circulation results in carbon dioxide accumulation and carbonic acid build up, which may participate in the decrease of tissue pH^[39]. During ischemia, decreases of brain pH to ~6.5 are commonly observed. It can also fall to 6.0 or below during severe ischemia or under hyperglycemic conditions^[37, 40, 41, 44, 45].

Decrease of brain pH or acidosis has long been known to play an important role in ischemic brain injury^[39, 42, 43, 46-48]. A direct correlation between the degree of brain acidosis and infarct size has also been described^[39, 49]. However, the exact mechanism underlying acidosis-mediated neuronal injury remained vague. Acidosis may cause non-selective denaturation of proteins and nucleic acids^[50]; trigger cell swelling and osmolysis via stimulation of Na^+/H^+ and $\text{Cl}^-/\text{HCO}_3^-$ exchange-

ers^[51]; hinder postischemic metabolic recovery by inhibiting mitochondrial energy metabolism and impairing postischemic blood flow via vascular edema^[52]; or stimulate pathologic free radical formation^[53]. At the neurotransmitter level, profound acidosis inhibits astrocytic glutamate uptake, which may contribute to excitatory neuronal injury^[54].

Interestingly, mild acidosis has been considered to be beneficial in protecting neurons from excitotoxic injury^[55-57]. This may be explained by proton inhibition of NMDA channel activity^[58, 59]. In contrast to its modulating effect on other ion channels, protons can activate a distinct family of ligand-gated channels, the acid-sensing ion channels (ASICs)^[60-71]. ASICs belong to the amiloride-sensitive epithelial Na⁺-channel/degenerin (ENaC/Deg) superfamily^[60, 72], which are formed with homomultimeric or heteromultimeric subunits. Each subunit contains two transmembrane spanning regions (TM1 and TM2) flanked by a large cysteine-rich extracellular loop and short intracellular N and C termini^[60, 61, 73-78]. To date, four genes encoding seven ASIC subunits have been cloned and characterized. ASIC1a subunits (originally named ASIC or BNaC2) are widely expressed in peripheral sensory neurons and in CNS neurons^[61, 65, 79, 80]. Pertinent to brain ischemia, these channels are activated by moderate decreases of pH_o with a threshold pH of ~7.0 and a pH for half maximal activation (pH_{0.5}) at ~6.2^[61, 81]. In addition to Na⁺, homomeric ASIC1a channels are permeable to Ca²⁺ ions^[61, 82, 83]. ASIC1 β and its longer form variant ASIC1b are expressed only in sensory neurons^[84, 85]. Similar to ASIC1a, homomeric ASIC1 β channels have high sensitivity to H⁺ with a pH_{0.5} at ~5.9^[85]. Unlike ASIC1a, however, ASIC1b or ASIC1 β has no detectable Ca²⁺ permeability^[84, 85]. ASIC2a subunits (originally named MDEG, or BNaC1) have widespread distribution in both peripheral sensory and central neurons^[63, 79, 86]. However, homomeric ASIC2a channels have very low sensitivity to H⁺ with a pH_{0.5} of 4.4^[63, 86, 87]. It is unlikely that homomeric ASIC2a channels can be activated in any physiological or pathological conditions in the brain. Similarly, ASIC2b subunits (originally named MDEG2) are expressed in peripheral sensory and central neurons^[87]. However, they do not form functional homomeric channels, but may associate with other ASIC subunits (eg ASIC3) to form heteromultimeric channels^[87]. ASIC3 subunits (originally also named DRASIC) are predominantly expressed in neurons of dorsal root ganglia^[88, 89], though its expression in the brain has been reported^[90]. Homomeric ASIC3 channels respond to pH drops biphasically, with a fast desensitizing current followed by a sustained component^[88, 89, 91]. ASIC4 subunits are highly expressed in the pituitary gland^[92, 93]. Similar to ASIC2b, they do not seem to form functional homomeric channels^[93]. ASICs were initially believed to be assembled as tetramers^[61, 77]. However, recent analysis of crystal structure suggested that ASICs existed as trimers^[94].

ASICs in peripheral sensory neurons are implicated in nociception, mechanosensation, and taste transduction^[95-107]. The presence of ASICs in the brain, which lacks nociceptors, suggests that these channels have functions beyond nociception. Indeed, ASIC1a has been shown to be involved in

synaptic plasticity, learning and memory^[64, 108]. Both ASIC1a and ASIC2a are implicated in the maintenance of retinal integrity^[109-111]. In pathological conditions, activation of Ca²⁺-permeable ASIC1a is involved in glutamate-independent, acidosis mediated, ischemic brain injury^[71, 82, 112], and in axon degeneration associated with multiple sclerosis^[113]. In contrast, increased expression of ASIC2a is associated with neuronal survival following global ischemia^[114], while reduced expression of ASIC1a is associated with neuroprotection elicited by ischemic pre- and post-conditioning^[115].

The presence of ASIC1a in the brain, its activation by pH drops to the levels commonly seen during brain ischemia, and its permeability to Ca²⁺ make it a potential player in ischemic brain injury. A series of recent studies, performed *in vitro* in neuronal cell culture and *in vivo* in whole animal models of ischemia, have provided strong evidence supporting this hypothesis^[71, 82, 112]. In cultured neurons, for example, brief acid incubations induced significant neuronal injury. This acid-induced neuronal injury was glutamate-independent, but was inhibited by amiloride, a non-specific ASIC blocker, or PcTX1, a specific ASIC1a inhibitor. In contrast to the neurons from ASIC1^{+/+} mice, neurons cultured from ASIC1^{-/+} mice were resistant to acid injury. Reducing the concentration of extracellular Ca²⁺, which lowers the driving force for Ca²⁺ entry through ASICs, also decreased acid-induced injury of CNS neurons^[71, 82]. Thus, activation of ASICs, and subsequent Ca²⁺ entry, participates in acidosis-mediated injury of neurons.

While homomeric ASIC1a can conduct Ca²⁺, some studies have suggested that, a significant portion of acid-evoked increases of intracellular Ca²⁺ is not due to Ca²⁺ entry directly through ASIC1a homomers. Rather, acidosis might induce Ca²⁺ accumulation through secondary activation of voltage-gated Ca²⁺ channels due to ASIC-mediated membrane depolarization and/or Ca²⁺ release from intracellular stores^[116-118].

In vivo studies also support a role for ASIC1a activation in acidosis-mediated, ischemic brain injury^[71, 112, 119]. In rats and mice, intracerebral ventricular injection of ASIC1a inhibitors reduced the infarct volume by up to 60%. Similarly, ASIC1a gene knockout protected the mouse brain from ischemic injury. Furthermore, ASIC1a blockade and ASIC1 gene knockout provided additional protection in the presence of glutamate receptor antagonist^[71]. The protection by ASIC1a blockade has an effective time window of >5 h, and the protection persists for at least 7 d^[119]. Attenuating brain acidosis by intracerebroventricular administration of NaHCO₃ is also protective, further suggesting that acidosis is a mediator of ischemic brain injury.

Interactions between ASIC1a and hypoxia/ischemia related signals contribute to ischemic brain injury

In the normal condition, ASIC1a current desensitizes rapidly in the continuous presence of acidosis. This property of ASIC1a argues against its role in brain ischemia in which acidosis is, in general, long-lasting. Recent findings showing that the properties of ASICs, particularly the ASIC1a channels, can be dramatically modulated by ischemia per se and/

or ischemia-related signals have provided good explanation supporting the role of ASIC1a channels in ischemic brain injury^[71, 112, 120-122]. In cultured mouse cortical neurons, for example, brief OGD not only increased the amplitude but also reduced the desensitization of the ASIC current. Accordingly, OGD treatment enhanced acidosis-mediated neuronal injury^[71]. The cellular and molecular mechanisms underlying ischemia-induced increase of ASIC activity has been investigated extensively by several studies. Allen and Attwell demonstrated that arachidonic acid, a lipid metabolite released in ischemia, increased the amplitude of the ASIC current in rat cerebellar Purkinje neurons^[122]. Gao and colleagues demonstrated that an increased phosphorylation of ASIC1a channels by CaMKII, mediated by NMDA receptor activation, was involved in ischemia-induced enhancement of the ASIC responses^[112]. Sherwood and Askwith demonstrated that dynorphins, the most basic neuropeptides abundantly expressed in the central nervous system, could increase the activities of ASIC1a channels and enhance neuronal damage following ischemia^[120]. They do so by reducing the steady-state desensitization of the ASIC1a channels. Very recent studies by Duan and colleagues also showed that, spermine, one of the endogenous polyamines, exacerbated ischemic neuronal injury through sensitization of ASIC1a channels to extracellular acidosis^[121]. Spermine slows down the desensitization of these channels in the open state, shifting steady-state desensitization to more acidic pH, and accelerating recovery of the channels between repeated periods of acid stimulation. Thus, therapeutic interventions for brain ischemia may target ASICs directly by using ASIC blockers/inhibitors or indirectly by blocking the ischemia-related signals which enhance the activation of ASICs.

Perspectives

Stroke/brain ischemia is a leading health problem worldwide. Although in recent years enormous progresses have been made in the prevention of stroke, unfortunately, there is still no effective treatment for stroke patients. Searching for new cell injury mechanisms and effective therapeutic strategies is therefore a major challenge in the field. Brain ischemia initiates various biochemical changes such as increased glutamate release, production of oxygen free radicals, lactic acidosis, and reduced ATP synthesis, *etc.* These changes may facilitate the opening of various Ca²⁺-permeable ion channels such as glutamate-receptor-gated channels, voltage-gated Ca²⁺ channels, TRPM7 channels, acid-sensing ion channels, *etc.* Activation of these channels induces entry of Ca²⁺ and accumulation of intracellular Ca²⁺. Intracellular Ca²⁺ accumulation can also occur through other pathways, *eg* release of Ca²⁺ from intracellular stores, or entry of Ca²⁺ through reversed Na⁺/Ca²⁺ exchange system (Figure 1). Overload of neurons with Ca²⁺ activates a panel of enzymes including proteases, phospholipases and endonucleases, leading to destruction of neurons either through necrotic or apoptotic process. Targeting the pathways responsible for Ca²⁺ overload may lead to effective neuroprotective interventions for stroke patients. The recent

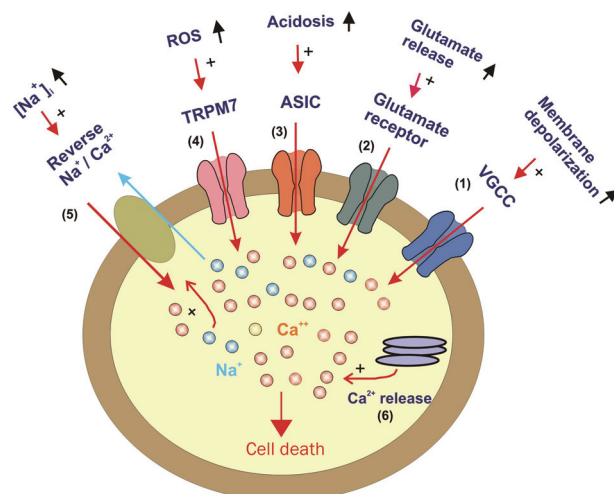


Figure 1. Potential pathways responsible for intracellular Ca²⁺ accumulation in neurons in ischemic condition. VGCC: voltage-gated Ca²⁺ channel; ASIC: acid-sensing ion channel; ROS: reactive oxygen species; TRPM7: transient receptor potential melastatin 7; Na⁺/Ca²⁺: sodium-calcium exchanger.

failure of clinical trials using the antagonists of glutamate receptors, however, suggests that future effort should also consider glutamate-independent Ca²⁺ toxicity in ischemia, *eg* through activation of TRPM7 channels or ASICs.

Acknowledgements

The work in author's laboratories were supported by grants from National Institute of Health (R01NS47506) and American Heart Association (0840132N)

References

- Weintraub MI. Thrombolysis (tissue plasminogen activator) in stroke: a medicolegal quagmire. *Stroke* 2006; 37: 1917-22.
- Wang X, Tsuji K, Lee SR, Ning M, Furie KL, Buchan AM, et al. Mechanisms of hemorrhagic transformation after tissue plasminogen activator reperfusion therapy for ischemic stroke. *Stroke* 2004; 35: 2726-30.
- Choi DW. Calcium-mediated neurotoxicity: relationship to specific channel types and role in ischemic damage. *Trends Neurosci* 1988; 11: 465-9.
- Lee JM, Zipfel GJ, Choi DW. The changing landscape of ischaemic brain injury mechanisms. *Nature* 1999; 399: A7-14.
- Simonian NA, Coyle JT. Oxidative stress in neurodegenerative diseases. *Annu Rev Pharmacol Toxicol* 1996; 36: 83-106.
- Coyle JT, Puttfarcken P. Oxidative stress, glutamate, and neurodegenerative disorders. *Science* 1993; 262: 689-95.
- Zoratti M, Szabo I. The mitochondrial permeability transition. *Biochim Biophys Acta* 1995; 1241: 139-76.
- Bernardi P, Colonna R, Costantini P, Eriksson O, Fontaine E, Ichas F, et al. The mitochondrial permeability transition. *Biofactors* 1998; 8: 273-81.
- Liu X, Kim CN, Yang J, Jemmerson R, Wang X. Induction of apoptotic program in cell-free extracts: requirement for dATP and cytochrome c. *Cell* 1996; 86: 147-57.
- Hengartner MO. The biochemistry of apoptosis. *Nature* 2000; 407:

- 770–6.
- 11 Polster BM, Fiskum G. Mitochondrial mechanisms of neural cell apoptosis. *J Neurochem* 2004; 90: 1281–9.
 - 12 Nakanishi S. Molecular diversity of glutamate receptors and implications for brain function. *Science* 1992; 258: 597–603.
 - 13 Curtis DR, Watkins JC. Acidic amino acids with strong excitatory actions on mammalian neurones. *J Physiol* 1963; 166: 1–14.
 - 14 Krnjevic K. Glutamate and gamma-aminobutyric acid in brain. *Nature* 1970; 228: 119–24.
 - 15 Gasic GP, Hollmann M. Molecular neurobiology of glutamate receptors. *Ann Rev Physiol* 1992; 54: 507–36.
 - 16 Hollmann M, Heinemann S. Cloned glutamate receptors. *Annu Rev Neurosci* 1994; 17: 31–108.
 - 17 Mori H, Mishina M. Structure and function of the NMDA receptor channel. *Neuropharmacology* 1995; 34: 1219–37.
 - 18 Sucher NJ, Awobuluyi M, Choi YB, Lipton SA. NMDA receptors: from genes to channels. *Trends Pharmacol Sci* 1996; 17: 348–55.
 - 19 Tymianski M, Charlton MP, Carlen PL, Tator CH. Source specificity of early calcium neurotoxicity in cultured embryonic spinal neurons. *J Neurosci* 1993; 13: 2085–104.
 - 20 Rothman SM, Olney JW. Excitotoxicity and the NMDA receptor – Still lethal after eight years. *Trends Neurosci* 1995; 18: 57–8.
 - 21 Gladstone DJ, Black SE, Hakim AM. Toward wisdom from failure: lessons from neuroprotective stroke trials and new therapeutic directions. *Stroke* 2002; 33: 2123–6.
 - 22 Ikonomidou C, Turski L. Why did NMDA receptor antagonists fail clinical trials for stroke and traumatic brain injury? *Lancet Neurol* 2002; 1: 383–6.
 - 23 Hoyte L, Barber PA, Buchan AM, Hill MD. The rise and fall of NMDA antagonists for ischemic stroke. *Curr Mol Med* 2004; 4: 131–6.
 - 24 Wahlgren NG, Ahmed N. Neuroprotection in cerebral ischaemia: facts and fancies—the need for new approaches. *Cerebrovasc Dis* 2004; 17: 153–66.
 - 25 Nilius B, Voets T. TRP channels: a TRP through a world of multi-functional cation channels. *Pflugers Arch* 2005; 451: 1–10.
 - 26 Venkatachalam K, Montell C. TRP channels. *Annu Rev Biochem* 2007; 76: 387–417.
 - 27 Kaneko S, Kawakami S, Hara Y, Wakamori M, Itoh E, Minami T, et al. A critical role of TRPM2 in neuronal cell death by hydrogen peroxide. *J Pharmacol Sci* 2006; 101: 66–76.
 - 28 Aarts MM, Tymianski M. TRPM7 and ischemic CNS injury. *Neuroscientist* 2005; 11: 116–23.
 - 29 Nicotera P, Bano D. The enemy at the gates. Ca²⁺ entry through TRPM7 channels and anoxic neuronal death. *Cell* 2003; 115: 768–70.
 - 30 Aarts M, Iihara K, Wei WL, Xiong ZG, Arundine M, Cerwinski W, et al. A key role for TRPM7 channels in anoxic neuronal death. *Cell* 2003; 115: 863–77.
 - 31 Sun HS, Jackson MF, Martin LJ, Jansen K, Teves L, Cui H, et al. Suppression of hippocampal TRPM7 protein prevents delayed neuronal death in brain ischemia. *Nat Neurosci* 2009; 12: 1300–7.
 - 32 Miller BA. The role of TRP channels in oxidative stress-induced cell death. *J Membr Biol* 2006; 209: 31–41.
 - 33 Kiedrowski L, Costa E, Wroblewski JT. Glutamate receptor agonists stimulate nitric oxide synthase in primary cultures of cerebellar granule cells. *J Neurochem* 1992; 58: 335–41.
 - 34 Grassi F, Giovannelli A, Fucile S, Eusebi F. Activation of the nicotinic acetylcholine receptor mobilizes calcium from caffeine-insensitive stores in C2C12 mouse myotubes. *Pflugers Arch* 1993; 422: 591–8.
 - 35 Inoue K, Branigan D, Xiong ZG. Zinc-induced neurotoxicity mediated by transient receptor potential melastatin 7 channels. *J Biol Chem* 2010; 285: 7430–9.
 - 36 Crowell JW, Kaufmann BN. Changes in tissue pH after circulatory arrest. *Am J Physiol* 1961; 200: 743–5.
 - 37 Ljunggren B, Norberg K, Siesjo BK. Influence of tissue acidosis upon restitution of brain energy metabolism following total ischemia. *Brain Res* 1974; 77: 173–86.
 - 38 Thorn W, Heitmann R. Hydrogen ion concentration of cerebral cortex of rabbit in situ during peracute total ischemia; pure anoxia and during recuperation. *Pflugers Arch* 1954; 258: 501–10.
 - 39 Siesjo BK. Acidosis and ischemic brain damage. *Neurochem Pathol* 1988; 9: 31–88.
 - 40 Rehnrcrona S. Brain acidosis. *Ann Emerg Med* 1985; 14: 770–6.
 - 41 Nedergaard M, Kraig RP, Tanabe J, Pulsinelli WA. Dynamics of interstitial and intracellular pH in evolving brain infarct. *Am J Physiol* 1991; 260: R581–R588.
 - 42 Siesjo BK, Katsura K, Kristian T. Acidosis-related damage. *Adv Neurol* 1996; 71: 209–33.
 - 43 Tombaugh GC, Sapolsky RM. Evolving concepts about the role of acidosis in ischemic neuropathology. *J Neurochem* 1993; 61: 793–803.
 - 44 Kraig RP, Pulsinelli WA, Plum F. Hydrogen ion buffering during complete brain ischemia. *Brain Res* 1985; 342: 281–90.
 - 45 Siemkowicz E, Hansen AJ. Brain extracellular ion composition and EEG activity following 10 minutes ischemia in normo- and hyperglycemic rats. *Stroke* 1981; 12: 236–40.
 - 46 Kraig RP, Petito CK, Plum F, Pulsinelli WA. Hydrogen ions kill brain at concentrations reached in ischemia. *J Cereb Blood Flow Metab* 1987; 7: 379–86.
 - 47 Kristian T, Katsura K, Gido G, Siesjo BK. The influence of pH on cellular calcium influx during ischemia. *Brain Res* 1994; 641: 295–302.
 - 48 Goldman SA, Pulsinelli WA, Clarke W Y, Kraig RP, Plum F. The effects of extracellular acidosis on neurons and glia *in vitro*. *J Cereb Blood Flow Metab* 1989; 9: 471–7.
 - 49 Back T, Hoehn M, Mies G, Busch E, Schmitz B, Kohno K, et al. Penumbra tissue alkalosis in focal cerebral ischemia: relationship to energy metabolism, blood flow, and steady potential. *Ann Neurol* 2000; 47: 485–92.
 - 50 Kalimo H, Rehnrcrona S, Soderfeldt B, Olsson Y, Siesjo BK. Brain lactic acidosis and ischemic cell damage: 2. Histopathology. *J Cereb Blood Flow Metab* 1981; 1: 313–27.
 - 51 Kimelberg HK, Barron KD, Bourke RS, Nelson LR, Cragoe EJ. Brain anti-cyotoxic edema agents. *Prog Clin Biol Res* 1990; 361: 363–85.
 - 52 Hillered L, Smith ML, Siesjo BK. Lactic acidosis and recovery of mitochondrial function following forebrain ischemia in the rat. *J Cereb Blood Flow Metab* 1985; 5: 259–66.
 - 53 Rehnrcrona S, Hauge HN, Siesjo BK. Enhancement of iron-catalyzed free radical formation by acidosis in brain homogenates: differences in effect by lactic acid and CO₂. *J Cereb Blood Flow Metab* 1989; 9: 65–70.
 - 54 Swanson RA, Farrell K, Simon RP. Acidosis causes failure of astrocyte glutamate uptake during hypoxia. *J Cereb Blood Flow Metab* 1995; 15: 417–24.
 - 55 Giffard RG, Monyer H, Christine CW, Choi DW. Acidosis reduces NMDA receptor activation, glutamate neurotoxicity, and oxygen-glucose deprivation neuronal injury in cortical cultures. *Brain Res* 1990; 506: 339–42.
 - 56 Kaku DA, Giffard RG, Choi DW. Neuroprotective effects of glutamate antagonists and extracellular acidity. *Science* 1993; 260: 1516–8.
 - 57 Sapolsky RM, Trafton J, Tombaugh GC. Excitotoxic neuron death, acidotic endangerment; and the paradox of acidotic protection. *Adv*

- Neurol 1996; 71: 237–44.
- 58 Tang CM, Dichter M, Morad M. Modulation of the *N*-methyl-*D*-aspartate channel by extracellular H⁺. *Proc Natl Acad Sci U S A* 1990; 87: 6445–9.
- 59 Traynelis SF, Cull-Candy SG. Proton inhibition of *N*-methyl-*D*-aspartate receptors in cerebellar neurons. *Nature* 1990; 345: 347–50.
- 60 Waldmann R, Lazdunski M. H⁺-gated cation channels: neuronal acid sensors in the ENaC/DEG family of ion channels. *Curr Opin Neurobiol* 1998; 8: 418–24.
- 61 Waldmann R, Champigny G, Bassilana F, Heurteaux C, Lazdunski M. A proton-gated cation channel involved in acid-sensing. *Nature* 1997; 386: 173–7.
- 62 Baron A, Waldmann R, Lazdunski M. ASIC-like, proton-activated currents in rat hippocampal neurons. *J Physiol* 2002; 539: 485–94.
- 63 Price MP, Snyder PM, Welsh MJ. Cloning and expression of a novel human brain Na⁺ channel. *J Biol Chem* 1996; 271: 7879–82.
- 64 Wemmie JA, Chen J, Askwith CC, Hruska-Hageman AM, Price MP, Nolan BC, et al. The acid-activated ion channel ASIC contributes to synaptic plasticity, learning, and memory. *Neuron* 2002; 34: 463–77.
- 65 De La Rosa DA, Krueger SR, Kolar A, Shao D, Fitzsimonds RM, Canessa CM. Distribution, subcellular localization and ontogeny of ASIC1 in the mammalian central nervous system. *J Physiol* 2003; 546: 77–87.
- 66 Krishtal OA, Pidoplichko VI. A receptor for protons in the nerve cell membrane. *Neuroscience* 1980; 5: 2325–7.
- 67 Kovalchuk Y, Krishtal OA, Nowycky MC. The proton-activated inward current of rat sensory neurons includes a calcium component. *Neurosci Lett* 1990; 115: 237–42.
- 68 Grantyn R, Perouansky M, Rodriguez-Tebar A, Lux HD. Expression of depolarizing voltage- and transmitter-activated currents in neuronal precursor cells from the rat brain is preceded by a proton-activated sodium current. *Brain Res Dev Brain Res* 1989; 49: 150–5.
- 69 Ueno S, Nakaye T, Akaike N. Proton-induced sodium current in freshly dissociated hypothalamic neurones of the rat. *J Physiol (Lond)* 1992; 447: 309–27.
- 70 Varming T. Proton-gated ion channels in cultured mouse cortical neurons. *Neuropharmacology* 1999; 38: 1875–81.
- 71 Xiong ZG, Zhu XM, Chu XP, Minami M, Hey J, Wei WL, et al. Neuroprotection in ischemia: blocking calcium-permeable acid-sensing ion channels. *Cell* 2004; 118: 687–98.
- 72 Kellenberger S, Schild L. Epithelial sodium channel/degenerin family of ion channels: a variety of functions for a shared structure. *Physiol Rev* 2002; 82: 735–67.
- 73 Benos DJ, Stanton BA. Functional domains within the degenerin/epithelial sodium channel (Deg/ENaC) superfamily of ion channels. *J Physiol* 1999; 520: 631–44.
- 74 Bianchi L, Driscoll M. Protons at the gate: DEG/ENaC ion channels help us feel and remember. *Neuron* 2002; 34: 337–40.
- 75 Corey DP, Garcia-Anoveros J. Mechanosensation and the DEG/ENaC ion channels. *Science* 1996; 273: 323–4.
- 76 Alvarez d. IR, Canessa CM, Fyfe GK, Zhang P. Structure and regulation of amiloride-sensitive sodium channels. *Annu Rev Physiol* 2000; 62: 573–94.
- 77 Krishtal O. The ASICs: signaling molecules? Modulators? *Trends Neurosci* 2003; 26: 477–83.
- 78 Saugstad JA, Roberts JA, Dong J, Zeitouni S, Evans RJ. Analysis of the membrane topology of the acid-sensing ion channel 2a. *J Biol Chem* 2004; 279: 55514–9.
- 79 Garcia-Anoveros J, Derfler B, Neville-Golden J, Hyman BT, Corey DP. BNaC1 and BNaC2 constitute a new family of human neuronal sodium channels related to degenerins and epithelial sodium channels. *Proc Natl Acad Sci U S A* 1997; 94: 1459–64.
- 80 Grunder S, Chen X. Structure, function; pharmacology of acid-sensing ion channels (ASICs): focus on ASIC1a. *Int J Physiol Pathophysiol Pharmacol* 2010; 2: 73–94.
- 81 Chu XP, Wemmie JA, Wang WZ, Zhu XM, Saugstad JA, Price MP, et al. Subunit-dependent high-affinity zinc inhibition of acid-sensing ion channels. *J Neurosci* 2004; 24: 8678–89.
- 82 Yermolaieva O, Leonard AS, Schnizler MK, Abboud FM, Welsh MJ. Extracellular acidosis increases neuronal cell calcium by activating acid-sensing ion channel 1a. *Proc Natl Acad Sci U S A* 2004; 101: 6752–7.
- 83 Chu XP, Miesch J, Johnson M, Root L, Zhu XM, Chen D, et al. Proton-gated channels in PC12 cells. *J Neurophysiol* 2002; 87: 2555–61.
- 84 Bassler EL, Ngo-Anh TJ, Geisler HS, Ruppertsberg JP, Grunder S. Molecular and functional characterization of acid-sensing ion channel (ASIC) 1b. *J Biol Chem* 2001; 276: 33782–7.
- 85 Chen CC, England S, Akopian AN, Wood JN. A sensory neuron-specific, proton-gated ion channel. *Proc Natl Acad Sci U S A* 1998; 95: 10240–5.
- 86 Waldmann R, Champigny G, Voilley N, Lauritzen I, Lazdunski M. The mammalian degenerin MDEG, an amiloride-sensitive cation channel activated by mutations causing neurodegeneration in *Caenorhabditis elegans*. *J Biol Chem* 1996; 271: 10433–6.
- 87 Lingueglia E, De Weille JR, Bassilana F, Heurteaux C, Sakai H, Waldmann R, et al. A modulatory subunit of acid sensing ion channels in brain and dorsal root ganglion cells. *J Biol Chem* 1997; 272: 29778–83.
- 88 Waldmann R, Bassilana F, de Weille J, Champigny G, Heurteaux C, Lazdunski M. Molecular cloning of a non-inactivating proton-gated Na⁺ channel specific for sensory neurons. *J Biol Chem* 1997; 272: 20975–8.
- 89 Sutherland SP, Benson CJ, Adelman JP, McCleskey EW. Acid-sensing ion channel 3 matches the acid-gated current in cardiac ischemia-sensing neurons. *Proc Natl Acad Sci U S A* 2001; 98: 711–6.
- 90 Meng QY, Wang W, Chen XN, Xu TL, Zhou JN. Distribution of acid-sensing ion channel 3 in the rat hypothalamus. *Neuroscience* 2009; 159: 1126–34.
- 91 De Weille J, Bassilana F, Lazdunski M, Waldmann R. Identification, functional expression and chromosomal localisation of a sustained human proton-gated cation channel. *FEBS Lett* 1998; 433: 257–60.
- 92 Akopian AN, Chen CC, Ding Y, Cesare P, Wood JN. A new member of the acid-sensing ion channel family. *Neuroreport* 2000; 11: 2217–22.
- 93 Grunder S, Geisler HS, Bassler EL, Ruppertsberg JP. A new member of acid-sensing ion channels from pituitary gland. *Neuroreport* 2000; 11: 1607–11.
- 94 Jasti J, Furukawa H, Gonzales EB, Gouaux E. Structure of acid-sensing ion channel 1 at 1.9 Å resolution and low pH. *Nature* 2007; 449: 316–23.
- 95 Benson CJ, Eckert SP, McCleskey EW. Acid-evoked currents in cardiac sensory neurons: A possible mediator of myocardial ischemic sensation. *Circ Res* 1999; 84: 921–8.
- 96 Bevan S, Yeats J. Protons activate a cation conductance in a sub-population of rat dorsal root ganglion neurones. *J Physiol (Lond)* 1991; 433: 145–61.
- 97 Krishtal OA, Pidoplichko VI. A receptor for protons in the membrane of sensory neurons may participate in nociception. *Neuroscience* 1981; 6: 2599–601.
- 98 Ugawa S, Ueda T, Ishida Y, Nishigaki M, Shibata Y, Shimada S. Amiloride-blockable acid-sensing ion channels are leading acid

- sensors expressed in human nociceptors. *J Clin Invest* 2002; 110: 1185–90.
- 99 Sluka KA, Price MP, Breese NM, Stucky CL, Wemmie JA, Welsh MJ. Chronic hyperalgesia induced by repeated acid injections in muscle is abolished by the loss of ASIC3, but not ASIC1. *Pain* 2003; 106: 229–39.
- 100 Chen CC, Zimmer A, Sun WH, Hall J, Brownstein MJ, Zimmer A. A role for ASIC3 in the modulation of high-intensity pain stimuli. *Proc Natl Acad Sci U S A* 2002; 99: 8992–7.
- 101 Wu LJ, Duan B, Mei YD, Gao J, Chen JG, Zhuo M, et al. Characterization of acid-sensing ion channels in dorsal horn neurons of rat spinal cord. *J Biol Chem* 2004; 279: 43716–24.
- 102 Price MP, Lewin GR, McIlwrath SL, Cheng C, Xie J, Heppenstall PA, et al. The mammalian sodium channel BNC1 is required for normal touch sensation. *Nature* 2000; 407: 1007–11.
- 103 Price MP, McIlwrath SL, Xie J, Cheng C, Qiao J, Tarr DE, et al. The DRASIC cation channel contributes to the detection of cutaneous touch and acid stimuli in mice. *Neuron* 2001; 32: 1071–83.
- 104 Page AJ, Brierley SM, Martin CM, Price MP, Symonds E, Butler R, et al. Different contributions of ASIC channels 1a, 2, and 3 in gastrointestinal mechanosensory function. *Gut* 2005; 54: 1408–15.
- 105 Ugawa S, Yamamoto T, Ueda T, Ishida Y, Inagaki A, Nishigaki M, et al. Amiloride-insensitive currents of the acid-sensing ion channel-2a (ASIC2a)/ASIC2b heteromeric sour-taste receptor channel. *J Neurosci* 2003; 23: 3616–22.
- 106 Ugawa S. Identification of sour-taste receptor genes. *Anat Sci Int* 2003; 78: 205–10.
- 107 Lin W, Ogura T, Kinnamon SC. Acid-activated cation currents in rat vallate taste receptor cells. *J Neurophysiol* 2002; 88: 133–41.
- 108 Wemmie JA, Askwith CC, Lamani E, Cassell MD, Freeman JH Jr, Welsh MJ. Acid-sensing ion channel 1 is localized in brain regions with high synaptic density and contributes to fear conditioning. *J Neurosci* 2003; 23: 5496–502.
- 109 Ettaiche M, Guy N, Hofman P, Lazdunski M, Waldmann R. Acid-sensing ion channel 2 is important for retinal function and protects against light-induced retinal degeneration. *J Neurosci* 2004; 24: 1005–12.
- 110 Ettaiche M, Deval E, Cougnon M, Lazdunski M, Voilley N. Silencing acid-sensing ion channel 1a alters cone-mediated retinal function. *J Neurosci* 2006; 26: 5800–9.
- 111 Render JA, Howe KR, Wunsch AM, Guionaud S, Cox PJ, Wemmie JA. Histologic examination of the eye of acid-sensing ion channel 1a knockout mice. *Int J Physiol Pathophysiol Pharmacol* 2010; 2: 69–72.
- 112 Gao J, Duan B, Wang DG, Deng XH, Zhang GY, Xu L, et al. Coupling between NMDA receptor and acid-sensing ion channel contributes to ischemic neuronal death. *Neuron* 2005; 48: 635–46.
- 113 Friese MA, Craner MJ, Ezensperger R, Vergo S, Wemmie JA, Welsh MJ, et al. Acid-sensing ion channel-1 contributes to axonal degeneration in autoimmune inflammation of the central nervous system. *Nat Med* 2007; 13: 1483–9.
- 114 Johnson MB, Jin K, Minami M, Chen D, Simon RP. Global ischemia induces expression of acid-sensing ion channel 2a in rat brain. *J Cereb Blood Flow Metab* 2001; 21: 734–40.
- 115 Pignataro G, Cuomo O, Esposito E, Sirabella R, Di Renzo G, Annunziato L. ASIC1a contributes to neuroprotection elicited by ischemic preconditioning and postconditioning. *Int J Physiol Pathophysiol Pharmacol* 2011; 3: 1–8.
- 116 Zha XM, Wemmie JA, Green SH, Welsh MJ. Acid-sensing ion channel 1a is a postsynaptic proton receptor that affects the density of dendritic spines. *Proc Natl Acad Sci U S A* 2006; 103: 16556–61.
- 117 Samways DS, Harkins AB, Egan TM. Native and recombinant ASIC1a receptors conduct negligible Ca^{2+} entry. *Cell Calcium* 2009; 45: 319–25.
- 118 Herrera Y, Katnik C, Rodriguez JD, Hall AA, Willing A, Pennypacker KR, et al. Sigma-1 receptor modulation of acid-sensing ion channel a (ASIC1a) and ASIC1a-induced Ca^{2+} influx in rat cortical neurons. *J Pharmacol Exp Ther* 2008; 327: 491–502.
- 119 Pignataro G, Simon RP, Xiong ZG. Prolonged activation of ASIC1a and the time window for neuroprotection in cerebral ischaemia. *Brain* 2007; 130: 151–8.
- 120 Sherwood TW, Askwith CC. Dynorphin opioid peptides enhance acid-sensing ion channel 1a activity and acidosis-induced neuronal death. *J Neurosci* 2009; 29: 14371–80.
- 121 Duan B, Wang YZ, Yang T, Chu XP, Yu Y, Huang Y, et al. Extracellular spermine exacerbates ischemic neuronal injury through sensitization of ASIC1a channels to extracellular acidosis. *J Neurosci* 2011; 31: 2101–12.
- 122 Allen NJ, Attwell D. Modulation of ASIC channels in rat cerebellar Purkinje neurons by ischemia-related signals. *J Physiol (Lond)* 2002; 543: 521–9.

Review

Calcium binding protein-mediated regulation of voltage-gated calcium channels linked to human diseases

Nasrin NEJATBAKSH, Zhong-ping FENG*

Department of Physiology, Faculty of Medicine, University of Toronto, 3306 MSB, 1 King's College Circle, Toronto, Ontario, Canada M5S 1A8

Calcium ion entry through voltage-gated calcium channels is essential for cellular signalling in a wide variety of cells and multiple physiological processes. Perturbations of voltage-gated calcium channel function can lead to pathophysiological consequences. Calcium binding proteins serve as calcium sensors and regulate the calcium channel properties via feedback mechanisms. This review highlights the current evidences of calcium binding protein-mediated channel regulation in human diseases.

Keywords: calcium binding proteins; voltage-gated calcium channels; EF-hand motif; calmodulin; calcium binding protein; calcineurin; calpain; visinin-like protein

Acta Pharmacologica Sinica (2011) 32: 741–748; doi: 10.1038/aps.2011.64

Introduction

Calcium (Ca^{2+}) entry via voltage-gated calcium channels (VGCCs), conveys the electric signals to intracellular transduction cascades in a wide variety of cells including neurons, muscle cells and endocrine cells^[1]. Ca^{2+} dependent-signalling cascades are largely mediated by Ca^{2+} binding proteins^[2,3], and are essential for multiple cellular and subcellular processes in physiological conditions. Perturbations of VGCCs functions can cause abnormality of cellular events, leading to pathological consequences. Ca^{2+} binding proteins mediate Ca^{2+} -dependent signal transduction pathways and regulate Ca^{2+} influx via the VGCCs in Ca^{2+} -dependent feedback mechanisms.

VGCCs are classified into L-, N-, P/Q-, R-, and T-types, based on their distinct electrophysiological and pharmacological properties^[4,5]. VGCCs are heteromultimeric protein complexes composed of a pore forming α_1 and four distinct auxiliary subunits: α_2 , δ , β , and γ subunits^[4-7]. Mammalian α_1 subunits are encoded by at least 10 distinct genes^[6,7]. The high voltage-activated VGCCs include Ca_v1 and Ca_v2 subfamilies. The Ca_v1 subfamily ($\text{Ca}_v1.1$ to $\text{Ca}_v1.4$) conducts L-type Ca^{2+} current and includes the channels containing α_{1S} , α_{1C} , α_{1D} , and α_{1F} subunits. The Ca_v2 subfamily ($\text{Ca}_v2.1$ to $\text{Ca}_v2.3$) conducts P/Q-type, N-type, and R-type Ca^{2+} currents, through the chan-

nels containing α_{1A} , α_{1B} , and α_{1E} subunits, respectively. The Ca_v3 subfamily ($\text{Ca}_v3.1$ to $\text{Ca}_v3.3$) conducts low voltage-activated T-type Ca^{2+} current mediated by the channels containing α_{1G} , α_{1H} , and α_{1I} subunits, respectively. The cell- and tissue-specific expression of these subunits allows for a vast variety of the channel subtypes exhibiting distinct functions.

Ca^{2+} -binding proteins containing EF-hand Ca^{2+} binding motifs regulate mostly high voltage-activated VGCCs^[8-12]. The EF-hand motif is a conserved Ca^{2+} -binding structure, spanning a region of 30–35 amino acids containing a 12-residue Ca^{2+} binding loop flanked by the N- and C-terminal α -helix regions which are differentially exposed in the presence of Ca^{2+} ^[3,13,14]. Each EF-hand protein has distinct Ca^{2+} binding affinity and cellular localization. The EF-hand Ca^{2+} -binding protein super-families^[2,3,15], such as calmodulin (CaM), calcineurin, calcium binding proteins (CaBP), and neuronal Ca^{2+} sensors (NCSs), contains 2 to 4 functioning EF-hand Ca^{2+} binding domains. The EF-hand Ca^{2+} -binding proteins may achieve their cellular effects through Ca^{2+} -dependent or Ca^{2+} -independent signalling mechanisms^[16,17] (Figure 1). Many EF-hand Ca^{2+} -binding proteins alter Ca^{2+} kinetics directly through regulation of VGCC properties^[8-12]. With the availability of human genetic databases and advanced molecular technologies, growing evidences suggest that dysfunctions in Ca^{2+} -binding protein mediated VGCC regulation may be one of the mechanisms leading to human diseases.

* To whom correspondence should be addressed.

E-mail zp.feng@utoronto.ca

Received 2011-03-14 Accepted 2011-04-20

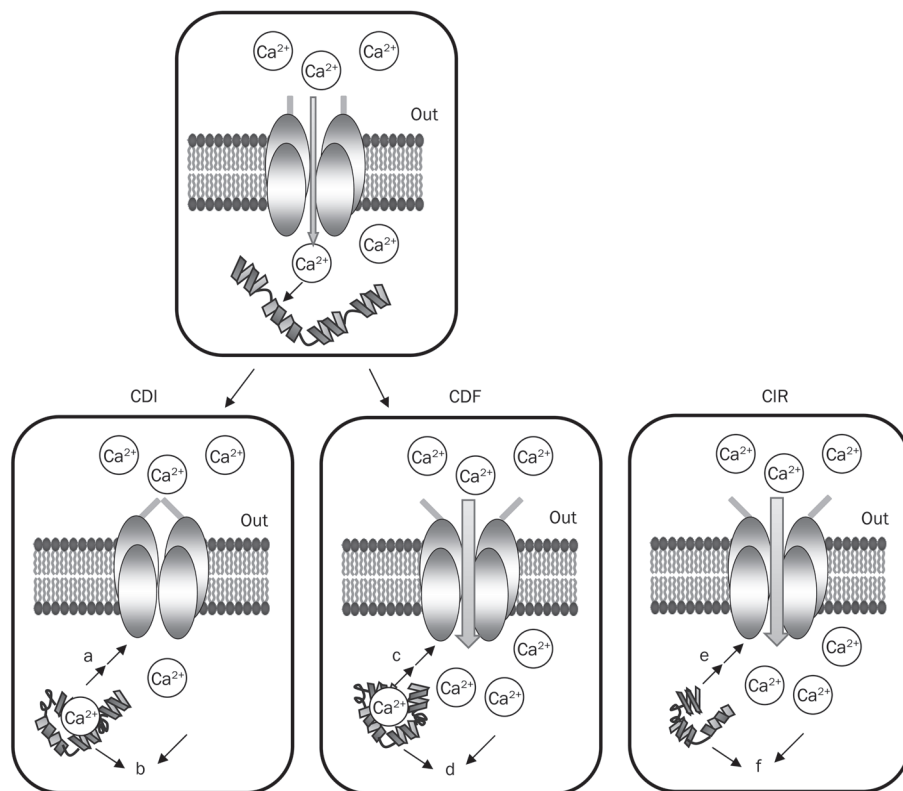


Figure 1. Ca^{2+} binding proteins regulate voltage-gated Ca^{2+} channels (VGCCs) via Ca^{2+} -dependent inactivation (CDI), Ca^{2+} -dependent facilitation (CDF) and Ca^{2+} -independent regulation (CIR) of the channels, hence contributing to Ca^{2+} homeostasis. Disrupting Ca^{2+} -binding protein-mediated VGCC regulation results in pathophysiological processes leading to human diseases. CDI: Ca^{2+} ions entering the cell through VGCCs bind to Ca^{2+} binding proteins to (a) inactivate the channel via negative feedback mechanism, reducing further Ca^{2+} entry through the channel and (b) lead to downstream mechanisms and pathways implicated in human diseases. CDF: Ca^{2+} ions entering the cell through VGCCs bind to Ca^{2+} binding proteins to (c) facilitate the channel via a positive feedback mechanism, thus enhancing further Ca^{2+} entry through the channel and (d) lead to downstream mechanisms and pathways implicated in human diseases. CIR: Ca^{2+} binding proteins, in absence of Ca^{2+} binding (e) regulate VGCCs and (f) lead to downstream mechanisms and pathways implicated in human diseases.

Calmodulin mediated P/Q-type regulation in familial hemiplegic migraine type 1

The best studied Ca^{2+} binding protein that regulates VGCCs is $\text{CaM}^{[18-20]}$. CaM contains 4 functional EF-hand motifs^[21, 22], and regulates VGCCs properties in an enzyme-inhibitor like fashion^[23]. CaM binds to various high-voltage activated VGCCs and causes the Ca^{2+} -dependent inactivation (CDI)^[8, 9, 24, 25] or Ca^{2+} -dependent facilitation (CDF)^[10, 12, 26] (Figure 1). In brief, CaM has a higher binding affinity to Ca^{2+} in the N-lobe than the C-lobe EF-hand motifs. This allows for antagonistic regulation of the Ca^{2+} channel through differential Ca^{2+} binding to $\text{CaM}^{[27]}$. Specifically, CDI of $\text{Ca}_v1.2$ channels^[8, 9, 24] and CDF of $\text{Ca}_v2.1$ channels depend on Ca^{2+} binding to the C-lobe of $\text{CaM}^{[10, 27]}$. Conversely, Ca^{2+} binding to the N-lobe of CaM induces CDI of $\text{Ca}_v2.1$ ^[10, 12, 28], $\text{Ca}_v2.2$ ^[10, 12], and $\text{Ca}_v2.3$ ^[10] type channels. The differential regulatory effects of CaM on VGCCs are likely due to different conformational changes in the structure of CaM following Ca^{2+} binding at alternate sites. CaM -mediated regulation of the presynaptic VGCCs results in a dual feedback regulation. The cellular and molecular mechanisms underlying CaM mediated VGCC regulation have been extensively reviewed previously^[18-20].

FHM is characterized by recurrent migraines and includes visual disturbance, sensory loss, hemiparesis and ataxia. FHM type 1 is an autosomal dominant type of migraine with aura and hemiparesis, which is linked to the VGCC α_1 -subunit gene, *CACNL1A4* encoding $\text{Ca}_v2.1$ ^[29-31]. All five FHM1 mutations change the biophysical properties of $\text{Ca}_v2.1$ channels, leading to both gain and loss of P/Q-type channel

function^[32, 33]. Specifically, single channel recording showed that the mutations enhanced the open probability of the $\text{Ca}_v2.1$ channels and shifted the activation gating of the channel to more negative voltages, allowing increased Ca^{2+} influx at more negative membrane potentials in cerebellar neurons^[33, 34]. Common treatments with Ca^{2+} channel blockers, such as verapamil, is effective in some FHM1 patients, carrying the *CACNA1A* mutations due to decreased open probability of P/Q-type $\text{Ca}_v2.1$ channels and reduced Ca^{2+} influx^[35].

Consistent with reports of increased open-channel probability^[32, 33], a recent study showed that FHM-1 missense mutants of the C-terminus in $\text{Ca}_v2.1$ subunit, R192Q and S218L, permitted a larger Ca^{2+} influx during action potentials than the wildtype channels in the cerebellar neurons^[36]. Interestingly, these FHM-1 gain-of-function missense mutations characteristically occlude CDF of human $\text{Ca}_v2.1$ channels in both recombinant preparations and the cerebellar Purkinje cells. The altered CDF of $\text{Ca}_v2.1$ channels coincided with a decrease in short-term synaptic facilitation at the parallel fiber-to-purkinje cell synapse in the cerebellum in FHM-1 mutant mice^[36]. The compelling evidence suggests that FHM-1 gain-of-function missense mutations of $\text{Ca}_v2.1$ channels favour a constitutively facilitated state that prevents further Ca^{2+} -dependent CaM -mediated channel facilitation. It is hypothesized that disruption of $\text{Ca}_v2.1$ CDF may cause the cerebellar ataxia-associated FHM-1 due to an imbalance between excitatory and inhibitory inputs to the cerebellar Purkinje cells. This disruption suppresses the intrinsic pacemaker activity of these cells, thus leading to motor deficits^[36]. The knock-in

mouse model carrying FHM-1 R192Q mutation exhibited an enhanced velocity of cortical spreading depression *in vivo*^[34], and it is thus important to demonstrate whether the cortical hyper-excitability is also associated with perturbation of CDF of the mutant Ca_v2.1 in future studies.

CaBPs mediated L-type channel inactivation

CaBPs consist of 8 members (CaBP 1–8) and are considered similar to CaM in that they bear four recognizable, but not necessarily functional EF-hands^[37]. CaBP1, also known as caldendrin (a splice variant of CaBP1)^[38], has ~50% sequence homology to CaM and is widely expressed in the brain, including the cerebral cortex, hippocampus, in the cone bipolar and amacrine cells of the retina^[39], and in the inner hair cells. CaBP1 interacts with Ca_v2.1 P/Q -type channels^[40, 41], and L-type channels^[42]. CaBP1 accelerates inactivation kinetics, prevents CaM-induced Ca_v2.1 channel facilitation, and shifts the voltage-dependent activation of Ca_v2.1 channels^[40]. These effects of CaBP1 are mediated by binding to the CaM-binding IQ-domain in the α_{1A} subunit of Ca_v2.1 channels. CaBP1 binding to the CaM binding domain (CBD) of α_{1A} causes a significantly faster inactivation of Ca_v2.1 channel than CaM.

CaBPs regulate L-type channels in a Ca²⁺-independent manner^[40, 42–44] (Figure 1), in contrast to CaM. CaBP1 and CaBP4 act as negative regulators to compete with CaM binding to the C-terminal IQ motif in the Ca_v1.2 and Ca_v1.3 subunit^[42, 44–46]. CaBP1 also interacts with the N-terminal domain of Ca_v1.2 to prolong the channel activation, independent of CaM effect^[42, 44]. Some CaBPs, such as CaBP1 and CaBP4, have the capacity to negatively regulate influx of Ca²⁺ through a direct inhibitory interaction with plasma member P/Q-type channels in cochlear cells^[45–47]. In the inner ear, at least 4 CaBPs have been found in hair cells, including CaBP1, CaBP2, CaBP4 and CaBP5. Sustained activation of presynaptic Ca_v1.3 channels triggers graded changes in neurotransmitter release which is required for sound detection^[46]. CaBP1 binding to Ca_v1.3 channels on CaM interaction sites, induced a stronger, than CaBP4, inhibition of Ca²⁺-dependent channel inactivation^[46]. Closely co-localization between CaBP1 and Ca_v1.3 at the presynaptic ribbon synapse of adult inner hair cells further suggests CaBP1-mediated inhibitory effect on Ca²⁺-dependent inactivation of Ca_v1.3 channel is critical for auditory transmission^[46].

CaBP4^[48] and CaBP5^[49] regulates L-type channels in photoreceptors. CaBP4 is located at the photoreceptor synaptic terminals in the retina, and is important for developing and sustaining synaptic transmission to bipolar cells^[43]. CaBP4 regulates Ca_v1.4 channel and shifts the activation of Ca_v1.4 to more hyperpolarized potentials through a direct interaction with the C-terminal domain of the Ca_v1.4 channel protein. CaBP4^{-/-} mice exhibited visual deficits similar to that caused by dysfunction of Ca_v1.4 channels^[43, 50, 51]. CaBP4, like CaBP1, is found to interact with CaM-binding IQ domain in Ca_v1.3 to dampen the inactivation of the channel^[40, 46]. CaBP4 has the capacity to eliminate even the baseline Ca²⁺ dependent inactivation of Ca_v1.3^[45]. Phosphorylation of S37 of CaBP4 by pro-

tein kinase C ζ in retina regulates Ca_v1.3, likely by facilitating the low-affinity interaction which exerts inhibitory regulation of Ca_v1.3 channel inactivation^[48]. Phosphorylation of CaBP4 is critical for tuning presynaptic Ca²⁺ signals required for light-induced neurotransmitter release. Incomplete congenital stationary night blindness (CSNB2) is linked to mutations in both CaBP4^[52, 53] and Ca_v1.4^[54–56]. Interrelation between CaBP4 and Ca_v1.4 in CSNB2 remains to be determined.

Bestrophin-1 mediated Ca_v1.3 modulation in macular degeneration

Bestrophins are a family of calcium-activated chloride channels^[57] encoded with VMD2 (Best vitelliform macular dystrophy-2) gene on chromosome 11q13^[58]. Human bestrophin-1 (hBest1) is a founding member of the family and contains one EF-hand (EF1, 350–390) at the C-terminal and a regulatory domain adjacent to EF1 that is required for Ca²⁺ activation of the channel^[59]. EF1 has a slightly higher Ca²⁺-binding affinity than the third EF hand of CaM and lower affinity than the second EF hand of troponin C. Mutations in hBest1 are involved in ~100 human diseases^[58].

Retinal cell death, induced by glaucoma, diabetic retinopathy and age-related macular degeneration are primarily caused by a form of metabolic stress which results from a lack of nutrient supply. This process is initiated primarily through the activation of NMDA receptors with a subsequent influx of Ca²⁺ and Na⁺ ions into the cells^[60]. The close relationship between ataxia and macular degeneration suggests that these disorders may share a common molecular network^[61]. Oxidative stress, an important cause of retinal pigment epithelium death and subsequent age-related macular degeneration, induces calcium overload and leads to cell injury^[62]. Oxidative stress induced elevation of Ca²⁺ level is sensitive to VGCC blocker^[62], suggesting the role of VGCCs in retinal cell death.

The hBest1 is localized at the basolateral plasma membrane of the retinal pigment epithelium cells^[63]. Mutations of the *hBest1* gene are associated with macular degeneration^[58]. Bestrophin-1 is co-localized with Ca_v1.3 channels and the auxiliary β_4 -subunit in the cell membrane in the retinal pigment epithelium, and inhibits Ca_v1.3 channels via a direct interaction with the Ca_v β_4 subunit^[64, 65]. Mutations of hBest1 on P330 and P334 prevented Best1-mediated inhibition of Ca_v1.3^[64, 65]. These findings provide new insights into the mechanisms of the retinal degeneration involved in hBest1-mediated Ca_v1.3 channel regulation.

Calcineurin regulation of Ca²⁺ channels in human diseases

Calcineurin is a calcium-dependent phosphatase activated by Ca²⁺/CaM^[66]. It is a heterodimer and consisted of a 59 kDa catalytic subunit and a 19 kDa Ca²⁺-binding regulatory subunit. Calcineurin regulatory subunit is encoded with four putative EF-hand Ca²⁺-binding motifs^[33]. The high-affinity Ca²⁺ binding site has a K_d of ~24 nmol/L to Ca²⁺ whereas three low-affinity binding sites have a K_d of 15 μ mol/L to Ca²⁺^[33]. Calcineurin regulates L-type channels in both myocytes^[67] and

neurons^[68, 69].

Calcineurin regulation of Ca_v1.2 L-type channel in cardiac hypertrophy

Ca²⁺ signalling pathways play a critical role in the development of cardiac hypertrophy, one of the predisposing factors related to hypertension and development of heart failure. The downstream effector of calcineurin, NFAT signalling transduction pathway, plays a critical role in pathological cardiac hypertrophy response^[70, 71]. L-type Ca_v1.2 channels play an important role in blood pressure and development of myogenic tone. In cardiac muscles, L-type currents through Ca_v1.2 channels stimulate the excitation-contraction coupling. The C-terminus of this channel serves an autoinhibitory role to mediate the fight-or-flight response. Inactivation of Ca_v1.2 was found to reduce mean arterial blood pressure in mice and there was a severe dampening of response to penylephrine and angiotensin II, due to a significant portion of penylephrine-induced resistance being dependent on calcium influx through the Ca_v1.2 channel^[72]. The truncation in the distal C-terminus of the α₁ subunit of Ca_v1.2 leads to 10–15 fold increase in channel activity in mammalian cell lines^[73]. The increased force of contraction during the fight-or-flight response is thought to be mediated by regulation of Ca_v1.2 channels via activation of secondary systems which act to phosphorylate the channel^[74]. Deletion of this C-terminus causes a reduction in Ca²⁺ currents, as a result of lower surface expression of the channel, and leads to development of cardiac hypertrophy and premature death after E15 during embryonic development in mice^[25].

Recently, an EF-hand containing Ca²⁺ and integrin-binding protein-1 (CIB1) was found to specifically enhance cardiac pathological hypertrophy, without a role in altering physiological hypertrophy, through a regulation of calcineurin interaction with the sarcolemma^[75]. One mechanism of calcineurin function is thought to be via L-type channels, which mediates Ca²⁺ influx into cardiomyocytes. Transgenic mice expressing an activated form of calcineurin were found to exhibit an enhanced I_{Ca} density compared with the non-transgenic littermates and to have a faster kinetics of I_{Ca} inactivation^[67]. Calcineurin can directly bind to both N- and C-termini (a.a. 1943–1971) of Ca_v1.2 channels, and dephosphorylate the channels, which in turn increase the channel conductance^[76]. Magnesium ions (Mg²⁺) bind to the C-terminal EF-hand to inhibit Ca_v1.2 channels, thereby reducing Ca²⁺ influx to maintain the intracellular Ca²⁺ at low levels^[77]. Supplement of Mg²⁺ during global ischemia resulted in myocardial protection and improved functional recovery^[78]. These evidences suggest that calcineurin serves as a key modulator of Ca²⁺-dependent pathways via regulation of Ca_v1.2 activities and in turn mediates the pathological electrical remodelling in cardiac hypertrophy.

Calcineurin regulation of L-type channels in neurodegenerative diseases

Calcineurin selectively enhances L-type channel activity in hippocampal neurons^[68, 69]. Application of FK506, an

inhibitor of calcineurin, reduces high-voltage-activated Ca²⁺ current via L-type, but not P/Q- or N-type channels^[68]. PKA and calcineurin bind to A-kinase anchoring protein 79/150 (AKAP79/150), which interact with endogenous and recombinant Ca_v1.2 channels in hippocampal neurons and HEK293 cells, respectively^[66]. Disruption of AKAP79/150-calcineurin anchoring increases Ca²⁺ current amplitude^[66]. In contrast to CaM, calcineurin does not affect Ca²⁺-dependent inactivation of the neuronal L- or N-type channels; this conclusion is based on the findings that FK506 has no effect on the time-course of Ca²⁺ current inactivation of L-type channel in rat pituitary tumor cell line (GH3) and N-type channels in chicken dorsal root ganglion neurons, while Ca²⁺-dependent inactivation of the channels is prevented by Ca²⁺ chelator EGTA^[79]. Calcineurin promotes dephosphorylation of 3', 5'-cyclic AMP response element binding protein (CREB)^[29]. Overexpression of calcineurin prevents^[30] and inhibition of calcineurin enhances long-term memory formation^[31, 80]. The activity of calcineurin increases in the hippocampus during aging, and L-type channel block reduces calcineurin activity^[81]. Cleavage of calcineurin by Ca²⁺-sensitive protease calpain^[82] enhances its phosphatase activity, which coincides with an increase in the number of neurofibrillary tangles in human brains of patients with Alzheimer's disease^[83]. Interestingly, amyloid-β protein also increases the activity of calcineurin, leading to dephosphorylation of the proapoptotic protein BAD (Bcl-2/Bcl-X_L-antagonist) causing cell death^[84] and subsequent activation of apoptotic pathways in Alzheimer's disease^[85]. Calcineurin activity is implicated in age-related Ca²⁺ dysregulation in neurodegenerative disorders^[69]. However, the role of EF-hand motifs in calcineurin-enhanced L-type channel activation, and the causal relation between calcineurin and VGCC regulation in degenerative disorders remain to be further investigated.

Perspectives and future directions

Functional diversity within related Ca²⁺-binding proteins may enhance the specificity of Ca²⁺ signalling by VGCCs in different cellular contexts. These channels undergo feedback mechanisms by Ca²⁺-dependent facilitation or inactivation. Such feedback is largely mediated by Ca²⁺ binding proteins. Increasing evidences demonstrate that the diverse and integrative roles of the abundant calcium binding proteins in VGCC regulation and Ca²⁺ signalling may be attributed to human diseases. However, our understanding of the role of such regulation in human diseases is rather limited, due to the complexity of the intracellular protein networks in which integrative functions of Ca²⁺ binding proteins must alter continuously to fit to the dynamic changes of Ca²⁺ signalling.

Many Ca²⁺ binding proteins have been found to regulate VGCCs, however, little is known about how such regulations are related to the pathophysiological processes. For instance, neuronal Ca²⁺ sensor-1/frequenin-1 (NCS-1/frq1) containing three functional EF-hand Ca²⁺ binding motifs^[15, 86–88] exhibits a 10 fold higher affinity for Ca²⁺ than CaM^[89]. NCS-1 is highly localized at the presynaptic terminal of the vertebrates^[90–95] and

invertebrates^[88, 96-98], and facilitates synaptic transmission. It increases the P/Q-type Ca^{2+} current in the Calyx of Held of the giant presynaptic terminal^[90], and regulates the presynaptic N-type channels in motoneurons^[99] and growth cone VGCCs in *Lymnaea neurons*^[100, 101]. Another example is visinin-like protein-2 (VILIP-2), a highly homologous subfamily of NCS proteins and capable of undergoing Ca^{2+} -myristoyl switch^[102, 103]. VILIP-2 slows inactivation^[104] and enhances facilitation^[105] of the presynaptic P/Q-type Ca^{2+} channels, by a direct interaction with the CBD of the C-terminus of $\text{Ca}_v2.1$. However, whether and how NCS-1 or VILIP-2-mediated VGCC regulation contributes to human diseases remain unclear. Conversely, down-regulation of VILIP-1 has been reported in several types of human cancers^[106, 107], and in heart failure/cardiac hypertrophy^[108]. However, whether VILIP-1 effect is associated with VGCC regulation is unknown. Thus, it is necessary to further investigate if there is interrelation between VGCC regulation by Ca^{2+} binding proteins and human diseases.

Dysregulation of Ca^{2+} homeostasis leads to pathophysiological processes related to human diseases. For instance, a disruption of basal and stimulus-dependent Ca^{2+} levels has been reported in brains of patients suffering from Alzheimer's disease^[109]. The level of Ca^{2+} -sensitive protease calpain-1 in the prefrontal cortex is 3-fold higher in the postmortem brains of individuals with Alzheimer's disease, than those with other neurodegenerative disorders, such as Huntington's or Parkinson's disease. Calpain-1 activates Ca^{2+} -sensitive phosphatase calcineurin by cleaving lysine501 at the C-terminal^[83]. The abnormally enhanced calpain and truncated calcineurin activities correlate with the level of secreted amyloid precursor protein and progression of Alzheimer's disease^[110, 111]. Thus, disruption of Ca^{2+} homeostasis in neuropathology of Alzheimer's disease may be mediated by hyperactivity of calpain-1 and calcineurin. Similarly, α -synuclein, a key protein in the pathophysiology of Parkinson's disease^[112, 113], binds to calmodulin in a Ca^{2+} -dependent manner^[114]. α -Synuclein-calmodulin interaction accelerates fibrilization of synuclein, crucial for forming the core of Lewy bodies. α -Synuclein also colocalizes with other Ca^{2+} -binding proteins, including calbindin and parvalbumin^[115], implicating the significance of Ca^{2+} -dependent signalling in the development of Parkinson's disease. One implication of these findings is that a tight regulation of Ca^{2+} homeostasis by Ca^{2+} / Ca^{2+} -sensitive proteins serves as a compelling mechanism for pathophysiological processes in neurodegenerative and/or cardiovascular disorders. Understanding such mechanisms allows us to identify potential drug targets for delaying or prevention of the onset of the related human diseases. However, this line of research is still at its infancy, and deserves further attention. With current advancement in genetic and epigenetic sequencing techniques and increased availability of the gene and protein databases of human diseases, exploring the role of Ca^{2+} binding proteins in VGCC regulation and their involvement in human diseases are becoming feasible in future studies.

Acknowledgements

This work was supported by an operating grant to ZPF from the Canadian Institutes of Health Research (CIHR MOP62738). NN is the recipient of an NSERC CGS-PhD studentship. ZPF holds a New Investigator Award from the Heart and Stroke Foundation of Canada.

References

- 1 Spitzer NC. Calcium: first messenger. *Nat Neurosci* 2008; 11: 243-4.
- 2 Schaub MC, Heizmann CW. Calcium, troponin, calmodulin, S100 proteins: from myocardial basics to new therapeutic strategies. *Biochem Biophys Res Commun* 2008; 369: 247-64.
- 3 Yap KL, Ames JB, Swindells MB, Ikura M. Diversity of conformational states and changes within the EF-hand protein superfamily. *Proteins* 1999; 37: 499-507.
- 4 Stea A, Soong TW, Snutch TP. Voltage-gated calcium channels in ligand- and voltage-gated ion channels (ed North, RA). Boca Raton (FL): CRC Press; 1995. p113-141.
- 5 Catterall WA. Structure and regulation of voltage-gated Ca^{2+} channels. *Annu Rev Cell Dev Biol* 2000; 16: 521-55.
- 6 Catterall WA, Perez-Reyes E, Snutch TP, Striessnig J. International Union of Pharmacology. XLVIII. Nomenclature and structure-function relationships of voltage-gated calcium channels. *Pharmacol Rev* 2005; 57: 411-25.
- 7 Dolphin AC. Calcium channel diversity: multiple roles of calcium channel subunits. *Curr Opin Neurobiol* 2009; 19: 237-44.
- 8 Zuhlke RD, Pitt GS, Tsien RW, Reuter H. Ca^{2+} -sensitive inactivation and facilitation of L-type Ca^{2+} channels both depend on specific amino acid residues in a consensus calmodulin-binding motif in the(α)1C subunit. *J Biol Chem* 2000; 275: 21121-9.
- 9 Pitt GS, Zuhlke RD, Hudmon A, Schulman H, Reuter H, Tsien RW. Molecular basis of calmodulin tethering and Ca^{2+} -dependent inactivation of L-type Ca^{2+} channels. *J Biol Chem* 2001; 276: 30794-802.
- 10 Liang H, DeMaria CD, Erickson MG, Mori MX, Alseikhan BA, Yue DT. Unified mechanisms of Ca^{2+} regulation across the Ca^{2+} channel family. *Neuron* 2003; 39: 951-60.
- 11 Lee A, Catterall WA. Ca^{2+} -dependent modulation of voltage-gated Ca^{2+} channels in voltage-gated calcium channels (ed Gerald Zamponi). Texas (USA): Landes Bioscience; 2005. p183-193.
- 12 Dick IE, Tadross MR, Liang H, Tay LH, Yang W, Yue DT. A modular switch for spatial Ca^{2+} selectivity in the calmodulin regulation of Ca_v channels. *Nature* 2008; 451: 830-4.
- 13 Kretsinger RH, Nockolds CE. Carp muscle calcium-binding protein. II. Structure determination and general description. *J Biol Chem* 1973; 248: 3313-26.
- 14 Garipey J, Hodges RS. Primary sequence analysis and folding behavior of EF hands in relation to the mechanism of action of troponin C and calmodulin. *FEBS Lett* 1983; 160: 1-6.
- 15 Burgoyne RD, Weiss JL. The neuronal calcium sensor family of Ca^{2+} -binding proteins. *Biochem J* 2001; 353: 1-12.
- 16 Burgoyne RD, O'Callaghan DW, Hasdemir B, Haynes LP, Tepikin AV. Neuronal Ca^{2+} -sensor proteins: multitasking regulators of neuronal function. *Trends Neurosci* 2004; 27: 203-9.
- 17 Burgoyne RD. Neuronal calcium sensor proteins: generating diversity in neuronal Ca^{2+} signalling. *Nat Rev Neurosci* 2007; 8: 182-93.
- 18 Halling DB, Racena-Parks P, Hamilton SL. Regulation of voltage-gated Ca^{2+} channels by calmodulin. *Sci STKE* 2006; er1.
- 19 Zamponi GW. Calmodulin lobotomized: novel insights into calcium regulation of voltage-gated calcium channels. *Neuron* 2003; 39:

- 879–81.
- 20 Catterall WA, Few AP. Calcium channel regulation and presynaptic plasticity. *Neuron* 2008; 59: 882–901.
- 21 Dalgarno DC, Klevit RE, Levine BA, Williams RJ, Dobrowolski Z, Drabikowski W. ^1H NMR studies of calmodulin. Resonance assignments by use of tryptic fragments. *Eur J Biochem* 1984; 138: 281–9.
- 22 Klevit RE, Dalgarno DC, Levine BA, Williams RJ. ^1H -NMR studies of calmodulin. The nature of the Ca^{2+} -dependent conformational change. *Eur J Biochem* 1984; 139: 109–14.
- 23 Liu X, Yang PS, Yang W, Yue DT. Enzyme-inhibitor-like tuning of Ca^{2+} channel connectivity with calmodulin. *Nature* 2010; 463: 968–72.
- 24 Mori MX, Erickson MG, Yue DT. Functional stoichiometry and local enrichment of calmodulin interacting with Ca^{2+} channels. *Science* 2004; 304: 432–5.
- 25 Fu Y, Westenbroek RE, Yu FH, Clark JP III, Marshall MR, Scheuer T, *et al.* Deletion of the distal C-terminus of Cav1.2 channel leads to loss of beta-adrenergic regulation and heart failure *in vivo*. *J Biol Chem* 2011;
- 26 DeMaria CD, Soong TW, Alseikhan BA, Alvania RS, Yue DT. Calmodulin bifurcates the local Ca^{2+} signal that modulates P/Q-type Ca^{2+} channels. *Nature* 2001; 411: 484–9.
- 27 Erickson MG, Alseikhan BA, Peterson BZ, Yue DT. Preassociation of calmodulin with voltage-gated Ca^{2+} channels revealed by FRET in single living cells. *Neuron* 2001; 31: 973–85.
- 28 Lee A, Zhou H, Scheuer T, Catterall WA. Molecular determinants of Ca^{2+} /calmodulin-dependent regulation of Ca(v)2.1 channels. *Proc Natl Acad Sci U S A* 2003; 100: 16059–64.
- 29 Pietrobon D. Familial hemiplegic migraine. *Neurotherapeutics* 2007; 4: 274–84.
- 30 Pietrobon D. Insights into migraine mechanisms and Cav2.1 calcium channel function from mouse models of familial hemiplegic migraine. *J Physiol* 2010; 588: 1871–8.
- 31 Ophoff RA, Terwindt GM, Vergouwe MN, van ER, Oefner PJ, Hoffman SM, *et al.* Familial hemiplegic migraine and episodic ataxia type-2 are caused by mutations in the Ca^{2+} channel gene CACNL1A4. *Cell* 1996; 87: 543–52.
- 32 Hans M, Luvisetto S, Williams ME, Spagnolo M, Urrutia A, Tottene A *et al.* Functional consequences of mutations in the human alpha1A calcium channel subunit linked to familial hemiplegic migraine. *J Neurosci* 1999; 19: 1610–9.
- 33 Tottene A, Fellin T, Pagnutti S, Luvisetto S, Striessnig J, Fletcher C, *et al.* Familial hemiplegic migraine mutations increase Ca^{2+} influx through single human Cav2.1 channels and decrease maximal Cav2.1 current density in neurons. *Proc Natl Acad Sci U S A* 2002; 99: 13284–9.
- 34 van den Maagdenberg AM, Pietrobon D, Pizzorusso T, Kaja S, Broos LA, Cesetti T, *et al.* A Cacna1a knockin migraine mouse model with increased susceptibility to cortical spreading depression. *Neuron* 2004; 41: 701–10.
- 35 Knierim E, Leisle L, Wagner C, Weschke B, Lucke B, Bohner G, *et al.* Recurrent stroke due to a novel voltage sensor mutation in Cav2.1 responds to verapamil. *Stroke* 2011; 42: e14–7.
- 36 Adams PJ, Rungta RL, Garcia E, van den Maagdenberg AM, MacVicar BA, Snutch TP. Contribution of calcium-dependent facilitation to synaptic plasticity revealed by migraine mutations in the P/Q-type calcium channel. *Proc Natl Acad Sci U S A* 2010; 107: 18694–9.
- 37 Haeseleer F, Palczewski K. Calmodulin and Ca^{2+} -binding proteins (CaBPs): variations on a theme. *Adv Exp Med Biol* 2002; 514: 303–17.
- 38 Laube G, Seidenbecher CI, Richter K, Dieterich DC, Hoffmann B, Landwehr M, *et al.* The neuron-specific Ca^{2+} -binding protein caldendrin: gene structure, splice isoforms, and expression in the rat central nervous system. *Mol Cell Neurosci* 2002; 19: 459–75.
- 39 Haeseleer F, Sokal I, Verlinde CL, Erdjument-Bromage H, Tempst P, Pronin AN, *et al.* Five members of a novel Ca^{2+} -binding protein (CABP) subfamily with similarity to calmodulin. *J Biol Chem* 2000; 275: 1247–60.
- 40 Lee A, Westenbroek RE, Haeseleer F, Palczewski K, Scheuer T, Catterall WA. Differential modulation of Ca(v)2.1 channels by calmodulin and Ca^{2+} -binding protein 1. *Nat Neurosci* 2002; 5: 210–7.
- 41 Haynes LP, Tepikin AV, Burgoyne RD. Calcium-binding protein 1 is an inhibitor of agonist-evoked, inositol 1,4,5-trisphosphate-mediated calcium signaling. *J Biol Chem* 2004; 279: 547–55.
- 42 Zhou H, Yu K, McCoy KL, Lee A. Molecular mechanism for divergent regulation of Cav1.2 Ca^{2+} channels by calmodulin and Ca^{2+} -binding protein-1. *J Biol Chem* 2005; 280: 29612–9.
- 43 Haeseleer F, Imanishi Y, Maeda T, Possin DE, Maeda A, Lee A, *et al.* Essential role of Ca^{2+} -binding protein 4, a Cav1.4 channel regulator, in photoreceptor synaptic function. *Nat Neurosci* 2004; 7: 1079–87.
- 44 Zhou H, Kim SA, Kirk EA, Tippens AL, Sun H, Haeseleer F, *et al.* Ca^{2+} -binding protein-1 facilitates and forms a postsynaptic complex with Cav1.2 (L-type) Ca^{2+} channels. *J Neurosci* 2004; 24: 4698–708.
- 45 Yang PS, Alseikhan BA, Hiel H, Grant L, Mori MX, Yang W, *et al.* Switching of Ca^{2+} -dependent inactivation of Ca(v)1.3 channels by calcium binding proteins of auditory hair cells. *J Neurosci* 2006; 26: 10677–89.
- 46 Cui G, Meyer AC, Calin-Jageman I, Neef J, Haeseleer F, Moser T, *et al.* Ca^{2+} -binding proteins tune Ca^{2+} -feedback to Cav1.3 channels in mouse auditory hair cells. *J Physiol* 2007; 585: 791–803.
- 47 Lee S, Briklín O, Hiel H, Fuchs P. Calcium-dependent inactivation of calcium channels in cochlear hair cells of the chicken. *J Physiol* 2007; 583: 909–22.
- 48 Lee A, Jimenez A, Cui G, Haeseleer F. Phosphorylation of the Ca^{2+} -binding protein CaBP4 by protein kinase C zeta in photoreceptors. *J Neurosci* 2007; 27: 12743–54.
- 49 Rieke F, Lee A, Haeseleer F. Characterization of Ca^{2+} -binding protein 5 knockout mouse retina. *Invest Ophthalmol Vis Sci* 2008; 49: 5126–35.
- 50 Mansergh F, Orton NC, Vessey JP, Lalonde MR, Stell WK, Tremblay F, *et al.* Mutation of the calcium channel gene *Cacna1f* disrupts calcium signaling, synaptic transmission and cellular organization in mouse retina. *Hum Mol Genet* 2005; 14: 3035–46.
- 51 Chang B, Heckenlively JR, Bayley PR, Brecha NC, Davisson MT, Hawes NL, *et al.* The nob2 mouse, a null mutation in *Cacna1f*: anatomical and functional abnormalities in the outer retina and their consequences on ganglion cell visual responses. *Vis Neurosci* 2006; 23: 11–24.
- 52 Zeitz C, Labs S, Lorenz B, Forster U, Uksti J, Kroes HY, *et al.* Genotyping microarray for CSNB-associated genes. *Invest Ophthalmol Vis Sci* 2009; 50: 5919–26.
- 53 Zeitz C, Kloeckener-Gruissem B, Forster U, Kohl S, Magyar I, Wissinger B, *et al.* Mutations in CABP4, the gene encoding the Ca^{2+} -binding protein 4, cause autosomal recessive night blindness. *Am J Hum Genet* 2006; 79: 657–67.
- 54 Lodha N, Bonfield S, Orton NC, Doering CJ, McRory JE, Mema SC *et al.* Congenital stationary night blindness in mice — a tale of two *cacna1f* mutants. *Adv Exp Med Biol* 2010; 664: 549–58.
- 55 Strom TM, Nyakatura G, pfelstedt-Sylla E, Hellebrand H, Lorenz B, Weber BH, *et al.* An L-type calcium-channel gene mutated in incomplete X-linked congenital stationary night blindness. *Nat Genet* 1998; 19: 260–3.

- 56 Hoda JC, Zaghetto F, Koschak A, Striessnig J. Congenital stationary night blindness type 2 mutations S229P, G369D, L1068P, and W1440X alter channel gating or functional expression of Ca(v)1.4 L-type Ca²⁺ channels. *J Neurosci* 2005; 25: 252–9.
- 57 Kunzelmann K, Milenkovic VM, Spitzner M, Soria RB, Schreiber R. Calcium-dependent chloride conductance in epithelia: is there a contribution by Bestrophin? *Pflugers Arch* 2007; 454: 879–89.
- 58 Petrukhin K, Koisti MJ, Bakall B, Li W, Xie G, Marknell T, *et al*. Identification of the gene responsible for Best macular dystrophy. *Nat Genet* 1998; 19: 241–7.
- 59 Xiao Q, Prussia A, Yu K, Cui YY, Hartzell HC. Regulation of bestrophin Cl channels by calcium: role of the C terminus. *J Gen Physiol* 2008; 132: 681–92.
- 60 Schmidt KG, Bergert H, Funk RH. Neurodegenerative diseases of the retina and potential for protection and recovery. *Curr Neuropharmacol* 2008; 6: 164–78.
- 61 Kahle JJ, Gulbahce N, Shaw CA, Lim J, Hill DE, Barabasi AL, *et al*. Comparison of an expanded ataxia interactome with patient medical records reveals a relationship between macular degeneration and ataxia. *Hum Mol Genet* 2011; 20: 510–27.
- 62 Li GY, Fan B, Zheng YC. Calcium overload is a critical step in programmed necrosis of ARPE-19 cells induced by high-concentration HO. *Biomed Environ Sci* 2010; 23: 371–7.
- 63 Marmorstein AD, Marmorstein LY, Rayborn M, Wang X, Hollyfield JG, Petrukhin K. Bestrophin, the product of the Best vitelliform macular dystrophy gene (VMD2), localizes to the basolateral plasma membrane of the retinal pigment epithelium. *Proc Natl Acad Sci U S A* 2000; 97: 12758–63.
- 64 Yu K, Xiao Q, Cui G, Lee A, Hartzell HC. The best disease-linked Cl⁻ channel hBest1 regulates Ca V 1 (L-type) Ca²⁺ channels via src-homology-binding domains. *J Neurosci* 2008; 28: 5660–70.
- 65 Reichhart N, Milenkovic VM, Halsband CA, Cordeiro S, Strauss O. Effect of bestrophin-1 on L-type Ca²⁺ channel activity depends on the Ca²⁺ channel beta-subunit. *Exp Eye Res* 2010; 91: 630–9.
- 66 Oliveria SF, Dell'Acqua ML, Sather WA. AKAP79/150 anchoring of calcineurin controls neuronal L-type Ca²⁺ channel activity and nuclear signaling. *Neuron* 2007; 55: 261–75.
- 67 Yatani A, Honda R, Tymitz KM, Lalli MJ, Molkentin JD. Enhanced Ca²⁺ channel currents in cardiac hypertrophy induced by activation of calcineurin-dependent pathway. *J Mol Cell Cardiol* 2001; 33: 249–59.
- 68 Norris CM, Blalock EM, Chen KC, Porter NM, Landfield PW. Calcineurin enhances L-type Ca²⁺ channel activity in hippocampal neurons: increased effect with age in culture. *Neuroscience* 2002; 110: 213–25.
- 69 Norris CM, Blalock EM, Chen KC, Porter NM, Thibault O, Kraner SD, *et al*. Hippocampal 'zipper' slice studies reveal a necessary role for calcineurin in the increased activity of L-type Ca²⁺ channels with aging. *Neurobiol Aging* 2010; 31: 328–38.
- 70 Bueno OF, van RE, Molkentin JD, Doevendans PA, De Windt LJ. Calcineurin and hypertrophic heart disease: novel insights and remaining questions. *Cardiovasc Res* 2002; 53: 806–21.
- 71 Wilkins BJ, Dai YS, Bueno OF, Parsons SA, Xu J, Plank DM, *et al*. Calcineurin/NFAT coupling participates in pathological but not physiological cardiac hypertrophy. *Circ Res* 2004; 94: 110–8.
- 72 Moosmang S, Schulla V, Welling A, Feil R, Feil S, Wegener JW, *et al*. Dominant role of smooth muscle L-type calcium channel Cav1.2 for blood pressure regulation. *EMBO J* 2003; 22: 6027–34.
- 73 Gao T, Cuadra AE, Ma H, Bunemann M, Gerhardstein BL, Cheng T, *et al*. C-terminal fragments of the alpha 1C (CaV1.2) subunit associate with and regulate L-type calcium channels containing C-terminal-truncated alpha 1C subunits. *J Biol Chem* 2001; 276: 21089–97.
- 74 Emrick MA, Sadilek M, Konoki K, Catterall WA. Beta-adrenergic-regulated phosphorylation of the skeletal muscle Ca(V)1.1 channel in the fight-or-flight response. *Proc Natl Acad Sci U S A* 2010; 107: 18712–7.
- 75 Heineke J, Uger-Messier M, Correll RN, Xu J, Benard MJ, Yuan W, *et al*. CIB1 is a regulator of pathological cardiac hypertrophy. *Nat Med* 2010; 16: 872–9.
- 76 Tandan S, Wang Y, Wang TT, Jiang N, Hall DD, Hell JW, *et al*. Physical and functional interaction between calcineurin and the cardiac L-type Ca²⁺ channel. *Circ Res* 2009; 105: 51–60.
- 77 Brunet S, Scheuer T, Klevit R, Catterall WA. Modulation of CaV1.2 channels by Mg²⁺ acting at an EF-hand motif in the COOH-terminal domain. *J Gen Physiol* 2005; 126: 311–23.
- 78 McCully JD, Levitsky S. Mechanisms of *in vitro* cardioprotective action of magnesium on the aging myocardium. *Magnes Res* 1997; 10: 157–68.
- 79 Zeilhofer HU, Blank NM, Neuhuber WL, Swandulla D. Calcium-dependent inactivation of neuronal calcium channel currents is independent of calcineurin. *Neuroscience* 2000; 95: 235–41.
- 80 Christie-Fougere MM, rby-King A, Harley CW, McLean JH. Calcineurin inhibition eliminates the normal inverted U curve enhances acquisition and prolongs memory in a mammalian 3', 5'-cyclic AMP-dependent learning paradigm. *Neuroscience* 2009; 158: 1277–83.
- 81 Foster TC, Sharrow KM, Masse JR, Norris CM, Kumar A. Calcineurin links Ca²⁺ dysregulation with brain aging. *J Neurosci* 2001; 21: 4066–73.
- 82 Tallant EA, Brumley LM, Wallace RW. Activation of a calmodulin-dependent phosphatase by a Ca²⁺-dependent protease. *Biochemistry* 1988; 27: 2205–11.
- 83 Liu F, Grundke-Iqbal I, Iqbal K, Oda Y, Tomizawa K, Gong CX. Truncation and activation of calcineurin A by calpain I in Alzheimer disease brain. *J Biol Chem* 2005; 280: 37755–62.
- 84 Wang HG, Pathan N, Ethell IM, Krajewski S, Yamaguchi Y, Shibasaki F, *et al*. Ca²⁺-induced apoptosis through calcineurin dephosphorylation of BAD. *Science* 1999; 284: 339–43.
- 85 Agostinho P, Lopes JP, Velez Z, Oliveira CR. Overactivation of calcineurin induced by amyloid-beta and prion proteins. *Neurochem Int* 2008; 52: 1226–33.
- 86 Brackmann M, Schuchmann S, Anand R, Braunewell KH. Neuronal Ca²⁺ sensor protein VILIP-1 affects cGMP signalling of guanylyl cyclase B by regulating clathrin-dependent receptor recycling in hippocampal neurons. *J Cell Sci* 2005; 118: 2495–505.
- 87 Ames JB, Ishima R, Tanaka T, Gordon JI, Stryer L, Ikura M. Molecular mechanics of calcium-myristoyl switches. *Nature* 1997; 389: 198–202.
- 88 Pongs O, Lindemeier J, Zhu XR, Theil T, Engelkamp D, Krah-Jentgens I, *et al*. Frequenin — a novel calcium-binding protein that modulates synaptic efficacy in the *Drosophila* nervous system. *Neuron* 1993; 11: 15–28.
- 89 Cox JA, Durussel I, Comte M, Nef S, Nef P, Lenz SE, *et al*. Cation binding and conformational changes in VILIP and NCS-1 two neuron-specific calcium-binding proteins. *J Biol Chem* 1994; 269: 32807–13.
- 90 Tsujimoto T, Jeromin A, Saitoh N, Roder JC, Takahashi T. Neuronal calcium sensor 1 and activity-dependent facilitation of P/Q-type calcium currents at presynaptic nerve terminals. *Science* 2002; 295: 2276–9.
- 91 Jinno S, Jeromin A, Roder J, Kosaka T. Immunocytochemical localization of neuronal calcium sensor-1 in the hippocampus and cerebellum of the mouse with special reference to presynaptic terminals.

- Neuroscience 2002; 113: 449–61.
- 92 Blasiolo B, Kabbani N, Boehmler W, Thisse B, Thisse C, Canfield V, *et al.* Neuronal calcium sensor-1 gene *ncs-1a* is essential for semicircular canal formation in zebrafish inner ear. *J Neurobiol* 2005; 64: 285–97.
- 93 Reynolds AJ, Bartlett SE, Morgans C. The distribution of neuronal calcium sensor-1 protein in the developing and adult rat retina. *Neuroreport* 2001; 12: 725–8.
- 94 Bergmann M, Grabs D, Roder J, Rager G, Jeromin A. Differential expression of neuronal calcium sensor-1 in the developing chick retina. *J Comp Neurol* 2002; 449: 231–40.
- 95 Genin A, Davis S, Meziane H, Doyere V, Jeromin A, Roder J, *et al.* Regulated expression of the neuronal calcium sensor-1 gene during long-term potentiation in the dentate gyrus *in vivo*. *Neuroscience* 2001; 106: 571–7.
- 96 Rivosecchi R, Pongs O, Theil T, Mallart A. Implication of frequenin in the facilitation of transmitter release in *Drosophila*. *J Physiol* 1994; 474: 223–32.
- 97 Jeromin A, Shayan AJ, Msghina M, Roder J, Atwood HL. Crustacean frequenins: molecular cloning and differential localization at neuromuscular junctions. *J Neurobiol* 1999; 41: 165–75.
- 98 Dason JS, Romero-Pozuelo J, Marin L, Iyengar BG, Klose MK, Ferrus A, *et al.* Frequenin/NCS-1 and the Ca²⁺-channel $\alpha 1$ -subunit co-regulate synaptic transmission and nerve-terminal growth. *J Cell Sci* 2009; 122: 4109–21.
- 99 Wang CY, Yang F, He X, Chow A, Du J, Russell JT, *et al.* Ca²⁺ binding protein frequenin mediates GDNF-induced potentiation of Ca²⁺ channels and transmitter release. *Neuron* 2001; 32: 99–112.
- 100 Hui K, Fei GH, Saab BJ, Su J, Roder JC, Feng ZP. Neuronal calcium sensor-1 modulation of optimal calcium level for neurite outgrowth. *Development* 2007; 134: 4479–89.
- 101 Hui K, Feng ZP. NCS-1 differentially regulates growth cone and somata calcium channels in *Lymnaea* neurons. *Eur J Neurosci* 2008; 27: 631–43.
- 102 Brauneuwel KH, Klein-Szanto AJ. Visinin-like proteins (VSNLs): interaction partners and emerging functions in signal transduction of a subfamily of neuronal Ca²⁺-sensor proteins. *Cell Tissue Res* 2009; 335: 301–16.
- 103 Brauneuwel KH, Gundelfinger ED. Intracellular neuronal calcium sensor proteins: a family of EF-hand calcium-binding proteins in search of a function. *Cell Tissue Res* 1999; 295: 1–12.
- 104 Lautermilch NJ, Few AP, Scheuer T, Catterall WA. Modulation of CaV2.1 channels by the neuronal calcium-binding protein visinin-like protein-2. *J Neurosci* 2005; 25: 7062–70.
- 105 Few AP, Lautermilch NJ, Westenbroek RE, Scheuer T, Catterall WA. Differential regulation of CaV2.1 channels by calcium-binding protein 1 and visinin-like protein-2 requires N-terminal myristoylation. *J Neurosci* 2005; 25: 7071–80.
- 106 Gonzalez Guerrero AM, Jaffer ZM, Page RE, Brauneuwel KH, Chernoff J, Klein-Szanto AJ. Visinin-like protein-1 is a potent inhibitor of cell adhesion and migration in squamous carcinoma cells. *Oncogene* 2005; 24: 2307–16.
- 107 Fu J, Jin F, Zhang J, Fong K, Bassi DE, Lopez De CR, *et al.* VILIP-1 expression *in vivo* results in decreased mouse skin keratinocyte proliferation and tumor development. *PLoS One* 2010; 5: e10196.
- 108 Buttgerit J, Qadri F, Monti J, Langenickel TH, Dietz R, Brauneuwel KH, *et al.* Visinin-like protein 1 regulates natriuretic peptide receptor B in the heart. *Regul Pept* 2010; 161: 51–7.
- 109 Palotas A, Kalman J, Palotas M, Juhasz A, Janka Z, Penke B. Fibroblasts and lymphocytes from Alzheimer patients are resistant to beta-amyloid-induced increase in the intracellular calcium concentration. *Prog Neuropsychopharmacol Biol Psychiatry* 2002; 26: 971–4.
- 110 Saito K, Elce JS, Hamos JE, Nixon RA. Widespread activation of calcium-activated neutral proteinase (calpain) in the brain in Alzheimer disease: a potential molecular basis for neuronal degeneration. *Proc Natl Acad Sci U S A* 1993; 90: 2628–32.
- 111 Nixon RA, Saito KI, Grynspan F, Griffin WR, Katayama S, Honda T, *et al.* Calcium-activated neutral proteinase (calpain) system in aging and Alzheimer's disease. *Ann NY Acad Sci* 1994; 747: 77–91.
- 112 Spillantini MG, Schmidt ML, Lee VM, Trojanowski JQ, Jakes R, Goedert M. Alpha-synuclein in Lewy bodies. *Nature* 1997; 388: 839–40.
- 113 Polymeropoulos MH, Lavedan C, Leroy E, Ide SE, Dehejia A, Dutra A, *et al.* Mutation in the alpha-synuclein gene identified in families with Parkinson's disease. *Science* 1997; 276: 2045–7.
- 114 Martinez J, Moeller I, Erdjument-Bromage H, Tempst P, Luring B. Parkinson's disease-associated alpha-synuclein is a calmodulin substrate. *J Biol Chem* 2003; 278: 17379–87.
- 115 Ubeda-Banon I, Saiz-Sanchez D, de la Rosa-Prieto C, Argandona-Palacios L, Garcia-Munozguren S, Martinez-Marcos A. alpha-Synucleinopathy in the human olfactory system in Parkinson's disease: involvement of calcium-binding protein- and substance P-positive cells. *Acta Neuropathol* 2010; 119: 723–35.

Review

Targeting ryanodine receptors for anti-arrhythmic therapy

Mark D McCAULEY^{1,2}, Xander H T WEHRENS^{1,2,*}

¹Department of Molecular Physiology and Biophysics; ²Department of Medicine (Cardiology), Baylor College of Medicine, Houston, TX, USA

Antiarrhythmic drugs are a group of pharmaceuticals that suppress or prevent abnormal heart rhythms, which are often associated with substantial morbidity and mortality. Current antiarrhythmic drugs that typically target plasma membrane ion channels have limited clinical success and in some cases have been described as being pro-arrhythmic. However, recent studies suggest that pathological release of calcium (Ca^{2+}) from the sarcoplasmic reticulum via cardiac ryanodine receptors (RyR2) could represent a promising target for antiarrhythmic therapy. Diastolic SR Ca^{2+} release has been linked to arrhythmogenesis in both the inherited arrhythmia syndrome ‘catecholaminergic polymorphic ventricular tachycardia’ and acquired forms of heart disease (eg, atrial fibrillation, heart failure). Several classes of pharmaceuticals have been shown to reduce abnormal RyR2 activity and may confer protection against triggered arrhythmias through reduction of SR Ca^{2+} leak. In this review, we will evaluate the current pharmacological methods for stabilizing RyR2 and suggest treatment modalities based on current evidence of molecular mechanisms.

Keywords: arrhythmias; atrial fibrillation; calcium; heart failure; ryanodine receptor; sarcoplasmic reticulum

Acta Pharmacologica Sinica (2011) 32: 749–757; doi: 10.1038/aps.2011.44

Introduction

The cardiac ryanodine receptor (RyR2) is a homotetrameric Ca^{2+} release channel located in the sarcoplasmic reticulum (SR) membrane^[1,2]. During the normal cardiac cycle, plasma membrane depolarization initiates opening of L-type Ca^{2+} channels (LTCC), by which extracellular Ca^{2+} enters the cytoplasm. Ca^{2+} influx acts as a trigger that subsequently activates RyR2 channels, leading to a ten-fold greater release of SR Ca^{2+} into the cytoplasm. During systolic contraction of the heart, elevated cytoplasmic Ca^{2+} binds to troponin-C, allowing actin and myosin to interdigitate and cause sarcomere shortening, thus causing myocardial contraction. Diastolic relaxation occurs when cytoplasmic $[\text{Ca}^{2+}]$ decreases as Ca^{2+} is extruded through the $\text{Na}^+/\text{Ca}^{2+}$ -exchanger (NCX) or is actively pumped back into the SR through the sarco/endoplasmic reticulum Ca^{2+} -ATPase (SERCA2a)^[3]. Concomitantly, myocardial relaxation is directly associated with diastolic reduction in Ca^{2+} levels. Thus, physiologic control of Ca^{2+} release from the SR is necessary for timely contraction and relaxation during the cardiac cycle. Pathological ‘leak’ of Ca^{2+} during diastole may be detrimental

and lead to cardiac arrhythmias^[4,5].

There is now considerable evidence that abnormal RyR2-mediated Ca^{2+} release from the SR can lead to both atrial^[6,7] and ventricular arrhythmias associated with sudden cardiac death^[8–10]. Increased SR Ca^{2+} release during diastole can lead to activation of the $\text{Na}^+/\text{Ca}^{2+}$ -exchanger^[11], which in turn generates a transient inward current that can cause afterdepolarizations and triggered action potentials. These afterdepolarizations have been observed in humans and have been directly linked to arrhythmogenesis in animal models of arrhythmias^[12].

Genetic susceptibility to cardiac arrhythmias may arise directly from genetic mutations in RyR2, such as in patients with catecholaminergic polymorphic ventricular tachycardia (CPVT)^[9,13]. Mutations in other proteins that bind to the pore-forming subunits within the RyR2 macromolecular complex (eg, calsequestrin, junctophilin) also have been reported to confer genetic susceptibility to cardiac arrhythmias and/or cardiomyopathy^[14,15]. These observations provide direct evidence that a perturbation in RyR2 function can facilitate the development of cardiac arrhythmias.

Additionally, acquired structural heart disease, for example heart failure or myocardial ischemia, has been shown to modify the post-translational regulation of RyR2 through

* To whom correspondence should be addressed.

E-mail wehrens@bcm.edu

Received 2011-03-01 Accepted 2011-04-07

nitrosylation, oxidation, and phosphorylation, which might also increase susceptibility to diastolic Ca^{2+} release and arrhythmias^[16–20]. Given that there are many excellent reviews on strategies to modify intracellular signaling to reduce RyR2 activation^[21, 22], we will restrict the scope of this review mainly to pharmacological strategies to stabilize RyR2 directly to reduce arrhythmic potential.

Because RyR2 also plays an important role during excitation-contraction coupling, it is important that antiarrhythmic compounds targeting the RyR2 channel complex will not interfere with systolic SR Ca^{2+} release. At the same time, inhibition of diastolic SR Ca^{2+} release is a desirable feature of compounds that could prevent arrhythmias^[22]. RyR2 activity can be modulated by numerous natural and pharmacological compounds, as reviewed elsewhere in more detail^[22–24]. These compounds may modulate RyR2 in various ways, including by modulating channel gating, ion channel translocation, RyR2 subunit composition, or posttranslational modifications. Some of these compounds have emerged as strong candidates for antiarrhythmic drugs, and will be discussed in more detail below.

Dantrolene

Dantrolene sodium is a hydrantoin derivative that was initially described as a muscle relaxant^[25], but later found to be a potent therapeutic agent for patients suffering from the rare life-threatening condition known as malignant hyperthermia (MH)^[26]. Patients susceptible to MH typically have inherited mutations in the type 1 ryanodine receptor (RyR1) primarily found in skeletal muscle^[27]. Exposure to inhaled halogenated anesthetics during surgery can trigger massive RyR1-mediated Ca^{2+} release associated with muscle breakdown, elevation of serum creatinine kinase (CK), hypotension, hyperthermia, and tachycardia, which often results in intraoperative death^[28]. Dantrolene has been shown to directly bind to the N-terminus of RyR1 and to prevent SR Ca^{2+} leak in skeletal muscle, thereby improving clinical outcomes^[29]. Dantrolene is believed to stabilize interdomain interactions between the N-terminal and central domains of RyR1^[30] and RyR2^[31], although the effects of dantrolene on single RyR channels remains controversial^[32].

Given that dantrolene improves the stability of both RyR1 and RyR2, dantrolene has become a molecule of interest for preventing cardiac arrhythmias. Dantrolene has previously been described as an inhibitor of arrhythmias in animal models of ischemia-reperfusion^[33–35]. More recently, dantrolene was demonstrated to inhibit catecholaminergic polymorphic ventricular tachycardia in a knock-in mouse model heterozygous for mutation R2474S in RyR2^[36] (Figure 1). Dantrolene was shown to suppress isoproterenol-induced spontaneous SR Ca^{2+} releases (ie, sparks) in intact myocytes isolated from RyR2-R2474A/+ mice. The mechanisms by which dantrolene prevented CPVT was attributed to stabilization of mutant RyR2 channels, and possibly also by preventing the PKA-induced reduction in calmodulin binding to RyR2^[37]. In this study, dantrolene did not exert any appreciable effects on cardiac function in hearts of wild-type mice. However, dan-

tolene did correct defective interdomain interactions within RyR2 isolated from dogs with heart failure, associated with suppression of delayed afterdepolarizations^[31].

In other studies, dantrolene has been described to improve cardiac contractility in failing hearts, which may contribute to its role in reducing arrhythmias in structural heart disease. Congestive heart failure (CHF) has been associated with a negative force-frequency relationship (Bowditch effect) in failing myocardium. Dantrolene has been shown to ameliorate the negative force-frequency relationship in explanted failing myocardial muscle strips by improving inotropic response to isoproterenol^[38]. This improved contractility was not associated with overall changes in cytoplasmic $[\text{Ca}^{2+}]$, and was postulated to be associated with improvement of diastolic Ca^{2+} release. Further evidence for reduction of Ca^{2+} release events in improved contractility was shown by Kobayashi *et al*^[31], who examined the effects of dantrolene on cardiac function on failing hearts. Dantrolene was shown to directly bind near the N-terminal domain in RyR2 at amino acids 601–620, a site critical for N-terminal and central domain interactions. Whereas unzipping of N-terminal and central domains was associated with spontaneous SR Ca^{2+} leak, dantrolene suppressed both unzipping and SR Ca^{2+} leak (sparks) and ultimately delayed afterdepolarizations, which are common in heart failure. Additionally, dantrolene restores calmodulin (CaM) binding to RyR2, which is usually attenuated in heart failure^[39]. Thus, dantrolene appears to be a promising molecule to treat arrhythmias in patients with CPVT and may attenuate cardiac Ca^{2+} handling dysfunction associated with heart failure.

1,4-Benzothiazepines

The benzothiazepine derivative JTV519 (4-[3(1-(4-benzyl)piperidinyl)propionyl]-7-methoxy-2,2,4,5-tetrahydro-1,4-benzothiazepine; also known as K201) was first identified as a compound able to suppress intracellular Ca^{2+} overload associated with cardiac cell death^[40]. The drug has been reported to have antiarrhythmic effects in a canine model of atrial fibrillation due to sterile pericarditis^[41] and Langendorff-perfused rat hearts subjected to ischemia-reperfusion^[42, 43]. JTV519 interacts with annexin-V and at higher doses inhibits various voltage-gated ion channels in the heart^[44, 45]. Subsequently, it has become clear that RyR2 represents an important target of JTV519^[46, 47].

JTV519 was described to normalize RyR2 gating in dogs with tachycardia-induced heart failure^[48]. In this study, Kohno *et al*^[48] demonstrated that JTV519 reversed the SR Ca^{2+} release defects indicative of RyR2 dysfunction. The concept of RyR2 stabilization by FKBP12.6 was further supported by the findings that JTV519 treatment of dogs with pacing-induced heart failure increased the amount of FKBP12.6 immunoprecipitated with RyR2^[46]. Moreover, JTV519 was shown to prevent lethal ventricular arrhythmias in mice haploinsufficient for FKBP12.6 by increasing FKBP12.6 binding to RyR2^[47] (Figure 2). The lack of efficacy of JTV519 in FKBP12.6 deficient mice suggests that FKBP12.6 binding to RyR2 is associated with the therapeutic effects of this compound^[47]. On the other hand,

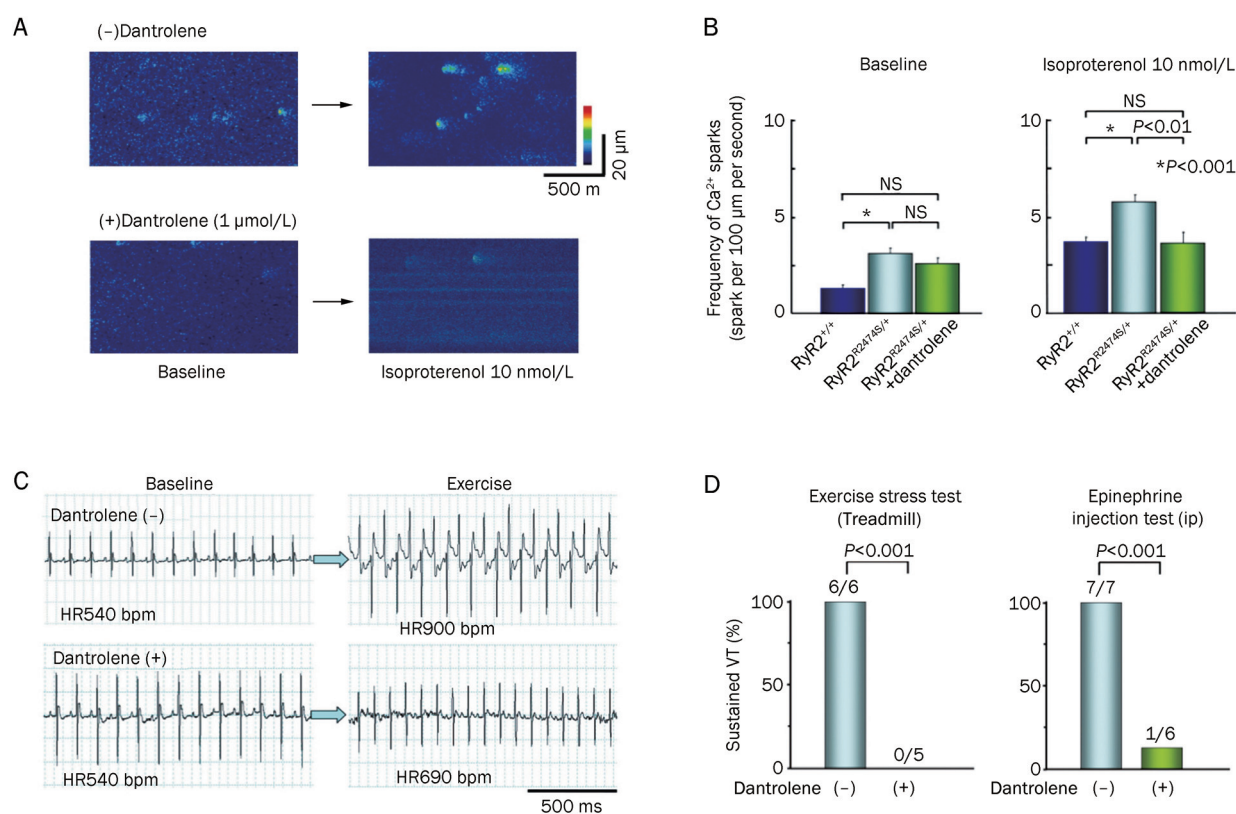


Figure 1. Dantrolene inhibits catecholaminergic polymorphic ventricular tachycardia in mice. (A) Representative images of Ca²⁺ sparks in cardiomyocytes isolated from heterozygous RyR2-R2474S/+ knock-in mice, showing that dantrolene reduces Ca²⁺ spark frequency following isoproterenol exposure. (B) Bar graph showing that dantrolene suppresses abnormal Ca²⁺ spark frequency in RyR2-R2474S/+ mutant mice after isoproterenol exposure. (C) Telemetric ECG recordings reveal exercise-induced ventricular tachycardia in a RyR2-R2474S/+ mouse, which was suppressed by dantrolene. (D) Bar graphs revealing that dantrolene suppresses the incidence of exercise or epinephrine induced ventricular tachycardia (VT) in RyR2-R2474S/+ mice. Adapted from Kobayashi et al^[36].

normalizing FKBP12.6 levels within the RyR2 macromolecular complex stabilizes the closed state of the channel, thereby preventing aberrant openings during diastole^[5]. Follow-up *in vitro* studies of human RyR2 mutations found in patients with CPVT (P2328S, Q4201R, and V4653F) showed that JTV519 can also normalize mutant channel gating as evidenced by single channel recordings^[49].

There has been some controversy whether the antiarrhythmic effects of JTV519 require modification of RyR2-FKBP12.6 interactions^[50]. In a mouse model of CPVT caused by the R4496C mutation in RyR2, it was shown that this mutation did not alter FKBP12.6 binding affinity for RyR2. Moreover, JTV519 did not prevent delayed afterdepolarizations in myocytes isolated from heterozygous RyR2-R4496C/+ mice^[51]. However, subsequent studies by other groups have shown that JTV519 did reduce the occurrence of spontaneous action potentials in ouabain-treated WT and RyR2-R4496/+ mouse myocytes, presumably independent of FKBP12.6^[52]. Additionally, *in vitro* studies in HEK293 cells suggest that JTV519 suppresses store-overload induced Ca²⁺ release independently of FKBP12.6 binding, though the relevance of these observations have yet to be determined *in vivo*^[50]. Also, Yamamoto et al^[53]

reported that JTV519 directly bound to RyR2 between amino acids 2114 and 2149, and that JTV519 can normalize defective interdomain interactions associated with RyR2 dysfunction.

Recently S107, a new 1,4-benzothiazepine similar to JTV519, has been found to prevent ventricular arrhythmias in a CPVT mouse model heterozygous for mutation R2474S in RyR2^[54]. In contrast to JTV519, S107 has been reported to lack off-target activity for ion channels other than RyR2 at concentrations up to 10 mmol/L^[54, 55]. S107 provided protection against epinephrine-induced ventricular tachycardias caused by abnormal SR Ca²⁺ leak in RyR2-R2474S/+ mice^[54]. Further, S107 was recently shown to be effective at preventing ventricular arrhythmias in the *mdx* mouse model of muscular dystrophy^[56]. Thus, 1,4-benzothiazepine derivatives JTV519 and S107 hold promise as RyR2-stabilizing molecules that could reduce the risk of arrhythmias^[57].

Flecainide

Flecainide is a trifluoroethoxybenzamide that was discovered to be a potent antiarrhythmic agent in 1977^[58]. Flecainide initially showed promise as an antiarrhythmic agent against both ventricular^[59] and atrial arrhythmias^[60]. Because a predomi-

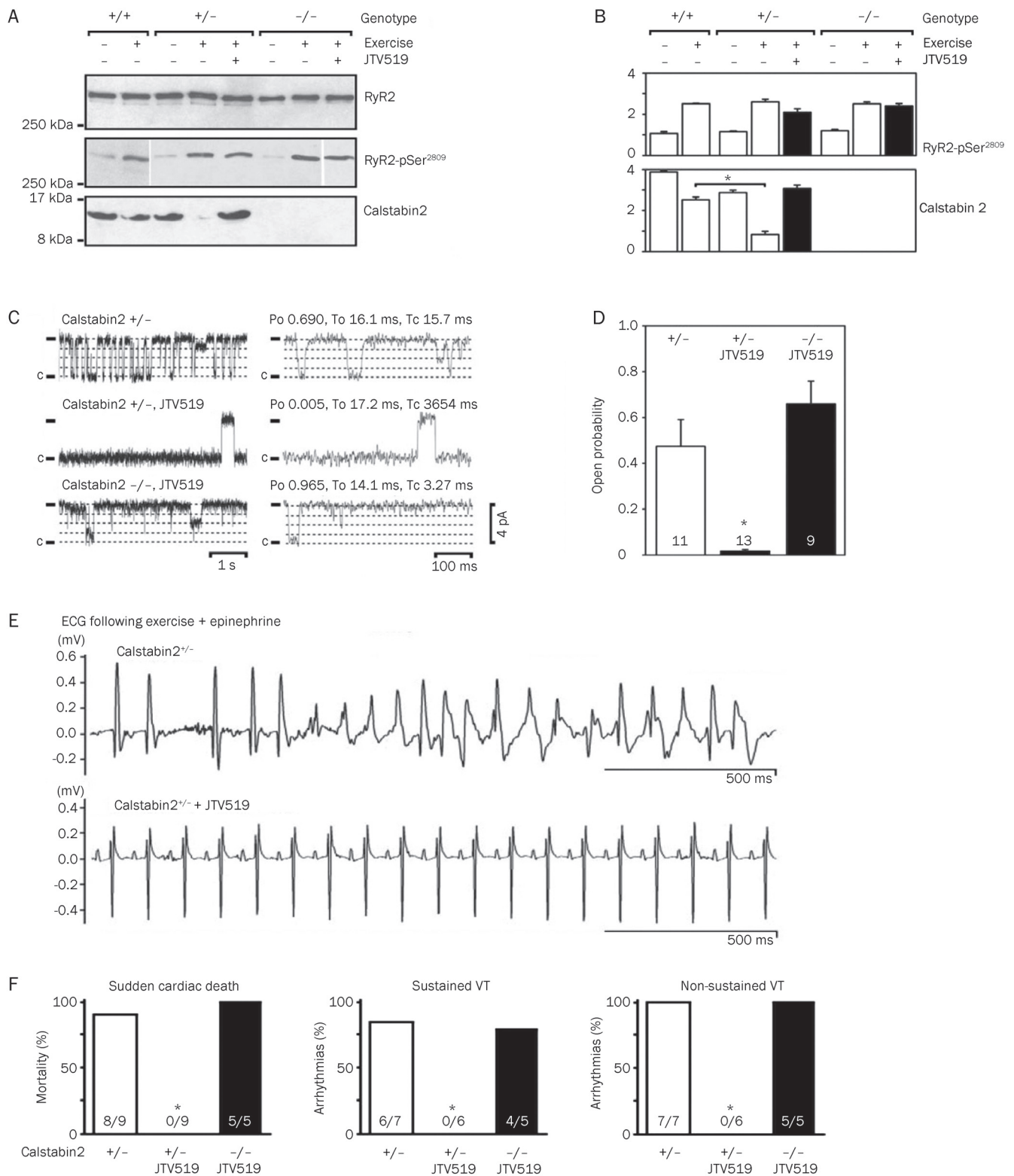


Figure 2. Anti-arrhythmic effects of 1,4-benzothiazepine JTV-519 in FKBP12.6^{+/-} mice. (A–B) Representative immunoblots and quantifications for RyR2, RyR2-pSer²⁸⁰⁹ (PKA phosphorylation site on RyR2), and calstabin2 (FKBP12.6) from wildtype (WT), calstabin2^{+/-} heterozygous, and calstabin2^{-/-} (FKBP12.6^{-/-}) knockout mice. Whereas exercise increased PKA phosphorylation of RyR2 and decreased calstabin2 (FKBP12.6) binding to RyR2, JTV-519 prevented calstabin2 dissociation. (C–D) Representative single channel recordings in planar lipid bilayers showing that JTV519 reduced the open probability of RyR2 isolated from calstabin2^{+/-} but not calstabin2^{-/-} mice, consistent with calstabin2 (FKBP12.6) being required for the therapeutic effects of JTV519. (E–F) ECG tracings showing that JTV-519 reduces ventricular arrhythmias in calstabin2^{+/-} but not calstabin2^{-/-} mice. **P*<0.05. Adapted from Wehrens et al^[47].

nant mechanism of action on inactivation of voltage-gated Na⁺ channels, it was classified as a type IC anti-arrhythmic drug. However, clinical trial results indicated that in patients with structural heart disease susceptible to ventricular arrhythmias, flecainide might in fact be pro-arrhythmogenic^[61, 62].

Recently, there has been a resurgence of enthusiasm for the use of flecainide in a select group of CPVT patients with genetic predisposition to ventricular arrhythmias and SCD. Watanabe *et al*^[63] found that flecainide inhibited the RyR2 channel by reducing the duration of RyR2 channel openings without affecting closed channel duration. Flecainide reduced SR Ca²⁺ release events and triggered arrhythmic beats in a calsequestrin deficient (*Casq2*^{-/-}) mouse model of CPVT^[63] (Figure 3). Moreover, it was shown that flecainide significantly reduced the incidence of exercise-induced arrhythmias in patients with mutations in *CASQ2*^[63]. Follow-up studies from the same group showed that flecainide reduced Ca²⁺ spark mass but increased spark frequency, resulting in a net neutral effect on SR Ca²⁺ leak and SR Ca²⁺ content^[64]. This finding is distinct from the reported mechanism of tetracaine, another RyR2 channel blocking agent, which reduces Ca²⁺ sparks and SR leak, thereby increasing SR Ca²⁺ content. Therefore, it was concluded that flecainide promoted block of the RyR2 open state, reducing the “probability of saltatory wave propagation between adjacent Ca²⁺ release units”^[64].

Other groups have applied these findings to further delineate the mechanism of arrhythmogenesis in another mouse model of CPVT. Knock-in mice heterozygous for mutation R4496/+ in RyR2 were crossed with *Cntn2-EGFP* transgenic mice expressing a fluorescent marker for the cardiac conduction system^[65]. Whereas tetracaine reduced spontaneous SR Ca²⁺ release events in ventricular myocytes and Purkinje cells equally, flecainide more specifically targeted mutant RyR2 in Purkinje cells, implicating the Purkinje conduction system as a potent mediator of ventricular arrhythmias in CPVT. Thus, flecainide may have a unique role in the prevention and suppression of ventricular arrhythmias in patients with genetically inherited CPVT.

Modulation of RyR2 posttranslational modification

In addition to inherited mutations, RyR2 channel function may also be perturbed due to acquired changes in, for example, channel posttranslational modulation^[2]. Xu *et al*^[20] demonstrated that increased S-nitrosylation leads to enhanced RyR2 activity and promotes SR Ca²⁺ release. Increased S-nitrosylation of RyR2 has been associated with cardiac arrhythmias in a mouse model of Duchenne’s muscular dystrophy, and inhibition with S107 (see above) was shown to normalize both RyR1 and RyR2 function and prevent arrhythmias^[56, 66]. In contrast, Gonzalez *et al*^[17] demonstrated that decreased rather

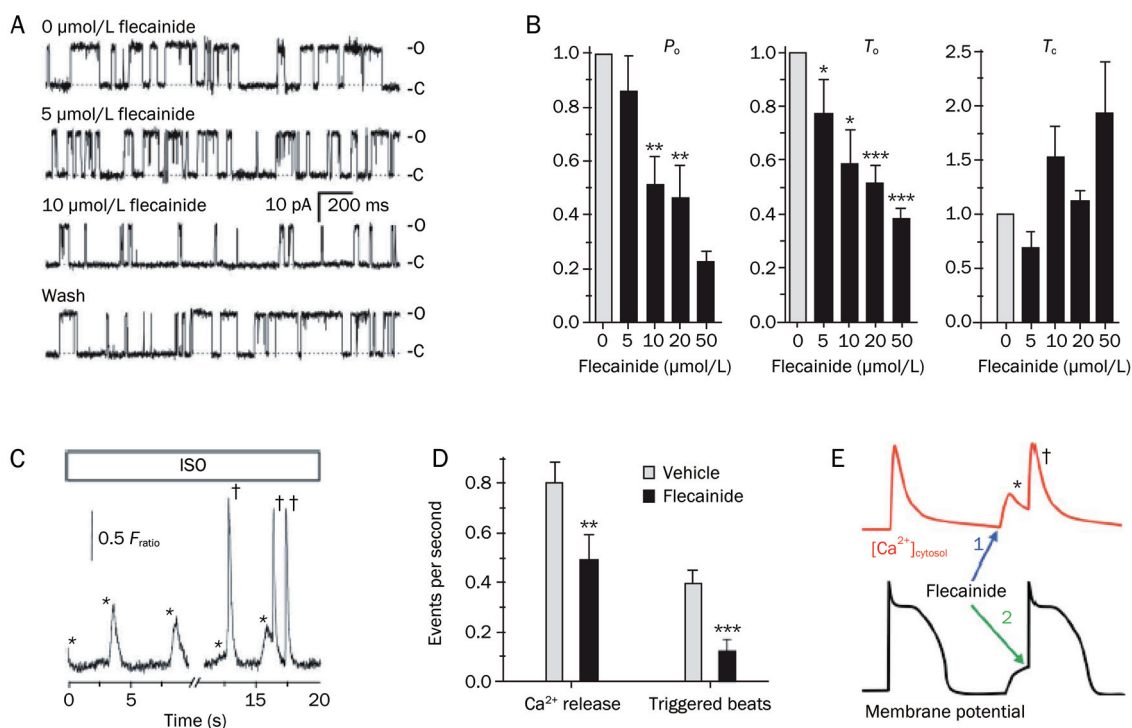


Figure 3. Prevention of triggered arrhythmias by flecainide. (A–B) Concentration-dependent effects of flecainide on single sheep RyR2 channels in lipid bilayers. Flecainide decreases open probability (P_o) and mean open time (T_o), and does not significantly alter the mean closed time (T_c) of RyR2. * $P < 0.02$, ** $P < 0.01$ and *** $P < 0.001$. (C–D) Effects of flecainide on isoproterenol (ISO) stimulated calsequestrin-deficient cardiomyocytes. Whereas ISO evoked spontaneous SR Ca²⁺ release events (*), flecainide reduced the number of Ca²⁺ releases and triggered beats (†). ** $P = 0.0078$ and *** $P < 0.001$. (E) Cartoon illustrating dual effects of flecainide action on SR Ca²⁺ release (red tracing) and inhibition of premature beats triggered by delayed after depolarization (black tracing). Adapted from Watanabe *et al*^[63].

than increased S-nitrosylation of RyR2 might promote SR Ca²⁺ leak and arrhythmogenesis. One explanation of this apparent paradox relates to nitroso-redox imbalance, a condition in which excess formation of reactive oxygen species (ROS) can modify the same thiols that are also target of S-nitrosylation^[67]. Indeed, Gonzalez *et al*^[67] reported evidence for increased oxidation of RyR2 associated with an increased tendency towards SR Ca²⁺ leak in rats with heart failure. In this particular study, increased oxidative stress was primarily the result of enhanced xanthine oxidase (XO) activity. Pharmacological inhibition of XO restored both the nitroso-redox imbalance and intracellular Ca²⁺ release defects in these rats with heart failure^[67]. Moreover, Niggli's group showed that anti-oxidants (ie, MPG and Mn-cpx3) normalized abnormal RyR sensitivity and hypersensitive E-C coupling in dystrophic cardiomyocytes^[68].

Increased oxidative stress might also promote activation of Ca²⁺/calmodulin-dependent protein kinase, which can phosphorylate RyR2 along with other Ca²⁺ handling proteins, and increase the propensity towards cardiac arrhythmias^[69]. We have previously shown that CaMKII phosphorylation of RyR2 leads to increased channel open probability^[19]. Recently, we demonstrated that constitutive phosphorylation of RyR2 by CaMKII in RyR2-S2814D knock-in mice promoted abnormal SR Ca²⁺ release events associated with ectopic activity and ventricular arrhythmias^[10]. On the other hand, genetic inhibition of RyR2 phosphorylation at S2814 in RyR2-S2814A knock-in mice conferred protection against ventricular arrhythmias in mice with heart failure induced by transverse aortic banding^[10]. These studies suggest that inhibition of RyR2 phosphorylation by CaMKII might provide a very specific way of preventing ventricular and also atrial arrhythmias^[6]. Moreover, pharmacological inhibition of the enzyme CaMKII itself might also provide protection against arrhythmias^[6, 70, 71].

RyR2 is also regulated by protein kinase A (PKA) phosphorylation, and increased PKA phosphorylation of RyR2 has been observed in patients with atrial fibrillation^[7]. Shan *et al*^[57] demonstrated that mice in which RyR2 was constitutively phosphorylated by PKA (RyR2-S2808D knock-in mice) exhibited an increased open probability, more calcium sparks, and increased SR Ca²⁺ leak. Inhibition of PKA phosphorylation of RyR2 in RyR2-S2808A mice was shown to protect against catecholamine-induced ventricular arrhythmias^[72]. Although there are currently no drugs that specifically reduce RyR2 phosphorylation, beta blockers such as carvedilol have been shown to reduce RyR2 phosphorylation and thereby RyR2 open probability in patients with atrial fibrillation^[73]. In addition, some beta blockers such as carvedilol also have antioxidant properties in addition to beta-adrenergic blockade, and may be useful in prolongation of arrhythmia-free survival in patients with congestive heart failure versus beta blockers lacking anti-oxidant properties^[74]. Clearly, further pharmacological studies would be needed to determine whether modulating post-translational modifications of RyR2 represents a suitable anti-arrhythmic strategy.

Conclusions

Cardiac arrhythmias is a potentially life-threatening complication of genetic and structural heart disease. Recent insights into excitation-contraction coupling have implicated release of SR Ca²⁺ through RyR2 as a key mechanism for the initiation and maintenance of both atrial and ventricular arrhythmias. RyR2-mediated release of SR Ca²⁺ is a tightly regulated process that involves discrete release of Ca²⁺ during systole, and cessation of Ca²⁺ release during diastole. For timely rhythmic release of Ca²⁺ from RyR2, the channel must succinctly open in response to cytoplasmic Ca²⁺ flux, but remain closed during diastolic SR Ca²⁺ filling. Destabilization of RyR2 may occur as a result of genetic mutations (ie, CPVT) or acquired (eg, oxidation, nitrosylation, phosphorylation) modifications, resulting in pathologic diastolic Ca²⁺ release, and subsequent arrhythmias.

Given the prominent role of RyR2 in SR Ca²⁺ release, pharmacological strategies to modulate RyR2 stability and gating have shown great promise as a therapy for cardiac arrhythmias. Several drugs targeting RyR2, such as benzothiazepine derivatives and flecainide, bind RyR2 directly and reduce the open probability of RyR2, thereby reducing pathological SR Ca²⁺ "leak". As benzothiazepines and flecainide have an additional role in blockade of voltage-gated sodium channels and delayed rectifier potassium channels, there may be an additive effect on anti-arrhythmic action, however further studies are necessary to evaluate whether this may occur independently of RyR2 blockade or enhancement of RyR2-FKBP12.6 binding. Additionally, dantrolene has been shown to bind directly to RyR2 and stabilize inter-domain regions, although the effects on RyR2 open probability are still controversial. Each of these drugs has a unique mechanism of action, as dantrolene stabilizes N-terminal and central domain interactions, benzothiazepines increase FKBP12.6 (calstabin2) binding to RyR2 (among other mechanisms), and flecainide blocks the open state of the channel. These drugs have proven particularly helpful in CPVT, in which stabilization of RyR2 reduces diastolic SR Ca²⁺ leak, and therefore reduces delayed afterdepolarizations.

In patients with structural heart disease, such as in congestive heart failure, acquired alterations in RyR2 function occur primarily due to post-translational modification of the channel. There is extensive evidence that hyperphosphorylation of RyR2 in heart failure also promotes the occurrence of SR Ca²⁺ leak^[10, 18, 72, 75]. By genetic or pharmacological blockade of RyR2 phosphorylation at CaMKII or PKA site, animal models have shown that effective arrhythmia prophylaxis is possible, especially under catecholaminergic conditions or after stress exercise. Recent insights also indicate that adverse redox remodeling of RyR2 may predispose to cardiac arrhythmias. Emerging data suggest that certain beta-adrenergic blocking agents, such as carvedilol, may also exert a redox-stabilizing effect on RyR2, which may potentially increase survival in patients with acquired heart disease. Ultimately, these insights will guide the design of future studies in human patients, whereby stabilization of the RyR2 channel might lead to improved outcomes in morbidity and mortality.

Acknowledgements

Dr McCauley is supported by NHLBI training grant 5T32HL066991-07. Dr WEHRENS is a WM Keck Foundation Distinguished Young Scholar in Medical Research and is supported by NHLBI grants R01-HL089598 and R01-HL091947, and Muscular Dystrophy Association grant 186531. This work was also supported in part by the Fondation Leducq Alliance for CaMKII Signaling in Heart.

References

- 1 Bers DM. Cardiac excitation-contraction coupling. *Nature* 2002; 415: 198–205.
- 2 Wehrens XH, Lehnart SE, Marks AR. Intracellular calcium release and cardiac disease. *Annu Rev Physiol* 2005; 67: 69–98.
- 3 Dobrev D, Wehrens XH. Calmodulin kinase II, sarcoplasmic reticulum Ca²⁺ leak, and atrial fibrillation. *Trends Cardiovasc Med* 2010; 20: 30–4.
- 4 Laitinen PJ, Brown KM, Piippo K, Swan H, Devaney JM, Brahmabhatt B, *et al*. Mutations of the cardiac ryanodine receptor (RyR2) gene in familial polymorphic ventricular tachycardia. *Circulation* 2001; 103: 485–90.
- 5 Wehrens XH, Lehnart SE, Huang F, Vest JA, Reiken SR, Mohler PJ, *et al*. FKBP12.6 deficiency and defective calcium release channel (ryanodine receptor) function linked to exercise-induced sudden cardiac death. *Cell* 2003; 113: 829–40.
- 6 Chelu MG, Sarma S, Sood S, Wang S, van Oort RJ, Skapura DG, *et al*. Calmodulin kinase II-mediated sarcoplasmic reticulum Ca²⁺ leak promotes atrial fibrillation in mice. *J Clin Invest* 2009; 119: 1940–51.
- 7 Vest JA, Wehrens XH, Reiken SR, Lehnart SE, Dobrev D, Chandra P, *et al*. Defective cardiac ryanodine receptor regulation during atrial fibrillation. *Circulation* 2005; 111: 2025–32.
- 8 Mathur N, Sood S, Wang S, van Oort RJ, Sarma S, Li N, *et al*. Sudden infant death syndrome in mice with an inherited mutation in RyR2. *Circ Arrhythm Electrophysiol* 2009; 2: 677–85.
- 9 Priori SG, Napolitano C, Tiso N, Memmi M, Vignati G, Bloise R, *et al*. Mutations in the cardiac ryanodine receptor gene (hRyR2) underlie catecholaminergic polymorphic ventricular tachycardia. *Circulation* 2001; 103: 196–200.
- 10 van Oort RJ, McCauley MD, Dixit SS, Pereira L, Yang Y, Respress JL, *et al*. Ryanodine receptor phosphorylation by calcium/calmodulin-dependent protein kinase II promotes life-threatening ventricular arrhythmias in mice with heart failure. *Circulation* 2010; 122: 2669–79.
- 11 Lehnart SE, Terrenoire C, Reiken S, Wehrens XH, Song LS, Tillman EJ, *et al*. Stabilization of cardiac ryanodine receptor prevents intracellular calcium leak and arrhythmias. *Proc Natl Acad Sci U S A* 2006; 103: 7906–10.
- 12 Paavola J, Viitasalo M, Laitinen-Forsblom PJ, Pasternack M, Swan H, Tikkanen I, *et al*. Mutant ryanodine receptors in catecholaminergic polymorphic ventricular tachycardia generate delayed afterdepolarizations due to increased propensity to Ca²⁺ waves. *Eur Heart J* 2007; 28: 1135–42.
- 13 McCauley MD, Wehrens XH. Animal models of arrhythmogenic cardiomyopathy. *Dis Model Mech* 2009; 2: 563–70.
- 14 Landstrom AP, Weisleder N, Batalden KB, Bos JM, Tester DJ, Ommen SR, *et al*. Mutations in JPH2-encoded junctophilin-2 associated with hypertrophic cardiomyopathy in humans. *J Mol Cell Cardiol* 2007; 42: 1026–35.
- 15 Song L, Alcalai R, Arad M, Wolf CM, Toka O, Conner DA, *et al*. Calsequestrin 2 (CASQ2) mutations increase expression of calreticulin and ryanodine receptors, causing catecholaminergic polymorphic ventricular tachycardia. *J Clin Invest* 2007; 117: 1814–23.
- 16 Belevych AE, Terentyev D, Viatchenko-Karpinski S, Terentyeva R, Sridhar A, Nishijima Y, *et al*. Redox modification of ryanodine receptors underlies calcium alternans in a canine model of sudden cardiac death. *Cardiovasc Res* 2009; 84: 387–95.
- 17 Gonzalez DR, Beigi F, Treuer AV, Hare JM. Deficient ryanodine receptor S-nitrosylation increases sarcoplasmic reticulum calcium leak and arrhythmogenesis in cardiomyocytes. *Proc Natl Acad Sci U S A* 2007; 104: 20612–7.
- 18 Marx SO, Reiken S, Hisamatsu Y, Jayaraman T, Burkhoff D, Rosembly N, *et al*. PKA phosphorylation dissociates FKBP12.6 from the calcium release channel (ryanodine receptor): defective regulation in failing hearts. *Cell* 2000; 101: 365–76.
- 19 Wehrens XH, Lehnart SE, Reiken SR, Marks AR. Ca²⁺/calmodulin-dependent protein kinase II phosphorylation regulates the cardiac ryanodine receptor. *Circ Res* 2004; 94: e61–70.
- 20 Xu L, Eu JP, Meissner G, Stamler JS. Activation of the cardiac calcium release channel (ryanodine receptor) by poly-S-nitrosylation. *Science* 1998; 279: 234–7.
- 21 Anderson ME, Higgins LS, Schulman H. Disease mechanisms and emerging therapies: protein kinases and their inhibitors in myocardial disease. *Nat Clin Pract Cardiovasc Med* 2006; 3: 437–45.
- 22 Santonastasi M, Wehrens XH. Ryanodine receptors as pharmacological targets for heart disease. *Acta Pharmacol Sin* 2007; 28: 937–44.
- 23 Dulhunty AF, Beard NA, Pouliquin P, Casarotto MG. Agonists and antagonists of the cardiac ryanodine receptor: potential therapeutic agents? *Pharmacol Ther* 2007; 113: 247–63.
- 24 Wehrens XH, Lehnart SE, Marks AR. Ryanodine receptor-targeted anti-arrhythmic therapy. *Ann N Y Acad Sci* 2005; 1047: 366–75.
- 25 Snyder HR Jr, Davis CS, Bickerton RK, Halliday RP. 1-[(5-aryl(furfurylidene)amino)hydantoin]. A new class of muscle relaxants. *J Med Chem* 1967; 10: 807–10.
- 26 Harrison GG. Control of the malignant hyperpyrexia syndrome in MHS swine by dantrolene sodium. *Br J Anaesth* 1975; 47: 62–5.
- 27 Durham WJ, Aracena-Parks P, Long C, Rossi AE, Goonasekera SA, Boncompagni S, *et al*. RyR1 S-nitrosylation underlies environmental heat stroke and sudden death in Y522S RyR1 knockin mice. *Cell* 2008; 133: 53–65.
- 28 Denborough M. Malignant hyperthermia. *Lancet* 1998; 352: 1131–6.
- 29 Paul-Pletzer K, Yamamoto T, Bhat MB, Ma J, Ikemoto N, Jimenez LS, *et al*. Identification of a dantrolene-binding sequence on the skeletal muscle ryanodine receptor. *J Biol Chem* 2002; 277: 34918–23.
- 30 Kobayashi S, Bannister ML, Gangopadhyay JP, Hamada T, Parness J, Ikemoto N. Dantrolene stabilizes domain interactions within the ryanodine receptor. *J Biol Chem* 2005; 280: 6580–7.
- 31 Kobayashi S, Yano M, Suetomi T, Ono M, Tateishi H, Mochizuki M, *et al*. Dantrolene, a therapeutic agent for malignant hyperthermia, markedly improves the function of failing cardiomyocytes by stabilizing interdomain interactions within the ryanodine receptor. *J Am Coll Cardiol* 2009; 53: 1993–2005.
- 32 Szentesi P, Collet C, Sarkozi S, Szegedi C, Jona I, Jacquemond V, *et al*. Effects of dantrolene on steps of excitation-contraction coupling in mammalian skeletal muscle fibers. *J Gen Physiol* 2001; 118: 355–75.
- 33 Balam Ortiz EO, Carvajal K, Cruz D. Protective effect of dantrolene in post-ischemic reperfusion myocardial damage. *Arch Inst Cardiol Mex* 1999; 69: 311–9.
- 34 Boys JA, Toledo AH, Anaya-Prado R, Lopez-Nebolina F, Toledo-Pereyra LH. Effects of dantrolene on ischemia-reperfusion injury in animal

- models: a review of outcomes in heart, brain, liver, and kidney. *J Investig Med* 2010; 58: 875–82.
- 35 Pelleg A, Roth A, Shargordsky B, Belhassen B, Chagnac A, Laniado S. Effects of dantrolene sodium on occlusion and reperfusion arrhythmias in the canine heart. *Methods Find Exp Clin Pharmacol* 1985; 7: 239–43.
- 36 Kobayashi S, Yano M, Uchinoumi H, Suetomi T, Susa T, Ono M, et al. Dantrolene, a therapeutic agent for malignant hyperthermia, inhibits catecholaminergic polymorphic ventricular tachycardia in a RyR2(R2474S/+) knock-in mouse model. *Circ J* 2010; 74: 2579–84.
- 37 Xu X, Yano M, Uchinoumi H, Hino A, Suetomi T, Ono M, et al. Defective calmodulin binding to the cardiac ryanodine receptor plays a key role in CPVT-associated channel dysfunction. *Biochem Biophys Res Commun* 2010; 394: 660–6.
- 38 Meissner A, Min JY, Haake N, Hirt S, Simon R. Dantrolene sodium improves the force-frequency relationship and beta-adrenergic responsiveness in failing human myocardium. *Eur J Heart Fail* 1999; 1: 177–86.
- 39 Ono M, Yano M, Hino A, Suetomi T, Xu X, Susa T, et al. Dissociation of calmodulin from cardiac ryanodine receptor causes aberrant Ca²⁺ release in heart failure. *Cardiovasc Res* 2010; 87: 609–17.
- 40 Kaneko N. New 1,4-benzothiazepine derivative, K201, demonstrates cardioprotective effects against sudden cardiac cell death and intracellular calcium blocking action. *Drug Dev Res* 1994; 33: 429–38.
- 41 Kumagai K, Nakashima H, Gondo N, Saku K. Antiarrhythmic effects of JTV-519, a novel cardioprotective drug, on atrial fibrillation/flutter in a canine sterile pericarditis model. *J Cardiovasc Electrophysiol* 2003; 14: 880–4.
- 42 Hachida M, Lu H, Kaneko N, Nonoyama M, Koyanagi H. Protective effect of JTV519 on prolonged myocardial preservation. *Transplant Proc* 1999; 31: 1094.
- 43 Inagaki K, Kihara Y, Hayashida W, Izumi T, Iwanaga Y, Yoneda T, et al. Anti-ischemic effect of a novel cardioprotective agent, JTV519, is mediated through specific activation of delta-isoform of protein kinase C in rat ventricular myocardium. *Circulation* 2000; 101: 797–804.
- 44 Kimura J, Kawahara M, Sakai E, Yatabe J, Nakanishi H. Effects of a novel cardioprotective drug, JTV-519, on membrane currents of guinea pig ventricular myocytes. *Jpn J Pharmacol* 1999; 79: 275–81.
- 45 Nakaya H, Furusawa Y, Ogura T, Tamagawa M, Uemura H. Inhibitory effects of JTV-519, a novel cardioprotective drug, on potassium currents and experimental atrial fibrillation in guinea-pig hearts. *Br J Pharmacol* 2000; 131: 1363–72.
- 46 Yano M, Kobayashi S, Kohno M, Doi M, Tokuhisa T, Okuda S, et al. FKBP12.6-mediated stabilization of calcium-release channel (ryanodine receptor) as a novel therapeutic strategy against heart failure. *Circulation* 2003; 107: 477–84.
- 47 Wehrens XH, Lehnart SE, Reiken SR, Deng SX, Vest JA, Cervantes D, et al. Protection from cardiac arrhythmia through ryanodine receptor-stabilizing protein calstabin2. *Science* 2004; 304: 292–6.
- 48 Kohno M, Yano M, Kobayashi S, Doi M, Oda T, Tokuhisa T, et al. A new cardioprotective agent, JTV519, improves defective channel gating of ryanodine receptor in heart failure. *Am J Physiol Heart Circ Physiol* 2003; 284: H1035–42.
- 49 Lehnart SE, Wehrens XH, Laitinen PJ, Reiken SR, Deng SX, Cheng Z, et al. Sudden death in familial polymorphic ventricular tachycardia associated with calcium release channel (ryanodine receptor) leak. *Circulation* 2004; 109: 3208–14.
- 50 Hunt DJ, Jones PP, Wang R, Chen W, Bolstad J, Chen K, et al. K201 (JTV519) suppresses spontaneous Ca²⁺ release and [³H]ryanodine binding to RyR2 irrespective of FKBP12.6 association. *Biochem J* 2007; 404: 431–8.
- 51 Liu N, Colombi B, Memmi M, Zissimopoulos S, Rizzi N, Negri S, et al. Arrhythmogenesis in catecholaminergic polymorphic ventricular tachycardia: insights from a RyR2 R4496C knock-in mouse model. *Circ Res* 2006; 99: 292–8.
- 52 Sedej S, Heinzel FR, Walther S, Dybkova N, Wakula P, Groborz J, et al. Na⁺-dependent SR Ca²⁺ overload induces arrhythmogenic events in mouse cardiomyocytes with a human CPVT mutation. *Cardiovasc Res* 2010; 87: 50–9.
- 53 Yamamoto T, Yano M, Xu X, Uchinoumi H, Tateishi H, Mochizuki M, et al. Identification of target domains of the cardiac ryanodine receptor to correct channel disorder in failing hearts. *Circulation* 2008; 117: 762–72.
- 54 Lehnart SE, Mongillo M, Bellinger A, Lindegger N, Chen BX, Hsueh W, et al. Leaky Ca²⁺ release channel/ryanodine receptor 2 causes seizures and sudden cardiac death in mice. *J Clin Invest* 2008; 118: 2230–45.
- 55 Bellinger AM, Reiken S, Dura M, Murphy PW, Deng SX, Landry DW, et al. Remodeling of ryanodine receptor complex causes “leaky” channels: a molecular mechanism for decreased exercise capacity. *Proc Natl Acad Sci U S A* 2008; 105: 2198–202.
- 56 Fauconnier J, Thireau J, Reiken S, Cassan C, Richard S, Matecki S, et al. Leaky RyR2 trigger ventricular arrhythmias in Duchenne muscular dystrophy. *Proc Natl Acad Sci U S A* 2010; 107: 1559–64.
- 57 Shan J, Betzenhauser MJ, Kushnir A, Reiken S, Meli AC, Wronska A, et al. Role of chronic ryanodine receptor phosphorylation in heart failure and beta-adrenergic receptor blockade in mice. *J Clin Invest* 2010; 120: 4375–87.
- 58 Banitt EH, Bronn WR, Coyne WE, Schmid JR. Antiarrhythmics. 2. Synthesis and antiarrhythmic activity of N-(piperidylalkyl)trifluoroethoxybenzamides. *J Med Chem* 1977; 20: 821–6.
- 59 Anderson JL, Stewart JR, Perry BA, Van Hamersveld DD, Johnson TA, Conard GJ, et al. Oral flecainide acetate for the treatment of ventricular arrhythmias. *N Engl J Med* 1981; 305: 473–7.
- 60 Anderson JL, Gilbert EM, Alpert BL, Henthorn RW, Waldo AL, Bhandari AK, et al. Prevention of symptomatic recurrences of paroxysmal atrial fibrillation in patients initially tolerating antiarrhythmic therapy. A multicenter, double-blind, crossover study of flecainide and placebo with transtelephonic monitoring. Flecainide Supraventricular Tachycardia Study Group. *Circulation* 1989; 80: 1557–70.
- 61 Muhiddin K, Nathan AW, Hellestrand KJ, Banim SO, Camm AJ. Ventricular tachycardia associated with flecainide. *Lancet* 1982; 2: 1220–1.
- 62 Preliminary report: effect of encainide and flecainide on mortality in a randomized trial of arrhythmia suppression after myocardial infarction. The Cardiac Arrhythmia Suppression Trial (CAST) Investigators. *N Engl J Med* 1989; 321: 406–12.
- 63 Watanabe H, Chopra N, Laver D, Hwang HS, Davies SS, Roach DE, et al. Flecainide prevents catecholaminergic polymorphic ventricular tachycardia in mice and humans. *Nat Med* 2009; 15: 380–3.
- 64 Hilliard FA, Steele DS, Laver D, Yang Z, Le Marchand SJ, Chopra N, et al. Flecainide inhibits arrhythmogenic Ca²⁺ waves by open state block of ryanodine receptor Ca²⁺ release channels and reduction of Ca²⁺ spark mass. *J Mol Cell Cardiol* 2010; 48: 293–301.
- 65 Kang G, Giovannone SF, Liu N, Liu FY, Zhang J, Priori SG, et al. Purkinje cells from RyR2 mutant mice are highly arrhythmogenic but responsive to targeted therapy. *Circ Res* 2010; 107: 512–9.
- 66 Bellinger AM, Reiken S, Carlson C, Mongillo M, Liu X, Rothman L, et al. Hypernitrosylated ryanodine receptor calcium release channels are leaky in dystrophic muscle. *Nat Med* 2009; 15: 325–30.
- 67 Gonzalez DR, Treuer AV, Castellanos J, Dulce RA, Hare JM. Impaired

- S-nitrosylation of the ryanodine receptor caused by xanthine oxidase activity contributes to calcium leak in heart failure. *J Biol Chem* 2010; 285: 28938–45.
- 68 Ullrich ND, Fanchaouy M, Gusev K, Shirokova N, Niggli E. Hypersensitivity of excitation-contraction coupling in dystrophic cardiomyocytes. *Am J Physiol Heart Circ Physiol* 2009; 297: H1992–2003.
- 69 Erickson JR, Joiner ML, Guan X, Kutschke W, Yang J, Oddis CV, *et al*. A dynamic pathway for calcium-independent activation of CaMKII by methionine oxidation. *Cell* 2008; 133: 462–74.
- 70 Sag CM, Wadsack DP, Khabbazzadeh S, Abesser M, Grefe C, Neumann K, *et al*. Calcium/calmodulin-dependent protein kinase II contributes to cardiac arrhythmogenesis in heart failure. *Circ Heart Fail* 2009; 2: 664–75.
- 71 Erickson JR, Anderson ME. CaMKII and its role in cardiac arrhythmia. *J Cardiovasc Electrophysiol* 2008; 19: 1332–6.
- 72 Lehnart SE, Wehrens XH, Reiken S, Warriar S, Belevych AE, Harvey RD, *et al*. Phosphodiesterase 4D deficiency in the ryanodine-receptor complex promotes heart failure and arrhythmias. *Cell* 2005; 123: 25–35.
- 73 Reiken S, Wehrens XH, Vest JA, Barbone A, Klotz S, Mancini D, *et al*. Beta-blockers restore calcium release channel function and improve cardiac muscle performance in human heart failure. *Circulation* 2003; 107: 2459–66.
- 74 Poole-Wilson PA, Swedberg K, Cleland JG, Di Lenarda A, Hanrath P, Komajda M, *et al*. Comparison of carvedilol and metoprolol on clinical outcomes in patients with chronic heart failure in the Carvedilol Or Metoprolol European Trial (COMET): randomised controlled trial. *Lancet* 2003; 362: 7–13.
- 75 Wehrens XH, Lehnart SE, Reiken S, Vest JA, Wronska A, Marks AR. Ryanodine receptor/calcium release channel PKA phosphorylation: a critical mediator of heart failure progression. *Proc Natl Acad Sci U S A* 2006; 103: 511–8.

Review

A role of stretch-activated potassium currents in the regulation of uterine smooth muscle contraction

Iain L O BUXTON*, Nathanael HEYMAN, Yi-ying WU, Scott BARNETT, Craig ULRICH

Myometrial Research Laboratory, University of Nevada School of Medicine, Reno, Nevada 89557–0573, USA

Rates of premature birth are alarming and threaten societies and healthcare systems worldwide. Premature labor results in premature birth in over 50% of cases. Preterm birth accounts for three-quarters of infant morbidity and mortality. Children that survive birth before 34 weeks gestation often face life-long disability. Current treatments for preterm labor are wanting. No treatment has been found to be generally effective and none are systematically evaluated beyond 48 h. New approaches to the treatment of preterm labor are desperately needed. Recent studies from our laboratory suggest that the uterine muscle is a unique compartment with regulation of uterine relaxation unlike that of other smooth muscles. Here we discuss recent evidence that the mechanically activated 2-pore potassium channel, TREK-1, may contribute to contraction-relaxation signaling in uterine smooth muscle and that *TREK-1* gene variants associated with human labor and preterm labor may lead to a better understanding of preterm labor and its possible prevention.

Keywords: stretch-activated potassium currents; preterm labor; uterine muscle; nitric oxide; arachidonic acid; pregnancy; TREK-1

Acta Pharmacologica Sinica (2011) 32: 758–764; doi: 10.1038/aps.2011.62

Introduction

Preterm labor and delivery of an under-developed fetus affect approximately 13 million births worldwide each year^[1]. The number of babies that die annually due solely to their prematurity ranges from 20 000 (4%) in the US to 336 000 of the 1.2 million newborn deaths (28%) in Sub-Saharan Africa^[2]. Those that survive their prematurity have numerous chronic health disabilities that constitute a major human tragedy, are enormously costly to societies and cripple the third world development. Advanced medical care makes it possible for premature fetuses (some as early as 22–24 weeks) to survive, but at huge cost often resulting in life-long disability for survivors. Prematurity, whether due to infection or occurring spontaneously, threatens global health and must be addressed.

Despite decades of interest, the majority of cases of preterm labor are unexplained, and there is currently no effective medication to prevent uterine contractions at the time of labor as evidenced by a lack of an FDA approved indication in the US for any treatment for preterm labor (PTL). Challenging also is the absence of a useful animal model in which to propose studies for PTL since there is no animal that experiences this uniquely human problem. The impact of delivery of a pre-

term fetus on society is very high; the Institute of Medicine estimates that this costs the American economy \$26.2 billion annually (in 2006 dollars).

In the last several years it has become clear that uterine smooth muscle mechanisms of relaxation differ significantly from those of other human smooth muscles. In this review we explore the nature of contractile regulation of myometrial smooth muscle and describe a channel target that we posit may be of significant interest as a therapeutic target for tocolysis.

The onset of labor

The signal(s) that initiate labor at term in women are unknown. This is an embarrassing truth when viewed in the context of what we have learned in a relatively short time about diseases such as AIDS. Our current ability to treat HIV-AIDS with highly active antiretroviral therapy has drastically changed HIV infection from an acute, very deadly disease, to a chronic, long-lasting, manageable disease^[3]. Such truth offers lessons; among the truths is that targeted research funding can yield results rapidly and the embarrassment surely is that we still don't understand our own reproductive physiology very well.

Theories of the proximate cause of labor have varied over time as we have learned more about what is not, rather than what is responsible for the regulation of uterine contractions.

* To whom correspondence should be addressed.

E-mail ibuxton@medicine.nevada.edu

Received 2011-03-16 Accepted 2011-04-18

For example, quite logical might be the notion that maternal nervous regulation initiates labor. However, we have known for some time that the uterus becomes essentially denervated during gestation^[4] and as a result, it is unlikely that any coordinated nervous regulation of the myometrium is centrally orchestrated^[5]. As a result, views of the origin of onset of labor turned early on to examine endocrine and paracrine mechanism of myometrial regulation. A role for corticotrophin releasing hormone (CRH) posits that the hormone, generated in the placenta, builds in the serum and amniotic fluid as pregnancy progresses^[6]. The human fetus also has a pituitary-adrenal axis by mid-trimester and CRH, although present in lower concentrations than in the maternal circulation, stimulates adrenocorticotrophic hormone (ACTH) secretion from the fetal pituitary. ACTH is also synthesized in the placenta under the influence of CRH^[7]. Fetal ACTH stimulates production of the androgenic steroids dehydroepiandrosterone (DHEA) and dehydroepiandrosterone sulphate (DHEAS). Cortisol secretion is induced by ACTH and an increase in fetal cortisol production in late pregnancy is responsible for fetal organ maturation including lung maturation^[8]. DHEA and DHEAS production in the fetus is thought to lead to initiation of parturition through their metabolism by the placenta to estrogen^[9], which acts on the myometrium, cervix and fetal membranes. While estrogen is thought to up-regulate the expression of myometrial genes associated with contraction^[10], it is progesterone that is thought to modulate parturition timing through its withdrawal. In a number of animal models, progesterone disappearance from the circulation is associated with onset^[11]. However, maternal progesterone levels in the blood stream do not fall at the time of onset in humans and so research has focused on the notion of changes in progesterone locally in the uterine compartment not reflected in the maternal circulation such that progesterone withdrawal could occur due to local progesterone metabolism^[12] or receptor-based heterologous regulation of steroid hormone receptors that leads to a functional withdrawal of the action of progesterone as recently reviewed by Mitchell and Taggart^[13]. Whatever the fact of progesterone withdrawal, it is not at all clear that administering progesterone exogenously will serve as an effective treatment of preterm labor^[14].

Quiescence is key

Relaxation of the myometrium is required for pregnancy to proceed in the face of ever increasing tension on uterine muscle as the fetus grows^[15, 16]. Approaches to understanding PTL have examined the notion that there is an inappropriate activation of contractile influences that initiate labor too soon, as well as a failure of relaxation influences on the myometrium^[17-19]. While both may operate, we assert that successful therapeutic intervention will come from probing relaxation mechanisms. This assertion is supported by the finding that the first drug designed specifically for preterm labor, Tractocile® (atosiban) that blocks the actions of oxytocin (OT), is not superior to conventional approaches to the treatment of preterm labor^[20, 21], albeit it may pose fewer side

effects and is only evaluated at 48 h. This agent is not yet FDA approved in the US. Examination of its development reveals the unimaginative model of an OT receptor blocker to block the actions of OT^[22]. In humans however, labor is not just the result of stimulation of the myometrium by oxytocin^[23].

NO-mediated relaxation

Nitric oxide (NO) is particularly effective in relaxing the myometrium and in fact has a lower inhibitory concentration 50% (K_i) in human than guinea pig or non-human primate myometrium^[24]. We have examined the heretical notion that relaxation of the myometrium by NO is independent of cGMP elevation as a result of soluble guanylyl cyclase. Although this notion was initially rejected by many on the basis that the dogma established by the 1998 Nobel for Physiology or Medicine^[25] demanded that NO signals through cGMP in smooth muscle, it is now clearly established from our work and that of others that NO-mediated relaxation of uterine muscle is independent of global cGMP elevation no matter whether this is studied in animal^[26], primate^[27] or human^[28].

Cyclic GMP is not without effect however. When the uterus is relaxed by uroquanylin, cGMP elevation secondary to activation of the guanylyl cyclase activity of the uroquanylin receptor, particulate guanylyl cyclase type C does relax the uterus. The presence of a uroquanylin-particulate cyclase-cGMP relaxation pathway in myometrium taken together with the failure of soluble cGMP elevation to relax the muscle leads to the inevitable conclusion that cGMP is compartmented in the myometrium^[29].

The importance of the fact that an effect of NO to relax the uterus is independent of global cGMP accumulation is two-fold. First, data supporting the cGMP-independence of nitro-agent mediated relaxation of uterine muscle that were first introduced by the pioneering work of Jack Diamond^[30-32] and later by our lab as cited above, establish more dramatically than any other type of study we are aware of that the uterus, particularly the human uterus, is regulated in a disparate manner compared to other smooth muscles^[19, 29].

The notion that the uterine smooth muscle biochemistry of relaxation signaling is fundamentally different than vascular or gastrointestinal muscle means that there is hope for discovery of therapeutic targets in the myometrium that are absent or disparately regulated in other smooth muscles and thus, can permit a reasoned line of investigation to find uterine-specific tocolytics. Whatever is learned must impact the final mediator of muscle contraction, calcium availability in the uterine myocyte and while beyond the scope of this perspective, the reader is guided to a recent expert review^[33].

The second point highlighted by the unique nature of NO-mediated relaxation of uterine muscle is that since NO relaxes uterine smooth muscle, NO must act in a fashion other than through activation of the soluble guanylyl cyclase. Thus, NO must directly nitrosylate or indirectly modify one or more proteins in the myometrium that regulate relaxation. Our interest that a stretch-activated potassium channel (K2P) may play a role in normal myometrial relaxation is peaked by the persua-

sive model that gestational growth means continual myometrial stretch along with the possibility that K2P channels, or their expression is(are) a target for NO or consequences of NO signaling.

The notion that NO is generated in myometrium and responsible for regulation of uterine quiescence has been controversial^[19] and yet high levels of myometrial expression of nitric oxide synthase(s) correlated with gestation until the time of labor need not be the only source of NO to affect the myometrium. Indeed, recent studies have examined the presence of NO-synthase (NOS) in uterine tissues including myometrium^[34] and actions of NO in reproductive tissues suggest its critical role in normal reproduction^[35]. A source for myometrial NO may not come from smooth muscle generation directly, but rather from the ability of NO generated in the uterine membranes or the vasculature to bind free cysteine forming cysteine-NO (Cys-NO) or hemoglobin-NO and be transported to the muscle where it may be released as nitrosyl ion (NO⁺) and bind to reduced glutathione (GSH) to generate GSNO^[36]. Such small molecule S-nitrosothiols (SNO) offer a scientifically more satisfying way to view the preservation of the signaling actions on NO since now the functional nitrosylation of proteins by SNO may be coupled to the redox state of the cell coupling extracellular and intracellular mechanisms mediating contraction-relaxation.

Nitric oxide as Cys-NO can travel through the plasma membrane in this way as a second messenger and hence transduce stimuli and initiate responses in adjacent cells. Of the known NO-mediated reactions with biological materials, nitrosylation is the major form of protein modification under physiological conditions and constitutes an important signal transduction mechanism. S-Nitrosylation is the covalent attachment of NO to the sulfur moiety of cysteine. This chemical reaction constitutes a redox sensitive post-translational, reversible modification of protein in response to stimuli outside the cell^[37]. Rather than free diffusion of NO from a NOS, S-nitrosylation allows for the compartmentation of the source of NO and the site of nitrosylation (Cysteine). The formation of SNOs is a critical pathway in the signaling of NO between cellular compartments since it maintains the availability of NO generated in one cell to act in another preserving the action of NO in time and space^[38]. Small molecular weight SNOs such as Cys-NO and GSNO constitute the major determinants of subsequent transnitrosylation of target proteins to alter cellular response^[39] and cell-cell transfer of NO.

Once accumulated in a target cell such as the uterine myocyte, GSNO may provide a source of both NO for protein transnitrosylation as well as glutathione for glutathionylation via the action of glutathione-S transferase reactions^[40]. Thus regulation of protein targets in myocytes such as membrane channels in a reversible fashion to activate or inactivate current may have profound influence on uterine quiescence. It is possible that actions of NO or glutathione may accumulate as a consequence of vascular NO generation and redox reactions in uterine myocytes that then manage contractile force. The notion that pregnancy physiology and preterm birth may in

part involve an inflammatory-like state^[41] fits with this notion and provides a testable platform for these ideas.

Given then that NO nitrosylates one or more regulatory proteins in myometrial smooth muscle to produce relaxation, we developed a method for showing S-nitrosylation in whole tissue lysates. This method has allowed us to elucidate the human myometrial smooth muscle nitroproteome and to test the effect of these post-secondary modifications on relaxation. Our method, which we are calling Nitro-DIGE, selectively labels S-nitrosylated proteins in a cell extract using spectrally resolvable Alexa Fluor maleimide dyes. Labeled extracts are then analyzed using 2-dimensional difference gel electrophoresis (2D DIGE). With this powerful technique we can identify differences in levels of S-nitrosylation between term and preterm myometrium. These identified proteins are regulatory in nature and preliminary results have identified candidates such as heat shock protein beta-1, desmin, alpha actinin which have been shown to regulate contraction in smooth muscle tissue. Importantly, we have found nitrosylation of the K2P channel TREK-1 and confirmed the identity of this protein by LC-MS/MS. Current work is directed at both hypothesis-directed examination of the function of nitrosylated TREK channels and the smooth muscle thin filament contraction-relaxation pathway, as well as identifying prominent proteins that are selectively nitrosylated by pregnancy progression and/or in response to experimental NO-stimulation of tissues in functional assays where relaxation/contraction can be correlated with protein nitrosylation.

TRAAK-family channels

Two-pore-domain K⁺ (K2P) channel subunits are made up of four transmembrane segments and two pore-forming domains that are arranged in tandem and function as either homo- or heterodimeric channels (Figure 1). This structural motif is associated with unique gating properties that would well serve quiescence in myometrium, including background channel activity (so-called leak current) and sensitivity to membrane stretch. Moreover, TRAAK-family K2P channels are modulated by cellular lipids and pharmacological agents, including polyunsaturated fatty acids such as arachidonic acid and volatile general anesthetics^[42]. Acidity and heat have also been suggested to activate the channel^[43, 44], while antipsychotics such as fluphenazine have been shown to block TREK-1 but not the related TRAAK channels^[45].

Arachidonic acid and acidic pH in pregnancy myometrium

Blood flow is temporarily compromised during forceful uterine contractions during labor^[46]. This transient ischemia is associated with intracellular acidosis and has been proffered as a mechanism for contractile regulation in myometrium^[47]. Myocyte signaling domains may be acidic on the basis of their construction *per se*, independent of relative ischemia^[48]. Relative acidification at the myocyte membrane activating TREK-1 during gestation would fit with hyperpolarization of the membrane and decreased uterine activity. An abundance of

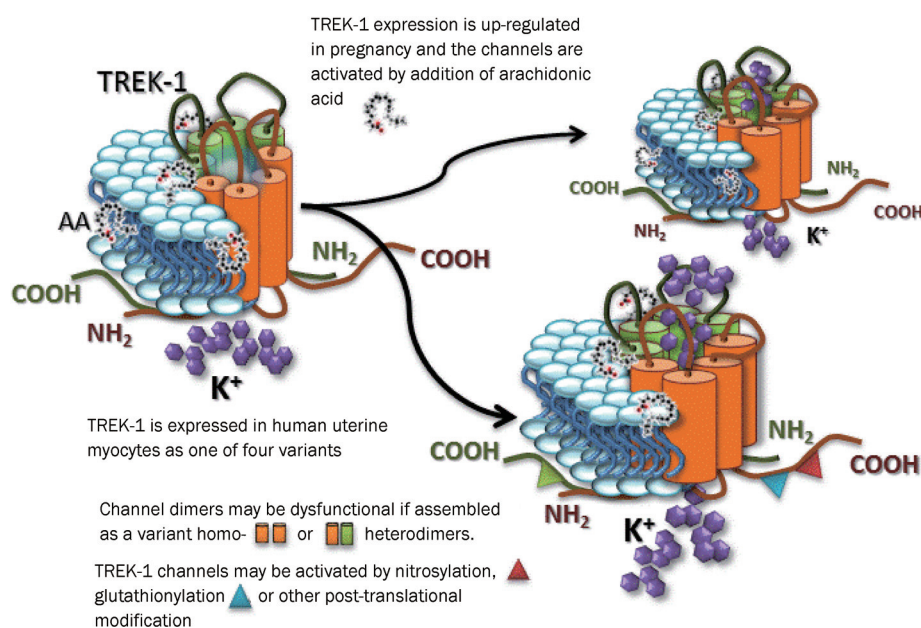


Figure 1. TREK-1 concept. Pregnancy results in up-regulation of channel number and provides for activation by stretch (right-hand figures) and arachidonic acid. The presence of channel variants (depicted as 2, 4-transmembrane units of disparate color) could result in assembly of channels that exhibit altered function or are dysfunctional. Altered conductance may be accompanied by disparate activation characteristics. Posttranslational alteration by nitrosylation, glutathionylation and or phosphorylation may confer sites of disparate regulation in preterm labor. Multimodal activation by stretch, heat, depolarization, intracellular acidosis, lipids and volatile anesthetics has been reviewed^[42]. TREK-1 is tonically inhibited by the actin cytoskeleton opening the possibility that pregnancy releases such inhibition through cytoskeletal reorganization. Protonation of a glutamic acid residue within the C-terminus of TREK-1 increases the affinity of this domain for inner leaflet phospholipids and increases activity. Stimulation of Gq-coupled extracellular receptors can inhibit TREK-1. A variety of possibilities for regulation of the TREK-1 channel in the uterine myocyte suggests that studies of TREK-1 may reveal a therapeutic target for preterm labor.

arachidonic acid in pregnant myometrium^[49] also would signal TREK-1 activation. Together, these influences may contribute to gestational uterine quiescence.

TREK-1

Other than our description of TREK-1 channels in human myometrium in 2005^[50] and the work of Bai *et al* in the same year^[51], very little was known about these channels in the myometrium until recently. Despite early claims that little TREK-1 was expressed in human^[52] or that no expression could be seen in mouse^[53] myometrium, we have shown the importance of these channels in human myometrium^[50, 54]. Recent studies in mice have now also appeared^[55]. Electrophysiological currents can readily be measured in human uterine myocytes as well as cells overexpressing the human protein (Figure 2). These currents are recorded under conditions that block other potassium channels and are themselves blocked by fluphenazine underscoring their identity as TREK-1 currents. Our ability to determine channel expression and functionally measure these channels in freshly isolated myocytes as well as cells overexpressing cloned channels, permits a thorough examination of the possibility that genetic channel variants underlie cases of preterm labor in women.

Recent *in vivo* studies have shown that TREK-1 has a key role in anesthesia, neuroprotection, pain, depression^[56], and

vascular regulation^[57]. Since it is known in rat heart that TREK-1 splice variants result in two different operating modes of the channel^[58], and since channel dysfunction could correlate with early labor, we tested the hypothesis that TREK-1 in human myometrium may also be alternatively spliced. We are aware that other data is available, describing TREK-1 variants associated with failure to respond to antidepressants^[56] and a variant in rat brain that is thought to code for a channel by alternative translation initiation that is permeable to both Na⁺ and K⁺ ions^[59]. Such a channel, if expressed in human myometrium, could readily depolarize the cell based on the Na⁺ gradient and contribute to early initiation of labor. Thus, a careful examination of TREK-1 regulation in human myometrium is particularly important.

TREK-1 variant expression

Because *TREK-1* gene expression is regulated by pregnancy increasing at term and falling at the time of labor^[54], it stands to reason that TREK-1 could be important in regulating relaxation until labor and may or may not participate in the intercontractile period during labor as suggested by the continued presence of the protein during the laboring period. If TREK-1 currents activated by the biochemistry of pregnancy (*eg*, progesterone dominance, arachidonic acid production) are important in uterine quiescence, then dysfunctional channels or low-

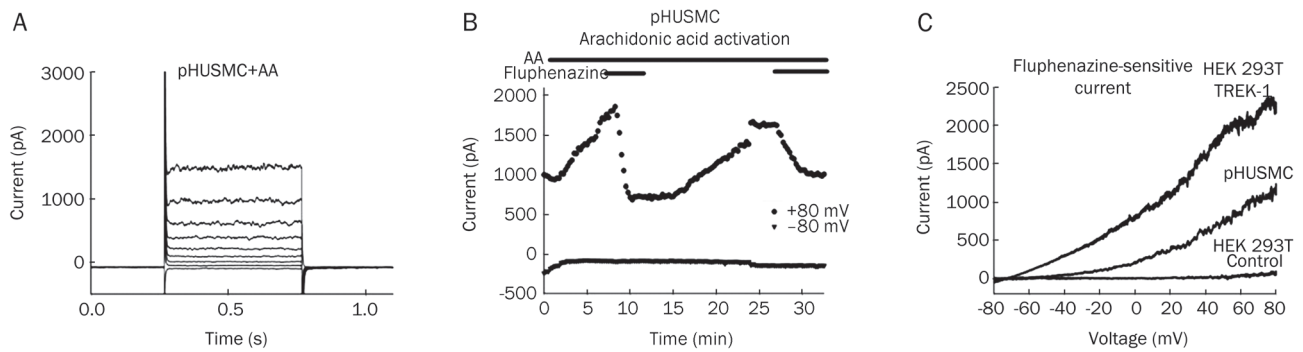


Figure 2. TEA-insensitive K^+ current in isolated uterine myocytes from gravid myometrium. (A) Whole cell currents elicited by voltage steps (-80 to +80 mV) under 10 $\mu\text{mol/L}$ arachidonic acid (AA). (B) Whole cell current activated by 10 $\mu\text{mol/L}$ AA and blocked by 10 $\mu\text{mol/L}$ fluphenazine. (C) Fluphenazine-sensitive, AA-activated whole cell currents (AA-AA+Fluphenazine) elicited by 1 s voltage ramps (reversal potential $\approx 70\text{mV}$ for HEK 293T (human embryonic kidney) cells over expressing human TREK-1 and isolated pregnant myocytes [pHUSMC] indicates K^+ current).

ered TREK-1 expression could underlie cases of spontaneous PTL. We found a high level of variation between samples in the extreme 5'-end of the mRNA.

We identified TREK-1 splice variants in human myometrium (Figure 3) using PCR. We have now cloned each of these putative channels and are expressing them in HEK cells in order to perform electrophysiological measurement of TREK-1 currents that we have examined in isolated uterine myocytes. The variability of expression differences including samples (patients) that express only one variant of the channel such as several of the preterm laboring samples we have collected, suggests the possibility that functional correlations between TREK-1 channel variants and TREK-1 variant channel function will be possible for human TREK-1. Human brain (hB) was amplified as a positive control and expressed only one of the variants seen (α , as expected) in one or more myometrial samples. This is exciting because it suggests a tissue-specific regulated expression is likely in myometrium and may have functional significance. We have tentatively named these variant transcripts from myometrium α , β , γ , δ (Figure 3). The possibility that each of these (β , γ , δ) corresponds to an expressed channel is being pursued.

Whatever the final outcome of preterm labor research, there is not a more significant human research imperative than to understand and prevent preterm delivery. If one considers the energy and treasure we expend on studying diseases of the aged only to cripple our healthcare systems with expensive medications and technology for the last years of life, and contrasts this with the relative ignorance we share about the beginning of life, it is possible to imagine we are failing. It is well past time to make preventing premature birth a priority.

Acknowledgements

Project was supported by National Institutes of Health (NIH) grant HD053028 and March of Dimes Prematurity Research Initiative #21-FY10-176 to ILOB.

References

- 1 Beck S, Wojdyla D, Say L, Betran AP, Merialdi M, Requejo JH, et al. The worldwide incidence of preterm birth: a systematic review of maternal mortality and morbidity. *Bull World Health Organ* 2010; 88: 31–8.
- 2 Kinney MV, Kerber KJ, Black RE, Cohen B, Nkrumah F, Coovadia H, et al. Sub-Saharan Africa's mothers, newborns, and children: where and why do they die? *PLoS Med* 2010; 7: e1000294.

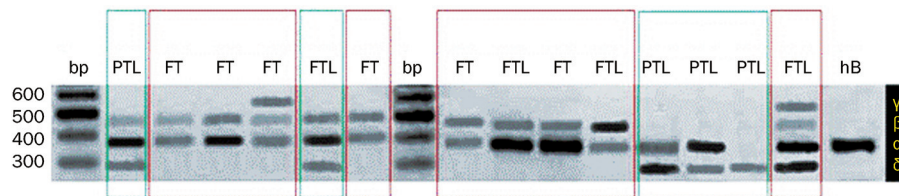


Figure 3. Expression of TREK-1 variants in human pregnant myometrium. We used the GenBank accession sequence NT_021877.18 to generate forward [AGG AAA CAG TAT GGG ACG ATG GCT] and reverse primers [CTG CTC CAA TGC TTT GAA CAC GGT] to examine expression of KCNK2 (K2P) TREK-1 in myometrium. The predicted product was 373 bp. Tissues from women who were in spontaneous preterm labor (PTL); at full term (38–41 weeks) but not in labor (FT); or who were at full term in labor (FTL) were collected under informed consent. A composite gel from several experiments is shown. Human brain cDNA was employed as a positive control (hB) and non-template controls run with water instead of cDNA were included with each experiment and verified the PCR (not shown). α – δ are a tentative identification by our lab of unique channel variants in myometrium based on these experiments. These variants have now been cloned and expressed in human embryonic kidney cells for electrophysiological and signal transduction studies.

- 3 Scotti N, Buonaguro L, Tornesello ML, Cardi T, Buonaguro FM. Plant-based anti-HIV-1 strategies: vaccine molecules and antiviral approaches. *Expert Rev Vaccines* 2010; 9: 925–36.
- 4 Haase EB, Buchman J, Tietz AE, Schramm LP. Pregnancy-induced uterine neuronal degeneration in the rat. *Cell Tissue Res* 1997; 288: 293–306.
- 5 Latini C, Frontini A, Morroni M, Marzoni D, Castellucci M, Smith PG. Remodeling of uterine innervation. *Cell Tissue Res* 2008; 334: 1–6.
- 6 Majzoub JA, Karalis KP. Placental corticotropin-releasing hormone: function and regulation. *Am J Obstet Gynecol* 1999; 180: S242–6.
- 7 Petraglia F, Giardino L, Coukos G, Calza L, Vale W, Genazzani AR. Corticotropin-releasing factor and parturition: plasma and amniotic fluid levels and placental binding sites. *Obstet Gynecol* 1990; 75: 784–9.
- 8 Majzoub JA, McGregor JA, Lockwood CJ, Smith R, Taggart MS, Schulkin J. A central theory of preterm and term labor: putative role for corticotropin-releasing hormone. *Am J Obstet Gynecol* 1999; 180: S232–41.
- 9 Challis JRG, Matthews SG, Gibb W, Lye SJ. Endocrine and paracrine regulation of birth at term and preterm. *Endocr Rev* 2000; 21: 514–50.
- 10 Arthur P, Taggart MJ, Zielnik B, Wong S, Mitchell BF. Relationship between gene expression and function of uterotonic systems in the rat during gestation, uterine activation and both term and preterm labour. *J Physiol* 2008; 586: 6063–76.
- 11 Csapo AI, Wiest WG. An examination of the quantitative relationship between progesterone and the maintenance of pregnancy. *Endocrinology* 1969; 85: 735–46.
- 12 Mitchell BF, Challis JR, Lukash L. Progesterone synthesis by human amnion, chorion, and decidua at term. *Am J Obstet Gynecol* 1987; 157: 349–53.
- 13 Mitchell BF, Taggart MJ. Are animal models relevant to key aspects of human parturition? *Am J Physiol Regul Integr Comp Physiol* 2009; 297: R525–45.
- 14 Rittenberg C, Newman RB, Istwan NB, Rhea DJ, Stanziano GJ. Preterm birth prevention by 17 alpha-hydroxyprogesterone caproate vs daily nursing surveillance. *J Reprod Med* 2009; 54: 47–52.
- 15 Anderson AB, Turnbull AC, Murray AM. The relationship between amniotic fluid pressure and uterine wall tension in pregnancy. *Am J Obstet Gynecol* 1967; 97: 992–7.
- 16 Scudiero R, Khoshnood B, Pryde PG, Lee KS, Wall S, Mittendorf R. Perinatal death and tocolytic magnesium sulfate. *Obstet Gynecol* 2000; 96: 178–82.
- 17 Challis JR, Lye SJ, Gibb W, Whittle W, Patel F, Alfaidy N. Understanding preterm labor. *Ann NY Acad Sci* 2001; 943: 225–34.
- 18 Hertelendy F, Zakar T. Regulation of myometrial smooth muscle functions. *Curr Pharm Des* 2004; 10: 2499–517.
- 19 Buxton IL. Regulation of uterine function: a biochemical conundrum in the regulation of smooth muscle relaxation. *Mol Pharmacol* 2004; 65: 1051–9.
- 20 Husslein P, Fuchs AR, Fuchs F. Oxytocin and the initiation of human parturition I. Prostaglandin release during induction of labor by oxytocin. *Am J Obstet Gynecol* 1981; 141: 688–93.
- 21 Lin CH, Lin SY, Shyu MK, Chen SU, Lee CN. Randomized trial of oxytocin antagonist atosiban versus beta-adrenergic agonists in the treatment of spontaneous preterm labor in Taiwanese women. *J Formos Med Assoc* 2009; 108: 493–501.
- 22 Lamont RF. The development and introduction of anti-oxytocic tocolytics. *BJOG* 2003; 110: 108–12.
- 23 Kamel RM. The onset of human parturition. *Arch Gynecol Obstet* 2010; 281: 975–82.
- 24 Buxton IL, Kaiser RA, Malmquist NA, Tichenor S. NO-induced relaxation of labouring and non-labouring human myometrium is not mediated by cyclic GMP. *Br J Pharmacol* 2001; 134: 206–14.
- 25 Furchgott RF. Endothelium-derived relaxing factor: discovery, early studies, and identification as nitric oxide. *BiosciRep* 1999; 19: 235–51.
- 26 Kuenzli KA, Bradley ME, Buxton IL. Cyclic GMP-independent effects of nitric oxide on guinea-pig uterine contractility. *Br J Pharmacol* 1996; 119: 737–43.
- 27 Kuenzli KA, Buxton IL, Bradley ME. Nitric oxide regulation of monkey myometrial contractility. *Br J Pharmacol* 1998; 124: 63–8.
- 28 Bradley KK, Buxton IL, Barber JE, McGaw T, Bradley ME. Nitric oxide relaxes human myometrium by a cGMP-independent mechanism. *Am J Physiol* 1998; 275: C1668–73.
- 29 Buxton IL, Milton D, Barnett S, Tichenor SD. Agonist-specific compartmentation of cGMP action in guinea pig myometrium. *J Pharmacol Exp Ther* 2010; 335: 256–63.
- 30 Diamond J. Lack of correlation between cyclic GMP elevation and relaxation of nonvascular smooth muscle by nitroglycerin, nitroprusside, hydroxylamine and sodium azide. *J Pharmacol Exp Ther* 1983; 225: 422–6.
- 31 Diamond J, Hartle DK. Cyclic nucleotide levels during spontaneous uterine contractions. *Can J Physiol Pharmacol* 1974; 52: 763–67.
- 32 Hennen JK, Diamond J. Evidence that spontaneous contractile activity in the rat myometrium is not inhibited by NO-mediated increases in tissue levels of cyclic GMP. *Br J Pharmacol* 1998; 123: 959–67.
- 33 Aguilar HN, Mitchell BF. Physiological pathways and molecular mechanisms regulating uterine contractility. *Hum Reprod Update* 2010; 16: 725–44.
- 34 Suzuki T, Mori C, Yoshikawa H, Miyazaki Y, Kansaku N, Tanaka K, *et al*. Changes in nitric oxide production levels and expression of nitric oxide synthase isoforms in the rat uterus during pregnancy. *Biosci Biotechnol Biochem* 2009; 73: 2163–6.
- 35 Poniedzialek-Czajkowska E, Marciniak B, Kimber-Trojnar Z, Leszczynska-Gorzela B, Oleszczuk J. Nitric oxide in normal and preeclamptic pregnancy. *Curr Pharm Biotechnol* 2011; 12: 743–9.
- 36 Allen BW, Demchenko IT, Piantadosi CA. Two faces of nitric oxide: implications for cellular mechanisms of oxygen toxicity. *J Appl Physiol* 2009; 106: 662–7.
- 37 Hess DT, Matsumoto A, Kim SO, Marshall HE, Stamler JS. Protein S-nitrosylation: purview and parameters. *Nat Rev Mol Cell Biol* 2005; 6: 150–66.
- 38 Matsumoto A, Gow AJ. Membrane transfer of S-nitrosothiols. *Nitric Oxide* 2011 Mar 4 [Epub ahead of print].
- 39 Liu L, Yan Y, Zeng M, Zhang J, Hanes MA, Ahearn G, *et al*. Essential roles of S-nitrosothiols in vascular homeostasis and endotoxic shock. *Cell* 2004; 116: 617–28.
- 40 Laborde E. Glutathione transferases as mediators of signaling pathways involved in cell proliferation and cell death. *Cell Death Differ* 2010; 17: 1373–80.
- 41 Wei SQ, Fraser W, Luo ZC. Inflammatory cytokines and spontaneous preterm birth in asymptomatic women: a systematic review. *Obstet Gynecol* 2010; 116: 393–401.
- 42 Dedman A, Sharif-Naeini R, Folgering JH, Duprat F, Patel A, Honore E. The mechano-gated K(2P) channel TREK-1. *Eur Biophys J* 2009; 38: 293–303.
- 43 Goldstein SA, Bockenhauer D, O’Kelly I, Zilberberg N. Potassium leak channels and the KCNK family of two-P-domain subunits. *Nat Rev Neurosci* 2001; 2: 175–84.
- 44 Cohen A, Ben-Abu Y, Hen S, Zilberberg N. A novel mechanism for human K2P2.1 channel gating. Facilitation of C-type gating by

- protonation of extracellular histidine residues. *J Biol Chem* 2008; 283: 19448–55.
- 45 Thummler S, Duprat F, Lazdunski M. Antipsychotics inhibit TREK but not TRAAK channels. *Biochem Biophys Res Commun* 2007; 354: 284–9.
- 46 Greiss FC Jr. Effect of labor on uterine blood flow. Observations on gravid ewes. *Am J Obstet Gynecol* 1965; 93: 917–23.
- 47 Larcombe-McDouall J, Buttell N, Harrison N, Wray S. *In vivo* pH and metabolite changes during a single contraction in rat uterine smooth muscle. *J Physiol* 1999; 518: 783–90.
- 48 Anderson RG. The caveolae membrane system. *Annu Rev Biochem* 1998; 67: 199–225.
- 49 Egarter CH, Husslein P. Biochemistry of myometrial contractility. *Baillieres Clin Obstet Gynaecol* 1992; 6: 755–69.
- 50 Tichenor JN, Hansen ET, Buxton IL. Expression of stretch-activated potassium channels in human myometrium. *Proc West Pharmacol Soc* 2005; 48: 44–8.
- 51 Bai X, Bugg GJ, Greenwood SL, Glazier JD, Sibley CP, Baker PN, *et al*. Expression of TASK and TREK, two-pore domain K⁺ channels, in human myometrium. *Reproduction* 2005; 129: 525–30.
- 52 Medhurst AD, Rennie G, Chapman CG, Meadows H, Duckworth MD, Kelsell RE, *et al*. Distribution analysis of human two pore domain potassium channels in tissues of the central nervous system and periphery. *Brain Res Mol Brain Res* 2001; 86: 101–14.
- 53 Koh SD, Monaghan K, Sergeant GP, Ro S, Walker RL, Sanders KM, *et al*. TREK-1 regulation by nitric oxide and cGMP-dependent protein kinase. An essential role in smooth muscle inhibitory neurotransmission. *J Biol Chem* 2001; 276: 44338–46.
- 54 Buxton ILO, Singer CA, Tichenor JN. Regulation of stretch-activated two-pore potassium channels in human myometrium in pregnancy and labor. *PLoS One* 2010; 5: e12372.
- 55 Mongahan K, Baker SA, Dwyer L, Hatton WC, Park KS, Sanders KM, *et al*. The stretch-dependent potassium conductance TREK-1 and its function in murine myometrium. *J Physiol* 2011; 589: 1221–33.
- 56 Perlis RH, Moorjani P, Fagerness J, Purcell S, Trivedi MH, Fava M, *et al*. Pharmacogenetic analysis of genes implicated in rodent models of antidepressant response: association of TREK1 and treatment resistance in the STAR(*)D study. *Neuropsychopharmacology* 2008; 33: 2810–9.
- 57 Bryan RM Jr, Joseph BK, Lloyd E, Rusch NJ. Starring TREK-1: the next generation of vascular K⁺ channels. *Circ Res* 2007; 101: 119–21.
- 58 Xian TL, Dyachenko V, Zuzarte M, Putzke C, Preisig-Muller R, Isenberg G, *et al*. The stretch-activated potassium channel TREK-1 in rat cardiac ventricular muscle. *Cardiovasc Res* 2006; 69: 86–97.
- 59 Thomas D, Plant LD, Wilkens CM, McCrossan ZA, Goldstein SA. Alternative translation initiation in rat brain yields K2P2.1 potassium channels permeable to sodium. *Neuron* 2008; 58: 859–70.

Review

Current understanding of K_{ATP} channels in neonatal diseases: focus on insulin secretion disorders

Yi QUAN¹, Andrew BARSZCZYK¹, Zhong-ping FENG^{1,*}, Hong-shuo SUN^{1,2,3,4,*}

Departments of ¹Physiology, ²Surgery, and ³Pharmacology, ⁴Institute of Medical Science, Faculty of Medicine, University of Toronto, 1 King's College Circle, Toronto, Ontario, Canada, M5S 1A8

ATP-sensitive potassium (K_{ATP}) channels are cell metabolic sensors that couple cell metabolic status to electric activity, thus regulating many cellular functions. In pancreatic beta cells, K_{ATP} channels modulate insulin secretion in response to fluctuations in plasma glucose level, and play an important role in glucose homeostasis. Recent studies show that gain-of-function and loss-of-function mutations in K_{ATP} channel subunits cause neonatal diabetes mellitus and congenital hyperinsulinism respectively. These findings lead to significant changes in the diagnosis and treatment for neonatal insulin secretion disorders. This review describes the physiological and pathophysiological functions of K_{ATP} channels in glucose homeostasis, their specific roles in neonatal diabetes mellitus and congenital hyperinsulinism, as well as future perspectives of K_{ATP} channels in neonatal diseases.

Keywords: ATP-sensitive potassium (K_{ATP}) channels; channelopathy; neonatal diabetes; congenital hyperinsulinism; glucose homeostasis; diazoxide; sulfonylureas

Acta Pharmacologica Sinica (2011) 32: 765–780; doi: 10.1038/aps.2011.57; published online 23 May 2011

Introduction

Adenosine triphosphate (ATP)-sensitive potassium (K_{ATP}) channels function as metabolic sensors that are capable of coupling a cell's metabolic status to electrical activity in order to regulate many cellular functions. The K_{ATP} channels are expressed extensively in various cell types, including pancreatic beta cells, skeletal muscles, smooth muscles, adipose tissue, cardiomyocytes and neurons, where they regulate cell excitability. In pancreatic beta cells, K_{ATP} channels are capable of modulating insulin secretion in response to fluctuations in plasma glucose levels, and thus are an important regulator of glucose homeostasis. K_{ATP} channel mutations mediated dysfunctions are associated with a variety of insulin secretion disorders, including neonatal diabetes mellitus and congenital hyperinsulinism. Fortunately, the identification of the role of K_{ATP} channels in these diseases has led to the implementation of new and improved clinical diagnoses and treatment practices. This review provides an overview of K_{ATP} channels, the role they play in the pathophysiology of neonatal diabetes and congenital hyperinsulinism, and the new therapeutic approaches developed based on our current understanding of

these diseases. It also discusses the current issues associated with the use of K_{ATP} channel modulators in treating these neonatal diseases.

Structure of K_{ATP} channel subunits

Functional K_{ATP} channels are octomeric protein structures composed of four Kir6.x subunits that form the channel pore, surrounded by four sulfonylurea receptors (SURs) that regulate the channel pore activity^[1] (Figure 1). The Kir6.x subunits (either Kir6.1 or Kir6.2) belong to the superfamily of weak inwardly rectifying, voltage independent potassium (K^+) channels^[2]. These channels generate large K^+ conductance at potentials negative to the equilibrium potential of potassium (E_K), but permit less current flow at more positive potentials. This, in conjunction with their voltage-independence, makes Kir channels one of the major regulators of resting membrane potentials. Furthermore, the unique sensitivity to ATP/ADP levels makes K_{ATP} channels the ideal cell metabolic sensors^[3]. That is, K_{ATP} channels are able to regulate the membrane excitability in response to the metabolic status of the cell, thus, regulating many cellular functions, such as insulin secretion, excitability and cytoprotection.

K_{ATP} channels were first discovered in cardiomyocytes^[4], and their expression was subsequently confirmed in pancreatic beta cells^[5, 6], skeletal muscles^[7, 8], vascular smooth muscles^[9], adipose tissue^[10], glial cells^[11], and neurons^[12–14]. In the major-

* To whom correspondence should be addressed.

E-mail zp.feng@utoronto.ca (Zhong-ping FENG);

hss.sun@utoronto.ca (Hong-shuo SUN)

Received 2011-03-11 Accepted 2011-04-13

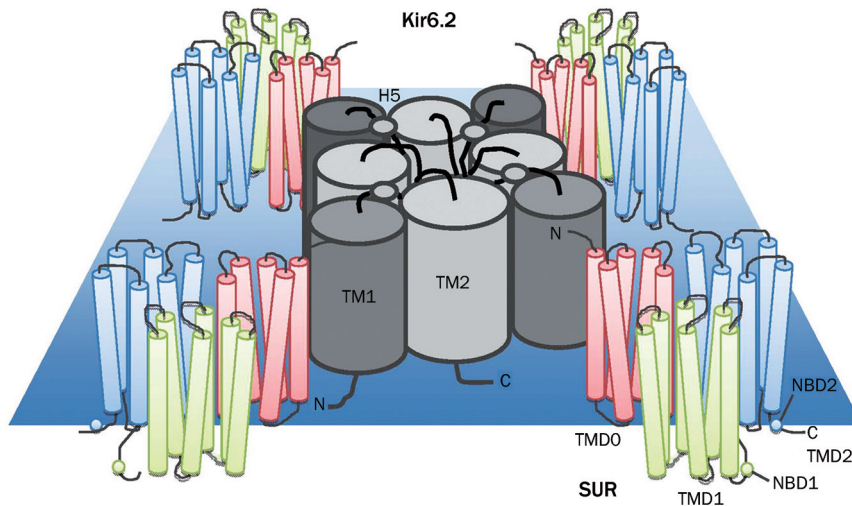


Figure 1. Schematic of the domain structure of a K_{ATP} channel. Four Kir6.2 subunits form the channel pore, and are surrounded by four sulfonylurea receptors (SURs) that regulate pore activity. Each Kir6.2 subunit has two domains (TM1 and TM2), linked by an extracellular pore-forming region (H5). Each SUR subunit has 17 transmembrane regions grouped into three domains: TMD0 (TM1-5), TMD1 (TM 6-11), and TMD2 (TM 12-17). Each SUR subunit also has two nucleotide binding domains (NBD).

ity of these tissues, the channel pore is formed by four Kir6.2 subunits^[15]. Each Kir6.2 subunit has two transmembrane (TM) domains (TM1 and TM2) linked by an extracellular pore-forming region (H5)^[2, 3]. The four TM2 domains in a K_{ATP} channel form the channel pore and the H5 region serves as the potassium selectivity filter, which contains the Kir6.2 channel signature sequence GFG (rather than GYG in the K^+ channel)^[2]. The amino and carboxyl terminals are both found cytoplasmically, and join together to form the cytoplasmic domain that is responsible for channel gating and ATP binding^[2, 3, 16]. Like other Kir subunits, it lacks the S4 voltage sensor region that is critical for gating in all voltage dependent calcium (Ca^{2+}), sodium (Na^+) and potassium (K^+) channels. Therefore, K_{ATP} channels are constitutively active if other regulatory mechanisms, such as SUR subunits, or ATP are absent.

The SUR regulatory subunits belong to the ATP-binding cassette (ABC) transporter family^[17]. Each SUR subunit has 17 TM regions, grouped into three transmembrane domains (TMDs). TMD1 (TM6-11) and TMD2 (TM12-17) are conserved among members of the ABC family. TMD0 (TM1-5) is unique to SUR, and is essential for trafficking Kir6.2 subunits to the membrane surface^[18]. Similar to all other ABC transporters, SUR subunits contain two nucleotide binding domains (NBDs). Dimerization of these two NBDs creates one single nucleotide binding site and catalytic site. Mg-dependent hydrolysis at this site provides the power stroke necessary to overcome the inhibitory effect of ATP on Kir6.2^[3]. Unlike traditional ABC transporters, the SUR regulatory subunits cannot conduct a functional current^[17].

Two types of SUR regulatory subunits have been identified to date^[17, 19]. They differ primarily in their affinity for sulfonylurea, their tissue distribution and genetic source. SUR1, encoded by the *ABCC8* gene located at ch11p15.1, has higher affinity for sulfonylurea and is mainly found in pancreatic beta cells and most neurons. SUR2, encoded by the *ABCC9* gene located at ch12p12.1, has lower affinity for sulfonylureas and is expressed mainly in the heart, skeletal muscle and some neurons^[2, 3]. SUR2 has two splice variants, SUR2A and

SUR2B. They differ only in the last 42 C-terminal amino acid residues. Interestingly, the C42 of SUR2B shows high homology to the C42 of SUR1^[20]. Since most K_{ATP} channels identified to date contain the Kir6.2 subunit, the heterogeneity observed between different K_{ATP} channels mainly arises from the differential expression of SUR regulatory subunits.

Biophysical properties and regulation of K_{ATP} channels

Gating and channel kinetics

Two independent types of gates for K_{ATP} channels have been described^[3, 21, 22]. The fast gating is due to the action of the selectivity filter. This ligand-independent gate is affected by mutations near the selectivity filter^[21]. The slow ligand-dependent gate describes changes in the TM2 helices induced by ATP binding^[22]. Mutations in TM2 near the cytoplasmic end have been shown to affect the slow gating in multiple Kir channels^[3, 23-25]. The kinetics of K_{ATP} channels consists of 1 open state and multiple closed states^[3, 21, 26, 27]. The channel only conducts current if all four Kir6.2 subunits are in the open conformation. ATP binding to any one subunit will induce a closed conformation in that subunit, and subsequent channel closure. Therefore the channel has multiple closed states and only one open state.

Trafficking of K_{ATP} channels

The membrane expression of K_{ATP} channels follows the strict 4:4 SUR:Kir stoichiometry, which has two implications. First, it allows only octameric channels expressed on the membrane, thus serves as quality control mechanisms that prevent expression of partial channels. Second, it indicates a tight coupling between the SUR and Kir subunits during the assembly and trafficking of K_{ATP} channels. Indeed, regulation of the membrane expression of the functional channels lies in the presence of a novel ER retention signal, RKR, which is present in both Kir6.2 and SUR subunits^[26]. Appropriate interactions between Kir6.2 and SUR subunits result in shielding of this RKR signal, allowing the complex to exit the ER and be trafficked to the plasma membrane. Furthermore, presence of this RKR signal

prevents the membrane expression of Kir tetramers (without SUR), SUR monomers or partial K_{ATP} channel complexes^[28]. As such, SUR subunits are the major regulator of the trafficking of Kir6.2 channels.

Numerous factors affect the efficiency of trafficking of K_{ATP} channels. Specifically, SUR regulation of Kir6.2 trafficking is dependent on the TMD0^[29] and NBD1^[30] domains of SUR, such that mutations (or deletions) at these regions result in significant decreases of membrane expression of K_{ATP} channels. Furthermore, mutations affecting the shielding of the RKR ER retention signal, such as L1544P on SUR1 that causes congenital hyperinsulinism, also decrease trafficking of K_{ATP} channels^[31]. Lastly, glucose deprivation stimulates trafficking of Kir6.2 subunits, possibly through an AMP kinase (AMPK)-dependent pathway^[32].

Regulation by intracellular ATP, Mg-ADP

The primary regulators of K_{ATP} channel activity are intracellular nucleotides, ATP and ADP. ATP has two major functions^[2]. First, it exerts a strong inhibitory effect on K_{ATP} channels via interaction with the cytoplasmic domain of Kir6.2 subunit^[33, 34]. Each Kir6.2 subunit has one ATP binding site, so the functional channel can accommodate four ATPs^[35]. The ATP binding pocket on each Kir6.2 subunit is formed by residues R50, I182, K185, R201, G334^[2, 3, 23, 33, 36-43]. Mutations at any one of these locations can reduce ATP mediated inhibitory effect on Kir6.2, resulting in increased K_{ATP} channel activity. For example, R201H is one of the most common mutations that cause neonatal diabetes^[44]. Decreased ATP mediated inhibition results in channel over-activity, and the cell remains hyperpolarized regardless of the ATP level. Other mutations that can alter the effect of ATP also change the intrinsic opening kinetics of the channels^[45]. ATP preferentially binds to the closed state of the channel^[2-3]. Thus mutations that alter the gating characteristics of the channel, such as I296 in neonatal diabetes, reduce the effectiveness of ATP binding and lead to channel overactivity^[45].

ATP, in the presence of Mg^{2+} , also exerts a weak stimulatory effect on K_{ATP} channels via its interaction with SUR regulatory subunits^[46]. It is important to note that the principal role of ATP is inhibition. Binding of ATP to any one of the four Kir6.2 subunits will render the channel closed. Under normal physiological ATP levels, the open probability of K_{ATP} channels is less than 0.1% if SUR regulatory subunits are absent^[2, 3].

Mg-ADP serves as the principle physiological activator of K_{ATP} channels, and allows them to operate in an ATP insensitive state. Mg-ADP exerts its stimulatory function via interaction with SUR regulatory subunits^[2]. Each SUR subunit has two nucleotide binding domains (NBDs), and dimerization of the two NBDs generates the catalytic sites for ATP hydrolysis, and thus dimerization is essential for successful transduction of ADP's stimulatory effect^[47-49]. Mutations that disrupt dimerization reduce ADP mediated activation of K_{ATP} channels^[50]. Mutations throughout the SUR1 subunit have been identified as one of the major contributors to the occurrence of congenital hyperinsulinemia hypoglycaemia^[51]. For exam-

ple, the point mutation G1479R^[52, 53] in the NBD2 of SUR1 or V187D^[54] in the TMD0 of SUR1, reduced the channel responsiveness to ADP. The decreased ADP-mediated channel activation leads to membrane depolarization in pancreatic beta cells, and continuous release of insulin into the bloodstream, even when plasma glucose levels are low, thus leading to hyperinsulinemic hypoglycaemia.

Regulation by protein interactions

SUR subunits are essential regulatory subunits of K_{ATP} channels. They are necessary for transducing the effect of Mg-ADP, and are the major target site for pharmacological substances. It is unclear how SUR subunits modulate Kir activity; however it has been proposed that the TMD0 domain of SUR anchors SUR to the outer TM1 helix and N-terminus of Kir6.2, thus providing a direct route for information transfer between SUR and the related Kir^[55-57].

K_{ATP} channel activity in pancreatic beta cells and cardiomyocytes can be suppressed by the SNARE protein syntaxin 1A via protein-protein interaction^[58]. Two specific mechanisms have been proposed. First, syntaxin 1A interacts with the NBD1 of SUR subunits via its C-terminal H3 domain to decrease the activity of existing plasma membrane K_{ATP} channels when ATP levels are lowered^[58-60]. This effect is subject to ATP regulation, such that ATP dose-dependently inhibits syntaxin 1A binding to SUR1 subunits at physiological concentrations^[61]. Second, it causes downregulation of K_{ATP} channel expression, either by accelerating endocytosis of existing surface channels, or by decreasing the biogenesis of K_{ATP} channels in the early secretory pathway^[62]. Syntaxin 1A binding to SUR1 subunit is able to counter the stimulatory effects exerted by potassium channel openers (KCOs) such as diazoxide, NNC55-0462, P1075 and cromakalim^[63, 64]. The physiological role of K_{ATP} channel regulation by syntaxin 1A is presently unclear. However, through modulating K_{ATP} channel activity, syntaxin 1A may play an important role in regulating insulin secretion and in pathologies related to glucose homeostasis.

Other mechanisms of regulation

Another modulator of K_{ATP} channel activity is phosphatidylinositol 4,5-bisphosphate (PIP₂). Two possible mechanisms may account for its activating effects^[2]. First, it sustains K_{ATP} channel activity by stabilizing the open state, thus decreasing ATP sensitivity and its ability to close the channel. Furthermore, the binding site for PIP₂ is also on the cytoplasmic domain of Kir6.2 (R54, R176, 177, R206) and is situated very close to the ATP binding site^[65-67]. Thus PIP₂ binding to the channel subunit may allosterically reduce ATP affinity for the channel. Other modulators of K_{ATP} channel activity include protein kinase A (PKA) in smooth muscle cells^[68, 69] and cytoskeletal actin in the cardiac atrium^[70]. Protein kinase C (PKC) activates the cardiac and pancreatic K_{ATP} channels by phosphorylating T180 at the pore-forming subunit Kir6.2^[71]. In the hypothalamus, PKC phosphorylation activates the neuronal Kir6.2/SUR1 K_{ATP} channels to inhibit hepatic glucose production^[72]. On the other hand, PKC phosphorylation

stimulates internalization of K_{ATP} channels in cardiomyocytes and CA1 hippocampal neurons, thus functionally decreases K_{ATP} channel activity^[73]. Lastly, PKC-mediated activation and upregulation of K_{ATP} channels also play an important role in ischemic preconditioning^[74–78].

Pharmacology

Sulfonylureas

Sulfonylureas reduce K_{ATP} channel activity by binding to SUR subunits. They include acetohexamide, tolbutamide, glipzide, glibenclamide and gliclazide. In pancreatic beta cells, the decreased K^+ efflux induced by sulfonylureas leads to membrane depolarization and activation of voltage-gated calcium channels (VGCCs), thus allowing Ca^{2+} influx and insulin release. As such, sulfonylureas have been used to treat diabetes and related diseases. Sulfonylureas therapy is one of the most established treatments for type 2 diabetes, as it is very effective and cost-efficient in achieving the targeted glycemic goals^[79]. Its major advantage is its rapid effectiveness, and its major side effects include hypoglycaemia and weight gain. With the discovery of the role of Kir6.2 mutations in causing neonatal diabetes mellitus, sulfonylureas have also become the main drug used to treat this disease. Patients achieve better glycemic control with sulfonylureas compared to insulin injections, and many of the side effects observed in type 2 diabetics (eg, hypoglycaemia) are not seen in patients with neonatal diabetes^[80].

Modulation of sulfonylureas

The effect of sulfonylureas is altered by the presence of cytoplasmic nucleotides such as Mg-ADP. It has been shown that in the cell-attached configuration, sulfonylureas can completely block K_{ATP} channels^[51]. In excised membrane patches however, the blockage is only 50%–70%. This difference is attributed to the presence of Mg-ADP, which can strongly activate K_{ATP} channels via its interaction with SUR1 and weakly inhibit K_{ATP} channel activity through the ATP binding site on Kir6.2. The strong stimulatory effect of Mg-ADP, but not the weak inhibitory effect, is counteracted by sulfonylureas. Therefore, the presence of Mg-ADP appears to enhance sulfonylureas' inhibitory effects^[51, 81].

Binding sites for tolbutamide and glibenclamide have been described. Both drugs share the high affinity binding site S1237 located in cytoplasmic loop 8 between TM15 and TM16 of SUR^[82, 83]. The other, low affinity binding site for tolbutamide is located on Kir6.2^[84, 85]. Another binding site for glibenclamide is located in cytoplasmic loop 3 between TM5 and TM6^[82, 83].

Potassium channel openers

The other class of drugs are K channel openers (KCOs) and these include cromakalim, pinacidil, nicorandil, diazoxide and minoxidil sulphate. Like their name suggests, these drugs bind to SUR regulatory subunits to stimulate K_{ATP} channel activity^[2]. In pancreatic beta cells, diazoxide binds to SUR1 subunits to increase K_{ATP} channel activity, promoting K^+ efflux

and cell hyperpolarization. This reduces the amount of insulin released. As such, this drug is currently one of the major drugs used to treat congenital hyperinsulinism^[86, 87].

Different K_{ATP} channels respond differently to these KCOs due to expression of different SUR regulatory subunits. Pancreatic beta cell K_{ATP} channels are composed of Kir6.2 and SUR1 subunits, and are readily activated by diazoxide, weakly activated by pinacidil, and unaffected by nicorandil or cromakalim^[88]. In contrast, cardiac K_{ATP} channels, which are composed of Kir6.2 and SUR2A subunits, are activated by pinacidil, nicorandil and cromakalim, but not affected by diazoxide^[89, 90]. Interestingly, K_{ATP} channels in smooth muscles respond to all of these drugs^[91]. The observed differences in KCO sensitivity is due to differences in SUR subunits. SUR1 shows high sensitivity to diazoxide, and SUR2A shows high sensitivity to pinacidil, nicorandil and cromakalim. The binding site for cromakalim, pinacidil and nicorandil resides within the second TM domain of SUR. The nucleotides L1249 and T1253 in SUR2A, and T1286 and M1290 in SUR2B are necessary and sufficient for KCO binding^[92–94]. These differences underscore the importance of SUR subunits in determining the function of K_{ATP} channels.

Physiological role of K_{ATP} channels in glucose homeostasis

K_{ATP} channels across several different tissues contribute to glucose homeostasis. In pancreatic beta cells, K_{ATP} channels consisting of Kir6.2 and SUR1 subunits^[95] promote insulin secretion and thus cause a reduction in blood glucose concentration^[96] (Figure 2). In their open state, K_{ATP} channels permit an efflux of K^+ ions to maintain the cell's polarized membrane potential. Following the metabolism of glucose, however, it is believed that the ATP that is produced causes K_{ATP} channels to close and thus no longer contribute to the polarization of the cell. The cell is now more depolarized and this triggers the influx of calcium via VGCCs and consequently the release of insulin-containing granules^[96].

K_{ATP} channels also play a role in regulating the release of glucagon. Insulin and zinc ions activate K_{ATP} channels on pancreatic alpha cells to hyperpolarize them and thus inhibit their ability to release glucagon^[97]. Alternatively, glucose can act to inhibit K_{ATP} channels in pancreatic alpha cells^[98]. However, unlike in beta cells where the inhibition of K_{ATP} channels is excitatory, the inhibition of K_{ATP} channels in alpha cells is inhibitory and therefore inhibits the release of glucagon^[96, 99]. This is because in alpha cells, the resting membrane potential is much closer to the threshold potential for action potential firing than in beta cells. Therefore, the depolarization resulting from K_{ATP} channel closure is sufficient to maintain VGSCs in a state where they are unable to reconfigure - thus inducing a depolarization block. In this way, the inactivation of K_{ATP} channels is excitatory in beta cells, but inhibitory in alpha cells.

K_{ATP} channels may regulate glucose concentration by mediating glucagon release at the level of the hypothalamus. Kir6.2 subunits are required for the increased spontaneous discharge rate of neurons in the ventromedial hypothalamus (VMH)

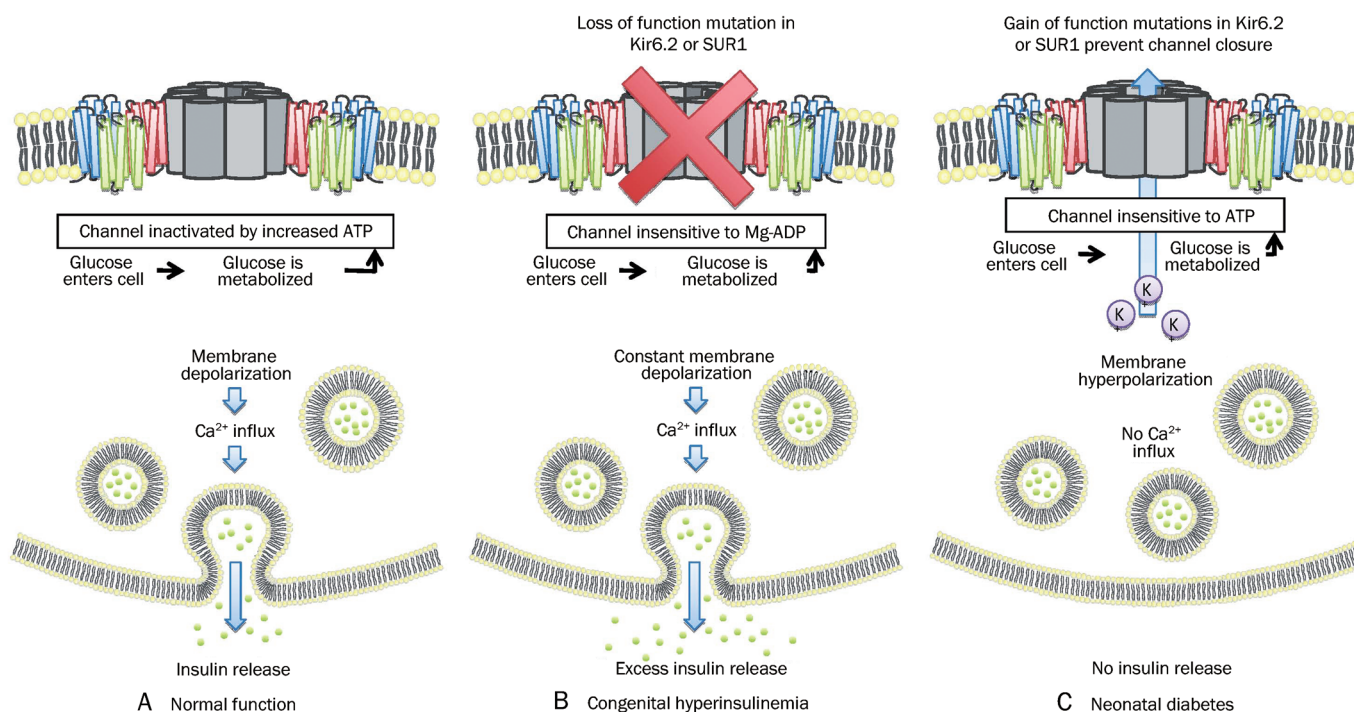


Figure 2. The role of K_{ATP} channels in insulin release from pancreatic β -cells. When glucose enters the cell it is metabolized to yield ATP. (A) During normal function, the K_{ATP} channel is inactivated, causing membrane depolarization and insulin release. (B) Loss of function mutations in Kir6.2 or SUR1 result in constant membrane depolarization leading to the excess insulin release characteristic of congenital hyperinsulinemia. (C) Gain of function mutations in Kir6.2 or SUR1 promotes the open state of the channel to cause membrane hyperpolarization and the lack of insulin release characteristic of neonatal diabetes.

following an increase in the concentration of extracellular glucose^[96]. This increase in VMH activity is likely a reflection of increased firing of glucose-responsive neurons (GRNs) within the VMH^[96, 100]. In addition, neurons within the VMH have been implicated in an autonomic pathway involving the release of adrenaline and terminating with the release of glucagon from pancreatic alpha cells^[99, 101]. VMH K_{ATP} channels are composed of Kir6.2 and SUR1 subunits, just like in pancreatic beta cells^[102]. Therefore, the ability for the body to regulate blood glucose levels by releasing both insulin and glucagon likely depends on these specific K_{ATP} channels in pancreatic beta cells and VMH cells, respectively. K_{ATP} channels in the hypothalamus may modulate the production of glucose^[103]. The infusion of the K^+ channel opener diazoxide into the hypothalamus inhibits gluconeogenesis in the liver, and a global knockout of SUR1 prevents the inhibition of gluconeogenesis by insulin^[103]. Insulin acts on K_{ATP} channels via the phosphatidylinositol 3-kinase (PI3K)/phosphatidylinositol 3,4,5-triphosphate (PIP₃) pathway in the arcuate nucleus of the hypothalamus to inhibit the release of glucose from the liver^[104]. Pro-opiomelanocortin-expressing neurons originating from this nucleus are sensitive to K_{ATP} channel activation and partial activation of these neurons results in impaired glucose tolerance^[105].

Finally, K_{ATP} channels may regulate glucose concentration by mediating the uptake of glucose into skeletal muscles.

The knockout of Kir6.2 subunits is associated with increased absorption of glucose into skeletal muscle (both basally and in response to insulin)^[106], as well as an increased sensitivity of blood glucose concentration to insulin^[102]. Similar effects are evident following the knockout of the SUR2 regulatory domain. Therefore, this K_{ATP} channel likely acts to inhibit glucose uptake in its open state and promote glucose uptake in its closed state^[107, 108]. Although the mechanism of such action is unknown, evidence suggests that this uptake of glucose is independent of the insulin receptor substrate-1/PI3K signaling pathway that underlies the sensitivity of skeletal muscles to insulin^[109-111]. It is also believed to be independent of the insulin-independent cAMP-activated protein kinase dependent pathway^[112, 113]. Taken together, K_{ATP} channels, acting through different mechanisms and from within various tissues, contribute to the regulation of blood glucose levels, and regulate glucose homeostasis under both physiological and pathological conditions.

Pathophysiological role of K_{ATP} channels in glucose homeostasis

Mutations in K_{ATP} channel subunits and neonatal diabetes mellitus

Neonatal diabetes mellitus (NDM) is defined as the occurrence of insulin-requiring monogenic diabetes in the first six months of life^[44, 114, 115]. It is a rare disease with incidence in the

range of 1/200000 live births^[115-118]. It can be transient, which is characterized by spontaneous remission within the first few months of life, or permanent, in which continuous treatment is required from the time of diagnosis. Transient neonatal diabetes mellitus (TNDM) is a result of chromosome abnormalities in the 6q24 locus^[80]. The *PLAGL1/ZAC* gene, a zinc finger protein that regulates apoptosis and cell cycle arrest and the *HYMAI* gene are believed to be involved in TNDM, although the mechanism of action is poorly understood^[80, 119, 120]. In contrast, permanent neonatal diabetes mellitus (PNDM) most commonly results from activating mutations in the genes encoding Kir6.2 (*KCNJ11*) and its regulatory subunit SUR1 (*ABCC8*)^[44]. Mutations in other genes, including insulin^[121-126], insulin promoter factor^[127-129], glucokinase^[130-139] and *FOXP3*^[140, 141] have also been reported to cause PNDM. Understanding the genetic basis of NDM in general has greatly facilitated the correct diagnosis and treatment of this disease. The following sections will focus on the role of K_{ATP} channel subunits in PNDM, and the current therapeutic approaches^[80].

Extensive clinical and molecular studies have firmly established the role of K_{ATP} channel subunits, specifically, Kir6.2 and SUR1 in neonatal diabetes. Overexpression of mutant Kir6.2 subunits with reduced ATP sensitivity causes mice to develop severe neonatal diabetes^[142]. More importantly, a polymorphism in Kir6.2 (E23K) is consistently linked with adult diabetes mellitus^[143-148]. The role of Kir6.2 in PNDM was confirmed in 2004, when Gloyn *et al* reported that activating dominantly inherited mutations in *KCNJ11* were found in 10 out of 29 patients with NDM^[44]. These patients did not secrete insulin in response to glucose or glucagon, but did secrete insulin in response to tolbutamide, which is a K_{ATP} channel blocker used to treat type 2 diabetes. Six heterozygous mutations of Kir6.2 were identified, among which the mutations R201H and V59M were most common. When the R201H mutant was co-expressed with SUR1 in *Xenopus* oocytes, the resulting mutant channels showed 40× decreased sensitivity to ATP inactivation compared to the wild type channels^[44].

Recent studies have identified more than 40 mutations in Kir6.2 and a similar number in SUR1 that lead to PNDM^[149]. All Kir6.2 mutations are heterozygous (dominantly inherited), but SUR1 mutations are more heterogeneous, with homozygous, heterozygous and compound heterozygous mutations being described^[80, 149]. About 80% of *KCNJ11* mutations and 50% of *ABCC8* mutations arise *de novo*^[150], however, there were two reports of germline mosaicism where two siblings with PNDM were born to unaffected parents^[151]. Interestingly, Kir6.2^[152-159] and SUR1^[160-166] mutations have also been found in TNDM patients, who do not have mutations at the 6q24 locus.

All mutations reported to date are missense mutations, with the exception of one in-frame *KCNJ11* nucleotide deletion^[167]. The functional consequence of Kir6.2 and SUR1 mutations is reduced metabolic sensing capacity of the K_{ATP} channel. All mutations on Kir6.2 decrease the channel's sensitivity to ATP^[2, 134, 168], either directly by interfering with ATP binding^[37, 44, 159, 169, 170], or indirectly by decreasing the intrinsic

open probability of the channel^[45, 170]. Mutations that affect ATP binding directly are clustered near the binding site, and these include the common R201H mutation, and also R50, I182, Y330, and F333^[2, 3, 44]. The second, indirect mechanism by which Kir6.2 mutations increase channel function lies in the fact that ATP sensitivity is decreased when the channel is in the open state. Thus mutations that drive the channel to the open state, such as I196H located at the channel pore, can decrease the ability of ATP to close the channel^[45]. Mutations in SUR1 function mainly increase the Mg-nucleotide mediated activation of the channel or change the intrinsic gating properties of the channel^[2, 3]. Overall, these mutations result in the gain of function of K_{ATP} channels so that they are persistently open, leading to beta cell hyperpolarization even in the presence of elevated plasma glucose levels. Hyperpolarization prevents the secretion of insulin, thus resulting in the diabetic phenotype.

Mutations in K_{ATP} channel subunits and DEND syndrome

About 20% of patients with PNDM exhibit developmental delay, epilepsy, muscle weakness in addition to neonatal diabetes (DEND syndrome)^[171]. Patients with a milder form, termed intermediate DEND (iDEND), do not have epilepsy. There are fifteen Kir6.2 mutations and two SUR1 mutations that may cause DEND and iDEND^[149-168]. In particular, the V59M mutation in Kir6.2 is the most common cause of iDEND^[44, 142, 168, 172]. The genetic basis of DEND suggests that mutation of this channel is responsible for all of the observed symptoms, and this notion is strengthened by the fact that K_{ATP} channel subunits are expressed in the affected tissues, namely the brain, muscle and pancreas.

The diabetic phenotype is the result of K_{ATP} channel overactivity in pancreatic beta cells, the same as that observed in PNDM. The muscle dysfunction is neural in origin^[172]. Several lines of evidence illustrate this. Muscle weakness is observed in one patient with a SUR1 mutation, despite the lack of SUR1 expression in skeletal muscles^[173]. Also, muscle weakness and ataxic gait in a patient with a Kir6.2 mutation was improved by treatment with gliclazide, which interacts only with SUR1^[174]. More definitive evidence comes from a recent study by Clark *et al*, in which hemizygous mice that selectively express the V59M Kir6.2 mutation in muscle or neurons were examined^[172]. Behaviourally, transgenic mice with the neuronal V59M Kir6.2 mutation display the same motor impairments as seen in human DEND. Electrophysiological studies show that V59M-carrying Purkinje neurons (output of cerebellum that regulates motor movement) were hyperpolarized and displayed suppressed electrical firing. This was reversed with the application of tolbutamide, suggesting that neuronal K_{ATP} channels containing V59M Kir6.2 were overactive mutants. In contrast, muscle-specific V59M mutation failed to alter muscle membrane properties, and mice with muscular V59M Kir6.2 mutation behave like their wild type counterparts. The differential effects of Kir6.2 V59M mutation on neurons and muscles may be due to the divergence in the identity of SUR regulatory subunits. Neurons, like pancreatic beta-cells, mostly contain

K_{ATP} channels made up of Kir6.2 and SUR1 subunits, whereas muscle K_{ATP} channels are composed of Kir6.2 and SUR2A subunits. In fact, it has been shown that the Kir6.2 V59M mutation specifically enhances the flow of current through K_{ATP} channels composed of Kir6.2/SUR1 subunits, but has no effect on Kir6.2/SUR2A K_{ATP} channels^[172]. Thus, the V59M mutation selectively targets the pancreas and neurons while sparing the muscle.

The last two symptoms of DEND, namely developmental delay and epilepsy, are neuronal in origin, but their exact causes are unknown. It has been proposed that epilepsy may result from decreased activity of inhibitory interneurons in the hippocampus, as there's a greater density of K_{ATP} channels in the inhibitory neurons compared to the excitatory ones^[11, 173]. The cause of developmental delay is unclear, but it may result directly from overactivity of K_{ATP} channels, or may be secondary to the symptom of diabetes. Motor and cognitive development requires dynamic changes in neuronal networks and balanced excitatory and inhibitory inputs within the network. Overactivity of K_{ATP} channels hinders the occurrence of excitatory synaptic connections, and thus may inhibit neuronal activity and development. On the other hand, developmental delay may be the result of diabetes-induced neuropathy. Therefore, further research is warranted to elucidate this matter.

Therapeutics of neonatal diabetes

Neonatal diabetes was originally thought to be an early onset form of type 1 diabetes and was therefore treated with insulin injections^[80]. However, after the discovery of the mutations of K_{ATP} channel subunits, more than 90% of patients were switched to treatments with sulfonylureas ($0.05\text{--}1.5\text{ mg}\cdot\text{kg}^{-1}\cdot\text{d}^{-1}$)^[175]. Most patients exhibited significant improvement in their clinical situations^[168]. Specifically, blood glucose levels were generally reduced, as indicated by HbA1C levels^[175-179]. There were also less fluctuation in plasma glucose levels, and hypoglycaemic episodes were less common^[173]. In addition, patients with iDEND also see improvement in extrapancreatic symptoms, such as reduced epileptic events, improved cognition and improved muscle tone and balance^[173, 180-183]. Unfortunately, patients suffering from the severe DEND syndrome are less responsive to sulfonylurea treatment^[184-186]. Side effects are minimal; a few patients have reported transient diarrhoea and tooth discoloration^[173, 187, 188].

Sulfonylureas work by interacting with SUR subunits to induce channel closure. This allows for the depolarization of the cell membrane and increased excitability. In pancreatic beta cells, cell depolarization allows for the activation of voltage-gated calcium channels, stimulating an influx of Ca^{2+} into the cytoplasm and subsequent release of insulin into the bloodstream. This is able to mitigate the diabetic symptoms. Interestingly, there was better insulin response to oral glucose intake than to intravenous glucose in NDM patients treated with sulphonylureas^[175-189]. The presence of food in the gut lumen stimulates the secretion of hormones and signalling molecules such as GLP-1, GIP and ACh, which can amplify the

insulin response and it appears that their proper action may require K_{ATP} channel closure^[189]. How sulphonylureas affect the secretion of such hormones is unclear at this moment. It has been proposed that secretion of these hormones requires Ca^{2+} influx, which in patients with PNDM is only possible after sulfonylurea treatment^[189].

The improvement of neurological symptoms of DEND and iDEND is most likely due to the action of sulfonylureas on neuronal K_{ATP} channels. Although there is enhanced cognition, improved muscle tone and abolition of seizures, development does not return to normal with sulfonylurea treatment^[173]. This could be the result of insufficient sulfonylurea potency or the irreversibility of neuronal damage caused by K_{ATP} channel overactivity.

A point of concern is that glibenclamide and glyburides, which interact with both SUR1 and SUR2A, are currently used to treat DEND and iDEND. The discovery of the neuronal origin of muscle impairment in DEND and iDEND suggests that more specific drugs, that only target SUR1, could be used in order to avoid unnecessary side effects, especially in the myocardium which also express SUR2A subunits^[172]. Indeed, it has been reported that gliclazide, which only interacts with SUR1, can alleviate the motor symptoms^[174].

Another minor drawback with sulfonylurea therapy is that its effectiveness decreases as the time between diagnosis and transfer to sulfonylurea therapy increases, although it is relatively successful when used at the early stage of the disease^[80, 175]. Prolonged hypoinsulinemia may result in a loss of beta cells and thus the insulin secreting machinery downstream of K_{ATP} channels may not be functional^[173]. In mouse models of neonatal diabetes, prolonged lack of insulin leads to a progressive decrease in beta cell mass and a loss of normal islet architecture is observed^[190]. In such cases, even though sulfonylurea may enhance K_{ATP} channel closure, it cannot relieve the hyperglycemia. Thus, it is beneficial to start sulfonylurea treatment as early as possible if neonatal diabetes is diagnosed. However, sulfonylurea treatment is only effective for those with mutations in K_{ATP} channel subunits, which only account for half of all NDM patients. For patients with mutations in other genes such as insulin and glucokinase, it may not be beneficial. Therefore, it may be advantageous for all diabetic patients to undergo genetic testing in the first six months of life in order to obtain a definitive diagnosis, and permit the earliest possible commencement of treatment^[80].

K_{ATP} channels and congenital hyperinsulinism

Congenital hyperinsulinism (CHI) is characterized by continuous and unregulated insulin secretion despite low plasma glucose levels^[51, 191, 192]. The incidence of CHI is 1/30 000 to 1/50 000 live births per year, however in some isolated areas where inbreeding is common, the disease incidence may reach 1/2500^[193]. This disease cannot be detected *in utero*, and babies with CHI have no gross characteristic differences from normal babies^[51]. The first clinical signs are vague, and include cyanosis, respiratory distress, sweating, hypothermia, poor feeding and hunger. It is important that the correct diagnosis is made

promptly, as delayed treatment will result in permanent brain damage and mental retardation due to insufficient energy supply for brain metabolism^[51].

There are two distinct forms of CHI, categorized based on their histological differences. Focal CHI is characterized by the presence of a small endocrine lesion in the pancreas. In the lesion area, the islets are normally structured, but hyperplastic; outside of the lesion, the islets are normal^[194–196]. Complete resection of the lesion can cure the patient. On the other hand, in patients with diffuse CHI, the islets of Langerhans show large beta cells with abnormally large nuclei, which is indicative of hyperactivity. Treatment for diffuse CHI patients usually involves partial pancreatectomy^[196], which often leads to pancreatic insufficiency and iatrogenic diabetes mellitus^[51].

Mutations in K_{ATP} channel subunits are the most common cause of CHI^[51]. The SUR1 gene *ABCC8* and Kir6.2 gene *KCNJ11* are located at ch11p15. Mutations at this genetic locus are linked to both diffuse and focal CHI^[197]. Diffuse CHI predominantly arises from autosomal recessive mutations of K_{ATP} channel subunits, although dominant ones have been reported^[51–193]. Focal CHI results from loss of heterozygosity at this locus^[198–204]. In the normal part of the pancreas, the cells inherit a mutated SUR1 gene from the father and a normal SUR1 gene from the mother. These cells have a normal phenotype, due to expression of the normal maternal SUR1 gene. In the focal lesion, the cells have lost the normal maternal chromosome during fetal life and contain two copies of the mutated SUR1 genes inherited from the father. They have also lost the maternally imprinted tumor suppressor genes *P57^{kip2}*, although they still express the paternally derived insulin-like growth factor II gene. This combination enables the growth of the focal lesion. About 40%–65% of patients with CHI have focal CHI^[51].

Mutations of K_{ATP} channels responsible for CHI are mostly found in SUR subunits, and a few in Kir6.2 subunits^[51, 168–205]. Indeed, over 150 mutations have been identified in the SUR1 subunit and these account for 50% of all CHI cases^[149]. These loss-of-function mutations have been grouped into two classes^[168]. In class I, there is a total loss of K_{ATP} channels in the plasma membrane, resulting in no K_{ATP} current^[51]. This type of mutation accounts for 10% of all diffuse CHI patients and 55% of focal CHI patients. The most common cause is defects in trafficking^[168]. For example, the mutation R1437Q(23)X in exon35 of *ABCC8* causes truncation of the C-terminus of SUR1, which contains the signal sequence necessary for exiting the ER^[51, 206]. Thus, the channel protein is retained in the ER and cannot be expressed in the membrane. In class II mutations, K_{ATP} channels are present in the membrane (although less than normal) but show reduced sensitivity to Mg-nucleotide activation or reduced intrinsic channel open probability^[51, 168]. These mutations account for more than 60% of diffuse CHI cases and 45% of focal CHI cases. For example, point mutations such as G1479R in NBD2 of SUR1^[52] or V187D in the TMD0 of SUR1^[207] lead to reduced responsiveness to ADP activation in the expressed channels. Overall, these mutations result in a loss-of-function of K_{ATP} channels in the pancreatic beta

cells, leading to constitutive exocytosis of insulin-containing secretory vesicles. In addition to K_{ATP} channel related mutations, CHI also arises from autosomal dominant mutations in genes involved in glucose metabolism, including mutations in glutamate dehydrogenase (GDH)^[208–216], glucokinase^[217, 218] and short-chain L-3-hydroxyacyl-CoA dehydrogenase (SCHAD)^[106–219].

Therapeutics of congenital hyperinsulinism

Understanding the molecular mechanisms that underlie CHI provides the basis for establishing effective treatment protocols. Of the utmost importance is the correct diagnosis of the type of CHI. Following the identification of K_{ATP} channels in the pathology of CHI, the K^+ channel opener, diazoxide, has become a diagnostic tool and a treatment method^[86, 87]. When CHI is suspected, the first step in diagnosis is to determine the diazoxide responsiveness. The diazoxide-responsive CHI patients can be managed with diazoxide treatment with regular monitoring. Non-responsive patients are given a genetic test of the *ABCC8* and *KCNJ11* genes to determine whether it is a case of focal or diffuse CHI. For the diffuse CHI patients, treatment involves a high calorie diet, somatostatin (Octreotide) therapy and a near-total pancreatectomy. Regular follow-up is required to monitor growth, development, as well as the occurrence of diabetes mellitus later in life. For focal CHI patients, a complete resection of the focal lesion is commonly used and can cure patients^[86, 87].

The mainstream drug used in CHI treatment, diazoxide (10–20 mg·kg⁻¹·d⁻¹), is a K_{ATP} channel opener and binds to SUR1 subunits to promote K_{ATP} channel opening^[51]. This prevents the depolarization of pancreatic beta cells and insulin secretion. Diazoxide is easily administered orally and provides significant relief for CHI caused by mutations in GDH, glucokinase and SCHAD. However, it is not effective for type I K_{ATP} -related CHI, in which a lack of K_{ATP} channels has been found. Therefore, diazoxide has no targets to exert its effects. More potent diazoxide analogues such as HEI713, BPDZ73, BPDZ44, and BPDZ154 have been synthesized^[51]. Although effective in stimulating K_{ATP} channel opening *in vitro*, their clinical potential has not yet been determined.

Diazoxide also poses serious side effects. It causes sodium/water retention that can lead to complications such as congestive heart defects, poor cardiac reserve, hyperuricemia and hypotension in patients with heart problems. Moreover, diazoxide can decrease immune function and long term use has been linked with hyperosmolar nonketotic coma^[51].

Other drugs used for CHI treatment include L-type Ca²⁺ channel antagonists (nifedipine, verapamil), glucagon, somatostatin and corticosteroids^[51]. VGCC antagonists prevent Ca²⁺ influx and may decrease insulin secretion. They have been shown to be therapeutically beneficial in some^[220–223], but not all CHI patients^[224]. Glucagon is used because it stimulates glycogenolysis and gluconeogenesis, but it is disfavoured because it also acts as an insulin secretagogue, thus promoting insulin hypersecretion. Long-term use of somatostatin is widely accepted, as it potently inhibits insulin release via acti-

vation of hyperpolarizing K^+ channels and it independently inhibits VGCCs. Short term use of steroids helps to maintain adequate blood glucose levels^[51].

Perspectives/future directions

Neonatal diabetes mellitus

The identification of the role of K_{ATP} channels in neonatal diabetes has revolutionized the treatment for this disease. With the groundbreaking report in 2004 by Gloyn *et al* that identified mutations in Kir6.2 subunits as one of the major causes of neonatal diabetes^[44], more than 90% of patients have been switched to treatment with sulfonylureas, which induce K_{ATP} channel closure. Sulfonylureas provide better glucose control than previous treatment methods, and to date, the side effects reported (*eg*, tooth discoloration) have been minimal. Hypoglycemic episodes, which is the major side effect associated with sulfonylurea treatment in type 2 diabetes, are not observed in patients with neonatal diabetes. However, long-term monitoring is needed to determine whether the other side effects previously reported with sulfonylurea use, such as liver dysfunction, skin allergic reactions, pancytopenia, hyponatremia or cardiovascular abnormalities will appear in patients with NDM. One possible way to minimize potential side effect is to develop derivatives of sulfonylureas specific to pancreatic cells, thus minimizing the unwanted effect on other tissues.

DEND and iDEND

For patients with DEND or iDEND, sulfonylurea treatment not only provides better glucose control, but also alleviates some of the extrapancreatic symptoms. As such, sulfonylurea therapy reduces occurrences of epileptic events, and improves muscle and cognitive functions^[173]. However, sulfonylureas do not improve developmental delay. The main difficulty is that the cause of developmental delay is unclear. It could arise from prolonged over-activity of neuronal K_{ATP} channels, or could be secondary to sustained high glucose levels prior to treatment. It is unclear how well sulfonylureas cross the blood brain barrier, thus the potency and efficacy of these drugs on neurons is unknown. It has been suggested that higher potency drugs may better improve the neural symptoms.

Another interesting point is that there are no cardiac symptoms observed in DEND or iDEND, even though K_{ATP} channels are widely expressed in cardiomyocytes. Pancreatic beta cells and neurons express Kir6.2 and SUR1 subunits while skeletal muscle and cardiomyocytes express SUR2A and Kir6.2 subunits. The study by Clark *et al* (2010) demonstrating the neural origin of motor symptoms suggest that skeletal muscle K_{ATP} channels, which are composed of SUR2A and Kir6.2 subunits, are not affected, thus, it is not surprising that DEND or iDEND patients have no cardiac symptoms^[172].

This differential response between K_{ATP} channels to the same genetic mutation has several implications. For one, it indicates that more specific sulfonylureas – ones that selectively target SUR1 – should be preferred over those that bind to both SUR2A and SUR1 when treating DEND/iDEND. Next,

it underlines the importance of neuronal K_{ATP} channels in DEND and iDEND. This area is relatively unexplored at this moment. Understanding the effect of these mutations on neuronal networks would provide a better idea about the molecular basis of the observed symptoms, and allow development of better therapeutic approaches. Lastly, it highlights the importance of SUR subunit regulation in K_{ATP} channel activity. Mutations implicated in DEND and iDEND are mostly found in the Kir6.2 subunit, and these subunits are expressed in most tissues. The expression of SUR subunits, however, is tissue-specific and thus SUR subunits have a better capability of regulating mutant channels.

Congenital hyperinsulinism

Identification of the role of K_{ATP} channels has improved the diagnostic and treatment process for many patients suffering with congenital hyperinsulinism (CHI). Since congenital CHI usually results from the loss of K_{ATP} function, K_{ATP} channel openers such as diazoxide are used to counteract the deficit in K_{ATP} function. In cases where K_{ATP} channels are not trafficked to membrane, diazoxide treatment may be ineffective. Nonetheless, diazoxide is useful in two ways. One, it serves as a diagnostic tool for determining the specific type of CHI. Patients in which diazoxide treatment is effective likely do not have mutations in K_{ATP} channel subunits and thus diazoxide can be administered as the key drug for these patients. Since diazoxide is not very effective for CHI patients with K_{ATP} channel mutations, alternative approaches for treating these patients may be to examine novel regulators of K_{ATP} channels. One such molecule is syntaxin 1A, which inhibits K_{ATP} channels^[61]. Therefore, decreases in syntaxin 1A levels can increase K_{ATP} channel activity. In contrast to diazoxide which only increases the activity of existing K_{ATP} channels, syntaxin 1A has been shown to regulate the membrane expression of wild-type K_{ATP} channels. Thus, it would be worthwhile to examine whether syntaxin 1A can provide additional regulation and therefore be effective for treating congenital hyperinsulinism.

Conclusion

Understanding the genetic basis of neonatal diabetes and congenital hyperinsulinism has significantly improved the diagnosis and treatment of patients with these diseases. The current use of K_{ATP} channel modulators by these patients has greatly alleviated their symptoms and improved their quality of life. However, assessment of the long-term effects of these treatment methods is warranted and better optimization of the treatment protocol is needed in order to deliver the best possible care to patients.

Acknowledgements

Zhong-ping FENG holds a New Investigator Award from the Heart and Stroke Foundation of Canada.

References

- 1 Shyng S, Nichols CG. Octameric stoichiometry of the K_{ATP} channel complex. *J Gen Physiol* 1997; 110: 655–64.

- 2 Hibino H, Inanobe A, Furutani K, Murakami S, Findlay I, Kurachi Y. Inwardly rectifying potassium channels: their structure, function, and physiological roles. *Physiol Rev* 2010; 90: 291–366.
- 3 Nichols CG. K_{ATP} channels as molecular sensors of cellular metabolism. *Nature* 2006; 440: 470–6.
- 4 Noma A. ATP-regulated K^+ channels in cardiac muscle. *Nature* 1983; 305: 147–8.
- 5 Ashcroft FM, Harrison DE, Ashcroft SJ. Glucose induces closure of single potassium channels in isolated rat pancreatic beta-cells. *Nature* 1984; 312: 446–8.
- 6 Cook DL, Hales CN. Intracellular ATP directly blocks K^+ channels in pancreatic beta-cells. *Nature* 1984; 311: 271–3.
- 7 Spruce AE, Standen NB, Stanfield PR. Studies of the unitary properties of adenosine-5'-triphosphate-regulated potassium channels of frog skeletal muscle. *J Physiol* 1987; 382: 213–36.
- 8 Spruce AE, Standen NB, Stanfield PR. Voltage-dependent ATP-sensitive potassium channels of skeletal muscle membrane. *Nature* 1985; 316: 736–8.
- 9 Standen NB, Quayle JM, Davies NW, Brayden JE, Huang Y, Nelson MT. Hyperpolarizing vasodilators activate ATP-sensitive K^+ channels in arterial smooth muscle. *Science* 1989; 245: 177–80.
- 10 Gabrielson BG, Karlsson AC, Lonn M, Olofsson LE, Johansson JM, Torgerson JS, *et al*. Molecular characterization of a local sulfonylurea system in human adipose tissue. *Mol Cell Biochem* 2004; 258: 65–71.
- 11 Zawar C, Plant TD, Schirra C, Konnerth A, Neumcke B. Cell-type specific expression of ATP-sensitive potassium channels in the rat hippocampus. *J Physiol* 1999; 514: 327–41.
- 12 Ashford ML, Sturgess NC, Trout NJ, Gardner NJ, Hales CN. Adenosine-5'-triphosphate-sensitive ion channels in neonatal rat cultured central neurones. *Pflugers Arch* 1988; 412: 297–304.
- 13 Ashford ML, Boden PR, Treherne JM. Glucose-induced excitation of hypothalamic neurones is mediated by ATP-sensitive K^+ channels. *Pflugers Arch* 1990; 415: 479–83.
- 14 Ashford ML, Boden PR, Treherne JM. Tolbutamide excites rat glucoreceptive ventromedial hypothalamic neurones by indirect inhibition of ATP- K^+ channels. *Br J Pharmacol* 1990; 101: 531–40.
- 15 Hattersley AT, Ashcroft FM. Activating mutations in Kir6.2 and neonatal diabetes: new clinical syndromes, new scientific insights, and new therapy. *Diabetes* 2005; 54: 2503–13.
- 16 Nishida M, Cadene M, Chait BT, MacKinnon R. Crystal structure of a Kir3.1-prokaryotic Kir channel chimera. *EMBO J* 2007; 26: 4005–15.
- 17 Aguilar-Bryan L, Nichols CG, Wechsler SW, Clement JP, Boyd AE III, Gonzalez G, *et al*. Cloning of the beta cell high-affinity sulfonylurea receptor: a regulator of insulin secretion. *Science* 1995; 268: 423–6.
- 18 Babenko AP, Bryan J. SUR-dependent modulation of K_{ATP} channels by an N-terminal KIR6.2 peptide. Defining intersubunit gating interactions. *J Biol Chem* 2002; 277: 43997–4004.
- 19 Inagaki N, Gono T, Clement JP, Wang CZ, Aguilar-Bryan L, Bryan J, *et al*. A family of sulfonylurea receptors determines the pharmacological properties of ATP-sensitive K^+ channels. *Neuron* 1996; 16: 1011–7.
- 20 Isomoto S, Kondo C, Yamada M, Matsumoto S, Higashiguchi O, Horio Y, *et al*. A novel sulfonylurea receptor forms with BIR (Kir6.2) a smooth muscle type ATP-sensitive K^+ channel. *J Biol Chem* 1996; 271: 24321–4.
- 21 Proks P, Capener CE, Jones P, Ashcroft FM. Mutations within the P-loop of Kir6.2 modulate the intraburst kinetics of the ATP-sensitive potassium channel. *J Gen Physiol* 2001; 118: 341–53.
- 22 Jiang Y, Lee A, Chen J, Cadene M, Chait BT, MacKinnon R. The open pore conformation of potassium channels. *Nature* 2002; 417: 523–6.
- 23 Enkvetchakul D, Nichols CG. Gating mechanism of K_{ATP} channels: function fits form. *J Gen Physiol* 2003; 122: 471–80.
- 24 Sackin H, Nanazashvili M, Palmer LG, Krambis M, Walters DE. Structural locus of the pH gate in the Kir1.1 inward rectifier channel. *Biophys J* 2005; 88: 2597–606.
- 25 Drain P, Geng X, Li L. Concerted gating mechanism underlying K_{ATP} channel inhibition by ATP. *Biophys J* 2004; 86: 2101–12.
- 26 Enkvetchakul D, Loussouarn G, Makhina E, Shyng SL, Nichols CG. The kinetic and physical basis of K_{ATP} channel gating: toward a unified molecular understanding. *Biophys J* 2000; 78: 2334–48.
- 27 Drain P, Li L, Wang J. K_{ATP} channel inhibition by ATP requires distinct functional domains of the cytoplasmic C terminus of the pore-forming subunit. *Proc Natl Acad Sci U S A* 1998; 95: 13953–8.
- 28 Zerangue N, Schwappach B, Jan YN, Jan LY. A new ER trafficking signal regulates the subunit stoichiometry of plasma membrane K_{ATP} channels. *Neuron* 1999; 22: 537–48.
- 29 Hosy E, Dupuis JP, Vivaudou M. Impact of disease-causing SUR1 mutations on the K_{ATP} channel subunit interface probed with a rhodamine protection assay. *J Biol Chem* 2010; 285: 3084–91.
- 30 Masia R, Caputa G, Nichols CG. Regulation of K_{ATP} channel expression and activity by the SUR1 nucleotide binding fold 1. *Channels (Austin)* 2007; 1: 315–23.
- 31 Taschenberger G, Mougey A, Shen S, Lester LB, LaFranchi S, Shyng SL. Identification of a familial hyperinsulinism-causing mutation in the sulfonylurea receptor 1 that prevents normal trafficking and function of K_{ATP} channels. *J Biol Chem* 2002; 277: 17139–46.
- 32 Lim A, Park SH, Sohn JW, Jeon JH, Park JH, Song DK, *et al*. Glucose deprivation regulates K_{ATP} channel trafficking via AMP-activated protein kinase in pancreatic beta-cells. *Diabetes* 2009; 58: 2813–9.
- 33 Antcliff JF, Haider S, Proks P, Sansom MS, Ashcroft FM. Functional analysis of a structural model of the ATP-binding site of the K_{ATP} channel Kir6.2 subunit. *EMBO J* 2005; 24: 229–39.
- 34 Dong K, Tang LQ, MacGregor GG, Leng Q, Hebert SC. Novel nucleotide-binding sites in ATP-sensitive potassium channels formed at gating interfaces. *EMBO J* 2005; 24: 1318–29.
- 35 Markworth E, Schwanstecher C, Schwanstecher M. ATP4-mediates closure of pancreatic beta-cell ATP-sensitive potassium channels by interaction with 1 of 4 identical sites. *Diabetes* 2000; 49: 1413–8.
- 36 Cukras CA, Jeliakova I, Nichols CG. The role of NH_2 -terminal positive charges in the activity of inward rectifier K_{ATP} channels. *J Gen Physiol* 2002; 120: 437–46.
- 37 John SA, Weiss JN, Xie LH, Ribalet B. Molecular mechanism for ATP-dependent closure of the K^+ channel Kir6.2. *J Physiol* 2003; 552: 23–34.
- 38 Li L, Wang J, Drain P. The I182 region of K(ir)6.2 is closely associated with ligand binding in K_{ATP} channel inhibition by ATP. *Biophys J* 2000; 79: 841–52.
- 39 Proks P, Gribble FM, Adhikari R, Tucker SJ, Ashcroft FM. Involvement of the N-terminus of Kir6.2 in the inhibition of the K_{ATP} channel by ATP. *J Physiol* 1999; 514: 19–25.
- 40 Reimann F, Ryder TJ, Tucker SJ, Ashcroft FM. The role of lysine 185 in the Kir6.2 subunit of the ATP-sensitive channel in channel inhibition by ATP. *J Physiol* 1999; 520: 661–9.
- 41 Tsuboi T, Lippiat JD, Ashcroft FM, Rutter GA. ATP-dependent interaction of the cytosolic domains of the inwardly rectifying K^+ channel Kir6.2 revealed by fluorescence resonance energy transfer. *Proc Natl Acad Sci U S A* 2004; 101: 76–81.
- 42 Tucker SJ, Gribble FM, Proks P, Trapp S, Ryder TJ, Haug T, *et al*. Molecular determinants of K_{ATP} channel inhibition by ATP. *EMBO J*

- 1998; 17: 3290–6.
- 43 Trapp S, Haider S, Jones P, Sansom MS, Ashcroft FM. Identification of residues contributing to the ATP binding site of Kir6.2. *EMBO J* 2003; 22: 2903–12.
- 44 Gloyn AL, Pearson ER, Antcliff JF, Proks P, Bruining GJ, Slingerland AS, et al. Activating mutations in the gene encoding the ATP-sensitive potassium-channel subunit Kir6.2 and permanent neonatal diabetes. *N Engl J Med* 2004; 350: 1838–49.
- 45 Proks P, Girard C, Haider S, Gloyn AL, Hattersley AT, Sansom MS, et al. A gating mutation at the internal mouth of the Kir6.2 pore is associated with DEND syndrome. *EMBO Rep* 2005; 6: 470–5.
- 46 Ashcroft FM, Kakei M. ATP-sensitive K⁺ channels in rat pancreatic beta-cells: modulation by ATP and Mg²⁺ ions. *J Physiol* 1989; 416: 349–67.
- 47 Campbell JD, Proks P, Lippiat JD, Sansom MS, Ashcroft FM. Identification of a functionally important negatively charged residue within the second catalytic site of the SUR1 nucleotide-binding domains. *Diabetes* 2004; 53: S123–7.
- 48 Masia R, Nichols CG. Functional clustering of mutations in the dimer interface of the nucleotide binding folds of the sulfonylurea receptor. *J Biol Chem* 2008; 283: 30322–9.
- 49 Vergani P, Lockless SW, Nairn AC, Gadsby DC. CFTR channel opening by ATP-driven tight dimerization of its nucleotide-binding domains. *Nature* 2005; 433: 876–80.
- 50 Yamada M, Kurachi Y. The nucleotide-binding domains of sulfonylurea receptor 2A and 2B play different functional roles in nicorandil-induced activation of ATP-sensitive K⁺ channels. *Mol Pharmacol* 2004; 65: 1198–207.
- 51 Dunne MJ, Cosgrove KE, Shepherd RM, Aynsley-Green A, Lindley KJ. Hyperinsulinism in infancy: from basic science to clinical disease. *Physiol Rev* 2004; 84: 239–75.
- 52 Nichols CG, Shyng SL, Nestorowicz A, Glaser B, Clement JP, Gonzalez G, et al. Adenosine diphosphate as an intracellular regulator of insulin secretion. *Science* 1996; 272: 1785–7.
- 53 Sharma N, Crane A, Gonzalez G, Bryan J, Aguilar-Bryan L. Familial hyperinsulinism and pancreatic beta-cell ATP-sensitive potassium channels. *Kidney Int* 2000; 57: 803–8.
- 54 Otonkoski T, Ammala C, Huopio H, Cote GJ, Chapman J, Cosgrove K, et al. A point mutation inactivating the sulfonylurea receptor causes the severe form of persistent hyperinsulinemic hypoglycemia of infancy in Finland. *Diabetes* 1999; 48: 408–15.
- 55 Babenko AP, Bryan J. Sur domains that associate with and gate K_{ATP} pores define a novel gatekeeper. *J Biol Chem* 2003; 278: 41577–80.
- 56 Fang K, Csanady L, Chan KW. The N-terminal transmembrane domain (TMD0) and a cytosolic linker (LO) of sulphonylurea receptor define the unique intrinsic gating of K_{ATP} channels. *J Physiol* 2006; 576: 379–89.
- 57 Hosi E, Derand R, Revilloud J, Vivaudou M. Remodelling of the SUR-Kir6.2 interface of the K_{ATP} channel upon ATP binding revealed by the conformational blocker rhodamine 123. *J Physiol* 2007; 582: 27–39.
- 58 Pasyk EA, Kang Y, Huang X, Cui N, Sheu L, Gaisano HY. Syntaxin-1A binds the nucleotide-binding folds of sulphonylurea receptor 1 to regulate the K_{ATP} channel. *J Biol Chem* 2004; 279: 4234–40.
- 59 Cui N, Kang Y, He Y, Leung YM, Xie H, Pasyk EA, et al. H3 domain of syntaxin 1A inhibits K_{ATP} channels by its actions on the sulfonylurea receptor 1 nucleotide-binding folds-1 and -2. *J Biol Chem* 2004; 279: 53259–65.
- 60 Kang Y, Leung YM, Manning-Fox JE, Xia F, Xie H, Sheu L, et al. Syntaxin-1A inhibits cardiac K_{ATP} channels by its actions on nucleotide binding folds 1 and 2 of sulfonylurea receptor 2A. *J Biol Chem* 2004; 279: 47125–31.
- 61 Kang Y, Zhang Y, Liang T, Leung YM, Ng B, Xie H, et al. ATP modulates interaction of Syntaxin-1A with sulfonylurea receptor 1 to regulate pancreatic [beta]-cell K_{ATP} channels. *J Biol Chem* 2011; 286: 5876–83.
- 62 Chen PC, Bruederle CE, Gaisano HY, Shyng SL. Syntaxin 1A regulates surface expression of [beta]-cell ATP-sensitive potassium channels. *Am J Physiol Cell Physiol* 2011; 300: C506–16.
- 63 Ng B, Kang Y, Xie H, Sun H, Gaisano HY. Syntaxin-1A inhibition of P-1075, cromakalim, and diazoxide actions on mouse cardiac ATP-sensitive potassium channel. *Cardiovasc Res* 2008; 80: 365–74.
- 64 Ng B, Kang Y, Elias CL, He Y, Xie H, Hansen JB, et al. The actions of a novel potent islet beta-cell specific ATP-sensitive K⁺ channel opener can be modulated by syntaxin-1A acting on sulfonylurea receptor 1. *Diabetes* 2007; 56: 2124–34.
- 65 Baukowitz T, Schulte U, Oliver D, Herlitz S, Krauter T, Tucker SJ, et al. PIP2 and PIP as determinants for ATP inhibition of K_{ATP} channels. *Science* 1998; 282: 1141–4.
- 66 Shyng SL, Cukras CA, Harwood J, Nichols CG. Structural determinants of PIP(2) regulation of inward rectifier K_{ATP} channels. *J Gen Physiol* 2000; 116: 599–608.
- 67 Shyng SL, Barbieri A, Gumusboga A, Cukras C, Pike L, Davis JN, et al. Modulation of nucleotide sensitivity of ATP-sensitive potassium channels by phosphatidylinositol-4-phosphate 5-kinase. *Proc Natl Acad Sci U S A* 2000; 97: 937–41.
- 68 Quinn KV, Giblin JP, Tinker A. Multisite phosphorylation mechanism for protein kinase A activation of the smooth muscle ATP-sensitive K⁺ channel. *Circ Res* 2004; 94: 1359–66.
- 69 Shi Y, Wu Z, Cui N, Shi W, Yang Y, Zhang X, et al. PKA phosphorylation of SUR2B subunit underscores vascular K_{ATP} channel activation by beta-adrenergic receptors. *Am J Physiol Regul Integr Comp Physiol* 2007; 293: R1205–14.
- 70 Van Wagoner DR. Mechanosensitive gating of atrial ATP-sensitive potassium channels. *Circ Res* 1993; 72: 973–83.
- 71 Light PE, Bladen C, Winkfein RJ, Walsh MP, French RJ. Molecular basis of protein kinase C-induced activation of ATP-sensitive potassium channels. *Proc Natl Acad Sci U S A* 2000; 97: 9058–63.
- 72 Ross R, Wang PY, Chari M, Lam CK, Caspi L, Ono H, et al. Hypothalamic protein kinase C regulates glucose production. *Diabetes* 2008; 57: 2061–5.
- 73 Hu K, Huang CS, Jan YN, Jan LY. ATP-sensitive potassium channel traffic regulation by adenosine and protein kinase C. *Neuron* 2003; 38: 417–32.
- 74 Speechly-Dick ME, Grover GJ, Yellon DM. Does ischemic preconditioning in the human involve protein kinase C and the ATP-dependent K⁺ channel? Studies of contractile function after simulated ischemia in an atrial *in vitro* model. *Circ Res* 1995; 77: 1030–5.
- 75 Hu K, Duan D, Li GR, Nattel S. Protein kinase C activates ATP-sensitive K⁺ current in human and rabbit ventricular myocytes. *Circ Res* 1996; 78: 492–8.
- 76 Light PE, Sabir AA, Allen BG, Walsh MP, French RJ. Protein kinase C-induced changes in the stoichiometry of ATP binding activate cardiac ATP-sensitive K⁺ channels. A possible mechanistic link to ischemic preconditioning. *Circ Res* 1996; 79: 399–406.
- 77 Zhuang JG, Zhang Y, Zhou ZN. Hypoxic preconditioning upregulates K_{ATP} channels through activation of protein kinase C in rat ventricular myocytes. *Acta Pharmacol Sin* 2000; 21: 845–9.
- 78 Hu K, Li GR, Nattel S. Adenosine-induced activation of ATP-sensitive K⁺ channels in excised membrane patches is mediated by PKC. *Am J Physiol* 1999; 276: H488–95.
- 79 Nathan DM, Buse JB, Davidson MB, Ferrannini E, Holman RR,

- Sherwin R, *et al*. Medical management of hyperglycemia in type 2 diabetes: a consensus algorithm for the initiation and adjustment of therapy: a consensus statement of the American Diabetes Association and the European Association for the Study of Diabetes. *Diabetes Care* 2009; 32: 193–203.
- 80 Greeley SA, Tucker SE, Naylor RN, Bell GI, Philipson LH. Neonatal diabetes mellitus: a model for personalized medicine. *Trends Endocrinol Metab* 2010; 21: 464–72.
- 81 Gribble FM, Reimann F. Sulphonylurea action revisited: the post-cloning era. *Diabetologia* 2003; 46: 875–91.
- 82 Ashfield R, Gribble FM, Ashcroft SJ, Ashcroft FM. Identification of the high-affinity tolbutamide site on the SUR1 subunit of the K_{ATP} channel. *Diabetes* 1999; 48: 1341–7.
- 83 Mikhailov MV, Mikhailova EA, Ashcroft SJ. Molecular structure of the glibenclamide binding site of the beta-cell K_{ATP} channel. *FEBS Lett* 2001; 499: 154–60.
- 84 Gribble FM, Tucker SJ, Ashcroft FM. The interaction of nucleotides with the tolbutamide block of cloned ATP-sensitive K^+ channel currents expressed in *Xenopus* oocytes: a reinterpretation. *J Physiol* 1997; 504: 35–45.
- 85 Gros L, Virsolvy A, Salazar G, Bataille D, Blache P. Characterization of low-affinity binding sites for glibenclamide on the Kir6.2 subunit of the beta-cell K_{ATP} channel. *Biochem Biophys Res Commun* 1999; 257: 766–70.
- 86 Arnoux JB, de LP, Ribeiro MJ, Hussain K, Blankenstein O, Mohnike K, *et al*. Congenital hyperinsulinism. *Early Hum Dev* 2010; 86: 287–94.
- 87 Kapoor RR, Flanagan SE, James C, Shield J, Ellard S, Hussain K. Hyperinsulinaemic hypoglycaemia. *Arch Dis Child* 2009; 94: 450–7.
- 88 Ashcroft FM, Gribble FM. New windows on the mechanism of action of K_{ATP} channel openers. *Trends Pharmacol Sci* 2000; 21: 439–45.
- 89 Isomoto S, Kurachi Y. Function, regulation, pharmacology, and molecular structure of ATP-sensitive K^+ channels in the cardiovascular system. *J Cardiovasc Electrophysiol* 1997; 8: 1431–46.
- 90 Terzic A, Jahangir A, Kurachi Y. Cardiac ATP-sensitive K^+ channels: regulation by intracellular nucleotides and K^+ channel-opening drugs. *Am J Physiol* 1995; 269: C525–45.
- 91 Quayle JM, Nelson MT, Standen NB. ATP-sensitive and inwardly rectifying potassium channels in smooth muscle. *Physiol Rev* 1997; 77: 1165–232.
- 92 Moreau C, Jacquet H, Prost AL, D'ahan N, Vivaudou M. The molecular basis of the specificity of action of K_{ATP} channel openers. *EMBO J* 2000; 19: 6644–51.
- 93 Moreau C, Gally F, Jacquet-Bouix H, Vivaudou M. The size of a single residue of the sulphonylurea receptor dictates the effectiveness of K_{ATP} channel openers. *Mol Pharmacol* 2005; 67: 1026–33.
- 94 Moreau C, Prost AL, Derand R, Vivaudou M. SUR, ABC proteins targeted by K_{ATP} channel openers. *J Mol Cell Cardiol* 2005; 38: 951–63.
- 95 Miki T, Nagashima K, Tashiro F, Kotake K, Yoshitomi H, Tamamoto A, *et al*. Defective insulin secretion and enhanced insulin action in K_{ATP} channel-deficient mice. *Proc Natl Acad Sci U S A* 1998; 95: 10402–6.
- 96 Minami K, Miki T, Kadowaki T, Seino S. Roles of ATP-sensitive K^+ channels as metabolic sensors: studies of Kir6.x null mice. *Diabetes* 2004; 53: S176–80.
- 97 Franklin I, Gromada J, Gjinovci A, Theander S, Wollheim CB. Beta-cell secretory products activate alpha-cell ATP-dependent potassium channels to inhibit glucagon release. *Diabetes* 2005; 54: 1808–15.
- 98 MacDonald PE, De Marinis YZ, Ramracheya R, Salehi A, Ma X, Johnson PR, *et al*. A K_{ATP} channel-dependent pathway within alpha cells regulates glucagon release from both rodent and human islets of Langerhans. *PLoS Biol* 2007; 5: e143.
- 99 Gromada J, Franklin I, Wollheim CB. Alpha-cells of the endocrine pancreas: 35 years of research but the enigma remains. *Endocr Rev* 2007; 28: 84–116.
- 100 Oomura Y, Ono T, Ooyama H, Wayner MJ. Glucose and osmosensitive neurones of the rat hypothalamus. *Nature* 1969; 222: 282–4.
- 101 Taborsky GJ Jr, Ahren B, Havel PJ. Autonomic mediation of glucagon secretion during hypoglycemia: implications for impaired alpha-cell responses in type 1 diabetes. *Diabetes* 1998; 47: 995–1005.
- 102 Miki T, Liss B, Minami K, Shiuchi T, Saraya A, Kashima Y, *et al*. ATP-sensitive K^+ channels in the hypothalamus are essential for the maintenance of glucose homeostasis. *Nat Neurosci* 2001; 4: 507–12.
- 103 Poci A, Lam TK, Gutierrez-Juarez R, Obici S, Schwartz GJ, Bryan J, *et al*. Hypothalamic K_{ATP} channels control hepatic glucose production. *Nature* 2005; 434: 1026–31.
- 104 Konner AC, Janoscsek R, Plum L, Jordan SD, Rother E, Ma X, *et al*. Insulin action in AgRP-expressing neurons is required for suppression of hepatic glucose production. *Cell Metab* 2007; 5: 438–49.
- 105 Parton LE, Ye CP, Coppari R, Enriori PJ, Choi B, Zhang CY, *et al*. Glucose sensing by POMC neurons regulates glucose homeostasis and is impaired in obesity. *Nature* 2007; 449: 228–32.
- 106 Hardy OT, Hohmeier HE, Becker TC, Manduchi E, Doliba NM, Gupta RK, *et al*. Functional genomics of the beta-cell: short-chain 3-hydroxyacyl-coenzyme A dehydrogenase regulates insulin secretion independent of K^+ currents. *Mol Endocrinol* 2007; 21: 765–73.
- 107 Chutkow WA, Samuel V, Hansen PA, Pu J, Valdivia CR, Makielski JC, *et al*. Disruption of Sur2-containing K_{ATP} channels enhances insulin-stimulated glucose uptake in skeletal muscle. *Proc Natl Acad Sci U S A* 2001; 98: 11760–4.
- 108 Miki T, Minami K, Zhang L, Morita M, Gono T, Shiuchi T, *et al*. ATP-sensitive potassium channels participate in glucose uptake in skeletal muscle and adipose tissue. *Am J Physiol Endocrinol Metab* 2002; 283: E1178–84.
- 109 Araki E, Lipes MA, Patti ME, Bruning JC, Haag B3, Johnson RS, *et al*. Alternative pathway of insulin signalling in mice with targeted disruption of the IRS-1 gene. *Nature* 1994; 372: 186–90.
- 110 Minami K, Morita M, Saraya A, Yano H, Terauchi Y, Miki T, *et al*. ATP-sensitive K^+ channel-mediated glucose uptake is independent of IRS-1/phosphatidylinositol 3-kinase signaling. *Am J Physiol Endocrinol Metab* 2003; 285: E1289–96.
- 111 Tamamoto H, Kadowaki T, Tobe K, Yagi T, Sakura H, Hayakawa T, *et al*. Insulin resistance and growth retardation in mice lacking insulin receptor substrate-1. *Nature* 1994; 372: 182–6.
- 112 Mu J, Brozinick JT Jr, Valladares O, Bucan M, Birnbaum MJ. A role for AMP-activated protein kinase in contraction- and hypoxia-regulated glucose transport in skeletal muscle. *Mol Cell* 2001; 7: 1085–94.
- 113 Musi N, Fujii N, Hirshman MF, Ekberg I, Froberg S, Ljungqvist O, *et al*. AMP-activated protein kinase (AMPK) is activated in muscle of subjects with type 2 diabetes during exercise. *Diabetes* 2001; 50: 921–7.
- 114 Shield JP, Gardner RJ, Wadsworth EJ, Whiteford ML, James RS, Robinson DO, *et al*. Aetiopathology and genetic basis of neonatal diabetes. *Arch Dis Child Fetal Neonatal Ed* 1997; 76: F39–42.
- 115 Sperling MA. ATP-sensitive potassium channels—neonatal diabetes mellitus and beyond. *N Engl J Med* 2006; 355: 507–10.
- 116 Stanik J, Gasperikova D, Paskova M, Barak L, Javorkova J, Jancova E, *et al*. Prevalence of permanent neonatal diabetes in Slovakia and successful replacement of insulin with sulphonylurea therapy in KCNJ11 and ABCC8 mutation carriers. *J Clin Endocrinol Metab*

- 2007; 92: 1276–82.
- 117 Wiedemann B, Schober E, Waldhoer T, Koehle J, Flanagan SE, Mackay DJ, *et al*. Incidence of neonatal diabetes in Austria—calculation based on the Austrian Diabetes Register. *Pediatr Diabetes* 2010; 11: 18–23.
- 118 Slingerland AS, Shields BM, Flanagan SE, Bruining GJ, Noordam K, Gach A, *et al*. Referral rates for diagnostic testing support an incidence of permanent neonatal diabetes in three European countries of at least 1 in 260 000 live births. *Diabetologia* 2009; 52: 1683–5.
- 119 Temple IK, James RS, Crolla JA, Sitch FL, Jacobs PA, Howell WM, *et al*. An imprinted gene(s) for diabetes? *Nat Genet* 1995; 9: 110–2.
- 120 Mackay DJ, Coupe AM, Shield JP, Storr JN, Temple IK, Robinson DO. Relaxation of imprinted expression of ZAC and HYMAI in a patient with transient neonatal diabetes mellitus. *Hum Genet* 2002; 110: 139–44.
- 121 Garin I, Edghill EL, Akerman I, Rubio-Cabezas O, Rica I, Locke JM, *et al*. Recessive mutations in the INS gene result in neonatal diabetes through reduced insulin biosynthesis. *Proc Natl Acad Sci U S A* 2010; 107: 3105–10.
- 122 Ahamed A, Unnikrishnan AG, Pendsey SS, Nampoothiri S, Bhavani N, Praveen VP, *et al*. Permanent neonatal diabetes mellitus due to a C96Y heterozygous mutation in the insulin gene. A case report. *JOP* 2008; 9: 715–8.
- 123 Molven A, Ringdal M, Nordbo AM, Raeder H, Stoy J, Lipkind GM, *et al*. Mutations in the insulin gene can cause MODY and autoantibody-negative type 1 diabetes. *Diabetes* 2008; 57: 1131–5.
- 124 Polak M, Dechaume A, Cave H, Nimri R, Crosnier H, Sulmont V, *et al*. Heterozygous missense mutations in the insulin gene are linked to permanent diabetes appearing in the neonatal period or in early infancy: a report from the French ND (Neonatal Diabetes) Study Group. *Diabetes* 2008; 57: 1115–9.
- 125 Edghill EL, Flanagan SE, Patch AM, Boustred C, Parrish A, Shields B, *et al*. Insulin mutation screening in 1 044 patients with diabetes: mutations in the INS gene are a common cause of neonatal diabetes but a rare cause of diabetes diagnosed in childhood or adulthood. *Diabetes* 2008; 57: 1034–42.
- 126 Stoy J, Edghill EL, Flanagan SE, Ye H, Paz VP, Pluzhnikov A, *et al*. Insulin gene mutations as a cause of permanent neonatal diabetes. *Proc Natl Acad Sci U S A* 2007; 104: 15040–4.
- 127 Stoffers DA, Zinkin NT, Stanojevic V, Clarke WL, Habener JF. Pancreatic agenesis attributable to a single nucleotide deletion in the human IPF1 gene coding sequence. *Nat Genet* 1997; 15: 106–10.
- 128 Schwitzgebel VM, Mamin A, Brun T, Ritz-Laser B, Zaiko M, Maret A, *et al*. Agenesis of human pancreas due to decreased half-life of insulin promoter factor 1. *J Clin Endocrinol Metab* 2003; 88: 4398–406.
- 129 Thomas IH, Saini NK, Adhikari A, Lee JM, Kasa-Vubu JZ, Vazquez DM, *et al*. Neonatal diabetes mellitus with pancreatic agenesis in an infant with homozygous IPF-1 Pro63fsX60 mutation. *Pediatr Diabetes* 2009; 10: 492–6.
- 130 Borowiec M, Antosik K, Fendler W, Deja G, Jarosz-Chobot P, Mysliwiec M, *et al*. Novel glucokinase mutations in patients with monogenic diabetes — clinical outline of *gck-md* and potential for founder effect in slavic population. *Clin Genet* 2011 Feb 23. doi: 10.1111/j.1399-0004.2011.01656.x
- 131 Hussain K. Mutations in pancreatic β -cell Glucokinase as a cause of hyperinsulinaemic hypoglycaemia and neonatal diabetes mellitus. *Rev Endocr Metab Disord* 2010; 11: 179–83.
- 132 Barbetti F, Cobo-Vuilleumier N, Dionisi-Vici C, Toni S, Ciampalini P, Massa O, *et al*. Opposite clinical phenotypes of glucokinase disease: Description of a novel activating mutation and contiguous inactivating mutations in human glucokinase (GCK) gene. *Mol Endocrinol* 2009; 23: 1983–9.
- 133 Osbak KK, Colclough K, Saint-Martin C, Beer NL, Bellanne-Chantelot C, Ellard S, *et al*. Update on mutations in glucokinase (GCK), which cause maturity-onset diabetes of the young, permanent neonatal diabetes, and hyperinsulinemic hypoglycemia. *Hum Mutat* 2009; 30: 1512–26.
- 134 Turkkahraman D, Bircan I, Tribble ND, Akcurin S, Ellard S, Gloyn AL. Permanent neonatal diabetes mellitus caused by a novel homozygous (T168A) glucokinase (GCK) mutation: initial response to oral sulphonylurea therapy. *J Pediatr* 2008; 153: 122–6.
- 135 Njolstad PR, Sagen JV, Bjorkhaug L, Odili S, Shehadeh N, Bakry D, *et al*. Permanent neonatal diabetes caused by glucokinase deficiency: inborn error of the glucose-insulin signaling pathway. *Diabetes* 2003; 52: 2854–60.
- 136 Gloyn AL. Glucokinase (GCK) mutations in hyper- and hypoglycemia: maturity-onset diabetes of the young, permanent neonatal diabetes, and hyperinsulinemia of infancy. *Hum Mutat* 2003; 22: 353–62.
- 137 Vaxillaire M, Samson C, Cave H, Metz C, Froguel P, Polak M. Glucokinase gene mutations are not a common cause of permanent neonatal diabetes in France. *Diabetologia* 2002; 45: 454–5.
- 138 Njolstad PR, Sovik O, Cuesta-Munoz A, Bjorkhaug L, Massa O, Barbetti F, *et al*. Neonatal diabetes mellitus due to complete glucokinase deficiency. *N Engl J Med* 2001; 344: 1588–92.
- 139 Rubio-Cabezas O, Diaz GF, Aragones A, Argente J, Campos-Barros A. Permanent neonatal diabetes caused by a homozygous nonsense mutation in the glucokinase gene. *Pediatr Diabetes* 2008; 9: 245–9.
- 140 Rubio-Cabezas O, Minton JA, Caswell R, Shield JP, Deiss D, Sumnik Z, *et al*. Clinical heterogeneity in patients with FOXP3 mutations presenting with permanent neonatal diabetes. *Diabetes Care* 2009; 32: 111–6.
- 141 Wildin RS, Ramsdell F, Peake J, Faravelli F, Casanova JL, Buist N, *et al*. X-linked neonatal diabetes mellitus, enteropathy and endocrinopathy syndrome is the human equivalent of mouse scurfy. *Nat Genet* 2001; 27: 18–20.
- 142 Girard CA, Wunderlich FT, Shimomura K, Collins S, Kaizik S, Proks P, *et al*. Expression of an activating mutation in the gene encoding the K_{ATP} channel subunit Kir6.2 in mouse pancreatic beta cells recapitulates neonatal diabetes. *J Clin Invest* 2009; 119: 80–90.
- 143 Hamming KS, Soliman D, Matemisz LC, Niazi O, Lang Y, Gloyn AL, *et al*. Coexpression of the type 2 diabetes susceptibility gene variants KCNJ11 E23K and ABCC8 S1369A alter the ATP and sulfonylurea sensitivities of the ATP-sensitive K^+ channel. *Diabetes* 2009; 58: 2419–24.
- 144 Villareal DT, Koster JC, Robertson H, Akrouh A, Miyake K, Bell GI, *et al*. Kir6.2 variant E23K increases ATP-sensitive K^+ channel activity and is associated with impaired insulin release and enhanced insulin sensitivity in adults with normal glucose tolerance. *Diabetes* 2009; 58: 1869–78.
- 145 Chistiakov DA, Potapov VA, Khodirev DC, Shamkhalova MS, Shestakova MV, Nosikov VV. Genetic variations in the pancreatic ATP-sensitive potassium channel, beta-cell dysfunction, and susceptibility to type 2 diabetes. *Acta Diabetol* 2009; 46: 43–9.
- 146 Riedel MJ, Steckley DC, Light PE. Current status of the E23K Kir6.2 polymorphism: implications for type-2 diabetes. *Hum Genet* 2005; 116: 133–45.
- 147 Riedel MJ, Boora P, Steckley D, de Vries G, Light PE. Kir6.2 polymorphisms sensitize beta-cell ATP-sensitive potassium channels to activation by acyl CoAs: a possible cellular mechanism for increased susceptibility to type 2 diabetes? *Diabetes* 2003; 52: 2630–5.
- 148 Gloyn AL, Weedon MN, Owen KR, Turner MJ, Knight BA, Hitman G, *et*

- al.* Large-scale association studies of variants in genes encoding the pancreatic beta-cell K_{ATP} channel subunits Kir6.2 (KCNJ11) and SUR1 (ABCC8) confirm that the KCNJ11 E23K variant is associated with type 2 diabetes. *Diabetes* 2003; 52: 568–72.
- 149 Flanagan SE, Clauin S, Bellanne-Chantelot C, de Lonlay P, Harries LW, Gloyn AL, *et al.* Update of mutations in the genes encoding the pancreatic beta-cell K_{ATP} channel subunits Kir6.2 (KCNJ11) and sulfonylurea receptor 1 (ABCC8) in diabetes mellitus and hyperinsulinism. *Hum Mutat* 2009; 30: 170–80.
- 150 Remedi MS, Koster JC. K_{ATP} channelopathies in the pancreas. *Pflugers Arch* 2010; 460: 307–20.
- 151 Gloyn AL, Cummings EA, Edghill EL, Harries LW, Scott R, Costa T, *et al.* Permanent neonatal diabetes due to paternal germline mosaicism for an activating mutation of the KCNJ11 gene encoding the Kir6.2 subunit of the beta-cell potassium adenosine triphosphate channel. *J Clin Endocrinol Metab* 2004; 89: 3932–5.
- 152 Ioannou YS, Ellard S, Hattersley A, Skordis N. KCNJ11 activating mutations cause both transient and permanent neonatal diabetes mellitus in Cypriot patients. *Pediatr Diabetes* 2011; 12: 133–7.
- 153 Kochar IP, Kulkarni KP. Transient neonatal diabetes due to Kcnj11 mutation. *Indian Pediatr* 2010; 47: 359–60.
- 154 Khadiolkar VV, Khadiolkar AV, Kapoor RR, Hussain K, Hattersley AT, Ellard S. KCNJ11 activating mutation in an Indian family with remitting and relapsing diabetes. *Indian J Pediatr* 2010; 77: 551–4.
- 155 Stanik J, Lethby M, Flanagan SE, Gasperikova D, Milosovicova B, Lever M, *et al.* Coincidence of a novel KCNJ11 missense variant R365H with a paternally inherited 6q24 duplication in a patient with transient neonatal diabetes. *Diabetes Care* 2008; 31: 1736–7.
- 156 D'Amato E, Tammaro P, Craig TJ, Tosi A, Giorgetti R, Lorini R, *et al.* Variable phenotypic spectrum of diabetes mellitus in a family carrying a novel KCNJ11 gene mutation. *Diabet Med* 2008; 25: 651–6.
- 157 Flanagan SE, Patch AM, Mackay DJ, Edghill EL, Gloyn AL, Robinson D, *et al.* Mutations in ATP-sensitive K^+ channel genes cause transient neonatal diabetes and permanent diabetes in childhood or adulthood. *Diabetes* 2007; 56: 1930–7.
- 158 Yorifuji T, Nagashima K, Kurokawa K, Kawai M, Oishi M, Akazawa Y, *et al.* The C42R mutation in the Kir6.2 (KCNJ11) gene as a cause of transient neonatal diabetes, childhood diabetes, or later-onset, apparently type 2 diabetes mellitus. *J Clin Endocrinol Metab* 2005; 90: 3174–8.
- 159 Gloyn AL, Reimann F, Girard C, Edghill EL, Proks P, Pearson ER, *et al.* Relapsing diabetes can result from moderately activating mutations in KCNJ11. *Hum Mol Genet* 2005; 14: 925–34.
- 160 Zhou Q, Garin I, Castano L, Argente J, Munoz-Calvo MT, Perez de NG, *et al.* Neonatal diabetes caused by mutations in sulfonylurea receptor 1: interplay between expression and Mg-nucleotide gating defects of ATP-sensitive potassium channels. *J Clin Endocrinol Metab* 2010; 95: E473–8.
- 161 de Wet H, Proks P, Lafond M, Aittoniemi J, Sansom MS, Flanagan SE, *et al.* A mutation (R826W) in nucleotide-binding domain 1 of ABCC8 reduces ATPase activity and causes transient neonatal diabetes. *EMBO Rep* 2008; 9: 648–54.
- 162 Vaxillaire M, Dechaume A, Busiah K, Cave H, Pereira S, Scharfmann R, *et al.* New ABCC8 mutations in relapsing neonatal diabetes and clinical features. *Diabetes* 2007; 56: 1737–41.
- 163 Babenko AP, Polak M, Cave H, Busiah K, Czernichow P, Scharfmann R, *et al.* Activating mutations in the ABCC8 gene in neonatal diabetes mellitus. *N Engl J Med* 2006; 355: 456–66.
- 164 Batra CM, Gupta N, Atwal G, Gupta V. Transient neonatal diabetes due to activating mutation in the ABCC8 gene encoding SUR1. *Indian J Pediatr* 2009; 76: 1169–72.
- 165 Flanagan SE, Patch AM, Mackay DJ, Edghill EL, Gloyn AL, Robinson D, *et al.* Mutations in ATP-sensitive K^+ channel genes cause transient neonatal diabetes and permanent diabetes in childhood or adulthood. *Diabetes* 2007; 56: 1930–7.
- 166 Patch AM, Flanagan SE, Boustred C, Hattersley AT, Ellard S. Mutations in the ABCC8 gene encoding the SUR1 subunit of the K_{ATP} channel cause transient neonatal diabetes, permanent neonatal diabetes or permanent diabetes diagnosed outside the neonatal period. *Diabetes Obes Metab* 2007; 9: 28–39.
- 167 Craig TJ, Shimomura K, Holl RW, Flanagan SE, Ellard S, Ashcroft FM. An in-frame deletion in Kir6.2 (KCNJ11) causing neonatal diabetes reveals a site of interaction between Kir6.2 and SUR1. *J Clin Endocrinol Metab* 2009; 94: 2551–7.
- 168 McTaggart JS, Clark RH, Ashcroft FM. The role of the K_{ATP} channel in glucose homeostasis in health and disease: more than meets the islet. *J Physiol* 2010; 588: 3201–9.
- 169 Ashcroft FM. ATP-sensitive potassium channelopathies: focus on insulin secretion. *J Clin Invest* 2005; 115: 2047–58.
- 170 Proks P, Antcliff JF, Lippiat J, Gloyn AL, Hattersley AT, Ashcroft FM. Molecular basis of Kir6.2 mutations associated with neonatal diabetes or neonatal diabetes plus neurological features. *Proc Natl Acad Sci U S A* 2004; 101: 17539–44.
- 171 De Leon DD, Stanley CA. Permanent neonatal diabetes mellitus. 1993. In: Pagon RA, Bird TD, Dolan CR, Stephens K, editors. *GeneReviews* [Internet]. Seattle (WA): University of Washington, Seattle; 1993–2008 Feb 08 [updated 2008 Mar 04].
- 172 Clark RH, McTaggart JS, Webster R, Mannikko R, Iberl M, Sim XL, *et al.* Muscle dysfunction caused by a K_{ATP} channel mutation in neonatal diabetes is neuronal in origin. *Science* 2010; 329: 458–61.
- 173 Ashcroft FM. New uses for old drugs: neonatal diabetes and sulphonylureas. *Cell Metab* 2010; 11: 179–81.
- 174 Koster JC, Cadario F, Peruzzi C, Colombo C, Nichols CG, Barbetti F. The G53D mutation in Kir6.2 (KCNJ11) is associated with neonatal diabetes and motor dysfunction in adulthood that is improved with sulfonylurea therapy. *J Clin Endocrinol Metab* 2008; 93: 1054–61.
- 175 Pearson ER, Flechtner I, Njolstad PR, Malecki MT, Flanagan SE, Larkin B, *et al.* Switching from insulin to oral sulfonylureas in patients with diabetes due to Kir6.2 mutations. *N Engl J Med* 2006; 355: 467–77.
- 176 Zung A, Glaser B, Nimri R, Zadik Z. Glibenclamide treatment in permanent neonatal diabetes mellitus due to an activating mutation in Kir6.2. *J Clin Endocrinol Metab* 2004; 89: 5504–7.
- 177 Wambach JA, Marshall BA, Koster JC, White NH, Nichols CG. Successful sulfonylurea treatment of an insulin-naive neonate with diabetes mellitus due to a KCNJ11 mutation. *Pediatr Diabetes* 2010; 11: 286–8.
- 178 Begum-Hasan J, Polychronakos C, Brill H. Familial permanent neonatal diabetes with KCNJ11 mutation and the response to glyburide therapy—a three-year follow-up. *J Pediatr Endocrinol Metab* 2008; 21: 895–903.
- 179 Klupa T, Skupien J, Mirkiewicz-Sieradzka B, Gach A, Noczynska A, Szalecki M, *et al.* Diabetic retinopathy in permanent neonatal diabetes due to Kir6.2 gene mutations: the results of a minimum 2-year follow-up after the transfer from insulin to sulphonylurea. *Diabet Med* 2009; 26: 663–4.
- 180 Mohamadi A, Clark LM, Lipkin PH, Mahone EM, Wodka EL, Plotnick LP. Medical and developmental impact of transition from subcutaneous insulin to oral glyburide in a 15-yr-old boy with neonatal diabetes mellitus and intermediate DEND syndrome: extending the age of KCNJ11 mutation testing in neonatal DM.

- Pediatr Diabetes 2010; 11: 203–7.
- 181 Stoy J, Greeley SA, Paz VP, Ye H, Pastore AN, Skowron KB, et al. Diagnosis and treatment of neonatal diabetes: a United States experience. *Pediatr Diabetes* 2008; 9: 450–9.
- 182 Slingerland AS, Nuboer R, Hadders-Algra M, Hattersley AT, Bruining GJ. Improved motor development and good long-term glycaemic control with sulfonylurea treatment in a patient with the syndrome of intermediate developmental delay, early-onset generalised epilepsy and neonatal diabetes associated with the V59M mutation in the KCNJ11 gene. *Diabetologia* 2006; 49: 2559–63.
- 183 Slingerland AS, Hurkx W, Noordam K, Flanagan SE, Jukema JW, Meiners LC, et al. Sulphonylurea therapy improves cognition in a patient with the V59M KCNJ11 mutation. *Diabet Med* 2008; 25: 277–81.
- 184 Masia R, Koster JC, Tumini S, Chiarelli F, Colombo C, Nichols CG, et al. An ATP-binding mutation (G334D) in KCNJ11 is associated with a sulfonylurea-insensitive form of developmental delay, epilepsy, and neonatal diabetes. *Diabetes* 2007; 56: 328–36.
- 185 Sumnik Z, Kolouskova S, Wales JK, Komarek V, Cinek O. Sulphonylurea treatment does not improve psychomotor development in children with KCNJ11 mutations causing permanent neonatal diabetes mellitus accompanied by developmental delay and epilepsy (DEND syndrome). *Diabet Med* 2007; 24: 1176–8.
- 186 Della MT, Battistini C, Radonsky V, Savodelli RD, Damiani D, Kok F, et al. Glibenclamide unresponsiveness in a Brazilian child with permanent neonatal diabetes mellitus and DEND syndrome due to a C166Y mutation in KCNJ11 (Kir6.2) gene. *Arq Bras Endocrinol Metabol* 2008; 52: 1350–5.
- 187 Kumaraguru J, Flanagan SE, Greeley SA, Nuboer R, Stoy J, Philipson LH, et al. Tooth discoloration in patients with neonatal diabetes after transfer onto glibenclamide: a previously unreported side effect. *Diabetes Care* 2009; 32: 1428–30.
- 188 Codner E, Flanagan SE, Ugarte F, Garcia H, Vidal T, Ellard S, et al. Sulfonylurea treatment in young children with neonatal diabetes: dealing with hyperglycemia, hypoglycemia, and sick days. *Diabetes Care* 2007; 30: e28–9.
- 189 Clark R, Proks P. ATP-sensitive potassium channels in health and disease. *Adv Exp Med Biol* 2010; 654: 165–92.
- 190 Remedi MS, Kurata HT, Scott A, Wunderlich FT, Rother E, Kleinridders A, et al. Secondary consequences of beta cell inexcitability: identification and prevention in a murine model of K_{ATP} -induced neonatal diabetes mellitus. *Cell Metab* 2009; 9: 140–51.
- 191 Hussain K. Congenital hyperinsulinism. *Semin Fetal Neonatal Med* 2005; 10: 369–76.
- 192 Hussain K, Cosgrove KE. From congenital hyperinsulinism to diabetes mellitus: the role of pancreatic beta-cell K_{ATP} channels. *Pediatr Diabetes* 2005; 6: 103–13.
- 193 Glaser B, Thornton P, Otonkoski T, Junien C. Genetics of neonatal hyperinsulinism. *Arch Dis Child Fetal Neonatal Ed* 2000; 82: F79–86.
- 194 Sempoux C, Guiot Y, Dubois D, Nollevaux MC, Saudubray JM, Nihoul-Fekete C, et al. Pancreatic beta-cell proliferation in persistent hyperinsulinemic hypoglycemia of infancy: an immunohistochemical study of 18 cases. *Mod Pathol* 1998; 11: 444–9.
- 195 Sempoux C, Guiot Y, Rahier J. The focal form of persistent hyperinsulinemic hypoglycemia of infancy. *Diabetes* 2001; 50: S182–3.
- 196 Sempoux C, Guiot Y, Jaubert F, Rahier J. Focal and diffuse forms of congenital hyperinsulinism: the keys for differential diagnosis. *Endocr Pathol* 2004; 15: 241–6.
- 197 Glaser B, Landau H, Permutt MA. Neonatal hyperinsulinism. *Trends Endocrinol Metab* 1999; 10: 55–61.
- 198 Fournet JC, Mayaud C, de Lonlay P, Verkarre V, Rahier J, Brunelle F, et al. Loss of imprinted genes and paternal SUR1 mutations lead to focal form of congenital hyperinsulinism. *Horm Res* 2000; 53: 2–6.
- 199 Fournet JC, Mayaud C, de Lonlay P, Gross-Morand MS, Verkarre V, Castanet M, et al. Unbalanced expression of 11p15 imprinted genes in focal forms of congenital hyperinsulinism: association with a reduction to homozygosity of a mutation in ABCC8 or KCNJ11. *Am J Pathol* 2001; 158: 2177–84.
- 200 Fournet JC, Junien C. Genetics of congenital hyperinsulinism. *Endocr Pathol* 2004; 15: 233–40.
- 201 de Lonlay P, Fournet JC, Touati G, Groos MS, Martin D, Sevin C, et al. Heterogeneity of persistent hyperinsulinaemic hypoglycaemia. A series of 175 cases. *Eur J Pediatr* 2002; 161: 37–48.
- 202 de Lonlay P, Fournet JC, Rahier J, Gross-Morand MS, Poggi-Travert F, Foussier V, et al. Somatic deletion of the imprinted 11p15 region in sporadic persistent hyperinsulinemic hypoglycemia of infancy is specific of focal adenomatous hyperplasia and endorses partial pancreatectomy. *J Clin Invest* 1997; 100: 802–7.
- 203 Glaser B, Ryan F, Donath M, Landau H, Stanley CA, Baker L, et al. Hyperinsulinism caused by paternal-specific inheritance of a recessive mutation in the sulfonylurea-receptor gene. *Diabetes* 1999; 48: 1652–7.
- 204 Verkarre V, Fournet JC, de Lonlay P, Gross-Morand MS, Devillers M, Rahier J, et al. Paternal mutation of the sulfonylurea receptor (SUR1) gene and maternal loss of 11p15 imprinted genes lead to persistent hyperinsulinism in focal adenomatous hyperplasia. *J Clin Invest* 1998; 102: 1286–91.
- 205 Huopio H, Shyng SL, Otonkoski T, Nichols CG. K_{ATP} channels and insulin secretion disorders. *Am J Physiol Endocrinol Metab* 2002; 283: E207–16.
- 206 James C, Kapoor RR, Ismail D, Hussain K. The genetic basis of congenital hyperinsulinism. *J Med Genet* 2009; 46: 289–99.
- 207 Chan KW, Zhang H, Logothetis DE. N-terminal transmembrane domain of the SUR controls trafficking and gating of Kir6 channel subunits. *EMBO J* 2003; 22: 3833–43.
- 208 Montero LC, Pozo RJ, Munoz Calvo MT, Martos MG, Donoso MA, Rubio CO, et al. Hyperinsulinism-hyperammonemia syndrome due to a *de novo* mutation in exon 7 (G979A) of the glutamate dehydrogenase gene with excellent response to diazoxide. *An Pediatr (Barc)* 2004; 61: 433–7.
- 209 Yasuda K, Koda N, Kadowaki H, Ogawa Y, Kimura S, Kadowaki T, et al. A Japanese case of congenital hyperinsulinism with hyperammonemia due to a mutation in glutamate dehydrogenase (GLUD1) gene. *Intern Med* 2001; 40: 32–7.
- 210 Marquard J, Palladino AA, Stanley CA, Mayatepek E, Meissner T. Rare forms of congenital hyperinsulinism. *Semin Pediatr Surg* 2011; 20: 38–44.
- 211 Palladino AA, Stanley CA. The hyperinsulinism/hyperammonemia syndrome. *Rev Endocr Metab Disord* 2010; 11: 171–8.
- 212 Chik KK, Chan CW, Lam CW, Ng KL. Hyperinsulinism and hyperammonemia syndrome due to a novel missense mutation in the allosteric domain of the glutamate dehydrogenase 1 gene. *J Paediatr Child Health* 2008; 44: 517–9.
- 213 de Lonlay P, Giurgea I, Sempoux C, Touati G, Jaubert F, Rahier J, et al. Dominantly inherited hyperinsulinaemic hypoglycaemia. *J Inher Metab Dis* 2005; 28: 267–76.
- 214 Stanley CA. Hyperinsulinism/hyperammonemia syndrome: insights into the regulatory role of glutamate dehydrogenase in ammonia metabolism. *Mol Genet Metab* 2004; 81: S45–51.
- 215 Fujioka H, Okano Y, Inada H, Asada M, Kawamura T, Hase Y, et al. Molecular characterisation of glutamate dehydrogenase gene

- defects in Japanese patients with congenital hyperinsulinism/hyperammonaemia. *Eur J Hum Genet* 2001; 9: 931–7.
- 216 Kelly A, Stanley CA. Disorders of glutamate metabolism. *Ment Retard Dev Disabil Res Rev* 2001; 7: 287–95.
- 217 Meissner T, Marquard J, Cobo-Vuilleumier N, Maringa M, Rodriguez-Bada P, Garcia-Gimeno MA, *et al*. Diagnostic difficulties in glucokinase hyperinsulinism. *Horm Metab Res* 2009; 41: 320–6.
- 218 Christesen HB, Tribble ND, Molven A, Siddiqui J, Sandal T, Brusgaard K, *et al*. Activating glucokinase (GCK) mutations as a cause of medically responsive congenital hyperinsulinism: prevalence in children and characterisation of a novel GCK mutation. *Eur J Endocrinol* 2008; 159: 27–34.
- 219 Molven A, Matre GE, Duran M, Wanders RJ, Rishaug U, Njolstad PR, *et al*. Familial hyperinsulinemic hypoglycemia caused by a defect in the SCHAD enzyme of mitochondrial fatty acid oxidation. *Diabetes* 2004; 53: 221–7.
- 220 Bas F, Darendeliler F, Demirkol D, Bundak R, Saka N, Gunoz H. Successful therapy with calcium channel blocker (nifedipine) in persistent neonatal hyperinsulinemic hypoglycemia of infancy. *J Pediatr Endocrinol Metab* 1999; 12: 873–8.
- 221 Eichmann D, Hufnagel M, Quick P, Santer R. Treatment of hyperinsulinaemic hypoglycaemia with nifedipine. *Eur J Pediatr* 1999; 158: 204–6.
- 222 Lindley KJ, Dunne MJ, Kane C, Shepherd RM, Squires PE, James RF, *et al*. Ionic control of beta cell function in nesidioblastosis. A possible therapeutic role for calcium channel blockade. *Arch Dis Child* 1996; 74: 373–8.
- 223 Shanbag P, Pathak A, Vaidya M, Shahid SK. Persistent hyperinsulinemic hypoglycemia of infancy-successful therapy with nifedipine. *Indian J Pediatr* 2002; 69: 271–2.
- 224 Straub SG, Cosgrove KE, Ammala C, Shepherd RM, O'Brien RE, Barnes PD, *et al*. Hyperinsulinism of infancy: the regulated release of insulin by K_{ATP} channel-independent pathways. *Diabetes* 2001; 50: 329–39.

Review

Activation of human ether-a-go-go related gene (hERG) potassium channels by small molecules

Ping-zheng ZHOU^{1,2}, Joseph BABCOCK³, Lian-qing LIU², Min LI^{1,3}, Zhao-bing GAO^{1,*}

¹State Key Laboratory of Drug Research, Shanghai Institute of Materia Medica, Chinese Academy of Sciences, Shanghai 201203, China; ²State Key Laboratory of Robotics, Shenyang Institute of Automation, Chinese Academy of Sciences, Shenyang 110016, China; ³Department of Neuroscience, High Throughput Biology Center and Johns Hopkins Ion Channel Center, School of Medicine, Johns Hopkins University, Baltimore, Maryland 21205, USA

Human ether-a-go-go related gene (hERG) potassium (K⁺) channels play a critical role in cardiac action potential repolarization. Mutations that reduce hERG conductance or surface expression may cause congenital long QT syndrome (LQTS). Moreover, the channels can be inhibited by structurally diverse small molecules, resulting in an acquired form of LQTS. Consequently, small molecules that increase the hERG current may be of value for treatment of LQTS. So far, nine hERG activators have been reported. The aim of this review is to discuss recent advances concerning the identification and action mechanism of hERG activators.

Keywords: Human ether-a-go-go related gene (hERG); ion channel; long QT syndrome (LQTS); activator

Acta Pharmacologica Sinica (2011) 32: 781–788; doi: 10.1038/aps.2011.70; published online 30 May 2011

Discovery and structure of hERG

In 1994, Warmke and Ganetzky first identified the human ether-a-go-go related gene (hERG) K⁺ channel by screening a human hippocampal cDNA library with a mouse homologue of “ether-a-go-go” (EAG), a *Drosophila* K⁺ channel gene^[1]. Subsequently, Sanguinetti and colleagues reported similarities between the biophysical properties of the heterologously expressed hERG channel and the rapidly activating delayed rectifier K⁺ current (*I_{Kr}*), a critical current in the phase 3 repolarization of the cardiac action potential, and confirmed that hERG encodes the α subunit of *I_{Kr}*^[2,3]. While hERG is predominately expressed in the heart, it is also found in diverse tissues including neurons, neuroendocrine glands and smooth muscle^[3].

hERG (Kv11.1) was the 11th member of the voltage-gated K⁺ channel family (Kv). Like other Kv channels, hERG is an obligate homotetramer, with each subunit containing six transmembrane domains (S1–S6): S1–S4 compose the voltage sensor domain, while the S5, P-loop, and S6 segments form the channel pore (Figure 1). However, hERG has several features that distinguish it from other Kv family members. First, a conserved tyrosine found in the GYG motif of other Kv channel pores is replaced by a phenylalanine^[4]. This aromatic

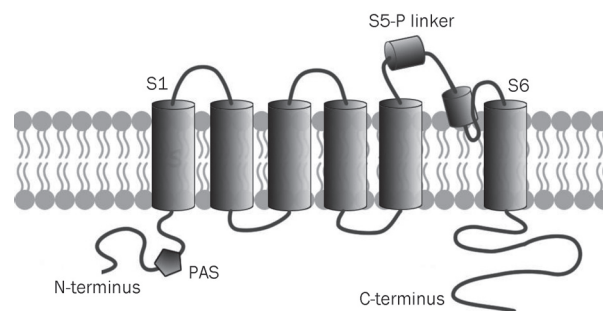


Figure 1. The basic structure of hERG channels. S1–S4 is the voltage sensor domain. S5, the P-loop, and S6 compose the pore of the channel; the termini of the protein are both intracellular.

residue, along with others lining the hERG pore, has been proposed as a determinant of promiscuous small-molecule interaction. Second, hERG’s protein sequence lacks the proline-X-proline (PXP) motif that often flanks the S6 helices of other Kv channels. It is generally believed that the PXP domain “kinks” this helix to reduce the volume of the pore cavity, and its absence in hERG has been suggested to play a role in promiscuous drug interactions as well. Finally, the hERG channel has a large “S5-P linker” domain between the S5 and P-loop segments that assumes an amphipathic helical arrangement in membrane mimetic sodium dodecyl sulfate (SDS) micelles and is believed to affect channel inactivation^[5].

* To whom correspondence should be addressed.

E-mail zb.gao@mail.shcnc.ac.cn

Received 2011-04-01 Accepted 2011-04-25

The intracellular termini of the hERG channel are also important for function. The N-terminus contains a Per-Arnt-Sim (PAS) domain (about 135 amino acids), which, despite being a common motif in signaling proteins found in bacteria and plants, appears in no other mammalian ion channels. In hERG, the PAS domain modulates the deactivation of the channel following membrane depolarization. The C-terminus of the channel contains a cyclic nucleotide binding domain (CNBD), which has been linked to mutations affecting trafficking^[5].

Gating of hERG K⁺ channels

Although the overall structure of hERG is homologous to that of other potassium channels, its kinetic behavior is quite distinct and is characterized by comparatively slow activation and deactivation kinetics (on the order of hundreds of ms to s) but very rapid, voltage-dependent inactivation kinetics (on the order of ms to tens of ms)^[5, 6]. The unusual kinetics of hERG are compatible with its function in cardiac repolarization. In the ascending phase of the action potential, as a result of slow activation and simultaneous fast inactivation, little outward current flows through hERG during depolarization. As the membrane repolarizes, hERG channels recover from inactivation much faster than they deactivate, thereby generating an outward current that peaks at about -40 mV. This outward current through hERG is the key determinant for termination of the plateau phase of the action potential^[5] (Figure 2). Due to the importance and uniqueness of hERG gating kinetics, much of the recent work on hERG has focused on understanding the molecular rearrangements of the channel protein during the cardiac action potential.

Slow activation

As noted above, the voltage sensor of the hERG channel is the S1-S4 segment, in which the S4 helix is particularly important.

Like other Kv channels, the hERG S4 has four periodically spaced arginine residues whose positive charges, which are repelled by changes in membrane potential, are thought to drive structural rearrangement of the protein during depolarization via the S4-S5 linker^[7]. Sequence alignments and hydrophathy plots suggest that the overall structure of this voltage sensor domain (VSD) is homologous to that of other K⁺ channels. Why then are the kinetics of activation so different in hERG? To answer this question, Smith and Yellen (2002) attached a fluorescent molecule to the extracellular domain of S4 and examined the movement of this helix by fluorescence resonance energy transfer (FRET). They found that the fluorescence signal changed very slowly in response to membrane depolarization, suggesting that slow voltage sensor movement is responsible for the unusual activation gating kinetics of the channel^[6, 8]. However, there still is no mechanistic explanation for the slow movement of the hERG S4 helix, though Subbiah and colleagues have identified residues K525, R528, and K538 as molecular determinants of this behavior using tryptophan scanning mutagenesis^[9].

Fast voltage-dependent inactivation

Two major mechanisms have been proposed for the inactivation of voltage-gated potassium channels^[10]. The first is N-type (also called “ball and chain” type), which involves rapid occlusion of the open channel by an intracellular segment of the protein. The second is C-type, which involves a slower change in channel conformation at the extracellular mouth. There is evidence that inactivation of hERG is similar to C-type and shows voltage-dependency, even though hERG inactivation is several orders of magnitude faster than C-type inactivation in Shaker K⁺ channels^[3, 5, 11]. Some studies have shown that this fast inactivation limits K⁺ efflux during depolarization, allowing hERG to function as an inward rectifier of potassium concentration^[11].

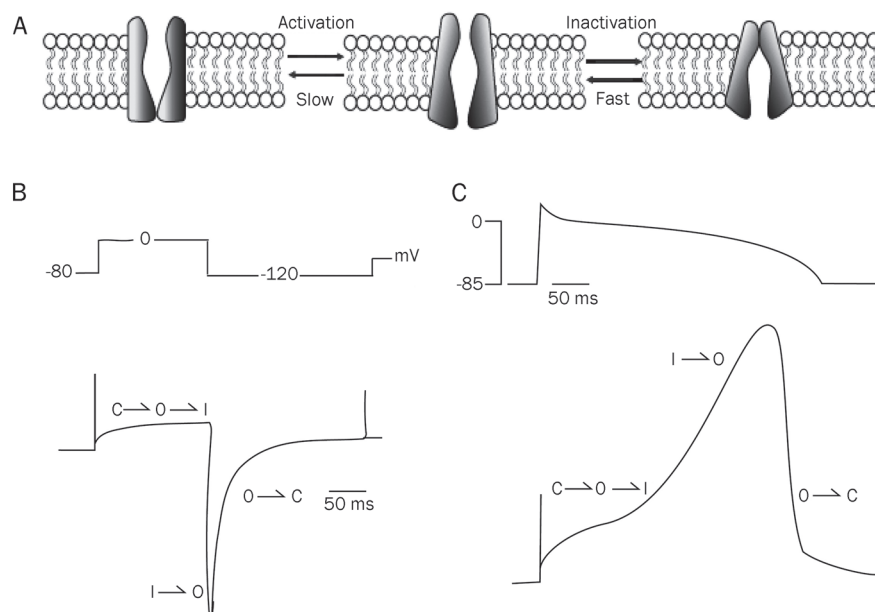


Figure 2. Gating of hERG channels. (A) The three main conformational states of hERG K⁺ channels: closed (C), open (O), and inactive (I). Transitions between these states are voltage dependent. The transition from closed to open involves the opening of an intracellular gate, whereas transition from open to inactive involves the closing of a gate at the extracellular face of the permeation pathway. (B) Representative traces showing characteristic kinetics: slow activation and deactivation, coupled with rapid inactivation. (C) hERG currents recorded during cardiac ventricular action potential. (B&C adapted from Vandenberg, JI, et al. *Eur Biophys J* 2004; 32: 89-97).

The S5-P-loop region is critical for inactivation of hERG. Many mutations in this region, most critically at S620 and S621, will inhibit inactivation^[5,6]. S620T abolishes the inactivation of hERG, while S620A left-shifts the voltage-dependent inactivation approximately +100 mV. Besides S620 and S621, other residues such as W585, L586, H587, L589, G590, D591, I593, and G594 have also been reported as molecular determinants of hERG channel inactivation. Furthermore, Jiang *et al* reported that dynamic conformational changes in the S5-P linker occur during channel gating, suggesting that this domain's mobility is critically important for hERG kinetics^[12].

It is currently still unclear why inactivation of hERG is much faster than C-type inactivation in other Kv channels. One explanation is that the previously mentioned tyrosine to phenylalanine substitution in the GYG pore motif may explain this isoform specific kinetics. This hypothesis comes from two experimental results: that mutation of the selectivity filter tyrosine to a phenylalanine (Y445F) in Shaker channels results in a channel with accelerated C-type inactivation and that members of the inward rectifier K⁺ channel family, Kir6.x, contain a GFG selectivity filter and also undergo a rapid gating process that is analogous to C-type inactivation^[6].

hERG and LQTS

hERG and congenital long QT syndrome

So far, at least 13 genes have been associated with congenital LQTS^[13], including KCNQ1(LQT1), hERG(LQT2), SCN5A(LQT3), ANK2(LQT4), KCNE1(LQT5), KCNE2(LQT6), KCNJ2(LQT7), CACNA1C(LQT8), CAV3(LQT9), SCN4B(LQT10), AKAP9(LQT11), SNTA1(LQT12), and GIRK(LQT13)^[13,14]. Among these, hERG was the first reported and is the most prevalent. To date, nearly 300 different hERG mutations linked to LQT2 have been identified. Such mutations may cause loss of hERG function by one of four main effects: reduced or defective synthesis; defective trafficking from the endoplasmic reticulum (ER) to the plasma membrane (resulting in decreased surface expression); defective gating; or defective ion permeation^[5].

hERG trafficking rapidly became a focus of interest for two reasons: (1) most hERG mutations cause trafficking defects, and (2) these trafficking defective mutants can be restored by high-affinity hERG channel-blocking drugs, which then give rise to a functional I_{Kr} current^[15,16]. Inhibitors of hERG act as molecular chaperones to rescue transport defective mutants^[16]. However, the molecular mechanism by which these small molecules function as hERG chaperones is still largely unclear, with only a single report in 2005 linking E-4031 rescue of the N470D mutant to interactions with calnexin^[17]. However, the mechanism of rescue by hERG blockers is likely heterogeneous, as evidenced by the fact that molecules such as E-4031, astemizole, and cisapride are able to restore trafficking of mutants N470D and G601S but not mutations in the C-terminal such as R752W, F805C, and R823W^[17]. Based on this evidence, Elizabeth S Kaufman suggests that, although restoration of intracellular processing and transport is theoretically an attractive therapeutic strategy, most LQTS patients

are heterozygous, and thus pharmacologic interventions that enhance the production and function of the healthy wild-type gene product may be more feasible^[16].

hERG and acquired long QT syndrome

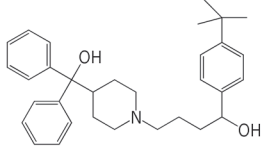
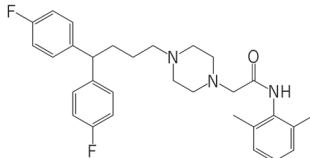
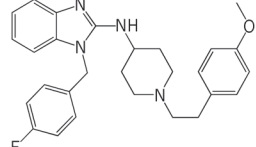
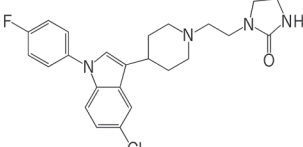
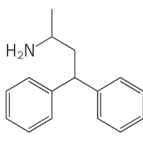
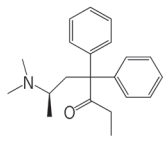
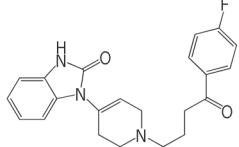
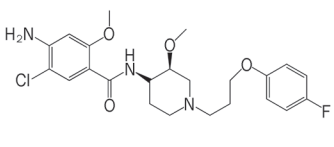
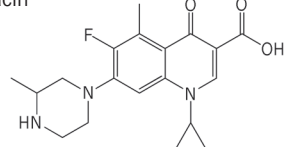
Unlike congenital LQTS, which may result from defects in numerous genes, almost all cases of pharmacologically induced LQTS (acquired long QT syndrome: aLQTS) have been linked to chemical blockade of the hERG channel. There is a recent paper reporting that single-nucleotide polymorphisms in other proteins that interact with hERG may be inhibited by small molecules, and thus also cause a LQTS^[18]. Indeed, it is thought that hERG is a promiscuous target that binds structurally diverse small molecules.

Until now, aLQTS has resulted in many drugs being removed from the market or terminated during clinical development. Examples include several non-cardiac drugs that have been withdrawn or given strict limitation for use, including terfenadine, lidoflazine, astemizole, sertindole, levomethadyl, droperidol, cisapride and grepafloxacin (Table 1)^[19]. Thus, potential blockade of cardiac I_{Kr} becomes a necessary pre-clinical assessment for candidate drugs. Structural determinants for this chemical blockade include a tyrosine at position 652 and a phenylalanine at 656^[5]. Alanine scanning mutagenesis has demonstrated that these two residues dictate the high-affinity binding of many drugs that inhibit hERG. However, the docking mode of different drugs is not the same, and computational modeling suggests that many drugs may utilize diverse binding conformations, coordinating multiple residues both within and between the subunits of the channel. Thus, the complex interactions between drugs and hERG complicate *in silico* predictions of the hERG inhibition by novel therapeutic compounds.

hERG activators

As mentioned above, hERG mutations cause congenital LQTS and a wide variety of drugs of different classes and structures bind to hERG, leading to aLQTS. However, hERG defects have also been linked to other diseases such as stress-mediated arrhythmias, diabetes and myocardial ischemia induced arrhythmias^[20]. Physiologically potentiating hERG would accelerate action potential repolarization and shorten the duration of the action potential. hERG channel activators can enhance channel function by accelerating myocardial repolarization, an effect that has been demonstrated by animal experiments, and they are considered potential therapeutics for LQTS. Indeed, hERG activators may become a novel class of antiarrhythmics, as reports have suggested that such compounds can reduce electrical heterogeneity in the myocardium and thereby the possibility of re-entry^[20,21]. However, due to the limitations of existing high throughput screening methods and difficulties in assaying the channel on a large scale, few activators have been reported. Most of the existing activators originated from combinatorial chemistry libraries, including RPR260243^[22-24], PD-118057^[25], PD-307243^[26], NS1643^[27], NS3623^[28], A-935142^[29], ICA-105574^[30], and KB130015^[31]. Addi-

Table 1. Summary of nine non-cardiac drugs withdrawn for hERG toxicity.

Terfenadine		Lidoflazine		Astemizole	
Sertindole		Grepafloxacin		Levomethadyl	
Droperidol		Cisapride		Grepafloxacin	

tionally, a natural product, mallotoxin, has also been shown to activate hERG^[32]. Below, we review the literature on individual compounds.

RPR260243

RPR260243 [(3*R*,4*R*)-4-[3-(6-methoxy-quinolin-4-yl)-3-oxo-propyl]-1-[3-(2,3,5-trifluoro-phenyl)-prop-2-yn-1-yl]-piperidine-3-carboxylic acid] was the first reported hERG channel activator. RPR260243 dramatically slows current deactivation in patch-clamp experiments, and its effect is temperature and voltage dependent. Though it is a weak inhibitor of the L-type Ca²⁺ channel, RPR260243 has no significant effects on the human cardiac Na⁺ channel or the KCNQ1/KCNE1 cardiac K⁺ channel, which are also linked with LQTS, thus showing high selectivity for hERG^[22]. Interestingly, RPR260243 inhibits the erg3 channel, which is in the same family as hERG, and a single S5 residue may account for this difference in pharmacology (Thr556 in hERG, Ile558 in rERG3). A Thr in this position favors agonist activity, whereas an Ile reveals a secondary blocking effect of RPR260243^[23]. Additionally, RPR260243 enhances the delayed rectifier current in guinea pig myocytes and can, to some extent, reverse dofetilide-induced prolongation of action potential. Physiologically, it has been reported that RPR260243 can increase the T-wave amplitude, prolong the PR interval and shorten the QT interval in guinea pig hearts^[22].

PD-118057

PD-118057 [2-(4-[2-(3,4-dichloro-phenyl)-ethyl]-phenylamino)-benzoic acid] was first reported by Zhou and colleagues^[25]. It primarily enhances the peak amplitude of the hERG tail current in a dose-dependent manner. PD-118057 shows no major effect on I_{Na} , I_{Ca} , I_{K1} or I_{Ks} , and it shortens the action potential duration and QT interval in arterially perfused rabbit ven-

tricular wedge preparations and prevents QT prolongation by dofetilide. Mechanistically, Zhou *et al* reported that the compound did not affect the voltage dependence or kinetics of gating, nor did its activity require the open conformation of the channel. Later results by Sanguinetti and colleagues suggest that PD-118057 activates the hERG channel mainly by attenuating inactivation^[33]. They also found that 10 μmol/L PD-118057 shifted the half-point of hERG channel inactivation by +19 mV, increased peak outward current amplitude by 136%, and enhanced K⁺ conductance.

PD-307243

PD-307243 [2-[2-(3,4-dichloro-phenyl)-2,3-dihydro-1*H*-isoindolin-5-ylamino]-nicotinic acid] significantly enhances hERG currents by slowing channel deactivation and inactivation. At potentials from -120 to -40 mV, PD-307243 induces instantaneous hERG current with little decay. When the membrane potential is higher than -40 mV, PD-307243 induces an I_{to} -like upstroke of hERG current. This I_{to} -like current may result from slowed channel inactivation and deactivation, and this effect can be only observed once the channel is in the open state, which may also explain the compound's use dependence. Additionally, hERG reversal potential was not altered in the presence of 3 μmol/L PD-307243, suggesting that the compound does not affect the selectivity filter of the channel^[26].

NS1643

Casis and colleagues (2006) reported that NS1643 [1,3-bis-(2-hydroxy-5-trifluoromethyl-phenyl)-urea] activates hERG channels expressed in *Xenopus* oocytes in a concentration- and voltage-dependent manner^[27]. At a depolarization voltage of -10 mV, the compound's EC₅₀ value is 10.4 μmol/L. While NS1643 strongly affects channel inactivation by right

shifting the voltage-inactivation curve by +21 mV at 10 $\mu\text{mol/L}$ and +35 mV at 30 $\mu\text{mol/L}$, it has no effect on the activation of the channel. In the absence of inactivation, NS1643 does not enhance outward current magnitude^[27]. However, Xu *et al* (2008) reported that NS1643 can also left-shift the voltage-dependent activation curve^[34]. In guinea pig cardiac myocytes, 10 $\mu\text{mol/L}$ NS1643 can activate I_{Kr} and significantly shorten the action potential duration^[27].

NS3623

NS3623 [N-(4-bromo-2-(1H-tetrazol-5-yl)phenyl)-N'-(3-trifluoromethyl-phenyl)urea], originally identified as a chloride channel blocker^[35], activates hERG channels expressed in *Xenopus* oocytes, with an EC_{50} value of 79.4 $\mu\text{mol/L}$ ^[28]. NS3623 mainly affects the voltage dependence of channel inactivation by right-shifting the half point of inactivation by +17.7 mV. NS3623 also slows channel inactivation. Similar to results found using NS1643, inactivation defective mutants S620T and S631A are not sensitive to NS3623, supporting the conclusion that these two compounds have similar mechanisms of action on hERG^[28].

A-935142

A-935142 [4-[4-(5-trifluoromethyl-1H-pyrazol-3-yl)-phenyl]-cyclohexyl]-acetic acid] was reported in 2009 as a hERG channel activator that enhances the amplitude of step and tail current in a concentration- and voltage-dependent manner. Current-voltage curves in the presence of 60 $\mu\text{mol/L}$ A-935142 suggest that the compound enhances both the outward and the inward K^+ currents. Unlike previously reported activators, A-935142 simultaneously affects channel activation, deactivation and inactivation. Specifically, 60 $\mu\text{mol/L}$ of A-935142 significantly accelerates the activation time constant of hERG channels from 164 ± 24 ms to 100 ± 17 ms and left-shifts the voltage-dependence of activation. A-935142 also reduces the rate of inactivation, right-shifts the voltage-dependence of inactivation, and slows hERG channel deactivation at voltage potentials from -120 to -70 mV^[29].

ICA-105574

Gerlach and colleagues recently described a compound, ICA-105574 [3-nitro-N-(4-phenoxyphenyl) benzamide], that activates hERG channels, mainly by affecting channel inactivation, with a magnitude much larger than that of previously reported activators. Two micromolar ICA-105574 shifts the mid-point of the voltage-dependent inactivation by >180 mV from -86 mV to +96 mV. Consistent with this observation, 2 $\mu\text{mol/L}$ ICA-105574 potentiates outward current amplitude ten fold, with an EC_{50} of 0.5 ± 0.1 $\mu\text{mol/L}$. In addition to effects on channel inactivation, high concentrations of the compound (3 $\mu\text{mol/L}$) can also left-shift the voltage dependence of channel activation by -11 mV and slow channel deactivation 2-fold. Finally, ICA-105574 induces a concentration-dependent shortening of action potential duration (>70% at 3 $\mu\text{mol/L}$) in isolated guinea pig ventricular cardiac myocytes. This effect can be prevented by hERG inhibitor E-4031, supporting the

conclusion that ICA-105574 increases hERG channel function through direct action on the protein^[30].

KB130015

KB130015 [(2-methyl-3-(3,5-diiodo-4-carboxymethoxybenzyl) benzofuran)] is a derivative of amiodarone, a potent hERG blocker^[36]. Because of the similarity, Gessner *et al* assumed KB130015 inhibited hERG^[31]. Unexpectedly, they found that, while KB130015 does inhibit native and recombinant hERG at high voltages, it can activate both forms of the channel at low voltages. KB130015 accelerates activation by 4-fold and left-shifts the voltage-dependent activation curve by -16 mV, with an EC_{50} value of 12 $\mu\text{mol/L}$. Based on its similarity to amiodarone, KB130015 presumably binds to the hERG pore from the cytosolic side and functionally competes with blockade by amiodarone and other canonical inhibitors at this site^[31].

Mallotoxin

Mallotoxin (MTX) [1-(6-(3-acetyl-2,4,6-trihydroxy-5-methylbenzyl)-7-hydroxy-2,2-dimethyl-2H-chromen-8-yl)-3-phenylprop-2-en-1-one], an extract of the tree *Mallotus philippinensis*, is the only natural product reported to activate hERG. It was previously shown to inhibit protein kinase C (PKC), Ca^{2+} /calmodulin-dependent protein kinase II and III, and elongation factor-2 kinase. Zeng *et al* (2006) discovered that MTX can enhance both step and tail hERG current, with EC_{50} values of 0.34 and 0.52 $\mu\text{mol/L}$, respectively^[32]. The potency of MTX is at least ten fold higher than previously reported hERG activators, including PD-118057, NS1643, and RPR260243. Furthermore, the mechanism by which MTX potentiates hERG is unique in comparison to these synthetic molecules. It mainly affects channel activation (left-shifting the activation curve by +24 mV at 2.5 $\mu\text{mol/L}$ MTX) and deactivation without modulating inactivation. Using pre-recorded cardiac action potentials, 2.5 $\mu\text{mol/L}$ MTX increases the total number of potassium ions passed through hERG channels by ~5-fold^[32].

Binding site of small-molecule hERG activators

Understanding the binding site of agonists is helpful for investigating channel conformation and gating, particularly for rational drug design. However, the exact molecular determinants of hERG activator function remain unresolved, with most of the knowledge about possible binding sites derived from mutagenesis experiments.

Sangunetii *et al* found that two groups of residues have different effects on RPR260243^[24, 37]. One group, including L553, F557 (S5), and N658, V659 (S6), affects the inactivation and deactivation effect of RPR260243 on the hERG channel, while mutations in the other group of residues, including V549, L550 (S4-S5 linker), and I662, L666, Y667 (intracellular S6 segment), only hinder the transition to the closed state of the channel. In another study by Sangunetii *et al* about possible binding sites of PD-118057^[33], they focused on the S5-P-S6 domain. Through alanine scanning mutagenesis of this region, four mutants (F619A, L622C, I639A, and L646A) were identified that display the lowest agonist activity in all tested mutants. Molecular

simulations suggested that PD-118057 interacted with F619 in the pore domain of one subunit and L646 (S6) of an adjacent subunit, which together form a hydrophobic binding pocket, reducing channel inactivation and increasing channel open possibility.

Limited binding site information about PD-307243 and NS1643 was reported by Xu and Tseng in 2008^[34]. Because both compounds act on the extracellular side of the channel and significantly slow channel inactivation, the authors speculated that these compounds may act on the pore domain. Perturbation of the conformation of the outer vestibule/external pore entrance (by cysteine substitution at high-impact positions or cysteine side chain modification at intermediate-impact positions) prevented the activation effect of NS1643 but not that of PD-307243, suggesting that NS1643 may bind to this domain. Further pharmacological experiments showed that the effects of PD-307243 could be abolished by TPpA⁺ and dofetilide (both hERG inhibitors that block the pore), which supports the conclusion that PD-307243 may be a “pore-modifier” (Table 2)^[34].

Outlook and challenges

LQTS is responsible for many sudden deaths before age 20. Current treatments for LQTS include beta-adrenergic receptor blockers, left cardiac sympathetic denervation or, in the worst cases, implantation of cardiac defibrillators^[24, 38]. However, pharmacologic treatment is not always effective, and both surgery and implanted devices are expensive and require invasive procedures^[24, 39]. Acute episodes of drug-induced LQTS are treated with magnesium sulfate administration and discontinued use of the suspect medication. Activation of hERG could provide an alternative and more specific treatment for acquired or congenital LQTS. In addition, hERG activators may become a novel class of antiarrhythmics because, as mentioned above, they can reduce electrical heterogeneity in the myocardium and, thereby, the possibility of re-entry^[20, 21]. However, this idea has yet to be confirmed clinically. A recent report in PubChem described a co-drug screen aiming to protect against the development of aLQTS by a high-throughput method (AID: 1680). Compounds that exhibit such activity would be expected to include neutral antagonists that bind to the same site as hERG blockers but do not favor the “blocked conformation” of the pore. Alternatively, these compounds may be hERG agonists that competitively bind to the same site as hERG inhibitors or compounds that prevent the access of a hERG inhibitor to its cognate binding site at the intracellular aspect of the pore region. Although it remains to be verified whether these compounds would be effective, this strategy does provide a new idea for the treatment of aLQTS.

The structural and mechanistic heterogeneity of the currently reported hERG activators suggests that hERG channels may have different agonist binding sites, a phenomenon that has been observed in voltage-gated KCNQ channel activators. However, so far, studies on the binding site by hERG agonists are still descriptive, mostly relying on inference from mutagenesis data for RPR260243 and PD118057. However,

activation of hERG by small molecules may be a double-edged sword from a clinical perspective because excessive potentiation may chemically induce short QT syndrome^[40]. Moreover, there are no reports from animal models or human clinical data about drug-induced short QT syndrome, indicating that the safety of hERG agonists remains to be tested.

Acknowledgements

This work was supported by National Natural Science Foundation of China grant 81072579 and open funds of State Key Laboratory of Robotics RLO201013.

We thank Dr Guo-yuan HU for valuable discussions and comments on the manuscript.

References

- 1 Warmke JW, Ganetzky B. A family of potassium channel genes related to eag in *Drosophila* and mammals. *Proc Natl Acad Sci U S A* 1994; 91: 3438–42.
- 2 Sanguinetti MC, Jiang C, Curran ME, Keating MT. A mechanistic link between an inherited and an acquired cardiac arrhythmia: HERG encodes the I_{Kr} potassium channel. *Cell* 1995; 81: 299–307.
- 3 Shen XZ, Wu J, Lin JJ. HERG and arrhythmia. *Adv Cardiovasc Dis* 2008; 29: 436–40.
- 4 Lagrutta AA, Trepakova ES, Salata JJ. The hERG channel and risk of drug-acquired cardiac arrhythmia: an overview. *Curr Top Med Chem* 2008; 8: 1102–12.
- 5 Perrin MJ, Subbiah RN, Vandenberg JI, Hill AP. Human ether-a-go-go related gene (hERG) K⁺ channels: function and dysfunction. *Prog Biophys Mol Biol* 2008; 98: 137–48.
- 6 Vandenberg JI, Torres AM, Campbell TJ, Kuchel PW. The hERG K⁺ channel: progress in understanding the molecular basis of its unusual gating kinetics. *Eur Biophys J* 2004; 33: 89–97.
- 7 Piper DR, Sanguinetti MC, Tristani-Firouzi M. Voltage sensor movement in the hERG K⁺ channel. *Novartis Found Symp* 2005; 266: 46–52.
- 8 Smith PL, Yellen G. Fast and slow voltage sensor movements in hERG potassium channels. *J Gen Physiol* 2002; 119: 275–93.
- 9 Subbiah RN, Kondo M, Campbell TJ, Vandenberg JI. Tryptophan scanning mutagenesis of the hERG K⁺ channel: the S4 domain is loosely packed and likely to be lipid exposed. *J Physiol* 2005; 569: 367–79.
- 10 Baukrowitz T, Yellen G. Modulation of K⁺ current by frequency and external [K⁺]: a tale of two inactivation mechanisms. *Neuron* 1995; 15: 951–60.
- 11 Smith PL, Baukrowitz T, Yellen G. The inward rectification mechanism of the hERG cardiac potassium channel. *Nature* 1996; 379: 833–6.
- 12 Jiang M, Zhang M, Maslennikov IV, Liu J, Wu DM, Korolkova YV, et al. Dynamic conformational changes of extracellular S5-P linkers in the hERG channel. *J Physiol* 2005; 569: 75–89.
- 13 Hedley PL, Jørgensen P, Schlamowitz S, Wangari R, Moolman-Smook J, Brink PA, et al. The genetic basis of long QT and short QT syndromes: a mutation update. *Hum Mutat* 2009; 30: 1486–511.
- 14 Roden DM, Lazzara R, Rosen M, Schwartz PJ, Towbin J, Vincent GM. Multiple mechanisms in the long-QT syndrome. Current knowledge, gaps, and future directions. The SADS Foundation Task Force on LQTS. *Circulation* 1996; 94: 1996–2012.
- 15 Charpentier F, Merot J, Loussouarn G, Baro I. Delayed rectifier K⁺ currents and cardiac repolarization. *J Mol Cell Cardiol* 2010; 48: 37–44.

Table 2. Summary of 8 HERG K⁺ channels activators.

Compound name	Structure	Mechanism of action	Binding site	Selectivity on channels	Refs
RPR260243		Slows deactivation	Interacts with residues in the S4–S5 linker or cytoplasmic ends of the S5 and S6 domains	No effect on human cardiac Na ⁺ channel, KCNQ1/KCNE1 channels, weakly inhibits L-type Ca ²⁺ channels, inhibits erg3 channel	[22–24]
PD-118057		Attenuates inactivation	Contacts the pore helix of hERG channels to attenuates inactivation and enhances K ⁺ conductance	No effect on <i>I</i> _{Na} , <i>I</i> _{Ca, L} , <i>I</i> _{K1} , and <i>I</i> _{ks}	[25, 33]
PD-307243		Slows channel deactivation and inactivation	May works as a “pore-modifier” of the hERG channels	Activates <i>I</i> _{ks} and <i>I</i> _{Ca, L} ; no effect on <i>I</i> _{to} and Nav1.5	[26, 34]
NS1643		Attenuates inactivation	Binds to the outer vestibule/pore entrance of hERG	No report	[27, 34]
NS3623		Attenuates inactivation	No report	No effect on <i>I</i> _{Ks} , <i>I</i> _{Kur} , Kv4.3, <i>I</i> _{Ca, T} , <i>I</i> _{Na} , activates <i>I</i> _{Ca, L}	[28]
A-935142		Accelerates activation Attenuates inactivation and slow deactivation	No report	No report	[29]
ICA-10557		Mainly attenuates or remove channel inactivation, besides at high concentration it also accelerates activation and slows deactivation	No report	No report	[30]
KB130015		Accelerates activation	Presumably binds to pore domain from the cytosolic-side	No report	[31]
Mallotoxin (MTX)		Left-shifts the activation curve, and slows deactivation process	No report	No report	[32]

16 Kaufman ES, Ficker E. Is restoration of intracellular trafficking clinically feasible in the long QT syndrome? The example of HERG mutations. *J Cardiovasc Electrophysiol* 2003; 14: 320–2.

17 Gong Q, Jones MA, Zhou, Z. Mechanisms of pharmacological rescue

of trafficking-defective hERG mutant channels in human long QT syndrome. *J Biol Chem* 2006; 281: 4069–74.

18 Berger SI, Ma'ayan A, Iyengar R. Systems pharmacology of arrhythmias. *Sci Signal* 2010; 3: ra30.

- 19 Roden DM. Drug-induced prolongation of the QT interval. *N Engl J Med* 2004; 350: 1013–22.
- 20 Guan FY, Yang SJ. HERG K⁺ channel, the target of anti-arrhythmias drugs. *Yao Xue Xue Bao* 2007; 42: 687–91.
- 21 Wulff H, Castle NA, Pardo LA. Voltage-gated potassium channels as therapeutic targets. *Nat Rev Drug Discov* 2009; 8: 982–1001.
- 22 Kang J, Chen XL, Wang H, Ji J, Cheng H, Incardona J, *et al*. Discovery of a small molecule activator of the human ether-a-go-go-related gene (HERG) cardiac K⁺ channel. *Mol Pharmacol* 2005; 67: 827–36.
- 23 Perry M, Sanguinetti MC. A single amino acid difference between ether-a-go-go-related gene channel subtypes determines differential sensitivity to a small molecule activator. *Mol Pharmacol* 2008; 73: 1044–51.
- 24 Perry M, Sachse FB, Sanguinetti MC. Structural basis of action for a human ether-a-go-go-related gene 1 potassium channel activator. *Proc Natl Acad Sci U S A* 2007; 104: 13827–32.
- 25 Zhou J, Augelli-Szafran CE, Bradley JA, Chen X, Koci BJ, Volberg WA, *et al*. Novel potent human ether-a-go-go-related gene (hERG) potassium channel enhancers and their *in vitro* antiarrhythmic activity. *Mol Pharmacol* 2005; 68: 876–84.
- 26 Gordon E, Lozinskaya IM, Lin Z, Semus SF, Blaney FE, Willette RN, *et al*. 2-[2-(3,4-dichloro-phenyl)-2,3-dihydro-1*H*-isoindol-5-ylamino]-nicotinic acid (PD-307243) causes instantaneous current through human ether-a-go-go-related gene potassium channels. *Mol Pharmacol* 2008; 73: 639–51.
- 27 Casis O, Olesen SP, Sanguinetti MC. Mechanism of action of a novel human ether-a-go-go-related gene channel activator. *Mol Pharmacol* 2006; 69: 658–65.
- 28 Hansen RS, Diness TG, Christ T, Wettwer E, Ravens U, Olesen SP, *et al*. Biophysical characterization of the new human ether-a-go-go-related gene channel opener NS3623 [N-(4-bromo-2-(1*H*-tetrazol-5-yl)-phenyl)-*N'*-(3'-trifluoromethylphenyl)urea]. *Mol Pharmacol* 2006; 70: 1319–29.
- 29 Su Z, Limberis J, Souers A, Kym P, Mikhail A, Houseman K, *et al*. Electrophysiologic characterization of a novel hERG channel activator. *Biochem Pharmacol* 2009; 77: 1383–90.
- 30 Gerlach AC, Stoehr SJ, Castle NA. Pharmacological removal of human ether-a-go-go-related gene potassium channel inactivation by 3-nitro-N-(4-phenoxyphenyl) benzamide (ICA-105574). *Mol Pharmacol* 2010; 77: 58–68.
- 31 Gessner G, Macianskiene R, Starkus JG, Schonherr R, Heinemann SH. The amiodarone derivative KB130015 activates hERG1 potassium channels via a novel mechanism. *Eur J Pharmacol* 2010; 632: 52–9.
- 32 Zeng H, Lozinskaya IM, Lin Z, Willette RN, Brooks DP, Xu X, *et al*. Mallotoxin is a novel human ether-a-go-go-related gene (hERG) potassium channel activator. *J Pharmacol Exp Ther* 2006; 319: 957–62.
- 33 Perry M, Sachse FB, Abbruzzese J, Sanguinetti MC. PD-118057 contacts the pore helix of hERG1 channels to attenuate inactivation and enhance K⁺ conductance. *Proc Natl Acad Sci U S A* 2009; 106: 20075–80.
- 34 Xu X, Recanatini M, Roberti M, Tseng GN. Probing the binding sites and mechanisms of action of two human ether-a-go-go-related gene channel activators, 1,3-bis-(2-hydroxy-5-trifluoromethyl-phenyl)-urea (NS1643) and 2-[2-(3,4-dichloro-phenyl)-2,3-dihydro-1*H*-isoindol-5-ylamino]-nicotinic acid (PD307243). *Mol Pharmacol* 2008; 73: 1709–21.
- 35 Bennekou P, de Franceschi L, Pedersen O, Lian L, Asakura T, Evans G, *et al*. Treatment with NS3623, a novel Cl⁻ conductance blocker, ameliorates erythrocyte dehydration in transgenic SAD mice: a possible new therapeutic approach for sickle cell disease. *Blood* 2001; 97: 1451–7.
- 36 Ridley JM, Milnes JT, Witchel HJ, Hancox JC. High affinity HERG K⁺ channel blockade by the antiarrhythmic agent dronedarone: resistance to mutations of the S6 residues Y652 and F656. *Biochem Biophys Res Commun* 2004; 325: 883–91.
- 37 Perry M, Sanguinetti M, Mitcheson J. Revealing the structural basis of action of hERG potassium channel activators and blockers. *J Physiol* 2010; 588: 3157–67.
- 38 Schwartz PJ. The congenital long QT syndromes from genotype to phenotype: clinical implications. *J Intern Med* 2006; 259: 39–47.
- 39 Gow RM. Effectiveness and limitations of beta-blocker therapy in congenital long-QT syndrome. *Circulation* 2001; 103: E24.
- 40 Bjerregaard P, Jahangir A, Gussak I. Targeted therapy for short QT syndrome. *Expert Opin Ther Targets* 2006; 10: 393–400.

Review

Role of the epithelial sodium channel in salt-sensitive hypertension

Yan SUN¹, Jia-ning ZHANG², Dan ZHAO², Qiu-shi WANG², Yu-chun GU³, He-ping MA⁴, Zhi-ren ZHANG^{2,*}

¹Department of General Surgery, the 2nd Affiliated Hospital, Harbin Medical University, Harbin 150086, China; ²Departments of Clinical Pharmacy and Cardiology, the 2nd Affiliated Hospital, Key Laboratories of Education Ministry for Myocardial Ischemia Mechanism and Treatment, Harbin Medical University, Harbin 150086, China; ³Molecular Pharmacology, IMM, Peking University, Beijing 100871, China; ⁴Department of Physiology, Emory University, USA

The epithelial sodium channel (ENaC) is a heteromeric channel composed of three similar but distinct subunits, α , β and γ . This channel is an end-effector in the rennin-angiotensin-aldosterone system and resides in the apical plasma membrane of the renal cortical collecting ducts, where reabsorption of Na^+ through ENaC is the final renal adjustment step for Na^+ balance. Because of its regulation and function, the ENaC plays a critical role in modulating the homeostasis of Na^+ and thus chronic blood pressure. The development of most forms of hypertension requires an increase in Na^+ and water retention. The role of ENaC in developing high blood pressure is exemplified in the gain-of-function mutations in ENaC that cause Liddle's syndrome, a severe but rare form of inheritable hypertension. The evidence obtained from studies using animal models and in human patients indicates that improper Na^+ retention by the kidney elevates blood pressure and induces salt-sensitive hypertension.

Keywords: epithelial sodium channel; salt-sensitive hypertension; high-salt intake; oxidative stress; sympathetic nervous system

Acta Pharmacologica Sinica (2011) 32: 789–797; doi: 10.1038/aps.2011.72; published online 30 May 2011

Introduction

Several studies have classified humans who are suffering from hypertension as salt-sensitive or salt-resistant based upon blood pressure (BP) responses to differences in sodium balance^[1, 2]. The increment in BP that is driven by a salt load is characteristic of salt-sensitive hypertension, a condition affecting more than two thirds of individuals with essential hypertension who are older than 60 years^[3]. Salt-sensitive hypertension may exacerbate mortality rates and worsen the manifestations of target organ damage^[1, 2]. The discovery of mutations in the β - and γ -subunits of epithelial sodium channel (ENaC) to understand Liddle's syndrome^[4, 5], a severe form of low-renin hypertension^[6], was followed by a search for common genetic variants in ENaC subunits. Several variants were identified^[7]. Interestingly, these variants were almost universally more common in black individuals, which correlate nicely with higher prevalence of low-renin, salt-sensitive hypertension in black individuals. The questions and issues addressed in the current review are whether ENaC that resides

in the renal distal nephron plays a role in the development of hypertension, particularly in salt-sensitive hypertension, how ENaC variants segregate with high BP, and whether high-salt intake induces oxidative stress and whether oxidative stress could activate ENaC, resulting in over reabsorption of Na^+ . We also briefly discuss the role of ENaC expressed in vascular endothelia and the central nervous system in the development of hypertension.

The topology and physiology of ENaC

Since 1994, when ENaC was initially cloned from the rat colon^[8], the biophysical properties and molecular structure of ENaC have been extensively studied. ENaC consists of at least three subunits including α , β , and γ , each of which possesses two transmembrane domains, a large extracellular loop, a cytoplasmic C-terminal domain and a N-terminal domain. All three subunits are required to form a functional α -, β -, γ -ENaC channel complex (Figure 1)^[8–15]. ENaC belongs to a member of the ENaC/Deg superfamily of ion channels that are responsible for sodium transport. The channel is typically located at the apical membrane of epithelial tissues throughout the body, including the colon, the sweat glands, the salivary duct, the airway, and the cortical collecting duct (CCD) of the kidney,

* To whom correspondence should be addressed.

E-mail zhirenz@yahoo.com

Received 2011-03-16 Accepted 2011-04-25

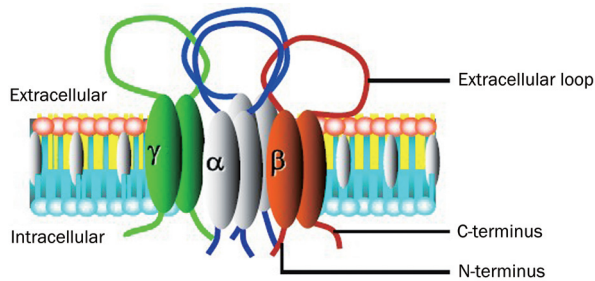


Figure 1. The topology of ENaC. ENaC consists of at least three subunits including α , β , and γ subunits, each of which possesses two transmembrane domains, a large extracellular loop, a cytoplasmic C-terminal domain and an N-terminal domain.

and this channel regulates sodium transport in tissues^[16–20]. Recent studies have shown that ENaC subunits are also present in the endothelial cells of the artery and may function as a vascular mechanosensor^[21–23].

ENaC α , β , and γ subunits share approximately 30% homology at the amino acid level, and each subunit corresponds to a molecular mass of 70–85 kDa. The three ENaC subunits are inserted into the plasma membrane with a proposed stoichiometry of 2:1:1^[24] or 3:3:3^[25, 26]. The α -subunit is critical to the formation of the ion permeating pore, whereas the β and γ subunits are required for the maximal channel activity and may play regulatory role. While α -ENaC is knocked out in mice, the mice would die within 40 h of birth because failure of pulmonary fluid clearance. This result clearly demonstrates the pivotal role of α -ENaC in forming a functional Na^+ channel complex *in vivo*^[27]. Moreover, decreased α -ENaC expression in mice causes a respiratory distress syndrome, whereas the β and γ have only a modest effect on pulmonary fluid clearance^[28]. The α -, β -, γ -ENaC channel complex is highly selective for Na^+ and mediates Na^+ entry through the apical membrane of distal renal epithelial cells with a slope single-channel conductance of approximately 5 pS. ENaC accounts for a small proportion of distal renal sodium reabsorption (<5%). However, there appears to be no further downstream sodium transport system beyond CCD, which places ENaC in a very critical position for the regulation (or homeostasis) of the extracellular fluid volume, electrolyte balance and long term BP^[7]. The factors such as high-salt intake that affect ENaC activity and the ENaC expression level at the apical membrane of CCD may constitute the critical role of ENaC in Na^+ over reabsorption and water retention.

The experiments assessed in animal models reveal the role of ENaC in developing salt-sensitive hypertension

The strains of rats were bred by Dr Lewis K Dahl for sensitivity or resistance to the hypertensive effect of a high-salt diet in the 1960s and were named Dahl salt-sensitive (DS) or Dahl salt-resistance (DR)^[29, 30]. When DS rats were placed on a high-salt (8% NaCl) diet at 21–23 d of age, they rapidly developed hypertension. All of the DS rats died by the 16th week of salt feeding. With similarly treated DR rats, the BP

remained in the normotensive range, and 80% of animals survived to the 48th week on a high-salt diet^[30]. Since then the kidney has been the focus of considerable attention in DS and DR rats because of the results obtained from the renal cross-transplantation assays, which involve the transplantation of a kidney from a DS rat into a DR rat that had the original kidneys removed, the results suggest that the DR rats develop a higher BP than DR rats with transplanted DR kidneys or DR rats with a unilateral nephrectomy. Conversely, a DR kidney that was transplanted into a DS rat ameliorated the increase in the BP that was seen in DR rats with transplanted DS kidneys or DS rats with a unilateral nephrectomy^[31–33]. Later studies revealed that the plasma renin and aldosterone concentrations were normal or lower in DS rats compared with that in control rats^[34, 35]. Aoi *et al* investigated the mechanisms by which quercetin, a plant extract, exerted an anti-hypertensive effect, and they found that quercetin diminished the α ENaC mRNA expression in the kidney, which was associated with the reduction of the systolic BP that was elevated by a high-salt diet in DS rats. These results suggest a role for ENaC in salt-sensitive hypertension^[36]. The same group attempted to determine whether a high-salt diet in DR rats stimulated the expression level of ENaC. These investigators divided the DS and DR rats into several salt diet groups as follows: DS and DR rats that were fed with a low-sodium diet (0.005% NaCl), a normal-sodium diet (0.3% NaCl), or a high-sodium diet (8% NaCl). Four weeks after the high-salt diet in DS rats, an increase in the systolic BP was observed. However, the BP was not altered in any of the other groups. Subsequently, these investigators examined the expression level of α -ENaC mRNA and serum and glucocorticoid-regulated kinase 1 (SGK1) mRNA. They found that the expression level of α -, β -, γ -ENaC, and the SGK1 mRNAs was significantly enhanced by the high-sodium diet in DS rats. Interestingly, the expression of SGK1 mRNA was down-regulated in DR rats that were fed a high sodium diet. These observations suggest that the expression of ENaC and SGK1 mRNAs is abnormally regulated by the dietary sodium in salt-sensitively hypertensive rats and that this abnormal expression may be a factor that causes salt-sensitive hypertension^[37]. Convincing evidence indicates that the aldosterone activated mineralocorticoid receptor increases SGK1 gene transcription in the CCD, and consequently, SGK1 strongly stimulates the activity and expression of the ENaC and renal Na^+/H^+ exchanger (NHE)^[38–43]. High-salt intake may up-regulate both ENaC and SGK1 in DS rats. However, functional studies that examine ENaC activity are required to evaluate the role of ENaC and SGK1 in salt-sensitive hypertension in DS rats and the mechanisms by which the high-salt intake regulates ENaC and SGK1.

Fenton and co-authors found that none of the ENaC subunits was increased in abundance in the inner medullas of DS rats compared with that of DR rats^[44]. In fact, the α -subunit was strongly down regulated, which may be a consequence of the marked increase in 11 β -HSD2 expression in the cells of the inner medulla. Consistent with this view, the protein abundance of α -ENaC was markedly elevated following the

carbenoxolone-induced inhibition of the 11β -HSD2 activity. These investigators also examined whether the ENaC subunits may be upregulated by a high-salt diet in DS rats. However, Husted and co-workers showed that the ENaC activity is doubled in the IMCD cells of DS rats *versus* in that of DR rats^[40, 45]. The reasons for this variability in ENaC activity and/or expression level in DS *versus* DR rats are poorly understood at the present time. Shehata and co-workers examined the complete coding sequences of three ENaC subunits and showed that there were no genetic differences within the 5' and 3' flanking regions in DS *vs* DR rats^[46]. The alternative splicing of α -ENaC may regulate α -ENaC by formation of coding RNA species (α -ENaC-a and -b) and non-coding RNA species (α -ENaC-c and -d). The α -ENaC-a and -b mRNA levels are significantly higher in DR *versus* DS rats. After 4 weeks of the high-salt intake, the level of α -ENaC-b was dramatically elevated compared to that in DR rats fed a normal-salt diet. These results suggest that α -ENaC-b is a salt-sensitive transcript. Furthermore, among the four α -ENaC transcripts (-a, -b, -c, and -d), α -ENaC-b is a predominant transcript that exceeds α -ENaC-wt abundance by approximately 32 fold. α -ENaC-b may potentially act as a dominant negative protein for ENaC activity and rescue DR rats from developing salt-sensitive hypertension on a high-salt diet^[47].

The molecular variations in ENaC and the risk for developing hypertension in humans

The search for common genetic variants in ENaC subunits that affect the susceptibility in less rare forms of hypertension took place soon after the discovery of mutations in α -, β -, and γ -ENaC that cause Liddle's syndrome (Table 1). The first variant that was associated with hypertension was T594M in the C-terminus of β -ENaC in black individuals. This variant was found in approximately 8% of hypertensive individuals, whereas the variant was detected in only approximately 2% of normotensive individuals^[48]. In another study, seven variants in β -ENaC, including G589S, T594M, R597H, R624C, E632G (last exon), G442V, and V434M (exon 8) were identified and almost found in black individuals^[49]. The functional properties of the variants were evaluated in *Xenopus* oocytes expressing these mutants. Interestingly, small but not significant differences were detected between the variants and wild-type ENaC. The clinical evaluation of the family bearing the G589S variant, which provided the highest relative ENaC activity, did not show any cosegregation between the mutation and hypertension^[49]. However, the lack of a significant increase in the Na^+ current that was observed in *Xenopus* oocytes that overexpressed these variants cannot completely rule out any functional impact of the ENaC mutants in developing hypertension^[49]. One possibility to explain why the association studies of ENaC variants are often inconclusive is that many factors influence the ENaC activity. Therefore, a variant that affects ENaC function *in vitro* may not necessarily cause Na^+ retention, unless at the same time, the regulatory factors do not adjust accordingly. The variants identified in the β - and γ -subunits of ENaC were almost exclusively identified

in individuals of African origin. However, the physiological significance of the β - and γ -subunit polymorphisms may partially explain the high incidence of salt-sensitive hypertension in African Americans. Among the black hypertensive population, approximately 75% is salt-sensitive, characterized by a BP increase after dietary salt intake^[2].

To determine whether SCNN1B or SCNN1G, which encode β and γ subunits, respectively, were present in a patient who was clinically suspected to have Liddle's syndrome with no familial history of hypertension, Wang and coworkers identified a mutation causing Liddle's syndrome. They demonstrated that a frameshift mutation of the γ subunit resulted in a new termination site at the 585 codon of the γ subunit and the deletion of its PY motif. Moreover, the parents of the patient, the other 50 randomly selected hypertensive patients, and 50 controls did not have the mutation that causes Liddle's syndrome. These results suggest that this frameshift mutation is a *de novo* mutation and not a common genetic variant^[50].

Several α -ENaC variants at the residues 334, 618 and 663 are possibly associated with the abnormal Na^+ handling by the kidney and the salt-sensitive hypertension that is prevalent in black populations^[51-54]. Several groups have studied whether these variants segregate with BP, and the outcomes are controversial^[51, 53]. Ambrosius and coworkers reported that the allele of T663A was twice as common in whites and that T663A was associated with being normotensive in black and white populations^[51]. The expression of T663A did not alter the basal Na^+ current^[51]. Kleyman's group used *Xenopus* oocytes expressing a mouse/human chimera (m(1-678)/h(650-669)/T663A), which was generated by the replacement of the distal C terminus of the mouse α -subunit with the distal C terminus of the human α -subunit, and determined that the human α T663 $\beta\gamma$ ENaC has increased activity in *Xenopus* oocytes when compared with human α T663A $\beta\gamma$ ENaC. The increase in the channel activity in human α T663 $\beta\gamma$ reflected an increase in surface expression^[55]. Stockand's group has reported that the polymorphic C618F and A663T ENaCs had greater activity compared with the wild-type channels in the excised patches with activity of channels increased 3.8- and 2.6-fold, respectively^[56]. This increase in the channel activity is associated with an increase in the surface expression of the polymorphisms. The results obtained by these studies are consistent with the C618F and A663T polymorphisms leading to an elevated ENaC activity with the possibility that these polymorphisms facilitate the altered Na^+ handling by the kidney^[55, 56]. Iwai *et al* reported that a polymorphism in the promoter region of the α -ENaC gene G2139A is associated with BP status and that the G2139 allele significantly increased the risk of hypertension in the general Japanese population^[57].

Does oxidative stress induced by high-salt intake activate ENaC?

ENaC activity depends upon the number of channels in the apical membrane, the permeation properties, and the open probability of the channel (P_o). One of the best examples is the salt-sensitive hypertension of Liddle's syndrome, in which

Table 1. Genetic variants of ENaC and risk for hypertension.

Genetic variation	Genetic variant location	Genetic variant frequency	Mutant gene function/ENaC activity	Risk for hypertension	Ref
G589S	Exon 12 of β -ENaC	1/475 W hypertension 8/347 hypertension, 2/175 normotension	↑ NS	NS OR=2.4	[49] [106]
i12-17CT	Intron 12 of β -ENaC	16/347 hypertension, 2/175 normotension	-	OR=4.6	[106]
T594M	Exon 12 of β -ENaC	3/50 B hypertension 17/206 hypertension, 3/142 normotension 7/126 B hypertension, 7/105 B normotension; 0/192 W hypertension	NS - NS	NS OR=4.17 NS	[49] [48] [107]
R597H	Exon 12 of β -ENaC	1/475 W hypertension	NS	NS	[49]
R624C	Exon 12 of β -ENaC	1/50 B hypertension	NS	NS	[49]
E632G	Exon 12 of β -ENaC	1/475 W hypertension	NS	NS	[49]
G442V	Exon 8 of β -ENaC	1/475 W hypertension, 18/50 B hypertension 0.002 W, 0.083 B normotension	NS NS	NS NS	[49] [51]
V434M	Exon 8 of β -ENaC	1/475 W hypertension	NS	NS	[49]
V546I	Exon 13 of γ -ENaC	8/347 hypertension, 1/175 normotension	NS	OR=2.4	[106]
T387C	Exon 3 of γ -ENaC	Similar frequencies in hypertension and normotension, similar frequencies in B and W	-	NS	[108]
T474C	Exon 3 of γ -ENaC	Similar frequencies in hypertension and normotension, similar frequencies in B and W	-	NS	[108]
C549C	Exon 3 of γ -ENaC	Similar frequencies in hypertension and normotension, similar frequencies in B and W	-	NS	[108]
C1990G	Last Exon of γ -ENaC	Similar frequencies in hypertension and normotension, similar frequencies in B and W	-	NS	[108]
594insP	Rare mutant located outside the PY motif of γ -ENaC	One case of mild hypertension	NS	-	[108]
R631H	Rare mutant located 39 to the PY motif of γ -ENaC	Two severe cases of severe hypertension	NS	-	[108]
A334T	Exon 6 of α -ENaC	0.031 W, 0.442 B normotension	-	NS	[51]
C618F	Exon 13 of α -ENaC	0.002 W, 0.080 B normotension	- ↑ 3.8-fold	NS -	[51] [56]
T663A	Exon 13 of α -ENaC	0.293 W, 0.146 B normotension	NS ↑ ↑ 2.6-fold	Aassociates with normotension - -	[51] [55] [56]
G2139A	Promoter region of α -ENaC	1719/3989 J hypertension	Promoter activity↑	OR _{total} =1.31 OR _{<60y} =1.77	[57]

Abbreviations and symbols: B, black; W, white; J, Japanese; NS, not significant; OR, odd ratio; ↑, increase; -, not determined.

a gain of function ENaC mutant enhances its trafficking to the plasma membrane and thereby increases its cell surface expression^[4-6, 58-61], which leads to over reabsorption of Na⁺ and water.

Evidence obtained in rats and humans suggest that high-salt diets also cause oxidative stress. This high-salt intake induced increase in oxidative stress is more obvious in salt-sensitive hypertension^[62, 63]. Furthermore, high-salt intake may also target the tissues and organs independent of hypertension via a mechanism of elevating reactive oxygen species (ROS)^[64]. In the absence of the prominent elevations of BP after salt-loading, salt sensitivity may be revealed by the structural and functional injuries of the targeting organs such as the heart and kidney^[65]. Recent studies have shown that hydrogen peroxide (H₂O₂), an isoform of ROS, stimulates ENaC and that high NaCl elevates ROS in CCD cells^[66]. However, the mechanism by which a high-salt diet induces an increase in ROS to stimulate ENaC is not known. A high-salt intake is known to induce the compensatory natriuresis to maintain sodium homeostasis. Reduced plasma aldosterone causes a decrease in α -ENaC mRNA level, which suggests an important role in the compensatory natriuresis^[40]. Previous electrophysiological experiments assessed in renal CCD have indicated that dietary sodium intake and variations in aldosterone plasma levels regulates the abundance of functional ENaC in the apical plasma membrane^[39]. A high or low Na⁺ diet for three weeks also influenced the distribution pattern of ENaC in the mouse kidney. The regulation of ENaC function *in vivo* involves shifting the β - and γ -subunits from the cytoplasm to the apical plasma membrane and *vice versa*, respectively^[12]. The insertion of these subunits into the apical plasma membrane coincides with the upregulation of the α -subunit and its insertion into the apical plasma membrane^[67]. These studies together suggest that dietary salt modulates the expression pattern of ENaC subunits in the kidney and may stimulate its activity via enhanced ROS level, which in turn leading to an increase in Na⁺ reabsorption.

Several studies have demonstrated that there is increased oxidative stress in animals with high-salt intake^[68-71]. In experimental models of salt-sensitive hypertension, high-salt intake increased the markers of vascular and systemic oxidative stress^[1]. Studies in essential hypertensive patients have suggested that high-salt intake and/or salt sensitivity is associated with impaired endothelial function^[72-75]. Miyoshi *et al*^[76] reported a decrease in acetylcholine-induced forearm vasodilation in salt-sensitive hypertensive subjects regardless of the level of salt intake. Increased ROS have a critical role in the initiation of hypertension and may be generated by the hypertension itself, suggesting a positive-feedback mechanism. In addition to the systemic effects of ROS, recent evidence demonstrated that oxidative stress within the kidney plays a central role in the pathophysiology of sodium retention by inducing the tubulointerstitial accumulation of Ang II-positive cells. The prohypertensive role of intrarenal ROS is suggested by the strong correlation between the renal superoxide-positive cells and the severity of hypertension in the spontaneously

hypertensive rats (SHR)^[77]. However, there is a lack of information at the present time regarding whether oxidative stress induced by high-salt intake affects the BP via influencing ENaC activity. In our preliminary studies, we found that the high-salt intake decreased the expression level of α -ENaC in the CCD cells of DR rats, but not that in DS rats (unpublished observations). When cultured CCD cells are treated with high NaCl, ROS accumulated within these cells. Using patch-clamp experiments, we found that H₂O₂ stimulates ENaC activity. These results suggest that high-salt intake may activate ENaC through an elevation of ROS [unpublished observations].

Does altered activity of ENaC affect the function of the vascular endothelium and sympathetic nervous system to influence BP?

Although ENaC was known as the typical sodium channel in the kidney, the colon and the lung, vascular endothelial cells were also shown to express ENaC and mineralocorticoid receptors^[21, 78, 79]. Endothelial cells are targets for aldosterone, which activates the apically located ENaC, and its activity modifies the biomechanical properties of the endothelium. Therefore, ENaC is proposed as the key mediator of aldosterone-dependent BP control in the endothelium^[80]. Several studies, in different cell types including CCD and endothelial cells, have suggested that ENaC may function as a mechanosensor and that mechanical stimuli may activate ENaC^[22, 81, 82]. Because endothelial ENaC inhibition may activate nitric oxide (NO) synthase^[83], it is completely possible that altered blood flow (shear stress), which is caused by over reabsorption of Na⁺ via ENaC located at distal nephron, may affect the NO production in endothelia. High-salt intake may cause an increase in plasma [Na⁺], which may or may not be detectable depending upon the extent of water intake and the timing of blood sampling relative to high-salt intake. Fang and coworkers showed that four days after 8% high-salt diet exposure, plasma [Na⁺] increased by 3–4 mmol/L in SHR and Wistar Kyoto rats^[84]. In normotensive rats, when salt intake increased from 10 to 250 mmol/d over 5 d, the plasma [Na⁺] increased by 3 mmol/L. In addition, reducing the salt intake from 350 to 12–20 mmol/d lowered the plasma [Na⁺] to a similar extent by 3–4 mmol/L^[85]. Huang and coworkers showed that high-salt intake increased [Na⁺] in the cerebrospinal fluid (CSF) up to 5 mmol/L in DS rats and SHR rats but not in DR rats^[86]. Similar to the results obtained from the animal models, [Na⁺] in CSF was increased by 2–3 mmol/L in patients with both salt-sensitive and non-salt-sensitive hypertension after a 7-d high-salt diet (16–18 g/d) compared to those given a low-salt diet (1–3 g/d)^[87]. Nevertheless, high-salt diets elevated the arterial pressure in salt-sensitive individuals. These results suggest that increases in plasma [Na⁺] may trigger this effect^[84] via a mechanism that has not been elucidated.

Previous studies have suggested that DS rats have abnormalities in the sympathetic nervous system (SNS)^[88, 89] and endothelial function^[90, 91], which causes significant vascular resistance. In addition, there is evidence that supports the hypothesis that abnormal modulation of SNS is involved in

salt-induced hypertension. Salt loading has been shown to augment the sympathetic activity in DS rats but not in DR rats^[92-94]. The intracerebroventricular (ICV) infusion of sodium caused sympathoexcitatory and pressor responses to a greater degree in DS rats than in DR rats^[85, 95]. The strict regulation of $[Na^+]$ in the CSF is crucial for the normal function of neurons. An increase in CSF $[Na^+]$ by as little as 2 mmol/L can increase the firing rate of neurons. A chronic 5 mmol/L increase in CSF $[Na^+]$ causes sympathetic hyperactivity and hypertension^[96-98]. Increases in CSF $[Cl^-]$ or the osmolarity of CSF did not cause such sympathoexcitation and hypertension^[99]. Because the role of ENaC in regulating sodium transport across the epithelia is important, investigators started to study whether ENaC in neural components also plays a role in salt-sensitive hypertension. Stoichiometrically different populations of ENaC may be present in both epithelial and neural components in the brain, which may contribute to the regulation of CSF and interstitial Na^+ concentrations and neuronal excitation^[90, 97]. ENaC subunits are also expressed in sensory nerve endings in the rat foot pad^[100] and in the trigeminal mechanosensory neurons^[101]. However, the function of the ENaC subunits in these tissues has not yet been elucidated. Functional studies have suggested the presence of specific Na^+ channels, presumably ENaC, in the brain that are activated by aldosterone or a high-salt diet and blocked by amiloride or benzamil. In Wistar rats, ICV infusion of aldosterone or Na^+ -rich artificial CSF increased BP and renal sympathetic nerve activity. In DS rats but not DR rats, a high-salt diet or ICV infusion of aldosterone caused sympathoexcitation and hypertension. The blood-brain barrier in DS rats is five to eight times more permeable to Na^+ than that in DR rats^[102]. Increases in CSF $[Na^+]$ are observed in DS rats but not DR rats on a high-salt diet and precede changes in BP by 1-2 d^[86]. Importantly, the responses to aldosterone or Na^+ -rich artificial CSF in Wistar rats and to aldosterone or a high-salt diet in DS rats can be prevented by ICV infusion of benzamil or spironolactone^[103-105]. These findings suggest that the mineralocorticoid receptor (MR)-mediated activation of sodium channels in the brain is responsible for the mechanisms leading to increased sympathetic outflow and hypertension.

Conclusion

We present evidence that places ENaC in a central position for Na^+ retention, which is necessary to achieve a state of high BP in the salt-sensitive population. The Na^+ reabsorptive site (ENaC) does not act alone in the mechanisms for developing hypertension. The emerging evidence is compelling for the consideration of ENaC as the additional requisite participant in endothelia and SNS (Figure 2). However, the mechanisms by which the activation of ENaC to induce Na^+ retention and the consequences in the vascular compartment and SNS require further investigation.

Acknowledgements

The current study was supported by the National Natural Science Foundation of China (No 81070217 and 30871007), the

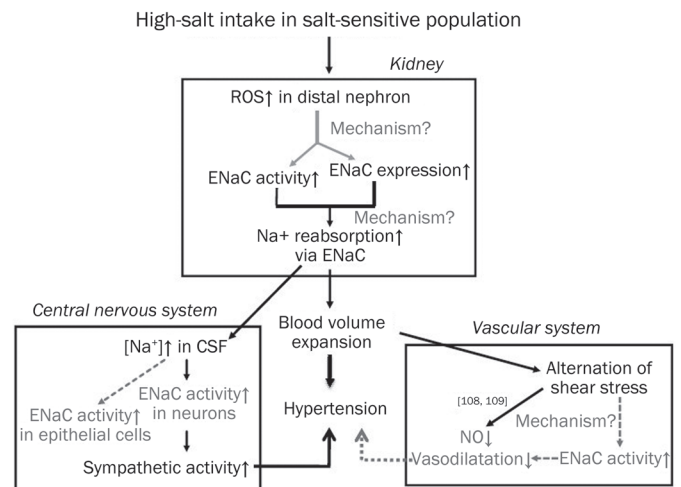


Figure 2. A schematic that illustrates the central role of ENaC in the development of salt-sensitive hypertension after the loss of compensatory natriuresis. High-salt intake in the salt-sensitive population induces oxidative stress in the kidney, which enhances the apical membrane expression of ENaC and ENaC activity with an unknown mechanism at the present time. This increased activity eventually causes Na^+ over-reabsorption in CCD followed by water retention and elevation of BP. The volume expansion in the vascular compartment alters blood flow (shear stress) and directly affects endothelial function by reducing the synthesis of NO^[109, 110]. ENaC may act as a mechanosensor in endothelial cells and may sense changes in shear stress. Alterations in shear stress may activate ENaC residing at the apical membrane of endothelial cells and may affect the regulation of vasoactive substances. Na^+ over-reabsorption in CCD elevates $[Na^+]$ in CSF, which in turn triggers sympathetic activity in neurons and contributes to hypertension. Stoichiometrically different populations of ENaC may be present in epithelial cells and neurons in the brain, which may contribute to the regulation of CSF and interstitial $[Na^+]$ as well as neuronal excitation. CCD: cortical collecting duct; CSF: cerebrospinal fluid; and NO: nitric oxide. Black solid lines with arrows: already known; grey dash lines with arrows and words in gray: open questions.

Natural Science Foundation of Heilongjiang Province (No ZD200807-01 and QC2010097), the Overseas Talent Foundation of the Department of Education, Heilongjiang Province (No 1154HZ11), the Key Research Program of the 2nd Affiliated Hospital of Harbin Medical University (No ZD2008-08), and the Postdoctoral Foundation of the 2nd Affiliated Hospital of Harbin Medical University (No ZD2010-01).

References

- Campese VM. Salt sensitivity in hypertension. Renal and cardiovascular implications. *Hypertension* 1994; 23: 531-50.
- Weinberger MH. Salt sensitivity of blood pressure in humans. *Hypertension* 1996; 27: 481-90.
- Staessen JA, Wang J, Bianchi G, Birkenhager WH. Essential hypertension. *Lancet* 2003; 361: 1629-41.
- Shimkets RA, Warnock DG, Bositis CM, Nelson-Williams C, Hansson JH, Schambelan M, et al. Liddle's syndrome: heritable human hypertension caused by mutations in the beta subunit of the epithelial sodium channel. *Cell* 1994; 79: 407-14.

- 5 Hansson JH, Nelson-Williams C, Suzuki H, Schild L, Shimkets R, Lu Y, et al. Hypertension caused by a truncated epithelial sodium channel gamma subunit: genetic heterogeneity of Liddle syndrome. *Nat Genet* 1995; 11: 76–82.
- 6 Liddle GW, Bledsoe T, Coppage WS Jr. Hypertension reviews. *J Tenn Med Assoc* 1974; 67: 669.
- 7 Pratt JH. Central role for ENaC in development of hypertension. *J Am Soc Nephrol* 2005; 16: 3154–9.
- 8 Canessa CM, Schild L, Buell G, Thorens B, Gautschi I, Horisberger JD, et al. Amiloride-sensitive epithelial Na⁺ channel is made of three homologous subunits. *Nature* 1994; 367: 463–7.
- 9 Lingueglia E, Voilley N, Waldmann R, Lazdunski M, Barbry P. Expression cloning of an epithelial amiloride-sensitive Na⁺ channel. A new channel type with homologies to *Caenorhabditis elegans* degenerins. *FEBS Lett* 1993; 318: 95–9.
- 10 McDonald FJ, Snyder PM, McCray PB Jr, Welsh MJ. Cloning, expression, and tissue distribution of a human amiloride-sensitive Na⁺ channel. *Am J Physiol* 1994; 266: L728–34.
- 11 McDonald FJ, Price MP, Snyder PM, Welsh MJ. Cloning and expression of the beta- and gamma-subunits of the human epithelial sodium channel. *Am J Physiol* 1995; 268: C1157–63.
- 12 Firsov D, Gautschi I, Merillat AM, Rossier BC, Schild L. The heterotetrameric architecture of the epithelial sodium channel (ENaC). *EMBO J* 1998; 17: 344–52.
- 13 Fyfe GK, Canessa CM. Subunit composition determines the single channel kinetics of the epithelial sodium channel. *J Gen Physiol* 1998; 112: 423–32.
- 14 Fyfe GK, Quinn A, Canessa CM. Structure and function of the Mec-ENaC family of ion channels. *Semin Nephrol* 1998; 18: 138–51.
- 15 Horisberger JD. Amiloride-sensitive Na channels. *Curr Opin Cell Biol* 1998; 10: 443–9.
- 16 Garty H, Benos DJ. Characteristics and regulatory mechanisms of the amiloride-blockable Na⁺ channel. *Physiol Rev* 1988; 68: 309–73.
- 17 Palmer LG. Epithelial Na channels: function and diversity. *Annu Rev Physiol* 1992; 54: 51–66.
- 18 Garty H, Palmer LG. Epithelial sodium channels: function, structure, and regulation. *Physiol Rev* 1997; 77: 359–96.
- 19 Benos DJ, Stanton BA. Functional domains within the degenerin/epithelial sodium channel (Deg/ENaC) superfamily of ion channels. *J Physiol* 1999; 520: 631–44.
- 20 Snyder PM. The epithelial Na⁺ channel: cell surface insertion and retrieval in Na⁺ homeostasis and hypertension. *Endocr Rev* 2002; 23: 258–75.
- 21 Golestaneh N, Klein C, Valamanesh F, Suarez G, Agarwal MK, Mirshahi M. Mineralocorticoid receptor-mediated signaling regulates the ion gated sodium channel in vascular endothelial cells and requires an intact cytoskeleton. *Biochem Biophys Res Commun* 2001; 280: 1300–6.
- 22 Drummond HA, Gebremedhin D, Harder DR. Degenerin/epithelial Na⁺ channel proteins: components of a vascular mechanosensor. *Hypertension* 2004; 44: 643–8.
- 23 Oberleithner H, Ludwig T, Riethmüller C, Hillebrand U, Albermann L, Schäfer C, et al. Human endothelium: target for aldosterone. *Hypertension* 2004; 43: 952–6.
- 24 Rossier BC, Pradervand S, Schild L, Hummler E. Epithelial sodium channel and the control of sodium balance: interaction between genetic and environmental factors. *Annu Rev Physiol* 2002; 64: 877–97.
- 25 Snyder PM, Cheng C, Prince LS, Rogers JC, Welsh MJ. Electrophysiological and biochemical evidence that DEG/ENaC cation channels are composed of nine subunits. *J Biol Chem* 1998; 273: 681–4.
- 26 Eskandari S, Snyder PM, Kreman M, Zampighi GA, Welsh MJ, Wright EM. Number of subunits comprising the epithelial sodium channel. *J Biol Chem* 1999; 274: 27281–6.
- 27 O'Brodovich HM. Immature epithelial Na⁺ channel expression is one of the pathogenetic mechanisms leading to human neonatal respiratory distress syndrome. *Proc Assoc Am Physicians* 1996; 108: 345–55.
- 28 Egli M, Duplain H, Lepori M, Cook S, Nicod P, Hummler E, et al. Defective respiratory amiloride-sensitive sodium transport predisposes to pulmonary oedema and delays its resolution in mice. *J Physiol* 2004; 560: 857–65.
- 29 Dahl LK, Heine M, Tassinari L. Role of genetic factors in susceptibility to experimental hypertension due to chronic excess salt ingestion. *Nature* 1962; 194: 480–2.
- 30 Dahl LK, Heine M, Tassinari L. Effects of chronic excess salt ingestion. Evidence that genetic factors play an important role in susceptibility to experimental hypertension. *J Exp Med* 1962; 115: 1173–90.
- 31 Dahl LK, Heine M, Thompson K. Genetic influence of renal homografts on the blood pressure of rats from different strains. *Proc Soc Exp Biol Med* 1972; 140: 852–6.
- 32 Dahl LK, Heine M, Thompson K. Genetic influence of the kidneys on blood pressure. Evidence from chronic renal homografts in rats with opposite predispositions to hypertension. *Circ Res* 1974; 40: 94–101.
- 33 Dahl LK, Heine M. Primary role of renal homografts in setting chronic blood pressure levels in rats. *Circ Res* 1975; 36: 692–6.
- 34 Rapp JP, Tan SY, Margolius HS. Plasma mineralocorticoids, plasma renin, and urinary kallikrein in salt-sensitive and salt-resistant rats. *Endocr Res Commun* 1978; 5: 35–41.
- 35 Baba K, Mulrow PJ, Franco-Saenz R, Rapp JP. Suppression of adrenal renin in Dahl salt-sensitive rats. *Hypertension* 1986; 8: 1149–53.
- 36 Aoi W, Niisato N, Miyazaki H, Marunaka Y. Flavonoid-induced reduction of ENaC expression in the kidney of Dahl salt-sensitive hypertensive rat. *Biochem Biophys Res Commun* 2004; 315: 892–6.
- 37 Aoi W, Niisato N, Sawabe Y, Miyazaki H, Tokuda S, Nishio K, et al. Abnormal expression of ENaC and SGK1 mRNA induced by dietary sodium in Dahl salt-sensitively hypertensive rats. *Cell Biol Int* 2007; 31: 1288–91.
- 38 Verrey F. Transcriptional control of sodium transport in tight epithelial by adrenal steroids. *J Membr Biol* 1995; 144: 93–110.
- 39 Chen SY, Bhargava A, Mastroberardino L, Meijer OC, Wang J, Buse P, et al. Epithelial sodium channel regulated by aldosterone-induced protein sgk. *Proc Natl Acad Sci U S A* 1999; 96: 2514–9.
- 40 Náray-Fejes-Tóth A, Canessa C, Cleaveland ES, Aldrich G, Fejes-Tóth G. sgk is an aldosterone-induced kinase in the renal collecting duct. Effects on epithelial Na⁺ channels. *J Biol Chem* 1999; 274: 16973–8.
- 41 Pearce D. The role of SGK1 in hormone-regulated sodium transport. *Trends Endocrinol Metab* 2001; 12: 341–7.
- 42 Yun CC, Chen Y, Lang F. Glucocorticoid activation of Na⁺/H⁺ exchanger isoform 3 revisited. The roles of SGK1 and NHERF2. *J Biol Chem* 2002; 277: 7676–83.
- 43 Kakizoe Y, Kitamura K, Ko T, Wakida N, Maekawa A, Miyoshi T, et al. Aberrant ENaC activation in Dahl salt-sensitive rats. *J Hypertens* 2009; 27: 1679–89.
- 44 Fenton RA, Chou CL, Ageloff S, Brandt W, Stokes JB, Knepper MA. Increased collecting duct urea transporter expression in Dahl salt-sensitive rats. *Am J Physiol Renal Physiol* 2003; 285: F143–51.

- 45 Husted RF, Takahashi T, Stokes JB. IMCD cells cultured from Dahl S rats absorb more Na⁺ than Dahl R rats. *Am J Physiol* 1996; 271: F1029–36.
- 46 Shehata MF, Leenen FH, Tesson F. Sequence analysis of coding and 3' and 5' flanking regions of the epithelial sodium channel alpha, beta, and gamma genes in Dahl S versus R rats. *BMC Genet* 2007; 8: 35.
- 47 Shehata MF. Characterization of the epithelial sodium channel alpha subunit coding and non-coding transcripts and their corresponding mRNA expression levels in Dahl R versus S rat kidney cortex on normal and high salt diet. *Int Arch Med* 2009; 2: 5.
- 48 Baker EH, Dong YB, Sagnella GA, Rothwell M, Onipinla AK, Markandu ND, *et al*. Association of hypertension with T594M mutation in beta subunit of epithelial sodium channels in black people resident in London. *Lancet* 1998; 351: 1388–92.
- 49 Persu A, Barbry P, Bassilana F, Houot AM, Mengual R, Lazdunski M, *et al*. Genetic analysis of the beta subunit of the epithelial Na⁺ channel in essential hypertension. *Hypertension* 1998; 32: 129–37.
- 50 Wang Y, Zheng Y, Chen J, Wu H, Zheng D, Hui R. A novel epithelial sodium channel gamma-subunit *de novo* frameshift mutation leads to Liddle syndrome. *Clin Endocrinol (Oxf)* 2007; 67: 801–4.
- 51 Ambrosius WT, Bloem LJ, Zhou L, Rebhun JF, Snyder PM, Wagner MA, *et al*. Genetic variants in the epithelial sodium channel in relation to aldosterone and potassium excretion and risk for hypertension. *Hypertension* 1999; 34: 631–7.
- 52 Su YR, Menon AG. Epithelial sodium channels and hypertension. *Drug Metab Dispos* 2001; 29: 553–6.
- 53 Sugiyama T, Kato N, Ishinaga Y, Yamori Y, Yazaki Y. Evaluation of selected polymorphisms of the Mendelian hypertensive disease genes in the Japanese population. *Hypertens Res* 2001; 24: 515–21.
- 54 Swift PA, Macgregor GA. Genetic variation in the epithelial sodium channel: a risk factor for hypertension in people of African origin. *Adv Ren Replace Ther* 2004; 11: 76–86.
- 55 Samaha FF, Rubenstein RC, Yan W, Ramkumar M, Levy DI, Ahn YJ, *et al*. Functional polymorphism in the carboxyl terminus of the alpha-subunit of the human epithelial sodium channel. *J Biol Chem* 2004; 279: 23900–7.
- 56 Tong Q, Menon AG, Stockand JD. Functional polymorphisms in the alpha-subunit of the human epithelial Na⁺ channel increase activity. *Am J Physiol Renal Physiol* 2006; 290: F821–7.
- 57 Iwai N, Baba S, Mannami T, Ogihara T, Ogata J. Association of a sodium channel alpha subunit promoter variant with blood pressure. *J Am Soc Nephrol* 2002; 13: 80–5.
- 58 Firsov D, Schild L, Gautschi I, Méritat AM, Schneeberger E, Rossier BC. Cell surface expression of the epithelial Na channel and a mutant causing Liddle syndrome: a quantitative approach. *Proc Natl Acad Sci U S A* 1996; 93: 15370–5.
- 59 Goulet CC, Volk KA, Adams CM, Prince LS, Stokes JB, Snyder PM. Inhibition of the epithelial Na⁺ channel by interaction of Nedd4 with a PY motif deleted in Liddle's syndrome. *J Biol Chem* 1998; 273: 30012–7.
- 60 Abriel H, Loffing J, Rebhun JF, Pratt JH, Schild L, Horisberger JD, *et al*. Defective regulation of the epithelial Na⁺ channel by Nedd4 in Liddle's syndrome. *J Clin Invest* 1999; 103: 667–73.
- 61 Rotin D, Kanelis V, Schild L. Trafficking and cell surface stability of ENaC. *Am J Physiol Renal Physiol* 2001; 281: F391–9.
- 62 Bayorh MA, Ganafa AA, Socci RR, Silvestrov N, Abukhalaf IK. The role of oxidative stress in salt-induced hypertension. *Am J Hypertens* 2004; 17: 31–6.
- 63 Laffer CL, Bolterman RJ, Romero JC, Elijovich F. Effect of salt on isoprostanes in salt-sensitive essential hypertension. *Hypertension* 2006; 47: 434–40.
- 64 Ritz E, Mehls O. Salt restriction in kidney disease – a missed therapeutic opportunity. *Pediatr Nephrol* 2009; 24: 9–17.
- 65 Frohlich ED, Varagic J. Sodium directly impairs target organ function in hypertension. *Curr Opin Cardiol* 2005; 20: 424–9.
- 66 Bayorh MA, Ganafa AA, Eatman D, Walton M, Feuerstein GZ. Simvastatin and losartan enhance nitric oxide and reduce oxidative stress in salt-induced hypertension. *Am J Hypertens* 2005; 18: 1496–502.
- 67 Loffing J, Vallon V, Loffing-Cueni D, Aregger F, Richter K, Pietri L, *et al*. Altered renal distal tubule structure and renal Na⁺ and Ca²⁺ handling in a mouse model for Gitelman's syndrome. *J Am Soc Nephrol* 2004; 15: 2276–88.
- 68 Swei A, Lacy F, DeLano FA, Schmid-Schönbein GW. Oxidative stress in the Dahl hypertensive rat. *Hypertension* 1997; 30: 1628–33.
- 69 Zhou MS, Adam AG, Jaimes EA, Raij L. In salt-sensitive hypertension, increased superoxide production is linked to functional upregulation of angiotensin II. *Hypertension* 2003; 42: 945–51.
- 70 Tian N, Moore RS, Braddy S, Rose RA, Gu JW, Hughson MD, *et al*. Interactions between oxidative stress and inflammation in salt-sensitive hypertension. *Am J Physiol Heart Circ Physiol* 2007; 293: H3388–95.
- 71 Jaimes EA, Zhou MS, Pearse DD, Puzis L, Raij L. Upregulation of cortical COX-2 in salt-sensitive hypertension: role of angiotensin II and reactive oxygen species. *Am J Physiol Renal Physiol* 2008; 294: F385–92.
- 72 Stein CM, Nelson R, Brown M, Wood M, Wood AJ. Dietary sodium intake modulates vasodilation mediated by nitroprusside but not by methacholine in the human forearm. *Hypertension* 1995; 25: 1220–3.
- 73 Campese VM, Tawadrous M, Bigazzi R, Bianchi S, Mann AS, Oparil S, *et al*. Salt intake and plasma atrial natriuretic peptide and nitric oxide in hypertension. *Hypertension* 1996; 28: 335–40.
- 74 Facchini FS, DoNascimento C, Reaven GM, Yip JW, Ni XP, Humphreys MH. Blood pressure, sodium intake, insulin resistance, and urinary nitrate excretion. *Hypertension* 1999; 33: 1008–12.
- 75 Fujiwara N, Osanai T, Kamada T, Katoh T, Takahashi K, Okumura K. Study on the relationship between plasma nitrite and nitrate level and salt sensitivity in human hypertension: modulation of nitric oxide synthesis by salt intake. *Circulation* 2000; 101: 856–61.
- 76 Miyoshi A, Suzuki H, Fujiwara M, Masai M, Iwasaki T. Impairment of endothelial function in salt-sensitive hypertension in humans. *Am J Hypertens* 1997; 10: 1083–90.
- 77 Rodríguez-Iturbe B, Pons H, Quiroz Y, Gordon K, Rincón J, Chávez M, *et al*. Mycophenolate mofetil prevents salt-sensitive hypertension resulting from angiotensin II exposure. *Kidney Int* 2001; 59: 2222–32.
- 78 Oberleithner H, Riethmüller C, Ludwig T, Shahin V, Stock C, Schwab A, *et al*. Differential action of steroid hormones on human endothelium. *J Cell Sci* 2006; 119: 1926–32.
- 79 Wang S, Meng F, Mohan S, Champaneri B, Gu Y. Functional ENaC channels expressed in endothelial cells: a new candidate for mediating shear force. *Microcirculation* 2009; 16: 276–87.
- 80 Kusche-Vihrog K, Callies C, Fels J, Oberleithner H. The epithelial sodium channel (ENaC): Mediator of the aldosterone response in the vascular endothelium. *Steroids* 2010; 75: 544–9.
- 81 Wei SP, Li XQ, Chou CF, Liang YY, Peng JB, Warnock DG, *et al*. Membrane tension modulates the effects of apical cholesterol on the renal epithelial sodium channel. *J Membr Biol* 2007; 220: 21–31.
- 82 Drummond HA, Welsh MJ, Abboud FM. ENaC subunits are molecular components of the arterial baroreceptor complex. *Ann N Y Acad Sci*

- 2001; 940: 42–7.
- 83 Pérez FR, Venegas F, González M, Andrés S, Vallejos C, Riquelme G, *et al*. Endothelial epithelial sodium channel inhibition activates endothelial nitric oxide synthase via phosphoinositide 3-kinase/Akt in small-diameter mesenteric arteries. *Hypertension* 2009; 53: 1000–7.
- 84 Fang Z, Carlson SH, Peng N, Wyss JM. Circadian rhythm of plasma sodium is disrupted in spontaneously hypertensive rats fed a high-NaCl diet. *Am J Physiol Regul Integr Comp Physiol* 2000; 278: R1490–5.
- 85 He FJ, Markandu ND, Sagnella GA, de Wardener HE, MacGregor GA. Plasma sodium: ignored and underestimated. *Hypertension* 2005; 45: 98–102.
- 86 Huang BS, Van Vliet BN, Leenen FH. Increases in CSF $[Na^+]$ precede the increases in blood pressure in Dahl S rats and SHR on a high-salt diet. *Am J Physiol Heart Circ Physiol* 2004; 287: H1160–6.
- 87 Kawano Y, Yoshida K, Kawamura M, Yoshimi H, Ashida T, Abe H, *et al*. Sodium and noradrenaline in cerebrospinal fluid and blood in salt-sensitive and non-salt-sensitive essential hypertension. *Clin Exp Pharmacol Physiol* 1992; 19: 235–41.
- 88 Gordon FJ, Mark AL. Mechanism of impaired baroreflex control in prehypertensive Dahl salt-sensitive rats. *Circ Res* 1984; 54: 378–87.
- 89 Osborn JL, Roman RJ, Ewens JD. Renal nerves and the development of Dahl salt-sensitive hypertension. *Hypertension* 1988; 11: 523–8.
- 90 Hayakawa H, Coffee K, Raji L. Endothelial dysfunction and cardiovascular injury in experimental salt-sensitive hypertension: effects of antihypertensive therapy. *Circulation* 1997; 96: 2407–13.
- 91 Zhou MS, Kosaka H, Tian RX, Abe Y, Chen QH, Yoneyama H, *et al*. L-Arginine improves endothelial function in renal artery of hypertensive Dahl rats. *J Hypertens* 2001; 19: 421–9.
- 92 Fujita T, Henry WL, Bartter FC, Lake CR, Delea CS. Factors influencing blood pressure in salt-sensitive patients with hypertension. *Am J Med* 1980; 69: 334–44.
- 93 Ono A, Kuwaki T, Kumada M, Fujita T. Differential central modulation of the baroreflex by salt loading in normotensive and spontaneously hypertensive rats. *Hypertension* 1997; 29: 808–14.
- 94 Huang BS, Leenen FH. Both brain angiotensin II and “ouabain” contribute to sympathoexcitation and hypertension in Dahl S rats on high salt intake. *Hypertension* 1998; 32: 1028–33.
- 95 Huang BS, Wang H, Leenen FH. Enhanced sympathoexcitatory and pressor responses to central Na^+ in Dahl salt-sensitive vs -resistant rats. *Am J Physiol Heart Circ Physiol* 2001; 281: H1881–9.
- 96 Masilamani S, Kim GH, Mitchell C, Wade JB, Knepper MA. Aldosterone-mediated regulation of ENaC alpha, beta, and gamma subunit proteins in rat kidney. *J Clin Invest* 1999; 104: R19–23.
- 97 Amin MS, Wang HW, Reza E, Whitman SC, Tuana BS, Leenen FH. Distribution of epithelial sodium channels and mineralocorticoid receptors in cardiovascular regulatory centers in rat brain. *Am J Physiol Regul Integr Comp Physiol* 2005; 289: R1787–97.
- 98 Ergonul Z, Frindt G, Palmer LG. Regulation of maturation and processing of ENaC subunits in the rat kidney. *Am J Physiol Renal Physiol* 2006; 291: F683–93.
- 99 Bunag RD, Miyajima E. Sympathetic hyperactivity elevates blood pressure during acute cerebroventricular infusions of hypertonic salt in rats. *J Cardiovasc Pharmacol* 1984; 6: 844–51.
- 100 Drummond HA, Abboud FM, Welsh MJ. Localization of beta and gamma subunits of ENaC in sensory nerve endings in the rat foot pad. *Brain Res* 2000; 884: 1–12.
- 101 Fricke B, Lints R, Stewart G, Drummond H, Dodt G, Driscoll M, *et al*. Epithelial Na^+ channels and stomatin are expressed in rat trigeminal mechanosensory neurons. *Cell Tissue Res* 2000; 299: 327–34.
- 102 Simchon S, Manger W, Golanov E, Kamen J, Sommer G, Marshall CH. Handling $22NaCl$ by the blood-brain barrier and kidney: its relevance to salt-induced hypertension in Dahl rats. *Hypertension* 1999; 33: 517–23.
- 103 Wang H, Leenen FH. Brain sodium channels mediate increases in brain “ouabain” and blood pressure in Dahl S rats. *Hypertension* 2002; 40: 96–100.
- 104 Wang H, Huang BS, Leenen FH. Brain sodium channels and ouabain-like compounds mediate central aldosterone-induced hypertension. *Am J Physiol Heart Circ Physiol* 2003; 285: H2516–23.
- 105 Wang H, Leenen FH. Brain sodium channels and central sodium-induced increases in brain ouabain-like compound and blood pressure. *J Hypertens* 2003; 21: 1519–24.
- 106 Hannila-Handelberg T, Kontula K, Tikkanen I, Tikkanen T, Fyhrquist F, Helin K, *et al*. Common variants of the beta and gamma subunits of the epithelial sodium channel and their relation to plasma renin and aldosterone levels in essential hypertension. *BMC Med Genet* 2005; 6: 4.
- 107 Su YR, Rutkowski MP, Klanke CA, Wu X, Cui Y, Pun RY, *et al*. A novel variant of the beta-subunit of the amiloride-sensitive sodium channel in African Americans. *J Am Soc Nephrol* 1996; 7: 2543–9.
- 108 Persu A, Coscoy S, Houot AM, Corvol P, Barbry P, Jeunemaitre X. Polymorphisms of the gamma subunit of the epithelial Na^+ channel in essential hypertension. *J Hypertens* 1999; 17: 639–45.
- 109 Nauli SM, Kawanabe Y, Kaminski JJ, Pearce WJ, Ingber DE, Zhou J. Endothelial cilia are fluid shear sensors that regulate calcium signaling and nitric oxide production through polycystin-1. *Circulation* 2008; 117: 1161–71.
- 110 AbouAlaiwi WA, Takahashi M, Mell BR, Jones TJ, Ratnam S, Kolb RJ, *et al*. Ciliary polycystin-2 is a mechanosensitive calcium channel involved in nitric oxide signaling cascades. *Circ Res* 2009; 104: 860–9.

Review

Beyond membrane channelopathies: alternative mechanisms underlying complex human disease

Konstantinos Dean BOUDOULAS^{1,2,*}, Peter J MOHLER^{1,2,3}¹The Dorothy M Davis Heart and Lung Research Institute; ²Departments of Internal Medicine (Cardiovascular Medicine); ³Physiology and Cell Biology; the Ohio State University Medical Center, Columbus, OH 43210, USA

Over the past fifteen years, our understanding of the molecular mechanisms underlying human disease has flourished in large part due to the discovery of gene mutations linked with membrane ion channels and transporters. In fact, ion channel defects (“channelopathies” – the focus of this review series) have been associated with a spectrum of serious human disease phenotypes including cystic fibrosis, cardiac arrhythmia, diabetes, skeletal muscle defects, and neurological disorders. However, we now know that human disease, particularly excitable cell disease, may be caused by defects in non-ion channel polypeptides including in cellular components residing well beneath the plasma membrane. For example, over the past few years, a new class of potentially fatal cardiac arrhythmias has been linked with cytoplasmic proteins that include sub-membrane adapters such as ankyrin-B (ANK2), ankyrin-G (ANK3), and alpha-1 syntrophin, membrane coat proteins including caveolin-3 (CAV3), signaling platforms including yotiao (AKAP9), and cardiac enzymes (GPD1L). The focus of this review is to detail the exciting role of lamins, yet another class of gene products that have provided elegant new insight into human disease.

Keywords: arrhythmia; channelopathy; heart disease; lamin; laminopathy; emerin; nesprin

Acta Pharmacologica Sinica (2011) 32: 798–804; doi: 10.1038/aps.2011.34

Introduction

In fact, ion channel defects (“channelopathies” – the focus of this review series) have been associated with a spectrum of serious human disease phenotypes including cystic fibrosis, cardiac arrhythmia, diabetes, skeletal muscle defects, and neurological disorders. However, we now know that human disease, particularly excitable cell disease, may be caused by defects in non-ion channel polypeptides including in cellular components residing well beneath the plasma membrane. For example, over the past few years, a new class of potentially fatal cardiac arrhythmias has been linked with cytoplasmic proteins that include sub-membrane adapters such as ankyrin-B (ANK2)^[1–5], ankyrin-G (ANK3)^[6–8], and alpha-1 syntrophin^[9], membrane coat proteins including caveolin-3 (CAV3)^[10], signaling platforms including yotiao (AKAP9)^[11, 12], and cardiac enzymes (GPD1L)^[13]. The focus of this review is to detail the exciting role of lamins, yet another class of gene products that have provided elegant new insight into human disease.

Lamins: critical intermediate filament components

Lamins are intermediate filament proteins and a major component of the nuclear lamina, a proteinaceous layer underlying the inner nuclear membrane, separating the nuclear envelope from the nuclear matrix. Lamins interact with proteins and chromatin, thus playing an important role in maintaining cell structure and cell regulation including apoptosis^[14–17]. Lamin is involved in DNA repair and replication, transcriptional regulation, and maintaining the organization and structure of heterochromatin, nuclear lamina, inner nuclear membrane and nuclear pore complexes^[14–19]. Further, lamin has been implicated to be involved in tumorigenesis and viral infections^[18, 20, 21].

Lamins are divided into two groups originally based on isoelectric points observed by two-dimensional gel electrophoresis: A-type lamins (almost neutral isoelectric point) and B-type lamins (acidic isoelectric point)^[22, 23]. A-type lamins are primarily located in differentiated cells while B-type lamins are located in all cells. Lamins have a conservative alpha helical central rod domain with an amino terminal globular head domain and carboxyl terminal globular tail domain^[21]. The lamin tail domain contains an approximate 120-residue immunoglobulin fold, CAAX motif (except lamin C as described below) and a nuclear localization signal^[24].

* To whom correspondence should be addressed.

E-mail Konstantinos.boudoulas@osumc.edu (Konstantinos Dean BOUDOULAS).

Received 2011-03-01 Accepted 2011-03-22

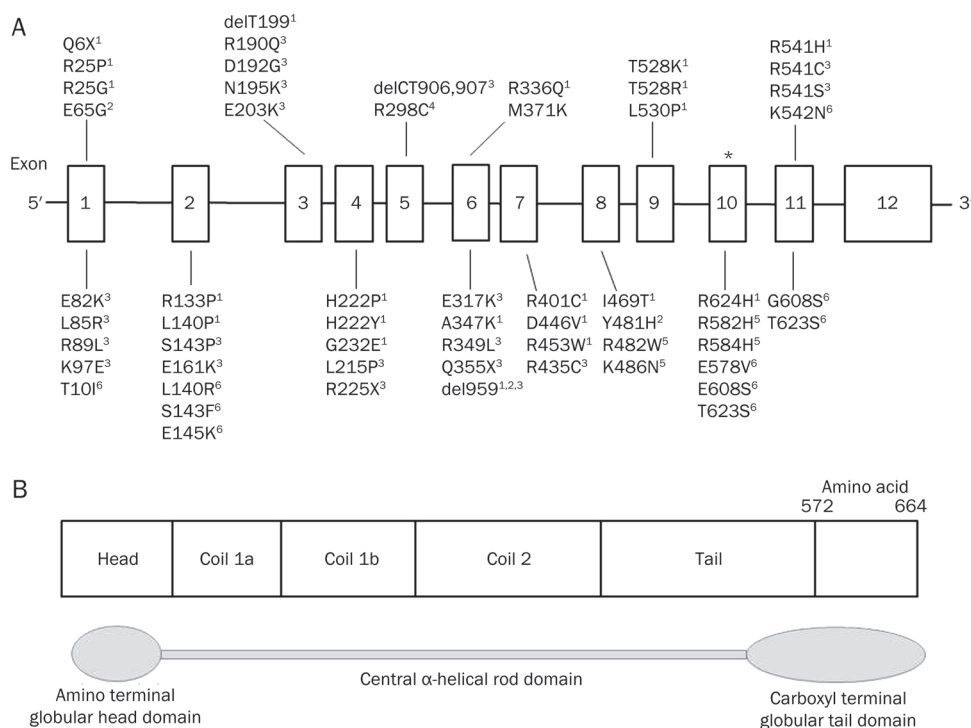


Figure 1. Schematic of (A) lamin gene (LMNA) and (B) lamin A/C protein. * indicates alternate splicing in exon 10 giving rise to the proteins lamin A (664 amino acids) and lamin C (572 amino acids). Shown are several mutations known to result in laminopathies with corresponding amino acid or nucleotide changes. 1=Emery-Dreifuss muscular dystrophy; 2=Limb girdle muscular dystrophy type 1B; 3=dilated cardiomyopathy; 4=Charcot-Marie Tooth type 2B1; 5=Familial partial lipodystrophy of the Dunnigan-type; 6=Hutchison-Gilford progeria syndrome.

In humans, the *LMNA* gene (Figure 1) codes for A-type lamins and is localized to chromosome 1q21.2^[25]. *LMNA* consists of 12 exons and at exon 10 alternative splicing occurs giving rise to the proteins lamin A (664 amino acids) and lamin C (572 amino acids). The first 566 amino acids (exon 1–10) of lamin A and C (lamin A/C) are identical which code for an amino terminal globular head domain, central rod domain (coil 1a, 1b, and 2), and a portion of the carboxyl terminal globular tail domain^[17, 26]. Mutations in the human *LMNA* gene encoding for lamin A/C results in several different clinical disorders referred to as “laminopathies”^[27–35]. Interestingly, certain cases of laminopathies primarily affect the heart resulting in dilated cardiomyopathy with or without conduction system disease even though lamin is found in all differentiated cells in the human body^[27–29]. *LMNA* also encodes the protein lamin C2 found in germ cells that is encoded by an alternative first exon^[36].

B-type lamins in humans are encoded by the genes *LMNB1* and *LMNB2*^[37]. *LMNB1* is localized to chromosome 5q23.3–q31.1 and encodes the protein lamin B1^[25, 38]. A mutation in the *LMNB1* gene has been found to result in autosomal dominant leukodystrophy^[39]. *LMNB2* is localized to chromosome 19p13.3 and encodes lamin B2 and lamin B3^[37, 40]. A mutation in the *LMNB2* gene has been found to result in acquired partial lipodystrophy^[41, 42]. Currently, these are the only two disorders discovered to be associated with mutations in the B-type lamins.

Laminopathies

Almost all lamin mutations discovered to-date resulting in human disease are located within the *LMNA* gene. These

mutations result in several different clinical disorders with various phenotypes referred to as laminopathies; there are more than 10 clinical phenotypes that can be divided into four broad categories: myopathy, neuropathy, lipodystrophy and progeria, with overlap between groups. Well over 100 mutations have been discovered in the *LMNA* gene with the majority resulting in cardiac involvement. Over 90% of laminopathies are due to a nucleotide substitution^[21, 43].

In a large French pedigree, Bonne *et al*, in 1999^[30] discovered for the first time that a mutation (nonsense and missense) in the *LMNA* gene resulted in an inherited disorder, autosomal dominant Emery-Dreifuss muscular dystrophy (EDMD). Since that time several mutations, mostly missense, have been discovered throughout the *LMNA* gene resulting in EDMD. EDMD is characterized by contractures of the elbows and Achilles, muscle wasting with humeroperoneal weakness and cardiomyopathy with conduction disease. Symptoms begin within the first few years of life with difficulty ambulating. Cardiac involvement usually occurs after the onset of skeletal myopathy between the first and fourth decades of life resulting in conduction system disease (atrioventricular block; atrial and ventricular arrhythmias), dilated cardiomyopathy and sudden cardiac death^[43, 44]. Autosomal recessive EDMD is much less common with a few reported cases demonstrating an earlier phenotypic expression of skeletal myopathy, however, cardiac involvement has not been seen^[45, 46].

Limb girdle muscular dystrophy type 1B (LGMD1B) results primarily from a missense mutation with an autosomal dominant inheritance; several missense mutations located throughout the *LMNA* gene resulting in LGMD1B have been identified. Affected individuals develop progressive limb

girdle weakness with or without calf hypertrophy and dilated cardiomyopathy with conduction system disease may occur^[47]. Interestingly, a single nucleotide deletion at position 959 has been identified within exon 6 of the *LMNA* gene in one family resulting in different phenotypic expressions within the same family including LGMD1B-like symptoms, autosomal dominant EDMD-like symptoms and isolated dilated cardiomyopathy with conduction system disease^[48].

Specific mutations in the *LMNA* gene can result in isolated cardiac involvement in which the affected individuals develop dilated cardiomyopathy with or without conduction system disease. Dilated cardiomyopathy is a disorder of the myocyte characterized by cardiac dilation and systolic dysfunction^[49, 50]. Lamin mutations are likely the most common cause of idiopathic dilated cardiomyopathies. Approximately 30% of idiopathic dilated cardiomyopathies are inherited^[51-53]. Several mutations have been discovered, mostly missense mutations, located throughout the *LMNA* gene^[43]. An example of the natural history of this disease and evolution to the discovery of one of the *LMNA* genetic mutations is illustrated by the immigration of a young couple from Bavaria, Germany to Maryland, United States of America and then to central Ohio in 1830. Descendants of this couple in the 1960s presented to The Ohio State University Medical Center with high-grade atrioventricular (AV) block; careful family history revealed autosomal dominant inheritance after reconstructing an extensive nine generations pedigree. Following the family members closely for several decades, it was found that affected patients between 30 to 70 years of age also developed non-ischemic dilated cardiomyopathy; sudden cardiac death may also occur. Autopsy in several cases demonstrated severe fibrosis in the sinus node, AV node, atria and ventricles. Fibrosis was more severe in the atria compared to the ventricles fibrosis. More recently, ventricular fibrosis has been seen on cardiac magnetic resonance imaging. Family wide genotyping performed in family members revealed a 2-nucleotide pair deletion in the *LMNA* gene (cytosine in position 906 and thymine in position 907 at exon 5) resulting in a sequence of amino acid changes beginning at position 302 and eventually leading to the amino acid substitution of cysteine for serine at position 328 forming a premature stop codon with protein truncation^[54].

Charcot-Marie Tooth (CMT) disorders are the most common group of inherited neuropathies affecting 10 to 40 per 100 000 individuals. One sub-type, CMT2B1, is a sensorimotor axonal neuropathy with an autosomal recessive inheritance that results from a missense mutation in the *LMNA* gene^[34, 55]; ten Algerian families with CMT2B1 have demonstrated a missense mutation resulting in the substitution of the amino acid arginine for cysteine at position 298 (R298C)^[34, 56]. Onset of symptoms ranges from early childhood to early adulthood with distal muscle weakness and wasting occurring in the distal extremities, more evident in the legs compared to the arms. A sensory deficit may occur in the feet and lower extremities^[57]. There is one family from south France found to have an axonal neuropathy with cardiac involvement and an autosomal dominant inheritance. In this family, a missense

mutation was found to result in the substitution of the amino acid glutamic acid for aspartic acid at position 33 (E33D) leading to CMT, cardiomyopathy with conduction system disease, muscular dystrophy and leuconychia^[58].

Familial partial lipodystrophy of the Dunnigan-type (FPLD) has an autosomal dominance inheritance. FPLD most commonly occurs from a missense mutation in exon 8 of the *LMNA* gene resulting in the substitution of the amino acid arginine for tryptophan at position 482 (R482W) that encodes primarily the carboxyl terminal globular tail domain^[59]. FPLD primarily affects adipocyte cells with progressive loss of fat from the extremities and trunk with accumulation of fat in the face and neck^[60]. Further, affected individuals develop metabolic abnormalities including insulin resistance and glucose intolerance. Hypertriglyceridaemia may also occur. Onset of symptoms usually occurs at puberty^[59, 61].

Hutchison-Gilford progeria syndrome (HGPS) is a multi-system disorder characterized by premature aging. Majority of affected individuals with HGPS results from a *de novo* heterozygous single base substitution of cytosine for thymine at position 1824. This substitution results in an abnormal splice donor site in exon 11 of the *LMNA* gene that produces a lamin A protein lacking 50 amino acids from the carboxyl terminal globular tail domain^[35]. Affected individuals demonstrate skeletal abnormalities, micrognathia, mid-face hypoplasia, alopecia, loss of subcutaneous fat and pre-mature atherosclerosis. Most affected individuals die between the first and second decades of life from cardiovascular complications^[43]. HGPS has also been found to have an autosomal recessive inheritance in one consanguineous family where a missense mutation results in the amino acid substitution of lysine for asparagine at position 542 (K542N)^[62].

Mechanisms underlying laminopathies

Researchers have strived to elucidate why certain laminopathies result in specific tissue phenotypes even though lamin A/C essentially is found in all differentiated cells within the human body. In addition, different mutations have been shown to result in the same clinical phenotype. Moreover, the same single mutation can result in various phenotypic expressions^[63]. Several hypotheses have been postulated to explain these observations including: structural, gene expression, cell proliferation and protein-protein interaction; however, a specific laminopathy may not be exclusive to one hypothesis.

Structural hypothesis

A mutation in the *LMNA* gene producing abnormal lamin weakens the nuclear envelope and develops abnormal nuclear-cytoplasmic interactions, thus decreasing the structural integrity of the cell. These changes make the cell susceptible to mechanical stress potentially leading to cell death, especially striated muscle or cardiomyocytes that are exposed to mechanical stress^[64]. Embryonic fibroblasts obtained from *Lmna* knockout mice demonstrate the inability of the nuclear envelope to withstand physical force easily rupturing as compared to controls^[65]. Skeletal muscle biopsies obtained from

patients with autosomal EDMD and cardiac biopsies from patients with dilated cardiomyopathies have shown physical damage to the cells including ruptured nuclear envelopes and localization of chromatin into the cytoplasm^[66, 67]. In addition, fibroblasts from patients with HGP have shown to have an abnormal nuclear envelope shape, clustering of nuclear pores and loss of peripheral heterochromatin that worsen as the cells age^[68]. Fibroblast from FPLD patients also revealed abnormal nuclei structure and when exposed to heat stress had an increase in cell death compared to controls^[69].

Gene expression hypothesis

Lamin plays an important role in DNA repair and replication as well as transcriptional regulation, thus abnormal lamin will affect these functions^[18, 19, 70]. The disruption of the normal organization of lamin in mammalian cells has been shown to inhibit RNA polymerase II-dependent transcription^[71]. The gene expression hypothesis may particularly provide some insight in adipocyte disorders like FPLD. Peroxisome proliferator activator receptor gamma (PPAR γ) and sterol regulatory element binding protein-1 (SREBP1) are two of several genes that regulate adipogenesis. SREBP1 binds to pre-lamin A and also activates PPAR γ . Pre-lamin A in fibroblasts from patients with FPLD has been shown to accumulate at the nuclear envelope sequestering SREBP1, thus decreasing PPAR γ activation and in turn inhibiting adipogenesis^[72-75]. These findings may partially explain the progressive loss of fat in the extremities and trunk of individuals with FPLD. Further, deficient SREBP1 has been associated with type 2 diabetes mellitus, also seen in individuals with FPLD^[76].

Cell proliferation hypothesis

Stem cells fail to differentiate properly due to abnormal lamin within the cell. Individuals with HGPS have an increased production of progerin, a mutant form of the lamin A protein. Progerin accumulates near the nucleus altering the structure of the nuclear lamina. Studies have demonstrated that progerin interferes with the normal function of human mesenchymal stem cells (MSC) altering their ability to differentiate appropriately. MSC typically undergo differentiation to form several of the tissues affected in HGPS including bone (osteogenesis) and fat (adipogenesis); these effects are mediated by progerin activating downstream effectors of the Notch signaling pathway, a major regulator of human MSCs^[77]. Further, studies have shown that the differentiation of mouse skeletal stem cells, satellite cells, is associated with the relocation of nucleoplasmic lamin A/C to the nuclear lamina and reorganization of the nucleoskeleton; C2C12 myoblasts transfected with a mutant lamin A, known to cause autosomal dominant EDMD, prevented the relocation of lamin and reorganization of the nucleoskeleton, resulting in the inhibition of myoblast differentiation^[78].

Protein-protein interaction hypothesis

Altered lamin due to a *LMNA* gene mutation will develop an abnormal interaction with associated proteins resulting in

disorganized cell structure and in-turn cell dysfunction^[79-82]. Nikolova *et al*, demonstrated that in lamin A/C deficient mice the intermediate filament protein desmin, important in maintaining structural integrity of the cell, became disorganized and detached from the nuclear surface^[79, 83]. In addition, the inner nuclear envelope proteins nesprin and emerin, both important in maintaining cell structure, mis-localized to the endoplasmic reticulum in SW-13 cells which lack lamin A and re-localized to the inner nuclear envelope in SW 13/20 cells that contain lamin A^[80]. Cardiomyocytes of *LMNA* knockout mice demonstrated an altered nuclear envelope, disorganization of nesprin-1 and changes in the expression and distribution of nuclear and cytoskeletal actin^[84]. Studies by Raharjo *et al*^[82], showed that point mutations in lamin A/C resulting in the substitution of amino acids leucine for arginine at position 85 (L85R) and asparagine for lysine at position 195 (N195K), both known to cause dilated cardiomyopathy, altered the assembly of lamin A/C resulting in the partial mis-localization of emerin in HeLa cells; these findings were also seen in the point mutation resulting in the substitution of amino acid leucine for proline at position 530 (L530P), known to cause autosomal dominant EDMD^[82]. Further, eliminating lamin A/C from the nuclear envelope of HeLa cells resulted in emerin mis-localization and the formation of aggregates within the endoplasmic reticulum^[81].

Conclusions and perspectives

Lamins are intermediate filament proteins and are major components of the nuclear lamina playing an important role in cell regulation and structural integrity^[14-17]. There are well over 100 mutations in the *LMNA* gene, encoding for the protein lamin A/C, that result in more than 10 clinical disorders collectively referred to as laminopathies^[37, 43]. The challenge remains to determine why certain *LMNA* mutations result in tissue specific diseases, even though lamin A/C is found in all differentiated cells in the human body.

The laminopathy story is an elegant example of the importance of close collaboration that must exist between the physician-scientist and basic research-scientist in the study of heritable disorders. Careful physical examination of affected individuals and meticulous investigation of their family history allows the physician-scientist to understand the complexity of the disease, while the basic research-scientist helps in defining molecular mechanisms of that disease. Animal models, including *Lmna* knockout mice and mice carrying various *LMNA* missense mutations, have provided much insight into the mechanisms of laminopathies^[85-87]. Knowledge gained from the clinic and bench will help to better understand the underlying mechanisms, and will result in therapeutic strategies to treat affected individuals and provide insight into molecular mechanisms of other human diseases.

Acknowledgements

This work was supported by NIH (HL084583, HL083422 to PJM), Pew Scholars Trust (PJM), and Fondation Leducq Award (Alliance for Calmodulin Kinase Signaling in Heart

Disease (PJM).

References

- 1 Bhasin N, Cunha SR, Mudannayake M, Gigena MS, Rogers TB, Mohler PJ. Molecular basis for PP2A regulatory subunit B56(alpha) targeting in cardiomyocytes. *Am J Physiol Heart Circ Physiol* 2007; 293: H109–19.
- 2 Le Scouarnec S, Bhasin N, Veyres C, Hund TJ, Cunha SR, Koval O, *et al.* Dysfunction in ankyrin-B-dependent ion channel and transporter targeting causes human sinus node disease. *Proc Natl Acad Sci U S A* 2008; 105: 15617–22.
- 3 Mohler PJ, Le Scouarnec S, Denjoy I, Lowe JS, Guicheney P, Caron L, *et al.* Defining the cellular phenotype of “ankyrin-B syndrome” variants: human ANK2 variants associated with clinical phenotypes display a spectrum of activities in cardiomyocytes. *Circulation* 2007; 115: 432–41.
- 4 Mohler PJ, Schott JJ, Gramolini AO, Dilly KW, Guatimosim S, duBell WH, *et al.* Ankyrin-B mutation causes type 4 long-QT cardiac arrhythmia and sudden cardiac death. *Nature* 2003; 421: 634–9.
- 5 Mohler PJ, Splawski I, Napolitano C, Bottelli G, Sharpe L, Timothy K, *et al.* A cardiac arrhythmia syndrome caused by loss of ankyrin-B function. *Proc Natl Acad Sci U S A* 2004; 101: 9137–42.
- 6 Hund TJ, Koval O, Li J, Wright PJ, Qian L, Snyder JS, *et al.* A beta1V spectrin/CaMKII signaling complex is essential for vertebrate membrane excitability in mice. *J Clin Invest* 2010; 120: 3508–19.
- 7 Lowe JS, Palygin O, Bhasin N, Hund TJ, Boyden PA, Shibata E, *et al.* Voltage-gated Nav channel targeting in the heart requires an ankyrin-G dependent cellular pathway. *J Cell Biol* 2008; 180: 173–86.
- 8 Mohler PJ, Rivolta I, Napolitano C, Lemaillet G, Lambert S, Priori SG, *et al.* Nav1.5 E1053K mutation causing Brugada syndrome blocks binding to ankyrin-G and expression of Nav1.5 on the surface of cardiomyocytes. *Proc Natl Acad Sci U S A* 2004; 101: 17533–8.
- 9 Ueda K, Valdivia C, Medeiros-Domingo A, Tester DJ, Vatta M, Farrugia G, *et al.* Syntrophin mutation associated with long QT syndrome through activation of the nNOS-SCN5A macromolecular complex. *Proc Natl Acad Sci U S A* 2008; 105: 9355–60.
- 10 Vatta M, Ackerman MJ, Ye B, Makielski JC, Ughanze EE, Taylor EW, *et al.* Mutant caveolin-3 induces persistent late sodium current and is associated with long-QT syndrome. *Circulation* 2006; 114: 2104–12.
- 11 Piippo K, Swan H, Pasternack M, Chapman H, Paavonen K, Viitasalo M, *et al.* A founder mutation of the potassium channel KCNQ1 in long QT syndrome: implications for estimation of disease prevalence and molecular diagnostics. *J Am Coll Cardiol* 2001; 37: 562–8.
- 12 Chen L, Marquardt ML, Tester DJ, Sampson KJ, Ackerman MJ, Kass RS. Mutation of an A-kinase-anchoring protein causes long-QT syndrome. *Proc Natl Acad Sci U S A* 2007; 104: 20990–5.
- 13 London B, Michalec M, Mehdi H, Zhu X, Kerchner L, Sanyal S, *et al.* Mutation in glycerol-3-phosphate dehydrogenase 1 like gene (GPD1-L) decreases cardiac Na⁺ current and causes inherited arrhythmias. *Circulation* 2007; 116: 2260–8.
- 14 Aebi U, Cohn J, Buhle L, Gerace L. The nuclear lamina is a meshwork of intermediate-type filaments. *Nature* 1986; 323: 560–4.
- 15 Hutchison CJ. Lamins: building blocks or regulators of gene expression? *Nat Rev Mol Cell Biol* 2002; 3: 848–58.
- 16 Mattout-Drubezki A, Gruenbaum Y. Dynamic interactions of nuclear lamina proteins with chromatin and transcriptional machinery. *Cell Mol Life Sci* 2003; 60: 2053–63.
- 17 Stuurman N, Heins S, Aebi U. Nuclear lamins: their structure, assembly, and interactions. *J Struct Biol* 1998; 122: 42–66.
- 18 Dechat T, Pflieger K, Sengupta K, Shimi T, Shumaker DK, Solimando L, *et al.* Nuclear lamins: major factors in the structural organization and function of the nucleus and chromatin. *Genes Dev* 2008; 22: 832–53.
- 19 Prokocimer M, Davidovich M, Nissim-Rafinia M, Wiesel-Motiuk N, Bar DZ, Barkan R, *et al.* Nuclear lamins: key regulators of nuclear structure and activities. *J Cell Mol Med* 2009; 13: 1059–85.
- 20 Foster CR, Przyborski SA, Wilson RG, Hutchison CJ. Lamins as cancer biomarkers. *Biochem Soc Trans* 2010; 38: 297–300.
- 21 Zaremba-Czogalla M, Dubinska-Magiera M, Rzepecki R. Lamino-pathies: the molecular background of the disease and the prospects for its treatment. *Cell Mol Biol Lett* 2011; 16: 114–48.
- 22 Krohne G, Benavente R. The nuclear lamins. A multigene family of proteins in evolution and differentiation. *Exp Cell Res* 1986; 162: 1–10.
- 23 Gerace L, Blobel G. The nuclear envelope lamina is reversibly depolymerized during mitosis. *Cell* 1980; 19: 277–87.
- 24 Herrmann H, Bar H, Kreplak L, Strelkov SV, Aebi U. Intermediate filaments: from cell architecture to nanomechanics. *Nat Rev Mol Cell Biol* 2007; 8: 562–73.
- 25 Wydner KL, McNeil JA, Lin F, Worman HJ, Lawrence JB. Chromosomal assignment of human nuclear envelope protein genes LMNA, LMNB1, and LBR by fluorescence *in situ* hybridization. *Genomics* 1996; 32: 474–8.
- 26 Lin F, Worman HJ. Structural organization of the human gene encoding nuclear lamin A and nuclear lamin C. *J Biol Chem* 1993; 268: 16321–6.
- 27 Kass S, MacRae C, Graber HL, Sparks EA, McNamara D, Boudoulas H, *et al.* A gene defect that causes conduction system disease and dilated cardiomyopathy maps to chromosome 1p1-1q1. *Nat Genet* 1994; 7: 546–51.
- 28 Taylor MR, Fain PR, Sinagra G, Robinson ML, Robertson AD, Carniel E, *et al.* Natural history of dilated cardiomyopathy due to lamin A/C gene mutations. *J Am Coll Cardiol* 2003; 41: 771–80.
- 29 Fatkin D, MacRae C, Sasaki T, Wolff MR, Porcu M, Frenneaux M, *et al.* Missense mutations in the rod domain of the lamin A/C gene as causes of dilated cardiomyopathy and conduction-system disease. *N Engl J Med* 1999; 341: 1715–24.
- 30 Bonne G, Di Barletta MR, Varnous S, Becane HM, Hammouda EH, Merlini L, *et al.* Mutations in the gene encoding lamin A/C cause autosomal dominant Emery-Dreifuss muscular dystrophy. *Nat Genet* 1999; 21: 285–8.
- 31 di Barletta MR, Viatchenko-Karpinski S, Nori A, Memmi M, Terentyev D, Turcato F, *et al.* Clinical phenotype and functional characterization of CASQ2 mutations associated with catecholaminergic polymorphic ventricular tachycardia. *Circulation* 2006; 114: 1012–9.
- 32 Muchir A, Bonne G, van der Kooij AJ, van Meegen M, Baas F, Bolhuis PA, *et al.* Identification of mutations in the gene encoding lamins A/C in autosomal dominant limb girdle muscular dystrophy with atrioventricular conduction disturbances (LGMD1B). *Hum Mol Genet* 2000; 9: 1453–9.
- 33 Shackleton S, Lloyd DJ, Jackson SN, Evans R, Niermeijer MF, Singh BM, *et al.* LMNA, encoding lamin A/C, is mutated in partial lipodystrophy. *Nat Genet* 2000; 24: 153–6.
- 34 De Sandre-Giovannoli A, Chaouch M, Kozlov S, Vallat JM, Tazir M, Kassouri N, *et al.* Homozygous defects in LMNA, encoding lamin A/C nuclear-envelope proteins, cause autosomal recessive axonal neuropathy in human (Charcot-Marie-Tooth disorder type 2) and mouse. *Am J Hum Genet* 2002; 70: 726–36.
- 35 Eriksson M, Brown WT, Gordon LB, Glynn MW, Singer J, Scott L, *et al.* Recurrent *de novo* point mutations in lamin A cause Hutchinson-Gilford progeria syndrome [Research Support, Non-US Gov't]. *Nature* 2003; 423: 293–8.

- 36 Furukawa K, Inagaki H, Hotta Y. Identification and cloning of an mRNA coding for a germ cell-specific A-type lamin in mice. *Exp Cell Res* 1994; 212: 426–30.
- 37 Worman HJ, Bonne G. “Laminopathies”: a wide spectrum of human disease. *Exp Cell Res* 2007; 313: 2121–33.
- 38 Lin F, Worman HJ. Structural organization of the human gene (LMNB1) encoding nuclear lamin B1. *Genomics* 1995; 27: 230–6.
- 39 Padiath QS, Saigoh K, Schiffmann R, Asahara H, Yamada T, Koeppen A, *et al*. Lamin B1 duplications cause autosomal dominant leukodystrophy. *Nat Genet* 2006; 38: 1114–23.
- 40 Furukawa K, Hotta Y. cDNA cloning of a germ cell specific lamin B3 from mouse spermatocytes and analysis of its function by ectopic expression in somatic cells. *EMBO J* 1993; 12: 97–106.
- 41 Hegele RA, Cao H, Liu DM, Costain GA, Charlton-Menys V, Rodger NW, *et al*. Sequencing of the reannotated LMNB2 gene reveals novel mutations in patients with acquired partial lipodystrophy. *Am J Hum Genet* 2006; 79: 383–9.
- 42 Hegele RA, Oshima J. Phenomics and lamins: from disease to therapy. *Exp Cell Res* 2007; 313: 2134–43.
- 43 Rankin J, Ellard S. The laminopathies: a clinical review. *Clin Genet* 2006; 70: 261–74.
- 44 Emery AE. The muscular dystrophies. *Lancet* 2002; 359: 687–95.
- 45 Sanna T, Dello Russo A, Toniolo D, Vytopil M, Pelargonio G, De Martino G, *et al*. Cardiac features of Emery-Dreifuss muscular dystrophy caused by lamin A/C gene mutations. *Eur Heart J* 2003; 24: 2227–36.
- 46 Raffaele Di Barletta M, Ricci E, Galluzzi G, Tonali P, Mora M, Morandi L, *et al*. Different mutations in the LMNA gene cause autosomal dominant and autosomal recessive Emery-Dreifuss muscular dystrophy. *Am J Human Genet* 2000; 66: 1407–12.
- 47 Bushby KM. The limb-girdle muscular dystrophies-multiple genes, multiple mechanisms. *Hum Mol Genet* 1999; 8: 1875–82.
- 48 Brodsky GL, Muntoni F, Miodic S, Sinagra G, Sewry C, Mestroni L. Lamin A/C gene mutation associated with dilated cardiomyopathy with variable skeletal muscle involvement. *Circulation* 2000; 101: 473–6.
- 49 Kasper EK, Agema WR, Hutchins GM, Deckers JW, Hare JM, Baughman KL. The causes of dilated cardiomyopathy: a clinicopathologic review of 673 consecutive patients. *J Am Coll Cardiol* 1994; 23: 586–90.
- 50 Fatkin D, Graham RM. Molecular mechanisms of inherited cardiomyopathies. *Physiol Rev* 2002; 82: 945–80.
- 51 Michels VV, Moll PP, Miller FA, Tajik AJ, Chu JS, Driscoll DJ, *et al*. The frequency of familial dilated cardiomyopathy in a series of patients with idiopathic dilated cardiomyopathy. *New Engl J Med* 1992; 326: 77–82.
- 52 Grunig E, Tasman JA, Kucherer H, Franz W, Kubler W, Katus HA. Frequency and phenotypes of familial dilated cardiomyopathy. *J Am Coll Cardiol* 1998; 31: 186–94.
- 53 Keeling PJ, Gang Y, Smith G, Seo H, Bent SE, Murday V, *et al*. Familial dilated cardiomyopathy in the United Kingdom. *Br Heart J* 1995; 73: 417–21.
- 54 Sparks EA, Boudoulas KD, Raman SV, Sasaki T, Graber HL, Seidman CE, *et al*. Heritable cardiac conduction and myocardial disease: from the clinic to the laboratory and from the laboratory back to the clinic. *Cardiology* 2011; In Press.
- 55 Pareyson D, Marchesi C. Diagnosis, natural history, and management of Charcot-Marie-Tooth disease. *Lancet Neurol* 2009; 8: 654–67.
- 56 Tazir M, Azzedine H, Assami S, Sindou P, Nouioua S, Zemmouri R, *et al*. Phenotypic variability in autosomal recessive axonal Charcot-Marie-Tooth disease due to the R298C mutation in lamin A/C. *Brain* 2004; 127: 154–63.
- 57 Bienfait HM, Baas F, Koelman JH, de Haan RJ, van Engelen BG, Gabreels-Festen AA, *et al*. Phenotype of Charcot-Marie-Tooth disease type 2. *Neurology* 2007; 68: 1658–67.
- 58 Goizet C, Yaou RB, Demay L, Richard P, Bouillot S, Rouanet M, *et al*. A new mutation of the lamin A/C gene leading to autosomal dominant axonal neuropathy, muscular dystrophy, cardiac disease, and leukonychia. *J Med Genet* 2004; 41: e29.
- 59 Vantyghem MC, Pigny P, Maurage CA, Rouaix-Emery N, Stojkovic T, Cuisset JM, *et al*. Patients with familial partial lipodystrophy of the Dunnigan type due to a LMNA R482W mutation show muscular and cardiac abnormalities. *J Clin Endocrinol Metab* 2004; 89: 5337–46.
- 60 Garg A, Peshock RM, Fleckenstein JL. Adipose tissue distribution pattern in patients with familial partial lipodystrophy (Dunnigan variety). *J Clin Endocrinol Metab* 1999; 84: 170–4.
- 61 Speckman RA, Garg A, Du F, Bennett L, Veile R, Arioglu E, *et al*. Mutational and haplotype analyses of families with familial partial lipodystrophy (Dunnigan variety) reveal recurrent missense mutations in the globular C-terminal domain of lamin A/C. *Am J Hum Genet* 2000; 66: 1192–8.
- 62 Plasilova M, Chattopadhyay C, Pal P, Schaub NA, Buechner SA, Mueller H, *et al*. Homozygous missense mutation in the lamin A/C gene causes autosomal recessive Hutchinson-Gilford progeria syndrome. *J Med Genet* 2004; 41: 609–14.
- 63 Scharner J, Gnocchi VF, Ellis JA, Zammit PS. Genotype-phenotype correlations in laminopathies: how does fate translate? *Biochem Soc Trans* 2010; 38: 257–62.
- 64 Broers JL, Ramaekers FC, Bonne G, Yaou RB, Hutchison CJ. Nuclear lamins: laminopathies and their role in premature ageing. *Physiol Rev* 2006; 86: 967–1008.
- 65 Broers JL, Peeters EA, Kuijpers HJ, Ender J, Bouten CV, Oomens CW, *et al*. Decreased mechanical stiffness in LMNA^{-/-} cells is caused by defective nucleo-cytoskeletal integrity: implications for the development of laminopathies. *Hum Mol Genet* 2004; 13: 2567–80.
- 66 Fidzianska A, Hausmanowa-Petrusewicz I. Architectural abnormalities in muscle nuclei. Ultrastructural differences between X-linked and autosomal dominant forms of EDMD. *J Neurol Sci* 2003; 210: 47–51.
- 67 Arbustini E, Pilotto A, Repetto A, Grasso M, Negri A, Diegoli M, *et al*. Autosomal dominant dilated cardiomyopathy with atrioventricular block: a lamin A/C defect-related disease. *J Am Coll Cardiol* 2002; 39: 981–90.
- 68 Goldman RD, Shumaker DK, Erdos MR, Eriksson M, Goldman AE, Gordon LB, *et al*. Accumulation of mutant lamin A causes progressive changes in nuclear architecture in Hutchinson-Gilford progeria syndrome. *Proc Natl Acad Sci US A* 2004; 101: 8963–8.
- 69 Vigouroux C, Auclair M, Dubosclard E, Pouchelet M, Capeau J, Courvalin JC, *et al*. Nuclear envelope disorganization in fibroblasts from lipodystrophic patients with heterozygous R482Q/W mutations in the lamin A/C gene. *J Cell Sci* 2001; 114: 4459–68.
- 70 Bridger JM, Foeger N, Kill IR, Herrmann H. The nuclear lamina. Both a structural framework and a platform for genome organization. *FEBS J* 2007; 274: 1354–61.
- 71 Spann TP, Goldman AE, Wang C, Huang S, Goldman RD. Alteration of nuclear lamin organization inhibits RNA polymerase II-dependent transcription. *J Cell Biol* 2002; 156: 603–8.
- 72 Akerblad P, Mansson R, Lagergren A, Westerlund S, Basta B, Lind U, *et al*. Gene expression analysis suggests that EBF-1 and PPARgamma2 induce adipogenesis of NIH-3T3 cells with similar efficiency and kinetics. *Physiol Genomics* 2005; 23: 206–16.
- 73 Kim JB, Spiegelman BM. ADD1/SREBP1 promotes adipocyte differentiation and gene expression linked to fatty acid metabolism.

- Genes Dev 1996; 10: 1096–107.
- 74 Lloyd DJ, Trembath RC, Shackleton S. A novel interaction between lamin A and SREBP1: implications for partial lipodystrophy and other laminopathies. *Hum Mol Genet* 2002; 11: 769–77.
- 75 Capanni C, Mattioli E, Columbaro M, Lucarelli E, Parnaik VK, Novelli G, *et al*. Altered pre-lamin A processing is a common mechanism leading to lipodystrophy. *Hum Mol Genet* 2005; 14: 1489–502.
- 76 Sewter C, Berger D, Considine RV, Medina G, Rochford J, Ciaraldi T, *et al*. Human obesity and type 2 diabetes are associated with alterations in SREBP1 isoform expression that are reproduced *ex vivo* by tumor necrosis factor- α . *Diabetes* 2002; 51: 1035–41.
- 77 Scaffidi P, Misteli T. Lamin A-dependent misregulation of adult stem cells associated with accelerated ageing. *Nat Cell Biol* 2008; 10: 452–9.
- 78 Markiewicz E, Ledran M, Hutchison CJ. Remodelling of the nuclear lamina and nucleoskeleton is required for skeletal muscle differentiation *in vitro*. *J Cell Sci* 2005; 118: 409–20.
- 79 Nikolova V, Leimena C, McMahon AC, Tan JC, Chandar S, Jogia D, *et al*. Defects in nuclear structure and function promote dilated cardiomyopathy in lamin A/C-deficient mice. *J Clin Invest* 2004; 113: 357–69.
- 80 Zhang Q, Ragnauth CD, Skepper JN, Worth NF, Warren DT, Roberts RG, *et al*. Nesprin-2 is a multi-isomeric protein that binds lamin and emerin at the nuclear envelope and forms a subcellular network in skeletal muscle. *J Cell Sci* 2005; 118: 673–87.
- 81 Vaughan A, Alvarez-Reyes M, Bridger JM, Broers JL, Ramaekers FC, Wehnert M, *et al*. Both emerin and lamin C depend on lamin A for localization at the nuclear envelope. *J Cell Sci* 2001; 114: 2577–90.
- 82 Raharjo WH, Enarson P, Sullivan T, Stewart CL, Burke B. Nuclear envelope defects associated with LMNA mutations cause dilated cardiomyopathy and Emery-Dreifuss muscular dystrophy. *J Cell Sci* 2001; 114: 4447–57.
- 83 Paulin D, Li Z. Desmin: a major intermediate filament protein essential for the structural integrity and function of muscle. *Exp Cell Res* 2004; 301: 1–7.
- 84 Nikolova-Krstevski V, Leimena C, Xiao XH, Kesteven S, Tan JC, Yeo LS, *et al*. Nesprin-1 and actin contribute to nuclear and cytoskeletal defects in lamin A/C-deficient cardiomyopathy. *J Mol Cell Cardiol* 2011; 50: 479–86.
- 85 Sullivan T, Escalante-Alcalde D, Bhatt H, Anver M, Bhat N, Nagashima K, *et al*. Loss of A-type lamin expression compromises nuclear envelope integrity leading to muscular dystrophy. *J Cell Biol* 1999; 147: 913–20.
- 86 Mounkes LC, Kozlov SV, Rottman JN, Stewart CL. Expression of an LMNA-N195K variant of A-type lamins results in cardiac conduction defects and death in mice. *Hum Mol Genet* 2005; 14: 2167–80.
- 87 Wang Y, Herron AJ, Worman HJ. Pathology and nuclear abnormalities in hearts of transgenic mice expressing M371K lamin A encoded by an LMNA mutation causing Emery-Dreifuss muscular dystrophy. *Hum Mol Genet* 2006; 15: 2479–89.

Review

Drug discovery for polycystic kidney disease

Ying SUN, Hong ZHOU, Bao-xue YANG*

Department of Pharmacology, School of Basic Medical Sciences, Peking University, and Key Laboratory of Molecular Cardiovascular Sciences, Ministry of Education, Beijing 100191, China

In polycystic kidney disease (PKD), a most common human genetic diseases, fluid-filled cysts displace normal renal tubules and cause end-stage renal failure. PKD is a serious and costly disorder. There is no available therapy that prevents or slows down the cystogenesis and cyst expansion in PKD. Numerous efforts have been made to find drug targets and the candidate drugs to treat PKD. Recent studies have defined the mechanisms underlying PKD and new therapies directed toward them. In this review article, we summarize the pathogenesis of PKD, possible drug targets, available PKD models for screening and evaluating new drugs as well as candidate drugs that are being developed.

Keywords: polycystic kidney disease; drug discovery; kidney; candidate drugs; animal model

Acta Pharmacologica Sinica (2011) 32: 805–816; doi: 10.1038/aps.2011.29

Introduction

Polycystic kidney disease (PKD), an inherited human renal disease, is characterized by massive enlargement of fluid-filled renal tubular and/or collecting duct cysts^[1]. Progressively enlarging cysts compromise normal renal parenchyma, often leading to renal failure. The occurrence of autosomal dominant polycystic kidney disease (ADPKD) is estimated to be between 1 in 1000 and 1 in 400 individuals by a study in Olmsted Country, MN^[2]. ADPKD is caused by mutations in one of two genes (*Pkd1* and *Pkd2*) expressing the interacting polycystic proteins polycystin-1 (PC1) and polycystin-2 (PC2) in renal tubular epithelia^[3, 4]. Mutation of *Pkd1* accounts for approximately 85% cases in clinically identified patients^[5]. PC1 is a membrane receptor capable of binding and interacting with many proteins, including carbohydrates and lipids, and eliciting intracellular responses through phosphorylation pathways^[6, 7]. PC2 is thought to act as a calcium permeable channel^[8, 9]. PC1 and PC2 form a complex that localizes to primary cilia^[10, 11]. The polycystin complex has a role in the regulation of the proliferation, differentiation and morphogenesis of renal tubular cells through interactions with protein complexes linked to the actin cytoskeleton, intracellular signaling cascades, and the regulation of gene transcription^[12, 13] (Figure 1). In ADPKD, the thousands of large, spherical cysts of various sizes throughout the cortex and medulla are derived from

the segments of the nephron. Autosomal recessive polycystic kidney disease (ARPKD) results primarily from the mutations in a single gene, *Pkhd1*^[14]. Its frequency is estimated to be one per 20000 individuals. The PKHD1 protein, fibrocystin, has been found to be localized to primary cilia and the basal bodies. The exact function of fibrocystin has not been demonstrated. In ARPKD, smaller, elongated cysts arise as ecstatic expansions of collecting ducts. Patients with PKD often require dialysis and kidney transplantation, which are exceedingly costly. There are currently no approved drug or preventive strategies for PKD.

Mechanisms of renal cyst formation and enlargement in PKD

The development and growth of PKD cysts involve the abnormal proliferation and apoptosis of immature epithelial cells, accumulation of fluid within the cyst cavity, abnormal cell-cell/cell-matrix interactions and abnormal cilia function.

Role of epithelial cell proliferation and apoptosis in cyst development in PKD

Increased apoptosis and proliferative capacity in renal epithelial cells are essential processes in PKD. While the proliferation of renal tubular epithelial cells halts before birth in normal individuals, cystic epithelia proliferate throughout life in patients with ADPKD^[15]. Several genetic manipulations that increase the proliferation of tubular epithelial cells in mice result in PKD^[16–19].

Epidermal growth factor (EGF), transforming growth fac-

* To whom correspondence should be addressed.

E-mail baoxue@bjmu.edu.cn

Received 2011-02-06 Accepted 2011-03-17

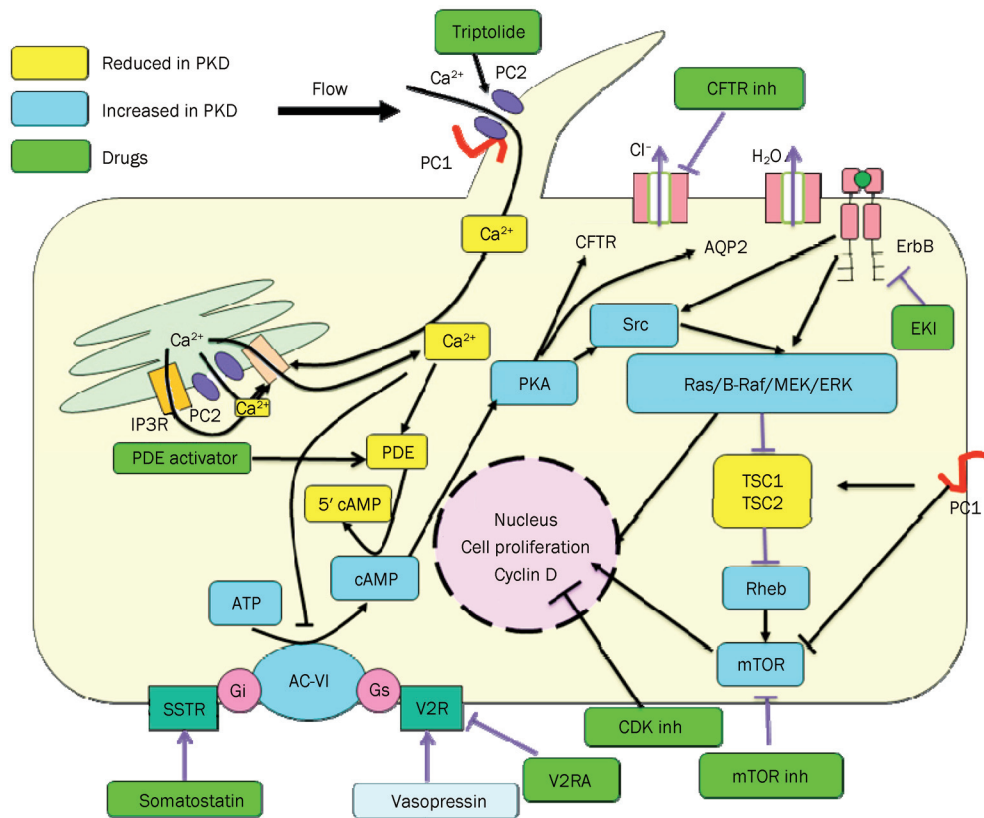


Figure 1. A diagram depicting the effects that PC1 and PC2 exert on signaling pathways. Multiple direct and indirect interactions allow the polycystin proteins to be inhibited or stimulated. Pathways involved in cell proliferation and liquid secretion.

tor alpha (TGF- α) and EGF receptor (EGFR) promote cystic epithelial proliferation and expand renal cysts. EGFR is over-expressed and mislocalized to the apical membranes of cystic epithelial cells, which leads to a sustained stimulation of cell proliferation in the cysts^[20]. Increased intracellular cAMP level also plays a crucial role in cystogenesis. The reduced calcium caused by mutation of Pkd1 or Pkd2 can inhibit adenylyl cyclase 6 leading to increased cAMP. Studies have demonstrated that cAMP inhibits the proliferation of normal renal epithelial cells. In contrast, cAMP promotes the proliferation of cells derived from PKD patients^[21]. The switch is caused by decreased intracellular calcium levels in a polycystic kidney leading to cAMP-mediated stimulation of the B-Raf/MEK/ERK pathway instead of inhibiting the Ras/Raf/MEK/ERK pathway like in the normal kidney^[22]. B-Raf is inhibited by Akt in normal cells, while it is activated because of decreased activation of Akt in calcium-restricted cells. Inhibitors of Akt and PI3K can reproduce the effects of calcium reduction. However, activation of Akt has been found in animal models of PKD, such as Pkd^{-/-} mice, Han:SPRD rats and jck mice. Additional growth factors, cytokines, lipid factors, and adenosine triphosphate (ATP) also participate in regulating the proliferation of renal epithelial cells^[23–25]. Cell apoptosis is also a key factor in the development of PKD. Knocking out the anti-apoptotic Bcl-2 and AP-2 genes or overexpression of the pro-apoptotic gene c-myc in mice results in renal cystogenesis^[26].

Role of fluid secretion in cyst development in PKD

Fluid secretion is a critical pathogenic mechanism associated with cyst formation and growth in PKD. Fluid secretion, coupled with epithelial hyperplasia, is necessary and sufficient to account for the dynamics of cyst growth. In PKD, a large number of cystic lesions lack afferent and efferent tubule connections, suggesting that cysts, which arise from tubular segments, become disconnected from the glomerular filtrate. The development and expansion of cystic lesions therefore requires net transepithelial fluid secretion. An extensive body of *in vitro* data implicates epithelial chloride secretion in the generation and maintenance of fluid-filled cysts^[27]. The fluid secretion is driven by mechanisms that are similar to those found in other secretory epithelia. Chloride movement drives fluid into the cyst lumen. Fluid accumulation causes cyst enlargement directly by swelling cysts and indirectly by stretching cells to promote cell division^[28].

Cystic fibrosis transmembrane conductance regulator (CFTR), a cAMP-regulated chloride channel, is present on the apical membranes of many secretory epithelia. Chloride secretion through the CFTR has been implicated in the pathway of fluid secretion in PKD. *In vitro* experiments have suggested that increased cAMP-mediated chloride secretion provides the electrochemical driving force for fluid secretion in cystic epithelia^[29]. CFTR is expressed in the apical membrane of intact cysts dissected from PKD kidneys^[30]. An important role of CFTR in PKD fluid secretion is also supported by the observation that interference with CFTR protein production

(by treatment of ADPKD monolayers with antisense oligonucleotide against human CFTR) dramatically reduced fluid secretion by these cells^[27]. Additional evidence supporting a role of CFTR in chloride secretion was obtained from immortalized cystic murine collecting duct cell lines isolated from CFTR mutant and CFTR wild-type mice. The wild-type cell lines formed numerous fluid-filled cysts in response to EGF and forskolin when cultured in three-dimensional collagen gels, whereas the CFTR mutant cell lines failed to form cysts under identical conditions^[31]. These results demonstrate that CFTR is required for *in vitro* cyst formation. In a single family affected with both ADPKD and cystic fibrosis (CF), individual members with both ADPKD and CF had less severe renal disease than those family members with only ADPKD^[32, 33]. These studies suggest that *in vivo*, defective CFTR function provides partial protection against renal cyst development and enlargement and suggests that modulation of epithelial chloride secretion may have therapeutic benefit in PKD. Using type I MDCK cells as a cell culture model of cyst development and growth, Sheppard's group found that the CFTR inhibitor CFTR_{inh}-172 (see below) retarded cyst growth. In contrast, blockers of other types of apical membrane Cl⁻ channels, which do not inhibit CFTR, failed to inhibit cyst growth^[28]. Inhibition of cyst growth by CFTR inhibitors correlated with inhibition of cAMP-stimulated Cl⁻ current, but not cell proliferation^[28]. Their studies strongly suggest that CFTR inhibitors might retard cyst growth predominantly by inhibiting fluid accumulation within the cyst lumen. In two ADPKD animal models, PCK rats and the pcy mice, renal cAMP levels were significantly higher compared to that in wild-type animals. Expression of the water channel AQP2 and vasopressin V2 receptor (VPV2R) was also increased. Administration of the VPV2R antagonist OPC-31260 lowered renal cAMP levels and halted progression or caused regression of established cysts^[33, 34].

Aquaporin (AQP)-mediated water permeability in cyst epithelia may also be involved in fluid secretion in cyst formation and progression, as fluid consists of salts and water. Normally, several AQPs are expressed in kidney: AQP1 in the proximal tubule, thin descending limb of Henle, and vasa recta; AQP2 in the apical membranes of collecting duct; AQP3 and AQP4 in the basolateral membranes of collecting duct. It has been reported that AQP1 and AQP2 are expressed in cyst epithelia from patients with PKD^[35]. Gattone *et al*^[36] found AQP2 and AQP3 expression in cysts in C57BL/6J-cpk/cpk mice with autosomal recessive-infantile polycystic kidney disease. High aquaporin-dependent water permeability in cyst epithelium may be important to facilitate near-isosmolar fluid secretion, particularly in growing cysts that have low surface-to-volume ratios.

Role of cell-cell/cell-matrix interactions in cyst development in PKD

PC1 has been detected in tight junctions, adhesions junctions, desmosomes, focal adhesions, apical vesicles, and primary cilia^[37, 38]. A study has shown that PC1 mediates cell-cell adhesion through the formation of strong homophilic interaction of

its Ig-like domains^[39]. A significant downregulation of Pkd1 mRNA is detected in MDCK cysts compared to tubules, which leads to a striking reduction of membrane PC1 and mislocalization to the cytoplasmic pools^[40]. It has been demonstrated that a controlled level of PC1 expressed at cell-cell junction is critical for normal tubular differentiation. In normal renal cells, PC1 forms a complex with the protein E-cadherin and its catenins. However, in primary cells from ADPKD patients, the PC1/E-cadherin/ β -catenin complex was disrupted and was accompanied by increased PC1 phosphorylation, reduced E-cadherin and upregulated normal mesenchymal N-cadherin^[41].

Renal epithelial cells in ADPKD show increased PC1 adhesion to type I collagen compared with normal human epithelia^[42]. The defects reduce the cell migratory capacity required for kidney morphogenesis^[43]. The PC1 protein has been proven to regulate the relationships between the cell and matrix through interacting with α 1 β 2 integrin, vinculin, paxillin, p130-cas, talin and focal adhesion kinase (FAK)^[42]. The basement-membrane composition and expression of matrix metalloproteases and their inhibitors are abnormal in PKD kidneys. It has been demonstrated that inactivation of several matrix adhesion receptors and focal adhesion complex-associated proteins result in cystogenesis^[44-46].

Role of cilia in cyst development in PKD

Renal cilia are microtubule-based, membrane-bound projections on the epithelia of the renal tubule and duct. Renal cilia have been reported to be mechanosensors and respond to flow by increasing intracellular calcium^[47]. Several studies support that PC1 and PC2 localize to primary cilia^[10, 38] and form a subfamily of transient receptor potential channels that are responsible for sensing flow and regulating levels of intracellular calcium^[48]. The bending of cilia causes calcium influx into the cell through the PC2 channel^[42]. The mechanosensory response is lost in cells with mutated PC1^[48]. Many cellular functions that are related to PKD, such as gene expression, cell cycle, differentiation and apoptosis, are regulated by intracellular calcium concentration.

The dysfunction of cilia has a close relationship with cell cycle progression^[49, 50]. PC1 upregulates p21 (waf1) through activating the JAK-STAT pathway and results in cell cycle arrest in G₀/G₁^[23]. The IFT88/Polaris protein, which is localized to cilia, has been demonstrated to be tightly associated with the centrosome during cell cycle transition^[51]. Overexpression of IFT88/Polaris prevents G₁/S transition and induces cell death. In contrast, deletion of IFT88/Polaris promotes cell cycle progression^[51]. PC2 also can regulate the cell cycle through direct interaction with Id2, a member of the helix-loop-helix (HLH) protein family, which has been proven to regulate cell proliferation and differentiation^[52].

Experimental models for screening and evaluating new drugs for PKD

Several common experimental models that have been used to screen and evaluate the new PKD drugs at the cell, organ and

whole animal levels are described in subsequent sections.

Madin-Darby canine kidney (MDCK) cyst model

MDCK type I cells provide a useful *in vitro* model of cystogenesis for screening candidate inhibitors of cyst formation and growth (Figure 2). MDCK cells cultured in three-dimensional collagen gels with forskolin produce a polarized, single-layer, thinned epithelium surrounding a fluid-filled space similar to the cysts in PKD^[53]. MDCK cells in cysts undergo proliferation, fluid transport and matrix remodeling, as seen in tubular epithelial cells cultured from PKD kidneys. Cyst formation and growth are cAMP-dependent, which is thought to independently increase cell proliferation and activate CFTR-facilitated transepithelial fluid secretion^[28]. Recognizing its limitations, such as differences between MDCK cells versus renal epithelial cells and cell cultures versus intact kidneys, the MDCK cyst model may be used to identify cyst inhibitors that reduce cyst formation and enlargement without demonstrable cell toxicity or inhibition of cell proliferation.

Embryonic kidney cyst model

The embryonic kidney culture model permits organotypic growth and differentiation of renal tissue in defined medium without the confounding effects of circulating hormones and glomerular filtration^[54]. In the absence of 8-Br-cAMP, kidneys cultured on porous cell culture inserts increase in size over 4 d, whereas numerous cystic structures were seen in the presence of 8-Br-cAMP (Figure 3). Although embryonic kidney cultures probably represent a better PKD model than MDCK cells, they are avascular and non-perfused and therefore are not exposed to the same environment as the *in vivo* kidney.

PKD mouse models

Pkd1^{flox/-};Ksp-Cre mice, are kidney-selective Pkd1 knockout mice that manifest a fulminant course with the development of large cysts (Figure 4), renal failure in the first 2 weeks of life and death by 20 d. This model is suitable to evaluate the efficacy of cyst inhibitors on retarding the growth of cysts in the distal segments of the nephron, including the medullary thick ascending limbs of the loops of Henle, distal convoluted tubule and collecting ducts. In humans, ADPKD develops slowly and causes renal failure at an average age of over 50 years. For experimental studies, this relatively severe model of ADPKD has been used, rather than mouse models in which disease develops more slowly because of the shorter time required for compound administration and the greater likelihood of observing an immediate benefit. Testing cyst inhibitors in the ADPKD mouse model should be of further utility in predicting efficacy in human ADPKD. The CFTR inhibitors significantly reduced cyst formation and clinical signs of PKD, as assessed by lower kidney weights and serum creatinine and urea concentrations in this mouse model^[55].

Pkd1^{flox} mice and Ksp-Cre transgenic mice have been generated as described^[56, 57]. Ksp-Cre mice express Cre recombinase in the kidney under the control of the Ksp-cadherin promoter^[58]. Pkd1^{flox/-}; Ksp-Cre mice were generated by cross-

breeding Pkd1^{flox/flox} mice with Pkd1^{+/-};Ksp-Cre mice^[56]. Neonatal mice (age 1 d) were genotyped by genomic PCR. Test compound or saline DMSO vehicle control were administered by subcutaneous injection on the backs of neonatal mice four times a day for 3 or 7 d using a 1 mL insulin syringe beginning at age 2 d. Pkd1^{flox/+}; Ksp-Cre or Pkd1^{flox/+} mice from the same litter were used as controls. Body weight was measured at d 5. Blood and urine samples were collected to measure the test compound concentration and renal function. The kidneys were removed, weighed, and fixed for histological examination or homogenized to determine the test compound content.

Many other mouse models of PKD have been described in which the mutant phenotypes result from spontaneous mutations or gene-specific targeting in mouse orthologs of human PKD genes. These murine phenotypes closely resemble human PKD with common abnormalities observed in the tubular epithelia, interstitial compartment, and extracellular matrix of cystic kidneys^[59].

Pkd1 and Pkd2 knockout mouse models, which are homologs of human genes, have been generated by targeted mutagenesis^[59, 60]. In most of these models, heterozygous mice develop renal, biliary, and pancreatic cysts at age 4–19 months. Disease progression is rapid, with embryonic lethality occurring in most homozygous mutants.

In the mouse models arising from spontaneous mutations, PKD is generally transmitted as an autosomal recessive trait. Several of these models with cysts distributed along the entire nephron and slower disease progression closely recapitulate human ADPKD^[59]. One of them is the murine autosomal recessive juvenile cystic kidney (jck)^[61]. The jck locus maps to chromosome 11. The mutant allele has a missense change in Nek8, which encodes NIMA (for 'never in mitosis' A)-related kinase 8^[62]. In homozygous mutant mice, focal renal cysts are evident as early as 3 d of life, and the renal cystic disease is slowly progressive but not evident by kidney palpation until age 4 to 5 weeks. Histological analysis of jck mutant kidney tubules showed the defects were specific to the connecting segment and collecting duct cells. The proximal tubule cells appeared morphologically normal. Cell membrane and cytoplasmic disruption could be observed in collecting ducts from mutant mice at 2–3 weeks of age. No histological abnormalities in other organs have been described. The mutant mice are fertile and generally survive for 4 months or more.

Another PKD mouse model arose spontaneously by mutation of the "congenital polycystic kidney" (cpk) gene with locus mapping to mouse chromosome 12^[63]. Cys1, the cpk gene, encodes cystin, which localizes to the primary apical cilia on collecting duct cells. Mutant mice develop massive renal cystic disease and progressive renal insufficiency in a pattern that resembles human ARPKD. Initial cystic changes are evident at approximately embryonic d 16 and localize primarily to the proximal tubule. With progressive postnatal age, the cystic changes predominantly involve the collecting duct. Death occurs by 3–4 weeks of age due to uremia^[64].

PKD in the kat mouse model is caused by a spontaneous mutation occurring in the Nek1 gene, which encodes NIMA-

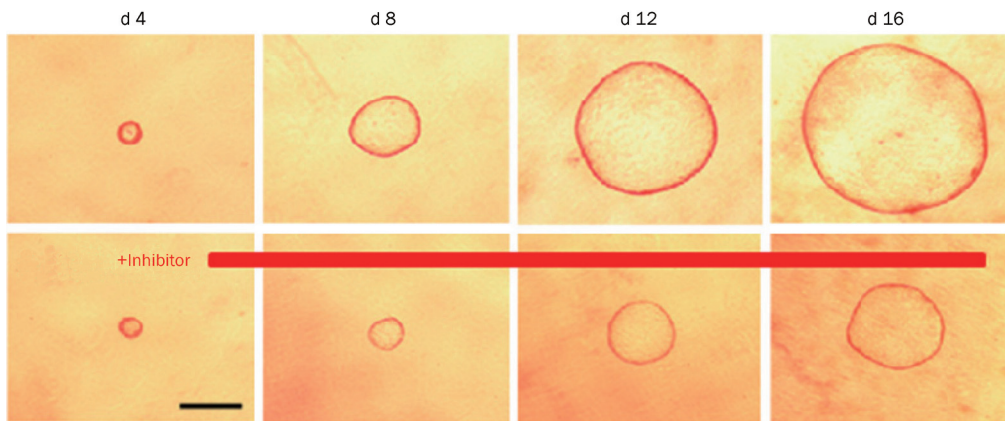


Figure 2. MDCK cyst growth in collagen gels. Light micrographs were taken at indicated days after cell seeding of MDCK cells exposed continuously to 10 $\mu\text{mol/L}$ forskolin without (top) or with cyst inhibitor (bottom). Each series of photographs shows the same cyst on successive days in culture.

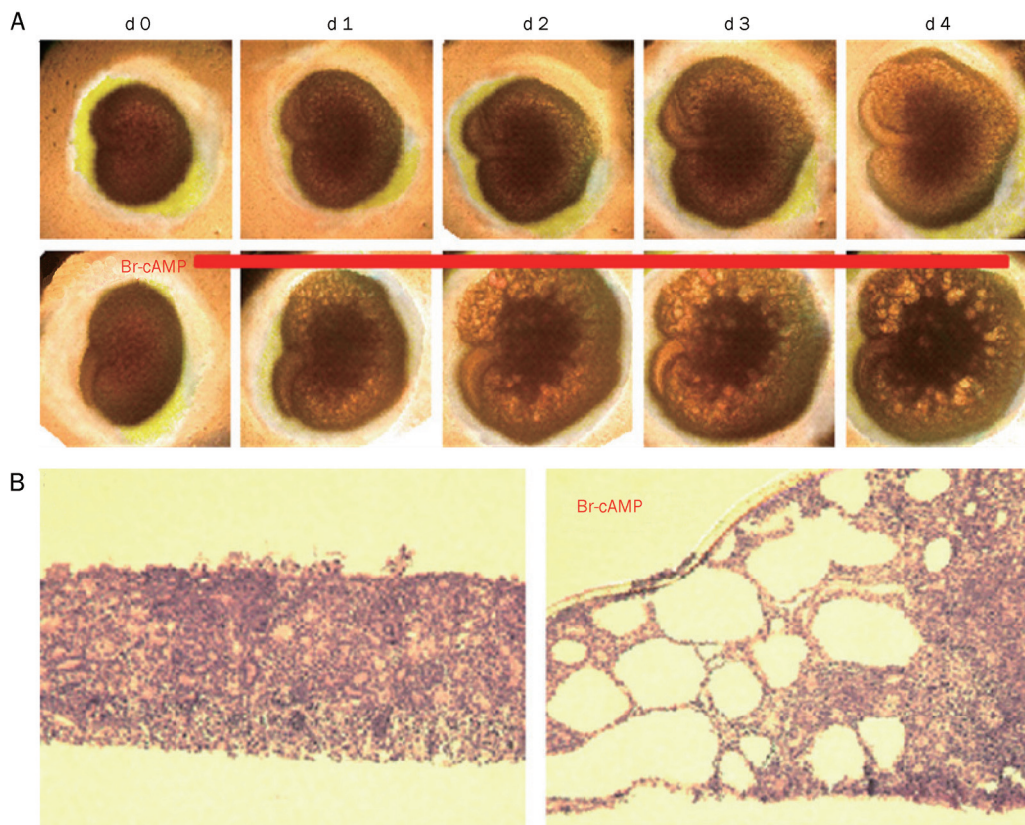


Figure 3. Embryonic kidney cyst model. Embryonic kidneys at d E13.5 were cultured for 4 d. (A) Kidney appearance by transmitted light microscopy for cultures in the absence (top) or continued presence (bottom) of 100 $\mu\text{mol/L}$ 8-Br-cAMP. Each series of photographs shows the same kidney on successive days in culture. (B) Histology (hematoxylin and eosin staining) of embryonic kidneys.

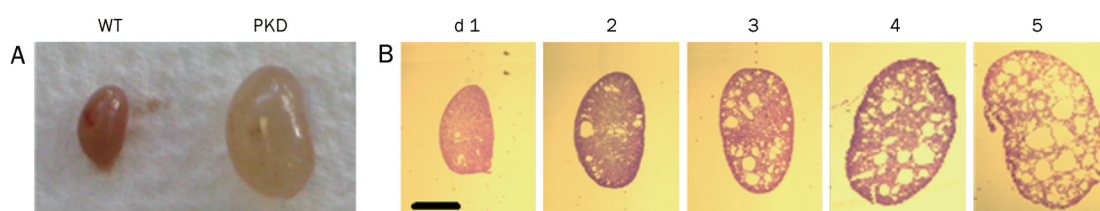


Figure 4. $\text{Pkd1}^{\text{flox}/-}; \text{Ksp-Cre}$ PKD mouse model. (A) Kidney from wildtype (left) and $\text{Pkd1}^{\text{flox}/-}; \text{Ksp-Cre}$ PKD mouse (right) at age 5 d. (B) Histology (hematoxylin and eosin staining) of kidneys from $\text{Pkd1}^{\text{flox}/-}; \text{Ksp-Cre}$ PKD mice at ages 1 to 5 d.

related kinase 1. In Nek1kat-2J homozygotes, fluid-filled cysts and dilated proximal tubules and Bowman spaces are found as early as 1 month of age. The bilateral renal cystic disease involves all levels of the nephron by 3 months of age. Disease progression, including growth of cysts and an increase in the number of cysts, is similar to that in ADPKD.

As a model of ADPKD, the Han:SPRD-cy rat has been used for research extensively^[65-67]. The gene locus maps to chromosome 5^[68]. The spontaneous mutation occurs in the Sprague-Dawley strain. In male Cy/+ rats, the kidneys enlarged more rapidly, and interstitial fibrosis is more pronounced^[69]. The Han:SPRD Cy/+ rat can be studied for the efficacy of long-term medical therapy. In this model, the renal cyst exclusively develops in the proximal tubules instead of the whole renal segment. Other mouse models, bpk, jcpk, orpk, inv and pcy, also resemble human PKD with respect to renal cyst pathology and disease progression^[60]. Because the murine models share common pathogenic features with human PKD, it is assumed that there are common molecular pathways involved in PKD progression in humans and mice. The jck, cpk, and kat mouse models are commercially available from the Jackson Laboratories.

The dynamics of cyst growth differ in the various models. These differences provide a unique opportunity to study the mechanism of cyst formation. The Nek8jck mouse model can be used mainly to test the preventive role of cyst inhibitors in the formation of cysts in collecting ducts of young mice. The Cys1cpk mouse model is suitable to test the role of cyst inhibitors on the progression of cysts and to compare the effects of treatments on cysts derived from different cell types in all levels of the nephron. The Nek1kat mouse model has been proposed to study the roles of cyst inhibitors on cysts derived from proximal tubules. Heterozygous Pkd2^{WS25} mice, an ADPKD model generated by targeted mutagenesis, can be used to test the prevention and the treatment with cyst inhibitors on the development of cysts in the kidney and other organs.

Cyst progression can be evaluated by measuring the size and number of cysts in the kidney. At first, the ratio of kidney weight to body weight can be measured. Development of cysts should increase kidney weight. For light microscopic analysis, transverse tissue sections, including cortex, medulla and papilla, can be stained with H&E to measure cyst size and number. The analysis can be performed by a reviewer who is blinded to the identity of the treatment modality. To quantitatively evaluate cyst growth, cyst size can be recorded on the following scale: 0, <0.05 mm (It is difficult to distinguish the cysts from normal renal tubules); 1, 0.05–0.3 mm; 2, 0.3–0.6 mm; 3, 0.6–0.9 mm; 4, 0.9 mm–1.2 mm; and 5, >1.2 mm. The number of cysts can be counted in the cortex, medulla and papilla. In some experiments, the origin of renal tubule cysts can be determined by segment-specific lectin binding using Dolichos biflorus agglutinin (DBA) as a marker for collecting ducts and Lotus tetragonolobus (LTA) as a marker for proximal tubules as described previously^[70]. The numbers of LTA-positive and DBA-positive cysts can be counted in serial

sections of bisected whole-mount kidneys from each animal. Proximal tubule cysts can be identified by LTA binding, and collecting duct cysts can be identified by DBA binding. A minimum of 10 sets of serial sections evenly spaced through the kidney from the cortex to the inner medulla can be used to determine the ratio of proximal tubule to collecting duct cysts.

Candidate drugs under research and development

Based on the mechanism of renal cyst development and the pathogenesis of PKD, some chemical and natural compounds have been discovered to have inhibitory activity on renal cysts and to slow PKD progression. Some classes of candidate PKD drugs have been described according to the drug targets in PKD as follows.

Vasopressin 2 receptor (V2R) antagonist

Studies were conducted to target cAMP pathways and take a step further by demonstrating the upregulation of vasopressin and the inhibition of cytotogenesis by V2R antagonists OPC-31260 in cpk mice, ARPKD (PCK rat), ADPKD (Pkd2WS25 mice) and adolescent nephronophthisis (pcy mouse)^[34, 35, 37]. As OPC-31260 is a weak antagonist for human V2R, clinical trials with tolvaptan, which has a higher affinity for human V2R, are underway. Tolvaptan was also effective in animal models of ARPKD, ADPKD, and nephronophthisis^[71-73]. The Tolvaptan Efficacy and Safety in Management of PKD and Outcomes (TEMPO) program is currently active^[74, 75]. Phase 2a studies to determine the response to increasing doses of tolvaptan (15, 30, 60, and 120 mg) in patients with ADPKD and normal renal function have been completed^[75, 76]. A 3-year phase 3, placebo-controlled, double-blind study in 18- to 50-year-old patients with ADPKD to determine long-term safety and efficacy has been initiated and will be completed in 2011.

Renin angiotensin aldosterone system (RAAS) antagonist

Angiotensin-II (AT-II) has been demonstrated to promote cellular proliferation, apoptosis, and the production of TNF- α and other pro-inflammatory cytokines^[77]. RAAS also plays an important role in hypertension. So, RAAS antagonism can prevent cellular proliferation and inflammation and treat hypertension in PKD. Angiotensin-converting enzyme (ACE) inhibitors, which are RAAS antagonists, have been proven to reduce cyst enlargement and blood pressure and improve renal function in Han:SPRD rats^[78, 79]. A randomized 7-year study showed that ACE inhibitors prevented left ventricular hypertrophy better than calcium channel blockers in 75 hypertensive ADPKD patients^[80]. An earlier longitudinal study has shown slower renal progression in those treated only with ACE inhibitor compared to only diuretics. Two HALT PKD trials that are randomized, double-blind, and placebo-controlled are underway to test the impact of intensive blockade of RAAS in ADPKD patients with ACE inhibitor or angiotensin receptor blocker (ARB)^[81].

Epidermal growth factor receptor (EGFR) tyrosine kinase inhibitor
EGF is an important factor in cyst epithelial cell proliferation

and cystogenesis. EKI-785, an EGFR tyrosine kinase inhibitor, has been shown to be effective in reducing cyst formation and decreasing mortality in murine ARPKD^[82]. EKI-785 and another EGFR tyrosine kinase inhibitor EKB-569 attenuate the development of PKD in Han:SPRD rats^[66]. Contrary to other murine models of ARPKD, overexpression and mislocalization of EGFR are not found at the apical membrane of cystic cells in PCK rats^[64]. This may be the reason that EKI-758 and EKI-569 have no efficacy in PCK rats^[64].

Peroxisome proliferator-activated receptor- γ (PPAR γ) agonist

Proliferation is recognized as an important factor for cysts development in PKD. PPAR γ , a member of the superfamily of nuclear hormone receptor transcription factors, has been demonstrated to suppress cell growth and promote differentiation and apoptosis in various cancer cells^[83]. Thus, it may be effective in treating PKD. A recent study showed that the expression of PPAR γ was greater in ADPKD kidneys and cyst-lining epithelial cells compared to normal kidneys and human kidney cortex cells^[84]. Rosiglitazone, a PPAR γ agonist, significantly inhibits the proliferation of ADPKD cystic epithelial cells by causing a G₀/G₁ arrest. Short-term treatment in Han:SPRD rats with rosiglitazone has been shown to attenuate the development of kidney cysts and improve renal function, while long-term administration with rosiglitazone can prolong survival in Han:SPRD rats^[67].

Somatostatin

Octreotide, a kind of somatostatin, has been shown to inhibit hepatic and renal cystogenesis in PCK rats by decreasing cAMP accumulation^[85]. A clinical trial has shown that octreotide safely slows renal volume expansion in 6-month therapy for 13 ADPKD patients^[86]. Recently, octreotide has been tested as long-term treatment for polycystic kidney and polycystic liver disease in a clinical trial.

Phosphodiesterase (PDE) activator

In PKD, cAMP has been proven to be a critical intracellular second messenger involved in cytotogenesis. The level of cAMP is largely regulated by the PDE superfamily through hydroxylation. In mixed cortical tubules and microdissected tubular segments, 50%–70% of PDE activity is inhibited by an inhibitor of the calcium-calmodulin-sensitive PDE1^[87]. PDE1 is responsible for cAMP and cGMP activity. The reduction of intracellular calcium in PKD may increase cAMP by dysregulating PDE1. PDE3 inhibited by increased cGMP are cAMP-specific PDEs. PDE3 may also be involved in cAMP accumulation in renal cells of PKD kidneys. In mesangial cells, PDE3 inhibitors increase cAMP levels and activate PKA, block phosphorylation of Raf-1 on serine 338 and suppress Raf-1 kinase activity^[88]. PDE inhibitors stimulate MDCK cell proliferation. A recent study showed that the protein levels of PDE1, PDE3, and PDE4 are significantly reduced in the cysts of PCK and Pkd2^{-1/WS25} kidneys compared with wild-type kidneys^[89], which indicates that a PDE activator may inhibit cystogenesis.

Src inhibitor

Src has been confirmed to be an important intermediary in cAMP pathways that promote epithelial proliferation in PKD and also a critical mediator in the activation of the EGFR axis. Src activity has a relationship with PKD progression in BPK mice and PCK rats^[90]. SKI-606 can inhibit Src activity in a highly specific manner. SKI-606, which is also in clinical trials for breast cancer and malignant tumors, significantly improves renal and biliary lesions in BPK and PCK rodent models of ARPKD^[90]. Thus, Src can be a prospective therapeutic target in PKD.

Raf inhibitor

Sorafenib, a small molecule Raf inhibitor, has been demonstrated to inhibit the proliferation of cells derived from the cysts of human ADPKD kidneys^[91]. Sorafenib has also been proven to treat renal cell carcinomas and prolong survival time^[92]. Cyst growth in human ADPKD cystic cells cultured within three dimensional collagen is completely inhibited by sorafenib^[91]. This study suggests that the inhibition of the Raf kinases may be an effective therapy for PKD.

Mitogen extracellular kinase (MEK) inhibitor

MEK is an important mediator in EGFR and cAMP signaling. PD98059, an inhibitor of MEK, has been shown to completely prevent ADPKD cellular proliferation in response to cAMP agonists^[21]. Another MEK inhibitor, PD184352, improved renal function and reduced the expression of P-ERK and ERK in pcy mice^[93]. However, U0126, an inhibitor of MEK1/2 that blocks phosphorylation of ERK, did not change the rate of cyst growth in Pkd1^{fllox/-}:ksp-Cre mice^[94]. More studies on MEK inhibitor efficiency in PKD are needed.

Mammalian target of rapamycin (mTOR) inhibitor

In human ADPKD patients and mouse models, the mTOR pathway is abnormally activated in cyst-lining epithelial cells. It has been shown that the cytoplasmic tail of PC1 interacts with tuberlin^[95]. Recently, another experiment^[96] directly showed that PC1 was able to inhibit the mTORC1(mTOR complex-1) cascade that regulates cell growth and proliferation, ribosome biogenesis and translation of a subset of mRNAs, cellular energy responses and autophagy^[97, 98]. Mutations in PC1 therefore lead to persistent activation of mTOR, which promotes cell growth and proliferation and cyst expansion in PKD. Also, mTOR is activated by increased ERKs through inhibiting tuberlin in the renal cells of ADPKD. Rapamycin, an inhibitor of mTOR, was shown to be highly effective in reducing renal cystogenesis in the bpk and orpk-rescue mouse models^[95]. In another study, long-term rapamycin treatment in Han:SPRD rats resulted in a normalization of kidney volume, renal function, blood pressure and heart weight^[65]. Treatment of human ADPKD transplant recipient patients with rapamycin showed a significant reduction in polycystic kidney volumes^[95]. A two-year, placebo-controlled trial of another mTOR inhibitor, everolimus, involving 433 patients with ADPKD has been finished. Everolimus slowed the increase in total kidney volume, but the estimated GFR was

not improved^[99].

Cystic fibrosis transmembrane conductance regulator (CFTR) inhibitor

CFTR_{inh}-172^[59], a thiazolidinone, has been shown to slow cyst growth in a MDCK cell culture model of PKD^[28] and in metanephric kidney organ cultures^[55]. CFTR_{inh}-172 maintains the channel closed state, probably by binding to a cytoplasmic domain of CFTR according to patch-clamp analysis^[100]. The other kind of CFTR inhibitors is the glycine hydrazides, which directly bind to the CFTR pore at a site near its external entrance^[101]. In an experiment screening CFTR inhibitors for PKD^[56], tetrazolo-CFTR_{inh}-172, a tetrazolo-derived thiazolidinone, and Ph-GlyH-101, a phenyl-derived glycine hydrazide, were found to almost completely suppress cyst growth without affecting cell proliferation. These compounds also showed a remarkable inhibition of cyst number and growth in an embryonic kidney cyst model. Subcutaneous delivery of tetrazolo-CFTR_{inh}-172 and Ph-GlyH-101 to neonatal kidney-specific Pkd1 knockout mice for 7 d prominently slowed kidney enlargement, cyst expansion and renal function impairment.

Cyclin-dependent kinase (CDK) inhibitor

As we discussed previously, cilia has a close link with the cell cycle progression. The CDK inhibitor roscovitine effectively inhibited cyst formation through cell cycle arrest in jck and cpk mouse models of PKD^[102]. Roscovitine has also been detected to be active against cysts originating from different parts of the nephron^[102]. Roscovitine significantly downregulates cAMP and aquaporin 2^[103] and increases p21^[104], leading to decreased renal tubular epithelial cell proliferation.

TNF- α interventions

A recent study has demonstrated that TNF- α promotes the progression of PKD^[105]. Treating inner medullary collecting duct (IMCD) cells with TNF- α increases the expression of FIP-2 and shows a striking loss of PC2 from its normal location. FIP-2 plays a role in transporting protein from the apical membrane and regulating epithelial cell polarity. TNF- α causes cystogenesis in the wild-type murine embryonic kidney, which is exacerbated in the Pkd2^{+/-} embryonic kidney. Pkd2^{+/-} mice injected with TNF- α have increased cyst development (the frequency was 6/14), while 50 Pkd2^{+/-} mice treated with the TNF- α inhibitor ethanercept did not develop cysts. Another study has found that TNF- α can activate the mTOR pathway^[106], which plays an important role in PKD development. These studies suggest that inhibition of TNF- α can slow cyst formation in PKD.

Glucosylceramide synthase inhibitor

Glucosphingolipids have been proven to play an important role in regulating cell proliferation and apoptosis^[107]. Recently, a study demonstrated that the glucosylceramide (GlcCer) synthase inhibitor Genz-123346 effectively inhibited cystogenesis in Pkd1^{-/-}, jck and pcy mice^[108]. GlcCer and ganglioside GM3 levels are higher in human and mouse PKD kidneys compared

to normal kidneys. Molecular analysis of jck mice and jck cells shows that Genz-123346 prevents cyst growth by dysregulating Akt-mTOR signaling^[108].

Matrix metalloproteinases (MMPs) inhibitor

MMPs are a large family of proteinases that play an important role in remodeling extracellular matrix components and cleaving a number of cell surface proteins. Kidney tubules derived from the C57BL/6J-cpk mouse contain higher levels of MMP-2 and -9 than normal mice^[109]. Serum MMP-1, -9, and tissue inhibitor of metalloproteinases-1 concentrations in patients with PKD were significantly higher compared to healthy controls^[110]. MMP-14 mRNA has a higher expression in cyst-lining epithelia and distal tubules in Han:SPRD rats^[111]. Treating Han:SPRD-cy/+ rats with the MMP inhibitor, batimastat, for 8 weeks caused a prominent reduction in cyst number and kidney weight^[111], which suggests that MMP inhibitor could be potential therapy for PKD.

HMG-CoA reductase inhibitor

Statins, which are HMG-CoA reductase inhibitors, are widely applied to decrease cholesterol in clinical settings. They can be used for improving renal function in PKD. Lovastatin significantly decreased cystic kidney size and improved function in heterozygous male Han:SPRD rats^[112]. It may be related with lovastatin reducing farnesyl pyrophosphate, which is important in cell proliferation^[112], and lovastatin can also cause actin filament disruption, which can induce apoptosis^[113]. In a double-blind cross-over study, 10 normocholesterolemic ADPKD patients treated with 40 mg/d simvastatin or placebo for 4 weeks showed that simvastatin significantly improved both glomerular filtration rate (GFR) and effective renal plasma flow^[47]. Another study of 16 ADPKD patients with well-preserved renal function treated with 40 mg/d simvastatin for six months proved that simvastatin ameliorated endothelial dysfunction in ADPKD patients using high resolution vascular ultrasound^[114]. A randomized open-label clinical trial was performed with 49 ADPKD patients who were treated with 20 mg/d pravastatin or no treatment for 2 years^[115]. There were no significant changes in the markers of kidney function or urinary protein excretion between the two groups.

Triptolide

Triptolide is a natural product isolated from the "Thunder God Vine". It has been demonstrated to promote an increase in PC2-mediated calcium release and cytosolic calcium in the murine kidney epithelial Pkd2^{-/-} cells and to inhibit cyst formation in Pkd1^{-/-} embryonic mice^[116]. Triptolide is an inhibitor of NF- κ B- and NF-AT-mediated transcription, which results in reduced gene products and cell growth arrest^[117, 118]. It has been proven to inhibit cell growth and increase p21 expression in Pkd1^{-/-} kidney cells. In another study, triptolide significantly inhibited the early phases of cyst expansion and improved renal function at postnatal d 8 in a kidney-specific Pkd1^{flox/-}; Ksp-cre mouse model of ADPKD^[119]. Recently, a study showed triptolide has a pronounced effect in reduc-

ing cyst formation in a Pkd1^{flox/flox}; Mx1Cre mouse model of ADPKD^[120].

Curcumin

Curcumin is a natural polyphenol derived from the plant *Curcuma longa*. Numerous studies have indicated that curcumin is a highly pleiotropic molecule capable of treating various cancers. Our studies have proven that curcumin also has a significant inhibitory effect on renal cyst development^[121]. Curcumin slowed cyst formation in both a MDCK cyst model and an embryonic kidney cyst model with a dose-dependent response. Curcumin inhibited forskolin-induced cell proliferation and promoted tubule formation in MDCK cells, which indicates that curcumin promotes MDCK cell differentiation. Curcumin affected intracellular signaling in the MDCK cells exposed to forskolin. Curcumin reduced signaling proteins Ras, B-raf, p-MEK, p-ERK, and c-fos and increased Raf-1 and NAB2 in MDCK cells.

Summary

PKD is a progressive disease with a decline in renal function. The cost of treatment, dialysis, and kidney transplantation related to PKD exceeds \$1 billion in USA each year according to the Polycystic Kidney Research Foundation. Up to now, the treatment options for PKD have been limited to renal replacement therapy by dialysis or transplantation. Based on the understanding of the pathogenesis of PKD, the inhibition of cyst epithelia and cyst fluid secretion may provide a new therapeutic option in PKD. Dual or triple therapies may be highly effective in slowing PKD progression. In addition to advancing the understanding of the mechanism in which PKD develops, the functional and morphological improvement in PKD, as seen with chemical compounds, could provide a proof-of-concept for the application of new drugs in treating PKD.

References

- 1 Chapin HC, Caplan MJ. The cell biology of polycystic kidney disease. *J Cell Biol* 2010; 191: 701–10.
- 2 Torres VE. Treatment strategies and clinical trial design in ADPKD. *Adv Chronic Kidney Dis* 2010; 17: 190–204.
- 3 Qian F, Watnick TJ, Onuchic LF, Germino GG. The molecular basis of focal cyst formation in human autosomal dominant polycystic kidney disease type I. *Cell* 1996; 87: 979–87.
- 4 Wilson P. Molecular and cellular aspects of polycystic kidney disease. *N Engl J Med* 2004; 350: 151–64.
- 5 Rossetti S, Consugar MB, Chapman AB, Torres VE, Guay-Woodford LM, Grantham JJ, et al. Comprehensive molecular diagnostics in autosomal dominant polycystic kidney disease. *J Am Soc Nephrol* 2007; 18: 2143–60.
- 6 Geng L, Segal Y, Peissel B, Deng N, Pei Y, Carone F, et al. Identification and localization of polycystin, the PKD1 gene product. *J Clin Invest* 1996; 98: 2674–82.
- 7 International Polycystic Kidney Disease Consortium. Polycystic kidney disease: the complete structure of the PKD1 gene and its protein. *Cell* 1995; 81: 289–98.
- 8 Cai Y, Maeda Y, Cedzich A, Torres VE, Wu GQ, Hayashi T, et al. Identification and characterization of polycystin-2, the PKD2 gene product. *J Biol Chem* 1999; 274: 28557–65.
- 9 Koulen P, Cai Y, Geng L, Maeda Y, Nishimura S, Witzgall R, et al. Polycystin-2 is an intracellular calcium release channel. *Nat Cell Biol* 2002; 4: 191–7.
- 10 Pazour GJ, San Agustin JT, Follit JA, Rosenbaum JL, Witman GB. Polycystin-2 localizes to kidney cilia and the ciliary level is elevated in orpk mice with polycystic kidney disease. *Curr Biol* 2002; 12: R378–80.
- 11 Yoder BK, Hou X, Guay-Woodford LM. The polycystic kidney disease proteins, polycystin-1, polycystin-2, polaris, and cystin, are colocalized in renal cilia. *J Am Soc Nephrol* 2002; 13: 2508–16.
- 12 Hanaoka K, Qian F, Boletta A, Bhunia AK, Piontek K, Tsiokas L, et al. Co-assembly of polycystin-1 and -2 produces unique cation-permeable currents. *Nature* 2000; 408: 990–4.
- 13 Wu G, Tian X, Nishimura S, Markowitz GS, D'Agati V, Park JH, et al. Trans-heterozygous Pkd1 and Pkd2 mutations modify expression of polycystic kidney disease. *Hum Mol Genet* 2002; 11: 1845–54.
- 14 Harris PC, Rossetti S. Molecular genetics of autosomal recessive polycystic kidney disease. *Mol Genet Metab* 2004; 81: 75–85.
- 15 Nadasdy T, Laszik Z, Lajoie G, Blick KE, Wheeler DE, Silva FG. Proliferative activity of cyst epithelium in human renal cystic diseases. *J Am Soc Nephrol* 1995; 5: 1462–8.
- 16 Trudel M, D'Agati V, Costantini F. C-myc as an inducer of polycystic kidney disease in transgenic mice. *Kidney Int* 1991; 39: 665–71.
- 17 MacKay K, Striker LJ, Pinkert CA, Brinster RL, Striker GE. Glomerulosclerosis and renal cysts in mice transgenic for the early region of SV40. *Kidney Int* 1987; 32: 827–37.
- 18 Schaffner DL, Barrios R, Massey C, Banez EI, Ou CN, Rajagopalan S, et al. Targeting of the rast24 oncogene to the proximal convoluted tubules in transgenic mice results in hyperplasia and polycystic kidneys. *Am J Pathol* 1993; 142: 1051–60.
- 19 Metcalf D, Mifsud S, Di Rago L, Nicola NA, Hilton DJ, Alexander WS. Polycystic kidneys and chronic inflammatory lesions are the delayed consequences of loss of the suppressor of cytokine signaling-1 (SOCS-1). *Proc Natl Acad Sci U S A* 2002; 99: 943–8.
- 20 Du J, Wilson PD. Abnormal polarization of EGF receptors and autocrine stimulation of cyst epithelial growth in human ADPKD. *Am J Physiol* 1995; 269: C487–95.
- 21 Yamaguchi T, Pelling JC, Ramaswamy NT. cAMP stimulates the *in vitro* proliferation of renal cyst epithelial cells by activating the extracellular signal-regulated kinase pathway. *Kidney Int* 2000; 57: 1460–71.
- 22 Yamaguchi T, Wallace DP, Magenheimer BS, Hempson SJ, Grantham JJ, Calvet JP. Calcium restriction allows cAMP activation of the B-Raf/ERK pathway, switching cells to a cAMP-dependent growth-stimulated phenotype. *J Biol Chem* 2004; 279: 40419–30.
- 23 Bhunia AK, Piontek K, Boletta A, Liu L, Qian F, Xu PN, et al. PKD1 induces p21 (waf1) and regulation of the cell cycle via direct activation of the JAK-STAT signaling pathway in a process requiring PKD2. *Cell* 2002; 109: 157–68.
- 24 Grantham JJ, Ye M, Davidow C, Holub BJ, Sharma M. Evidence for a potent lipid secretagogue in the cyst fluids of patients with autosomal dominant polycystic kidney disease. *J Am Soc Nephrol* 1995; 6: 1242–9.
- 25 Chatterjee S, Shi WY, Wilson P, Mazumdar A. Role of lactosylceramide and MAP kinase kinase in the proliferation of proximal tubular cells in human polycystic kidney disease. *J Lipid Res* 1996; 37: 1334–44.
- 26 Torres VE. Apoptosis in cystogenesis: hands on or hands off? *Kidney Int* 1999; 55: 334–5.
- 27 Davidow CJ, Maser RL, Rome LA, Calvet JP, Grantham JJ. The cystic fibrosis transmembrane conductance regulator mediates trans-epithelial fluid secretion by human autosomal dominant polycystic

- kidney disease epithelium *in vitro*. *Kidney Int* 1996; 50: 208–18.
- 28 Li H, Findlay IA, Sheppard DN. The relationship between cell proliferation, Cl⁻ secretion, and renal cyst growth: a study using CFTR inhibitors. *Kidney Int* 2004; 66: 1926–38.
- 29 Sullivan LP, Wallace DP, Grantham JJ. Epithelial transport in polycystic kidney disease. *Physiol Rev* 1998; 78: 1165–91.
- 30 Brill SR, Ross KE, Davidow CJ, Ye M, Grantham JJ, Caplan MJ. Immunolocalization of ion transport proteins in human autosomal dominant polycystic kidney epithelial cells. *Proc Natl Acad Sci U S A* 1996; 93: 10206–11.
- 31 Sweeney WE, Avner ED, Elmer HL, Cotton CU. CFTR is required for cAMP-dependent: *In vitro* renal cyst formation. *J Am Soc Nephrol* 1998; 9: 38A.
- 32 O'Sullivan DA, Torres VE, Gabow PA, Thibodeau SN, King BF, Bergstralh EJ. Cystic fibrosis and the phenotypic expression of autosomal dominant polycystic kidney disease. *Am J Kidney Dis* 1998; 32: 976–83.
- 33 Gattone VH, Wang X, Harris PC, Torres VE. Inhibition of renal cystic disease development and progression by a vasopressin V2 receptor antagonist. *Nat Med* 2003; 9: 1323–6.
- 34 Torres VE, Wang X, Qian Q, Somlo S, Harris PC, Gattone VH 2nd. Effective treatment of an orthologous model of autosomal dominant polycystic kidney disease. *Nat Med* 2004; 10: 363–4.
- 35 Devuyt O, Burrow CR, Smith BL, Agre P, Knepper MA, Wilson PD. Expression of aquaporins-1 and -2 during nephrogenesis and in autosomal dominant polycystic kidney disease. *Am J Physiol* 1996; 271: F169–83.
- 36 Gattone VH 2nd, Maser RL, Tian C, Rosenberg JM, Branden MG. Developmental expression of urine concentration-associated genes and their altered expression in murine infantile-type polycystic kidney disease. *Dev Genet* 1999; 24: 309–18.
- 37 Ong AC, Harris PC. Molecular pathogenesis of ADPKD: the polycystin complex gets complex. *Kidney Int* 2005; 67: 1234–47.
- 38 Yoder BK, Hou X, Guay-Woodford LM. The polycystic kidney disease proteins, polycystin-1, polycystin-2, polaris, and cystin, are colocalized in renal cilia. *J Am Soc Nephrol* 2002; 13: 2508–16.
- 39 Ibraghimov-Beskrovnaya O, Bukanov NO, Donohue LC, Dackowski WR, Klinger KW, Landes GM. Strong homophilic interactions of the Ig-like domains of polycystin-1, the protein product of an autosomal dominant polycystic kidney disease gene, PKD1. *Hum Mol Genet* 2000; 9: 1641–9.
- 40 Bukanov NO, Husson H, Dackowski WR, Lawrence BD, Clow PA, Roberts BL, *et al*. Functional polycystin-1 expression is developmentally regulated during epithelial morphogenesis *in vitro*: down-regulation and loss of membrane localization during cystogenesis. *Hum Mol Genet* 2002; 11: 923–36.
- 41 Roitbak T, Ward CJ, Harris PC, Bacallao R, Ness SA, Wandinger-Ness A. A polycystin-1 multiprotein complex is disrupted in polycystic kidney disease cells. *Mol Biol Cell* 2004; 15: 1334–46.
- 42 Wilson PD, Geng L, Li X, Burrow CR. The PKD1 gene product, "polycystin-1," is a tyrosine-phosphorylated protein that colocalizes with alpha2beta1-integrin in focal clusters in adherent renal epithelia. *Lab Invest* 1999; 79: 1311–23.
- 43 Hyink DP, Burrow CR, Blosswick B, Wilson PD. Reversal of the ADPKD epithelial cell decreased motility phenotype by lithium. *J Am Soc Nephrol* 2000; 11: 392A.
- 44 Lo SH, Yu QC, Degenstein L, Chen LB, Fuchs E. Progressive kidney degeneration in mice lacking tensin. *J Cell Biol* 1997; 136: 1349–61.
- 45 Shannon MB, Miner JH. Insertional mutation in laminin alpha 5: a new mouse model for polycystic kidney disease. *J Am Soc Nephrol* 2004; 15: 652A.
- 46 van Dijk MA, Kamper AM, van Veen S, Souverein JH, Blauw GJ. Effect of simvastatin on renal function in autosomal dominant polycystic kidney disease. *Nephrol Dial Transplant* 2001; 16: 2152–7.
- 47 Praetorius HA, Spring KR. Bending the MDCK cell primary cilium increases intracellular calcium. *J Membr Biol* 2001; 184: 71–9.
- 48 Nauli SM, Alenghat FJ, Luo Y, Caniains E, Vassilev P, Li X, *et al*. Polycystins 1 and 2 mediate mechanosensation in the primary cilium of kidney cells. *Nat Genet* 2003; 33: 129–37.
- 49 Pazour GJ. Intraflagellar transport and cilia-dependent renal disease: the ciliary hypothesis of polycystic kidney disease. *J Am Soc Nephrol* 2004; 15: 2528–36.
- 50 Otto EA, Schermer B, Obara T, O'Toole JF, Hiller KS, Ruf RG, *et al*. Mutations in INVS encoding inversin cause nephronophthisis type 2, linking renal cystic disease to the function of the primary cilia and left-right axis determination. *Nat Genet* 2003; 34: 413–20.
- 51 Robert A, Margall-Ducos G, Guidotti JE, Bregerie O, Celati C, Brechot C, *et al*. The intraflagellar transport component IFT88/polaris is a centrosomal protein regulating G1-S transition in non-ciliated cells. *J Cell Sci* 2007; 120: 628–37.
- 52 Li X, Luo Y, Starremans PG, McNamara CA, Pei Y, Zhou J. Polycystin-1 and polycystin-2 regulate the cell cycle through the helix-loop-helix inhibitor Id2. *Nat Cell Biol* 2005; 7: 1202–12.
- 53 Balkovetz DF. Hepatocyte growth factor and Madin-Darby canine kidney cells: *in vitro* models of epithelial cell movement and morphogenesis. *Microsc Res Tech* 1998; 43: 456–63.
- 54 Magenheimer BS, St John PL, Isom KS, Abrahamson DR, De Lisle RC, Wallace DP, *et al*. Early embryonic renal tubules of wild-type and polycystic kidney disease kidneys respond to cAMP stimulation with cystic fibrosis transmembrane conductance regulator/Na⁺, K⁺, 2Cl⁻ co-transporter-dependent cystic dilation. *J Am Soc Nephrol* 2006; 17: 3424–37.
- 55 Yang B, Sonawane ND, Zhao D, Somlo S, Verkman AS. Small-molecule CFTR inhibitors slow cyst growth in polycystic kidney disease. *J Am Soc Nephrol* 2008; 19: 1300–10.
- 56 Shibasaki S, Yu Z, Nishio S, Tian X, Thomson RB, Mitobe M, *et al*. Cyst formation and activation of the extracellular regulated kinase pathway after kidney specific inactivation of Pkd1. *Hum Mol Genet* 2008; 17: 1505–16.
- 57 Shao X, Somlo S, Igarashi P. Epithelial-specific Cre/lox recombination in the developing kidney and genitourinary tract. *J Am Soc Nephrol* 2002; 13: 1837–46.
- 58 Ma T, Thiagarajah JR, Yang H, Sonawane ND, Folli C, Galletta LJ, *et al*. Thiazolidinone CFTR inhibitor identified by high-throughput screening blocks cholera toxin-induced intestinal fluid secretion. *J Clin Invest* 2002; 110: 1651–8.
- 59 Guay-Woodford LM. Murine models of polycystic kidney disease: molecular and therapeutic insights. *Am J Physiol Renal Physiol* 2003; 285: F1034–49.
- 60 Pritchard L, Sloane-Stanley JA, Sharpe JA, Aspinwall R, Buckle V, Strmecki L, *et al*. A human PKD1 transgene generates functional polycystin-1 mice and is associated with a cystic phenotype. *Human Mol Genet* 2000; 9: 2617–27.
- 61 Atala A, Freeman MR, Mandell J, Beier DR. Juvenile cystic kidneys (jck): a new mouse mutation which causes polycystic kidneys. *Kidney Int* 1993; 43: 1081–5.
- 62 Liu S, Lu W, Obara T, Kuida S, Lehoczyk J, Dewar K, *et al*. A defect in a novel Nek-family kinase causes cystic kidney disease in the mouse and in zebrafish. *Development* 2002; 129: 5839–46.
- 63 Sommardahl C, Woychik R, Sweeney W, Avner E, Wilkinson J. Efficacy of taxol in the orpk mouse model of polycystic kidney disease.

- Pediatr Nephrol 1997; 11: 728–33.
- 64 Torres VE, Sweeney WE Jr, Wang X, Qian Q, Harris PC, Frost P, et al. Epidermal growth factor receptor tyrosine kinase inhibition is not protective in PCK rats. *Kidney Int* 2004; 66: 1766–73.
- 65 Zafar I, Belibi FA, He Z, Edelstein CL. Edelstein long-term rapamycin therapy in the Han:SPRD rat model of polycystic kidney disease. *Nephrol Dial Transplant* 2009; 24: 2349–53.
- 66 Torres VE, Sweeney WE Jr, Wang X, Qian Q, Harris PC, Frost P, et al. EGF receptor tyrosine kinase inhibition attenuates the development of PKD in Han:SPRD rats. *Kidney Int* 2003; 64: 1573–9.
- 67 Dai B, Liu Y, Mei C, Fu L, Xiong X, Zhang Y, et al. Rosiglitazone attenuates development of polycystic kidney disease and prolongs survival in Han:SPRD rats. *Clin Sci* 2010; 119: 323–33.
- 68 Bihoreau M, Ceccherini I, Browne J, Kranzlin B, Romeo G, Lathrop GM, et al. Location of the first genetic locus, PKD1, controlling autosomal dominant polycystic kidney disease in Han:SPRD *cy*/- rat. *Hum Mol Gen* 1997; 6: 609–13.
- 69 Gretz N, Ceccherini I, Kranzlin B, Kloting I, Devoto M, Rohmeiss P, et al. Gender-dependent disease severity in autosomal polycystic kidney disease of rats. *Kidney Int* 1995; 48: 496–500.
- 70 Nakanishi K, Sweeney WE Jr, Macrae Dell K, Cotton CU, Avner ED. Role of CFTR in autosomal recessive polycystic kidney disease. *J Am Soc Nephrol* 2001; 12: 719–25.
- 71 Wang X, Gattone VH 2nd, Harris PC, Torres VE. Effectiveness of vasopressin V2 receptor antagonists OPC-31260 and OPC-41061 on polycystic kidney disease development in the PCK rat. *J Am Soc Nephrol* 2005; 16: 846–51.
- 72 Gattone VH, Kinne Q, Torres VE. Efficacy of OPC-41061 in the treatment of murine nephronophthisis. *J Am Soc Nephrol* 2005; 16: 138A.
- 73 Wang S, Gattone VH, Somlo S, Harris PC, Torres VE. Effectiveness of OPC-41061 on polycystic kidney disease development in Pkd2WS25/-. *J Am Soc Nephrol* 2005; 16: 361A.
- 74 Grantham JJ, Chapman AB, Torres VE, Ouyang J, Shoaf SE, Czerwiec FS. Acute and chronic osmotic stress after vasopressin V2 receptor inhibition with tolvaptan in ADPKD. *J Am Soc Nephrol* 2005; 16: 361A.
- 75 Torres VE, Wang X, Ward CJ, Grantham JJ, Chapman AB, Ouyang J, et al. Urine aquaporin 2 and cyclic AMP responses to tolvaptan administration in autosomal dominant kidney disease. *J Am Soc Nephrol* 2005; 16: 361A.
- 76 Chapman AB, Torres VE, Grantham JJ, Shoaf SS, Ouyang JJ, Czerwiec FS. A phase IIB pilot study of the safety and efficacy of tolvaptan, a vasopressin V2 receptor antagonist (V2RA) in patients with ADPKD. *J Am Soc Nephrol* 2005; 16: 68A.
- 77 Cao Z, Cooper ME. Role of angiotensin II in tubulointerstitial injury. *Semin Nephrol* 2001; 21: 554–62.
- 78 Zafar I, Tao Y, Falk S, McFann K, Schrier RW, Edelstein CL. Effect of statin and angiotensin-converting enzyme inhibition on structural and hemodynamic alterations in autosomal dominant polycystic kidney disease model. *Am J Physiol Renal Physiol* 2007; 293: F854–9.
- 79 Kennefick TM, Al-Nimri MA, Oyama TT, Thompson MM, Kelly FJ, Chapman JG, et al. Hypertension and renal injury in experimental polycystic kidney disease. *Kidney Int* 1999; 56: 2181–90.
- 80 Schrier R, McFann K, Johnson A, Chapman A, Edelstein C, Brosnahan G, et al. Cardiac and renal effects of standard versus rigorous blood pressure control in autosomal-dominant polycystic kidney disease: results of a seven-year prospective randomized study. *J Am Soc Nephrol* 2002; 13: 1733–9.
- 81 Chapman AB, Torres VE, Perrone RD, Steinman TI, Bae KT, Miller JP, et al. The HALT polycystic kidney disease trials: design and implementation. *Cin J Am Soc Nephrol* 2010; 5: 102–9.
- 82 Sweeney WE, Chen Y, Nakanishi K, Frost P, Avner ED. Treatment of polycystic kidney disease with a novel tyrosine kinase inhibitor. *Kidney Int* 2000; 57: 33–40.
- 83 Grommes C, Landreth GE, Heneka MT. Antineoplastic effects of peroxisome proliferator-activated receptor gamma agonists. *Lancet Oncol* 2004; 5: 419–29.
- 84 Liu Y, Dai B, Fu L, Jia J, Mei C. Rosiglitazone inhibits cell proliferation by inducing G1 cell cycle arrest and apoptosis in ADPKD cyst-lining epithelia cells. *Basic Clin Pharmacol Toxicol* 2010; 106: 523–30.
- 85 Masyuk TV, Masyuk AI, Torres VE, Harris PC, Larusso NF. Octreotide inhibits hepatic cystogenesis in a rodent model of polycystic liver disease by reducing cholangiocyte adenosine 3',5'-cyclic monophosphate. *Gastroenterology* 2007; 132: 1104–16.
- 86 Ruggenenti P, Remuzzi A, Onfei P, Fasolini G, Antiga L, Ene-Iordache B, et al. Safety and efficacy of long-acting somatostatin treatment in autosomal-dominant polycystic kidney disease. *Kidney Int* 2005; 68: 206–16.
- 87 Kusano E, Yoshida I, Takeda S, Homma S, Yusufi AN, Dousa TP, et al. Nephron distribution of total low Km cyclic AMP phosphodiesterase in mouse, rat and rabbit kidney. *Tohoku J Exp Med* 2001; 193: 207–20.
- 88 Cheng J, Thompson MA, Walker HJ, Homma S, Yusufi AN, Dousa TP, et al. Differential regulation of mesangial cell mitogenesis by cAMP phosphodiesterase isozymes 3 and 4. *Am J Physiol Renal Physiol* 2004; 287: F940–53.
- 89 Wang X, Ward CJ, Harris PC, Torres VE. Cyclic nucleotide signaling in polycystic kidney disease. *Kidney Int* 2010; 77: 129–40.
- 90 Sweeney WE Jr, von Vigier RO, Frost P, Avner ED. Src inhibition ameliorates polycystic kidney disease. *J Am Soc Nephrol* 2008; 19: 1331–41.
- 91 Yamaguchi T, Reif GA, Calvet JP, Wallace DP. Sorafenib inhibits cAMP-dependent ERK activation, cell proliferation, and *in vitro* cyst growth of human ADPKD cyst epithelial cells. *Am J Physiol Renal Physiol* 2010; 299: F944–51.
- 92 Escudier B, Eisen T, Stadler WM, Szczylik C, Oudard S, Siebels M, et al. Sorafenib in advanced clear-cell renal-cell carcinoma. *N Engl J Med* 2007; 356: 125–34.
- 93 Omori S, Hida M, Fujita H, Takahashi H, Tanimura S, Kohno M, et al. Extracellular signal-regulated kinase inhibition slows disease progression in mice with polycystic kidney disease. *J Am Soc Nephrol* 2006; 17: 1604–14.
- 94 Shibasaki S, Yu Z, Nishio S, Tian X, Thomson RB, Mitobe M, et al. Cyst formation and activation of the extracellular regulated kinase pathway after kidney specific inactivation of Pkd1. *Hum Mol Genet* 2008; 17: 1505–16.
- 95 Shillingford JM, Murcia NS, Larson CH, Low SH, Hedgepeth R, Brown N, et al. The mTOR pathway is regulated by polycystin-1, and its inhibition reverses renal cystogenesis in polycystic kidney disease. *Proc Natl Acad Sci U S A* 2006; 103: 5466–71.
- 96 Distefano G, Boca M, Rowe I, Wodarczyk C, Ma L, Piontek KB, et al. Polycystin-1 regulates extracellular signal-regulated kinase-dependent phosphorylation of tuberlin to control cell size through mTOR and its downstream effectors S6K and 4EBP1. *Mol Cell Biol* 2009; 29: 2359–71.
- 97 Wullschlegel S, Loewith R, Hall MN. TOR signaling in growth and metabolism. *Cell* 2006; 124: 471–84.
- 98 Huang J, Manning BD. The TSC1-TSC2 complex: a molecular switchboard controlling cell growth. *Biochem J* 2008; 412: 179–90.
- 99 Walz G, Budde K, Mannaa M, Nurnberger J, Wanner C, Sommerer C, et al. Everolimus in patients with autosomal dominant polycystic

- kidney disease. *N Engl J Med* 2010; 363: 830–40.
- 100 Taddei A, Folli C, Zegarra-Moran O, Fanen P, Verkman AS, Galletta LJ. Altered channel gating mechanism for CFTR inhibition by a high affinity thiazolidinone blocker. *FEBS Lett* 2004; 558: 52–6.
- 101 Sonawane ND, Muanprasat C, Nagatani R Jr, Song Y, Verkman AS. *In vivo* pharmacology and antidiarrheal efficacy of a thiazolidinone CFTR inhibitor in rodents. *J Pharm Sci* 2004; 94: 134–43.
- 102 Bukanov NO, Smith LA, Klinger KW, Ledbetter SR, Ibraghimov-Beskrovnaya O. Long lasting arrest of murine polycystic kidney disease with CDK inhibitor roscovitine. *Nature* 2006; 444: 949–52.
- 103 Genzyme Corporation, Framingham, Massachusetts. Targeting dysregulated cell cycle and apoptosis for polycystic kidney disease therapy. *Cell Cycle* 2007; 6: 776–9.
- 104 Park JY, Schutzer WE, Lindsley JN, Bagby SP, Oyama TT, Anderson S, *et al*. p21 is decreased in polycystic kidney disease and leads to increased epithelial cell cycle progression: roscovitine augments p21 levels. *BMC Nephrol* 2007; 8: 12.
- 105 Li X, Magenheimer BS, Xia S, Johnson T, Wallace DP, Calvet JP, *et al*. A tumor necrosis factor- α -mediated pathway promoting autosomal dominant polycystic kidney disease. *Nat Med* 2008; 14: 863–8.
- 106 Lee DF, Kuo HP, Chen CT, Hsu JM, Chou CK, Wei Y, *et al*. IKK beta suppression of TSC1 links inflammation and tumor angiogenesis via the mTOR pathway. *Cell* 2007; 130: 440–55.
- 107 Bieberich E. Integration of glycosphingolipid metabolism and cell-fate decisions in cancer and stem cells: review and hypothesis. *Glycoconj J* 2004; 21: 315–27
- 108 Natoli TA, Smith LA, Rogers KA, Wang B, Komarnitsky S, Budman Y, *et al*. Inhibition of glucosylceramide accumulation results in effective blockade of polycystic kidney disease in mouse models. *Nat Med* 2010; 16: 788–92.
- 109 Rankin CA, Suzuki K, Itoh Y, Ziemer DM, Grantham JJ, Calvet JP, *et al*. Matrix metalloproteinases and TIMPS in cultured C57BL/6Jcpk kidney tubules. *Kidney Int* 1996; 50: 835–44.
- 110 Nakamura T, Ushiyama C, Suzuki S, Ebihara I, Shimada N, Koide H. Elevation of serum levels of metalloproteinase-1, tissue inhibitor of metalloproteinase-1 and type IV collagen, and plasma levels of metalloproteinase-9 in polycystic kidney disease. *Am J Nephrol* 2000; 20: 32–6.
- 111 Obermuller N, Morente N, Kranzlin B, Gretz N, Witzgall R. A possible role for metalloproteinases in renal cyst development. *Am J Physiol Renal Physiol* 2001; 280: F540–50.
- 112 Gile RD, Cowley BD Jr, Gattone VH 2nd, O'Donnell MP, Swan SK, Grantham JJ. Effect of lovastatin on the development of polycystic kidney disease in the Han:SPRD rat. *Am J kidney Dis* 1995; 26: 501–7.
- 113 Limura O, Vrtovsnik F, Terzi F, Friedlander G. HMG-CoA reductase inhibitors induce apoptosis in mouse proximal tubular cells in primary culture. *Kidney int* 1997; 52: 962–72.
- 114 Namli S, Oflaz H, Turgut F, Alisir S, Tufan F, Ucar A, *et al*. Improvement of endothelial dysfunction with simvastatin in patients with autosomal dominant polycystic kidney disease. *Ren Fail* 2007; 29: 55–9.
- 115 Fassett RG, Coombes JS, Packham D, Fairley KF, Kincaid-Smith P. Effect of pravastatin on kidney function and urinary protein excretion in autosomal dominant polycystic kidney disease. *Scand J Urol Nephrol* 2010; 44: 56–61.
- 116 Leuenroth SJ, Okuhara D, Shotwell JD, Markowitz GS, Yu Z, Somlo S, *et al*. Triptolide is a traditional Chinese medicine-derived inhibitor of polycystic kidney disease. *Proc Natl Acad Sci U S A* 2007; 104: 4389–94.
- 117 Lee KY, Chang W, Qiu D, Kao PN, Rosen GD. PG490 (triptolide) cooperates with tumor necrosis factor- α to induce apoptosis in tumor cells. *J Biol Chem* 1999; 274: 13451–5.
- 118 Liu H, Liu ZH, Chen ZH, Yang JW, Li LS. Triptolide: a potent inhibitor of NF- κ B in T-lymphocytes. *Acta Pharmacol Sin* 2000; 21: 782–6.
- 119 Leuenroth SJ, Bencivenga N, Igarashi P, Somlo S, Crews CM. Triptolide reduces cystogenesis in a model of ADPKD. *J Am Soc Nephrol* 2008; 19: 1659–62.
- 120 Leuenroth SJ, Bencivenga N, Chahboune H, Hyder F, Crews CM. Triptolide reduces cyst formation in a neonatal to adult transition Pkd1 model of ADPKD. *Nephrol Dial Transplant* 2010; 25: 2187–94.
- 121 Gao J, Zhou H, Lei T, Zhou L, Li W, Li X, *et al*. Curcumin inhibits renal cyst formation and enlargement *in vitro* by regulating intracellular signaling pathways. *Eur J Pharmacol* 2011; 654: 92–9.

Review

Propofol and arrhythmias: two sides of the coin

Qiang LIU¹, Ai-ling KONG^{1,§}, Rong CHEN¹, Cheng QIAN¹, Shao-wen LIU¹, Bao-gui SUN¹, Le-xin WANG², Long-sheng SONG³, Jiang HONG^{1,*}

¹Department of Cardiology, Shanghai First People's Hospital, School of Medicine, Shanghai Jiaotong University, Shanghai 200080, China; ²School of Biomedical Sciences, Charles Sturt University, Wagga Wagga, NSW, Australia; ³Division of Cardiology, Department of Internal Medicine, University of Iowa College of Medicine, Iowa City, IA, USA

The hypnotic agent propofol is effective for the induction and maintenance of anesthesia. However, recent studies have shown that propofol administration is related to arrhythmias. Propofol displays both pro- and anti-arrhythmic effects in a concentration-dependent manner. Data indicate that propofol can convert supraventricular tachycardia and ventricular tachycardia and may inhibit the conduction system of the heart. The mechanism of the cardiac effects remains poorly defined and may involve ion channels, the autonomic nervous system and cardiac gap junctions. Specifically, sodium, calcium and potassium currents in cardiac cells are suppressed by clinically relevant concentrations of propofol. Propofol shortens the action potential duration (APD) but lessens the ischemia-induced decrease in the APD. Furthermore, propofol suppresses both sympathetic and parasympathetic tone and preserves gap junctions during ischemia. All of these effects cumulatively contribute to the antiarrhythmic and proarrhythmic properties of propofol.

Keywords: propofol; arrhythmias; ion channels; gap junction; autonomic nervous system

Acta Pharmacologica Sinica (2011) 32: 817–823; doi: 10.1038/aps.2011.42

Introduction

The hypnotic agent propofol (2,6-diisopropylphenyl) is widely used during the induction and maintenance of anesthesia. It has the advantages of minimal side effects, a controllable anesthetic state, a quick onset, and rapid patient emergence from general anesthesia. Apart from these anesthetic properties, propofol has additional antiarrhythmic and proarrhythmic effects.

Antiarrhythmic property of propofol

Several case reports have documented the antiarrhythmic effects of propofol. Kannan and Sherwood^[1] reported that a 68-year-old man with a previous myocardial infarction experienced supraventricular tachycardia. In this patient, administration of adenosine or carotid sinus massage had no effect, but propofol converted the supraventricular arrhythmia to sinus rhythm before electrical cardioversion. Hermann and Vettermann reported another case of ectopic supraventricular tachycardia that was terminated by propofol^[2]. Propofol has also been shown to terminate ventricular tachycardia (VT)

storm^[3,4]. Burjorjee and Milne reported that propofol resolved the recurrent episodes of VT that were not terminated by maximal antiarrhythmic therapy in a 65-year-old man^[3]; similar results were observed in a second study of a patient with comparable disease^[4].

Additionally, propofol converted atrial fibrillation, which was not terminated by intravenous infusion of amiodarone, to sinus rhythm^[5]. Propofol can significantly decrease P-wave dispersion^[6], which may represent the reason for termination of atrial fibrillation. Furthermore, propofol may improve cardiac conduction. After propofol injection, the delta wave of Wolff-Parkinson-White syndrome has been shown to disappear and the P-R interval to normalize, though the delta wave returned immediately after propofol discontinuation^[7,8]. The Q-T interval of long Q-T syndrome was shortened when propofol was used; therefore, propofol may have the potential to prevent episodes of VT that are due to Q-T interval dispersion^[9,10].

Reperfusion of the heart after short-term ischemia may lead to potentially lethal arrhythmias, but propofol can alleviate reperfusion-induced arrhythmia. In the isolated rat myocardium, propofol had antiarrhythmic effects against reperfusion-induced arrhythmia at concentrations of 1, 10, and 20 $\mu\text{mol/L}$, and the incidence and duration of sustained arrhythmias were decreased significantly^[11]. From the above studies, we conclude that propofol is likely to inhibit arrhythmias. How-

[§] Now in Department of Cardiology, Yancheng First People's Hospital, Yancheng, China

* To whom correspondence should be addressed.

E-mail jhong.pku@163.com

Received 2011-02-16 Accepted 2011-04-07

ever, clinical conditions are often complex, and the general classification of propofol as a unique agent for antiarrhythmic therapy cannot yet be made. Thus, more studies are needed to understand the detailed mechanism by which propofol exerts its antiarrhythmic effects.

Proarrhythmic properties of propofol

Some studies have demonstrated that propofol has the potential to block the conduction system of the heart and thereby induce arrhythmia. A study of 60 children with paroxysmal supraventricular tachycardia undergoing radiofrequency catheter ablation showed that atrioventricular (AV) node (AVN) conduction was slowed with propofol^[12]. Atrial wavelength and AVN are electrophysiologic factors critical to the pathogenesis of supraventricular tachydysrhythmias. A study focusing on the effects of anesthetics on such electrophysiologic factors in guinea pig hearts has indicated that propofol does not change the atrial wavelength. However, this study revealed that propofol prolonged the AVN effective refractory period (ERP) in concentration- and frequency-dependent manners, though no significant effect on atrial conduction velocity was detected^[13]. Additionally, at concentrations greater than 25 $\mu\text{mol/L}$, propofol slowed the atrial rate and AVN conduction and prolonged the Wenckebach cycle length in a concentration-dependent manner. The frequency of propofol administration also correlated with stimulus-to-His bundle intervals, such that the higher the frequency, the longer the S-H interval^[14].

Propofol (3 $\mu\text{mol/L}$) significantly prolonged the rabbit AV conduction interval in a dose-dependent (3 to 100 $\mu\text{mol/L}$) manner. At higher concentrations (10 to 100 $\mu\text{mol/L}$), the AVN Wenckebach cycle length and its refractory period were also prolonged. In addition, conduction through the His-Purkinje system (HV interval) and the atrial tissue (SA interval), as well as the spontaneous cycle length, were lengthened in a dose-dependent manner (30 to 100 $\mu\text{mol/L}$). By contrast, propofol had no effect on the refractory period of the atrium, ventricle, or the His-Purkinje system^[15]. Therefore, propofol inhibits AV conduction in a concentration-dependent fashion.

Conversely, some research suggests that propofol does not affect the conduction system. For example, propofol had no effect on the electrophysiological properties of the AVN and pathway conduction in atrioventricular nodal reentrant tachycardia patients^[16]. Additionally, propofol did not cause sinoatrial node depression or a pathological increase in atrioventricular conduction^[17]. Studies in normal pig hearts demonstrate that propofol promotes a dose-related depression of sinus node and His-Purkinje system functions but has no effect on the AVN function or the conduction properties of atrial and ventricular tissues^[18].

The effects of propofol on the conduction system may be impacted by age and drug concentration. At a low concentration (3 $\mu\text{mol/L}$), propofol induced a significant lengthening of the AV conduction interval in adult rabbit hearts but not neonatal hearts. At a higher concentration (10 $\mu\text{mol/L}$ and above), propofol significantly prolonged the AV conduction

interval in hearts from both neonates and adults. The AV Wenckebach cycle length was also lengthened, with a more significant change in the adult hearts. However, with concentrations of propofol up to 100 $\mu\text{mol/L}$, the neonatal hearts progressed to complete AV block, which did not occur in the adults. The spontaneous heart rate and conduction through the atrial tissue (SA interval) and the His-Purkinje system (HV interval) were all slowed by propofol at 30 $\mu\text{mol/L}$ or above. Additionally, the lengthening of the SA interval was more pronounced in the neonatal hearts, where the atrial refractory period was prolonged by propofol at 10 $\mu\text{mol/L}$ and above^[19].

Based on the above study, the effects of propofol on the conduction system remain controversial. One reasonable explanation is that different concentrations promote divergent effects: at clinically relevant or low concentrations, propofol does not significantly suppress conduction, but at high concentrations, it blocks conduction.

In a canine study, propofol reduced the arrhythmogenic plasma concentration of epinephrine in a concentration-dependent manner, which suggests that propofol enhances epinephrine-induced arrhythmias^[20]. Furthermore, propofol can directly induce arrhythmia.

Rewari and Kaul^[21] have reported that one long Q-T interval syndrome patient undergoing surgery experienced ventricular premature beats immediately upon propofol administration and then progressed to polymorphic ventricular tachycardia that intermittently changed to ventricular fibrillation. Another report described a 78-year-old woman with normal cardiac function who suffered torsade de pointes and then progressed to ventricular fibrillation after propofol infusion^[22]. Prolonged high-dose propofol infusion can induce some particular arrhythmias. An infant also developed dramatic cardiac conduction disturbances and tachyarrhythmias after prolonged high-dose propofol infusion; this patient's electrocardiograph resembled that of a patient with Brugada syndrome^[23]. A study of a chronic propofol abuser with a propofol blood concentration as high as 0.73 $\mu\text{g/g}$ also revealed a Brugada-like electrocardiograph. This patient subsequently developed a long Q-T interval, idioventricular rhythm, and ventricular fibrillation^[24].

These cases demonstrate that propofol can block conduction and induce bradycardia. Polymorphic ventricular tachycardia and some particular arrhythmias similar to Brugada syndrome can also result from propofol treatment. It should be noted that the most common abnormality is bradycardia, whereas others, such as AV block, are relatively rare and only occur at high propofol concentrations. A systematic review showed that the incidence of bradycardia (<50 beats per minute) was 4.8% in the presence of propofol^[25]. The reason for the conduction block could be the ability of propofol to modify the activity of human atrial muscarinic cholinergic receptors, and this effect may be related to the drug-induced bradycardia^[26]. Further, an M-2-muscarinic receptor-mediated mechanism may be the reason for propofol-induced conduction block. In a study of isolated guinea pig hearts, the negative dromotropic effect of propofol was attenuated by a muscarinic receptor

antagonist^[14].

Propofol and action potential duration

Action potential duration (APD) is determined by several inward and outward ion currents, including I_{Na} , I_{Ca} , I_{KR} , and I_{KS} . Changes in any individual current may prolong or shorten the APD, and APD dispersion can produce ventricular arrhythmia. Propofol (25 and 50 $\mu\text{mol/L}$) shortened monophasic APD at 90% repolarization (MAPD_{90}) in Langendorff-perfused guinea pig hearts^[27]. With single guinea pig cardiac myocytes, propofol (10 and 100 $\mu\text{mol/L}$) shortened the APD. A concentration-dependent shortening of the APD was produced by propofol (1–100 $\mu\text{mol/L}$) in these cells^[28]. However, the concentration of propofol required to reduce the APD by 50% was at least 100 $\mu\text{mol/L}$, and neither resting membrane potential nor action potential amplitude was significantly affected^[29]. High-dose propofol (1000 $\mu\text{mol/L}$) also shortened the APD of single dog ventricular cells^[30]. Propofol reduced the APD_{20} and the APD_{90} (the time required for 20% or 90% repolarization, respectively) in guinea pig cardiomyocytes in a concentration-dependent manner, and the APD_{90} was reduced by 21% at 100 $\mu\text{mol/L}$ ^[31]. In seeming contrast, however, propofol lessened the ischemia-induced decrease in the APD_{90} at 1 $\mu\text{mol/L}$ and 10 $\mu\text{mol/L}$ and attenuated the APD dispersion around the “border zone”, which is between the normal and ischemic zones of guinea pig right ventricular muscle strips. Specifically, the APD was shortened by 27%, 31% and 3% at doses of 1, 10, and 20 $\mu\text{mol/L}$ propofol, respectively^[11]. This effect is of particular importance because the decrease in APD dispersion between the normal and ischemic areas results in a reduction in the incidence of reentrant tachycardia. These paradoxical findings indicate that the propofol-induced shortening or prolongation of the APD is related to the cell surroundings. In normal conditions, propofol reduces the APD, whereas in ischemic conditions, it lessens the shortening trend.

Propofol and ion channels

Propofol can influence some ion currents, including the ATP-sensitive potassium current, delayed rectifier K^+ current, transient outward rectifier K^+ channel current, inward rectifier K^+ current, sodium current, and L-type Ca^{2+} current. These effects cumulatively result in changes to the APD.

ATP-sensitive potassium channels (K_{ATP}), which are composed of the Kir6.x and SUR subunits, are regulated by cytosolic nucleotides and link cell metabolism to electrical activity and K^+ fluxes. There are two types: sarcolemmal K_{ATP} ($\text{sarcK}_{\text{ATP}}$) channels and mitochondrial K_{ATP} ($\text{mitoK}_{\text{ATP}}$) channels. A number of studies have examined the effect of propofol on $\text{mitoK}_{\text{ATP}}$ channels.

In isolated guinea pig myocardial cells, propofol alone had no significant effects on $\text{mitoK}_{\text{ATP}}$ channels at a concentration of 50 $\mu\text{mol/L}$, but it dose-dependently inhibited isoflurane-induced mitochondrial K_{ATP} channel opening^[32]. In isolated ischemia-reperfused guinea pig hearts, propofol (35 $\mu\text{mol/L}$) had no effect on $\text{mitoK}_{\text{ATP}}$ channels^[33]. A study of single rat

ventricular myocytes showed that propofol inhibited $\text{mitoK}_{\text{ATP}}$ channel activity, but the concentration required was very high (>31 $\mu\text{mol/L}$)^[34]. By contrast, propofol has differing effects on $\text{sarcK}_{\text{ATP}}$ channels. For example, studies^[35, 36] on recombinant cardiac $\text{sarcK}_{\text{ATP}}$ channels showed that propofol inhibited the channel with half the maximal inhibitory concentration (IC_{50}) more than 70 $\mu\text{mol/L}$; in the presence of MgADP, the IC_{50} was as high as 183 $\mu\text{mol/L}$.

Because propofol protein binding exceeds 95%, free fractions of propofol are less than 2 $\mu\text{mol/L}$ ^[34]. Hence, we can conclude that propofol inhibits K_{ATP} channels only at high concentrations and has no significant effect on either $\text{sarcK}_{\text{ATP}}$ or $\text{mitoK}_{\text{ATP}}$ channel activities at clinically relevant concentrations.

In the human heart, the delayed rectifier K^+ current (I_{K}) can be separated into at least three different components: ultra-rapid (I_{KUR}), rapid (I_{KR}) and slow (I_{KS}). The effects of low- and high-dose propofol on some of these components have been examined. Two independent studies assessed the effect of propofol treatment on I_{K} ^[31, 37]. In one, propofol (28 $\mu\text{mol/L}$) induced significant depression of the I_{K} component in single dispersed guinea pig ventricular myocytes. Data from the second study indicates that propofol inhibits I_{K} at a concentration of 50 $\mu\text{mol/L}$. In another study, propofol suppressed the I_{K} amplitude in a concentration-dependent manner (IC_{50} =36 $\mu\text{mol/L}$) in differentiated H9c2 cells. The H9c2 cell line was established from an embryonic rat cardiac ventricle, and it has properties similar to neonatal and adult cardiomyocytes^[38]. It is important to note that the concentrations required for I_{K} suppression are higher than what is currently used in the clinic.

The slowly activating component of the I_{KS} contributes to human atrium and ventricle repolarization, particularly during action potentials with a long duration, and is a dominant determinant of the physiological heart rate-dependent shortening of the APD^[39]. A study of guinea pig ventricular myocytes indicated that propofol inhibited the I_{KS} (IC_{50} =23 $\mu\text{mol/L}$)^[29], whereas data from another study in these cells demonstrated that propofol (100 $\mu\text{mol/L}$ and 300 $\mu\text{mol/L}$) selectively inhibited the I_{KS} of isolated guinea pig ventricular myocytes. Therefore, propofol was preferred as the agent to separate I_{K} into I_{KR} and I_{KS} ^[40]. Propofol also inhibited the I_{sK} (IC_{50} =250 $\mu\text{mol/L}$), which is the current induced by the mRNA that encodes the minK protein that has similar electrophysiological properties to I_{KS} . This particular study measured the channel activity after expression via injection into *Xenopus* oocytes^[41].

The rapid activating component of the delayed rectifier potassium current (I_{KR}) is characterized by rapid activation, rapid inactivation and strong inward rectification, which promotes phase 3 of repolarization. Thus, I_{KR} plays an important role in governing the cardiac APD and refractoriness. Pharmacologically, I_{KR} is the target of class III antiarrhythmic drugs; however, to the best of our knowledge, little research concerning the effects of propofol on the I_{KR} component has been published. Heath and Terrar^[40] showed that propofol had no effect on the channel, and it was selected as an agent

to differentiate I_{KR} and I_{KS} . Similarly, no group has reported how propofol modulates the ultrarapid activating component of the delayed rectifier potassium current (I_{KUR}), which exists only in human atria and not ventricular tissue. I_{KUR} is the predominant delayed rectifier current responsible for human atrial repolarization. Hence, studies of the effects of propofol on this component will be of great clinical value.

The transient outward rectifier K^+ channel current (I_{to}) is a voltage-gated channel current that is responsible for early rapid repolarization (phase 1). I_{to} also determines the height of the early plateau, thus influencing activation of other currents that control repolarization^[31]. Propofol (60 $\mu\text{mol/L}$) inhibited the I_{to} of canine ventricular cells, and the inhibition was not voltage dependent^[42]. Propofol (25 and 50 $\mu\text{mol/L}$) also significantly decreased the I_{to} in rat ventricular myocytes but did not affect the voltage-dependent manner and the outward rectifier character^[43]. In addition, the steady-state voltage-dependent inactivation curve of I_{to} was shifted to a more negative membrane potential, and the I_{to} of rabbit atrial myocytes was suppressed by propofol with a 50% effective dose (ED_{50}) of 5.7 $\mu\text{mol/L}$. At 3 $\mu\text{mol/L}$, propofol slightly inhibited I_{to} , suggesting that while propofol does inhibit I_{to} at high concentrations, the suppression is minimal or nonexistent at clinically relevant concentrations^[15].

The inward rectifier K^+ current (I_{K1}) plays a significant role in cardiac myocytes where it maintains the resting membrane potential and shapes the late repolarization phase (phase 3) of the action potential. Whether propofol inhibits the I_{K1} is not clear. Propofol (28 $\mu\text{mol/L}$) had no effect on the I_{K1} of single dispersed guinea pig ventricular myocytes^[37] nor was an effect observed using a higher concentration (60 $\mu\text{mol/L}$) on single dispersed canine ventricular cells^[42]. Further, propofol (2.5 $\mu\text{mol/L}$) did not alter I_{K1} conductance in rat ventricular myocytes^[44]. By contrast, another study indicated that propofol suppressed I_{K1} , although the decrease in I_{K1} occurred to a much lesser extent: the currents were decreased by only 18% when cells were exposed to 3 $\mu\text{mol/L}$ propofol, and the inward rectification was not affected^[15].

Cardiac sodium channels transmit a large inward depolarizing current (I_{Na}) during phase 0 of the cardiac action potential, and it has been shown that propofol inhibits sodium currents. For example, in isolated rabbit ventricular myocytes, the Na^+ current was decreased in dose-dependent and frequency-dependent manners by propofol with an ED_{50} for current inhibition of 6.9 $\mu\text{mol/L}$. In part, this suppression was due to a negative shift of the steady-state voltage-dependent inactivation and a decreased rate of recovery from inactivation^[15]. Propofol inhibited I_{Na} in isolated rat myocardial cells, and the effect was enhanced at depolarized resting potentials^[45]. In another study, single channel conductance was not changed by propofol, but a dose-dependent suppression of rat whole cell sodium currents (ED_{50} =14.8 $\mu\text{mol/L}$) was detected. The most reasonable explanation for this apparent dichotomy is that a shorter mean channel open time accompanied by an increased channel re-opening could result in slowed macroscopic inactivation^[46]. Hyperpolarization-activated, cyclic nucleotide-

gated (HCN) channels conduct a monovalent cationic current $I(f)$ that contributes to autorhythmicity in the heart. Propofol inhibited and slowed the activation of recombinant HCN1, HCN2, and HCN4 channels at clinically relevant concentrations, in which the HCN1 current was the most sensitive of the three. HCN4 is the predominant subtype in the sinoatrial node (SA node)^[47, 48]. In this study, HCN4 channel activation was decreased more significantly than other isoforms with 20 $\mu\text{mol/L}$ propofol. In addition, propofol reduced the heart rate in an isolated guinea pig heart preparation over the same range of concentrations. These data indicate that propofol modulation of HCN channel gating is an important molecular mechanism that contributes to the bradyarrhythmic effect of propofol^[49].

The L-type Ca^{2+} current (I_{Ca}) is important in heart function because it triggers excitation-contraction coupling, modulates action potential shape, and is involved in cardiac arrhythmia. The negative inotropic effect of propofol can therefore be best explained by inhibition of the L-type Ca^{2+} current (I_{Ca}). Though propofol did not alter steady-state I_{Ca} , it reduced the isoproterenol-stimulated increase in I_{Ca} in a dose-dependent manner (0.1–10 $\mu\text{mol/L}$)^[50]. Propofol caused a statistically significant decrease in the I_{Ca} of guinea pig cardiac myocytes in a concentration-dependent manner (1–100 $\mu\text{mol/L}$), even at low concentrations (1 $\mu\text{mol/L}$)^[29]. In single dog ventricular cells, propofol decreased the I_{Ca} at 100 $\mu\text{mol/L}$ ^[30]. Propofol (10 and 100 $\mu\text{mol/L}$) also inhibited the I_{Ca} of H9c2 cells and guinea pig cardiac myocytes^[28, 37]. In rat ventricular myocytes, propofol depressed the I_{Ca} by 28% and 57% at 25 and 50 $\mu\text{mol/L}$, respectively^[51]. These data from several different model systems definitively prove that propofol inhibits I_{Ca} even at concentrations used in the clinic (1 $\mu\text{mol/L}$).

In conclusion, propofol can inhibit sodium, calcium and potassium currents, but we should note that the concentrations needed for inhibition are much higher than clinically achievable concentrations. At clinically relevant concentrations, propofol is likely to inhibit I_{K1} , I_{Na} , and I_{Ca} . However, controversies still exist, most notably the fact that propofol shortened the APD but lessened the ischemia-induced decrease of the APD.

Propofol and gap junctions

Gap junctions comprise intercellular channels that couple cardiac myocytes electrically and metabolically by facilitating the intercellular exchange of ions, signaling molecules, and other molecular information between neighboring cells in the heart. The constituent proteins of gap junction channels, connexins, play a critical role in impulse propagation and electrical synchronization between myocytes. Multiple connexin types are expressed in the heart, among which connexin 43 (Cx43) is the principal gap junction protein in ventricular myocardium^[52, 53].

Ventricular arrhythmia following acute myocardial infarction is always lethal. Propofol preconditioning has the ability to prevent the ischemic heart from progressing to a lethal ventricular arrhythmia. Cx43 is a principal cardiac gap-junction channel protein that undergoes progressive dephosphoryla-

tion during acute myocardial infarction (MI). The dephosphorylation of Cx43 decreases gap junction conduction, which produces the substrate for reentrant arrhythmia. Propofol treatment preserved Cx43 phosphorylation during acute myocardial ischemia, and this might protect the heart from serious ventricular arrhythmias during acute coronary occlusion^[54]. However, one study showed that the electrical uncoupling correlated with an intercalated disk occurred 10–15 min after ischemia^[55]. In the study of Hirata *et al*, most of the severe arrhythmias occurred between 5 and 10 min in all groups^[54]. As such, the importance of the role played by Cx43 in arrhythmogenesis is debatable.

Propofol and the autonomic nervous system

The Bezold-Jarish reflex sensitivity is an index of vagal nerve activity. Activation of the Bezold-Jarish reflex by injection of some agents produced a profound reduction in heart rate. It has been postulated that propofol-induced bradycardia may be related to the Bezold-Jarish reflex. Vincze^[56] and Ebert^[57] indicated that propofol lowered the Bezold-Jarish reflex sensitivity, but other researches indicated that the cause of acute bradycardia after propofol administration did not involve the Bezold-Jarish reflex in humans^[58] or rabbits^[59].

Whether the block of cardiac conduction by propofol is due to direct or indirect effects by the autonomic nervous system is controversial. Ikeno^[60] reported that propofol did not affect the cardiac conduction system when the autonomic nervous system was completely blocked. Therefore, it was thought that the conductance change was an indirect effect of propofol. Propofol also reduced the cardiac parasympathetic tone in humans, depending on the depth of hypnosis^[61]. Propofol could protect the heart from serious ventricular arrhythmias during acute coronary occlusion, but the effect was absolutely blocked by atropine, indicating that the antiarrhythmic effect of propofol was due to a reduction in sympathetic tone leading to a dominance of parasympathetic tone^[27]. Research showed that propofol suppressed both sympathetic and parasympathetic tone, but the suppression of sympathetic tone was more than that of parasympathetic tone^[62, 63].

Conclusion

Though propofol can induce various types of arrhythmias, some of which are severe, the incidence of arrhythmia is relatively rare at clinically relevant concentrations of propofol. Numerous studies conclusively show that propofol has the potential to inhibit arrhythmia. The potential antiarrhythmic mechanisms of propofol include ion channel inhibition, uneven suppression of the autonomic nervous system, and protection of gap junctions during ischemia. The controversies in the field can be attributed in part to the use of different species and experimental conditions and the promiscuous effects of propofol at various concentrations. The currently available data regarding the effects of propofol on arrhythmogenesis are not sufficient. Previous studies mostly focused on normal conditions, but arrhythmias are always induced in abnormal conditions, such as ischemia and electrolyte disturbances. In

addition, there is no pharmacogenetic data on the opposing propofol effects at clinically used doses. Available clinical data largely came from sporadic reports rather than large-sized, blinded and controlled trials. We believe future studies will expand to these areas to fully characterize the arrhythmic and antiarrhythmic properties of propofol.

Acknowledgements

This study is granted by National 973 Project (2007CB512008).

References

- 1 Kannan S, Sherwood N. Termination of supraventricular tachycardia by propofol. *Br J Anaesth* 2002; 88: 874–5.
- 2 Hermann R, Vettermann J. Change of ectopic supraventricular tachycardia to sinus rhythm during administration of propofol. *Anesth Analg* 1992; 75: 1030–2.
- 3 Burjorjee JE, Milne B. Propofol for electrical storm; a case report of cardioversion and suppression of ventricular tachycardia by propofol. *Can J Anaesth* 2002; 49: 973–7.
- 4 Mulpuru SK, Patel DV, Wilbur SL, Vasavada BC, Furqan T. Electrical storm and termination with propofol therapy: a case report. *Int J Cardiol* 2008; 128: e6–8.
- 5 Miro O, de la Red G, Fontanals J. Cessation of paroxysmal atrial fibrillation during acute intravenous propofol administration. *Anesthesiology* 2000; 92: 910.
- 6 Owczuk R, Wujtewicz MA, Sawicka W, Polak-Krzeminska A, Suszynska-Mosiewicz A, Raczynska K, *et al*. Effect of anaesthetic agents on P-wave dispersion on the electrocardiogram: comparison of propofol and desflurane. *Clin Exp Pharmacol Physiol* 2008; 35: 1071–6.
- 7 Seki S, Ichimiya T, Tsuchida H, Namiki A. A case of normalization of Wolff-Parkinson-White syndrome conduction during propofol anesthesia. *Anesthesiology* 1999; 90: 1779–81.
- 8 Wakita R, Takahashi M, Ohe C, Kohase H, Umino M. Occurrence of intermittent Wolff-Parkinson-White syndrome during intravenous sedation. *J Clin Anesth* 2008; 20: 146–9.
- 9 Michaloudis D, Fraidakis O, Kanoupakis E, Flossos A, Manios E. Idiopathic prolonged QT interval and QT dispersion: the effects of propofol during implantation of cardioverter-defibrillator. *Eur J Anaesthesiol* 1999; 16: 842–7.
- 10 Kleinsasser A, Loeckinger A, Lindner KH, Keller C, Boehler M, Puehringer F. Reversing sevoflurane-associated Q-Tc prolongation by changing to propofol. *Anaesthesia* 2001; 56: 248–50.
- 11 Hanouz JL, Yvon A, Flais F, Rouet R, Ducouret P, Bricard H, *et al*. Propofol decreases reperfusion-induced arrhythmias in a model of “border zone” between normal and ischemic-reperfused guinea pig myocardium. *Anesth Analg* 2003; 97: 1230–8.
- 12 Erb TO, Kanter RJ, Hall JM, Gan TJ, Kern FH, Schulman SR. Comparison of electrophysiologic effects of propofol and isoflurane-based anesthetics in children undergoing radiofrequency catheter ablation for supraventricular tachycardia. *Anesthesiology* 2002; 96: 1386–94.
- 13 Napolitano CA, Raatikainen MJ, Martens JR, Dennis DM. Effects of intravenous anesthetics on atrial wavelength and atrioventricular nodal conduction in guinea pig heart. Potential antidysrhythmic properties and clinical implications. *Anesthesiology* 1996; 85: 393–402.
- 14 Alphin RS, Martens JR, Dennis DM. Frequency-dependent effects of propofol on atrioventricular nodal conduction in guinea pig isolated heart. Mechanism and potential antidysrhythmic properties. *Anesthesiology* 1995; 83: 382–94.

- 15 Wu MH, Su MJ, Sun SS. Comparative direct electrophysiological effects of propofol on the conduction system and ionic channels of rabbit hearts. *Br J Pharmacol* 1997; 121: 617–24.
- 16 Warpechowski P, Lima GG, Medeiros CM, Santos AT, Kruse M, Migloransa MH, et al. Randomized study of propofol effect on electrophysiological properties of the atrioventricular node in patients with nodal reentrant tachycardia. *Pacing Clin Electrophysiol* 2006; 29: 1375–82.
- 17 Romano R, Ciccaglioni A, Fattorini F, Quaglione R, Favaro R, Arcioni R, et al. Effects of propofol on the human heart electrical system: a transesophageal pacing electrophysiologic study. *Acta Anaesthesiol Scand* 1994; 38: 30–2.
- 18 Pires LA, Huang SK, Wagshal AB, Kulkarni RS. Electrophysiological effects of propofol on the normal cardiac conduction system. *Cardiology* 1996; 87: 319–24.
- 19 Wu MH, Su MJ, Sun SS. Age-related propofol effects on electrophysiological properties of isolated hearts. *Anesth Analg* 1997; 84: 964–71.
- 20 Kamibayashi T, Hayashi Y, Sumikawa K, Yamatodani A, Kawabata K, Yoshiya I. Enhancement by propofol of epinephrine-induced arrhythmias in dogs. *Anesthesiology* 1991; 75: 1035–40.
- 21 Rewari V, Kaul H. Sustained ventricular tachycardia in long QT syndrome: is propofol the culprit? *Anesthesiology* 2003; 99: 764.
- 22 Douglas RJ, Cadogan M. Cardiac arrhythmia during propofol sedation. *Emerg Med Australas* 2008; 20: 437–40.
- 23 Robinson JD, Melman Y, Walsh EP. Cardiac conduction disturbances and ventricular tachycardia after prolonged propofol infusion in an infant. *Pacing Clin Electrophysiol* 2008; 31: 1070–3.
- 24 Riezzo I, Centini F, Neri M, Rossi G, Spanoudaki E, Turillazzi E, et al. Brugada-like EKG pattern and myocardial effects in a chronic propofol abuser. *Clin Toxicol (Phila)* 2009; 47: 358–63.
- 25 Hug CC Jr, McLeskey CH, Nahrwold ML, Roizen MF, Stanley TH, Thisted RA, et al. Hemodynamic effects of propofol: data from over 25,000 patients. *Anesth Analg* 1993; 77: S21–9.
- 26 Aguero Pena RE, Pascuzzo-Lima C, Granado Duque AE, Bonfante-Cabarcas RA. Propofol-induced myocardial depression: possible role of atrial muscarinic cholinergic receptors. *Rev Esp Anestesiol Reanim* 2008; 55: 81–5.
- 27 Morey TE, Martynyuk AE, Napolitano CA, Raatikainen MJ, Guyton TS, Dennis DM. Ionic basis of the differential effects of intravenous anesthetics on erythromycin-induced prolongation of ventricular repolarization in the guinea pig heart. *Anesthesiology* 1997; 87: 1172–81.
- 28 Shigemura T, Hatakeyama N, Shibuya N, Yamazaki M, Masuda A, Chen FS, et al. Effects of propofol on contractile response and electrophysiological properties in single guinea-pig ventricular myocyte. *Pharmacol Toxicol* 1999; 85: 111–4.
- 29 Hatakeyama N, Sakuraya F, Matsuda N, Kimura J, Kinoshita H, Kemotsu O, et al. Pharmacological significance of the blocking action of the intravenous general anesthetic propofol on the slow component of cardiac delayed rectifier K⁺ current. *J Pharmacol Sci* 2009; 110: 334–43.
- 30 Shibuya N, Higuchi A, Hatakeyama N, Yamazaki M, Ito Y, Momose Y. Effects of propofol on contractility and electrophysiological properties of canine single cardiomyocytes. *Masui* 1996; 45: 408–14.
- 31 Puttick RM, Terrar DA. Effects of propofol and enflurane on action potentials, membrane currents and contraction of guinea-pig isolated ventricular myocytes. *Br J Pharmacol* 1992; 107: 559–65.
- 32 Kohro S, Hogan QH, Nakae Y, Yamakage M, Bosnjak ZJ. Anesthetic effects on mitochondrial ATP-sensitive K channel. *Anesthesiology* 2001; 95: 1435–40.
- 33 Kamada N, Kanaya N, Hirata N, Kimura S, Namiki A. Cardioprotective effects of propofol in isolated ischemia-reperfused guinea pig hearts: role of K_{ATP} channels and GSK-3beta. *Can J Anaesth* 2008; 55: 595–605.
- 34 Kawano T, Oshita S, Tsutsumi Y, Tomiyama Y, Kitahata H, Kuroda Y, et al. Clinically relevant concentrations of propofol have no effect on adenosine triphosphate-sensitive potassium channels in rat ventricular myocytes. *Anesthesiology* 2002; 96: 1472–7.
- 35 Kawano T, Oshita S, Takahashi A, Tsutsumi Y, Tomiyama Y, Kitahata H, et al. Molecular mechanisms of the inhibitory effects of propofol and thiamylal on sarcolemmal adenosine triphosphate-sensitive potassium channels. *Anesthesiology* 2004; 100: 338–46.
- 36 Yamada H, Kawano T, Tanaka K, Yasui S, Mawatari K, Takahashi A, et al. Effects of intracellular MgADP and acidification on the inhibition of cardiac sarcolemmal ATP-sensitive potassium channels by propofol. *J Anesth* 2007; 21: 472–9.
- 37 Baum VC. Distinctive effects of three intravenous anesthetics on the inward rectifier (I_{K1}) and the delayed rectifier (I_K) potassium currents in myocardium: implications for the mechanism of action. *Anesth Analg* 1993; 76: 18–23.
- 38 Liu YC, Wang YJ, Wu SN. The mechanisms of propofol-induced block on ion currents in differentiated H9c2 cardiac cells. *Eur J Pharmacol* 2008; 590: 93–8.
- 39 Tamargo J, Caballero R, Gomez R, Valenzuela C, Delpon E. Pharmacology of cardiac potassium channels. *Cardiovasc Res* 2004; 62: 9–33.
- 40 Heath BM, Terrar DA. Separation of the components of the delayed rectifier potassium current using selective blockers of I_{Kr} and I_{Ks} in guinea-pig isolated ventricular myocytes. *Exp Physiol* 1996; 81: 587–603.
- 41 Heath BM, Terrar DA. Block by propofol and thiopentone of the min K current (I_{sk}) expressed in *Xenopus* oocytes. *Naunyn Schmiedeberg's Arch Pharmacol* 1997; 356: 404–9.
- 42 Buljubasic N, Marijic J, Berczi V, Supan DF, Kampine JP, Bosnjak ZJ. Differential effects of etomidate, propofol, and midazolam on calcium and potassium channel currents in canine myocardial cells. *Anesthesiology* 1996; 85: 1092–9.
- 43 Zhou J, Tian M, Zhou ZN. Inhibition of transient outward potassium current in rat ventricular myocytes by propofol. *Sheng Li Xue Bao* 1997; 49: 99–101.
- 44 Carnes CA, Muir WW 3rd, Van Wagoner DR. Effect of intravenous anesthetics on inward rectifier potassium current in rat and human ventricular myocytes. *Anesthesiology* 1997; 87: 327–34.
- 45 Saint DA, Tang Y. Propofol block of cardiac sodium currents in rat isolated myocardial cells is increased at depolarized resting potentials. *Clin Exp Pharmacol Physiol* 1998; 25: 336–40.
- 46 Saint DA. The effects of propofol on macroscopic and single channel sodium currents in rat ventricular myocytes. *Br J Pharmacol* 1998; 124: 655–62.
- 47 Baruscotti M, Barbuti A, Bucchi A. The cardiac pacemaker current. *J Mol Cell Cardiol* 2010; 48: 55–64.
- 48 Nof E, Antzelevitch C, Glikson M. The contribution of HCN4 to normal sinus node function in humans and animal models. *Pacing Clin Electrophysiol* 2010; 33: 100–6.
- 49 Cacheaux LP, Topf N, Tibbs GR, Schaefer UR, Levi R, Harrison NL, et al. Impairment of hyperpolarization-activated, cyclic nucleotide-gated channel function by the intravenous general anesthetic propofol. *J Pharmacol Exp Ther* 2005; 315: 517–25.
- 50 Kurokawa H, Murray PA, Damron DS. Propofol attenuates beta-adrenoreceptor-mediated signal transduction via a protein kinase C-dependent pathway in cardiomyocytes. *Anesthesiology* 2002; 96: 688–98.
- 51 Zhou W, Fontenot HJ, Liu S, Kennedy RH. Modulation of cardiac

- calcium channels by propofol. *Anesthesiology* 1997; 86: 670–5.
- 52 Poelzing S, Rosenbaum DS. Altered connexin43 expression produces arrhythmia substrate in heart failure. *Am J Physiol Heart Circ Physiol* 2004; 287: H1762–70.
- 53 Saffitz JE, Laing JG, Yamada KA. Connexin expression and turnover: implications for cardiac excitability. *Circ Res* 2000; 86: 723–8.
- 54 Hirata N, Kanaya N, Kamada N, Kimura S, Namiki A. Differential effects of propofol and sevoflurane on ischemia-induced ventricular arrhythmias and phosphorylated connexin 43 protein in rats. *Anesthesiology* 2009; 110: 50–7.
- 55 Kleber AG, Riegger CB, Janse MJ. Electrical uncoupling and increase of extracellular resistance after induction of ischemia in isolated, arterially perfused rabbit papillary muscle. *Circ Res* 1987; 61: 271–9.
- 56 Vincze D, Farkas AS, Rudas L, Makra P, Csik N, Lepran I, et al. Relevance of anaesthesia for dofetilide-induced *torsades de pointes* in alpha1-adrenoceptor-stimulated rabbits. *Br J Pharmacol* 2008; 153: 75–89.
- 57 Ebert TJ. Sympathetic and hemodynamic effects of moderate and deep sedation with propofol in humans. *Anesthesiology* 2005; 103: 20–4.
- 58 Ma D, Chakrabarti MK, Whitwam JG. Propofol, bradycardia and the Bezold-Jarisch reflex in rabbits. *Br J Anaesth* 1999; 82: 412–7.
- 59 Cullen PM, Turtle M, Prys-Roberts C, Way WL, Dye J. Effect of propofol anesthesia on baroreflex activity in humans. *Anesth Analg* 1987; 66: 1115–20.
- 60 Ikeno S, Akazawa S, Shimizu R, Nakaigawa Y, Ishii R, Inoue S, et al. Propofol does not affect the canine cardiac conduction system under autonomic blockade. *Can J Anaesth* 1999; 46: 148–53.
- 61 Kanaya N, Hirata N, Kurosawa S, Nakayama M, Namiki A. Differential effects of propofol and sevoflurane on heart rate variability. *Anesthesiology* 2003; 98: 34–40.
- 62 Deutschman CS, Harris AP, Fleisher LA. Changes in heart rate variability under propofol anesthesia: a possible explanation for propofol-induced bradycardia. *Anesth Analg* 1994; 79: 373–7.
- 63 Hidaka S, Kawamoto M, Kurita S, Yuge O. Comparison of the effects of propofol and midazolam on the cardiovascular autonomic nervous system during combined spinal and epidural anesthesia. *J Clin Anesth* 2005; 17: 36–43.

Original Article

Characterization of a critical role for CFTR chloride channels in cardioprotection against ischemia/reperfusion injury

Sunny Yang XIANG^{1,§}, Linda L YE¹, Li-lu Marie DUAN¹, Li-hui LIU^{1,3}, Zhi-dong GE², John A AUCHAMPACH², Garrett J GROSS², Dayue Darrel DUAN^{1,*}

¹Department of Pharmacology, University of Nevada School of Medicine, Reno, NV 89557, USA; ²Department of Pharmacology and Toxicology, Medical College of Wisconsin, Milwaukee, WI 53226, USA; ³Institute of Clinical Pharmacology, Central South University Xiangya School of Medicine, Changsha 410078, China

Aim: To further characterize the functional role of cystic fibrosis transmembrane conductance regulator (CFTR) in early and late (second window) ischemic preconditioning (IPC)- and postconditioning (POC)-mediated cardioprotection against ischemia/reperfusion (I/R) injury.

Methods: CFTR knockout (*CFTR*^{-/-}) mice and age- and gender-matched wild-type (*CFTR*^{+/+}) and heterozygous (*CFTR*^{+/-}) mice were used. In *in vivo* studies, the animals were subjected to a 30-min coronary occlusion followed by a 40-min reperfusion. In *ex vivo* (isolate heart) studies, a 45-min global ischemia was applied. To evaluate apoptosis, the level of activated caspase 3 and TdT-mediated dUTP-X nick end labeling (TUNEL) were examined.

Results: In the *in vivo* I/R models, early IPC significantly reduced the myocardial infarct size in wild-type (*CFTR*^{+/+}) (from 40.4%±5.3% to 10.4%±2.0%, *n*=8, *P*<0.001) and heterozygous (*CFTR*^{+/-}) littermates (from 39.4%±2.4% to 15.4%±5.1%, *n*=6, *P*<0.001) but failed to protect CFTR knockout (*CFTR*^{-/-}) mice from I/R induced myocardial infarction (46.9%±6.2% vs 55.5%±7.8%, *n*=6, *P*>0.5). Similar results were observed in the *in vivo* late IPC experiments. Furthermore, in both *in vivo* and *ex vivo* I/R models, POC significantly reduced myocardial infarction in wild-type mice, but not in CFTR knockout mice. In *ex vivo* I/R models, targeted inactivation of *CFTR* gene abolished the protective effects of IPC against I/R-induced apoptosis.

Conclusion: These results provide compelling evidence for a critical role for CFTR Cl⁻ channels in IPC- and POC-mediated cardioprotection against I/R-induced myocardial injury.

Keywords: ischemia; preconditioning; postconditioning; apoptosis; cystic fibrosis transmembrane conductance regulator (CFTR)

Acta Pharmacologica Sinica (2011) 32: 824–833; doi: 10.1038/aps.2011.61

Introduction

Ischemia and reperfusion (I/R) induce myocardial injury and lead to infarction through increased apoptosis (programmed cell death) and necrosis^[1,2]. Ischemic preconditioning (IPC) is a phenomenon in which brief episodes of ischemia dramatically reduce myocardial infarct size produced by a subsequent sustained ischemia and reperfusion^[3]. IPC has an early phase (lasting 1–2 h) and a late phase or “second window” (lasting 24–72 h) of protection^[4]. The signaling pathways involved in both early IPC (EIPC) and late IPC (LIPC) have been the

subject of numerous intensive studies ever since IPC was first described by Murry *et al* in 1986^[5,6]. The end-effectors of these signaling pathways are believed to directly participate in protecting the myocardium from subsequent ischemia/reperfusion insults after IPC^[7–9]. Both sarcolemmal and mitochondrial ATP-sensitive potassium channels (sarc-K_{ATP} and mito-K_{ATP}, respectively) have been suggested to serve as mediators or end-effectors in EIPC and LIPC^[8,9]. Many other factors have also been proposed to be end-effectors, including the mitochondrial permeability transition pore (mPTP)^[10], the sodium/hydrogen exchanger^[11], and swelling-activated Cl⁻ channels^[12,13]. Although it has been shown that specific blockades of each proposed end-effector completely abolish the protection given by IPC, the identification of which factors are true end-effectors and the elucidation of possible interactions between these end-effectors have yet to be established^[5,14,15].

[§] Now in the Department of Pharmacology, University of California at San Diego, 9500 Gilman Drive, La Jolla, CA 92093-0636, USA

* To whom correspondence should be addressed.

E-mail dduan@medicine.nevada.edu

Received 2011-03-16 Accepted 2011-04-18

In 2003, Zhao *et al* reported that short episodes of I/R immediately after sustained ischemia and before full reperfusion reduced myocardial infarct size to a level equivalent to IPC in dogs. This phenomenon was named ischemic postconditioning (POC)^[16]. POC is as powerful as EIPC and LIPC in reducing myocardial infarction and preserving functional performance of the heart and also has the potential to be clinically applicable in the most common situations of unexpected coronary occlusion and acute myocardial infarction^[16-18]. To date, POC has been documented in dog, pig, rabbit, rat, and mouse models and in humans^[6, 16, 19-22]. This widespread occurrence of POC has aroused a renewed interest in understanding the mechanisms of cell death during I/R and identifying endogenous mediators of cardioprotection against I/R injury^[6, 17, 18, 22, 23]. Many studies suggest that POC shares some signaling pathways with IPC, including activation of PKC, PKA, PI3K-Akt, and the MEK1/2-Erk1/2 pathways. Both mito-K_{ATP} and mPTP are also thought to be key players or potential end-effectors in POC^[24, 25].

A recent study in isolated mouse hearts supports a potential role for the cystic fibrosis transmembrane-conductance regulator (CFTR) in acute IPC^[26]. The CFTR gene belongs to the ATP-binding cassette (ABC) transporter superfamily and encodes a PKC- and PKA-activated Cl⁻ channel in the heart^[27-30]. The sulfonylurea receptor (SUR) and mABC1 are also included in the same ABC superfamily. SUR combines with inward rectifier K⁺ (Kir6.1, Kir6.2) channel subunits to form functional sarc-K_{ATP} channels^[8, 9], and mABC1 was suggested to be a component of mito-K_{ATP}^[31]. While both sarc-K_{ATP} and mito-K_{ATP} channels have been extensively studied for their roles as important mediators of IPC and POC, the relative functional role of cardiac CFTR channels in EIPC, LIPC, and POC has not been studied. This study was designed to directly address this question with CFTR-knockout (*CFTR*^{-/-}) mice and age- and gender-matched wild-type (WT, *CFTR*^{+/+}) and heterozygous (*CFTR*^{+/-}) mice.

Materials and methods

This investigation conforms to the Guide for the Care and Use of Laboratory Animals (US National Institute of Health publication No 85-23, revised 1996) and was carried out in accordance with the Institutional Guidelines for Animal Care and Use approved by the University of Nevada Institutional Animal Care and Use Committee.

Breeding and genotyping of transgenic mice

STOCKCftrtm1Unc-TgN (FABPCFTR)1Jaw breeders obtained from Dr Jeffrey Whitsett (Children's Hospital Medical Center, Cincinnati, OH, USA) were bred in our transgenic animal facility as previously described^[26]. Eight- to twelve-week-old male *CFTR*^{-/-} offspring and age- and gender-matched *CFTR*^{+/+} and *CFTR*^{+/-} littermates were used. These mice were genotyped by performing polymerase chain reaction (PCR) on genomic DNA isolated from tail samples using a three-primer assay (5'-GAG AAC TGG AAG CTT CAG AGG-3', 5'-TCC ATC TTG TTC AAT GGC C-3', and 5'-TCC ATG TAG TGG TGT GAA

CG-3'), which resulted in a 357-bp band for *CFTR*^{-/-}, a 526-bp band for *CFTR*^{+/+}, and both bands for *CFTR*^{+/-}.

In vivo I/R injury

Mice were anesthetized with sodium pentobarbital (50 mg/kg, ip), placed on a 37 °C heated pad, intubated, and ventilated using a mouse ventilator (Harvard Apparatus, Germany) with air (respiration frequency 120 strokes/min). Body temperature was maintained at about 37 °C with the heating pad. Surface 12-lead ECG was recorded throughout the experiments on a Gould ACQ-7700 recorder (Gould Instrument Systems, Valley View, OH, USA). A left thoracotomy was performed, and the left anterior descending (LAD) coronary artery 2-3 mm from the tip of the left atrium was occluded with an Ethicon 8.0-silk suture (ETHICON, INC). Successful coronary occlusion was verified by the development of a pale color in the distal myocardium, which was observed using a Surgical Microscope system (Applied Fiberoptics, Southbridge, Massachusetts), and by S-T segment elevation and QRS widening on the ECG. Blood flow was restored by releasing the ligature. Successful reperfusion was confirmed when the bright red color of the left ventricle (LV) and the ECG returned to normal. A 30-min coronary occlusion (ischemia) was used in the *in vivo* studies. Either a 40-min or a 24-h reperfusion period was used according to different protocols.

In vivo EIPC, LIPC, and POC

To simulate EIPC, 3 I/R cycles of 4 min each were applied immediately before a sustained 30-min ischemia followed by a 40-min reperfusion, after which the chest was closed. Mice were allowed to recover for 24 h before their hearts were removed to measure infarct size. To simulate LIPC, 3 brief (4 min) I/R cycles (IPC) were applied on d 1, and a sustained ischemia (30 min) and reperfusion (40 min or 24 h) injury was created on d 2, while in the I/R controls, no IPC intervention was used on d 1. To simulate POC, 6 brief cycles (10 s) of LAD reflow/reocclusion were applied during the first minute of reperfusion immediately following a 30-min LAD coronary artery occlusion, while the control group received no interventions during reperfusion.

Ex vivo IPC and POC models (isolated Langendorff and working heart preparations)

The aorta and left atrium were cannulated and connected to the HSE isolated heart perfusion system (model IH-1, Harvard Apparatus, Inc) immediately after removal from mice to allow measurements to be obtained in the working-heart mode (afterload=60 mmHg, preload=10 mmHg) as described previously^[26]. Left ventricular pressure (LVP), LV developed pressure (LVDP), and LV end-diastolic pressure (LVEDP) were measured with a Millar tip catheter (1.4/0.8F pressure transducer, Millar) inserted into the LV cavity through the aorta. Measurements of functional performance, including aortic pressure (AP), heart rate (HR), left ventricular pressure (LVP), LV developed pressure (LVDP), first derivative of maximum and minimum LVDP ($\pm dp/dt$), and LV end-diastolic pressure

(LVEDP) were recorded continuously during the experiment and analyzed offline by an HSE data acquisition system (HSE Haemodyn, Harvard Apparatus). Total global ischemia, which was produced by clamping both atrial inflow and aortic outflow, was used to induce sustained ischemia and IPC and POC interventions. Myocardial infarct size was determined using 2,3,5-triphenyltetrazolium chloride (TTC) staining as described previously^[26].

Measurement of infarct size

At the end of each protocol, the heart was stained with 0.1 mL 5% Phthalo Blue (Heucotech LTD, USA) and 1 mL of 1% TTC and then removed. The area at risk and the infarct size of the left ventricle were quantified by a blinded observer using the image processing and analysis (IPA) module of Simple PCI image analysis software (Compic, Inc, USA)^[26]. The percent infarction was calculated for each slice and reported as the percent of infarct tissue divided by the total area at risk.

Active caspase 3 assay

Hearts from *CFTR*^{+/+} or *CFTR*^{-/-} mice were subjected to 45 min of ischemia and 180 min of reperfusion in the isolated Langendorff and working heart system to create I/R injury. Three brief 5-min cycles of I/R applied immediately before a sustained ischemic event were used for the IPC intervention. Control hearts were subjected to a 240-min perfusion to evaluate baseline activated caspase 3 activity. At the end of the experiments, the hearts were snap frozen in liquid nitrogen and stored at -80 °C. The hearts were then pulverized and homogenized in RIPA buffer in the presence of a protease inhibitor cocktail (Sigma, Saint Louis, MO, USA, P8340) with a Kontes-Duall glass homogenizer. The homogenates were incubated on ice for 30 min and centrifuged in a microcentrifuge at maximal speed (about 14000 r/min) for 10 min at 4 °C. The supernatant (whole lysate) was collected, and protein concentrations were determined using the BCA protein assay. The supernatants were incubated with SDS loading buffer at 95 °C for 5 min, separated by 12% SDS-PAGE, and transferred to a nitrocellulose (NC) membrane for immunoblot analysis. Following SDS-PAGE, the NC membrane was blocked with Odyssey blocking buffer (Li-COR, Lincoln, NA, USA, 927-40000) for 45 min and incubated with primary rabbit polyclonal anti-active caspase 3 antibody (1 µg/mL, Abcam, ab2302) overnight at 4 °C with rocking. To detect active caspase 3, the membrane was then incubated with Alexa Flour 680 goat anti-rabbit secondary antibody (dilution 1:50000, #A21076, Invitrogen, Carlsbad, CA, USA) for 45 min at room temperature, and the membranes were washed and then scanned with the Odyssey infrared imaging system at 700 nm and processed with Odyssey software (V1.2, Li-COR). GAPDH was used as an internal control.

TUNEL assay

To identify apoptotic cells containing DNA fragments, tissue samples (serial 8 µm cryosections) were immunohistochemically stained using terminal deoxynucleotidyl transferase

(TdT) and fluorescein conjugated nucleotides with the *in situ* cell death detection kit (Roche Applied Science, Indianapolis, IN) according to the manufacturer's instructions. Negative control sections were prepared without the TdT enzyme. Labeled nuclei were identified from the negative nuclei counterstained by propidium iodide (PI) (Vector Laboratories, Inc Burlingame, CA, USA) and counted after being photographed under a fluorescence microscope at 40× magnification. The percentage of TUNEL-positive nuclei (cell) was calculated as the number of TUNEL-labeled nuclei (green)/total nuclei (PI-labeled, red).

Statistical analysis

All group data are presented as the mean±SEM. ANOVA and Student's *t* test were used to determine statistical significance. A 2-tailed probability value of *P*<0.05 was considered statistically significant.

Results

Functional role of CFTR in EIPC-mediated cardioprotection

Age-matched male *CFTR*^{+/+}, *CFTR*^{+/-}, and *CFTR*^{-/-} mice were randomly divided into I/R (control) and EIPC groups following the experimental protocols depicted in Figure 1A. In the control group, mice were subjected to 24 min of open-chest exposure (sham) followed by a sustained 30-min occlusion and a 40-min reperfusion. In the EIPC group, 3 I/R cycles of 4 min each were applied immediately before a sustained 30-min ischemia followed by a 40-min reperfusion, and then the chest was closed. The mice were allowed to recover for 24 h before the hearts were removed to measure infarct size. Representative images of Phthalo Blue and TTC stained LV sections from each group are shown in Figure 1B. As seen in Figure 1C, EIPC significantly reduced the size of the infarcts caused by 30-min sustained ischemia and 24-h reperfusion (expressed as a percentage of the risk region) in the *CFTR*^{+/+} (from 40.4%±5.3% to 10.4%±2.0%, *n*=8, *P*<0.001) and *CFTR*^{+/-} mice (from 39.4%±2.4% to 15.4%±5.1%, *n*=6, *P*<0.001). However, EIPC failed to protect the hearts of *CFTR*^{-/-} mice (46.9%±6.2% in I/R control *vs* 55.5%±7.8% in EIPC, *n*=6, *P*>0.5). These results suggest that CFTR Cl⁻ channels are involved in the cardioprotective effects of EIPC *in vivo*.

Functional role of CFTR in LIPC-mediated cardioprotection

To test whether CFTR is involved in LIPC cardioprotection *in vivo*, age-matched male *CFTR*^{+/+}, *CFTR*^{+/-}, and *CFTR*^{-/-} mice were randomly divided into four groups following the experimental protocols depicted in Figure 2A. In the LIPC group, 3 brief (4 min) I/R cycles (IPC) were applied on d 1, and a sustained ischemia (30 min) and reperfusion (40 min or 24-h) injury was created on d 2, while in the I/R controls, no IPC intervention was used on d 1. The reason both a 40-min and a 24-h reperfusion were used in the LIPC protocols was to compare LIPC with EIPC and also to examine long term protection provided by LIPC. Similar to what was seen with EIPC, LIPC significantly reduced the size of the infarcts caused by sustained I/R injury in both *CFTR*^{+/+} (from 44.9%±5.1%

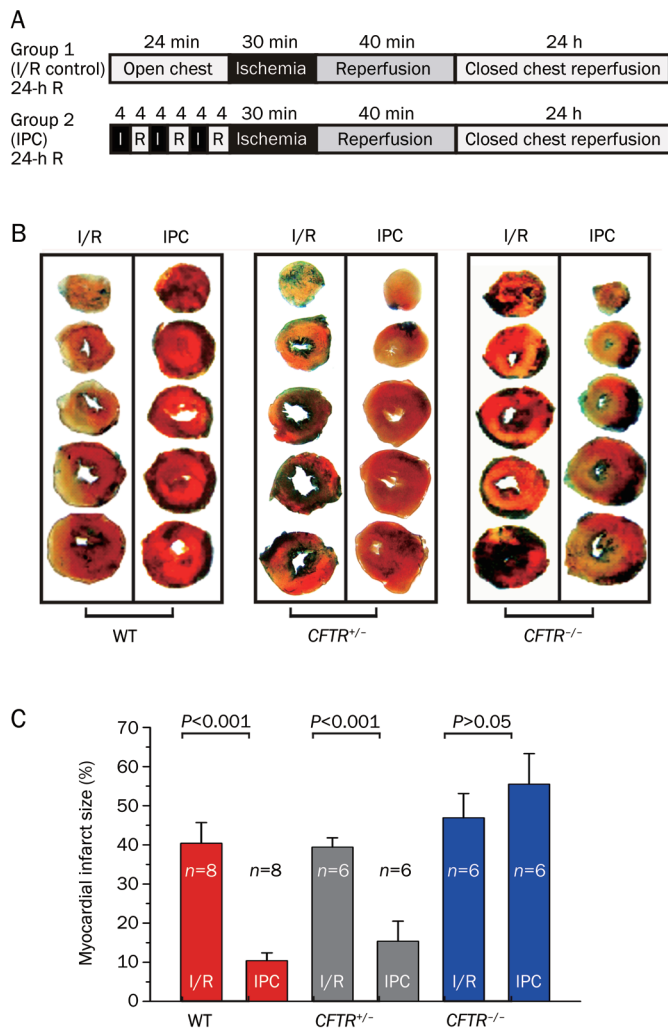


Figure 1. Effect of CFTR knockout on early preconditioning (EIPC). (A) Experimental protocols. Protocol for each group is applied to *CFTR*^{-/-} mice and age-matched *CFTR*^{+/+} (WT) and *CFTR*^{+/-} littermates. (B) Representative tissue staining of transverse slices from age-matched WT, *CFTR*^{+/-}, or *CFTR*^{-/-} mice. (C) Mean infarct size measured from age-matched WT, *CFTR*^{+/-}, or *CFTR*^{-/-} mouse heart in group 1 (I/R) and 2 (IPC).

to 20.6%±2.6%, *n*=7, *P*<0.001 in the groups with 40-min reperfusion and from 39.6%±4.1% to 18.3%±1.8%, *n*=6, *P*<0.001 in the groups with 24-h reperfusion) and *CFTR*^{+/-} mice (from 39.9%±4.1% to 19.4%±1.7%, *n*=6, *P*<0.001 in the groups with 40-min reperfusion, and from 40.2%±3.2% to 21.6%±2.0%, *n*=5, *P*<0.001 in the groups subjected to 24-h reperfusion). However, LIPC failed to provide protection against I/R injury in hearts from *CFTR*^{-/-} mice (42.6%±4.1% in control vs 40.8%±5.3% in LIPC with 40-min reperfusion, *n*=7, *P*>0.05, and 36.8%±3.2% in control vs 39.8%±4.7% in LIPC with 24-h reperfusion, *n*=5, *P*>0.05), as shown in Figures 2B and 2C. These results strongly indicate that CFTR may play a very important role in LIPC-mediated cardioprotection in the mouse heart.

Functional role of CFTR in POC-mediated cardioprotection

To examine whether CFTR Cl⁻ channels play a role in POC, we first established an *ex vivo* model of POC. Isolated Langendorff (retrograde) and working-heart (antegrade) perfusion preparations^[26] from *CFTR*^{-/-} and *CFTR*^{+/+} mice were subjected to the experimental protocols shown in Figure 3A. Functional and histological changes to the hearts during I/R and POC were studied. A 45-min period of ischemia was applied as the index ischemia. Six cycles of 10-s ischemia/reperfusion initiated in the first minute of reperfusion following the index ischemia were used as the POC intervention. I/R groups received no interventions during reperfusion. As shown in Table 1, I/R injury caused a significant decrease in heart function as evaluated by HR, LVDP, and ±dp/dt in both *CFTR*^{+/+} and *CFTR*^{-/-} mice; however, in hearts subjected to POC, post-ischemic cardiac function was restored to levels close to the baseline seen before the ischemic event in *CFTR*^{+/+} but not *CFTR*^{-/-} mice.

The infarct size was also measured to assess myocardial tissue injury and viability, and representative images of stained LV sections from each group are shown in Figure 3B. The size of infarcts caused by 45-min ischemia was significantly reduced from 37.5%±3.4% to 17%±2.0% (*P*<0.005, *n*=4) by POC in the hearts of *CFTR*^{+/+} mice but not *CFTR*^{-/-} mice (control, 40.4%±4.1% vs POC 45%±7.7%, *P*>0.1, *n*=5). These results strongly suggest that targeted inactivation of the *CFTR* gene in

Table 1. Effects of *CFTR* gene knockout on POC-induced changes in hemodynamics of the isolated perfused mouse heart. ^b*P*<0.05, ^c*P*<0.01, 40-min R vs baseline. Data are represented as mean±SEM.

	<i>CFTR</i> ^{+/+}				<i>CFTR</i> ^{-/-}			
	I/R		POC		I/R		POC	
	Baseline	40-min R	Baseline	40-min R	Baseline	40-min R	Baseline	40-min R
Heart rate (bpm)	387±29	312±14 ^b	397±10	379±15	378±20	295±5 ^b	419±18	303±6
LVDP (mmHg)	100.5±2.2	61.6±5.6 ^b	103.9±4.0	89.7±49	113.9±8.4	66.1±6.9 ^b	118.7±11.0	69.2±2.3 ^b
+dp/dt (mmHg/s)	7313±290	2874±125 ^c	8215±298	6451±476 ^b	8689±101	3088±234 ^c	7914±1042	3706±494 ^c
-dp/dt (mmHg/s)	5792±327	2618±177 ^b	5908±323	4707±483	6256±899	2233±104 ^c	5951±207	2673±649 ^c

I/R: ischemia/reperfusion; LVDP: left ventricular developed pressure; +dp/dt: maximum rate of change in LVDP; -dp/dt: minimum rate of change in LVDP. Hemodynamic parameters at baseline were measured at the end of the 10 min of working heart perfusion before ischemia/reperfusion protocol. Results measured at the end of 40 min of reperfusion (40-min R) after 45 min of global ischemia without postconditioning (I/R) or with postconditioning (POC) were compared with those measured at baseline.

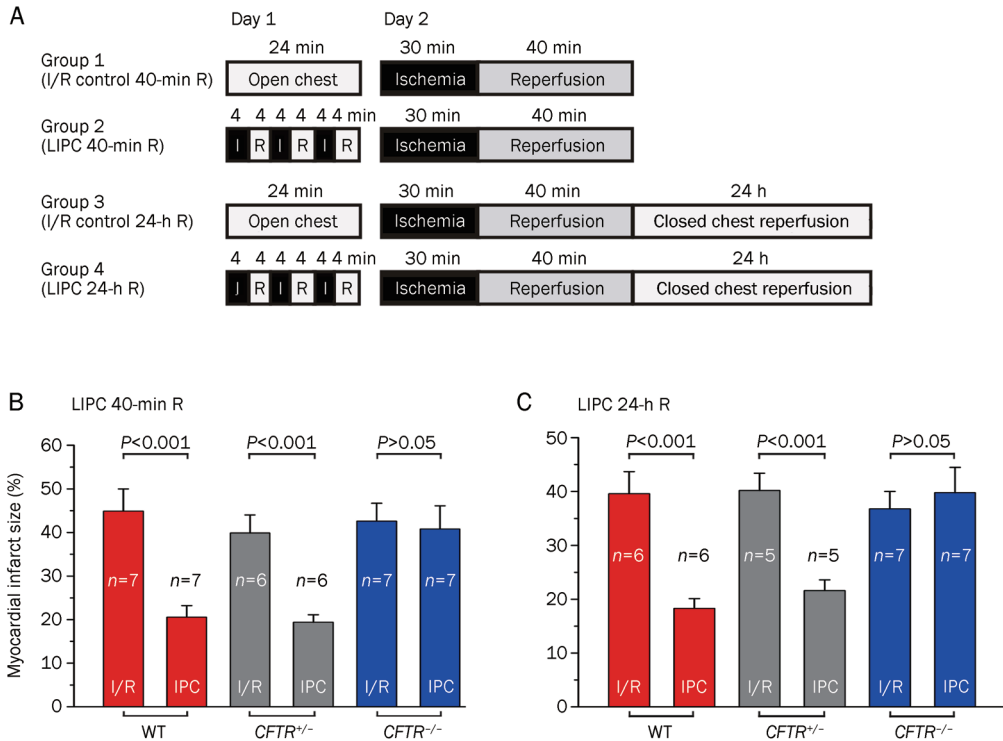


Figure 2. Effect of CFTR knockout on late (second window) preconditioning (LIPC). (A) Experimental protocols. Protocol for each group is applied to $CFTR^{-/-}$ mice and age-matched WT and $CFTR^{+/+}$ littermates. (B) Mean infarct size in Group 1 (I/R) & 2 (IPC) with 40-min reperfusion. (C) Mean infarct size in Group 3 (I/R) & 4 (IPC) with 24 h reperfusion.

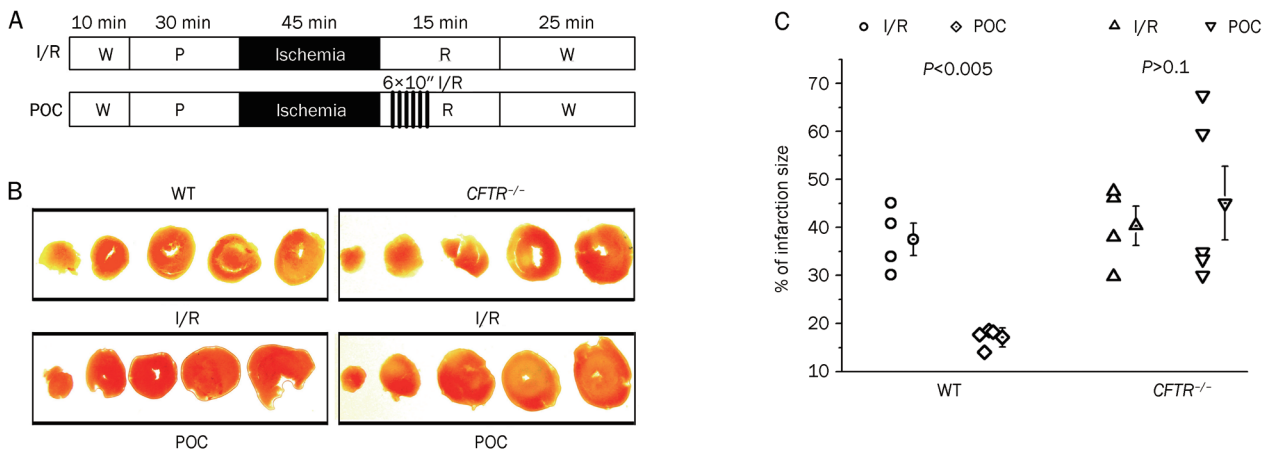


Figure 3. Effects of CFTR knockout on postconditioning (POC) in isolated hearts. (A) Experimental protocols. Protocol for each group is applied to $CFTR^{-/-}$ mice and age-matched WT littermates. W: working, P: perfusion, R: reperfusion. (B) Representative staining of ventricle transverse slices after ischemia/reperfusion (I/R) or postconditioning (POC). (C) Individual infarct size measured from each age- and gender-matched WT and $CFTR^{-/-}$ mouse hearts after control or POC, mean value with error bar (mean±SEM) were also shown for each group.

the mouse abolishes the cardioprotective effect of POC against sustained I/R in isolated hearts.

A “gold standard” for confirmation of the potential role of CFTR Cl⁻ channels in POC protection is to test whether POC also protects the heart from *in vivo* I/R injury. Therefore, an *in vivo* model of POC was established in $CFTR^{-/-}$ mice and their $CFTR^{+/+}$ littermates to test the effects of targeted inactivation of the CFTR gene on *in vivo* POC protection in mice.

Open-heart surgery was performed on male $CFTR^{-/-}$ mice

(8–12 week-old) and age-matched $CFTR^{+/+}$ and $CFTR^{+/-}$ littermates, and coronary artery occlusion and POC protocols were performed (Figure 4A). Immediately following a 30-min LAD coronary artery occlusion, which was applied as the index ischemia to induce about 40% infarct size in the hearts of mice in the control group, 6 brief cycles (10 s) of LAD reflow/reocclusion were applied in the first minute of reperfusion, while the control group received no interventions during reperfusion. At the end of each experimental protocol, the hearts

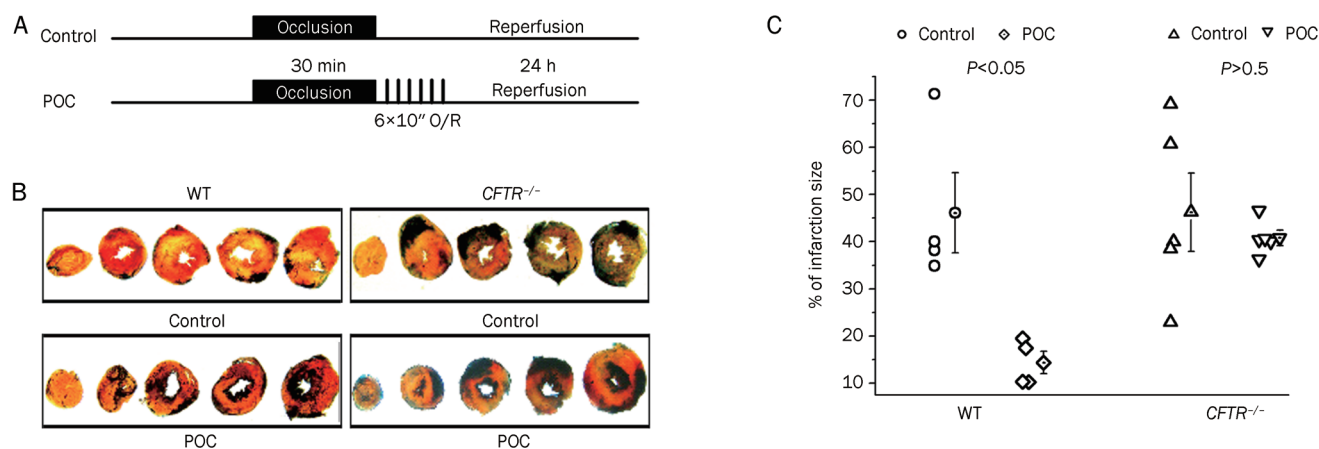


Figure 4. Effects of CFTR knockout on postconditioning (POC) *in vivo*. (A) Experimental protocols. Protocol for each group is applied to *CFTR*^{-/-} mice and age-matched WT littermates. O/R: occlusion/reperfusion. (B) Representative staining of ventricle transverse slices after ischemia/reperfusion (I/R) or postconditioning (POC). (C) Individual infarct size measured from each age- and gender-matched WT and *CFTR*^{-/-} mouse hearts after control or POC, mean value with error bar (mean±SEM) were also shown for each group.

were stained by TTC and Phthalo Blue (Figure 4B) and the infarct size (% of the region at risk) was calculated. As seen in Figure 4C, a 30-min ischemia/24-h reperfusion caused an infarct size of 46.1%±8.5% ($n=4$) in *CFTR*^{+/+} mice and an infarct size of 46.3%±8.3% ($n=5$) in *CFTR*^{-/-} mice. POC significantly reduced the infarct size within the risk zone to 14.4%±2.4% ($n=4$, $P<0.05$) in the *CFTR*^{+/+} mice but not in the *CFTR*^{-/-} mice (40.8%±1.2%, $n=5$, $P>0.5$). These results further confirm an important role of CFTR in POC-mediated cardioprotection against I/R injury in mouse hearts.

Effect of targeted inactivation of the CFTR gene on apoptosis

It has been demonstrated previously that apoptosis and necrosis are the major cell death pathways involved in I/R injury and myocardial infarction and that both IPC and POC can reduce I/R-induced apoptosis^[1, 2, 32, 33]. To test whether activation of CFTR Cl⁻ channels is important in IPC-mediated inhibition of apoptosis, isolated Langendorff and working heart preparations from *ex vivo* IPC models from age-matched male *CFTR*^{+/+} and *CFTR*^{-/-} mice were examined. As shown in Figure 5, post-ischemic functional performance, as estimated by LVDP, +dp/dt, and -dp/dt, was significantly improved by IPC in *CFTR*^{+/+} mouse hearts compared to non-preconditioned *CFTR*^{+/+} mouse hearts but not in *CFTR*^{-/-} mouse hearts (Figure 5B-5D). A separate group of control hearts was subjected to normal perfusions without I/R to investigate the amount of apoptosis that develops during I/R using the isolated heart perfusion system. Our results showed that a 240-min perfusion resulted in little caspase 3 activation (control) but that sustained I/R caused a significant increase in caspase 3 activation in both *CFTR*^{+/+} and *CFTR*^{-/-} mouse hearts. I/R induced caspase 3 activation, however, was significantly reduced by IPC in hearts of *CFTR*^{+/+} mice to a level similar to that of *CFTR*^{+/+} control mice. In hearts of *CFTR*^{-/-} mice, the level of active caspase 3 was not reduced by IPC, indicating loss of IPC-induced inhibition of apoptosis in these hearts (Figure 5A

and 5B).

To confirm our observations on the effects of knocking out *CFTR* on apoptosis of cardiac myocytes, TUNEL assays were performed to detect apoptotic cells under I/R and IPC conditions. Figure 5C shows a representative image of TUNEL assays in mouse heart sections. In these studies, the reperfusion time was increased to >360 min to allow DNA damage to develop. In control hearts not subjected to global I/R, 420 min of perfusion led to the appearance of some TUNEL-positive (TN-P) nuclei in the epicardium, but no TN-P nuclei were detected in the deeper layers of the myocardium (data not show). I/R resulted in the appearance of 26.1%±2.15% and 29.28%±4.98% TN-P nuclei in hearts of *CFTR*^{+/+} and *CFTR*^{-/-} mice, respectively. IPC significantly reduced TN-P nuclei in hearts of *CFTR*^{+/+} mice (3.77±0.28, $P<0.001$) but not hearts of *CFTR*^{-/-} mice (24.79%±3.17%, $P>0.1$) (Figure 5D). These results suggest that CFTR is very important for IPC-mediated inhibition of apoptosis in the heart.

Discussion

Although our previous study in isolated heart preparations suggested a potential role of CFTR in acute IPC, it is not clear what the exact function of CFTR is in *in vivo* EIPC and LIPC or whether CFTR is involved in POC^[26-28]. In this study, therefore, we investigated the relative role of CFTR Cl⁻ channels in *in vivo* EIPC and LIPC in the mouse heart. Our results demonstrate that CFTR Cl⁻ channels are important for both EIPC- and LIPC-mediated cardioprotection. In addition, our results provide strong evidence for a novel and critical role for CFTR Cl⁻ channels in POC-mediated cardioprotection. Furthermore, we found that CFTR may exert its cardioprotective effects through inhibition of apoptosis.

Functional role of Cl⁻ channels in IPC-mediated cardioprotection

For historical reasons, the potential role of Cl⁻ channels in cardiac physiology has been ignored^[27, 28]. The first evidence for

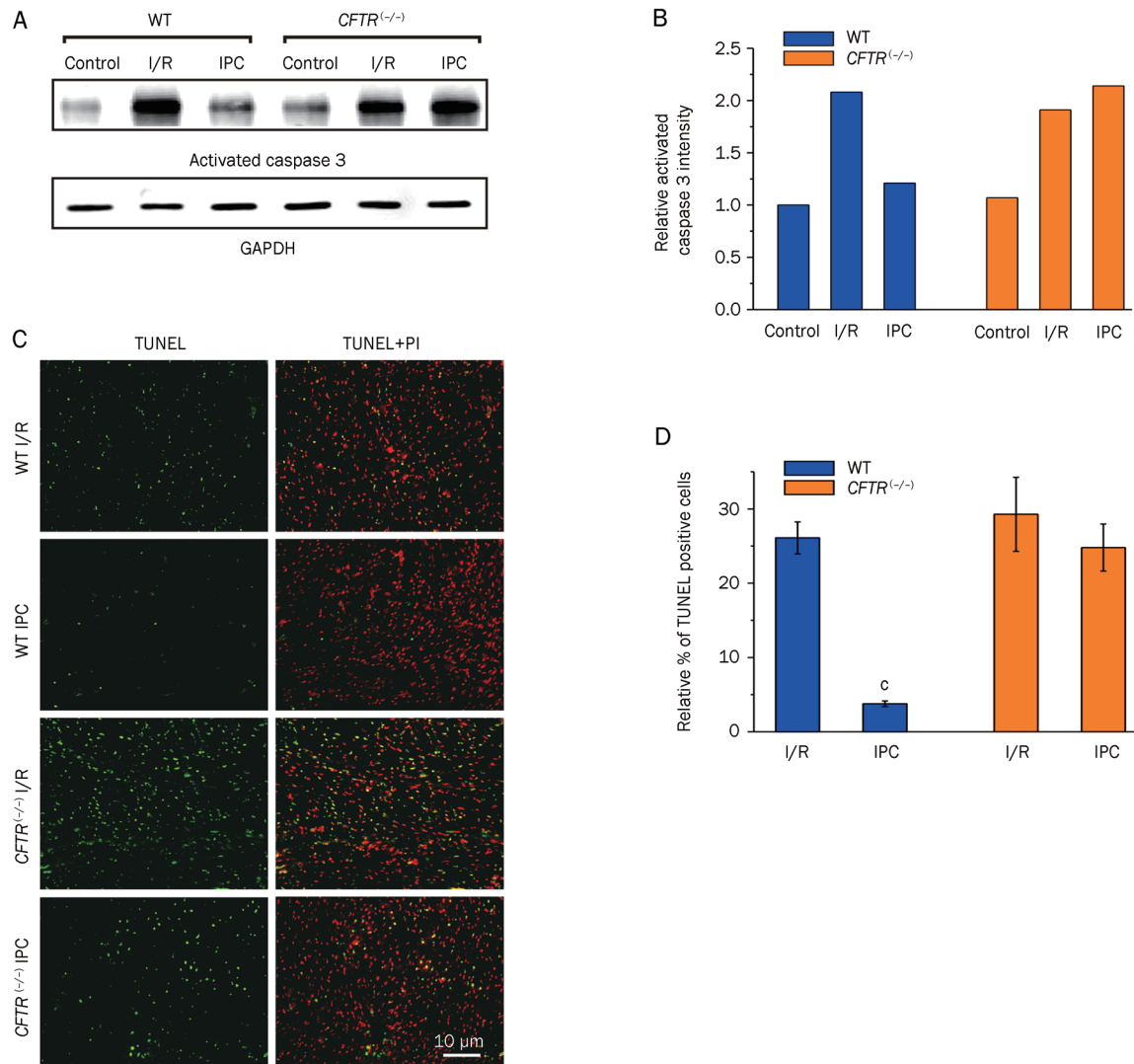


Figure 5. Effects of targeted inactivation of CFTR gene on apoptosis during I/R or IPC. (A) Western blots (WB) analysis of activated caspase 3 in an isolated perfusion heart model for either WT or *CFTR*^{-/-} mice exposed to reperfusion alone (control), ischemia/reperfusion (I/R) or ischemic preconditioning (IPC) protocols. After control (5 h perfusion), I/R (45 min ischemia/3 h reperfusion) or IPC (3 cycles of 5 min I/R right before the 45 min ischemia/3 h reperfusion) treatments, hearts lysates from each group were obtained and subjected to WB analysis for activated caspase 3. GAPDH was immunoblotted as a loading control. (B) Relative active caspase-3 density after normalized to GAPDH. (C) Representative images of heart longitudinal sections of TUNEL staining for each group of treatments: I/R (45 min ischemia/6 h reperfusion) or IPC (3 cycles of 5 min I/R right before the 45 min ischemia/6 h reperfusion). Green: TUNEL stained nuclei; red, propidium iodide (PI) stained nuclei. (D) Relative percentage of TUNEL positive (TP) cells calculated as 100% * (count of TP/count of PI), data presented as mean±SEM (error bar). *n*=6. ^c*P*=0.0027.

the potential involvement of Cl⁻ channels in IPC came from a study by Diaz *et al*, which demonstrated that the Cl⁻ channel blockers 5-nitro-2-(3-phenylpropyl-amino) benzoic acid (NPPB) and indanyloxyacetic acid 94 (IAA-94) not only block hypo-osmotic cell swelling induced by Cl⁻ current (*I*_{Cl,swell}) but also prevent IPC- and hypo-osmotic stress-mediated protection of isolated rabbit hearts^[13]. Subsequent studies from the same group provided further evidence supporting the notion that *I*_{Cl,swell} may be an important end-effector in IPC^[34,35], and it is believed that enhanced cell volume regulation may be a key mechanism for IPC protection^[12]. These observations by Diaz *et al* were, however, seriously questioned by Heusch *et al*^[36,37].

In an attempt to confirm the effects of the same Cl⁻ channel blockers on both Cl⁻ channel activity in isolated ventricular myocytes and cardioprotection by IPC in isolated perfused rabbit heart, Heusch *et al* found that the channel-blocking concentrations of both NPPB and IAA-94 were toxic in isolated perfused rabbit hearts, as evidenced by cessation of cardiac contraction and massive infarction. Thus, neither agent could be used to test the role of Cl⁻ channels on the anti-infarct effect of IPC. The doses used in the report by Diaz *et al*^[13] did not affect coronary flow, heart rate, or developed pressure and also failed to prevent infarct size reduction by IPC^[36]. Similar results were obtained with another VSOACs blocker, 4,4'-

diisothiocyanostilbene-2,2'-disulfonic acid (DIDS)^[36]. Therefore, whether cardiac Cl⁻ channels play a role in IPC remains controversial.

The difficulty in resolving these controversies stems from the fact that multiple types of Cl⁻ channels (CFTR, $I_{Cl,swell}$ *etc*) are concomitantly expressed in the same cardiac cell^[27, 28], and the Cl⁻ channel blockers used in these studies lack specificity towards any particular subgroup of Cl⁻ channels in the heart^[13, 35, 36]. Therefore, the use of a gene targeting technique to specifically inactivate Cl⁻ channel (*eg*, CFTR) gene expression in the mouse provides a unique and powerful approach to directly address the question of whether Cl⁻ channels play a role in the early and late phases of IPC.

Relationship between CFTR and sarc-K_{ATP} channels

CFTR belongs to the ABC transport superfamily^[38] and shares similar structural features, including transmembrane and nucleotide binding domains, with SUR, a subunit of functional sarc-K_{ATP} channels^[39]. However, CFTR is the only member of the ABC family that encodes a protein with a transport structure and Cl⁻ channel function^[38]. CFTR is unique in forming an anion channel gated by PKA and PKC phosphorylation and intracellular ATP^[29, 30]. Interestingly, sulfonylureas such as glibenclamide, which have long been used as specific blockers of sarc-K_{ATP} channels in IPC studies^[8, 9], can also block CFTR Cl⁻ channels^[40, 41]. However, a potential role for CFTR Cl⁻ channels as endogenous protective factors in IPC and POC has been ignored. In this study, we provide the first compelling experimental evidence for a novel and critical functional role of CFTR channels in IPC- and POC-mediated cardioprotection. Therefore, CFTR may represent a novel target for cardioprotection against I/R injury.

Mechanisms of activation of CFTR in IPC- and POC-mediated cardioprotection against I/R injury

CFTR Cl⁻ channels are expressed in many species ranging from mice to humans^[29]. It is well established that cardiac CFTR channels can be activated by PKA and PKC through a vast array of signaling pathways such as activation of β -adrenergic receptors^[29] and purinergic receptors^[42]. It is thus conceivable that cardiac CFTR channels can be activated by signaling mechanisms invoked during IPC and POC, including PKC ϵ activation via G-protein (possibly Gq and/or Gi)-coupled receptors^[17, 18].

Apoptosis and necrosis are the major cell death mechanisms involved in ischemia- and reperfusion-induced myocardial injury and infarction^[1, 2]. Considerable evidence has demonstrated that activation of CFTR channels may be an important modulator of apoptotic mechanism in non-cardiac cells^[43-45]. For example, glibenclamide, an inhibitor of CFTR Cl⁻ channels^[40, 41] that has been mistaken as a specific blocker of sarc-K_{ATP} channels^[8, 9], induces apoptosis in a dose- and time-dependent manner in HepG2 human hepatoblastoma cells^[43]. In this study, we found that targeted inactivation of CFTR abolished the protective effects of IPC on I/R-induced

apoptosis, suggesting that CFTR channels may be involved in IPC- and POC-mediated cardioprotection through inhibition of apoptosis. It has been suggested that the anti-apoptotic effect of CFTR may be a result of strengthened cell volume homeostasis during cell proliferation and apoptosis^[46]. Other mechanisms behind CFTR-mediated effects on apoptosis may involve the role of CFTR in the regulation of intracellular reactive oxygen species (ROS) and glutathione content (GSH/GSSG)^[47]. It should be pointed out, however, that in several other cell types, activation of CFTR has been reported to actually enhance apoptosis^[47-49]. The reason for the multifaceted role of CFTR in apoptosis is not currently known^[50]. However, Yalcin *et al* recently found that the majority of apoptotic cells in CF patients are alveolar epithelial cells, and apoptotic cells are not detected in other locations where CFTR expression is much more prominent than alveolar cells. They postulated, therefore, that increased apoptosis in the alveolar epithelium is related to the presence of chronic infections rather than CFTR dysfunction^[51].

In addition, activation of CFTR Cl⁻ channels may protect the heart against arrhythmogenesis by preventing excessive prolongation of action potential duration (APD) and protecting the heart against the development of early after depolarizations (EAD) and triggered activity caused by activation of Ca²⁺ channels in the presence of β -adrenergic stimulation^[28, 29]. It has been demonstrated that cardiac CFTR plays a role in early action potential shortening during hypoxia and ischemia^[52]. Activation of CFTR also decreases resting membrane potential and action potential duration, thereby limiting intracellular Ca²⁺ overload and cell damage^[29]. These beneficial effects of the activation of cardiac CFTR may serve as mechanisms behind the cardioprotection of CFTR against I/R injury during IPC or POC.

Numerous previous studies have demonstrated that CFTR is not only a Cl⁻ channel but also a transporter for many other molecules such as sphingosine-1-phosphate^[53], an important lipid messenger involved in IPC^[54]. CFTR may interact with many proteins that either directly or indirectly impact the function of other ion channels and transporters, such as epithelial Na⁺ channels (ENaC) and Ca²⁺- and volume-activated Cl⁻ channels^[55]. Evidence is emerging that CFTR assembles into large, dynamic macromolecular complexes that contain signaling molecules, kinases, transport proteins, PDZ-domain-containing proteins, myosin motors, and Rab GTPases^[56]. Therefore, CFTR may be involved in the regulation of a variety of cellular functions. The integrated versatile function and complex regulation of CFTR channels may be orchestrated by a number of proteins in the CFTR interactome^[57]. It is thus very important to further study the underlying molecular mechanisms behind CFTR-mediated cardioprotection and the interplay between CFTR and other cardioprotective factors such as sarc-K_{ATP}, mito-K_{ATP}, and mPTP. Such studies may shed new light on the functional role of CFTR Cl⁻ channels in the heart and increase our understanding of the complicated mechanisms behind endogenous cardioprotection.

Acknowledgements

We are grateful to Dr William HATTON and Dr Hong-lin TIAN for their excellent technical assistance. This study was supported by the National Center for Research Resources P-20 RR-15581 (Dayue Darrel DUAN); National Heart, Lung, and Blood Institute Grants HL106256 and HL63914 (Dayue Darrel DUAN), HL60051 (John A AUCHAMPACH), HL 077707 (John A AUCHAMPACH), and HL 08311 (Garrett J GROSS); American Diabetes Association Innovation Award #07-8-IN-08 (Dayue Darrel DUAN); and the National Basic Research Program of China Grant 2009CB521903 (Dayue Darrel DUAN).

References

- 1 Lopez-Neblina F, Toledo AH, Toledo-Pereyra LH. Molecular biology of apoptosis in ischemia and reperfusion. *J Invest Surg* 2005; 18: 335–50.
- 2 Zhao ZQ, Vinten-Johansen J. Myocardial apoptosis and ischemic preconditioning. *Cardiovasc Res* 2002; 55: 438–55.
- 3 Murry CE, Jennings RB, Reimer KA. Preconditioning with ischemia: a delay of lethal cell injury in ischemic myocardium. *Circulation* 1986; 74: 1124–36.
- 4 Guo Y, Wu WJ, Qiu Y, Tang XL, Yang Z, Bolli R. Demonstration of an early and a late phase of ischemic preconditioning in mice. *Am J Physiol* 1998; 275: H1375–87.
- 5 Ludman AJ, Yellon DM, Hausenloy DJ. Cardiac preconditioning for ischaemia: lost in translation. *Dis Model Mech* 2010; 3: 35–8.
- 6 Ovize M, Baxter GF, Di LF, Ferdinandy P, Garcia-Dorado D, Hausenloy DJ, et al. Postconditioning and protection from reperfusion injury: where do we stand? Position paper from the Working Group of Cellular Biology of the Heart of the European Society of Cardiology. *Cardiovasc Res* 2010; 87: 406–23.
- 7 Downey JM, Davis AM, Cohen MV. Signaling pathways in ischemic preconditioning. *Heart Fail Rev* 2007; 12: 181–8.
- 8 Gross GJ, Peart JN. K_{ATP} channels and myocardial preconditioning: an update. *Am J Physiol Heart Circ Physiol* 2003; 285: H921–30.
- 9 Gross GJ. Selective ATP-sensitive potassium channel openers: fact or fiction. *J Mol Cell Cardiol* 2003; 35: 1005–7.
- 10 Hausenloy DJ, Ong SB, Yellon DM. The mitochondrial permeability transition pore as a target for preconditioning and postconditioning. *Basic Res Cardiol* 2009; 104: 189–202
- 11 Xiao XH, Allen DG. Activity of the Na^+/H^+ exchanger is critical to reperfusion damage and preconditioning in the isolated rat heart. *Cardiovasc Res* 2000; 48: 244–53.
- 12 Diaz RJ, Armstrong SC, Batthish M, Backx PH, Ganote CE, Wilson GJ. Enhanced cell volume regulation: a key protective mechanism of ischemic preconditioning in rabbit ventricular myocytes. *J Mol Cell Cardiol* 2003; 35: 45–58.
- 13 Diaz RJ, Losito VA, Mao GD, Ford MK, Backx PH, Wilson GJ. Chloride channel inhibition blocks the protection of ischemic preconditioning and hypo-osmotic stress in rabbit ventricular myocardium. *Circ Res* 1999; 84: 763–75.
- 14 Downey JM, Cohen MV. Why do we still not have cardioprotective drugs? *Circ J* 2009; 73: 1171–7.
- 15 McIntosh VJ, Lasley RD. Adenosine receptor-mediated cardioprotection: are all 4 subtypes required or redundant? *J Cardiovasc Pharmacol Ther* 2011 doi:10.1177/1074248410396877.
- 16 Zhao ZQ, Corvera JS, Halkos ME, Kerendi F, Wang NP, Guyton RA, et al. Inhibition of myocardial injury by ischemic postconditioning during reperfusion: comparison with ischemic preconditioning. *Am J Physiol Heart Circ Physiol* 2003; 285: H579–88.
- 17 Zhao ZQ, Vinten-Johansen J. Postconditioning: reduction of reperfusion-induced injury. *Cardiovasc Res* 2006; 70: 200–11.
- 18 Gross GJ, Auchampach JA. Reperfusion injury: does it exist? *J Mol Cell Cardiol* 2007; 42: 12–8.
- 19 Philipp S, Yang XM, Cui L, Davis AM, Downey JM, Cohen MV. Postconditioning protects rabbit hearts through a protein kinase C-adenosine A2b receptor cascade. *Cardiovasc Res* 2006; 70: 308–14.
- 20 Heusch G, Buchert A, Feldhaus S, Schulz R. No loss of cardioprotection by postconditioning in connexin 43-deficient mice. *Basic Res Cardiol* 2006; 101: 354–6.
- 21 Skyschally A, van Caster P, Boengler K, Gres P, Musiolik J, Schilawa D, et al. Ischemic postconditioning in pigs: no causal role for RISK activation. *Circ Res* 2009; 104: 15–8.
- 22 Peart JN, Headrick JP. Clinical cardioprotection and the value of conditioning responses. *Am J Physiol Heart Circ Physiol* 2009; 296: H1705–20.
- 23 Heusch G. Postconditioning: old wine in a new bottle? *J Am Coll Cardiol* 2004; 44: 1111–2.
- 24 Burley DS, Baxter GF. Pharmacological targets revealed by myocardial postconditioning. *Curr Opin Pharmacol* 2009; 9: 177–88.
- 25 Granfeldt A, Lefer DJ, Vinten-Johansen J. Protective ischaemia in patients: preconditioning and postconditioning. *Cardiovasc Res* 2009; 83: 234–46.
- 26 Chen H, Liu LL, Ye LL, McGuckin C, Tamowski S, Scowen P, et al. Targeted inactivation of cystic fibrosis transmembrane conductance regulator chloride channel gene prevents ischemic preconditioning in isolated mouse heart. *Circulation* 2004; 110: 700–4.
- 27 Duan D. Phenomics of cardiac chloride channels: the systematic study of chloride channel function in the heart. *J Physiol* 2009; 587: 2163–77.
- 28 Duan DY, Liu LL, Bozeat N, Huang ZM, Xiang SY, Wang GL, et al. Functional role of anion channels in cardiac diseases. *Acta Pharmacol Sin* 2005; 26: 265–78.
- 29 Hume JR, Duan D, Collier ML, Yamazaki J, Horowitz B. Anion transport in heart. *Physiol Rev* 2000; 80: 31–81.
- 30 Sheppard DN, Welsh MJ. Structure and function of the CFTR chloride channel. *Physiol Rev* 1999; 79: S23–S45.
- 31 Burke MA, Ardehali H. Mitochondrial ATP-binding cassette proteins. *Transl Res* 2007; 150: 73–80.
- 32 Gateau-Roesch O, Argaud L, Ovize M. Mitochondrial permeability transition pore and postconditioning. *Cardiovasc Res* 2006; 70: 264–73.
- 33 Obal D, Dettwiler S, Favocchia C, Scharbatke H, Preckel B, Schlack W. The influence of mitochondrial K_{ATP} -channels in the cardioprotection of preconditioning and postconditioning by sevoflurane in the rat *in vivo*. *Anesth Analg* 2005; 101: 1252–60.
- 34 Batthish M, Diaz RJ, Zeng HP, Backx PH, Wilson GJ. Pharmacological preconditioning in rabbit myocardium is blocked by chloride channel inhibition. *Cardiovasc Res* 2002; 55: 660–71.
- 35 Diaz RJ, Batthish M, Backx PH, Wilson GJ. Chloride channel inhibition does block the protection of ischemic preconditioning in myocardium. *J Mol Cell Cardiol* 2001; 33: 1887–9.
- 36 Heusch G, Liu GS, Rose J, Cohen MV, Downey JM. No confirmation for a causal role of volume-regulated chloride channels in ischemic preconditioning in rabbits. *J Mol Cell Cardiol* 2000; 32: 2279–85.
- 37 Heusch G, Cohen MV, Downey JM. Ischemic preconditioning through opening of swelling-activated chloride channels? *Circ Res* 2001; 89: E48.
- 38 Riordan JR, Chang XB. CFTR, a channel with the structure of a transporter. *Biochim Biophys Acta* 1992; 1101: 221–2.
- 39 Nichols CG. K_{ATP} channels as molecular sensors of cellular metabo-

- lism. *Nature* 2006; 440: 470–6.
- 40 Sheppard DN, Welsh MJ. Effect of ATP-sensitive K^+ channel regulators on cystic fibrosis transmembrane conductance regulator chloride currents. *J Gen Physiol* 1992; 100: 573–91.
- 41 Yamazaki J, Hume JR. Inhibitory effects of glibenclamide on cystic fibrosis transmembrane regulator, swelling-activated, and Ca^{2+} -activated Cl^- channels in mammalian cardiac myocytes. *Circ Res* 1997; 81: 101–9.
- 42 Duan D, Ye L, Britton F, Miller LJ, Yamazaki J, Horowitz B, *et al*. Purinoceptor-coupled Cl^- channels in mouse heart: a novel, alternative pathway for CFTR regulation. *J Physiol (Lond)* 1999; 521: 43–56.
- 43 Kim JA, Kang YS, Lee SH, Lee EH, Yoo BH, Lee YS. Glibenclamide induces apoptosis through inhibition of cystic fibrosis transmembrane conductance regulator (CFTR) Cl^- channels and intracellular Ca^{2+} release in HepG2 human hepatoblastoma cells. *Biochem Biophys Res Commun* 1999; 261: 682–8.
- 44 Kim JA, Kang YS, Lee SH, Lee EH, Lee YS. Role of pertussis toxin-sensitive G-proteins in intracellular Ca^{2+} release and apoptosis induced by inhibiting cystic fibrosis transmembrane conductance regulator (CFTR) Cl^- channels in HepG2 human hepatoblastoma cells. *J Cell Biochem* 2001; 81: 93–101.
- 45 Xu Y, Krause A, Hamai H, Harvey BG, Worgall TS, Worgall S. Proinflammatory phenotype and increased caveolin-1 in alveolar macrophages with silenced CFTR mRNA. *PLoS One* 2010; 5: e11004.
- 46 Valverde MA, Vazquez E, Munoz FJ, Nobles M, Delaney SJ, Wainwright BJ, *et al*. Murine CFTR channel and its role in regulatory volume decrease of small intestine crypts. *Cell Physiol Biochem* 2000; 10: 321–8.
- 47 L'hoste S, Chargui A, Belfodil R, Corcelle E, Duranton C, Rubera I, *et al*. CFTR mediates apoptotic volume decrease and cell death by controlling glutathione efflux and ROS production in cultured mice proximal tubules. *Am J Physiol Renal Physiol* 2010; 298: F435–53.
- 48 Barriere H, Poujeol C, Tauc M, Blasi JM, Counillon L, Poujeol P. CFTR modulates programmed cell death by decreasing intracellular pH in Chinese hamster lung fibroblasts. *Am J Physiol Cell Physiol* 2001; 281: C810–24.
- 49 L'hoste S, Chargui A, Belfodil R, Duranton C, Rubera I, Mograbi B, *et al*. CFTR mediates cadmium-induced apoptosis through modulation of ROS level in mouse proximal tubule cells. *Free Radic Biol Med* 2009; 46: 1017–31.
- 50 Thevenod F. Multifaceted CFTR: novel role in ROS signaling and apoptotic cell death — a commentary on “CFTR mediates cadmium-induced apoptosis through modulation of ROS levels in mouse proximal tubule cells”. *Free Radic Biol Med* 2009; 46: 1014–6.
- 51 Yalcin E, Talim B, Ozcelik U, Dogru D, Cobanoglu N, Pekcan S, *et al*. Does defective apoptosis play a role in cystic fibrosis lung disease? *Arch Med Res* 2009; 40: 561–4.
- 52 Ruiz PE, Ponce ZA, Schanne OF. Early action potential shortening in hypoxic hearts: role of chloride current(s) mediated by catecholamine release. *J Mol Cell Cardiol* 1996; 28: 279–90.
- 53 Boujaoude LC, Bradshaw-Wilder C, Mao C, Cohn J, Ogretmen B, Hannun YA, *et al*. Cystic fibrosis transmembrane regulator regulates uptake of sphingoid base phosphates and lysophosphatidic acid: modulation of cellular activity of sphingosine 1-phosphate. *J Biol Chem* 2001; 276: 35258–64.
- 54 Karliner JS. Lysophospholipids and the cardiovascular system. *Biochim Biophys Acta* 2002; 1582: 216–21.
- 55 Kunzelmann K. CFTR: interacting with everything? *News Physiol Sci* 2001; 16: 167–70.
- 56 Guggino WB, Stanton BA. New insights into cystic fibrosis: molecular switches that regulate CFTR. *Nat Rev Mol Cell Biol* 2006; 7: 426–36.
- 57 Wang X, Venable J, LaPointe P, Hutt DM, Koulov AV, Coppinger J, *et al*. Hsp90 cochaperone Aha1 downregulation rescues misfolding of CFTR in cystic fibrosis. *Cell* 2006; 127: 803–15.

Original Article

CFTR chloride channel as a molecular target of anthraquinone compounds in herbal laxatives

Hong YANG^{1,*}, Li-na XU², Cheng-yan HE³, Xin LIU³, Rou-yu FANG², Tong-hui MA^{1,2}

¹School of Life Sciences, Liaoning Provincial Key Laboratory of Biotechnology and Drug Discovery, Liaoning Normal University, Dalian 116029, China; ²Central Research Laboratory, Jilin University Bethune Second Hospital, Changchun 130041, China; ³China-Japan Union Hospital, Jilin University, Changchun 130041, China

Aim: To clarify whether CFTR is a molecular target of intestinal fluid secretion caused by the anthraquinone compounds from laxative herbal plants.

Methods: A cell-based fluorescent assay to measure I⁻ influx through CFTR chloride channel. A short-circuit current assay to measure transcellular Cl⁻ current across single layer FRT cells and freshly isolated colon mucosa. A closed loop experiment to measure colon fluid secretion *in vivo*.

Results: Anthraquinone compounds rhein, aloe-emodin and 1,8-dihydroxyanthraquinone (DHAN) stimulated I⁻ influx through CFTR chloride channel in a dose-dependent manner in the presence of physiological concentration of cAMP. In the short-circuit current assay, the three compound enhanced Cl⁻ currents in epithelia formed by CFTR-expressing FRT cells with EC₅₀ values of 73±1.4, 56±1.7, and 50±0.5 μmol/L, respectively, and Rhein also enhanced Cl⁻ current in freshly isolated rat colonic mucosa with a similar potency. These effects were completely reversed by the CFTR selective blocker CFTR_{inh}-172. In *in vivo* closed loop experiments, rhein 2 mmol/L stimulated colonic fluid accumulation that was largely blocked by CFTR_{inh}-172. The anthraquinone compounds did not elevate cAMP level in cultured FRT cells and rat colonic mucosa, suggesting a direct effect on CFTR activity.

Conclusion: Natural anthraquinone compounds in vegetable laxative drugs are CFTR potentiators that stimulated colonic chloride and fluid secretion. Thus CFTR chloride channel is a molecular target of vegetable laxative drugs.

Keywords: cystic fibrosis transmembrane conductance regulator (CFTR) chloride channel; anthraquinone compounds; colonic fluid secretion; molecular pharmacology; drug discovery

Acta Pharmacologica Sinica advance (2011) 32: 834–839; doi: 10.1038/aps.2011.46; published online 23 May 2011

Introduction

Vegetable laxative drugs such as Aloe, cascara and senna are widely used all over the world for the treatment of constipation in both prescription and non-prescription forms^[1, 2]. Cathartic ingredients of these laxative drugs are anthranoid compounds (including anthraquinone, anthrone and dianthrone) and possibly their derivatives^[3]. It is generally regarded that anthranoid compounds work exclusively in the colon to stimulate colonic motility and increase electrolyte and fluid transport. These compounds exert their functions by both inhibiting absorption and inducing secretion of fluid in the intestine^[4]. Decrease of net absorption was generally attributed to accelerated intestinal transit^[5, 6]. The molecular mechanism of intestinal net fluid secretion is still unclear.

Intestinal fluid secretion is driven by active Cl⁻ transport from the basolateral to the apical side of enterocytes. Chloride enters the intestinal epithelial cells via Na⁺, K⁺, 2Cl⁻ cotransporter, and is secreted into the lumen through the cystic fibrosis transmembrane conductance regulator (CFTR) chloride channel. Both Na⁺ and water follow Cl⁻ paracellularly, resulting in a net iso-osmotic fluid secretion^[7]. Previous studies showed that rhein anthraquinone stimulated Cl⁻ secretion in colonic mucosa^[8, 9]. However, the precise molecular pathway of such Cl⁻ secretion has not yet been clarified. Because CFTR is the final common pathway for intestinal Cl⁻ secretion in response to various agonists^[10], and all stimulant laxatives act by altering fluid and electrolyte transport in the small and/or large intestines, we hypothesized that CFTR Cl⁻ channel activity played an important role in colonic fluid secretion stimulated by anthraquinone compounds.

In the present study, we determined the potentiating effects of anthraquinone compounds on CFTR chloride channel and

* To whom correspondence should be addressed.

E-mail hyanglnnu@gmail.com

Received 2011-02-16 Accepted 2011-04-07

characterized the role of CFTR in anthraquinone-stimulated colonic fluid secretion.

Materials and methods

Chemicals

Anthraquinone compounds were obtained from the National Institute for the Control of Pharmaceutical and Biological Products in China (purity >99% as determined by analytical HPLC). Compounds were dissolved in DMSO prior to use and stability of stock solution was verified during the study by HPLC analysis. Forskolin (FSK), genistein, F12 Coon's medium and *L*-glutamine were purchased from Sigma Chemical Co (St Louis, MO, USA); indomethacin, amiloride, amphotericin B were purchased from Sigma-Aldrich company (St Louis, MO, USA); fetal bovine serum (Characterized) was purchased from HyClone; CFTR_{inh}-172 were synthesized as reported before^[11]; other reagents were of analytical grade or higher. cAMP radioimmunoassay kit was purchased from Shanghai Traditional Chinese Medicine University.

Tissue preparation

All *in vivo* studies including isolation of rat colonic mucosa followed institutional guidelines for animal experiments. Rat colonic mucosa was obtained as described previously^[12]. Briefly, Sprague-Dawley (SD) rats (body weight about 200 g) were starved for 24 h prior. Two to three segments of colon were excised after the rat was euthanized with intravenous pentobarbital (100 mg/kg). The segments were immediately stripped of muscularis and bathed in Krebs-Henseleit (KH) solution (contained in mmol/L: NaCl 117, KCl 4.7, MgCl₂ 1.2, KH₂PO₄ 1.2, NaHCO₃ 24.8, CaCl₂ 2.5, glucose 11.1, pH 7.4).

Fluorescence assay of CFTR channel function

Fisher rat thyroid (FRT) epithelial cells coexpressing human wild type CFTR and halide sensitive yellow fluorescent protein YFP-H148Q were generated as described previously^[11, 13]. The FRT cells were seeded in black-walled, clear-bottomed 96-well tissue culture plates (Costar, Corning, NY, USA) and incubated at 37 °C to achieve confluence (about 24 h). After washing 3 times with phosphate-buffered saline (PBS), the FRT cells were incubated with 100 nmol/L FSK and test compounds in a final volume of 40 μL for 10 min. The fluorescence of each well was monitored in a fluorescence plate reader (Fluostar Optima; BMG Laboratory Technologies, Offenburg, Germany) with 2 s before and 12 s after injection of 120 μL of I⁻-containing solution (PBS in which 137 mmol/L Cl⁻ was replaced by equal concentration of I⁻). I⁻ influx rates (d[I⁻]/dt at *t*=0) were computed from fluorescence time course data by single exponential regression, as described previously^[13].

Electrophysiology

Transepithelial short-circuited current (*I*_{SC}) studies were done on both FRT cells and rat colonic mucosa.

The FRT cells grew on Snapwell inserts, formed monolayer epithelial cells (about 7–9 d) at an air liquid interface as described^[14, 15], and then were placed in a Ussing chamber

system (Vertical Diffusion Chamber, Physiological Instruments, San Diego, CA, USA). Measurements were performed in the presence of a transepithelial Cl⁻ gradient, in which the basolateral side solution contained (in mmol/L): NaCl 130, KCl 2.7, KH₂PO₄ 1.5, CaCl₂ 1, MgCl₂ 0.5, Na-HEPES 10, pH 7.3, and glucose 10; The apical side solution contained the same components but was modified by replacing 65 mmol/L NaCl with sodium gluconate and the concentration of CaCl₂ was increased to 2 mmol/L to compensate for calcium buffering caused by gluconate^[16]. The basolateral membrane of the FRT cells was permeabilized with 250 μg/mL amphotericin B.

For measurements of transepithelial *I*_{SC} on rat colonic mucosa, sheets of tissue were mounted in the Ussing chambers (area 1.03 cm²); the hemichambers were filled with a KH solution. *I*_{SC} values were measured after inhibition of Na⁺ current by the ENaC inhibitor amiloride (10 μmol/L) and prostaglandin synthesis using indomethacin (10 μmol/L), followed by stimulation by forskolin (20 μmol/L) and subsequent inhibitor addition^[12].

Measurements were performed at 37 °C, and solutions were continuously bubbled with air (FRT cells) or with 5% CO₂, 95% air (rat colonic mucosa) during experiments. *I*_{SC} values were recorded with a DVC-1000 voltage clamp (World Precision Instruments, Sarasota, FL, USA) via Ag/AgCl electrodes and 1 mol/L KCl agar bridges.

In vivo intestinal fluid secretion analysis

Fluid accumulation in rat colonic loops was measured as described previously^[11]. Briefly, SD rats were starved for 24 h prior to commencing experiments. Closed colonic loops proximal to cecum were isolated with ligature under intraperitoneal (60 mg/kg) anesthesia. Loops were injected with 100 μL of: PBS alone, PBS containing rhein (2 mmol/L), or PBS containing rhein (2 mmol/L) plus CFTR_{inh}-172 (40 μmol/L). The abdominal wall was then closed, and rats were allowed to recover from anesthesia. After 6 h the rats were euthanized with overdose intraperitoneal injection of pentobarbital (100 mg/kg). Loops were excised, and loop length and weight were measured.

Assay of cAMP activity

cAMP activity was determined by using the cAMP radioimmunoassay kit (Shanghai Traditional Chinese Medicine University).

FRT cells grown in 96-well plates were washed with PBS, then incubated with test compounds for 10 min, and then lysed. cAMP activities were measured in sextuplicate as the manufacture's instruction.

Rat colonic mucosa cAMP contents were measured as described in reference^[17] with some modifications. Briefly, freshly prepared rat colonic mucosa (50 mg) was washed and incubated in KH solution in a 37 °C incubator. The isolated mucosal sheets were exposed to test compounds for 15 min then rapidly frozen in liquid nitrogen and homogenized. The homogenates were centrifuged at 2000×g for 15 min at 4 °C. The supernatant was extracted three times with 3 volumes of

diethyl ether before lyophilization. The supernatants were collected and mixed with equal volume of ethanol, then dried in 37 °C incubator. cAMP levels were assayed by using the radioimmunoassay kit as done on the FRT cells.

Statistical analysis

Data are reported as mean±SEM. Statistical significance of the effects were determined by using the OriginPro 8.0 software.

Results

Anthraquinones potentiate the CFTR chloride channel

First, we analyzed the effect of 5 anthraquinone compounds (Figure 1A) on FRT cells stably expressing CFTR chloride

channel using an iodide-sensitive fluorescent assay. As shown in Figure 1B, three out of the five anthraquinone compounds (rhein, aloë-emodin and DHAN) significantly increased iodide influx into FRT cells in a dose-dependent manner in the presence of 100 nmol/L FSK. The potency and efficacy of the three compounds are lower than the known CFTR potentiator genistein.

To confirm the activity of the three anthraquinone compounds on CFTR, we further analyzed their effect by the more reliable short-circuit current assay in Ussing chamber. Measurements were performed on the FRT cells after basolateral membrane permeabilisation with amphotericin B to measure apical membrane Cl⁻ current. Representative recordings of

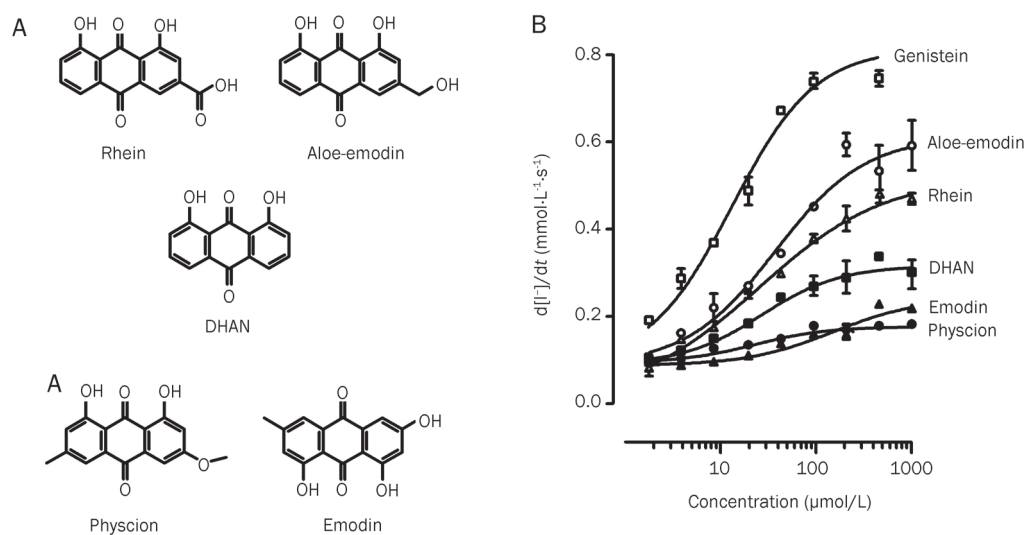


Figure 1. Functional analysis of anthraquinones in FRT cells expressing wild-type CFTR. (A) Chemical structures of the tested anthraquinone compounds; (B) Dose-dependent effects of the 5 anthraquinone compounds on CFTR with genistein as a positive control. Mean±SEM. *n*=6.

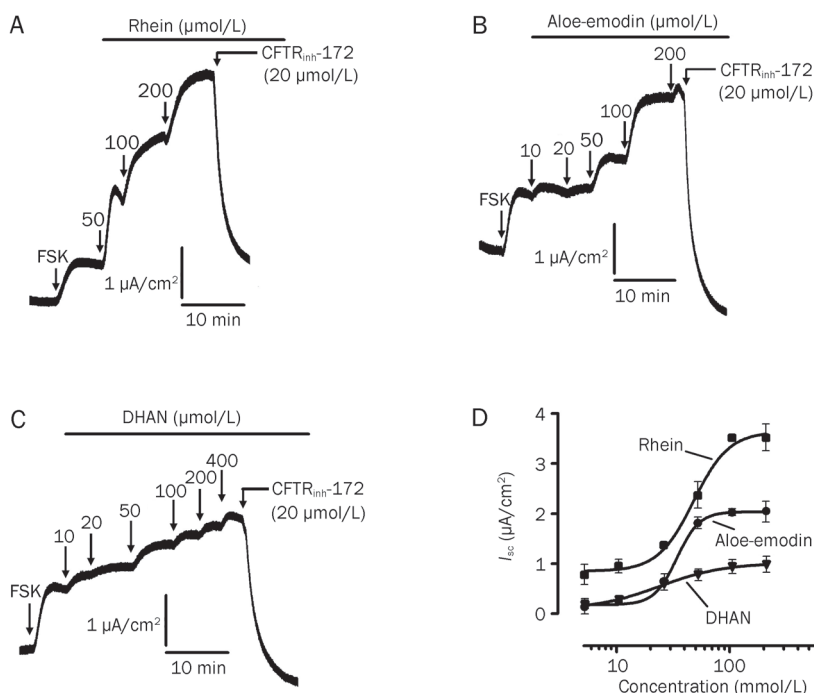


Figure 2. Short-circuit current analysis of anthraquinone compounds in FRT cells expressing wild-type CFTR. (A–C) representative recordings of short-circuit current potentiated by the indicated concentrations of aloë-emodin, rhein and DHAN in the presence of 100 nmol/L forskolin (FSK) and inhibited by CFTR_{mir-172} (20 μmol/L). (D) averaged dose-response relationships for potentiation of Cl⁻ currents by the three anthraquinones. Mean±SEM. *n*=6.

I_{sc} are shown in Figure 2A–2C and summarized in Figure 2D. The three positive compounds in the fluorescence assay all potentiated apical membrane I_{sc} in a concentration-dependent manner in the presence of forskolin. In each case, the increased I_{sc} was completely abolished by the specific CFTR blocker CFTR_{inh}-172^[11]. The potency of the three anthraquinone compounds is: Rhein>Aloe-emodin>DHAN. EC₅₀ values for CFTR activation by Rhein, Aloe-emodin and DHAN were (in $\mu\text{mol/L}$): 73 ± 1.4 , 56 ± 1.7 , and 50 ± 0.52 , respectively. Physicion and Emodin did not stimulate significant I_{sc} at 1 mmol/L in the short-circuit current assays (data not shown). Both potency and efficacy of these compounds are significantly lower than genistein.

Stimulation of mucosal short-circuit current and fluid secretion in rat colon by rhein

Further short-circuit current analysis was performed on isolated rat colonic mucosa. Experiments were done after inhibition of Na⁺ current by amiloride and inhibition of prostaglandin generation by indomethacin. Rhein was administered on the serosal and mucosal sides separately. As shown in Figure 3A, rhein stimulated Cl⁻ secretion across colonic mucosa in a dose-dependent manner. Although the EC₅₀s are similar in both cases (about 100 $\mu\text{mol/L}$), the serosal application appeared more effective. Addition of CFTR_{inh}-172 (20 $\mu\text{mol/L}$) to the mucosal solution completely abolished the chloride secretion. The effect of rhein on colonic fluid secretion was studied in a closed loop model of rat distal colon. As shown in Figure 3B, left, there was marked fluid accumulation

in rhein-treated loops, whereas control loops filled with saline remained empty. CFTR_{inh}-172 effectively prevented fluid accumulation in the rhein-treated colonic loops. Data from a series of experiments are summarized in Figure 3B, right.

Rhein has no effect on cAMP levels of rat colonic mucosa

To further characterize its mechanism of action, rhein was tested for its ability to elevate cAMP production. As shown in Figure 4, although rhein elicited a small increase of cAMP levels in FRT cells in the presence of 100 nmol/L FSK, it did not affect the cAMP level of rat colonic mucosa. These data suggest that rhein might interact directly with CFTR and potentiate its activity.

Discussion

The purpose of this study was to clarify whether CFTR was a molecular target of intestinal net fluid secretion induced by the anthraquinone compounds. Anthraquinones are a group of small molecules found in herbal laxatives. Previous studies have found that anthraquinone compounds stimulated Cl⁻ secretion in colonic mucosa, but molecular targets were not determined^[7, 8]. CFTR is predominantly expressed in colonic crypts where it plays vital roles in regulating the secretion of electrolytes and fluid across the epithelium^[18]. Abnormalities of CFTR function may result in diarrhea^[19–21] or constipation^[22, 23]. Therefore, CFTR modulators might be used to treat diarrhea and constipation^[24].

We demonstrated that natural anthraquinone compounds from laxative herbal plants stimulated CFTR activity both *in*

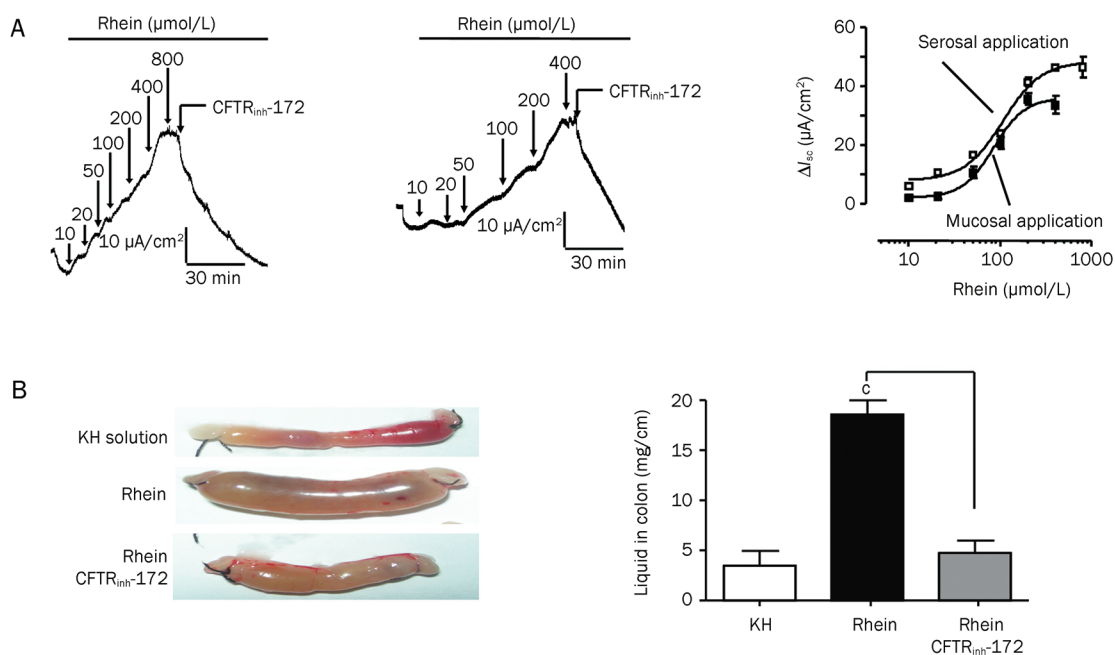


Figure 3. Stimulation of mucosal short-circuit current and fluid secretion in rat colon by rhein. (A) Representative recordings of rhein-stimulated short-circuit current (I_{sc}) across rat distal colonic mucosa. *Left*, when added from serosal side; *middle*, when added from mucosal side; *right*, data summary. Mean \pm SEM. $n=6$. (B) Stimulation of intestinal fluid secretion in rat intestinal closed loop experiments. *Left*: Photograph of isolated rat descending colon loops at 6 h after luminal injection of KH solution alone, rhein (2 mmol/L) and rhein (2 mmol/L) plus CFTR_{inh}-172 (40 $\mu\text{mol/L}$). *Right*: averaged luminal liquid weight at 6 h. Mean \pm SEM. $n=12$ loops from 6 rats. $^{\circ}P<0.01$.

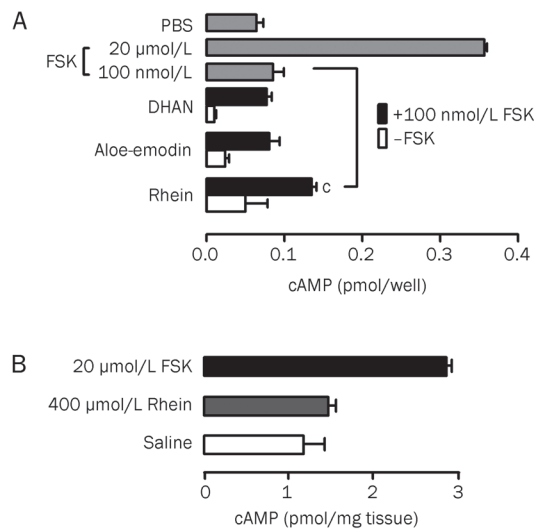


Figure 4. cAMP stimulating activities of anthraquinones. (A) cAMP content in FRT cells at 10 min after the addition of 400 $\mu\text{mol/L}$ test compounds with and without 100 nmol/L FSK. (B) cAMP content in rat colonic mucosa after the addition of 400 $\mu\text{mol/L}$ rhein. Mean \pm SEM. $n=6$. $^{\circ}P<0.01$.

vitro and *in vivo*. First, *in vitro* functional analysis using a cell-based fluorescent assay^[13] and a short-circuit current assay revealed that anthraquinone compounds potentiated CFTR chloride channel function in a dose-dependent manner in the presence of physiological concentration of cAMP. Second, the increase of chloride secretion across isolated rat colonic mucosa by rhein was completely reversed by CFTR specific blocker CFTR_{inh}-172, further supporting CFTR as the molecular target of anthraquinone compounds. Finally, colonic fluid accumulation stimulated by rhein in *in vivo* closed loop experiment was largely blocked by CFTR_{inh}-172, suggesting that CFTR activation is a major mechanism of anthraquinone-stimulated colonic fluid secretion.

The rhein-induced I_{SC} in rat colonic mucosa is not considered to be mediated by electrogenic Na^+ absorption because it was not inhibited by apical addition of amiloride. Though it is possible that rhein may affect generation of prostaglandins (PG) which are also known to be mediators of other secretagogues of intestinal secretion^[25], secretion of Cl^- stimulated by anthraquinone does not appear to be involved in this pathway, because rhein-induced I_{SC} response was unaffected by the presence of the prostaglandin synthesis inhibitor indomethacin.

CFTR is a cAMP-dependent Cl^- channel. An activator can stimulate CFTR activity by increasing cAMP-dependent phosphorylation of CFTR protein or direct interaction with CFTR. Our data support the idea that anthraquinone compounds interact directly with CFTR, because these compounds exhibited minimal effect on intracellular cAMP level in both FRT cells and rat colonic mucosal epithelial cells. Consistent with our results, Ai *et al* reported that anthracene compounds with similar structure increased P_o of CFTR by prolonging the

mean burst duration and shortening the interburst durations in excised inside-out patches, suggesting potentiation of CFTR activity by directly affecting CFTR gating^[26]. Therefore, it is likely that anthraquinone compounds potentiate CFTR function through direct binding to CFTR protein.

In conclusion, natural anthraquinone compounds in vegetable laxative drugs are CFTR potentiators that stimulated colonic chloride and fluid secretion. Anthraquinone compounds potentiate CFTR function most probably through direct interaction with CFTR protein. Thus CFTR chloride channel is a molecular target of vegetable laxative drugs.

Acknowledgements

This work was supported by National Natural Science Foundation of China (No 30973577), Dalian Municipal Science and Technology Fund (No 2008E11SF162), and National Basic Research Program of China ("973" Program, No 2009CB521900).

Author contribution

Hong YANG directed the research and wrote the paper; Li-na XU performed part of the research; Cheng-yan HE performed part of the research; Xin LIU performed part of the research; Rou-yu FANG performed part of the research; Tong-hui MA designed the research and helped writing the paper

References

- de Witte P. Metabolism and pharmacokinetics of anthranoids. *Pharmacology* 1993; 47: 86–97.
- Biggs WS, Dery WH. Evaluation and treatment of constipation in infants and children. *Am Fam Physician* 2006; 73: 469–77.
- van Gorkom BA, de Vries EG, Karrenbeld A, Kleibeuker JH. Review article: anthranoid laxatives and their potential carcinogenic effects. *Aliment Pharmacol Ther* 1999; 13: 443–52.
- Leng-Peschlow E. Dual effect of orally administered sennosides on large intestine transit and fluid absorption in the rat. *J Pharm Pharmacol* 1986; 38: 606–10.
- Wienbeck M, Kortenhaus E, Wallenfels M, Karaus M. Effect of sennosides on colon motility in cats. *Pharmacology* 1988; 36: 31–9.
- Leng-Peschlow E. Effect of sennosides and related compounds on intestinal transit in rat. *Pharmacology* 1988; 36: 40–8.
- Thiagarajah JR, Broadbent T, Hsieh E, Verkman AS. Prevention of toxin-induced intestinal ion and fluid secretion by a small-molecule CFTR inhibitor. *Gastroenterology* 2004; 126: 511–9.
- Goerg KJ, Wanitschke R, Schwarz M, Meyer zum Büschenfelde KH. Rhein stimulates active chloride secretion in the short-circuited rat colonic mucosa. *Pharmacology* 1988; 36: 111–9.
- Clauss W, Domokos G, Leng-Peschlow E. Effect of rhein on electrogenic chloride secretion in rabbit distal colon. *Pharmacology* 1988; 36: 104–10.
- Sheppard DN, Welsh MJ. Structure and function of the CFTR chloride channel. *Physiol Rev* 1999; 79: S23–45.
- Ma T, Thiagarajah JR, Yang H, Sonawane ND, Folli C, Galletta LJ, *et al*. Thiazolidinone CFTR inhibitor identified by high-throughput screening blocks cholera toxin-induced intestinal fluid secretion. *J Clin Invest* 2002; 110: 1651–8.
- He Q, Zhu JX, Xing Y, Tsang LL, Yang N, Rowlands DK, *et al*. Tetramethylpyrazine stimulates cystic fibrosis transmembrane conductance

- regulator-mediated anion secretion in distal colon of rodents. *World J Gastroenterol* 2005; 11: 4173-9.
- 13 Galietta LV, Jayaraman S, Verkman AS. Cell-based assay for high-throughput quantitative screening of CFTR chloride transport agonists. *Am J Physiol Cell Physiol* 2001; 281: C1734-42.
 - 14 Ma T, Vetrivel L, Yang H, Pedemonte N, Zegarra-Moran O, Galietta LJ, et al. High-affinity activators of cystic fibrosis transmembrane conductance regulator (CFTR) chloride conductance identified by high-throughput screening. *J Biol Chem* 2002; 277: 37235-41.
 - 15 Sheppard DN, Carson MR, Ostedgaard LS, Denning GM, Welsh MJ. Expression of cystic fibrosis transmembrane conductance regulator in a model epithelium. *Am J Physiol* 1994; 266: L405-13.
 - 16 Kenyon JL, Gibbons WR. Effects of low-chloride solutions on action potentials of sheep cardiac Purkinje fibers. *J Gen Physiol* 1977; 70: 635-60.
 - 17 Wu D, Hu Z. Rutaecarpine induces chloride secretion across rat isolated distal colon. *J Pharmacol Exp Ther* 2008; 325: 256-66.
 - 18 Strong TV, Boehm K, Collins FS. Localization of cystic fibrosis transmembrane conductance regulator mRNA in the human gastrointestinal tract by *in situ* hybridization. *J Clin Invest* 1994; 93: 347-54.
 - 19 Forte LR, Thorne PK, Eber SL, Krause WJ, Freeman RH, Francis SH, et al. Stimulation of intestinal Cl⁻ transport by heat-stable enterotoxin: activation of cAMP-dependent protein kinase by cGMP. *Am J Physiol* 1993; 263: C607-15.
 - 20 Lencer WI, Delp C, Neutra MR, Madara JL. Mechanism of cholera toxin action on a polarized human intestinal epithelial cell line: role of vesicular traffic. *J Cell Biol* 1992; 117: 1197-209.
 - 21 Grøndahl ML, Jensen GM, Nielsen CG, Skadhauge E, Olsen JE, Hansen MB. Secretory pathways in Salmonella Typhimurium-induced fluid accumulation in the porcine small intestine. *J Med Microbiol* 1998; 47: 151-7.
 - 22 Tenore A, Fasano A, Gasparini N, Sandomenico ML, Ferrara A, Di Carlo A, et al. Thyroxine effect on intestinal Cl⁻/HCO₃⁻ exchange in hypo- and hyperthyroid rats. *J Endocrinol* 1996; 151: 431-7.
 - 23 Ewe K. Intestinal transport in constipation and diarrhoea. *Pharmacology* 1988; 36: 73-84.
 - 24 Verkman AS, Galietta LJ. Chloride channels as drug targets. *Nat Rev Drug Discov* 2009; 8: 153-71.
 - 25 Mall M, Bleich M, Schurlein M, Kuhr J, Seydewitz HH, Brandis M, et al. Cholinergic ion secretion in human colon requires coactivation by cAMP. *Am J Physiol Gastrointest Liver Physiol* 1998; 275: G1274-81.
 - 26 Ai T, Bompadre SG, Sohma Y, Wang X, Li M, Hwang TC. Direct effects of 9-anthracene compounds on cystic fibrosis transmembrane conductance regulator gating. *Pflugers Arch* 2004; 449: 88-95.

Original Article

Pregnant phenotype in aquaporin 8-deficient mice

Xiao-yan SHA^{1, #}, Zheng-fang XIONG^{1, #}, Hui-shu LIU^{1, *}, Zheng ZHENG¹, Tong-hui MA^{2, *}¹Dept of Obstetrics, Guangzhou Women and Children's Medical Centre, Guangzhou Medical College, Guangzhou 510623, China;²Central Research Laboratory, Jilin University Bethune Second Hospital, Changchun 130024, China

Aim: Aquaporin 8 (AQP8) is expressed within the female reproductive system but its physiological function remains to be elucidated. This study investigates the role of AQP8 during pregnancy using AQP8-knockout (AQP8-KO) mice.

Methods: Homozygous AQP8-KO mice were mated, and the conception rate was recorded. AQP8-KO pregnant mice or their offspring were divided into 5 subgroups according to fetal gestational day (7, 13, 16, 18 GD) and newborn. Wild type C57 pregnant mice served as the control group. The number of pregnant mice, total embryos and atrophic embryos, as well as fetal weight, placental weight and placental area were recorded for each subgroup. The amount of amniotic fluid in each sac at 13, 16, and 18 GD was calculated. Statistical significance was determined by analysis of variance of factorial design and chi-square tests.

Results: Conception rates did not differ significantly between AQP8-KO and wild type mice. AQP8-KO pregnant mice had a significantly higher number of embryos compared to wild type controls. Fetal/neonatal weight was also significantly greater in the AQP8-KO group compared to age-matched wild type controls. The amount of amniotic fluid was greater in AQP8-KO pregnant mice than wild type controls, although the FM/AFA (fetal weight/amniotic fluid amount) did not differ. While AQP8-KO placental weight was significantly larger than wild type controls, there was no evidence of placental pathology in either group.

Conclusion: The results suggest that AQP8 deficiency plays an important role in pregnancy outcome.

Keywords: AQP8 gene; knockout mice; pregnancy outcome; female reproductive system

Acta Pharmacologica Sinica (2011) 32: 840–844; doi: 10.1038/aps.2011.45; published online 23 May 2011

Introduction

Aquaporins (AQPs) constitute a growing family of water-specific membrane channel proteins that transport water across cell membranes^[1, 2]. There are currently 13 known mammalian aquaporins (AQP0–12); a subset of these molecules are capable of increasing the permeability of small molecules such as glycerol (AQP3, 7, 9) and urea (AQP3, 7, 8, 9). AQP8 is reportedly permeable to ammonia^[3]. The majority of aquaporins are constitutively expressed in the plasma membrane (AQP0, 1, 3, 4, 7, 8, 9, 10), while others are almost exclusively restricted to intracellular membranes (AQP6, 11, 12)^[4].

AQP8 complementary DNAs (cDNAs) were cloned from rat and mouse^[5–7] in 1997 and human in 1998^[8]. When expressed in *Xenopus* oocytes, mouse, rat or human aquaporin 8 genes increase the water permeability of oocytes by 10 to 20 fold. In addition, the cytoplasmic localization of AQP8 may also hint at its involvement in intracellular osmoregulation^[9].

Subsequent studies^[10–16] have shown that AQP8 has a wide tissue distribution in mammals, with expression noted in the testis, kidney, heart, gastrointestinal tract, airway, salivary gland, pancreas and placenta. In the reproductive system, AQP8 is strongly expressed in the testis and sperm in the male and in the ovary, oviduct, uterus, placenta, amnion, chorion and cervix in the female^[16–25]. While an earlier study^[26] of AQP8 null mice reported no significant differences in comparison to wild type controls with the exceptions of an increase in testicular volume and a reduction in water permeability within the testes, we observed that AQP8 deficiency increased the number of mature follicles and the resulting fertility of female mice^[27]. The present study aims to survey the role of AQP8 during pregnancy in AQP8-KO mice.

Materials and methods

Mice

AQP8 null mice were generated by targeted gene disruption as described in a previous study^[26]. Wild type and AQP8-KO mice in a C57 genetic background were used at age 6–8 weeks. All animals were maintained in accordance with Institutional Guidelines for Care and Use of Laboratory Animals. Mice were housed under standard lighting (12-h light/dark cycle)

[#] These authors contributed equally to this work.

^{*} To whom correspondence should be addressed.

E-mail math108@gmail.com (Tong-hui MA);

huishuliu@hotmail.com (Hui-shu LIU)

Received 2011-02-12 Accepted 2011-04-07

and temperature (23 ± 1 °C) conditions, with free access to a nutritionally balanced diet and deionized water. Protocols for mouse experiments were approved by the Committee on Animal Research of Jilin University Bethune Second Hospital.

Homozygous AQP8-KO mice and wild type mice were mated. Gestational day (GD) 1 was assigned as the day a copulation plug was observed. Pregnant mice that delivered pups did so at term (19–21 GD); thus, there were no premature or post-term deliveries. Embryos or offspring from AQP8-KO pregnant mice and wild type C57 pregnant mice (control group) were divided into 5 subgroups according to gestational age (7 GD, 13 GD, 16 GD, 18 GD, and newborn).

Gestational age-dependent embryo quantification

In total, 225 sacs from 31 AQP8-KO pregnant mice and 212 sacs from 33 wild type pregnant mice were used for embryo quantification studies (including all subgroups).

Mice that had shown copulatory plugs were anesthetized, and a Cesarean section was performed. Pregnant or non-pregnant status was recorded. The number of embryos per female was recorded at 7 GD, 13 GD, 16 GD, and 18 GD. Evidence of macroscopic atrophies were counted and recorded. The number of newborns delivered from 13 pregnant females was also recorded.

Fetal, placental and amniotic fluid measurements

AQP8-KO and wild type C57 pregnant mice were anesthetized, and Cesarean sections were performed at 13 GD, 16 GD, and 18 GD. Parameters, including fetal weight, placental weight and placental area, were measured in each subgroup. A total of 260 sacs were measured in this study.

The entire gestational sac was weighed before rupture of the amniotic membrane. After rupture of the amniotic membrane and absorption of the amniotic fluid, the fetus, placenta and fetal membranes were weighed. The placental area was calculated by measuring the placental diameter. The weight of amniotic fluid was estimated as the difference in weight pre- and post-rupture.

Statistical analysis

Differences in conception rate were assessed by a chi-square test. Analysis of variance (ANOVA) of factorial design was used to determine differences in embryo number, fetal weight, placental area and weight, weight of amniotic fluid and the ratio of fetal weight (FW)/amniotic fluid weight (AFA) between AQP8-KO and wild type groups. Parameters with significant interactions were assessed by LSD (Least Significant Difference) *post hoc* tests. Statistical significance was set at $P<0.05$.

Results

Embryo number

Fifty-three mated AQP8-KO females successfully conceived 40 mice (75.47%), and 54 mated wild type females conceived 35 mice (64.81%) ($P=0.321$).

As pregnancy progressed, the number of embryos declined

in both AQP8-KO and wild type groups ($P=0.004$). However, the total number of embryos per female was significantly greater among the AQP8-KO group for all gestational days compared to the wild type group ($P=0.018$), without interactions between the AQP8 gene and gestational age ($P=0.93$). Gestational age-dependent results are shown in Figure 1.

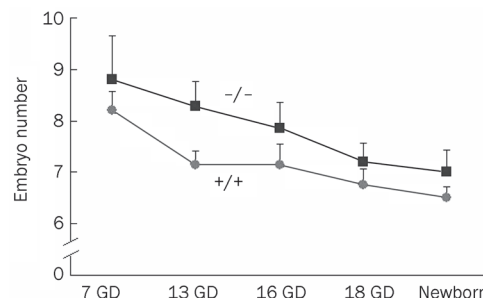


Figure 1. The mean number of embryos/pups at different gestational ages. The number of embryos per female decreased both in the AQP8-KO and wild type group as pregnancy progressed. The total number of embryos/pups of AQP8-KO mice during gestation was higher than wild type ($P=0.018$) although statistical significance was not achieved ($P_{7\text{ GD}}=0.54$, $P_{13\text{ GD}}=0.056$, $P_{16\text{ GD}}=0.293$, $P_{18\text{ GD}}=0.383$, $P_{\text{Newborn}}=0.354$). The number of pregnant mice examined at each checkpoint were 5, 7, 7, 5, 7 in AQP8-KO ($n_1=31$) and 5, 7, 7, 8, 6 in wild type ($n_2=33$) as pregnancy progressed. -/-: AQP8-KO; +/+ : Wild type.

While the number of macroscopic atrophic embryos was recorded for each gestational age investigated, no differences were observed among groups or during pregnancy.

Fetal/neonatal weight (mg)

Fetal weight varied as a result of both the presence/absence of the AQP8 gene and gestational age ($P<0.001$). Fetal weight progressively increased with gestational age ($P<0.001$) and was greater in AQP8-KO mice when compared to age-matched wild type controls ($P<0.001$) for gestational days 16, 18, and newborn (Table 1; $P_{16\text{ GD}}=0.001$, $P_{18\text{ GD}}<0.001$, $P_{\text{New born}}<0.001$) but not 13 ($P_{13\text{ GD}}=0.072$).

Amniotic fluid

Amniotic fluid amount

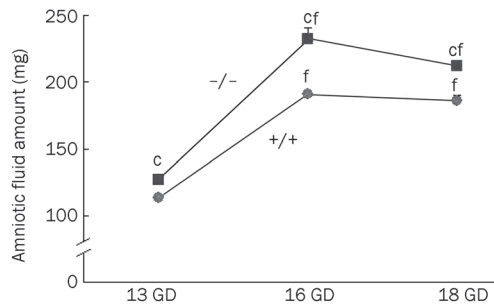
The weight of calculated amniotic fluid increased progressively during pregnancy for both AQP8-KO and wild type groups ($P<0.001$), although the increase in AQP8-KO mice was greater than that of wild type for each gestational age investigated ($P<0.001$). There were also significant interactions between the AQP8 gene and gestational age ($P<0.001$). As seen in Figure 2, the amount of amniotic fluid in AQP8-KO pregnant mice was elevated above wild type at each gestational age ($P_{13\text{ GD}}<0.001$, $P_{16\text{ GD}}<0.001$, $P_{18\text{ GD}}<0.001$).

Fetal weight (FW)/amniotic fluid amount (AFA)

There was no interaction between the AQP8 gene and ges-

Table 1. Fetal weight (mg) of AQP8-KO and wild type mice at 13, 16, 18 GD and newborn. Values are reported as Mean±SEM.

Mice type	Gestational age			
	13 GD (n=49, 33)	16 GD (n=47, 45)	18 GD (n=42, 44)	Newborn (n=43, 49)
AQP8-KO (n=181)	68.500±1.59	395.750±4.80	838.674±9.08	964.6±13.3
C57 (n=171)	65.027±1.05	368.065±6.80	777.984±7.60	885.2±10.7
P	0.072	0.001	<0.001	<0.001

**Figure 2.** The amniotic fluid amount (AFA) differed both between groups and during gestation. AFA in AQP8-KO mice was significantly greater than wild type throughout pregnancy ($P_{13\text{ GD}} < 0.001$, $P_{16\text{ GD}} < 0.001$, $P_{18\text{ GD}} < 0.001$). The number (n) of embryos examined at each checkpoint was in Table 2. -/-: AQP8-KO; +/+ : wild type. ^c $P < 0.01$ vs wild type. ^f $P < 0.01$ vs 13 GD.

tational age ($P=0.35$), and no difference in FM/AFA was observed between the two groups ($P=0.157$). As pregnancy progressed, FM/AFA did increase ($P < 0.001$).

Placenta

Placental area

Calculated placental area did not differ between AQP8-KO pregnant and wild type mice ($P=0.862$). Placental area visibly increased from 13 GD to 18 GD ($P < 0.001$). However, an interaction between the AQP8 gene and gestational age for placental area was not observed ($P=0.815$).

Placental weight

Placental weight was dependent on both the AQP8 gene and gestational age ($P < 0.001$). The placenta grew heavier as pregnancy progressed ($P < 0.001$). As summarized in Table 2, the placental weight of AQP8-KO mice was greater in

Table 2. Placenta weight (mg) of AQP8-KO and wild type mice at 13, 16 and 18 GD. Values are reported as Mean±SEM.

Mice type	Gestational age		
	13 GD (n=49, 33)	16 GD (n=47, 45)	18 GD (n=42, 44)
AQP8-KO (n=138)	60.275±1.15	101.317±1.67	101.949±1.55
C57 (n=122)	58.568±1.77	87.357±0.99	84.138±1.20
P	0.401	<0.001	<0.001

comparison to age-matched wild type controls, specifically at 16 GD and 18 GD ($P_{13\text{ GD}} = 0.401$, $P_{16\text{ GD}} < 0.001$, $P_{18\text{ GD}} < 0.001$).

Pathology of the placenta

Placental hematoxylin and eosin staining revealed no differences in structure between AQP8-KO and wild type placentas and no signs of pathology in either genetic background. Placentas of both groups were composed of three trophoblast cell layers: trophoblast giant cells, spongiotrophoblasts and labyrinthine trophoblasts.

Discussion

Findings reported in the present study suggest that AQP8 deficiency plays an important role in pregnancy outcome. Comparison of the pregnant phenotype of AQP8-deficient mice with that of wild type controls revealed elevations in embryo number, fetus/newborn weight (16 GD, 18 GD, and newborn), and the amount of amniotic fluid at each gestational age.

While a broad tissue distribution of AQP8 has been reported in rat, mouse and human, strong expression has been reported within the female reproductive system, in particular in the placentas and fetal membranes of sheep, human and mouse and in the cervix of the mouse^[16–19]. The reproductive impact of AQP8 deficiency has been addressed previously. Yang *et al*^[26] reported that the weight and size of the testes in AQP8-KO mice were remarkably elevated, and a recent study^[27] from our laboratory has shown elevated fertility in female AQP8-KO mice. Consistent with these studies, data presented here suggested an AQP8-mediated effect on female fertility. A nonsignificant increase in conception rate for AQP8-KO mice (75.47%) was observed compared to wild type mice (64.81%). Furthermore, while embryo number progressively decreased with advancing gestational age in both groups, embryo number was greater in the AQP8-KO group compared to wild type, with a comparable incidence of atrophic embryos. These results may be associated with an increase in follicular maturation and ovulation, as an increase in corpus luteum number has previously been reported in mature AQP8-KO ovaries^[27].

Importantly, previous studies^[26, 28] on AQP8-KO mice have shown that the number, survival, and growth of offspring, as well as urinary concentrating ability, salivary gland fluid secretion ability, pancreatic function and organ weight, do not differ in comparison to wild type mice, with the notable exception of increased testicular weight in AQP8 null mice. Further, osmotically driven water transport, active fluid absorption,

and cholera toxin-driven fluid secretion are unimpaired in AQP8 null mice, with the exception of mild hypertriglyceridemia in null mice in closed intestinal loop measurements^[26]. However, data presented here indicate that fetal weight increased, together with an enlarged and structurally normal placenta in AQP8 null mice.

The placenta is a special organ, constructed and utilized only during pregnancy. Nearly all material exchanges between mother and fetus take place via the placenta, including those involving nutrients and waste. Our results suggest that AQP8 plays a direct or indirect role in fetal and placental growth, as the fetuses of AQP8-KO mice were significantly heavier than those of wild type controls.

Mann *et al*^[29] reported that AQP1-KO pregnant mice had a greater volume of amniotic fluid than wild type and heterozygous groups; they speculated that idiopathic polyhydramnios might contribute to amniotic fluid volume regulation and that the AQP1 knockout mice provided a polyhydramnios animal model. In our research, although the amniotic fluid amount also increased in AQP8-KO pregnant mice, the increase in fluid was related to fetal weight, which was confirmed by the consistent and comparable FW/AFA ratios between the two groups.

Ye *et al*^[30] detected that the embryos from LPA₃-deficient (lysophosphatidic acid, LPA) uteri were consistently smaller than those from wild-type/heterozygote controls on embryonic days 10.5 and 18.5; however, newborns from LPA₃-deficient females were heavier. Prolonged pregnancy and/or smaller litter size were presumed to induce the above results. Regarding our research, the number of embryos per female was elevated in AQP8-KO mice, as were fetal/neonatal weights, without post-term delivery. The rise in number of embryos per female may be associated with an increase in follicular maturation and ovulation in AQP8-KO mice^[27], and the increase in amniotic fluid and larger placentas may provide a superior environment in utero as well as more nutrients to the fetuses to allow higher fetal/neonatal weights.

Our previous study^[27] suggested that AQP8-KO mice displayed a greater number of mature follicles via reduced granulosa cell apoptosis, thus increasing the fertility of female mice. However, it remains unclear whether the findings reported here, namely, elevation in fetal/neonatal weight, amount of amniotic fluid and placental weight, are related to reduced apoptosis of placental cells. Further studies are needed to elucidate the molecular mechanism and cellular events occurring in the AQP8-KO placenta.

In conclusion, our collective results provide evidence that AQP8 deficiency plays an important role in pregnancy outcome.

Acknowledgements

The authors thank Dr Alan S VERKMAN, Dr Xue-chao FENG, Lei GUO, and Wei-heng SU for their help and Song-ying SHEN and Xiao-yan XIA for data analysis assistance. This study was supported by the National Natural Sciences Foundation of China (No 30471828, 30973206) and the National

Natural Science Funds for Distinguished Young Scholar (No 30325011).

Author contribution

Hui-shu LIU and Tong-hui MA designed research; Zheng-fang XIONG, Xiao-yan SHA, and Zheng ZHENG performed the research; Hui-shu LIU and Tong-hui MA contributed new analytical tools and reagents; Xiao-yan SHA analyzed the data; Xiao-yan SHA, Zheng-fang XIONG, and Hui-hu LIU wrote the paper.

References

- 1 Liu H, Wintour EM. Aquaporins in development – a review. *Reprod Biol Endocrinol* 2005; 3: 18–28.
- 2 Liu H, Zheng Z, Wintour EM. Aquaporins and fetal fluid balance. *Placenta* 2008; 29: 840–7.
- 3 Saparov SM, Liu K, Agre P, Pohl P. Fast and selective ammonia transport by aquaporin-8. *J Biol Chem* 2007; 282: 5296–301.
- 4 Itoh T, Rai T, Kuwahara M, Ko SB, Uchida S, Sasaki S, *et al*. Identification of a novel aquaporin, AQP12, expressed in pancreatic acinar cells. *Biochem Biophys Res Commun* 2005; 330: 832–8.
- 5 Ishibashi K, Kuwahara M, Kageyama Y, Tohsaka A, Marumo F, Sasaki S. Cloning and functional expression of a second new aquaporin abundantly expressed in testis. *Biochem Biophys Res Commun* 1997; 237: 714–8.
- 6 Koyama Y, Yamamoto T, Kondo D, Funaki H, Yaoita E, Kawasaki K, *et al*. Molecular cloning of a new aquaporin from rat pancreas and liver. *J Biol Chem* 1997; 272: 30329–33.
- 7 Ma T, Yang B, Verkman AS. Cloning of a novel water and urea-permeable aquaporin from mouse expressed strongly in colon, placenta, liver, and heart. *Biochem Biophys Res Commun* 1997; 240: 324–8.
- 8 Koyama N, Ishibashi K, Kuwahara M, Inase N, Ichioka M, Sasaki S, *et al*. Cloning and functional expression of human aquaporin 8 cDNA and analysis of its gene. *Genomics* 1998; 54: 169–72.
- 9 Calamita G, Mazzone A, Bizzoca A, Cavalier A, Cassano G, Thomas D, *et al*. Expression and immunolocalization of the aquaporin-8 water channel in rat gastrointestinal tract. *Eur J Cell Biol* 2001; 80: 711–9.
- 10 Calamita G, Mazzone A, Bizzoca A, Svelto M. Possible involvement of aquaporin-7 and -8 in rat testis development and spermatogenesis. *Biochem Biophys Res Commun* 2001; 288: 619–25.
- 11 Calamita G, Mazzone A, Cho YS, Valenti G, Svelto M. Expression and localization of the aquaporin-8 water channel in rat testis. *Biol Reprod* 2001; 64: 1660–6.
- 12 Elkjaer ML, Nejsum LN, Gresz V, Kwon TH, Jensen UB, Frokiaer J, *et al*. Immunolocalization of aquaporin-8 in rat kidney, gastrointestinal tract, testis, and airways. *Am J Physiol Renal Physiol* 2001; 281: F1047–57.
- 13 Hoque AT, Yamano S, Liu X, Swaim WD, Goldsmith CM, Delporte C, *et al*. Expression of the aquaporin 8 water channel in a rat salivary epithelial cell. *J Cell Physiol* 2002; 191: 336–41.
- 14 Hurley PT, Ferguson CJ, Kwon TH, Andersen ML, Norman AG, Steward MC, *et al*. Expression and immunolocalization of aquaporin water channels in rat exocrine pancreas. *Am J Physiol Gastrointest Liver Physiol* 2001; 280: G701–9.
- 15 Tani T, Koyama Y, Nihei K, Hatakeyama S, Ohshiro K, Yoshida Y, *et al*. Immunolocalization of aquaporin-8 in rat digestive organs and testis. *Arch Histol Cytol* 2001; 64: 159–68.
- 16 Liu H, Koukoulas I, Ross MC, Wang S, Wintour EM. Quantitative comparison of placental expression of three aquaporin genes. *Placenta* 2004; 25: 475–8.

- 17 Wang S, Chen J, Au KT, Ross MG. Expression of aquaporin 8 and its up-regulation by cyclic adenosine monophosphate in human WISH cells. *Am J Obstet Gynecol* 2003; 188: 997–1001.
- 18 Beall MH, Wang S, Yang B, Chaudhri N, Amidi F, Ross MG. Placental and membrane aquaporin water channels: correlation with amniotic fluid volume and composition. *Placenta* 2007; 28: 421–8.
- 19 Anderson J, Brown N, Mahendroo MS, Reese J. Utilization of different aquaporin water channels in the mouse cervix during pregnancy and parturition and in models of preterm and delayed cervical ripening. *Endocrinology* 2006; 147: 130–40.
- 20 Yeung CH, Callies C, Rojek A, Nielsen S, Cooper TG. Aquaporin isoforms involved in physiological volume regulation of murine spermatozoa. *Biol Reprod* 2009; 80: 350–7.
- 21 Yeung CH, Callies C, Tüttelmann F, Kliesch S, Cooper TG. Aquaporins in the human testis and spermatozoa – identification, involvement in sperm volume regulation and clinical relevance. *Int J Androl* 2010; 33: 629–41.
- 22 McConnell NA, Yunus RS, Gross SA, Bost KL, Clemens MG, Hughes FM Jr. Water permeability of an ovarian antral follicle is predominantly transcellular and mediated by aquaporins. *Endocrinology* 2002; 143: 2905–12.
- 23 Brañes MC, Morales B, Ríos M, Villalón MJ. Regulation of the immunoeexpression of aquaporin 9 by ovarian hormones in the rat oviductal epithelium. *Am J Physiol Cell Physiol* 2005; 288: C1048–57.
- 24 Jablonski EM, McConnell NA, Hughes FM Jr, Huet-Hudson YM. Estrogen regulation of aquaporins in the mouse uterus: potential roles in uterine water movement. *Biol Reprod* 2003; 69: 1481–7.
- 25 Wang S, Kallichanda N, Song W, Ramirez BA, Ross MG. Expression of aquaporin-8 in human placenta and chorioamniotic membranes: evidence of molecular mechanism for intramembranous amniotic fluid resorption. *Am J Obstet Gynecol* 2001; 185: 1226–31.
- 26 Yang B, Song Y, Zhao D, Verkman AS. Phenotype analysis of aquaporin-8 null mice. *Am J Physiol Cell Physiol* 2005; 288: C1161–70.
- 27 Su W, Qiao Y, Yi F, Guan X, Zhang D, Zhang S, *et al*. Increased female fertility in aquaporin 8-deficient mice. *IUBMB Life* 2010; 62: 852–7.
- 28 Burghardt B, Nielsen S, Steward MC. The role of aquaporin water channels in fluid secretion by the exocrine pancreas. *J Membr Biol* 2006; 210: 143–53.
- 29 Mann SE, Ricke EA, Torres EA, Taylor RN. A novel model of polyhydramnios: amniotic fluid volume is increased in aquaporin 1 knockout mice. *Am J Obstet Gynecol* 2005; 192: 2041–6.
- 30 Ye X, Hama K, Contos JJ, Anliker B, Inoue A, Skinner MK, *et al*. LPA₃-mediated lysophosphatidic acid signalling in implantation and embryo spacing. *Nature* 2005; 435: 104–8.

Original Article

Enhanced salt sensitivity following shRNA silencing of neuronal TRPV1 in rat spinal cord

Shuang-quan YU¹, Donna H WANG^{1, 2, *}

¹Department of Medicine, Michigan State University, East Lansing, Michigan, USA; ²Neuroscience Program and Cell and Molecular Biology Program, Michigan State University, East Lansing, Michigan, USA

Aim: To investigate the effects of selective knockdown of TRPV1 channels in the lower thoracic and upper lumbar segments of spinal cord, dorsal root ganglia (DRG) and mesenteric arteries on rat blood pressure responses to high salt intake.

Methods: TRPV1 short-hairpin RNA (shRNA) was delivered using intrathecal injection ($6 \mu\text{g}\cdot\text{kg}^{-1}\cdot\text{d}^{-1}$, for 3 d). Levels of TRPV1 and tyrosine hydroxylase expression were determined by Western blot analysis. Systolic blood pressure and mean arterial pressure (MAP) were examined using tail-cuff and direct arterial measurement, respectively.

Results: In rats injected with control shRNA, high-salt diet (HS) caused higher systolic blood pressure compared with normal-salt diet (NS) (HS: 149 ± 4 mmHg; NS: 126 ± 2 mmHg, $P < 0.05$). Intrathecal injection of TRPV1 shRNA significantly increased the systolic blood pressure in both HS rats and NS rats (HS: 169 ± 3 mmHg; NS: 139 ± 2 mmHg). The increases was greater in HS rats than in NS rats (HS: $13.9\% \pm 1.8\%$; NS: 9.8 ± 0.7 , $P < 0.05$). After TRPV1 shRNA treatment, TRPV1 expression in the dorsal horn and DRG of T8-L3 segments and in mesenteric arteries was knocked down to a greater extent in HS rats compared with NS rats. Blockade of $\alpha 1$ -adrenoceptors abolished the TRPV1 shRNA-induced pressor effects. In rats injected with TRPV1 shRNA, level of tyrosine hydroxylase in mesenteric arteries was increased to a greater extent in HS rats compared with NS rats.

Conclusion: Selective knockdown of TRPV1 expression in the lower thoracic and upper lumbar segments of spinal cord, DRG, and mesenteric arteries enhanced the prohypertensive effects of high salt intake, suggesting that TRPV1 channels in these sites protect against increased salt sensitivity, possibly via suppression of sympatho-excitatory responses.

Keywords: blood pressure; high salt intake; intrathecal injection; short-hairpin RNA; sympathetic nerve; TRPV1

Acta Pharmacologica Sinica (2011) 32: 845–852; doi: 10.1038/aps.2011.43

Introduction

Accumulating evidence indicates that sensory nerves play a key role in regulating blood pressure^[1–3]. The transient receptor potential vanilloid type 1 (TRPV1) channel is abundantly expressed in sensory nerves^[4, 5] and conveys the intricate task of modulating the function of these nerves. Thus, defining the role of TRPV1-positive sensory nerves in the regulation of blood pressure and salt sensitivity will be useful. We have shown previously that the degeneration of TRPV1-expressing sensory nerves throughout the neonatal body by subcutaneous injection of capsaicin, a selective TRPV1 agonist, leads to increased salt sensitivity of arterial pressure, indicating that TRPV1-positive sensory nerves play a counter-regulatory role against salt-induced increases in blood pressure^[6–20]. The underlying mechanism of anti-hypertensive effects of TRPV1

may involve its counter-balancing role against the activation of the renin-angiotensin-aldosterone system^[7–9], sympathetic nervous system^[10], endothelin system^[11, 12], superoxide generation system^[13, 14], and epithelial sodium transporters^[15]. Our previous approach using systemic sensory denervation does, however, have two major limitations. First, systemic sensory denervation obliterates not only TRPV1 but also other components that colocalize with TRPV1 in the same neuron, which may regulate blood pressure independently of TRPV1^[21, 22]. Second, systemic sensory denervation prevents elucidation of the role of specific organ(s) or tissue(s) in regulating blood pressure.

To bypass these limitations, we developed a new model with improved approaches and validation. We applied TRPV1 shRNA to selectively knock down TRPV1 expression without affecting other components that colocalize with TRPV1 in the same neuron. The strategy of using shRNA to selectively silence TRPV channels *in vivo* has been successfully used in our previous study to effectively knock down the

* To whom correspondence should be addressed.

E-mail donna.wang@ht.msu.edu

Received 2011-02-22 Accepted 2011-04-07

expression and function of TRPV4 channels^[23]. In the present study, we used an intrathecal injection technique to target the T8-L3 segments of the dorsal root ganglia (DRG) and their central (dorsal horn) and peripheral (mesenteric arteries and kidneys) terminals without affecting other regions. The T8-L3 segments were chosen as targets because they innervate mesenteric resistance arteries and the kidneys, which are known for their involvement in blood pressure regulation^[24–29].

Using this strategy, we sought to determine whether selective knockdown of TRPV1 expressed in DRG of lower thoracic and upper lumbar segments (T8-L3) and their central and periphery projections enhances the prohypertensive effects induced by salt loading. Furthermore, to assess whether the sympathetic nervous system is involved in TRPV1 shRNA-induced blood pressure regulation, the content of tyrosine hydroxylase (TH), a marker of sympathetic nerves, and blood pressure responses to prazosin, a blocker of α 1-adrenoceptors, were examined.

Materials and methods

Animals

Male Wistar rats (201–225 g, Charles River Laboratory, Wilmington, Massachusetts, USA) were housed in a standard facility. Rats received either a normal-salt (NS) diet (1% NaCl by weight, Harlan Teklad, Madison, Wisconsin, USA) or a high-salt (HS) diet (8% NaCl by weight, Harlan Teklad, Madison, Wisconsin, USA). One week after dietary treatment, rats underwent surgery for intrathecal catheter implantation and removal of the right kidney. One week after surgery, rats began receiving intrathecal injections of either TRPV1 shRNA or control shRNA once per day for 3 d and were randomly divided into 4 groups: NS diet+control shRNA, NS diet+TRPV1 shRNA, HS diet+control shRNA, or HS diet+TRPV1 shRNA. Measurement of systolic blood pressure, mean arterial pressure, water intake, and urine excretion and tissue sample collection for immunohistochemistry and Western blot analysis were performed on d 3 after the beginning of shRNA treatment. All experiments were performed in accordance with the protocols approved by the Institutional Animal Care and Use Committee of Michigan State University.

Surgery for intrathecal catheter implantation and uninephrectomy

Under anesthetization with ketamine/xylazine (85/5 mg/kg, ip), the nape skin was cut open and a small incision was made in the atlanto-occipital membrane. The muscles were separated, and a PE-10 catheter was inserted into the subarachnoid space as far as the T8 segment of the spinal cord (the length of the catheter from the inside end to the atlanto-occipital membrane was about 7.5 cm) and sutured in place, and the incision was closed. About 5 cm of the catheter remained external for injection of shRNA and was sealed with parafilm to stop the outflow of cerebrospinal fluid when not used for injection. Uninephrectomy was performed by making a right flank incision and then removing the right kidney.

Preparation of TRPV1 shRNA or control shRNA and intrathecal injection

TRPV1 shRNA or control shRNA (KR42959N, SABiosciences, Frederick, Maryland, USA) were mixed with i-FectTM (NI35150, Neuromics, Edina, Minnesota, USA) in a 1:5 ratio (*w/v*) for intrathecal injection. Rats received 6 μ g/kg in a 10- μ L volume of either TRPV1 shRNA or control shRNA once daily for three consecutive days. The catheter was immediately flushed with 10 μ L of saline following every injection to ensure that all drugs reached the subarachnoid space.

Measurements of systolic blood pressure, water intake, and urine excretion

Systolic blood pressure of conscious rats was measured by the indirect tail-cuff method with a sphygmomanometer (Hatteras Instruments, Cary, North Carolina, USA). Rats were accustomed to the testing environment for 3 d prior to the measurement, and the blood pressure value for each rat was calculated as the average of nine separate measurements. Twenty-four-hour water intake and urine excretion were determined by the use of metabolic cages one day before and three days after intrathecal injection.

Measurement of mean arterial pressure (MAP) and its response to intravenous injection of capsaicin

The jugular vein and carotid artery of pentobarbital (50 mg/kg, ip) anesthetized rats were cannulated for administration of capsaicin (30 μ g/kg, Sigma, M2028, dissolved in saline with 0.1% ethanol) and for monitoring of MAP (Gould Instruments, Valley View, Ohio, USA), respectively. MAP was recorded 30 min after the cannulation and recorded every 3 s. The MAP value for each rat was calculated as the average of 10 min of continuous measurements.

Blockade of α 1-adrenoceptor by prazosin

Prazosin (P7791, Sigma-Aldrich, St Louis, Missouri, USA, dissolved in saline), an α 1-adrenoceptor blocker, was intragastrically administered via gavage, at a dose of 0.5 mg/kg of each administration dose, twice per day for 7 d starting 3 d before shRNA injection.

Immunohistochemistry

For TRPV1 staining, samples of the spinal cord and DRG of T8-L3 segments, mesenteric arteries, and kidneys were fixed in 4% paraformaldehyde dissolved in phosphate-buffered saline and then cut into 20- μ m sections using a cryostat (Leica CM 1850, Leica Biosystems Nussloch GmbH, Nussloch, Germany). The sections were incubated with guinea pig anti-TRPV1 polyclonal antibody (1:500, AB5566, Millipore, Billerica, Massachusetts, USA) for 1 h at room temperature, and then they were incubated with rhodamine redTM-X donkey anti-guinea pig IgG (1:100, 711-295-152, Jackson ImmunoResearch Laboratories, West Grove, Pennsylvania, USA) for 1 h at room temperature. Pictures were taken with a fluorescent microscope (Olympus BX41 model, Olympus Optical Co, Ltd, Tokyo, Japan; Olympus MicroSuiteTM-Basic software, Olympus Soft

Imaging Solutions GmbH, Münster, Germany).

For tyrosine hydroxylase staining, whole-mount mesenteric second-order arteries were fixed in 70% acetone (in saline) for 3 h. The primary antibody was mouse anti-TH monoclonal antibody (1:1000, Calbiochem 657010, EMD Chemicals, Gibbstown, New Jersey, USA, 1:1000, 1 h at room temperature), and the secondary antibody was rhodamine redTM-X donkey anti-mouse IgG (1:100, 715-295-151, Jackson ImmunoResearch Laboratories, West Grove, Pennsylvania, USA, 1 h at room temperature).

Western blot analysis

Samples were homogenized in 10 mmol/L Tris buffer (pH 7.6) that included protein inhibitors. After centrifugation at 500×g for 5 min, the supernatant was added to 20 μL of 0.5 mol/L EDTA and centrifuged at 50 000×g for 1 h. The pellet was resuspended with lysis buffer on ice for 45 min and centrifuged at 14 000×g for 20 min. After denaturation for 10 min at 100 °C, 30 μg protein of each supernatant was electrophoresed on a 10% SDS-PAGE gel and transferred to a PVDF membrane (162-0180, Bio-Rad Laboratories, Hercules, California, USA). Membranes were incubated with rabbit anti-TRPV1 (1:1000, PA1-29421, Affinity BioReagents, Golden, Colorado, USA) or mouse anti-TH (1:1000, 657010, Calbiochem, EMD Chemicals Inc, Gibbstown, New Jersey, USA) at 4 °C overnight, followed by incubation with HRP-donkey anti-rabbit IgG (1:10 000, 711-035-152, Jackson ImmunoResearch Laboratories, West Grove, Pennsylvania) or HRP-donkey anti-mouse IgG (1:10 000, 711-035-151, Jackson ImmunoResearch Laboratories, West Grove, Pennsylvania, USA) for 2 h at room temperature. The intensity of the bands was determined using ImageJ software (NIH, Bethesda, Maryland, USA). Protein loading on the membrane was normalized to β-actin (mouse anti-β-actin monoclonal antibody, 1:1000, sc-69879, Santa Cruz Biotechnology, Santa Cruz, California, USA).

Statistical analysis

Data are expressed as mean±SEM. Differences between paired groups were analyzed using an unpaired Student's *t*-test. Differences among groups were analyzed using a one-way ANOVA followed by a Bonferroni adjustment for multiple comparisons. Differences were considered statistically significant at *P*<0.05.

Results

Body weight in all groups increased with age. No difference in body weight was found between NS and HS diet-treated rats administered control or TRPV1 shRNA before dietary treatment, at the day of intrathecal injection, or 3 d after intrathecal injection (data not shown), which indicates that the general growth and condition of the rats were not affected by dietary or intrathecal treatment.

TRPV1 shRNA treatment resulted in a greater pressor effect in HS rats compared with NS rats

HS diet intake for 2 weeks, without shRNA treatment,

increased systolic blood pressure when compared with NS-treated rats (Figure 1A). Systolic blood pressure was elevated 3 d after intrathecal injection of TRPV1 shRNA in both NS- and HS-treated rats (in NS rats, control shRNA: 126±2 vs TRPV1 shRNA: 139±2 mmHg, *P*<0.05; in HS rats, control shRNA: 149±4 vs TRPV1 shRNA: 169±3 mmHg, *P*<0.05, Figure 1A). Moreover, the increases in systolic blood pressure after TRPV1 shRNA treatment were greater in HS- than in NS-treated rats (NS: 9.8%±0.7% vs HS: 13.9%±1.8%, *P*<0.05, Figure 1B).

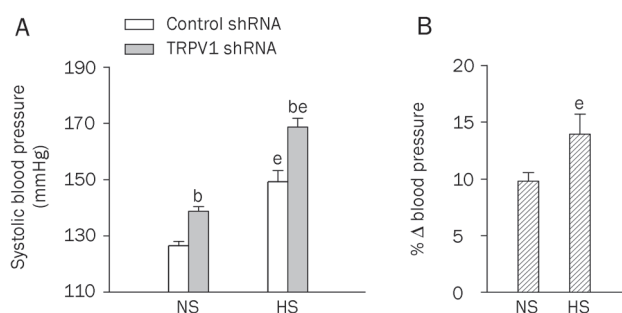


Figure 1. Effects of intrathecal injection of TRPV1 shRNA on systolic blood pressure in rats fed a normal-sodium (NS) or high-sodium (HS) diet. (A) The systolic blood pressure at d 3 after control or TRPV1 shRNA treatment. (B) The percentage change in systolic blood pressure of TRPV1 shRNA compared to that of corresponding control shRNA. Values are expressed as mean±SEM (*n*=11 to 14). ^b*P*<0.05 compared with the corresponding control shRNA-treated group; ^e*P*<0.05 compared with the corresponding NS diet group.

TRPV1 shRNA treatment led to greater TRPV1 downregulation in targeted tissues in HS rats compared with NS rats

Immunohistochemistry studies revealed that TRPV1 expression in the dorsal horn of the spinal cord (T8-L3 segments), DRG (T8-L3 segments), and mesenteric arteries was attenuated in TRPV1 shRNA-treated rats fed either an NS or a HS diet compared with corresponding control shRNA-treated rats (Figure 2). Consistently, quantitative measurement of TRPV1 content by Western blot analysis revealed that TRPV1 expression was knocked down by TRPV1 shRNA treatment in both NS rats and HS rats in the dorsal horn of the spinal cord (T8-L3 segments), DRG (T8-L3 segments), and mesenteric arteries (Figure 3). Western blot analysis revealed that TRPV1 expression was also knocked down by TRPV1 shRNA in the kidney (NS, control shRNA: 0.37±0.02 vs TRPV1 shRNA: 0.29±0.01, *P*<0.05; HS, control shRNA: 0.50±0.03 vs TRPV1 shRNA: 0.29±0.02, *P*<0.05). In contrast, no significant change was found in TRPV1 levels in the cervical spinal cord in NS or HS rats after TRPV1 shRNA treatment (NS, control shRNA: 0.35±0.02 vs TRPV1 shRNA: 0.32±0.03, *P*>0.05; HS, control shRNA: 0.45±0.01 vs TRPV1 shRNA: 0.44±0.02, *P*>0.05), indicating that shRNA suppression occurred only in the targeted segments/tissues. Moreover, TRPV1 expression in the dorsal horn, DRG, and mesenteric arteries was higher in HS rats

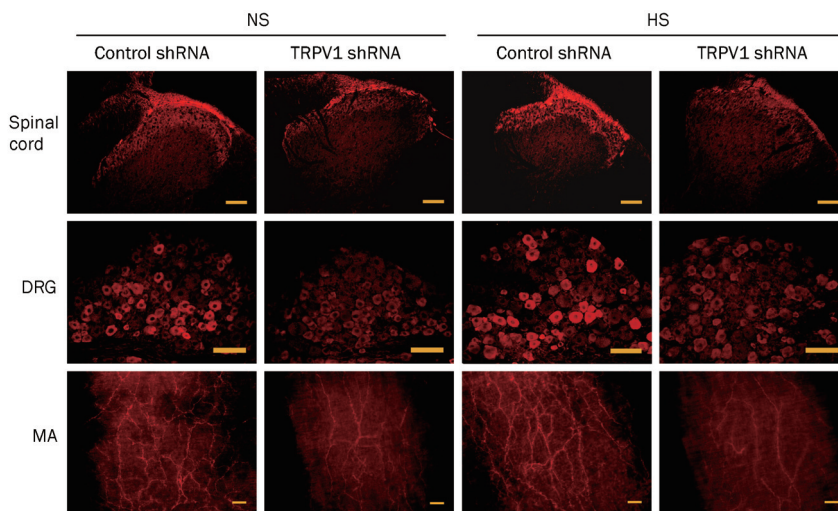


Figure 2. Immunohistochemistry staining showing TRPV1 expression in the dorsal horn of the spinal cord (T8-L3), dorsal root ganglia (DRG) (T8-L3) and mesenteric arteries (MA) of rats fed a NS or HS diet 3 d after control or TRPV1 shRNA treatment. Scale bars, 100 μ m.

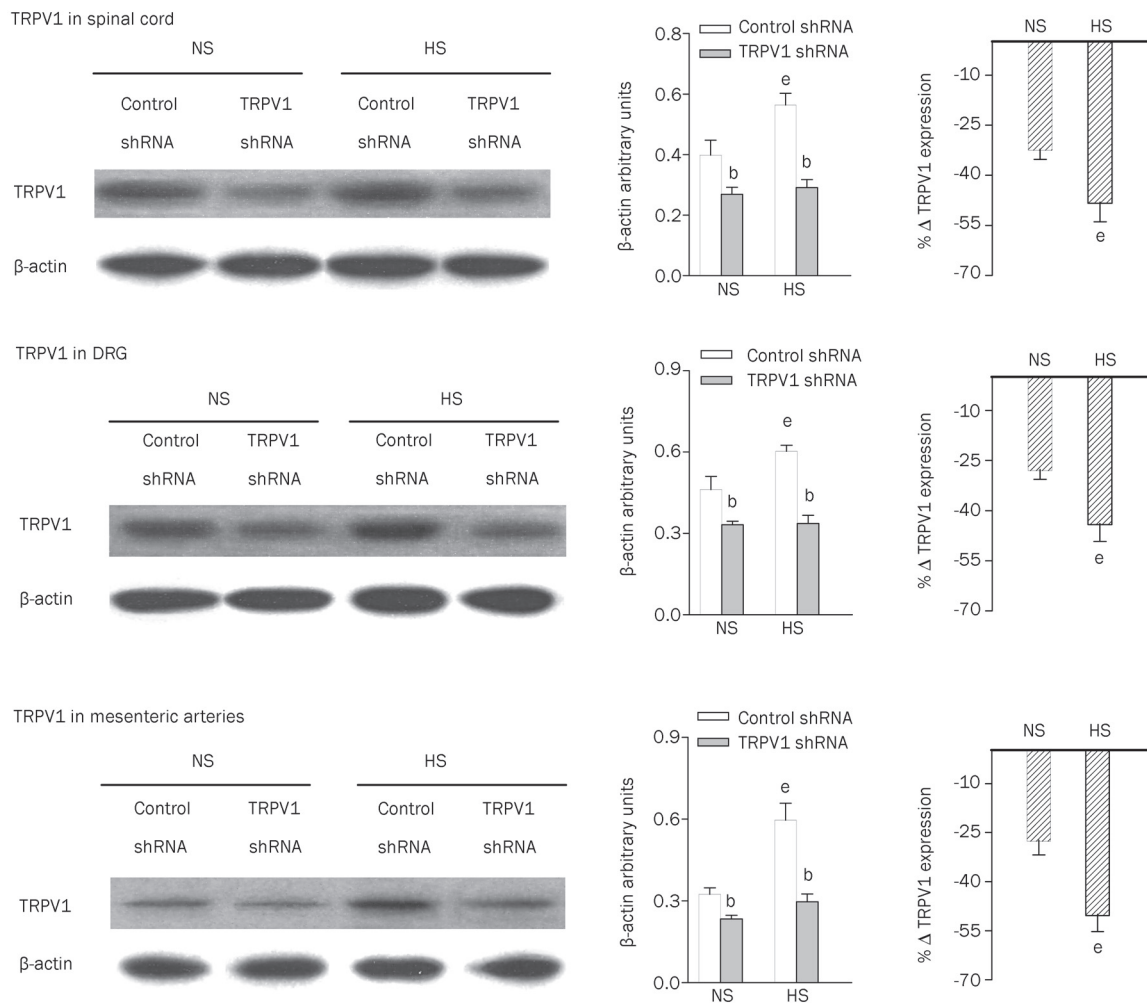


Figure 3. Western blot analysis showing TRPV1 expression in the dorsal horn of the spinal cord (T8-L3), DRG (T8-L3), and mesenteric arteries of rats fed a NS or HS diet 3 d after control or TRPV1 shRNA treatment. The left, middle, and right panels indicate representative Western blots, quantification results (β -actin arbitrary units), and the percentage change of TRPV1 expression of TRPV1 shRNA from that of corresponding control shRNA, respectively. Values are expressed as mean \pm SEM ($n=5$). ^b $P<0.05$ compared with the corresponding control shRNA-treated group; ^e $P<0.05$ compared with the corresponding NS diet group.

administered control shRNA compared with NS rats given control shRNA, and the magnitude of TRPV1 down-regulation by TRPV1 shRNA treatment was greater in HS than in NS rats (dorsal horn, NS: $-32\% \pm 3\%$ vs HS: $-48\% \pm 6\%$, $P < 0.05$; DRG, NS: $-28\% \pm 3\%$ vs HS: $-44\% \pm 5\%$, $P < 0.05$; mesenteric arteries, NS: $-28\% \pm 4\%$ vs HS: $-50\% \pm 5\%$, $P < 0.05$).

TRPV1 shRNA treatment resulted in a greater degree of inhibition of capsaicin-induced depressor effects in HS rats compared with NS rats

To further confirm TRPV1 suppression induced by TRPV1 shRNA, we examined blood pressure responses to iv injection of capsaicin, a selective TRPV1 agonist. The magnitude of the prolonged depression phase of MAP in response to capsaicin was attenuated in both NS and HS rats (Figure 4A) that received TRPV1 shRNA compared with rats that received control shRNA. The magnitude of inhibition of capsaicin-induced depressor effects by TRPV1 shRNA treatment was greater in HS rats than in NS rats (NS: $-34\% \pm 3\%$ vs HS: $-50\% \pm 3\%$, $P < 0.05$) (Figure 4B).

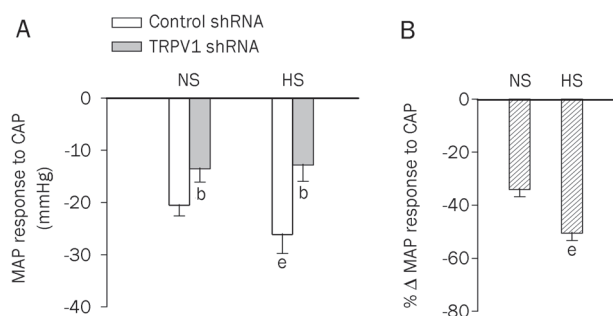


Figure 4. The response of mean arterial pressure (MAP) at 36 s to a bolus injection of capsaicin (30 $\mu\text{g}/\text{kg}$, iv) in NS rats and HS rats 3 d after administration of control or TRPV1 shRNA (A) and the percentage change of MAP in response to capsaicin following TRPV1 shRNA treatment compared with corresponding control shRNA (B). Values are expressed as mean \pm SEM ($n=6$ to 7). ^b $P < 0.05$ compared with the corresponding control shRNA-treated group; ^e $P < 0.05$ compared with the corresponding NS diet group.

TRPV1 shRNA treatment had no effect on urinary excretion in HS- or NS-treated rats

HS intake increased urine excretion, water intake, and the ratio of urine/water intake compared with NS-treated rats both before shRNA treatment and 3 d after. However, no significant differences were found between control shRNA and TRPV1 shRNA-treated rats fed a NS or HS diet in 24-h urine excretion (NS rats, control shRNA: 30 ± 1 vs TRPV1 shRNA: 27 ± 2 mL, $P > 0.05$; HS rats, control shRNA: 106 ± 7 vs TRPV1 shRNA: 106 ± 9 mL, $P > 0.05$), 24-h water intake (NS rats, control shRNA: 53 ± 2 vs TRPV1 shRNA: 50 ± 4 , $P > 0.05$; HS rats, control shRNA: 135 ± 9 vs TRPV1 shRNA: 131 ± 10 , $P > 0.05$), or the ratio of 24-h urine/water intake (NS rats, control shRNA: 0.58 ± 0.02 vs TRPV1 shRNA: 0.54 ± 0.02 , $P > 0.05$; HS rats, control shRNA:

0.79 ± 0.01 vs TRPV1 shRNA: 0.80 ± 0.02 , $P > 0.05$).

Depressor effects induced by blockade of α_1 -adrenoceptors following treatment with TRPV1 shRNA were greater in HS rats compared with NS rats

In both NS and HS rats, blockade of the α_1 -adrenoceptor by prazosin pretreatment prevented TRPV1 shRNA-induced elevation of blood pressure (Figure 5A). Moreover, prazosin played a greater depressor role in HS-treated rats given TRPV1 shRNA compared with NS-treated rats given TRPV1 shRNA (NS: $-7\% \pm 1\%$ vs HS: $-12\% \pm 1\%$, $P < 0.05$, Figure 5B).

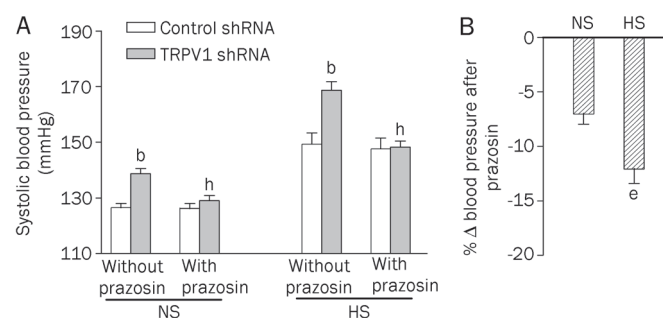


Figure 5. Pretreatment with prazosin prevented TRPV1 shRNA-induced elevation of blood pressure in rats fed NS or HS diets (A) and the percentage change of systolic blood pressure induced by prazosin compared with controls that did not receive prazosin (B). Values are expressed as mean \pm SEM ($n=6$ to 7). ^b $P < 0.05$ compared with the corresponding control shRNA-treated group; ^e $P < 0.05$ compared with the corresponding NS diet group; ^h $P < 0.05$ compared with the corresponding "without prazosin group."

TRPV1 shRNA treatment led to enhanced upregulation of mesenteric tyrosine hydroxylase in HS rats compared with NS rats

Immunohistochemistry staining (Figure 6A) and Western blot analysis (Figure 6B) revealed that TH levels in mesenteric arteries were enhanced in both NS and HS rats administered TRPV1 shRNA compared with corresponding control shRNA-treated rats. In control shRNA-treated rats, HS intake increased TH expression in mesenteric arteries compared with the NS diet. TRPV1 shRNA treatment produced a greater increase in TH in HS rats than in NS rats (NS: $46\% \pm 9\%$ vs HS: $77\% \pm 6\%$, $P < 0.05$) (Figure 6B). In contrast, no significant differences were found in TH levels in the kidney in NS or HS rats administered TRPV1 shRNA compared with rats receiving the control shRNA (NS, control shRNA: 0.22 ± 0.01 vs TRPV1 shRNA: 0.24 ± 0.01 , $P > 0.05$; HS, control shRNA: 0.25 ± 0.02 vs TRPV1 shRNA: 0.30 ± 0.02 , $P > 0.05$).

Discussion

The goal of this study was to determine whether selective knockdown of TRPV1 expressed in the DRG of lower thoracic and upper lumbar segments (T8-L3) and their central and periphery projections enhances prohypertensive effects induced by salt loading. We observed that (1) TRPV1 shRNA

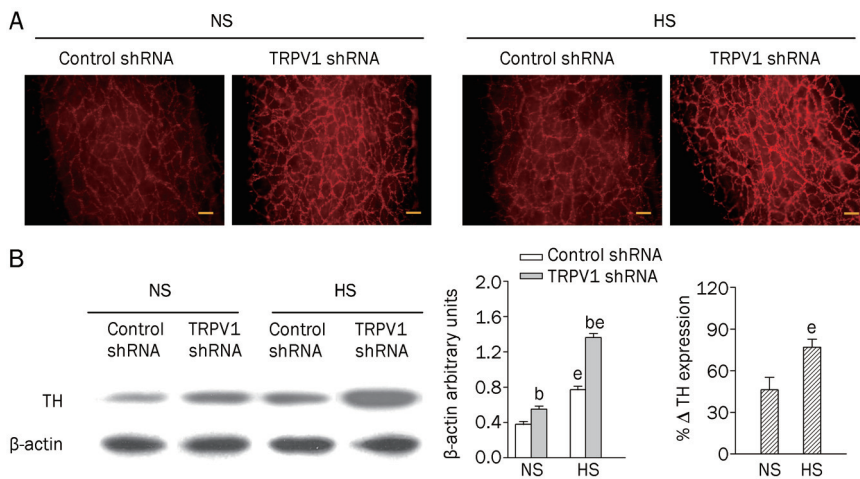


Figure 6. Immunohistochemistry staining (A) and Western blot analysis (B) showing tyrosine hydroxylase expression in mesenteric arteries of rats fed a NS or HS diet 3 d after either control or TRPV1 shRNA treatment. The left, middle, and right panels in (B) indicate representative Western blots, quantification results (% β -actin arbitrary units), and the percentage change of TH expression in rats receiving TRPV1 shRNA compared with control shRNA, respectively. Values are expressed as mean \pm SEM ($n=5$). ^b $P<0.05$ compared with the corresponding control shRNA-treated group; ^e $P<0.05$ compared with the corresponding NS diet group. Scale bars, 100 μ m.

treatment increased blood pressure to a greater extent in HS rats compared with NS rats; (2) HS diet enhanced TRPV1 expression in the dorsal horn, DRG, mesenteric arteries, and kidneys, which was suppressed by TRPV1 shRNA treatment; (3) TRPV1 shRNA treatment attenuated the depressor action of capsaicin with a greater effect in HS rats compared with NS rats; (4) TRPV1 shRNA treatment had no effect on urinary excretion, water intake, or the ratio of urine/water intake in rats fed a NS or HS diet; (5) blockade of α 1-adrenoceptors led to a greater depressor effect in HS rats compared with NS rats treated with TRPV1 shRNA; and (6) TRPV1 shRNA treatment produced a greater increase in TH in mesenteric arteries, but not kidneys, in HS rats compared with NS rats. These data show that selective knockdown of neuronal TRPV1 enhances prohypertensive effects induced by salt loading and that pressor effects of TRPV1 shRNA may be mediated, at least in part, by enhancement of the sympatho-excitatory response.

We have previously shown that neonatal degeneration of TRPV1-expressing sensory nerves increased salt sensitivity of arterial pressure as these rats grew into adulthood^[6–20]. However, the systemic sensory denervation used in these previous studies precluded us from making conclusions about whether the observed effect was due to the removal of TRPV1 or other proteins co-expressed in the same nerves innervating any specific organs or tissues^[21, 22]. In the present study, we anatomically limited the TRPV1 affected by intrathecally injecting TRPV1 shRNA to selectively knockdown TRPV1 in an attempt to answer the question of whether impairment of TRPV1 in selective tissues is sufficient to enhance salt sensitivity of blood pressure. shRNA knocks down the expression of a specific gene by RNA interference, and its transfection efficacy can be further enhanced by the use of the transfection reagent iFectTM, which is particularly designed for facilitating effective transfection for neuronal cells. We did not observe any neuron damage or other side effects following intrathecal injection of shRNA (data not shown), which is consistent with observations made by other laboratories^[30]. Our results show that knocking down TRPV1 expression in T8-L3 DRG and their central and periphery projections, without affecting other

segments such as the cervical spinal cord, significantly modulated the development of hypertension, especially during salt loading. These results indicate that intrathecal injection with shRNA is a viable strategy of conditional knockdown, which can be used to study the role of a given gene or protein.

Although TRPV1 expression in the kidney was suppressed, no changes occurred for 24-h urine excretion, water intake, or the ratio of urine/water intake after TRPV1 shRNA treatment. Although unexpected, these results suggest that mechanisms other than altered renal function are responsible for the prohypertensive effect of TRPV1 shRNA. Given that the peripheral projections of T8-L3 DRGs innervate mesenteric arteries, we examined mesenteric TRPV1 levels. Indeed, TRPV1 levels in mesenteric resistant arteries were suppressed by TRPV1 shRNA treatment. Interestingly, levels of tyrosine hydroxylase, a sympathetic nerve marker, were markedly upregulated after TRPV1 shRNA treatment in mesenteric resistant arteries but not kidneys. Furthermore, blockade of α 1-adrenoceptors completely abolished TRPV1 shRNA-induced prohypertensive effects. These data suggest that heightened sympathetic nerve activity occurred, which contributed to TRPV1 shRNA-induced hypertension. The pressor effect of TRPV1 shRNA may be mediated by enhanced vasoconstriction of mesenteric resistant arteries via at least two potential mechanisms. First, knockdown of TRPV1 in the dorsal horn would decrease signal input from periphery organs to the central nervous system via afferent primary neurons and, as a result, diminish the inhibitory effect of afferent nerves on sympathetic nerve activity in mesenteric resistant arteries^[31–34]. Second, knockdown of TRPV1 expressed in mesenteric resistant arteries would reduce the release of vasodilator neuropeptides such as CGRP and, as a result, diminish the counter-regulatory role of afferent nerves against vasoconstriction^[24, 35, 36].

Our data show that HS intake led to compensatory increases in mesenteric TRPV1 levels, which is consistent with previous reports^[36–38]. Moreover, the depressor effect of TRPV1 activation after capsaicin administration was much greater in HS rats compared with NS rats, supporting the notion that TRPV1 plays a counter-regulatory role against salt-induced increases

in blood pressure. The counter-regulatory effect of TRPV1 has been shown to involve enhanced CGRP release from sensory nerves that cause vasodilation, sodium and water excretion, and decreases in blood pressure^[39–43]. TRPV1 shRNA treatment resulted in enhanced suppression of mesenteric TRPV1 levels but enhanced up-regulation of mesenteric tyrosine hydroxylase contents. The combination of these effects would lead to a more pronounced pressor action in HS rats. Indeed, as shown in the present study, HS rats displayed a greater degree of pressor effects after TRPV1 shRNA treatment when compared with NS rats receiving the same treatment.

In conclusion, the present study shows that intrathecal injection of TRPV1 shRNA selectively knocks down TRPV1 expression in the DRG of T8-L3 segments and their central and periphery projections in rats, which enhances the prohypertensive effects induced by salt loading. The pressor effect of TRPV1 shRNA may be mediated, at least in part, by enhancement of the sympatho-excitatory response.

Acknowledgements

This work was supported in part by the NIH (grants HL-57853, HL-73287, and DK67620).

Author contribution

Donna H WANG designed research, secured funding, and interpreted the data; Shuang-quan YU performed the experiments and analyzed the data; Donna H WANG and Shuang-quan YU wrote the paper.

References

- 1 Zygmunt PM, Petersson J, Andersson DA, Chuang H, Sorgard M, Di Marzo V, et al. Vanilloid receptors on sensory nerves mediate the vasodilator action of anandamide. *Nature* 1999; 400: 452–7.
- 2 Zahner MR, Li DP, Chen SR, Pan HL. Cardiac vanilloid receptor 1-expressing afferent nerves and their role in the cardiogenic sympathetic reflex in rats. *J Physiol* 2003; 551: 515–23.
- 3 Kopp UC, Jones SY, DiBona GF. Afferent renal denervation impairs baroreflex control of efferent renal sympathetic nerve activity. *Am J Physiol Regul Integr Comp Physiol* 2008; 295: R1882–90.
- 4 Caterina MJ, Schumacher MA, Tominaga M, Rosen TA, Levine JD, Julius D. The capsaicin receptor: a heat-activated ion channel in the pain pathway. *Nature* 1997; 389: 816–24.
- 5 Tominaga M, Caterina MJ, Malmberg AB, Rosen TA, Gilbert H, Skinner K, et al. The cloned capsaicin receptor integrates multiple pain-producing stimuli. *Neuron* 1998; 21: 531–43.
- 6 Wang DH, Li J, Qiu J. Salt-sensitive hypertension induced by sensory denervation: introduction of a new model. *Hypertension* 1998; 32: 649–53.
- 7 Wang DH, Li J. Antihypertensive mechanisms underlying a novel salt-sensitive hypertensive model induced by sensory denervation. *Hypertension* 1999; 33: 499–503.
- 8 Huang Y, Wang DH. Role of AT1 and AT2 receptor subtypes in salt-sensitive hypertension induced by sensory nerve degeneration. *J Hypertens* 2001; 19: 1841–6.
- 9 Huang Y, Wang DH. Role of renin-angiotensin-aldosterone system in salt-sensitive hypertension induced by sensory denervation. *Am J Physiol Heart Circ Physiol* 2001; 281: H2143–9.
- 10 Wang DH, Wu W, Lookingland KJ. Degeneration of capsaicin-sensitive sensory nerves leads to increased salt sensitivity through enhancement of sympathoexcitatory response. *Hypertension* 2001; 37: 440–3.
- 11 Ye DZ, Wang DH. Function and regulation of endothelin-1 and its receptors in salt sensitive hypertension induced by sensory nerve degeneration. *Hypertension* 2002; 39: 673–8.
- 12 Wang Y, Chen AF, Wang DH. ETA receptor blockade prevents renal dysfunction in salt-sensitive hypertension induced by sensory denervation. *Am J Physiol Heart Circ Physiol* 2005; 289: H2005–11.
- 13 Song WZ, Chen AF, Wang DH. Increased salt sensitivity induced by sensory denervation: role of superoxide. *Acta Pharmacol Sin* 2004; 25: 1626–32.
- 14 Wang Y, Chen AF, Wang DH. Enhanced oxidative stress in kidneys of salt-sensitive hypertension: role of sensory nerves. *Am J Physiol Heart Circ Physiol* 2006; 291: H3136–43.
- 15 Li J, Wang DH. Function and regulation of epithelial sodium transporters in the kidney of a salt-sensitive hypertensive rat model. *J Hypertens* 2007; 25: 1065–72.
- 16 Vaishnav P, Wang DH. Capsaicin sensitive-sensory nerves and blood pressure regulation. *Curr Med Chem Cardiovasc Hematol Agents* 2003; 1: 177–88.
- 17 Wang DH. The vanilloid receptor and hypertension. *Acta Pharmacol Sin* 2005; 26: 286–94.
- 18 Wang Y, Wang DH. Neural control of blood pressure: focusing on capsaicin-sensitive sensory nerves. *Cardiovasc Hematol Disord Drug Targets* 2007; 7: 37–46.
- 19 Wang DH. Transient receptor potential vanilloid channels in hypertension, inflammation, and end organ damage: an imminent target of therapy for cardiovascular disease? *Curr Opin Cardiol* 2008; 23: 356–63.
- 20 Rayamajhi S, Contractor T, Wang DH. The potential of TRPV1 agonists for treating ischemia/reperfusion-induced renal injuries. *Curr Opin Investig Drugs* 2009; 10: 963–70.
- 21 Kobayashi K, Fukuoka T, Obata K, Yamanaka H, Dai Y, Tokunaga A, et al. Distinct expression of TRPM8, TRPA1, and TRPV1 mRNAs in rat primary afferent neurons with delta/c-fibers and colocalization with trk receptors. *J Comp Neurol* 2005; 493: 596–606.
- 22 Price TJ, Flores CM. Critical evaluation of the colocalization between calcitonin gene-related peptide, substance P, transient receptor potential vanilloid subfamily type 1 immunoreactivities, and isolectin B4 binding in primary afferent neurons of the rat and mouse. *J Pain* 2007; 8: 263–72.
- 23 Gao F, Sui D, Garavito RM, Worden RM, Wang DH. Salt intake augments hypotensive effects of transient receptor potential vanilloid 4: functional significance and implication. *Hypertension* 2009; 53: 228–35.
- 24 Kawasaki H, Takasaki K, Saito A, Goto K. Calcitonin gene-related peptide acts as a novel vasodilator neurotransmitter in mesenteric resistance vessels of the rat. *Nature* 1988; 335: 164–7.
- 25 Mayer G. An update on the relationship between the kidney, salt and hypertension. *Wien Med Wochenschr* 2008; 158: 365–9.
- 26 Ciriello J, Calaresu FR. Central projections of afferent renal fibers in the rat: an anterograde transport study of horseradish peroxidase. *J Auton Nerv Syst* 1983; 8: 273–85.
- 27 Donovan MK, Wyss JM, Winternitz SR. Localization of renal sensory neurons using the fluorescent dye technique. *Brain Res* 1983; 259: 119–22.
- 28 Chevendra V, Weaver LC. Distribution of splenic, mesenteric and renal neurons in sympathetic ganglia in rats. *J Auton Nerv Syst* 1991; 33: 47–53.
- 29 Huang J, Chowdhury SI, Weiss ML. Distribution of sympathetic

- preganglionic neurons innervating the kidney in the rat: PRV trans-neuronal tracing and serial reconstruction. *Auton Neurosci* 2002; 95: 57–70.
- 30 Zou W, Song Z, Guo Q, Liu C, Zhang Z, Zhang Y. Intrathecal lentiviral-mediated RNA interference targeting PKC γ attenuates chronic constriction injury-induced neuropathic pain in rats. *Hum Gene Ther* 2011; 22: 465–75.
- 31 Vizzard MA, Standish A, Ammons WS. Renal afferent input to ventrolateral medulla of the cat. *Am J Physiol* 1992; 263: R412–22.
- 32 Solano-Flores LP, Rosa-Arellano MP, Ciriello J. Fos induction in central structures after afferent renal stimulation. *Brain Res* 1997; 753: 102–19.
- 33 Bard P. Anatomical organization of the central nervous system in relation to control of the heart and blood vessels. *Physiol Rev Suppl* 1960; 4: 3–26.
- 34 Barman SM, Gebber GL. Brain stem neuronal types with activity patterns related to sympathetic nerve discharge. *Am J Physiol* 1981; 240: R335–47.
- 35 Wang LH, Luo M, Wang Y, Galligan JJ, Wang DH. Impaired vasodilation in response to perivascular nerve stimulation in mesenteric arteries of TRPV1-null mutant mice. *J Hypertens* 2006; 24: 2399–408.
- 36 Wang Y, Wang DH. Increased depressor response to N-arachidonoyl-dopamine during high salt intake: role of the TRPV1 receptor. *J Hypertens* 2007; 25: 2426–33.
- 37 Li J, Wang DH. Function and regulation of the vanilloid receptor in rats fed a high salt diet. *J Hypertens* 2003; 21: 1525–30.
- 38 Wang Y, Kaminski NE, Wang DH. VR1-mediated depressor effects during high-salt intake: role of anandamide. *Hypertension* 2005; 46: 986–91.
- 39 Wang Y, Novotny M, Quaiserová-Mocko V, Swain GM, Wang DH. TRPV1-mediated protection against endotoxin-induced hypotension and mortality in rats. *Am J Physiol Regul Integr Comp Physiol* 2008; 294: R1517–23.
- 40 Wang Y, Wang DH. A novel mechanism contributing to development of Dahl salt-sensitive hypertension: role of the transient receptor potential vanilloid type 1. *Hypertension* 2006; 47: 609–14.
- 41 Wang DH, Zhao Y. Increased salt sensitivity induced by impairment of sensory nerves: is nephropathy the cause? *J Hypertens* 2003; 21: 403–9.
- 42 Li J, Wang DH. High-salt-induced increase in blood pressure: role of capsaicin-sensitive sensory nerves. *J Hypertens* 2003; 21: 577–82.
- 43 Wang Y, Kaminski NE, Wang DH. Endocannabinoid regulates blood pressure via activation of the transient receptor potential vanilloid type 1 in Wistar rats fed a high-salt diet. *J Pharmacol Exp Ther* 2007; 321: 763–9.

Original Article

Nanomechanical analysis of insulinoma cells after glucose and capsaicin stimulation using atomic force microscopy

Rui-guo YANG¹, Ning XI¹, King Wai-chiu LAI¹, Bei-hua ZHONG^{2,3}, Carmen Kar-man FUNG¹, Chen-geng QU¹, Donna H WANG^{2,4,*}

¹College of Engineering, Department of Electrical and Computer Engineering, Michigan State University, East Lansing, MI 48824, USA; ²Department of Medicine, Michigan State University, East Lansing, MI 48824, USA; ³Guangzhou Medical College, Guangzhou 510182, China; ⁴Neuroscience Program, Cell and Molecular Biology Program, Michigan State University, USA

Aim: Glucose stimulates insulin secretion from pancreatic islet β cells by altering ion channel activity and membrane potential in the β cells. TRPV1 channel is expressed in the β cells and capsaicin induces insulin secretion similarly to glucose. This study aims to investigate the biophysical properties of the β cells upon stimulation of membrane channels using an atomic force microscopic (AFM) nanoindentation system.

Methods: ATCC insulinoma cell line was used. Cell stiffness, a marker of reorganization of cell membrane and cytoskeleton due to ion channel activation, was measured in real time using an integrated AFM nanoindentation system. Cell height that represented structural changes was simultaneously recorded along with cell stiffness.

Results: After administration of glucose (16, 20, and 40 mmol/L), the cell stiffness was markedly increased in a dose-dependent manner, whereas cell height was changed in an opposite way. Lower concentrations of capsaicin (1.67×10^{-9} and 1.67×10^{-8} mol/L) increased the cell stiffness without altering cell height. In contrast, higher concentrations of capsaicin (1.67×10^{-6} and 1.67×10^{-7} mol/L) had no effect on the cell physical properties.

Conclusion: A unique bio-nanomechanical signature was identified for characterizing biophysical properties of insulinoma cells upon general or specific activation of membrane channels. This study may deepen our understanding of stimulus-secretion coupling of pancreatic islet cells that leads to insulin secretion.

Keywords: AFM nanoindentation; cellular stiffness; insulin secretion; glucose; capsaicin; cellular height

Acta Pharmacologica Sinica (2011) 32: 853–860; doi: 10.1038/aps.2011.56; published online 30 May 2011

Introduction

Pancreatic β -cell responses to glucose and capsaicin stimulation

Pancreatic β -cells are one of the main physiological units of the endocrine pancreas^[1], and they constitute about 65 to 90 percent of the islet cell population. Insulin, produced and released from pancreatic β -cells, is an important hormone that is involved in blood glucose homeostasis. In response to glucose stimulation, insulin is secreted from β -cells, a process known as stimulus-secretion coupling^[2]. The resting potential of the β -cell membrane is determined primarily by the activity of ATP-dependent potassium channels (K_{ATP}). When the plasma glucose level increases, glucose uptake and the β -cell

metabolic rate will be enhanced, leading to the closure of K_{ATP} as the ATP/ADP ratio increases. As a result of the closure of K_{ATP} , the membrane potential changes, leading to the opening of voltage-gated calcium channels due to membrane depolarization. The increased cytoplasmic calcium concentration will ultimately result in insulin secretion (Figure 1). In addition, β -cell responses are synchronized with an oscillatory pattern, displaying pulse-like insulin secretion^[3].

Capsaicin, the main ingredient of hot peppers, is a specific activator of the transient receptor potential vanilloid type 1 (TRPV1) channel, also known as the capsaicin receptor. Accumulating evidence showed that capsaicin-sensitive afferent nerves play a regulatory role in insulin secretion^[4]. Studies also showed that activation of TRPV1 expressed in pancreatic islet β cells may modulate insulin secretion^[5]. Despite the fact that capsaicin may activate TRPV1 leading to altered insulin

* To whom correspondence should be addressed.

E-mail donna.wang@hc.msu.edu

Received 2011-03-10 Accepted 2011-04-13

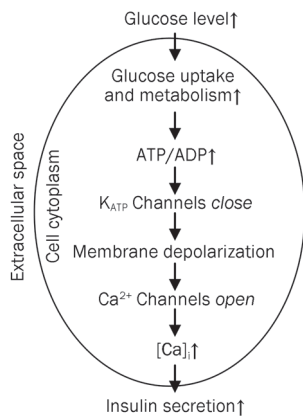


Figure 1. The stimulus-secretion coupling model of β -cells. Increased plasma glucose levels will increase the intracellular ATP/ADP ratio after glucose uptake by cells, which leads to the closure of ATP-dependent potassium channels, membrane depolarization, and the increase in intracellular Ca^{2+} concentrations that result in insulin secretion.

secretion, the mechanisms underlying capsaicin mediated insulin secretion are largely unknown.

The electrophysiological properties of ion channels are important for cellular and organ function, and an ion channel defect in pancreatic islet β cells may lead to metabolic disorders. As such, these ion channels have been widely studied from various perspectives, most of which have made use of the patch-clamp technique to study the electrical activities of cells. While effective, the patch-clamp technique is very time consuming and demands highly skilled workers. Alternatively, other biophysical features may serve as biomarkers for assessing ion channel activities. Indeed, it has been shown that alterations in ion channel activity leading to insulin secretion would change the physical state of the cell membrane^[6] and cytoskeleton^[7]. Membrane bilayer stiffness depends on membrane protein configuration and deformation. The activation of ion channels can alter protein formation, the curvature of the membrane bilayer, and possibly the overall mechanical behavior of the cell^[8, 9]. Accordingly, this study was intended to develop a new technique to study the physical properties of pancreatic insulin secreting cells by characterizing the nanomechanical properties of a single cell or cell population in order to identify unique biomarkers that respond to general or specific channel activators.

Mechanical property characterization using an atomic force microscopic (AFM) nanoindentation system

AFM utilizes a cantilever with a sharp tip to probe the surface topography of various materials. AFM operates the cantilever to move across the sample surface in a raster scan. The fine scan motion was driven by a piezoelectric actuator with a high step resolution. During the scan, the interaction force between the scanning AFM tip and the sample surface bends the cantilever. A laser, which reflects back from the cantilever, records the deflection by readings of the laser spot position on a position sensitive device. The vertical movement of the piezoac-

tuator, which keeps either the tip at a constant distance from the sample (contact mode) or the cantilever in constant oscillation amplitude (tapping mode), forms the topography image. The schematic drawing of the working principle of AFM is shown in Figure 2A. AFM works perfectly well in liquid and makes measurements in real time, features that are ideal for biological applications and have unparalleled advantages over other high resolution imaging systems, including electron microscopy. Obtaining nanometer resolution images of cell membranes, DNA molecules and other biological structures has become possible with the recent development of AFM systems.

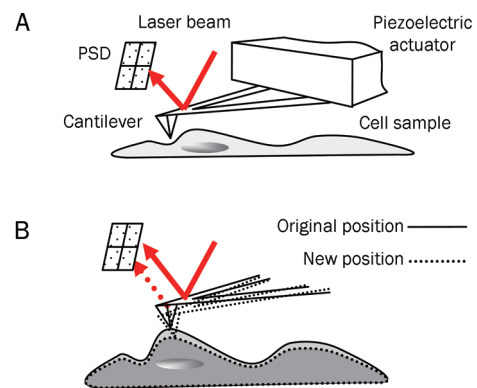


Figure 2. (A) AFM working principle. Briefly, the piezoelectric actuator drives the cantilever with a sharp tip at the end to perform a raster scan on sample surfaces. As it scans across the surface, the interaction force will bend the cantilever, and the bending is recorded by a laser reflected back from the cantilever. By maintaining the tip at a constant distance from the sample, a topography image is formed. (B) The initial contact point, indicated in Figure 2 as a square, indicates the relative height of the sample. By recording the laser position of the contact point, the dynamic cell height can be obtained.

In addition to imaging, AFM is a natural nanoindenter, a feature that can be employed to probe the mechanical properties of materials. In nanoindentation mode, AFM drives a sharp tip into contact with the cell membrane and, consequently, deforms the membrane. By evaluating the indentation force and the indentation depth, the mechanical properties of the cell membrane may be obtained. The process will generate force-displacement curves as shown in Figure 3. A Hertzian model is often used to fit the curve and to generate the Young's modulus value^[10].

When performing the force measurement on the same location of the cell, the AFM tip is drawn into contact by the interaction force (mainly van der Waals adhesive forces) between the tip and cell membrane. The contact point is indicated schematically by the square in the force curve shown in Figure 3. When there are changes in the sample height, the contact point in the following force-displacement curves will correspondingly change in position as indicated by the laser spot (Figure 2B). Therefore, the relative cell height can be obtained

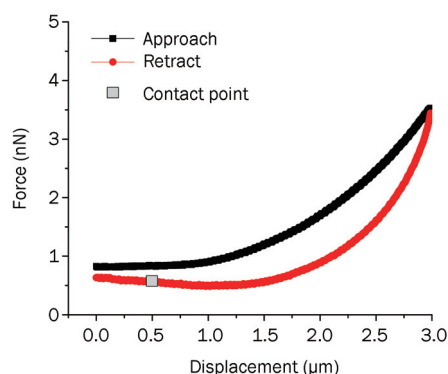


Figure 3. A typical force displacement curve with the contact point marked. The vertical motion will bring the AFM tip into contact with the cell and deform the cell (approach curve), followed by a retraction of the tip (retract curve). During the process, by recording the cantilever deflection (Y axis) with regard to the vertical displacement of the scanner (X axis), the force displacement curve is formed. The contact point is marked schematically as a square in the figure showing the point where the initial contact between the AFM tip and the sample is established.

by the continuous recording of the contact point. Normally, the absolute cell height and volume are measured by a topographical image, and it takes approximately 15 min to capture a single image. Given that the change in response to glucose stimulation happens rapidly, we considered the contact point measurement to be a faster method for monitoring height change.

AFM for the study of β cell ion channel activities

AFM has been applied to study biomarkers for a number of biological events^[11-13]. In these events, changes in physiological conditions led to the reconfiguration of cell membranes and cytoskeleton structures. Cells exhibited distinct mechanical properties, including stiffness and viscosity, due to an altered cellular structure. Thus, AFM-based high resolution imaging and high sensitivity force measurements for characterizing structural and mechanical biomarkers are feasible. For example, AFM has been used for the dynamic observation of mechanical property changes during the loss of cellular adhesion and apoptosis^[13]. Using a similar strategy, this study aims to observe the physical changes of cell membranes in response to glucose and capsaicin stimulation in real time. The ability of AFM to record interaction forces and cell stiffness changes in the nanoscale in real time would provide a fresh perspective on these events.

Materials and methods

Cell culture

The insulinoma cells (ATCC, Manassas, VA, USA) were cultured to confluence in RPMI-1640 medium (Gibco-Invitrogen, Carlsbad, CA, USA) supplemented with 10% fetal calf serum and 1% penicillin and streptomycin at 37 °C in a humidified atmosphere containing 5% CO₂. The cells were then seeded onto glass coverslips until reaching confluency.

Glucose stimulation

Before each glucose stimulation experiment, the coverslips were placed in a petri dish with 5 mL of low glucose medium (2 mmol/L) for 90 min until equilibrium was reached. For glucose stimulation, volumes of 100 μ L, 50 μ L, or 40 μ L of high glucose medium (2 mol/L) were added to the petri dish to make the final glucose concentrations 40 mmol/L, 20 mmol/L, or 16 mmol/L, respectively. A total of 100 μ L of low glucose medium was added to a separate petri dish as a control.

Capsaicin stimulation

Before each capsaicin stimulation experiment, the coverslips were placed in a petri dish containing 5 mL of Hanks' buffered salt solution (HBSS) for 90 min until equilibrium was reached. For capsaicin stimulation, 1 mL of HBSS medium with capsaicin concentrations of 10 nmol/L, 100 nmol/L, 1 μ mol/L, and 10 μ mol/L were added to the petri dish to obtain final concentrations of 1.67×10^{-9} mol/L, 1.67×10^{-8} mol/L, 1.67×10^{-7} mol/L, and 1.67×10^{-6} mol/L, respectively. HBSS 1 mL was added to a separate petri dish as control.

AFM measurements

The insulinoma cells at equilibrium in the low glucose medium or HBSS were directly observed under the AFM equipped with an inverted microscope underneath. For statistical analysis, AFM nanoindentations were performed on 100 randomly selected cells before and after the stimulation. For the dynamic observation, 20 force displacement curves were taken as the baseline before the addition of glucose or capsaicin. After stimulation, force displacement curves were taken at a frequency of 1 Hz to dynamically monitor the stiffness change in real time for 1 h. To obtain higher sensitivity and to prevent the potential damage of the delicate cell membrane by the sharp AFM tip, the force applied to indent the cell was kept at a minimum. The maximum force applied was maintained below 10 nN, with the resulting deformation less than 100 nm, and all force curves were taken at a loading rate of 1 Hz. Meanwhile, the contact point of the cantilever with the cell membrane was recorded to denote the relative cell height. Figure 4 shows an optical image with the AFM cantilever

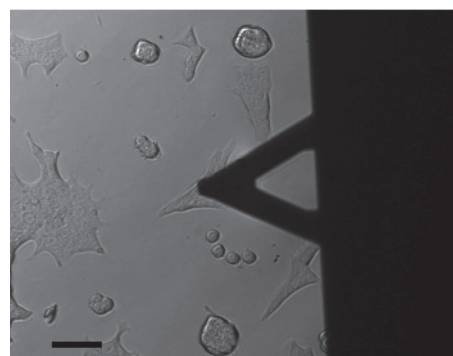


Figure 4. Optical image of an AFM cantilever above an insulinoma cell for nanomechanical property measurement obtained by an inverted optical microscope below the AFM. Scale bar: 50 μ m.

above a single insulinoma cell before the force measurement.

Force displacement curve processing

In the AFM nanoindentation experiment, a conically shaped AFM tip with a silicon nitride cantilever (Bruker-nano, Santa Barbara, CA, USA) was used. The spring constant, which was 0.06 N/m, was calibrated using the thermal tune method. The applied force can be calculated by Hooke's law where: $F=kd$, where d is the deflection of the cantilever and k is the spring constant of the cantilever. According to the Hertzian model, for a conical shaped tip, the relationship between indentation and deformation is defined as:

$$F = \frac{2}{\pi} \frac{E}{1-\nu^2} \delta^2 \tan \alpha$$

where α is the half angle of the cone-shaped tip, ν is the Poisson ratio, F is the applied force, δ is the indentation depth and E is the Young's modulus value. Young's moduli can be generated by fitting a force displacement curve. The half open angle of the tip is 17.5° and we used 0.5 as the Poisson ratio. A Matlab routine was developed to automate the calculation process.

Results

Glucose stimulation and stiffness measurement

For elasticity measurements, the Young's moduli calculated from the first 20 force curves before switching to high glucose were averaged as the baseline. The moduli from the first 20 min of measurements after the addition of high glucose medium were averaged as the positive results. As shown in Figure 5A, the normal Young's modulus value for insulinoma in low glucose medium was around 7.0 kPa. The addition of high glucose medium increased the cell stiffness, and the increase displayed a dose-dependent pattern. The modulus increase resulting from the 40 mmol/L glucose stimulation was more than one fold, reaching 14.8 kPa. The 16 mmol/L glucose stimulation increased the stiffness to 13.9 kPa, while

the 20 mmol/L glucose stimulation increased the stiffness to 14.2 kPa. The control showed no significant changes in stiffness in response to low glucose stimulation.

For the relative height capture, dynamic monitoring showed that there was a sharp decrease in cell height around 120 nm at the onset of stimulation as indicated by the point scatter in Figure 5B. The decrease of cell height was accompanied by the sharp increase of stiffness as shown in Figure 5B. The addition of high glucose medium occurred at 11 min, and the final glucose level was 20 mmol/L. As the experiment continued, the cell height gradually recovered, and the stiffness gradually decreased. Figure 6 shows the relationship between glucose concentration and cell height and stiffness, demonstrating that the increase in glucose concentration causes substantial changes in cell height and increases cell stiffness.

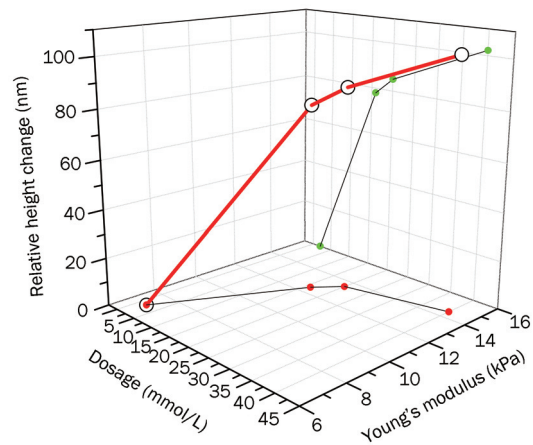


Figure 6. Glucose dosage is related to Young's modulus and change in cell height, with projections on each plane (bottom plane, stiffness vs dosage; right plane, height change vs dosage). There is a substantial increase in both height and stiffness in response to the glucose dosages of 16, 20, and 40 mmol/L compared to the baseline glucose concentration of 2 mmol/L.

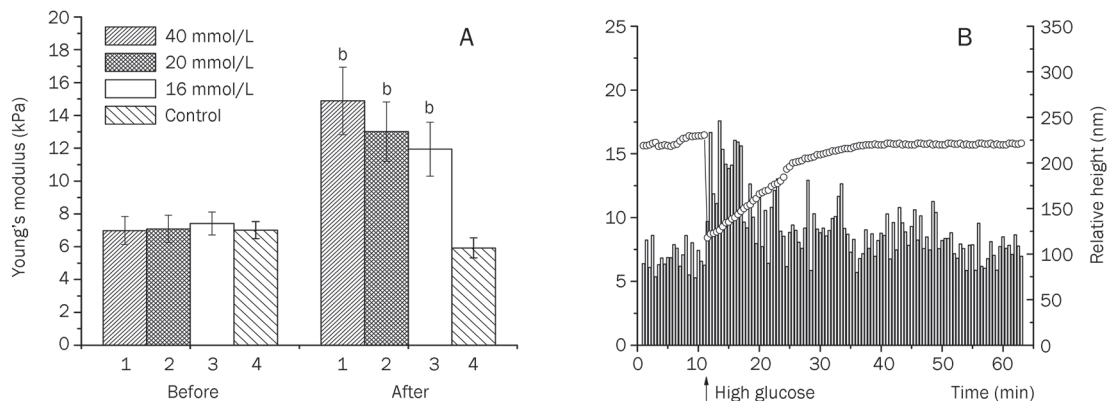


Figure 5. (A) The change in stiffness before and after administration of three different glucose levels: 16, 20, and 40 mmol/L, plus the control. Each datum was expressed as mean \pm SEM. ^b $P < 0.05$ for 40, 20, and 16 mmol/L vs the control ($n=20$). (B) Dynamic stiffness (bar) and cell height change (point scatters) after 20 mmol/L glucose stimulation.

Capsaicin stimulation and stiffness measurement

Nanomechanical property measurement of cell population

The capsaicin stimulation experiment was carried out in a similar fashion as the glucose stimulation experiment. However, unlike the glucose experiment, changes in stiffness after capsaicin stimulation were absent in some cells because they did not respond to capsaicin. Thus, we adopted a statistical approach by measuring the nanomechanical properties of a cell population from which the general cell property might be drawn. This approach has been used by a number of nanomedicine related studies^[12, 14]. A total of 100 randomly selected cells were used prior to stimulation for baseline measurements. Thirty minutes after the addition of capsaicin, measurements were made on the same number of cells. Dose-dependent experiments of capsaicin were performed in the same fashion as in the glucose studies, and capsaicin was added in the following concentrations: 1.67×10^{-9} , 1.67×10^{-8} , 1.67×10^{-7} and 1.67×10^{-6} mol/L. Note that the Young's moduli of the insulinoma cell population has a normal distribution with one peak value (population mean) around 7.0 kPa, as indicated above. The dose studies showed that 1.67×10^{-9} mol/L and 1.67×10^{-8} mol/L capsaicin caused changes in the physical properties of the cell population. The change was displayed as the change in peak percentile and the emergence of another peak at a higher Young's modulus value in the cell population (Figure 7A3 and 7A4), indicating that stiffness was increased in a portion of the cell population after stimulation. Thus, based on the responses, two groups had been identified: cells incapable of responding to capsaicin stimulation sitting in the lower stiffness value peak and cells with responses to capsaicin stimulation residing in the higher stiffness value peak. In contrast, higher concentrations of capsaicin (1.67×10^{-7} and 1.67×10^{-6} mol/L) had no effect on the cell physical properties as shown by the histogram in Figure 7A1 and 7A2. The dose-dependent experiments were summarized in the cumulative distribution in Figure 7B with the horizontal line indicating the 50th percentile. As shown in Figure 7, there was a clear stiffness shift at the 50th percentile line for 1.67×10^{-9} mol/L and 1.67×10^{-8} mol/L capsaicin stimulation compared to the unstimulated cells and the control. This was also confirmed by performing the mean value and deviation analysis as shown in Figure 7C.

Dynamic observation of stiffness and cell height after stimulation

The dose-dependent statistical analysis indicated that subgroups in the cell population responded differently to capsaicin stimulation. We next aimed to define the dynamic changes of cellular nanomechanical properties. A single cell was observed through the whole stimulation process with continuous measurement. This time-lapse experiment was similar to the glucose stimulation experiment for monitoring dynamic stiffness changes and height changes. The stimulation was carried out with 1.67×10^{-9} mol/L capsaicin that was added at 21 min. Before the addition of capsaicin buffer, the cell was observed for 20 min to obtain a baseline. The stiffening effect was not observed immediately following the stimulation, but

it occurred about 10 min after capsaicin administration (Figure 8, bar). The cell Young's modulus increased from 7.0 kPa to 11 kPa and was maintained at this value throughout the experiment. However, the stiffening effect of capsaicin was not accompanied by a change in cell height (Figure 8, point scatter), as an overlaid point scatter plot indicated that the cell maintained the same height during the experiment.

Given the inhomogeneous nature of a cell body where different sites of a cell may respond differently to the applied indentation force, we wanted to ensure that inhomogeneity *per se* would not overshadow the true physiological state of the cell. To reach this goal, each cell was examined at three different locations on the membrane as depicted in Figure 9: at the nucleus located at center of the cell, at the midpoint between the center and boundary of the cell, and at the boundary of the cell. Cells were examined in this fashion, and the results were plotted along with the mean of three measurements (Figure 10A). The mean value of the three measurements for each cell was then plotted in a histogram (Figure 10B) displaying a normal distribution with the peak value at 7.0 kPa, which is consistent with previous observations.

Discussion

As elucidated in Figure 1, it is known that increased glucose concentrations lead to changes in membrane potential and insulin secretion through glucose uptake^[15]. The process is known as stimulus-secretion coupling^[2, 16, 17]. With nanomechanical analysis, the results from the present study show for the first time that cell stiffness increases in a dose-dependent manner in insulinoma cells subjected to glucose stimulation. In addition, cell height decreases with increased glucose concentrations in a synchronized fashion with stiffness changes as revealed by real time AFM nanoindentation measurements. Moreover, capsaicin has been shown to induce insulin secretion either via capsaicin-sensitive afferent neuron-mediated effects^[4] or through activation of TRPV1 expressed in pancreatic islet β cells^[5, 18]. AFM nanomechanical analysis of capsaicin stimulation in the present study reveals a distinct pattern of stiffness changes and dose-dependent effects from glucose stimulation; capsaicin at low (10^{-9} mol/L and 10^{-8} mol/L), but not high, concentrations was able to increase stiffness without altering cellular heights in insulinoma cells.

Accumulating evidence has shown that altered ion channel activities occur and lead to insulin secretion^[17, 19-21]. Altered ion channel activity may cause reorganization of the cellular membrane and cytoskeleton, resulting in changes of cellular stiffness^[6-8]. Using an integrated AFM imaging system, we were able to measure cell stiffness and structural changes simultaneously upon stimulation of glucose and capsaicin (both known to alter ion channel activity and insulin secretion) on the nanoscale in real time. Distinct nanomechanical properties of insulinoma cell responses to glucose and capsaicin have been identified, which may indicate that a unique bio-nanomechanical signature is linked to a specific stimulus-secretion coupling of pancreatic islet cells that leads to insulin secretion.

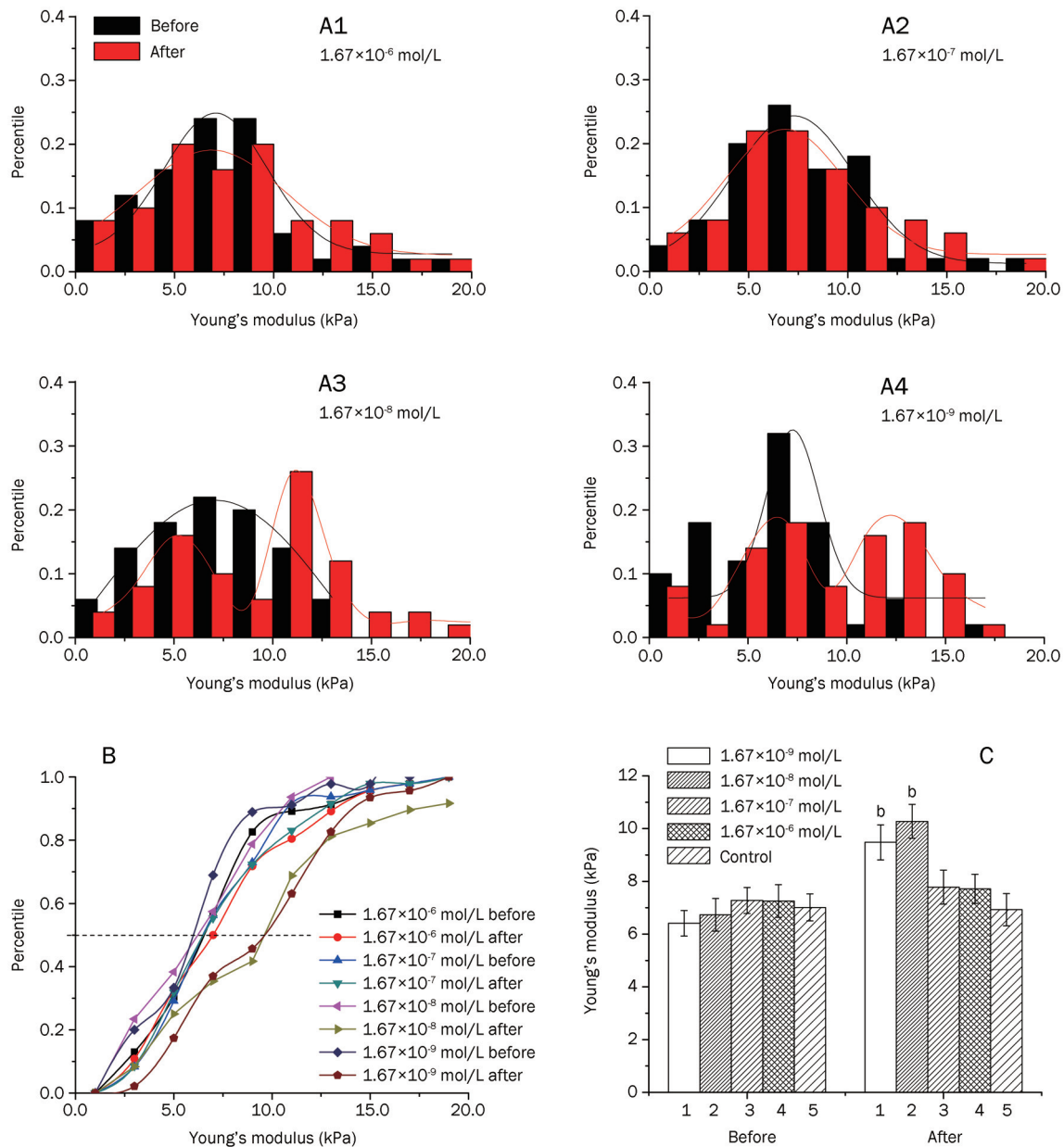


Figure 7. (A) Dose-dependent experimental results obtained from four different capsaicin concentrations: A1: 1.67×10^{-6} mol/L, A2: 1.67×10^{-7} mol/L, A3: 1.67×10^{-8} mol/L, and A4: 1.67×10^{-9} mol/L. (B) Summarized dose-dependent experiment with cumulative histogram. (C) Mean comparison of different doses with $^bP < 0.05$ for 1.67×10^{-9} mol/L and 1.67×10^{-8} mol/L vs the control and $^bP < 0.05$ for 1.67×10^{-9} mol/L and 1.67×10^{-8} mol/L vs 1.67×10^{-6} mol/L and 1.67×10^{-7} mol/L, respectively. Each datum is expressed as the mean \pm SEM ($n=100$).

Following glucose stimulation, we observed rapid decreases in cellular height. This physical change of cells may be explained by a number of glucose effects. In addition to altering ion channel activity, glucose may also change osmolarity, which may affect the configuration of the cellular structure. Before reaching equilibrium by glucose uptake, osmolarity outside of cells may be higher than that inside after glucose administration, which may lead to cellular shrinkage and contribute to increased cellular stiffness. Thus, increased cell stiffness after glucose administration may be attributed to altered ion channel activity and changes in osmolarity. In

contrast, cells remain the same height in response to capsaicin administration, indicating that the shrinkage of cells due to altered osmolarity was absent in the capsaicin experiments. Moreover, cell stiffness increased only at low doses of capsaicin without altering cell height, further ruling out the possibility that concentrations of capsaicin may alter osmolarity and, therefore, cell stiffness. These results are consistent with a previous report where capsaicin induces insulin secretion only at low doses^[5].

The nature of small changes in cell stiffness presents a daunting challenge for detecting and capturing these changes.

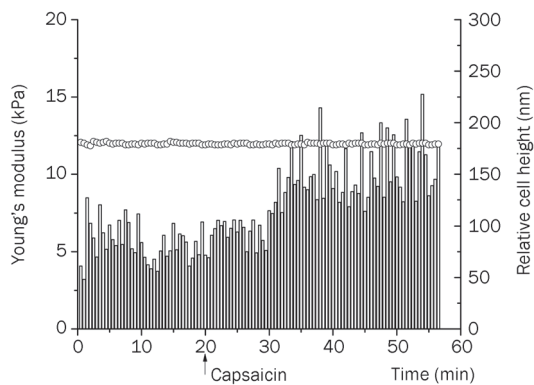


Figure 8. Dynamic stiffness (bar) and cell height change (point scatter) after 1.67×10^{-9} mol/L capsaicin stimulation.

With the use of the AFM nanoindentation system, forces less than 10 nN can be applied, and the resulting changes in cell stiffness can be detected. Such a unique capability and the ultra-high sensitivity of the AFM nanoindentation system are indeed advantageous for studies focused on the cellular and molecule levels. Such an approach may provide insight into pancreatic β -cell stimulation secretion responses with a fresh perspective. With future development aimed at integrating AFM with traditional capabilities, including patch-clamp aptitude for measurement of ion channel activity and fluorescence

optical microscopy assessment of intracellular Ca^{2+} concentrations, the next generation of the AFM system would indeed be a powerful tool to not only study pathophysiological events of ion channels and other molecules but also facilitate drug discovery.

Acknowledgements

This research was partially supported by NSF Grants IIS-0713346 and DMI-0500372, ONR Grants N00014-04-1-0799 and N00014-07-1-0935, NIH Grant R43 GM084520, HL-57853, HL-73287, and DK67620.

Author contribution

Ning XI and Donna H WANG designed the research. Rui-guo YANG performed the experiments, analyzed the data and wrote the manuscript. Donna H WANG and King Wai-chiu LAI revised the paper. King Wai-chiu LAI, Bei-hua ZHONG, Carmen Kar-man FUNG, and Chen-geng QU assisted with the experiments.

References

- 1 Leung YM, Ahmed I, Sheu L, Tsushima RG, Diamant NE, Hara M, *et al*. Electrophysiological characterization of pancreatic islet cells in the mouse insulin promoter–green fluorescent protein mouse. *Endocrinology* 2005; 146: 4766–75.
- 2 Juan-Pico P, Fuentes E, Bermudez-Silva FJ, Diaz-Molina FJ, Ripoll C, de Fonseca FR, *et al*. Cannabinoid receptors regulate Ca^{2+} signals

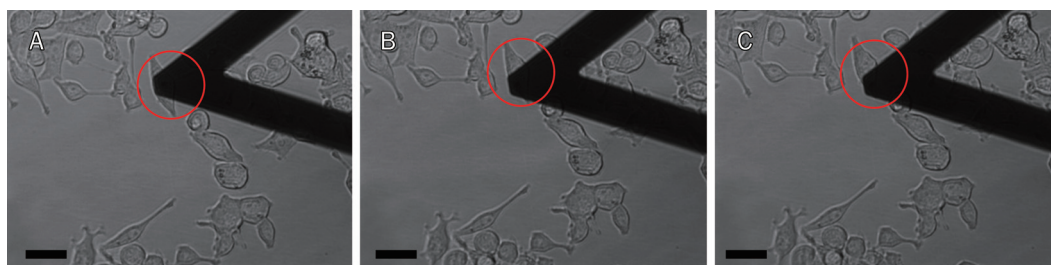


Figure 9. Position of measurement with AFM tip on top of an insulinoma cell: (A) nucleus; (B) middle between nucleus and boundary; and (C) boundary. Scale bar: 20 μm .

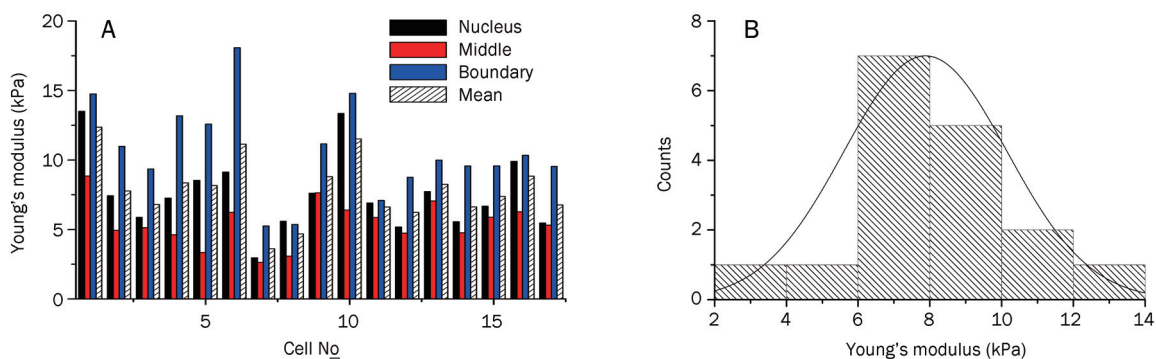


Figure 10. Measurement results on 17 cells at three different locations for each cell. (A) The mean of the three values for each cell, and (B) the distribution of the mean value with the peak at a similar value as previously established.

- and insulin secretion in pancreatic beta-cell. *Cell Calcium* 2006; 39: 155–62.
- 3 Nilius B, Owsianik G, Voets T, Peters JA. Transient receptor potential cation channels in disease. *Physiol Rev* 2007; 87: 165–217.
 - 4 Karlsson S, Scheurink AJ, Steffens AB, Ahren B. Involvement of capsaicin-sensitive nerves in regulation of insulin secretion and glucose tolerance in conscious mice. *Am J Physiol* 1994; 267: R1071–7.
 - 5 Akiba Y, Kato S, Katsube K, Nakamura M, Takeuchi K, Ishii H, *et al*. Transient receptor potential vanilloid subfamily 1 expressed in pancreatic islet beta cells modulates insulin secretion in rats. *Biochem Biophys Res Commun* 2004; 321: 219–25.
 - 6 Lundbaek JA, Birn P, Girshman J, Hansen AJ, Andersen OS. Membrane stiffness and channel function. *Biochemistry* 1996; 35: 3825–30.
 - 7 Cantiello HF. Role of the actin cytoskeleton on epithelial Na⁺ channel regulation. *Kidney Int* 1995; 48: 970–84.
 - 8 Lundbaek JA, Andersen OS. Spring constants for channel-induced lipid bilayer deformations estimates using gramicidin channels. *Biophys J* 1999; 76: 889–95.
 - 9 Lim CT, Zhou EH, Quek ST. Mechanical models for living cells — A review. *J Biomech* 2006; 39: 195–216.
 - 10 Touhami A, Nysten B, Dufrene YF. Nanoscale mapping of the elasticity of microbial cells by atomic force microscopy. *Langmuir* 2003; 19: 4539–43.
 - 11 Pelling AE, Veraitch FS, Chu CP, Mason C, Horton MA. Mechanical dynamics of single cells during early apoptosis. *Cell Motil Cytoskeleton* 2009; 66: 409–22.
 - 12 Cross SE, Jin YS, Rao J, Gimzewski JK. Nanomechanical analysis of cells from cancer patients. *Nat Nanotechnol* 2007; 2: 780–3.
 - 13 Fung CKM, Seiffert-Sinha K, Lai KWC, Yang RG, Panyard D, Zhang JB, *et al*. Investigation of human keratinocyte cell adhesion using atomic force microscopy. *Nanomedicine* 2010; 6: 191–200.
 - 14 Hammerick KE, Huang Z, Sun N, Lam MT, Prinz FB, Wu JC, *et al*. Elastic properties of induced pluripotent stem cells. *Tissue Eng Part A* 2011; 17: 495–502.
 - 15 Henquin JC. Triggering and amplifying pathways of regulation of insulin secretion by glucose. *Diabetes* 2000; 49: 1751–60.
 - 16 Malaisse WJ, Sener A, Koser M, Ravazzola M, Malaisse-Lagae F. The stimulus-secretion coupling of glucose-induced insulin release due to glycogenolysis in glucose-deprived islets. *Biochem J* 1977; 164: 447–54.
 - 17 Henquin JC, Meissner HP. Significance of ionic fluxes and changes in membrane potential for stimulus-secretion coupling in pancreatic B-cells. *Experientia* 1984; 40: 1043–52.
 - 18 Schmidt PT, Tornøe K, Poulsen SS, Rasmussen TN, Holst JJ. Tachykinins in the porcine pancreas: potent exocrine and endocrine effects via NK-1 receptors. *Pancreas* 2000; 20: 241–7.
 - 19 Kilpatrick DL. Ion channels and membrane potential in stimulus-secretion coupling in adrenal paraneurons. *Can J Physiol Pharmacol* 1984; 62: 477–83.
 - 20 Ammala C, Kane C, Cosgrove KE, Chapman JC, Aynsley-Green A, Lindley KJ, *et al*. Characterization of ion channels in stimulus-secretion coupling in pancreatic islets. *Digestion* 1997; 58: 81–5.
 - 21 Petersen OH. Stimulus-secretion coupling: cytoplasmic calcium signals and the control of ion channels in exocrine acinar cells. *J Physiol* 1992; 448: 1–51.